frontiers | Research Topics

Microbial co-cultures: A new era of synthetic biology and metabolic engineering

Edited by
Durgesh K. Jaiswal, Jay Prakash Verma, Tarun Belwal,
Arthur Prudêncio De Araujo Pereira and Avinash Bapurao Ade

Published in
Frontiers in Microbiology

FRONTIERS EBOOK COPYRIGHT STATEMENT

The copyright in the text of individual articles in this ebook is the property of their respective authors or their respective institutions or funders. The copyright in graphics and images within each article may be subject to copyright of other parties. In both cases this is subject to a license granted to Frontiers.

The compilation of articles constituting this ebook is the property of Frontiers.

Each article within this ebook, and the ebook itself, are published under the most recent version of the Creative Commons CC-BY licence. The version current at the date of publication of this ebook is CC-BY 4.0. If the CC-BY licence is updated, the licence granted by Frontiers is automatically updated to the new version.

When exercising any right under the CC-BY licence, Frontiers must be attributed as the original publisher of the article or ebook, as applicable.

Authors have the responsibility of ensuring that any graphics or other materials which are the property of others may be included in the CC-BY licence, but this should be checked before relying on the CC-BY licence to reproduce those materials. Any copyright notices relating to those materials must be complied with.

Copyright and source acknowledgement notices may not be removed and must be displayed in any copy, derivative work or partial copy which includes the elements in question.

All copyright, and all rights therein, are protected by national and international copyright laws. The above represents a summary only. For further information please read Frontiers' Conditions for Website Use and Copyright Statement, and the applicable CC-BY licence.

ISSN 1664-8714
ISBN 978-2-8325-2956-0
DOI 10.3389/978-2-8325-2956-0

About Frontiers

Frontiers is more than just an open access publisher of scholarly articles: it is a pioneering approach to the world of academia, radically improving the way scholarly research is managed. The grand vision of Frontiers is a world where all people have an equal opportunity to seek, share and generate knowledge. Frontiers provides immediate and permanent online open access to all its publications, but this alone is not enough to realize our grand goals.

Frontiers journal series

The Frontiers journal series is a multi-tier and interdisciplinary set of open-access, online journals, promising a paradigm shift from the current review, selection and dissemination processes in academic publishing. All Frontiers journals are driven by researchers for researchers; therefore, they constitute a service to the scholarly community. At the same time, the *Frontiers journal series* operates on a revolutionary invention, the tiered publishing system, initially addressing specific communities of scholars, and gradually climbing up to broader public understanding, thus serving the interests of the lay society, too.

Dedication to quality

Each Frontiers article is a landmark of the highest quality, thanks to genuinely collaborative interactions between authors and review editors, who include some of the world's best academicians. Research must be certified by peers before entering a stream of knowledge that may eventually reach the public - and shape society; therefore, Frontiers only applies the most rigorous and unbiased reviews. Frontiers revolutionizes research publishing by freely delivering the most outstanding research, evaluated with no bias from both the academic and social point of view. By applying the most advanced information technologies, Frontiers is catapulting scholarly publishing into a new generation.

What are Frontiers Research Topics?

Frontiers Research Topics are very popular trademarks of the *Frontiers journals series*: they are collections of at least ten articles, all centered on a particular subject. With their unique mix of varied contributions from Original Research to Review Articles, Frontiers Research Topics unify the most influential researchers, the latest key findings and historical advances in a hot research area.

Find out more on how to host your own Frontiers Research Topic or contribute to one as an author by contacting the Frontiers editorial office: frontiersin.org/about/contact

Microbial co-cultures: A new era of synthetic biology and metabolic engineering

Topic editors

Durgesh K. Jaiswal — Savitribai Phule Pune University, India
Jay Prakash Verma — Banaras Hindu University, India
Tarun Belwal — Texas A and M University, United States
Arthur Prudêncio De Araujo Pereira — Federal University of Ceara, Brazil
Avinash Bapurao Ade — Savitribai Phule Pune University, India

Citation

Jaiswal, D. K., Verma, J. P., Belwal, T., Pereira, A. P. D. A., Ade, A. B., eds. (2023). *Microbial co-cultures: A new era of synthetic biology and metabolic engineering*. Lausanne: Frontiers Media SA. doi: 10.3389/978-2-8325-2956-0

Table of contents

frontiers | Frontiers in Microbiology

TYPE Editorial
PUBLISHED 23 June 2023
DOI 10.3389/fmicb.2023.1235565

Check for updates

OPEN ACCESS

EDITED AND REVIEWED BY
William James Hickey,
University of Wisconsin-Madison, United States

*CORRESPONDENCE
Durgesh Kumar Jaiswal
✉ durgesh.jaiswal9@gmail.com;
✉ durgesh.jaiswal1@bhu.ac.in

RECEIVED 06 June 2023
ACCEPTED 12 June 2023
PUBLISHED 23 June 2023

CITATION
Jaiswal DK, Verma JP, Belwal T, Pereira APDA and Ade AB (2023) Editorial: Microbial co-cultures: a new era of synthetic biology and metabolic engineering.
Front. Microbiol. 14:1235565.
doi: 10.3389/fmicb.2023.1235565

COPYRIGHT
© 2023 Jaiswal, Verma, Belwal, Pereira and Ade. This is an open-access article distributed under the terms of the Creative Commons Attribution License (CC BY). The use, distribution or reproduction in other forums is permitted, provided the original author(s) and the copyright owner(s) are credited and that the original publication in this journal is cited, in accordance with accepted academic practice. No use, distribution or reproduction is permitted which does not comply with these terms.

Editorial: Microbial co-cultures: a new era of synthetic biology and metabolic engineering

Durgesh Kumar Jaiswal[1]*, Jay Prakash Verma[2], Tarun Belwal[3], Arthur Prudêncio De Araujo Pereira[4] and Avinash Bapurao Ade[1]

[1]Department of Botany, Savitribai Phule Pune University, Pune, Maharashtra, India, [2]Plant-Microbe Interaction Lab, Institute of Environment and Sustainable Development, Banaras Hindu University, Varanasi, Uttar Pradesh, India, [3]Texas A&M University, College Station, TX, United States, [4]Federal University of Ceará, Soil Science Department, Soil Microbiology Laboratory, Fortaleza, Ceará, Brazil

KEYWORDS

synthetic microbial consortia, metabolic engineering, sustainable agriculture, industrial, environment

Editorial on the Research Topic
Microbial co-cultures: a new era of synthetic biology and metabolic engineering

This special issue explores the field of microbial engineering consortia and its potential applications in agriculture, industrial, and environmental restoration. Microbial consortia are communities of diverse groups of microorganisms that collaborate to achieve collective goals. By harnessing symbiotic interactions and synergistic behaviors, scientists aim to unlock various applications beyond what single organisms can accomplish. In the realm of agriculture, microbial consortia hold tremendous promise. They can enhance nutrient availability, suppress diseases, improve soil health, promote plant growth, manage abiotic stress, increase crop productivity, and support sustainable farming methods. However, further research is needed to optimize consortia composition, stability, and functionality for multiple crops' productivity, environmental sustainability, and cost-effectiveness concerns. Microbial consortia also show immense potential for ecological restoration and revitalization. They can be utilized for bioremediation of contaminated sites, restoration of soil health, wastewater treatment, ecological restoration, climate change mitigation, and environmental health assessment. However, similar to agricultural applications, further research is necessary to optimize their application in specific contexts. This special issue features cutting-edge research articles and reviews that delve into various aspects of microbial engineering consortia. The articles cover topics such as industrial enzyme production, plant growth promotion under stress conditions, utilizing CO_2 as a feedstock for chemical manufacturing, understanding community dynamics and phenotypes, function-driven co-cultures for tobacco quality improvement, desiccation-tolerant bacteria for crop resilience, artificial plant-bacteria systems, biocontrol of crop diseases, and the development of nano-pesticides. Additionally, the issue explores using bacterial biosensors for environmental pollution detection and creating synthetic consortia for the sustainable production of ethylene and isoprene. Overall, this special issue provides insights into the exciting and rapidly advancing field of microbial engineering consortia and highlights the potential applications, challenges, and prospects in agricultural fields.

Synthetic biology has emerged as a transformative field, revolutionizing the way we approach complex biological systems. Synthetic biology aims to design, construct, and manipulate biological components to create novel functionalities and address real-world challenges (Andrianantoandro et al., 2006; Liang et al., 2022). Over the years, researchers made remarkable progress in engineering individual microorganisms to perform specific tasks. However, the true potential of synthetic biology lies in the collaborative efforts of microbial consortia–a new frontier that holds immense promise in various domains (Brenner et al., 2008; Ben Said and Or, 2017).

In this special issue, we delve into the exciting world of engineering microbial consortia and explore its potential applications, challenges, and prospects in agriculture and the environment. Microbial consortia refer to communities of diverse microorganisms that interact and work together to achieve collective objectives. By harnessing symbiotic interactions and synergistic behaviors, scientists' main aim is to unlock a range of applications that go beyond what single organisms can achieve (Hays et al., 2015; Liu et al., 2023).

Indeed, microbial consortia hold tremendous promise in agriculture. The use of these communities of microorganisms can revolutionize agricultural practices by improving nutrient availability (Yadav et al., 2014; Shukla et al., 2020; Vishwakarma et al., 2020; Jaiswal et al., 2022b; Islam et al., 2023); disease suppression (Sarma et al., 2015; Gómez Expósito et al., 2017; Dheeman et al., 2023); soil health (Khan et al., 2023; Nabi, 2023); plant growth promotion (Verma et al., 2014a, 2023; Méndez-Bravo et al., 2023); crop protection (Jaiswal et al., 2022a); management abiotic stress (Krishna et al., 2022; Prajapati et al., 2022; Hett et al., 2023; Mahreen et al., 2023); sustainable crop productivity (Singh et al., 2016; Mukherjee et al., 2022; Kaushal et al., 2023; Paravar et al., 2023), and promoting sustainable farming methods (Jha et al., 2013; Kong et al., 2018; Gehlot et al., 2021). It is worth noting that engineering microbial consortia for agricultural applications is still in its early stages. Further research is needed to optimize consortia composition, stability, and functionality for multiple crops under different environments and agroclimatic regions. Additionally, the scalability and cost-effectiveness of implementing microbial consortia in agricultural systems need consideration.

In addition, one more area where microbial consortia have immense potential for environmental restoration and revitalization (Verma et al., 2014b; Abhilash et al., 2016; Pankaj and Pandey, 2022; Singh et al., 2023). The complex interactions within these communities can be harnessed to address ecological challenges and restore ecosystems (Liang et al., 2022). Researchers explore the study in which microbial consortia show promise in environmental revival: bioremediation of contaminated sites (Jaiswal et al., 2019; Zhang et al., 2020; Li et al., 2023; Wu et al., 2023); restoration of Soil Health (Lebrun et al., 2021); wastewater Treatment (Mazzucotelli et al., 2014; Heredia et al., 2022); ecological restoration (Singh et al., 2023); climate change mitigation (Hamilton et al., 2016; Silverstein et al., 2023) and monitoring and environmental health assessment (Bhatia et al., 2018; Chandran et al., 2020). The field of engineering microbial consortia for environmental revival is still evolving, and further research is needed to optimize their application in specific contexts.

However, in this special issue, we have a collection of 13 cutting-edge research articles and two review articles that shed light on the diverse aspects of engineering microbial consortia and their functional attributes for agricultural productivity and environmental & industrial sustainability.

Engineering microbial consortia: sustainable agriculture

The engineering of microbial consortiums for sustainable agriculture has great promise for increasing yields while reducing negative environmental effects. These coalitions can enhance nutrient cycling, disease control, soil health, and plant resilience by harnessing the strength of microbial interactions. However, the full potential of microbial consortia in attaining sustainable and resilient agricultural systems relies on further study and innovation in this sector. Furthermore, the widespread use of engineered microbial consortia in sustainable agriculture still faces obstacles like scaling up from laboratory to field conditions, ensuring stability and persistence of the consortia, and addressing regulatory and ethical considerations. In this Research Topic, the following articles collection addresses the current need for research to promote sustainable agriculture.

Gupta et al. claimed that integrated and balanced nutrient management inspired the trial. Organic manures with N_2-fixing, P-, and K-solubilizing microbial inoculants improved the crop growth, root development, and soil health. The study's findings may help to manage crop wastes and animal bio-products by encouraging microbial consortia and organic manure-based agro-industries, vital to microbial inoculants and integrated nutrient management (INM). Thus, the study would sustain agricultural growth by producing high-quality crops, sustaining agro-biodiversity, and making soils healthy, fertile, and productive.

Zeyad et al. observed that applying *Streptomyces araujoniae* strains (TN11 and TN19) individually and as a consortium reduces wilt severity in chickpea plants. Reduction in disease development was supported by the production of antifungal metabolites at a higher level by *S araujoniae* strains. The results on disease development, plant growth parameters, physiological and biochemical parameters, and gene expression studies suggest that the consortium of TN11 and TN19 can act as an efficient biocontrol tool against chickpea wilt caused by *Fusarium oxysporum* f. sp. ciceris (Foc).

Mageshwaran et al. recorded that the bacterial endophytes had biocontrol capability. Three promising isolates inhibited all three soil-borne fungal infections (*R. solani*, S. *rolfsii*, and *F. oxysporum* f.sp. ciceri) *in-vitro*. *Bacillus subtilis* strains TRO4 and CLO5-treated chickpea seeds increased plant development and reduced complex wilt disease incidence in the in-planta assay. This study explores chickpea plant complex wilt disease management with possible endophytes. Eco-friendly wilt disease management would improve plant and soil health.

Shahid et al. studied that natural and human-induced stresses affect crop plant growth and yield. Plant stress hormone ethylene can hinder growth and survival. However, ACC deaminase, an enzyme that decreases ethylene levels, can reduce stress and

increase crop yield. According to the researchers, plant growth-promoting rhizobacteria (PGPR) with ACC deaminase activity enhance plant growth under unfavorable conditions like salt stress, water deprivation, extreme temperatures, waterlogging, heavy metals, pesticides, and organic pollutants. They also used molecular biotechnology and omics methods like proteomics, transcriptomics, metagenomics, and NGS to find and characterize stress-tolerant PGPR strains that produce ACC deaminase. These microorganisms can help crops flourish and tolerate harsh environmental conditions.

Shankar and Prasad observed that desiccation-tolerant plant growth-promoting rhizobacteria (DT-PGPR) may reduce the deleterious effects of water stress on wheat yield and physiology. Under desiccation stress, five DT-PGPR isolates—*Enterobacter cloacae* BHUAS1, *Bacillus cereus* BHUAS2, *Bacillus megaterium* BHUIESDAS3, 4, and 5—grew and promoted plant growth. In a pot experiment with water-stressed wheat plants, inoculation with Enterobacter cloacae BHUAS1, *Bacillus cereus* BHUAS2, and *Bacillus megaterium* BHUIESDAS3 improved growth, chlorophyll and carotenoid content, antioxidant enzyme activity, and oxidative stress markers. These DT-PGPR strains may boost wheat growth and yield under water stress.

Engineering microbial consortia: industrial application

The versatility and potential of engineered microbial consortia in various industrial applications. Researchers and engineers can develop innovative solutions for sustainable production (biofuel production, biodegradable plastic production, antibiotics, enzymes, and bioactive compounds), waste management, and resource utilization by leveraging the interactions and synergies among microorganisms. Continued research and technological advancements in this field promise to unlock further opportunities for industrial applications of microbial consortia. Under this Research Topic, the following collected articles have to address research industrial applications by harnessing the multi-facility potential of microbial consortia.

Benito-Vaquerizo et al. explored using one-carbon (C1) compounds, particularly CO_2, as a sustainable feedstock for producing valuable chemicals. They demonstrated that acetogens, microorganisms capable of utilizing CO_2/H_2 gas mixtures, can convert these substrates into ethanol and acetate. A wider range of products, including butyrate, can be obtained by co-cultivating acetogens with solventogens, which produce medium-chain fatty acids (MCFA) and alcohols. Their study employed metabolic modeling to design a co-culture of specific microbial species, and experimental validation confirmed the feasibility and potential of utilizing such microbial consortia to produce chemicals from renewable resources.

Lobo-Moreira et al. stated that the industrial microalgae-fungi consortia use hinders research. Science explored fungi's involvement in microalgae study. Database searches found 1,452 publications from 1950 to 2020, rising sharply after 2006. Chinese writers and organizations topped publications rankings in China, the US, and Germany. Microalgae-fungi consortia focused on biodiesel, lipid accumulation, anaerobic digestion, and biogas upgrading. Industrial-scale microalgae-based biofuel biorefineries still need work. Microalgae-fungi applications for greenhouse gas abatement are intriguing ideas.

Pawar et al. provides a comprehensive overview of the expanding use of microbial enzymes to replace chemical processes in industrial applications. Due to their versatility and alkaline stability, proteases, especially fungi-derived ones, are used in many sectors. Fungi have a wider range of proteases and are safer for industrial application than bacterial alkaline proteases. This study discusses the classification, generation, and usage of alkaline proteases from diverse fungi, emphasizing more research on alkaline-tolerant and alkaliphilic fungi and their biotechnological potential.

Wu et al. conducted a study to address the need for improved quality in flue-cured tobacco (FCT) by developing a function-driven co-culture of microorganisms. They identified *Bacillus kochii* SC, which reduces tobacco irritation, and *Filobasidium magnum* F7, which enhances aroma and flavor. Co-cultivating these strains at a specific ratio significantly improved FCT quality within just 2 days, surpassing the efficiency and cost of the traditional spontaneous aging process that takes over 2 years. The study demonstrated the effectiveness of the function-driven co-culture in achieving desired tobacco quality and suggested its potential application in the tobacco industry through bioaugmentation.

Engineering microbial consortia: environmental application

It provides innovative solutions to a variety of environmental problems. These consortia can help rehabilitate damaged areas, sustainable waste management, and ecological restoration by using the collective capacities of various microorganisms.

Barman et al. explained that *Bemisia tabaci* (whitefly) is a major agricultural pest and plant virus vector. The genetic variation of whiteflies from West Bengal, India, revealed cryptic species. Most endosymbionts were *Arsenophonus*. Thiamethoxam was the most susceptible pesticide. Insecticide resistance genes were upregulated, and *Arsenophonus* and Wolbachia titers were linked with resistance. The study implies that symbiont-oriented management could reduce whitefly populations and pesticide resistance.

Cui et al. found that ethylene and isoprene production, necessary for polymers and materials, is inefficient and polluting; thus, generating these compounds from biomass or CO_2 is essential for a more sustainable economy. This study created artificial consortia of *E. coli* strains producing ethylene, isoprene, and sucrose-producing cyanobacteria. In addition, they increased sucrose yields by introducing the sucrose transport gene into cyanobacteria strains, which shuttled carbon and electrons amongst community components. These artificial consortia produced more ethylene and isoprene than *E. coli* cultures alone, indicating their benefit to platform chemical synthesis.

Danish et al. synthesized silver nanoparticles (Ag-NPs) from *Cassia fistula* leaf extract and test them as nano-pesticides against main tomato phytopathogens. The synthesized Ag-NPs were spherical using diverse methods with an average diameter of 16 nm. Ag-NPs reduced bacterial and fungal pathogen

viability, morphology, and biofilm formation. They also increased phytopathogen-challenged tomato plant growth, physiological indices, and antioxidant enzyme activity. These findings suggest that *Cassia fistula* leaf extract-synthesized Ag-NPs could be useful and sustainable nano-pesticides in green agriculture for disease management and plant health.

Guo et al. observed that bioavailable lead is essential for forecasting ecological risks and protecting human health from environmental lead pollution. This work develops low-equipment environmental pollution biosensors using bacterial biosensors with visual pigment output signals. Reconstructing *Escherichia coli's* PbrR-based Pb(II) sensing element's anthocyanin biosynthesis pathway creates a metabolic-engineered biosensor. This biosensor uses colored anthocyanin derivatives as a visual signal and better detect low Pb(II) concentrations than fluorescent protein-based biosensors. The biosensor also has a large linear dose-response range and is unaffected by organic and inorganic water samples. These results show that the metabolic engineering of natural colorants can create visible, sensitive, and cost-effective bacterial biosensors for heavy metal pollution detection.

Astafyeva et al. created an artificial plant-bacteria system utilizing the microalga *Micrasterias radians* MZCH 672 and *Dyadobacter* sp. HH091. In pure algal cultures, Bacteroidota phylum member HH091 greatly increased microalga growth. They found HH091 genes linked to the type IX secretion system (T9SS) in transcriptome and genome analysis, which may be involved in the bacterium-microalga interaction. This research will aid symbiotic microalgal–bacteria studies. Additionally, the co-farming of microalgae and bacteria will have favorable commercial and environmental effects on microalgal cultivation.

McClure et al. conducted a comprehensive study on a chitin-degrading synthetic community of soil microbes and examined how it responds to losing key members. They found that the absence of a primary degrader, even if other members can potentially fill the same metabolic niche, led to a collapse in community growth and respiration. The study highlighted that diversity and redundancy alone are insufficient for community resilience; the emerging species must possess the same sharing phenotype and interaction network to support community growth. The findings contribute to our understanding of how keystone species and genomic redundancy changes can impact soil microbiomes and their ability to adapt to a changing climate.

As we embark on this new frontier in synthetic biology, interdisciplinary collaborations, and knowledge sharing will be vital. Engineers, biologists, computer scientists, and ethicists must come together to address the scientific, technical, and ethical challenges that lie ahead. Additionally, interdisciplinary collaborations between biologists, ecologists, and environmental scientists are essential for unlocking the full potential of microbial consortia in environmental restoration. By embracing this innovative approach, we can move toward a more sustainable and environmentally conscious agricultural sector that meets the growing demands for food production while preserving our natural resources. We are excited to present this special issue on Engineering Microbial Consortia, and we hope that the articles published in this issue will inspire researchers, policymakers, and industrial partners to further explore and unlock the potential of complex biological communities for multiple applications. Together, we can harness the power of microbial consortia to address global challenges, improve human health, and pave the way for a more sustainable future.

Author contributions

DJ, JV, TB, AP, and AA contributed to writing this Editorial on the Research Topic and approved it for publication. All authors contributed to the article and approved the submitted version.

Funding

DJ was supported by UGC-Dr. D.S. Kothari Postdoctoral Fellowship [No. F.4 – 2/2006 (BSR)/BL/20–21/0082] to carry out the research work at the Department of Botany, Savitribai Phule Pune University, Pune, India. JV is thankful to SERB (EEQ/2021/001083) and DST (DST/INT/SL/P-31/2021) for financial support for research work for developing microbial consortium for sustainable agricultural productivity.

Acknowledgments

The authors would like to thank the senior editor of Frontier Microbiology Journals for her highly valuable input during the preparation of the collection. The authors would like to thank the Department of Botany, Savitribai Phule Pune University, Pune, India; Institute of Environment and Sustainable Development, Banaras Hindu University, Varanasi, India; College of Biosystems Engineering and Food Science, Zhejiang University, Hangzhou, People's Republic of China and the Federal University of Ceará, Soil Science Department, Soil Microbiology Laboratory, Fortaleza, Ceará, Brazil, which form a large part of setting the scene behind this collection.

Conflict of interest

The authors declare that the research was conducted in the absence of any commercial or financial relationships that could be construed as a potential conflict of interest.

Publisher's note

All claims expressed in this article are solely those of the authors and do not necessarily represent those of their affiliated organizations, or those of the publisher, the editors and the reviewers. Any product that may be evaluated in this article, or claim that may be made by its manufacturer, is not guaranteed or endorsed by the publisher.

References

Abhilash, P. C., Dubey, R. K., Tripathi, V., Gupta, V. K., and Singh, H. B. (2016). Plant growth-promoting microorganisms for environmental sustainability. *Tren. Biotechnol.* 34, 847–850. doi: 10.1016/j.tibtech.2016.05.005

Andrianantoandro, E., Basu, S., Karig, D. K., and Weiss, R. (2006). Synthetic biology: new engineering rules for an emerging discipline. *Mol. Syst. Biol.* 2, 2006–0028. doi: 10.1038/msb4100073

Ben Said, S., and Or, D. (2017). Synthetic microbial ecology: engineering habitats for modular consortia. *Front. Microbiol.* 8, 1125. doi: 10.3389/fmicb.2017.01125

Bhatia, S. K., Bhatia, R. K., Choi, Y. K., Kan, E., Kim, Y. G., Yang, Y. H., et al. (2018). Biotechnological potential of microbial consortia and future perspectives. *Crit. Rev. Biotechnol.* 38, 1209–1229. doi: 10.1080/07388551.2018.1471445

Brenner, K., You, L., and Arnold, F. H. (2008). Engineering microbial consortia: a new frontier in synthetic biology. *Trends Biotechnol.* 26, 483–489. doi: 10.1016/j.tibtech.2008.05.004

Chandran, H., Meena, M., and Sharma, K. (2020). Microbial biodiversity and bioremediation assessment through omics approaches. *Front. Environ. Chem.* 1, 570326. doi: 10.3389/fenvc.2020.570326

Dheeman, S., Kumar, M., and Maheshwari, D. K. (2023). "Beneficial microbial mixtures for efficient biocontrol of plant diseases: impediments and success," in *Sustainable Agrobiology: Design and Development of Microbial Consortia*. (Singapore: Springer Nature Singapore), pp. 23-40. doi: 10.1007/978-981-19-9570-5_2

Gehlot, P., Pareek, N., and Vivekanand, V. (2021). Development of biofertilizers and microbial consortium an approach to sustainable agriculture practices. *Plant Soil Microbe. Trop. Ecosyst.* 3, 315–348. doi: 10.1007/978-981-16-3364-5_15

Gómez Expósito, R., De Bruijn„ Postma, I. J., and Raaijmakers, J. M. (2017). Current insights into the role of rhizosphere bacteria in disease suppressive soils. *Front. Microbiol.* 8, 2529. doi: 10.3389/fmicb.2017.02529

Hamilton, C. E., Bever, J. D., Labbe, J., Yang, X., and Yin, H. (2016). Mitigating climate change through managing constructed-microbial communities in agriculture. *Agric. Ecosyst. Environ*. 216, 304–308. doi: 10.1016/j.agee.2015.10.006

Hays, S. G., Patrick, W. G., Ziesack, M., Oxman, N., and Silver, P. A. (2015). Better together: engineering and application of microbial symbioses. *Curr. Opin. Biotechnol.* 36, 40–49. doi: 10.1016/j.copbio.2015.08.008

Heredia, M., Layedra-Almeida, A. P., Torres, Y., and Toulkeridis, T. (2022). Evaluation of a microbial consortium and selection of a support in an anaerobic reactor directed to the bio-treatment of wastewater of the textile industry. *Sustainability* 14, 8889. doi: 10.3390/su14148889

Hett, J., Döring, T. F., Bevivino, A., and Neuhoff, D. (2023). Impact of microbial consortia on organic maize in a temperate climate varies with environment but not with fertilization. *Eur. J. Agron.* 144, 126743. doi: 10.1016/j.eja.2023.126743

Islam, M. M., Rengel, Z., Storer, P., Siddique, K. H., and Solaiman, Z. M. (2023). Microbial consortium inoculant and rock mineral fertiliser differentially improved yield and nutrient uptake of industrial hemp (*Cannabis sativa* L.) varieties. *Ind. Crop. Prod.* 197, 116599. doi: 10.1016/j.indcrop.2023.116599

Jaiswal, D. K., Gawande, S. J., Soumia, P. S., Krishna, R., Vaishnav, A., Ade, A. B., et al. (2022a). Biocontrol strategies: an eco-smart tool for integrated pest and diseases management. *BMC Microbiol.* 22, 1–5. doi: 10.1186/s12866-022-02744-2

Jaiswal, D. K., Krishna, R., Chouhan, G. K., Araujo Pereira, d. e., Ade, A. P., Prakash, A. B. J., et al. (2022b). Bio-fortification of minerals in crops: current scenario and future prospects for sustainable agriculture and human health. *Plant Growth Regul.* 98, 5–22. doi: 10.1007/s10725-022-00847-4

Jaiswal, D. K., Verma, J. P., Krishna, R., Gaurav, A. K., and Yadav, J. (2019). Molecular characterization of monocrotophos and chlorpyrifos tolerant bacterial strain for enhancing seed germination of vegetable crops. *Chemosphere* 223, 636–650. doi: 10.1016/j.chemosphere.2019.02.053

Jha, M., Chourasia, S., and Sinha, S. (2013). Microbial consortium for sustainable rice production. *Agroecol. Sustain. Food Syst*. 37, 340–362. doi: 10.1080/10440046.2012.672376

Kaushal, M., Devi, S., Kumawat, K. C., and Kumar, A. (2023). "Microbial consortium: a boon for a sustainable agriculture," in *Climate Change and Microbiome Dynamics: Carbon Cycle Feedbacks*. (Cham: Springer International Publishing), pp. 15-31. doi: 10.1007/978-3-031-21079-2_2

Khan, A., Panthari, D., Sharma, R. S., Punetha, A., Singh, A. V., Upadhayay, V. K., et al. (2023). "Biofertilizers: a microbial-assisted strategy to improve plant growth and soil health," in *Advanced Microbial Techniques in Agriculture, Environment, and Health Management*. (Academic Press), pp. 97-118. doi: 10.1016/B978-0-323-91643-1.00007-7

Kong, Z., Hart, M., and Liu, H. (2018). Paving the way from the lab to the field: using synthetic microbial consortia to produce high-quality crops. *Front. Plant Sci.* 9, 1467. doi: 10.3389/fpls.2018.01467

Krishna, R., Jaiswal, D. K., Ansari, W. A., Singh, S., Soumia, P. S., Singh, A. K., et al. (2022). Potential microbial consortium mitigates drought stress in tomato (*Solanum lycopersicum* L.) Plant by up-regulating stress-responsive genes and improving fruit yield and soil properties. *J. Soil Sci. Plant Nutr.* 3, 1–18. doi: 10.1007/s42729-022-00929-2

Lebrun, M., Michel, C., Joulian, C., Morabito, D., and Bourgerie, S. (2021). Rehabilitation of mine soils by phytostabilization: does soil inoculation with microbial consortia stimulate Agrostis growth and metal (loid) immobilization?. *Sci. Total Environ.*791, 148400. doi: 10.1016/j.scitotenv.2021.148400

Li, X., Wu, S., Fan, H., Dong, Y., Wang, Y., Bai, Z., et al. (2023). Phylogenetic distance affects the artificial microbial consortia's effectiveness and colonization during the bioremediation of polluted soil with Cr (VI) and atrazine. *J. Hazard. Mater.* 4, 131460. doi: 10.1016/j.jhazmat.2023.131460

Liang, Y., Ma, A., and Zhuang, G. (2022). Construction of environmental synthetic microbial consortia: based on engineering and ecological principles. *Front. Microbiol.* 13, 829717. doi: 10.3389/fmicb.2022.829717

Liu, X., Mei, S., and Salles, J. F. (2023). Do inoculated microbial consortia perform better than single strains in living soil? A meta-analysis. *BioRxiv* 2023, 3. doi: 10.1101/2023.03.17.533112

Mahreen, N., Yasmin, S., Asif, M., Yahya, M., Ejaz, K., Yousaf, S., et al. (2023). Mitigation of water scarcity with sustained growth of Rice by plant growth promoting bacteria. *Front. Plant Sci.* 14, 1081537. doi: 10.3389/fpls.2023.1081537

Mazzucotelli, C. A., Durruty, I., Kotlar, C. E., Moreira, M. D. R., Ponce, A. G., Roura, S. I., et al. (2014). Development of a microbial consortium for dairy wastewater treatment. *Biotechnol. Bioprocess Eng.* 19, 221–230. doi: 10.1007/s12257-013-0517-8

Méndez-Bravo, A., Herrera-Cornelio, L. C., García-Toscano, D. F., Kiel-Martínez, A. L., Guevara-Avendaño, E., Ramírez-Vázquez, M., et al. (2023). Beneficial effects of selected rhizospheric and endophytic bacteria, inoculated individually or in combination, on non-native host plant development. *Rhizosphere* 26, 100693. doi: 10.1016/j.rhisph.2023.100693

Mukherjee, A., Singh, S., Gaurav, A. K., Chouhan, G. K., Jaiswal, D. K., Araujo Pereira, d. e. A. P., et al. (2022). Harnessing of phytomicrobiome for developing potential biostimulant consortium for enhancing the productivity of chickpea and soil health under sustainable agriculture. *Sci. Total Environ.* 836, 155550. doi: 10.1016/j.scitotenv.2022.155550

Nabi, M. (2023). Role of microorganisms in plant nutrition and soil health. In *Sustainable Plant Nutrition* (pp. 263-282). Academic Press. doi: 10.1016/B978-0-443-18675-2.00016-X

Pankaj, U., and Pandey, V. C. (Eds.). (2022). *Microbial Based Land Restoration Handbook*, Vol. 1: Plant-Microbial Interaction and Soil Remediation. CRC Press. doi: 10.1201/9781003147091

Paravar, A., Piri, R., Balouchi, H., and Ma, Y. (2023). Microbial seed coating: an attractive tool for sustainable agriculture. *Biotechnol. Rep.* 37, e00781. doi: 10.1016/j.btre.2023.e00781

Prajapati, J., Yadav, J., Jaiswal, D. K., Prajapati, B., Tiwari, S., Yadav, J., et al. (2022). Salt tolerant indigenous zn solubilizing bacteria isolated from forest organic soils promotes yield and root growth in oryza sativa under zinc deficient alluvial soil. *Geomicrobiol. J.* 39, 465–476. doi: 10.1080/01490451.2022.2028941

Sarma, B. K., Yadav, S. K., Singh, S., and Singh, H. B. (2015). Microbial consortium-mediated plant defense against phytopathogens: readdressing for enhancing efficacy. *Soil Biol. Biochem.* 87, 25–33. doi: 10.1016/j.soilbio.2015.04.001

Shukla, S. K., Sharma, L., Jaiswal, V. P., Pathak, A. D., Tiwari, R., Awasthi, S. K., et al. (2020). Soil quality parameters vis-a-vis growth and yield attributes of sugarcane as influenced by integration of microbial consortium with NPK fertilizers. *Sci. Rep.*10, 19180. doi: 10.1038/s41598-020-75829-5

Silverstein, M. R., Segrè, D., and Bhatnagar, J. M. (2023). Environmental microbiome engineering for the mitigation of climate change. *Glob. Change Biol.* 29, 2050–2066. doi: 10.1111/gcb.16609

Singh R. V., Kaur, J., Bhagwat, S., Arora Pandit, M., and Dogra Rawat, C. (2023). Deploying microbes as drivers and indicators in ecological restoration. *Restor. Ecol.* 31, e13688. doi: 10.1111/rec.13688

Singh, J. S., Abhilash, P. C., and Gupta, V. K. (2016). Agriculturally important microbes in sustainable food production. *Trends Biotechnol.* 34, 773–775. doi: 10.1016/j.tibtech.2016.06.002

Verma, J. P., Jaiswal, D. K., Gaurav, A. K., Mukherjee, A., Krishna, R., Araujo Pereira, d. e., et al. A. P. (2023). Harnessing bacterial strain from rhizosphere to develop indigenous PGPR consortium for enhancing lobia (*Vigna unguiculata*) production. *Heliyon* 9, e13804. doi: 10.1016/j.heliyon.2023.e13804

Verma, J. P., Jaiswal, D. K., and Sagar, R. (2014b). Pesticide relevance and their microbial degradation: a-state-of-art. *Rev. Environ. Sci.* 13, 429–466. doi: 10.1007/s11157-014-9341-7

Verma, J. P., Yadav, J., Tiwari, K. N., and Jaiswal, D. K. (2014a). Evaluation of plant growth promoting activities of microbial strains and their effect on growth

and yield of chickpea (*Cicer arietinum* L.) in India. *Soil Biol. Biochem.* 70, 33–37. doi: 10.1016/j.soilbio.2013.12.001

Vishwakarma, K., Kumar, N., Shandilya, C., Mohapatra, S., Bhayana, S., Varma, A., et al. (2020). Revisiting plant–microbe interactions and microbial consortia application for enhancing sustainable agriculture: a review. *Front. Microbiol.* 11, 560406. doi: 10.3389/fmicb.2020.560406

Wu, S., Li, X., Fan, H., Dong, Y., Wang, Y., Bai, Z., et al. (2023). Engineering artificial microbial consortia based on division of labor promoted simultaneous removal of Cr (VI)-atrazine combined pollution. *J. Hazard. Mater.* 443, 130221. doi: 10.1016/j.jhazmat.2022.130221

Yadav, J., Verma, J. P., Jaiswal, D. K., and Kumar, A. (2014). Evaluation of PGPR and different concentration of phosphorus level on plant growth, yield and nutrient content of rice (*Oryza sativa*). *Ecol. Eng.* 62, 123–128. doi: 10.1016/j.ecoleng.2013.10.013

Zhang, C., Wu, D., and Ren, H. (2020). Bioremediation of oil contaminated soil using agricultural wastes via microbial consortium. *Sci. Rep.* 10, 9188. doi: 10.1038/s41598-020-66169-5

frontiers | Frontiers in Microbiology

ORIGINAL RESEARCH
published: 26 May 2022
doi: 10.3389/fmicb.2022.903737

Trends on Microalgae-Fungi Consortia Research: An Alternative for Biofuel Production?

Ana Beatriz Lobo-Moreira[1]*, *Solange Xavier-Santos*[2], *Luciana Damacena-Silva*[3] and *Samantha Salomão Caramori*[4]

[1] Post Graduate Program in Natural Resources of Cerrado, State University of Goiás, Anápolis, Brazil, [2] Laboratory of Basic, Applied and Mycology and Scientific Dissemination (FungiLab), State University of Goiás, Anápolis, Brazil, [3] Laboratory of Host-Parasite Interactions, State University of Goiás, Anápolis, Brazil, [4] Laboratory of Biotechnology, State University of Goiás, Anápolis, Brazil

The utilization of microalgae and fungi on an industrial scale is a challenge for researchers. Based on the question "how fungi have contributed to microalgae research?," we verified the scientific trends on microalgae-fungi consortia focused on biofuels production by searching for articles on the Web of Science and Scopus databases through the terms "microalgae*" or phytoplankton and "fung*." We found 1,452 articles published between 1950 and 2020; since 2006, the publication numbers have increased rapidly. The articles were published in 12 languages, but most were written in English (96.3%). Among 72 countries, China (360 articles), USA (344), and Germany (155) led the publication rank. Among the 10 most-prolific authors, 8 were Chinese, like 5 of the most-productive institutions, whereas the National Cheng Kung University was on the top of the list. The sources that published the most on the subject were: Bioresource Technology (96), PLoS ONE (28), and Science of the Total Environment (26). The keyword analysis emphasized the magnitude of applications in microalgae-fungi consortia research. Confirming this research question, biofuels appeared as a research trend, especially biodiesel, biogas, and related terms like lipid, lipid accumulation, anaerobic digestion, and biogas upgrading. For 70 years, articles have been published, where China and the United States seem to dominate the research scenario, and biodiesel is the main biofuel derived from this consortium. However, microalgae-based biofuel biorefinery is still a bottleneck on an industrial scale. Recent environmental challenges, such as greenhouse gas mitigation, can be a promising field for that microalgae-fungi application.

Keywords: phytoplankton, fungus, scientometric, microbial co-cultivation, biotechnology

OPEN ACCESS

Edited by:
Tarun Belwal,
Zhejiang University, China

Reviewed by:
Chunpeng Wan,
Jiangxi Agricultural University, China
T. Sharma,
Punjab Agricultural University, India
Ruyuan Zhang,
Zhejiang University, China

***Correspondence:**
Ana Beatriz Lobo-Moreira
lobo.anab@gmail.com

Specialty section:
This article was submitted to Microbiotechnology, a section of the journal Frontiers in Microbiology

Received: *24 March 2022*
Accepted: *11 April 2022*
Published: *26 May 2022*

Citation:
Lobo-Moreira AB, Xavier-Santos S, Damacena-Silva L and Caramori SS (2022) Trends on Microalgae-Fungi Consortia Research: An Alternative for Biofuel Production? Front. Microbiol. 13:903737. doi: 10.3389/fmicb.2022.903737

INTRODUCTION

Microalgae (also referred to as phytoplankton) is a generic term used to determine a group of microscopic photosynthetic unicellular or multicellular algae and cyanobacteria that can convert sunlight, water, and carbon dioxide (CO_2) into biomass and double their body weight in 24 h (Zabed et al., 2020). They can grow in freshwater, seawater, and under harsh conditions, such as brackish water and wastewater (Serejo et al., 2019). The diversity of microalgae ranges from 50,000 (Alam et al., 2015) to 1 million species (Rumin et al., 2020), and they have been studied for more than 100 years (Spier et al., 2020). Among various human applications, microalgae are used in the medicine and pharmaceutical industry, food and nutrition, wastewater treatment, and as a renewable source of energy (Baicha et al., 2016).

Likewise, fungi comprise the most diversified living organisms Kingdom; being estimated that the funga (Kuhar et al., 2018) is composed of 2.2–3.8 million species (Hawksworth and Lücking, 2017). They can be micro or macroscopic organisms, they are all eukaryotic and heterotrophic, and most of them form structures called hypha, except for yeasts (Alexopoulos et al., 1996). Fungi can form mutualistic and symbiotic consortia with other living organisms (Richards et al., 2017). Humans also exploit fungus, especially in biological systems for food and drugs, and to reduce the environmental impacts of chemical industrial processes (Rai et al., 2021).

Microalgae-fungi co-cultivation has gained emphasis in research and industry once it improves the main bottlenecks and barriers to using microalgae biomass, e.g., upgrading organic compounds concentration and assisting in the harvesting process, considered the most energetic and financially costly steps of microalgae culture (Li et al., 2020). Despite this, co-cultivation appears as an alternative to increasing the manufacturing ecological footprint (Brasil et al., 2017), which is a low-cost and low-energy input and chemical-free harvesting method for biofuel production (Chen et al., 2018; Mathimani and Mallick, 2020). Many researchers have quantified the scientific production of microalgae in the biofuel scenario (Coelho et al., 2014; Azadi et al., 2017; Ma et al., 2018; Konur, 2020a) in science, technology, and medicine (Konur, 2020b) worldwide (Garrido-Cardenas et al., 2018), particularly in Europe (Rumin et al., 2020) and Brazil (Nabout et al., 2015; Moreira, 2021). Still, none of them comprised the consortia with fungi.

Based on these findings, a question was left: How fungi have contributed to microalgae research? The answers to this question can provide an overview of the present published bibliography and the gaps in the research as a tool to spread the current technologies and guide future research. That being said, in this research, we aimed to map the microalgae-fungi consortia research focused on the following: (a) the amount of literature produced and when did the interest start in this consortium culture, (b) the countries, institutions, and authors who have published about co-cultivation and how was the collaboration dynamic, (c) the most-relevant articles published about this consortium, and lastly (d) the enclosed topics by these studies and the trend for biofuel production research.

METHODS

Microalgae-fungi consortia data was obtained in the Web of Science (Thomson Reuters) and Scopus databases. We searched for "microalga*" or phytoplankton and "fung*" on titles, keywords, and abstracts. The search attempts were limited to *articles* comprising the first publication in each database until 2020. All data were downloaded in June of 2021. Several publications, journals, institutions, countries, and idioms were analyzed using Microsoft Office Excel 2016. Authors, countries, institutions collaboration, and keywords associations were made using Bibliometrix (Aria and Cuccurullo, 2017) for RStudio version 2021.09.0 Build 351 (R Core Team, 2022) and SigmaPlot 12.0 (Systat Software and Inc, 2011).

Amongst the limitations of scientometric research (Andreo-Martínez et al., 2020), bias in results can be due to the database chosen and the option to only analyze articles. For example, microalgae is a generic term commonly used in biotechnology research (Rumin et al., 2020), while phytoplankton is mostly used by studies in ecology (Nabout et al., 2015). In this way, the searching terms also contributed to bias in the result analyses, delimitating the comprehension of the courses that the research is taking in each specific study field (Cheng et al., 2020).

RESULTS

Publication Outputs

A total of 1,995 articles were downloaded from the two databases, including 902 from the Web of Science and 1,093 in the Scopus database. After removing 543 duplicities, we analyzed about 1,452 articles. The temporal distribution of publication on microalgae-fungi consortia can be observed in **Figure 1**. The publication increase presented an exponential growth, whereby the average number of publications per year was 20.7 articles.

In reinforcing English as an official scientific publication idiom (Parkinson, 2013), 96.3% of articles were published in English. The remaining 3.7% (53 articles) were published in 11 languages, including German, Chinese, Korean, Spanish, French, Japanese, Persian, Polish, Portuguese, Russian, and Turkish. Citations are also a good measure to quantify the publications. In the case of microalgae-fungi consortia articles, there was a rising tendency in the citation numbers that reached the citation peak in 2010 (**Figure 1**). Only 6% of the articles did not show citations, while 34.2% showed <10 citations during the time-lapse analyzed. Considering the language, the articles published in English were also the most cited, followed by articles in French (74), Spanish (57), Chinese (52), and Portuguese (32).

All the 1,452 articles summed 49,052 citations, corresponding to an average of 33.7 citations per article. The 10 most-cited articles are described in **Table 1**, counting 6,021 citations. Confirming the trend for biofuel research using microalgae-fungi consortia, the 3rd and the 6th most-cited articles stated Biodiesel in the title. In the same way, the 2nd and 5th most-cited articles mentioned lipid accumulation, which is one important step in biofuel manufacture.

Country and Collaboration

China, the United States (USA), and Germany were the most prolific countries publishing about microalgae-fungi consortia, counting 360, 344, and 155 publications each. They were followed by France (148), India (113), Japan (103), Spain (101), the United Kingdom (UK) (94), and Brazil (70). **Figure 2** presents the country collaboration map. The thicker the red line between the countries, the stronger teamwork between them. European countries showed intense collaboration among them and with the USA. Accordingly, the USA (9,803 citations), China (5,580), and France (3,215) were the countries that accumulated more article citations without taking into account the publication language.

Despite the collaboration between countries, it was evidenced that amongst the 10 most prolific countries, the single country publications (SCP) still count a higher number of articles than

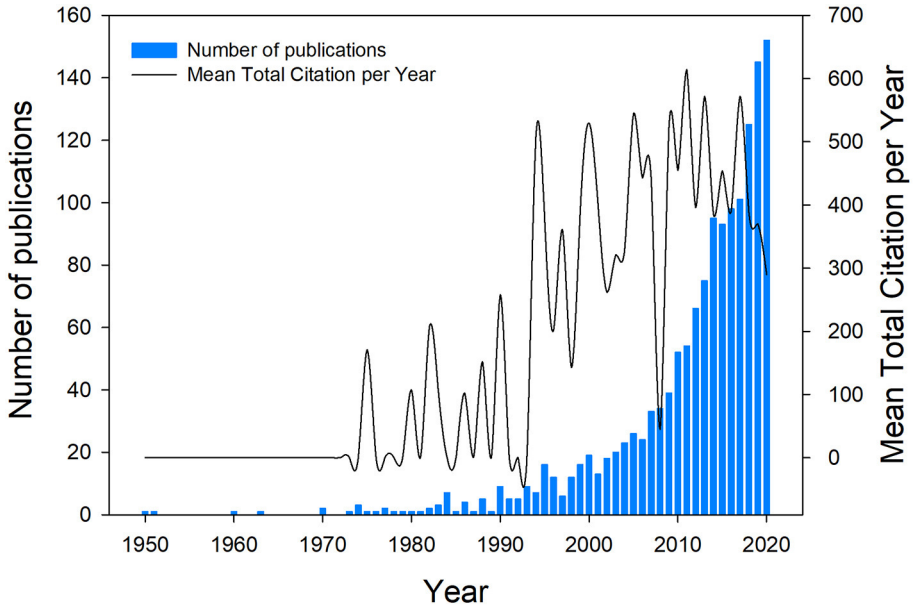

FIGURE 1 | Microalgae-fungi consortia publication and citation outputs among 70 years (1950–2020).

TABLE 1 | The 10 most-cited articles about microalga-fungi consortia.

	Title	Source (Country)	Year	Citations
1	Microbial carbonates: the geological record of calcified bacterial algal mats and biofilms	Sedimentology (United Kingdom)	2000	1,035
2	Effects of nitrogen sources on cell growth and lipid accumulation of green alga *Neochloris oleoabundans*	Applied Microbiology and Biotechnology (Germany)	2008	821
3	High-quality biodiesel production from a microalga *Chlorella protothecoides* by heterotrophic growth in fermenters	Journal of Biotechnology (Netherlands)	2006	775
4	High-value products from microalgae—their development and commercialization	Journal of Applied Phycology (Netherlands)	2013	645
5	Lipid accumulation and CO_2 utilization of *Nannochloropsis oculata* in response to CO_2 aeration	Bioresource Technology (United Kingdom)	2009	577
6	Characterization of a microalga *Chlorella* sp. well-adapted to highly concentrated municipal wastewater for nutrient removal and biodiesel production	Bioresource Technology (United Kingdom)	2011	482
7	Omega-3/6 fatty acids: Alternative sources of production	Process Biochemistry (United Kingdom)	2005	442
8	Amino Acid Absorption by Arctic Plants: Implications for Plant Nutrition and Nitrogen Cycling	Ecology (United States)	1994	438
9	Progress in the biological and chemical treatment technologies for emerging contaminant removal from wastewater: A critical review	Journal of Hazardous Materials (Netherlands)	2017	413
10	Mapping of picoeucaryotes in marine ecosystems with quantitative PCR of the 18S rRNA gene	FEMS Microbiology Ecology (United Kingdom)	2005	393

the ones on which multiple countries (MCP) have collaborated (**Figure 3**). In this regard, the country that most collaborated internationally was the USA, even though it was the 2nd in the number of total publications. India was the only country that did not present any MCP.

Authors and Institutions

The articles were signed by 4,974 authors, an average of 3.3 authors per article. Single authored articles summed 5.9%, and 71 distinct authors individually signed these. Of the 10 most-prolific authors, 8 were from China, and 2 were from the Netherlands. A timeline of the 10 most-prolific authors is displayed in **Figure 4**. Most of the authors started to publish on the subject after 2000.

Chinese institutions also figured between the top 10 ranks of the most-productive institutions. The National Cheng Kung University was the 1st in several publications (25 articles), followed by the University of Chinese Academy of Science

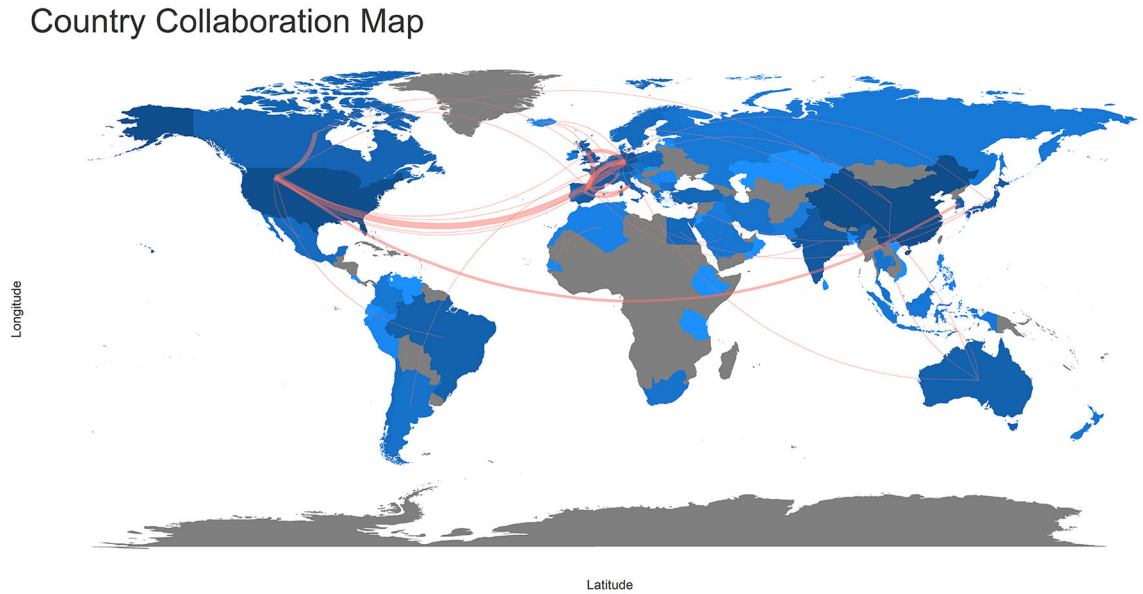

FIGURE 2 | Country collaboration map of microalgae-fungi consortia publications.

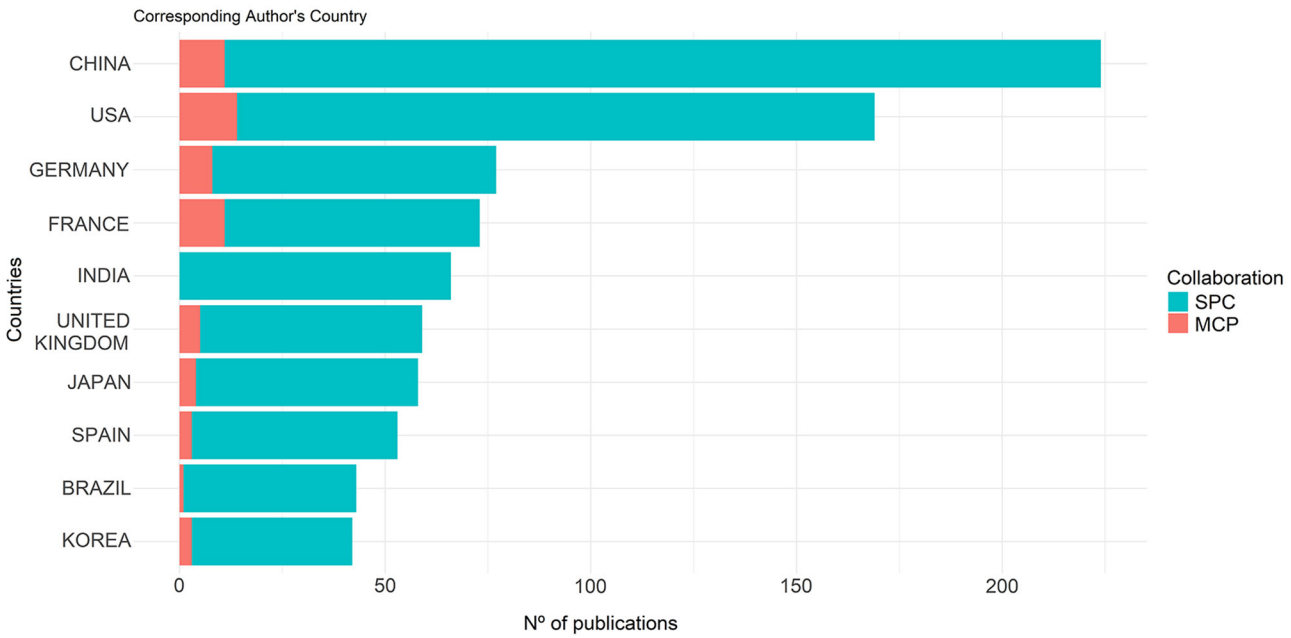

FIGURE 3 | Single and multiple countries' publications on microalgae-fungi consortia.

(21). The USA appeared twice on the rank occupying the 5th (University of Minnesota−17) and the 9th (University of California−15) positions. France represented Europe in the 3rd position (Centre National de la Recherche Scientifique – 19) and Italy in the 10th position (University of Naples Federico II−15). No countries from Central and South America appeared on the rank, like Asia and Oceania.

Sources

Articles were cataloged in 575 journals, but 62.7% of these only published 1 article each. Bioresource Technology was, by far, the most-productive journal with 96 articles published, followed by PLoS ONE (28) and Science of the Total Environment (26) (**Table 2**). The top 10 journals published 19.6% of the articles. The increase in publications by the 10 most-productive sources

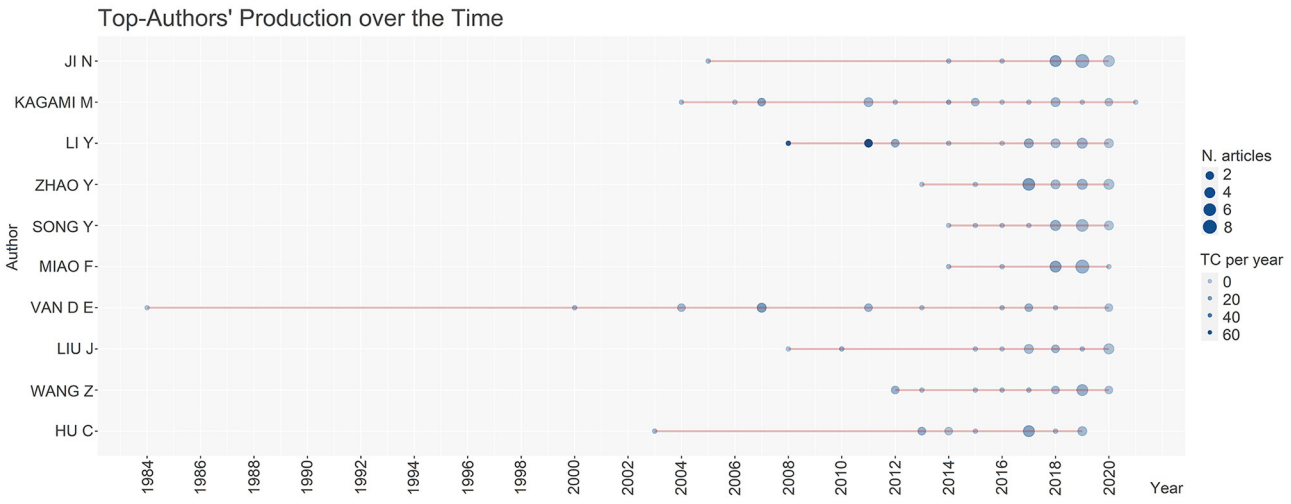

FIGURE 4 | Publication timeline of the 10 most-prolific authors on microalgae-fungi consortia.

TABLE 2 | The 10 most-productive journals in microalgae-fungi consortia.

	Source	Articles	Country
1	Bioresource technology	96	United Kingdom
2	PLoS ONE	28	United States
3	Science of the total environment	26	Netherlands
4	Frontiers in microbiology	23	Switzerland
5	Hydrobiologia	22	Netherlands
6	Applied and environmental microbiology	21	United States
7	Journal of applied phycology	18	Netherlands
8	Algal research	17	Netherlands
9	Marine drugs	17	Switzerland
10	Scientific reports	17	United Kingdom
	Other (475)	1,167	

over the last 50 years is shown in **Figure 5**. All journals increased their publication rates in the last decade, detaching Bioresource Technology, PLoS ONE, and Frontiers in Microbiology, which exhibited leverage on the number of publications after 2010.

Keywords

To reveal the main publication trends and subjects, we analyzed 3,794 keywords. A word cloud showing the most-cited keywords is presented in **Figure 6**. The "x" following the numbers after the keywords mentioned means the times they were cited. The word Microalgae was cited 204 times, followed by Fungi (67×), Algae (57×), Phytoplankton (55×), and Cyanobacteria (47×). To complete the top 10 ranks of the most-cited keywords, Biodiesel (44×), Bacteria (35×), Lipid (34×), Biofuel (31×), and *Chlorella vulgaris* (27×) emerged from the 1,452 articles. After biodiesel, biogas-related words (e.g., biogas upgrading and anaerobic digestion) were mentioned 26 times and ranked in the 64th position of the most-cited.

Summing the 2nd most-cited keyword (Fungi) and Filamentous fungi (27th position), this group of organisms counted 80 mentions in the articles. In Biology, the association between algae and fungi can be called Lichen (15×) (Srinuanpan et al., 2018), and their co-culture (21×) is a promising topic in Biotechnology. Filamentous fungi (the most cited genus in this investigation were *Trichoderma* sp. and *Aspergillus* sp.) have been used to assist microalgae biomass harvesting (27×) through bioflocculation (25×) (Zhou et al., 2013), seen as a low-cost technique (Jiang et al., 2021) for bioproducts and biofuel production (Zhou et al., 2012).

Another important step for the utilization of microalgae biomass is the pre-treatment (11×) performed by fungal enzymes (11×) that break the microalgae hard cell wall (Mahdy et al., 2016; Rai et al., 2021). The two most-cited microalgae species in the keyword analysis were also the most well-studied (Garrido-Cardenas et al., 2018). The *C. Vulgaris* and *Chlamydomonas reindhardtii* (19×) are characterized by different aspects. At the same time, the first is the most-studied species and presents a hard cell wall composed of cellulose, hemicellulose, and glycoproteins (Passos et al., 2016), while the cell wall is unprovided on the latter (Mahdy et al., 2016).

As evidenced by the keyword analysis, we found a bias for biofuel research in the articles, especially biodiesel and biogas. The connection between the most prolific authors, journals, and most-cited keywords is displayed in **Figure 7**. For example, confirming Nabout et al. (2015) and Rumin et al. (2020), microalgae, biodiesel, lipid, and *C. Vulgaris* were keywords strongly connected to the journal Bioresource Technology, which focused on biotechnology and bioenergy [also discussed in Zhang et al. (2018)]. On the contrary, phytoplankton was linked to Hydrobiologia, a journal focused on ecological studies.

DISCUSSION

Economic interests, biorefinery, and the research around microalgae-fungi consortia have raised since 1950

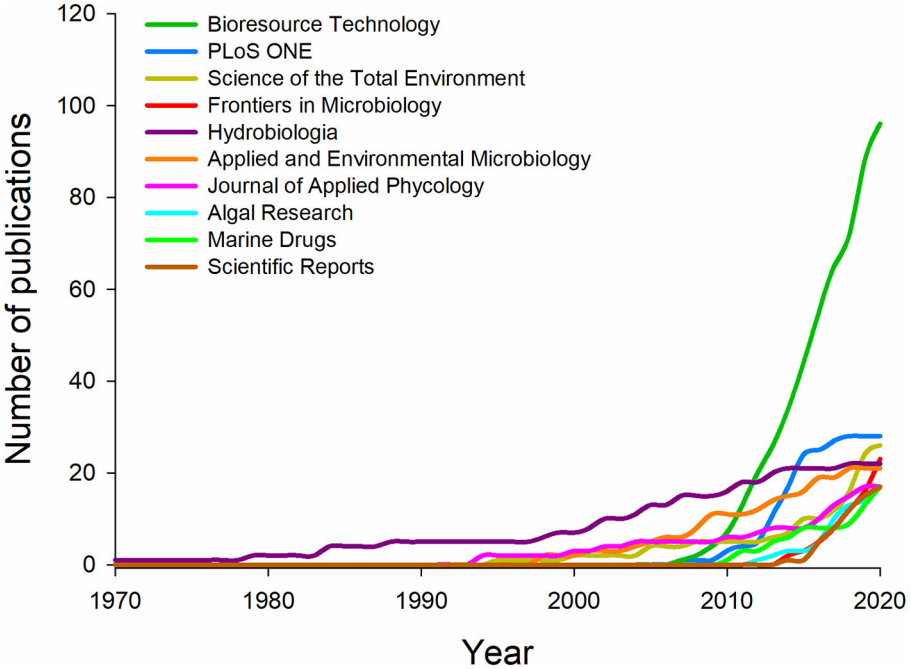

FIGURE 5 | Microalgae-fungi consortia publication increased in the 10 most-productive journals in the last 50 years.

FIGURE 6 | Most-cited keywords of microalgae-fungi consortia publications.

(Cheng et al., 2020), and during the oil crisis in the 1970 decade microalgae was considered a potential source for energy production (Baicha et al., 2016). Notwithstanding, the number of publications found in this investigation was smaller than in other research focused only on microalgae, which counted from 20,000 and 70,000 publications (Garrido-Cardenas et al., 2018; Rumin et al., 2020). Different from studying each group of organisms individually, we expected a lower number of publications while investigating this microbial consortium. Comparing, a review focused on microalgae fungal-assisted bioflocculation included only 18 articles (Nazari et al., 2020).

Since the technology outbreak, globalization, and software development in Computer Science, the English language has become part of political and economic confluence. In the twentieth century, high investments in education were made by developed nations, and the hegemony of the English language was certified as the Science language (Hamel, 2007). Not surprisingly, English dominated the publications about microalgae-fungi consortia in our results (96.3%). It confirms

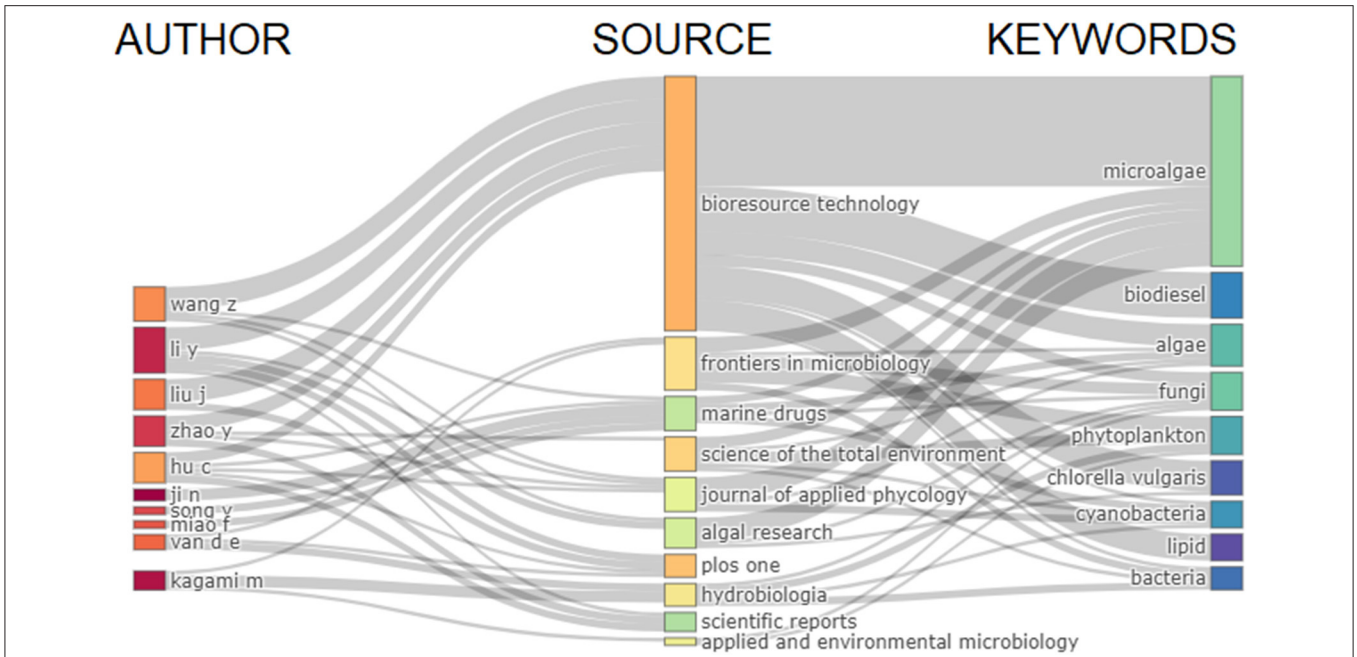

FIGURE 7 | The connection between authors, journals, and keywords.

that even for researchers, whose mother tongue is not English, publishing in English is an important factor in ensuring their results' wide distribution and comprehension.

Publishing the results is the main goal for researchers that worked hard to confirm or refute their hypothesis. The 1,452 articles found in our results counted almost 50 thousand citations until 2020. We observed that the publication numbers have grown over the years and also the article citations (see **Figure 1**). It can be considered evidence of the subject's relevance among the scientific community and the advances in biotechnological development of microalgae-fungi co-culture. Furthermore, these citations represent a good means to spread the new findings published, enriching the discussion of the upcoming publications worldwide (Larsen and von Ins, 2010).

The collaboration between countries reinforced the significance that microalgae-fungi consortia are gaining. Scientists are summing efforts to develop new knowledge in the field and exchange their findings, technologies, and research results with other researchers and society. Even though the most published country was China, the USA showed more collaboration with different countries on their publications. In general science, the USA has been the leading country in several publications since the 1990 decade (King, 2004), and here we also stated its collaboration strength. Garrido-Cardenas et al. (2018) found a similar pattern of collaboration between the USA and European countries while mapping the microalgae research worldwide.

Despite that, China was the country with the most prolific authors. The country has implemented high investments in education and funding; many Chinese researchers left the country to study abroad and then came back, helping to sustain the country's rapid economic growth (King, 2004). Also, the increase in investments in Research & Development (R&D) in China has contributed to the rising of Science (Gonzalez-Brambila et al., 2016). In 2017, the Chinese government invested 2.15% of the Gross Domestic Product (GDP) in R&D. This amount is only lower than that found in South Korea, Japan, Germany, the USA, and France's R&D investments (Chiarini et al., 2020).

Azadi et al. (2017) reported that the number of scientists and engineers in China has tripled in 20 years (between 1990- and 2010). Similar to this study, Cheng et al. (2020) evidenced that half of the most-fruitful institutions were also from China. Finally, Garrido-Cardenas et al. (2018) found that 4 of the most-productive institutions were Chinese, including the Chinese Academy of Sciences and the National Cheng Kung University, which also ranked in our results. It is notable the progress and the innovation capacity of Chinese universities and authors over the last years (Gonzalez-Brambila et al., 2016).

Different from the biotechnological profile of Chinese authors, 2 of the most prolific authors were from the Netherlands and linked to the Netherlands Institute of Ecology. Nabout et al. (2015) stated that the term phytoplankton is broadly studied in Ecology, and the Netherlands figures as the 7th most-contributive country in algae ecology research (Konur, 2020c) and also on bioenergy/biofuels publications (Konur, 2020a). European countries have strong participation in research involving microalgae and phytoplankton, registering 33% of the world's publications (Rumin et al., 2020). Likewise, the USA and China published around 3,000 articles each (Garrido-Cardenas et al., 2018).

To reinforce the tendency of using the keyword "microalgae" in biotechnology publications, Bioresource Technology was

the journal that published the most about microalgae-fungi consortia. In the same way, Garrido-Cardenas et al. (2018) searched for "microalga*" and the same source was also ranked as the most prolific. Similar to the observed in this study, Rumin et al. (2020) ranked 4 of the most-productive journals focused on Ecology, while Bioresource Technology occupied only the 5th position when searched for "microalgae" and "phytoplankton" keywords.

When the keyword "phytoplankton" was not included in the search, Konur (2020a) ranked only 2 of the 10 most-productive journals ranked in this study (Bioresource Technology and Journal of Applied Phycology). It confirmed that the keyword "phytoplankton" used in our search has influenced the publication outputs presenting results related to Ecology besides Biotechnology. Otherwise, when the search was done only for the genus *Chlorella* sp., Cheng et al. (2020) ranked 7 of the 10 most-productive journals in this research, evidencing the importance of this microalgae genus to current investigations about algae in Biotechnology.

Algae biofuels have turned into one of the most rising topics in the renewable energy scenario. Nowadays, China is the country that most contributed to the crescent propagation of this thematic (Azadi et al., 2017), differently from what happened in the past 10 years, when the USA and European countries were responsible for 70% of the total publication in this research field (Adenle et al., 2013). In our search, the word "biofuel*" appeared as a trend among microalgae-fungi consortia research, especially focused on "Biodiesel" and "Biogas." The energy production of microalgae-based biofuels can be 100 times higher than most crops used in the first and second generations of biofuels (Kirrolia et al., 2013).

It is known that more than a few types of biofuels can be produced from microalgae, e.g., lipids can be converted to biodiesel through transesterification; carbohydrates can be used for bioethanol production through fermentation, biogas is produced *via* anaerobic digestion, and finally, biohydrogen through biophotolysis (Bahadar and Bilal-Khan, 2013; Kiran et al., 2014; Zhu et al., 2017; Sankaran et al., 2018). In all these processes, fungi can cooperate in harvesting microalgal biomass through bioflocculation. However, this is one of the most expensive steps, costing up to 20–30% of biofuel production costs (Molina-Grima et al., 2003), and is still a bottleneck on microalgae-based biofuel biorefinery (Gerde et al., 2014).

Biodiesel was first reported on databases in 1991, while the microalgae-based biodiesel concept appeared in 1993 (Ma et al., 2018). The high lipid content of microalgae is one of the most attractive features of its use in biofuel biorefinery (Kiran et al., 2014; Hwang et al., 2016). Considering the required cultivation area, some microalgae species can produce 300 times more oil than some edible crops from the first generation of biofuels (Alam et al., 2015). Even though liquid biofuels have been more explored than gaseous (Yaoyang and Boeing, 2013). Anaerobic digestion of algae for biogas production, in its turn has been an established technology being studied and utilized for more than 60 years from the 1950 decade until nowadays (Golueke et al., 1957; Zabed et al., 2020). Biogas is a biofuel commonly derived from the second generation of biomass for biofuels (Azadi et al., 2017), but it has considerably emerged as a hot topic in the microalgae-based biofuel scenario (Córdova et al., 2018).

Figuring between the most-cited species in this investigation, *C. vulgaris* is one of the most studied and cultivated microalgae species worldwide for biofuel production (Garrido-Cardenas et al., 2018). This genus was widely studied during the 2nd World War as a nutritional supplement. Then, its ability to remove recalcitrant compounds through bioremediation started to be investigated, and the high lipid content is an extremely valuable compound to the biofuel industry (Cheng et al., 2020). Filamentous fungi also appeared on the top-cited keywords, and the most species applied to the bioflocculation of microalgae are *Aspergillus* sp., *Trichoderma* sp., *Penicillium* sp., *Rhizopus* sp., and *Mucor* sp (see Chu et al., 2021).

Rajendran and Hu (2016) defined this synthetic association called "Mycoalgae"; the co-cultivation of microalgae-fungi is advantageous in many biorefinery processes, reducing the energetic and financial costs of the harvesting process. Also, this topic has gained emphasis in the scientific community, reflected by the increase in the number of publications, likewise on the citation parameters, and the range broad of countries, institutions, and authors investigating this consortium. Finally, the analysis of the keywords revealed the main trends related to the topic, highlighting the terms associated with biofuel production, especially biodiesel and biogas.

CONCLUSION

Through the analysis of 1,452 articles, an increase in the number of publications is observed between 1950 and 2020, especially highlighted from the year 2006 onward, the same period where an increase for microalgae-derived products took place. In addition to the publication trends, the languages of the publications were also evaluated, and 96.3% of the articles are in English. All the articles summed 49,052 citations; the 10 most-cited are published in English, while 2 are are related to biodiesel manufacture. That confirms the trend for biofuel research sought in this investigation. The country publishing the most is China (360), followed by the USA (344), and far behind in the 3rd position is Germany (155).

On the other hand, the USA has the highest number of multiple countries' collaboration. Unlike those observed in other microalgae research, the most participative institutions are Chinese (1st and 2nd positions), while the others are from the USA and Europe. The most-prolific authors are Chinese, except for 2 authors from the Netherlands. The results evidence that China occupies a very prominent spot in microalgae-fungi research. The sources publishing the most about this consortium are distributed between Biotechnology (as Bioresource Technology) and Ecology (e.g., Hydrobiologia) fields, confirming the bias of using the terms microalgae and phytoplankton in the search. The analysis of the keywords also indicates the trends for biofuel production expected in this investigation. Biodiesel is the 6th most cited keyword, confirming that biodiesel is the most studied biofuel type, like lipid, the main microalgae byproduct used for biodiesel production. Also, but

in a distant position, Biogas (64th) is another type of biofuel that emerged from the keyword analysis. Finally, coupled with a range of filamentous fungi species, *Chlorella* sp., ranks as the most-studied microalgae genus in the keywords.

These findings can collaborate on understanding how microalgae-fungi co-cultivation is being investigated and guide future research on exploring the potential of this consortium for biotechnology, bioproducts, and biofuels. Through this effort, we conclude that there is a gap in exploring new microbial-consortia actors, including fungi and microalgae, that are not yet bioprospecting. Moreover, applications for carbon-mitigation emissions using microalgae-fungi consortia are welcome.

DATA AVAILABILITY STATEMENT

The original contributions presented in the study are included in the article/supplementary material, further inquiries can be directed to the corresponding authors.

AUTHOR CONTRIBUTIONS

AL-M: conceptualization (lead), writing—original draft (lead), formal analysis (lead), investigation (lead), and writing—review and editing (equal). SX-S: conceptualization (supporting), writing—review and editing (equal), investigation (supporting), and financial resource (equal). LD-S: review and editing (equal) and financial resource (equal). SC: conceptualization (supporting), investigation (supporting), writing—review, editing (equal), and financial resource (equal).

FUNDING

AL-M scholarship was provided by the Fundação de Amparo à Pesquisa do Estado de Goiás, process n° 202110267000890. This study was financed in part by the Coordenação de Aperfeiçoamento de Pessoal de Nível Superior - Brasil (CAPES) - Finance Code 001 (Convênio n° 817164/2015 CAPES/PROAP).

REFERENCES

Adenle, A. A., Haslam, G. E., and Lee, L. (2013). Global assessment of research and development for algae biofuel production and its potential role for sustainable development in developing countries. *Energy Policy* 61, 182–195. doi: 10.1016/j.enpol.2013.05.088

Alam, F., Mobin, S., and Chowdhury, H. (2015). Third generation biofuel from algae. *Procedia Eng.* 105, 763–768. doi: 10.1016/j.proeng.2015.05.068

Alexopoulos, C. J., Mims, C. W., and Blackwell, M. (1996). *Introductory Mycology*, *4th Edn.* New York, NY: John Wiley and *Sons*. 880p.

Andreo-Martínez, P., Ortiz-Martínez, V. M., García-Martínez, N., A. P., Hernández-Fernández, F. J., and Quesada-Medina, J. (2020). Production of biodiesel under supercritical conditions: state of the art and bibliometric analysis. *Appl. Energy* 264:114753. doi: 10.1016/j.apenergy.2020.114753

Aria, M., and Cuccurullo, C. (2017). Bibliometrix: an R-Tool for comprehensive science mapping analysis. *J. Informetr.* 11, 959–975. doi: 10.1016/j.joi.2017.08.007

Azadi, P., Malina, R., Barrett, S. R. H., and Kraft, M. (2017). The evolution of the biofuel science. *Renew. Sustain. Energy Rev.* 76, 1479–1484. doi: 10.1016/j.rser.2016.11.181

Bahadar, A., and Bilal-Khan, M. (2013). Progress in energy from microalgae: a review. *Renew. Sustain. Energy Rev.* 27, 128–148. doi: 10.1016/j.rser.2013.06.029

Baicha, Z., Salar-García, M. J., Ortiz-Martínez, V. M., Hernández-Fernández, F. J., de los Ríos, A. P., Labjar, N., et al. (2016). A critical review on microalgae as an alternative source for bioenergy production: a promising low-cost substrate for microbial fuel cells. *Fuel Process. Technol.* 154, 104–116. doi: 10.1016/j.fuproc.2016.08.017

Brasil, B. S. A. F., Silva, F. C. P., and Siqueira, F. G. (2017). *Microalgae biorefineries*: the Brazilian scenario in perspective. *N. Biotechnol.* 39, 90–98. doi: 10.1016/j.nbt.2016.04.007

Chen, J., Leng, L., Ye, C., Lu, Q., Addy, M., Wang, J., et al. (2018). A comparative study between fungal pellet- and spore-assisted microalgae harvesting methods for algae bioflocculation. *Bioresour. Technol.* 259, 181–190. doi: 10.1016/j.biortech.2018.03.040

Cheng, Z., Kong, W., Cheng, Z., Qi, H., Yang, S., Zhang, A., et al. (2020). A bibliometric-based analysis of the high-value application of Chlorella. *3 Biotech* 10:106. doi: 10.1007/s13205-020-2102-0

Chiarini, T., Cimini, F., Rapini, M. S., and Silva, L. A. (2020). The political economy of innovation why is Brazil stuck in the technology ladder?. *Braz. Polit. Sci. Rev.* 14:14. doi: 10.1590/1981-3821202000020001

Chu, R., Li, S., Zhu, L., Yin, Z., Hu, D., Liu, C., et al. (2021). A review on co-cultivation of microalgae with filamentous fungi: efficient harvesting, wastewater treatment, and biofuel production. *Renew. Sustain. Energy Rev.* 139:110689. doi: 10.1016/j.rser.2020.110689

Coelho, M. S., Barbosa, F. G., and Souza, M. R. A. Z. (2014). The scientometric research on macroalgal biomass as a source of biofuel feedstock. *Algal Res.* 6, 132–138. doi: 10.1016/j.algal.2014.11.001

Córdova, O., Santis, J., Ruiz-Fillipi, G., Zuñiga, M. E., Fermoso, F. G., and Chamy, R. (2018). Microalgae digestive pretreatment for increasing biogas production. *Renew. Sustain. Energy Rev.* 82, 2806–2813. doi: 10.1016/j.rser.2017.10.005

Garrido-Cardenas, J. A., Manzano-Agugliaro, F., Acien-Fernandez, F. G., and Molina-Grima, E. (2018). Microalgae research worldwide. *Algal Res.* 35, 50–60. doi: 10.1016/j.algal.2018.08.005

Gerde, J. A., Yao, L., Lio, J. Y., Wen, Z., and Wang, T. (2014). Microalgae flocculation: impact of flocculant type, algae species and cell concentration. *Algal Res.* 3, 30–35. doi: 10.1016/j.algal.2013.11.015

Golueke, C. G., Oswald, W. J., and Gotaas, H. B. (1957). Anaerobic digestion of algae. *Appl. Microbiol.* 5, 47–55. doi: 10.1128/am.5.1.47-55.1957

Gonzalez-Brambila, C. N., Reyes-Gonzalez, L., Veloso, F., and Perez-Angón, M. A. (2016). The scientific impact of developing nations. *PLoS ONE* 11:e0151328. doi: 10.1371/journal.pone.0151328

Hamel, R. E. (2007). The dominance of English in the international scientific periodical literature and the future of language use in science. *AILA Rev.* 20, 53–71. doi: 10.1075/aila.20.06ham

Hawksworth, D. L., and Lücking, R. (2017). Fungal diversity revisited: 2.2 to 3.8 million species. *Microbiol Spectr.* (2017) 5, 79–95. doi: 10.1128/microbiolspec.FUNK-0052-2016

Hwang, J. H., Church, J., Lee, S. J., Park, J., and Lee, W. H. (2016). Use of microalgae for advanced wastewater treatment and sustainable bioenergy generation. *Environ. Eng. Sci.* 33, 882–897. doi: 10.1089/ees.2016.0132

Jiang, J., Jin, W., Tu, R., Han, S., Ji, Y., and Zhou, X. (2021). Harvesting of Microalgae *Chlorella pyrenoidosa* by bio-flocculation with bacteria and filamentous fungi. *Waste Biomass Valorization* 12, 145–154. doi: 10.1007/s12649-020-00979-6

King, D. A. (2004). The scientific impact of nations. *Science* 430, 331–316. doi: 10.1038/430311a

Kiran, B., Kumar, R., and Deshmukh, D. (2014). Perspectives of microalgal biofuels as a renewable source of energy. *Energy Conversion Manage.* 88, 1228–1244. doi: 10.1016/j.enconman.2014.06.022

Kirrolia, A., Bishnoi, N. R., and Singh, R. (2013). Microalgae as a boon for sustainable energy production and its future research and development aspects. *Renew. Sustain. Energy Rev.* 20, 642–656. doi: 10.1016/j.rser.2012.12.003

Konur, O. (2020a). "The scientometric analysis of the research on the algal bioenergy and biofuels," in *Handbook of Algal Science, Technology and Medicine*. ed O. Konur (London: Elsevier Academic Press). doi: 10.1016/B978-0-12-818305-2.00020-6

Konur, O. (2020b). "The scientometric analysis of the research on the algal science, technology, and medicine," in *Handbook of Algal Science, Technology and Medicine*, ed. O. Konur (London: Elsevier Academic Press) doi: 10.1016/B978-0-12-818305-2.00001-2

Konur, O. (2020c). "The scientometric analysis of the research on the algal ecology," in *Handbook of Algal Science, Technology and Medicine*, ed. O. Konur (London: Elsevier Academic Press). doi: 10.1016/B978-0-12-818305-2.00016-4

Kuhar, F., Furci, G., Drechsler-Santos, E. R., and Pfister, D. H. (2018). Delimitation of funga as a valid term for the diversity of fungal communities: the Fauna, Flora and Funga Proposal (FF and F). *IMA Fungus* 9, 71–74. doi: 10.1007/BF03449441

Larsen, P. O., and von Ins, M. (2010). The rate of growth in scientific publication and the decline in coverage provided by science citation index. *Scientometrics* 84, 575–603. doi: 10.1007/s11192-010-0202-z

Li, S., Hu, T., Xu, Y., Wang, J., Chu, R., Yin, Z., et al. (2020). A review on flocculation as an efficient method to harvest energy microalgae: mechanisms, performances, influencing factors and perspectives. *Renew. Sustain. Energy Rev.* 131:110005. doi: 10.1016/j.rser.2020.110005

Ma, X., Gao, M., Gao, Z., Wang, J., Zhang, M., Ma, Y., et al. (2018). Past, current, and future research on microalga-derived biodiesel: a critical review and bibliometric analysis. *Environ. Sci. Pollut. Res.* 25, 10596–10610. doi: 10.1007/s11356-018-1453-0

Mahdy, A., Mendez, L., Tomás-Pejó, E., Morales, M. M., Ballesteros, M., and González-Fernández, C. (2016). Influence of enzymatic hydrolysis on the biochemical methane potential of *Chlorella vulgaris* and *Scenedesmus Sp. J. Chem. Technol. Biotechnol.* 91, 1299–1305. doi: 10.1002/jctb.4722

Mathimani, T., and Mallick, N. (2020). A comprehensive review on harvesting of microalgae for biodiesel – Key challenges and future directions. *Renew. Sustain. Energy Rev.* 91, 1103–1120. doi: 10.1016/j.rser.2018.04.083

Molina-Grima, E., Belarbi, E. H., Acién-Fernández, F. G., Robles-Medina, A., and Chisti, Y. (2003). Recovery of microalgal biomass and metabolites: process options and economics. *Biotechnol. Adv.* 20, 491–515. doi: 10.1016/S0734-9750(02)00050-2

Moreira, A. B. L. (2021). Trends of microalgae research in Brazil. *Revista Brasileira de Engenharia e Sustentabilidade* 9, 18–25. doi: 10.15210/rbes.v9i2.21400

Nabout, J. C., Carneiro, F. M., Borges, P. P., Machado, K. B., and Huszar, V. L. M. (2015). Brazilian scientific production on phytoplankton studies: national determinants and international comparisons. *Braz. J. Biol.* 75, 216–223. doi: 10.1590/1519-6984.11713

Nazari, M. T., Freitag, J. F., Cavanhi, V. A. F., and Colla, L. M. (2020). Microalgae harvesting by fungal-assisted bioflocculation. *Rev. Environ. Sci. Biotechnol.* 19, 369–388. doi: 10.1007/s11157-020-09528-y

Parkinson, J. (2013). "English for science and technology," in *The Handbook of English for Specific Purposes*, eds B. Paltridge and S. Starfield (Chichester: John Wiley & Sons), 155–173. doi: 10.1002/9781118339855.ch8

Passos, F., Hom-Diaz, A., Blanquez, P., Vicent, T., and Ferrer, I. (2016). Improving biogas production from microalgae by enzymatic pretreatment. *Bioresour. Technol.* 199, 347–351. doi: 10.1016/j.biortech.2015.08.084

R Core Team (2022). *R: A language and environment for statistical computing*. Vienna: R Foundation for Statistical Computing. Available online at: https://www.R-project.org/.

Rai, M., Bonde, S., Golinska, P., Trzcińska-Wencel, J., Gade, A., Abd-Elsalam, K., et al. (2021). Fusarium as a novel fungus for the synthesis of nanoparticles: mechanism and applications. *J. Fungi* 7, 1–24. doi: 10.3390/jof7020139

Rajendran, A., and Hu, B. (2016). Mycoalgae biofilm: development of a novel platform technology using algae and fungal cultures. *Biotechnol. Biofuels* 9:112. doi: 10.1186/s13068-016-0533-y

Richards, T. A., Leonard, G., and Wideman, J. G. (2017). "What defines the 'Kingdom' Fungi?" *Microbiol. Spectr.* 5, 57–77. doi: 10.1128/microbiolspec.FUNK-0044-2017

Rumin, J., Nicolau, E., Oliveira, R. G., Fuentes-Grünewald, C., Flynn, K. J., and Picot, L. (2020). A bibliometric analysis of microalgae research in the World, Europe, and the European Atlantic Area. *Mar. Drugs* 18:79. doi: 10.3390/md18020079

Sankaran, R., Show, P. L., Nagarajan, D., and Chang, J. S. (2018). *Exploitation and Biorefinery of Microalgae*. Waste Biorefinery: Potential and Perspectives. Elsevier B.V. doi: 10.1016/B978-0-444-63992-9.00019-7

Serejo, M. L., Morgado, M. F., García, D., González-Sánchez, A., Méndez-Acosta, H. O., and Toledo-Cervantes, A. (2019). "Environmental resilience by microalgae," in *Microalgae Cultivation for Biofuels Production*, ed. A. Yousuf (London: Elsevier Inc.), Chap. 19, 293–315. doi: 10.1016/B978-0-12-817536-1.00019-9

Spier, M. R., Peron-Schlosser, B., Paludo, L. C., Gallo-García, L. A., and Zanette, C. M. (2020). "Microalgae as enzymes biofactories," in *Handbook of Microalgae-Based Processes and Products*, Chap. 25, eds E. Jacob-Lopes, M. M. Maroneze, M. I. Queiroz, and L. Q. Zepka (London: Academic Press), 687–706. doi: 10.1016/b978-0-12-818536-0.00025-7

Srinuanpan, S., Chawpraknoi, A., Chantarit, S., Cheirsilp, B., and Prasertsan, P. (2018). A rapid method for harvesting and immobilization of oleaginous microalgae using pellet-forming filamentous fungi and the application in phytoremediation of secondary effluent. *Int. J. Phytoremediation* 20, 1017–1024. doi: 10.1080/15226514.2018.1452187

Systat Software and Inc. (2011). *SigmaPlot for Windows, version 12.0*. San Jose: California. Available online at: www.systatsoftware.com.

Yaoyang, X., and Boeing, W. J. (2013). Mapping biofuel field: a bibliometric evaluation of research output. *Renew. Sustain. Energy Rev.* 28, 82–91. doi: 10.1016/j.rser.2013.07.027

Zabed, H. M., Akter, S., Yun, J., Zhang, G., Zhang, Y., and Qi, Q. (2020). Biogas from microalgae: technologies, challenges and opportunities. *Renew. Sustain. Energy Rev.* 117:109503. doi: 10.1016/j.rser.2019.109503

Zhang, M., Gao, Z., Zheng, T., Ma, Y., Wang, Q., Gao, M., et al. (2018). A bibliometric analysis of biodiesel research during 1991–2015. *J. Mater. Cycles Waste Manage.* 20, 10–18. doi: 10.1007/s10163-016-0575-z

Zhou, W., Cheng, Y., Li, Y., Wan, Y., Liu, Y., Lin, X., et al. (2012). Novel fungal pelletization-assisted technology for algae harvesting and wastewater treatment. *Appl. Biochem. Biotechnol.* 167, 214–228. doi: 10.1007/s12010-012-9667-y

Zhou, W., Min, M., Hu, B., Ma, X., Liu, Y., Wang, Q., et al. (2013). Filamentous fungi assisted bio-flocculation: a novel alternative technique for harvesting heterotrophic and autotrophic microalgal cells. *Sep. Purif. Technol.* 107, 158–165. doi: 10.1016/j.seppur.2013.01.030

Zhu, L., Nugroho, Y. K., Shakeel, S. R., Li, Z., Martinkauppi, B., and Hiltunen, E. (2017). Using microalgae to produce liquid transportation biodiesel: what is next? *Renew. Sustain. Energy Rev.* 78, 391–400. doi: 10.1016/j.rser.2017.04.089

Conflict of Interest: The authors declare that the research was conducted in the absence of any commercial or financial relationships that could be construed as a potential conflict of interest.

Publisher's Note: All claims expressed in this article are solely those of the authors and do not necessarily represent those of their affiliated organizations, or those of the publisher, the editors and the reviewers. Any product that may be evaluated in this article, or claim that may be made by its manufacturer, is not guaranteed or endorsed by the publisher.

Copyright © 2022 Lobo-Moreira, Xavier-Santos, Damacena-Silva and Caramori. This is an open-access article distributed under the terms of the Creative Commons Attribution License (CC BY). The use, distribution or reproduction in other forums is permitted, provided the original author(s) and the copyright owner(s) are credited and that the original publication in this journal is cited, in accordance with accepted academic practice. No use, distribution or reproduction is permitted which does not comply with these terms.

frontiers | Frontiers in Microbiology

ORIGINAL RESEARCH
published: 23 June 2022
doi: 10.3389/fmicb.2022.901793

Unraveling the Basis of Neonicotinoid Resistance in Whitefly Species Complex: Role of Endosymbiotic Bacteria and Insecticide Resistance Genes

Mritunjoy Barman[1†], Snigdha Samanta[1†], Gouranga Upadhyaya[2], Himanshu Thakur[3], Swati Chakraborty[4], Arunava Samanta[1] and Jayanta Tarafdar[4*]*

[1] Department of Agricultural Entomology, Bidhan Chandra Krishi Viswavidyalaya, Mohanpur, India, [2] Department of Biological Sciences, Indian Institute of Science Education and Research Kolkata, Kolkata, India, [3] Department of Entomology, C.S.K. Himachal Pradesh Krishi Vishvavidyalaya, Palampur, India, [4] Department of Plant Pathology, Bidhan Chandra Krishi Viswavidyalaya, Nadia, India

OPEN ACCESS

Edited by:
Durgesh K. Jaiswal,
Savitribai Phule Pune University, India

Reviewed by:
Jie Wang,
Fujian Agriculture and Forestry University, China
Pankaj Bhatt,
Purdue University, United States

***Correspondence:**
Gouranga Upadhyaya
gour.cubot@gmail.com
Jayanta Tarafdar
jayanta94bckv@gmail.com

[†] These authors have contributed equally to this work and share first authorship

Specialty section:
This article was submitted to Microbiotechnology, a section of the journal Frontiers in Microbiology

Received: 22 March 2022
Accepted: 25 May 2022
Published: 23 June 2022

Citation:
Barman M, Samanta S, Upadhyaya G, Thakur H, Chakraborty S, Samanta A and Tarafdar J (2022) Unraveling the Basis of Neonicotinoid Resistance in Whitefly Species Complex: Role of Endosymbiotic Bacteria and Insecticide Resistance Genes. Front. Microbiol. 13:901793. doi: 10.3389/fmicb.2022.901793

Bemisia tabaci (whitefly) is one of the most detrimental agricultural insect pests and vectors of many plant viruses distributed worldwide. Knowledge of the distribution patterns and insecticide resistance of this cryptic species is crucial for its management. In this study, genetic variation of mitochondrial cytochrome oxidase subunit 1 (*MtCol*) gene of *B. tabaci* was analyzed followed by a study of the infection profile of various endosymbionts in 26 whitefly populations collected from West Bengal, India. Phylogenetic analysis revealed Asia I as the major cryptic species (65.38%), followed by Asia II 5, China 3, and Asia II 7, which were diversified into 20 different haplotypes. In addition to the primary endosymbiont (*C. poriera*), each of the four whitefly species showed a variable population of three secondary endosymbionts, majorly *Arsenophonus* with the highest infection rate (73.07%), followed by *Wolbachia* and *Rickettsia*. Further phylogenetic analyses revealed the presence of two subgroups of *Arsenophonus*, *viz*., A1 and A2, and one each in *Wolbachia* (W1) and *Rickettsia* (R3). Resistance to thiamethoxam, imidacloprid, and acetamiprid insecticides was analyzed for a clear picture of pesticide resistance status. The highest susceptibility was noted toward thiamethoxam (LC_{50} = 5.36 mg/L), followed by imidacloprid and acetamiprid. The whitefly population from Purulia and Hooghly districts bearing Asia II 7 and Asia II 5 cryptic species, respectively, shows maximum resistance. The differences in mean relative titer of four symbiotic bacteria among field populations varied considerably; however, a significant positive linear correlation was observed between the resistance level and relative titer of *Arsenophonus* and *Wolbachia* in the case of imidacloprid and thiamethoxam, while only *Wolbachia* was found in case of acetamiprid. Expression analysis demonstrated differential upregulation of insecticide resistance genes with Purulia and Hooghly populations showing maximally upregulated P450 genes. Moreover, thiamethoxam and imidacloprid resistance ratio (RR) showed a significant correlation with CYP6CM1, CYP6DZ7, and CYP4C64 genes, while acetamiprid RR correlated with

CYP6CX1, CYP6DW2, CYP6DZ7, and CYP4C64 genes. Taken together, these findings suggested that P450 mono-oxygenase and symbiotic bacteria together affected whitefly resistance to neonicotinoids. Hence, a symbiont-oriented management programme could be a better alternative to control or delay resistance development in whitefly and can be used for pesticide clean-up in an agricultural field.

Keywords: whitefly, cryptic species, endosymbionts, genetic group, P450 monooxygenase, insecticide resistance, neonicotinoid, *mtCOI*

INTRODUCTION

The whitefly, *Bemisia tabaci,* is an economically important agricultural pest causing huge damage to crops worldwide. They inflict damage to plants directly and as a vector of several hundred viruses, with a majority (>320 species) of them belonging to the genus Begomovirus and other economically important viruses belonging to the genera Ipomovirus, Carlavirus, Crinivirus, Torradovirus, and Polerovirus (Jones, 2003; Mugerwa et al., 2021). Whitefly is composed of a complex group of genetically distinct species and/or biotypes that differ substantively by host plant preference, virus transmitting ability, and insecticide resistance (De Barro et al., 2011; Barman et al., 2022). It is listed as one of the top 100 dreadful alien invasive species due to its virus transmission ability and wide host adaptability (Lowe et al., 2000). Dinsdale et al. (2010) proposed a 3.5% pair-wise genetic divergence of mitochondrial cytochrome oxidase I (*MtCoI*), which led to the identification of 44 distinct species of *B. tabaci*. Additionally, two new species, Asia II 13 and Spain 1, have also been recently reported (Kanakala and Ghanim, 2019). The Indian geographical regions unveil a huge diversity of *B. tabaci* with the presence of 10 cryptic species out of 46 recorded species so far (Rehman et al., 2021). Precise knowledge of the distribution pattern of this cryptic species is crucial for the efficient management of this notorious pest worldwide.

Nonetheless, increasing reports of resistance development in *B. tabaci* to various organophosphates, synthetic pyrethroids, and other neonicotinoid compounds have been surfacing (Peshin and Zhang, 2014; Naveen et al., 2017; Wang et al., 2020). Several countries, namely, China (Wang et al., 2010), India (Kranthi et al., 2002), Iran (Basij et al., 2017), Israel (Alon et al., 2008), Malaysia (Shadmany et al., 2015), Pakistan (Ahmad et al., 2010), and the USA (Prabhaker et al., 2014), have reported the development of insecticide resistance in whitefly to even compounds of novel chemistry. Intensive and frequent use of insecticides, selection pressure, and choice of poor insecticides may be some of the other factors rendering resistance in whitefly both at field and laboratory levels (Sethi and Dilawari, 2008; Pietri and Liang, 2018). The neonicotinoid group of compounds, represented by imidacloprid, thiamethoxam, and others, are majorly used insecticides in controlling the whitefly population worldwide, including in India (Sethi and Dilawari, 2008; Yang et al., 2013; Pang et al., 2020). However, several countries reported neonicotinoid resistance in whitefly due to the overuse of this chemical compound (Nauen et al., 2002; Ma et al., 2007; Luo et al., 2010; Naveen et al., 2017).

Researchers have observed that increased metabolic detoxification may be due to gene amplification, overexpression, and modification of gene coding proteins of major detoxifying enzymes, such as cytochrome P450 and glutathione S-transferases (GSTs) (Karunker et al., 2008; Feyereisen, 2011; Elzaki et al., 2017). The involvement of P450 genes in conferring resistance to several insecticides has been listed in insects, such as *Drosophila melanogaster* to DDT and imidacloprid, brown planthopper (BPH) to imidacloprid, and so on (Daborn et al., 2001; Garrood et al., 2016). Another most notable aspect of this complex is the bacterial symbionts that infect its members. Considerable evidence exists regarding microbe-mediated effects in whitefly, ranging from host survival, development, and nutritional fitness to even insecticide resistance (Su et al., 2014; Li et al., 2018). The *B. tabaci* species complex carries a primary endosymbiont *Candidatus Portiera aleyrodidarum* that occurs in all individuals and is located in specialized cells termed as bacteriocytes (Sloan and Moran, 2012). The secondary symbionts, namely, *Rickettsia* (Gottlieb et al., 2006), *Wolbachia* (Nirgianaki et al., 2003), *Hamiltonella, Arsenophonus* (Thao and Baumann, 2004; Sloan and Moran, 2012), *Cardinium* (Weeks et al., 2003), *Fritschea* (Everett et al., 2005), and *Hemipteriphilus* (Bing et al., 2013) have been reported to be present in *B. tabaci* populations around the world. Unlike primary endosymbionts which have a direct mutualistic relationship with the host, the secondary symbionts form a less stable partnership with their host. The infection pattern of these secondary symbionts is highly complex and varies according to the geographical regions (Zchori-Fein et al., 2014) and the different genetic groups (Chiel et al., 2007; Ghosh et al., 2015; Lestari et al., 2021).

The development of resistance is generally manifested by a failure to control the pests at the field level. A very few studies from India were involved in determining the field level resistance in *B. tabaci*; however, there was no in-depth study explaining the exact mechanism behind such resistance development. Hence, a precise understanding of the mechanism of insecticide resistance is of great significance for the management or delay in the development of resistance. Within this framework, this work hypothesized that there are differences in the resistance levels of whitefly populations in different regions toward insecticides like neonicotinoids, and this variation might be affected by the expression of genes associated with cytochrome P450 mono-oxygenase or variation of symbiont titres, either separately or together. To test this hypothesis, the following objectives were considered: (1) characterization and resistance level of the whitefly field population toward imidacloprid, thiamethoxam,

and acetamiprid, (2) infection pattern and the relative titer of the endosymbiotic bacteria (*Portiera, Arsenophonus, Wolbachia,* and *Rickettsia*) associated with the whitefly field population, and (3) gene expression associated with cytochrome P450 mono-oxygenase (CYP6CM1, CYP6CX1, CYP6CX5, CYP6CX3, CYP6DZ4, CYP4C64, CYP6DZ7, and CYP6DW2) and their relationship with resistance level. Our finding, for the first time, shall shed light on field evolved resistance in different whitefly cryptic species toward popularly used neonicotinoids, further attempting to predict the mechanism behind such resistance development, in particular, the involvement of endosymbionts and P450 genes.

METHODS

Whitefly Collection

The samples of *B. tabaci* used in the current study were collected from different locations across Bengal province, India (as detailed in **Supplementary Table S1**). Adult whiteflies (mixed sex) were collected from various crop plants (chili, eggplant, cucumber, tomato, lady's finger, and pointed gourd) and weed plants (cida and wild brinjal). The flies were pooled together inside ventilated insect-proof cages on the basis of location and further reared in the Molecular Biology laboratory, Directorate of Research, BCKV.

Detection of Whitefly Genetic Groups and Endosymbionts

The genetic group identity of *B. tabaci* field population was examined by random sampling of 10 adult flies for each population using PCR amplification of the *MtCoI* gene and sequencing as described by Dinsdale et al. (2010). Genomic DNA was extracted from each specimen as per the manufacturer's instructions (Invitrogen, USA). PCR amplification using 20 ng of insect DNA was carried out in Veriti 96-Well Thermal Cycler (Applied Biosystems, USA). The endosymbionts (*Portiera*, *Wolbachia*, *Arsenophonus,* and *Rickettsia*) in the collected whitefly populations were also determined using specific primers (as listed in **Supplementary Table S2**). The amplified PCR products were excised from the gel and purified using the XcelGen DNA Gel/ PCR Purification mini kit (Xcelris genomics, India) following the manufacturer's instructions. The DNA sequence was obtained through Sanger dideoxy sequencing method from Chromus Biotech Laboratory, India.

Genetic Structuring and Phylogenetic Analysis

Different neutrality statistics were performed to examine the demographic history of whitefly and their endosymbionts. Tajima's *D* (Tajima, 1989) and Fu's Fs (Fu, 1997) statistics were subsequently calculated to check whether the *COI* conformed to the expectations of neutrality by DnaSP (Librado and Rozas, 2009). The population pair-wise *F*-statistics (F_{ST}) and analysis of molecular variance (AMOVA) were calculated with the help of Arlequin v.3.5 (Excofer and Lischer, 2010). The haplotype network of the sequences was examined using a minimum spanning network relationship with the help of popART software. Multiple alignments of all the nucleotide sequences of whiteflies and endosymbionts were conducted using ClustalW, and analysis was done in Mega-X (Kimura, 1980; Kumar et al., 2018). The tree was verified using the maximum likelihood (ML) model, and a total 1,000 of bootstrap replicates were performed. The tree was processed through iTol (version 6.4.3) for graphical representation. All the nucleotide sequences of the whitefly population and endosymbionts were submitted to the NCBI GenBank database.

Bioassay of Insecticides

To determine the current susceptibility status and resistant gene expression of whitefly, the field populations from the five most important regions (one population each from Kalimpong, Midnapore, Hooghly, Malda, and Purulia) were selected (as listed in **Supplementary Table S3**). For the bioassay, a total of approximately 800 adult flies were collected per location, and around 650 of them were used immediately in the bioassay study. The whitefly population collected from the university farm (B.C.K.V., Kalyani, India) was chosen to be reared for 10 additional generations without any exposure to insecticides in the laboratory and was considered as the susceptible population (SP). Three insecticides, namely, imidacloprid 17.8 SL (Confidor) obtained from Bayer Co., Ltd., thiamethoxam 25 WG (Actara) from Syngenta Chemical Ltd., and acetamiprid 20SP (Pyramid) from Hifield-AG Chem. Pvt. Ltd., were used for bioassay studies against the adult whitefly population. The toxicity of imidacloprid, thiamethoxam, and acetamiprid was evaluated following a modified leaf dip bioassay method by the Insecticide Resistance Action Committee (Naveen et al., 2017). To evaluate the toxicity, final doses were decided based on the prior experiments conducted on lab populations, and five different concentrations of each insecticide were used. In each insecticide treatment, fresh brinjal leaves (5×5 cm^2) were dipped in the respective insecticide dilutions for 30 ± 2 s in a corning glass Petri plate (dia. = 15 cm) and air-dried, whereas the control leaves were dipped in water alone. After drying the solution on the leaf surface, the treated leaves were transferred to the corning glass Petri plate (dia. = 9 cm) containing a thin 2% agar layer at the bottom. Each treatment was replicated five times, and six adult whiteflies were released per replication (thirty in each treatment) and plates were covered with ventilated lids. The experiment was conducted under laboratory conditions ($26 \pm 1^{\circ}$C, 70–80% RH, 16L: 8D photoperiod), and the observations regarding the mortality were taken at 72 h after feeding (HAF).

Symbiont Quantification and Expression Analyses of Insecticide Resistance Genes

Total genomic DNA (for quantification of symbiont titer) and RNA (for gene expression) were extracted from field-collected whitefly (adult) population using Insect DNA and RNA Isolation Kit (Thermo Fisher Scientific, USA) following the manufacturer's protocol. Quantity was assessed with a Qubit Flex Fluorometer, and cDNA was prepared using 1 μl of total RNA according to the manufacturer's instructions (GeneSure H-Minus First Strand cDNA Synthesis Kit, Genetix Biotech Asia Pvt. Ltd.).

The relative abundance of targeted symbionts (*Portiera*, *Arsenophonus*, *Wolbachia,* and *Rickettsia*) and expression pattern of cytochrome P450 genes, namely, CYP6CM1, CYP6CX1, CYP6CX5, CYP6CX3, CYP6DZ4, CYP4C64, CYP6DZ7, and CYP6DW2, were examined using qRT-PCR (Wang et al., 2020). qRT-PCR was performed in Agilent Technologies Stratagene (Model-Mx3000P) using SYBR Green Master Mix (Applied Biosystems, USA). Primer details and annealing temperatures are mentioned in **Supplementary Table S2**. The relative expression of each target gene was calculated by the $2^{-\Delta\Delta Ct}$ method (Livak and Schmittgen, 2001). The Actin gene was used as an internal control.

Statistical Analysis

To determine the lethal concentration (LC) values, the observations recorded on mortality data were corrected using Abbott's formula (Abbott, 1925). The data were subjected to probit analysis (Finney, 1971) using SPSS. The resistance ratio (RR) for each population was calculated by the ratio: LC_{50} value of the population/LC_{50} value of the susceptible population. The RRs were then classified as follows: RR $<$ 5 indicated low resistance; RR $=$ 5–10 indicated moderate resistance, and RR $>$ 10 indicated high resistance (Mazzarri and Georghiou, 1995; World Health Organization, 2016). The qRT-PCR experiments were conducted at least thrice with a minimum of three individual biological replicates. Data have been represented as mean $\pm$ SD ($n = 3$) values. Statistical significance was analyzed using the GraphPad Prism 8.0 software by one-way analysis of variance (ANOVA), followed by Dunnett's multiple comparison test. Significant differences with the susceptible population have been represented as $^{*}p < 0.01$, $^{**}p < 0.001$, and $^{***}p < 0.0001$. Linear Model II regression analysis was used to determine the functional relationship between the resistance level of the population and the mean normalized expression value of each gene and endosymbiont in different populations using SPSS (SPSS for Windows, Rel. 17.0.0 2009. Chicago: SPSS Inc.).

RESULTS

Exploring the Prevalence of Different Genetic Groups of Whitefly and Their Symbionts

In totality, 26 whitefly populations collected from different host crops across different regions of Bengal province (as shown in **Figure 1A**) were identified using the primer pair (C1-J-2195 F/L2-N-3014 R) of the universal *Mt-co1* gene. The phylogenetic analysis of the determined *COI* sequences divided *B. tabaci* into four different cryptic species, with Asia I being the most predominant species followed by Asia II 5, China 3, and Asia II 7 at rates of 65.38, 19.23, 11.53, and 3.84%, respectively (**Figure 1A** inset). To show the distribution of collected samples, a maximum likelihood phylogenetic tree of the *COI* sequences of *Bemisia tabaci* collected from different locations has been drawn with previously reported GenBank sequences, wherein the bold text *COI* sequences represent collected samples used in this study (**Figure 1B**). Subsequently, diagnostic PCR confirmed the presence of primary endosymbiont *Portiera* and secondary endosymbionts *Wolbachia*, *Arsenophonus,* and *Rickettsia* in the selected whitefly population.

Study of Evolutionary Relationship Advocates Evident Genetic Diversity and Expansion Nature of Whitefly Cryptic Species

The pair-wise divergence in the *MtCoI* nucleotide sequence among the four identified genetic groups varied both at intraspecific and interspecific levels (**Supplementary Table S4**). Intraspecific variation was recorded to be the highest in Asia I (0.24–2.66%), and the lowest was observed in China 3 (0.11–0.23%). While considering the interspecific variation, Asia I and Asia II 5 (17.47–20.80%) were higher than that of Asia I and China 3 (14.63–17.09%). However, the lowest variation was observed between China 3 and Asia II 7 (16.95–17.30%).

Among the 20 haplotypes (based on *MtCoI* sequence), the highest number was recorded in Asia I (12), followed by Asia II 5 (5) and China 3 (2) (**Supplementary Table S5**). Asia II 7 was excluded from the genetic diversity study, as only one such sample was found in our survey. Haplotype diversity was higher in Asia II 5 (1) when compared to Asia I (0.956), whereas nucleotide diversity was higher in Asia I (0.014) in comparison to Asia II 5 (0.008). Results obtained from the neutrality test (Fu and Li's D^{*}, Fu and Li's F^{*}, and Tajima's D) recorded a significant negative value for Asia II 5 and China 3, indicating that these two cryptic species across the regions might be undergoing expansion.

Minimum spanning network analysis indicated four cryptic species to be diversified into 20 haplotypes, which are quite distant from one another (**Figure 1C**). Among the 12 haplotypes of Asia I, H1 occupied the central position of the network and was the linking haplotype between China 3 (H13) and Asia II 7 (H15) with the mutational differences of 109 and 114, respectively. Furthermore, hierarchical AMOVA revealed that most of the evident genetic diversity is collectively accredited to highly significant genetic differences between the four whitefly cryptic species (Fst: 91.83%; $P < 0.001$), and the haplotypes within these cryptic species contributed to 8.16% of the variation (**Supplementary Table S6**). Moreover, the genetic differentiation among the population (pair-wise Fst value) was >0.90 for all the four cryptic species (**Supplementary Table S7**).

Variation in the Infection Pattern of Endosymbiotic Bacteria Is Governed by *B. tabaci* Genetic Group

Primary endosymbiont (*C. poriera*) was present in all the test samples; however, the infection profiles of three secondary endosymbionts (*Arsenophonus*, *Wolbachia,* and *Rickettsia*) showed a substantial variation in each of the four identified cryptic whitefly species. Overall, *Arsenophonus* showed the highest infection rate (73.07%), followed by *Rickettsia* (65.38%) and *Wolbachia* (53.84%). *Arsenophonus* infection was found

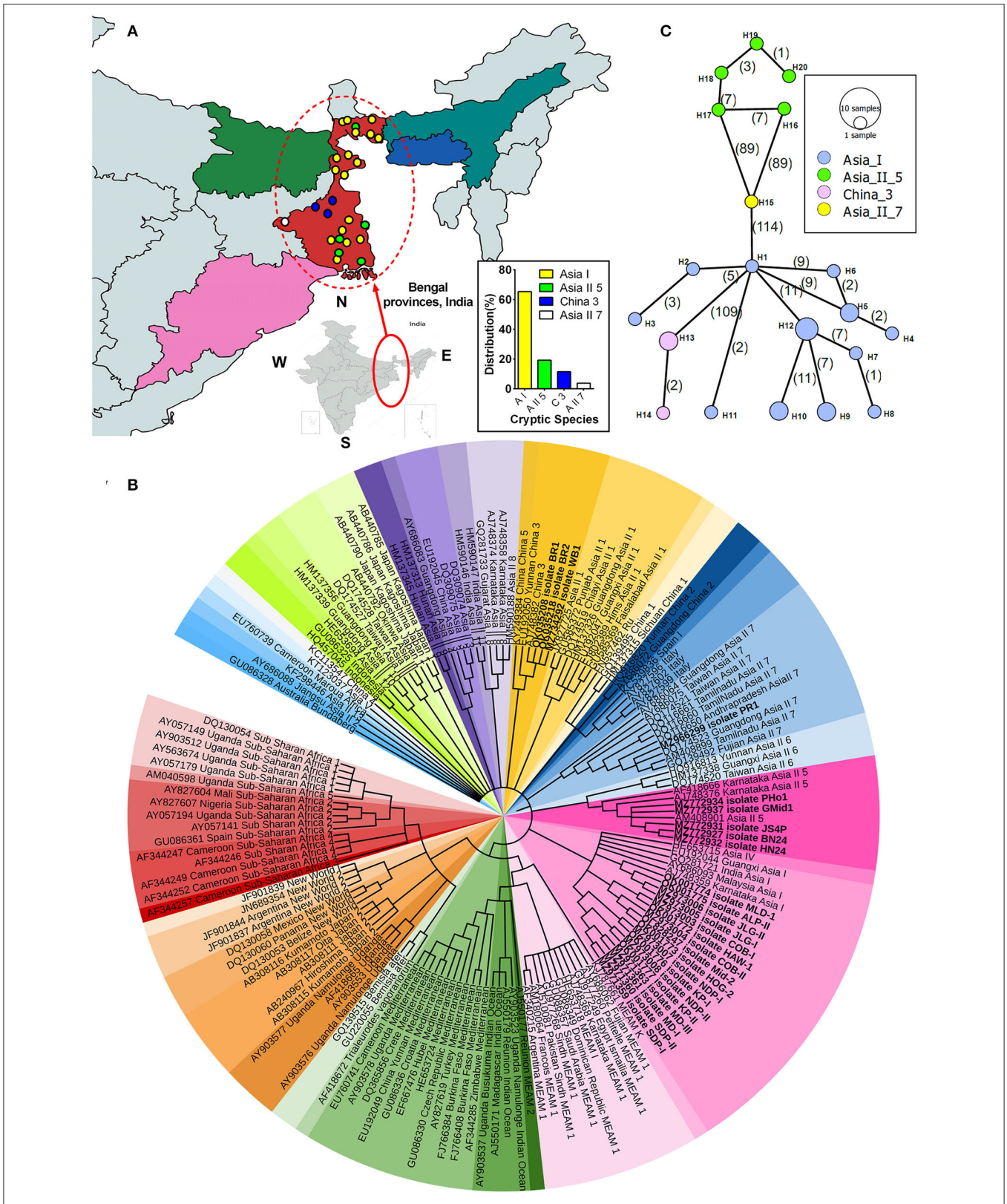

FIGURE 1 | Phylogenetic analysis of whitefly (*Bemisia tabaci*) based on *COI* gene. **(A)** Map indicating different locations of *B. tabaci* sampling and distribution across different genetic groups in Bengal provinces, India. Inset shows the percentage distribution of various cryptic species of *B. tabaci* from collected specimens. **(B)** The

(Continued)

FIGURE 1 | maximum likelihood phylogenetic tree of the *COI* sequences of *Bemisia tabaci* collected from different locations. The bold text *COI* sequences represent collected samples used in this study, and the rest represent reference sequences obtained from the GenBank database. A total of 159 nucleotide sequences were selected to construct the tree, wherein *Bemisia afer* and *Trialeurodes vaporariorom* were taken as an out-group. Different color sheds indicate the different cryptic species of whitefly distributed worldwide. Hasegawa-Kishnio-Yano HKY850 model and gamma distribution rate of variation among sites were implemented to construct the phylogenetic tree in MEGA X. **(C)** Minimum spanning network of different *B. tabaci* cryptic species haplotypes from the studied samples. The four different colors indicate the haplotype of *B. tabaci* cryptic species. Each circle represents a unique haplotype, the frequency of which is proportional to the diameter of the circle. The number of mutations is represented by numbers in parenthesis.

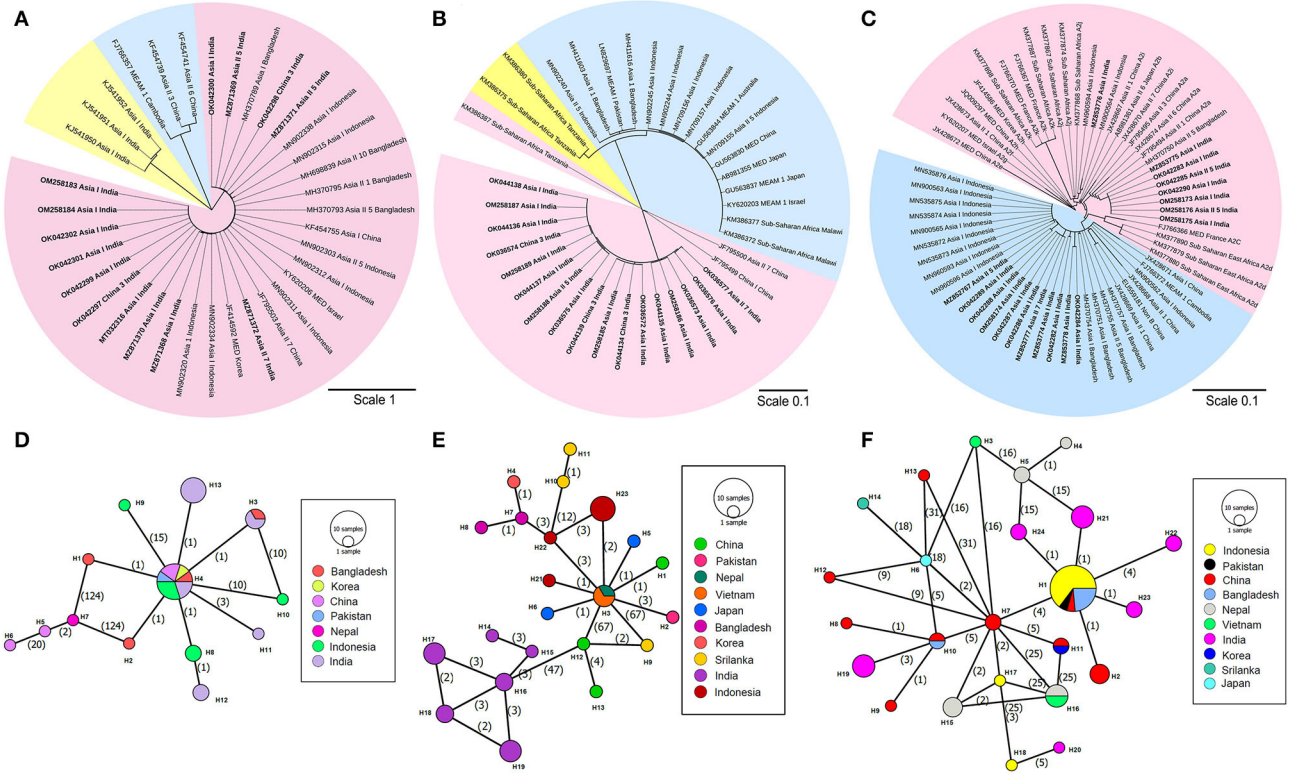

FIGURE 2 | Phylogenetic tree and network analysis of secondary endosymbiont based on 16S rDNA (*Wolbachia* and *Rickettsia*) and 23S rDNA (*Arsenophonus*) gene segments. **(A)** The maximum likelihood phylogenetic tree of the 16S rDNA sequences of *Wolbachia* sp. infecting different whitefly populations. Different color shades indicate the subgroup of *Wolbachia* species (W1 subgroup-pink shade, W2 subgroup-blue shade, W3 subgroup-yellow shade) distributed worldwide. **(B)** The maximum likelihood phylogenetic tree of the 16S rDNA sequences of *Rickettsia* sp. infecting different whitefly populations. Different color shades indicate the subgroup of *Rickettsia* species (R1 subgroup-blue shade, R2 subgroup-yellow shade, and R3 subgroup-pink shade) distributed worldwide. **(C)** The maximum likelihood phylogenetic tree of the 23S rDNA sequences of *Arsenophonus* sp. infecting different whitefly populations. Different color shades indicate the subgroup of *Arsenophonus* species (A1 subgroup-blue shade and A2 subgroup-pink shade) distributed worldwide. Hasegawa-Kishnio-Yano HKY850 model and gamma distribution rate of variation among sites were implemented to construct all the phylogenetic trees in MEGA X. Minimum spanning network of different *Wolbachia* species **(D)**, *Rickettsia* species **(E)**, and *Arsenophonus* species **(F)** present in collected whitefly samples from India and other Asian countries. The different colors indicate the haplotype of each species. Each circle represents a unique haplotype, the frequency of which is proportional to the diameter of the circle. The number of mutations is represented by numbers in parenthesis.

in Asia I, Asia II 5, and Asia II 7 population but not in China 3 population, with Asia I bearing the highest infection rate (**Supplementary Table S8**).

Furthermore, based on the criterion of Kanakala and Ghanim (2019), the secondary endosymbionts were classified at the subgroup level. The phylogenetic tree analysis revealed the presence of only one subgroup of *Wolbachia* (W1) and one subgroup of *Rickettsia* (R3) that infected all the four cryptic whitefly species (**Figures 2A,B**, respectively). The phylogenetic tree also revealed the presence of two subgroups of *Arsenophonus*: A1 and A2 (**Figure 2C**). The infection rate of A1 was always higher than A2 in Asia I population, which was in contrast to Asia II 5 population, where A2 was higher. The infection rate of *Wolbachia* was 40–100%, with the highest rate occurring in Asia II 7 and China 3 populations. The infection rate of *Rickettsia* was the highest in China 3 and Asia II 7 populations, followed by Asia I and Asia II 5 populations, respectively. Thus, as observed, all the whitefly individuals were infected with the variable combinations of the three secondary endosymbionts (**Supplementary Table S9**).

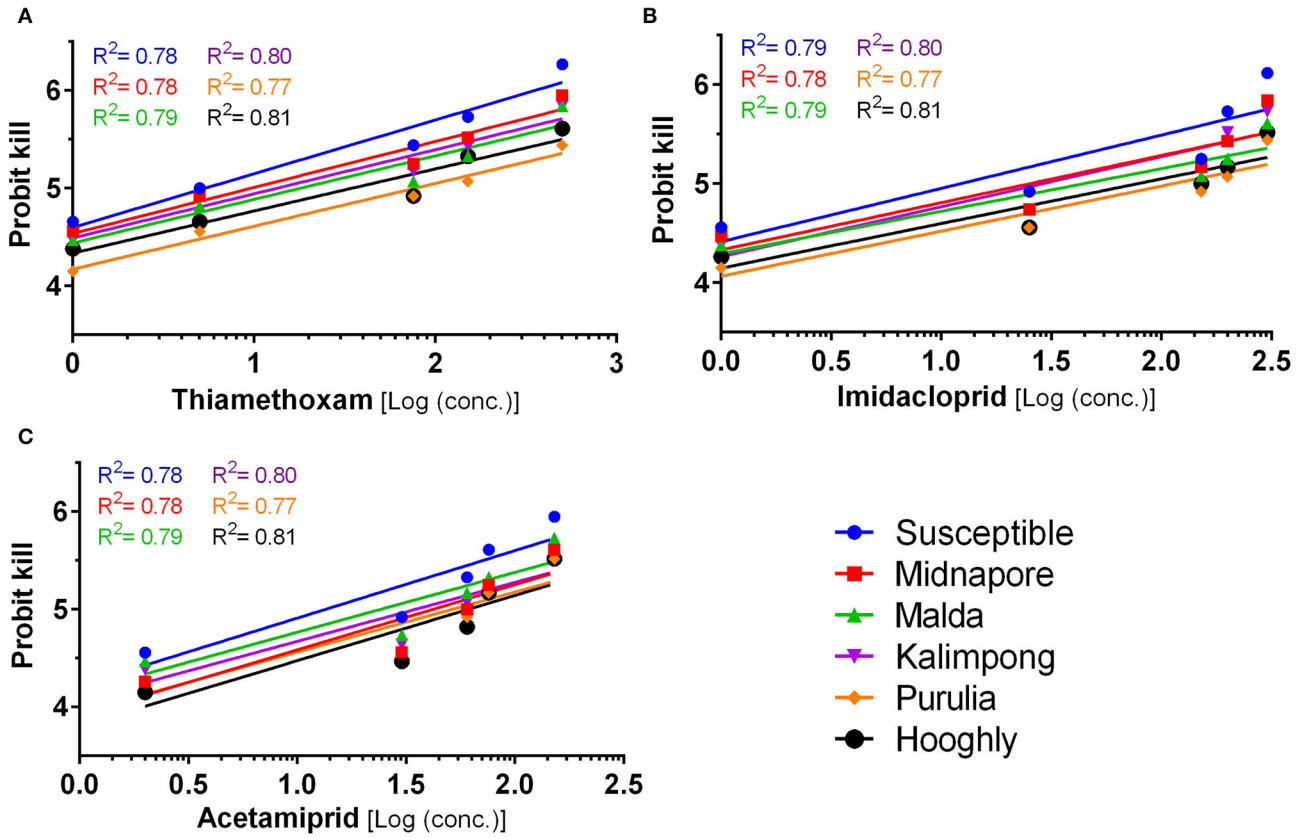

FIGURE 3 | Mortality response of whitefly (*Bemisia tabaci*) population to insecticides. Increasing concentrations of three insecticides, thiamethoxam **(A)**, imidacloprid **(B)**, and acetamiprid **(C)** was tested against different populations of whitefly labeled with separately colored lines, as marked in the legend to analyse the mortality response. The *X*-axis represents the logarithmic dose of every insecticide concentration tested, while the *Y*-axis represents the probit kill values. The straight line represents the best fitting probit regression line between insecticide log dose and mortality probits (working probits) for adult whitefly. The R^2 of each individual line in the graphs represents the regression coefficient. Slopes of the lines are given in **Supplementary Table S11**.

Comparative Network Analysis Revealed a Close Relationship Between the Symbiont Haplotypes

In the current study, an intriguing facet was to comprehend the genetic variation of secondary symbionts with that of the symbionts in other whitefly species complex. This is anticipated to further assist in the discovery of the population demography of whitefly and the relationship between different sub-populations. The haplotype diversity and nucleotide diversity of *Wolbachia* in our collected samples were 0.803 and 0.006, respectively (**Supplementary Table S10**), which further diversified into five different haplotypes (**Figure 2D**). On the other hand, the neutrality test revealed the haplotype and nucleotide diversity of *Rickettsia* to be 0.879 and 0.003, respectively, with the presence of six haplotypes (**Figure 2E**). Subsequently, the presence of six haplotypes was observed among the *Arsenophonus* sequences: the A2 subgroup of *Arsenophonus* had only two haplotypes, and the A1 subgroup consisted of four haplotypes (**Figure 2F**). Interestingly, the network analysis also revealed a considerable overlap among the symbiont haplotypes from different Asian countries, sometimes with a little variation.

The demographic history when analyzed using Fu and Li's D^*, Fu and Li's F^*, and Tajima's D tests, each returned a positive value for the sequences of *Arsenophonus* and *Rickettsia* (interpreted as a sudden population contraction) used in the current study, but since the value was not significant, the null hypothesis regarding the neutrality of the population is accepted. However, Tajima's D test statistic showed a negative but non-significant value for *Wolbachia* specimens. Overall, the Tajima's D values were negative but not significant in all the symbionts outside India. As a test for a recent population expansion, the mismatch distribution analysis indicated a non-significant multimodal distribution for the genes of three endosymbiotic bacteria. However, the distribution observed was higher than the expected one.

Bioassay Studies Indicate Variation in Toxicity of Selected Neonicotinoids Toward *B. tabaci* Field Population

The susceptibility of six whitefly populations has been evaluated against three different insecticides, namely, thiamethoxam, imidacloprid, and acetamiprid (**Figure 3**). The results (detailed

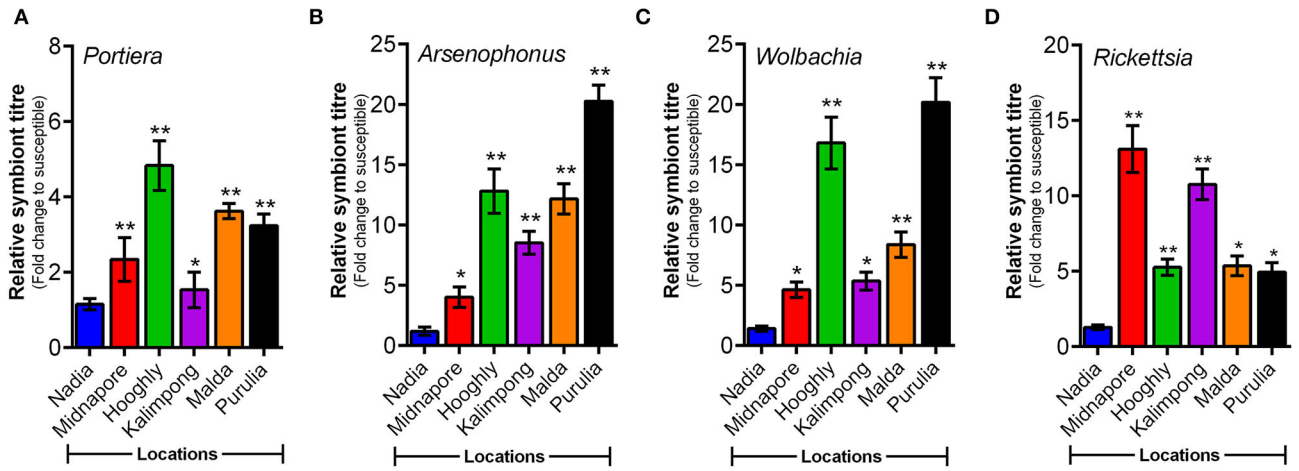

FIGURE 4 | Relative titer of endosymbiotic bacteria (normalized to the whitefly's nuclear β-actin gene) in different whitefly populations as quantified by qPCR. Titer of four endosymbiotic bacteria (*Portiera*, *Arsenophonus*, *Wolbachia,* and *Rickettsia*) in whitefly populations (as listed along the X-axes). **(A)** *Portiera*, **(B)** *Arsenophonus*, **(C)** *Wolbachia*, and **(D)** *Rickettsia.* Values represent mean ± SE values for three independent replicates. Statistical significance of the experimental sets as compared to the susceptible population has been marked with ***$p \leq 0.0001$, **$p \leq 0.001$, and *$p \leq 0.01$.

in **Supplementary Table S11**) indicate that the toxicity (LC_{50}) level varies between 5.36 and 52.14 mg/L for thiamethoxam, 12.87 and 112.09 mg/L for imidacloprid, and 13.49 and 60.04 mg/L for acetamiprid, signifying the varying susceptibility of these populations toward the neonicotinoid group of insecticides. Based on the LC_{50} value of the susceptible laboratory population, thiamethoxam (LC_{50} = 5.36 mg/L) was found to be the most toxic, followed by imidacloprid (12.87 mg/L) and acetamiprid (13.49 mg/L). The populations belonging to Midnapore and Kalimpong exhibited a similar toxicity trend against these insecticides (detailed in **Supplementary Table S11**). On the contrary, populations from Hooghly, Malda, and Purulia followed a slightly different trend, wherein the highest toxicity was observed in the case of thiamethoxam, followed by acetamiprid (LC_{50} = 60.04, 24.37, and 52.23 mg/L) and imidacloprid (LC_{50} = 77.79, 44.53, and 112.09 mg/L, respectively) (detailed in **Supplementary Table S11**).

On comparing the susceptibility of different populations against an insecticide, the data indicated that the resistance ratio (RR value) is in the range of 1.00–9.73, 1.00–8.71, and 1.00–4.45 for thiamethoxam, imidacloprid, and acetamiprid, respectively (**Supplementary Table S11**). The maximum RR value for thiamethoxam was recorded in the population of Purulia (9.73), where the lowest (1 ppm) and highest (300 ppm) tested concentration resulted in the working probit kill of 4.15 and 5.44, respectively. On the other hand, susceptible (Nadia population) working probit kill was 4.66 and 6.27, respectively, for the same concentrations (**Figure 3A**). Toxicity comparison with the laboratory population for imidacloprid indicated the highest RR value (8.71) for the Purulia population (**Supplementary Table S11**). The population of Purulia showed working probit kill values of 4.15 and 5.44 for the lowest (2 ppm) and highest (450 ppm) test concentrations of imidacloprid, respectively, whereas the susceptible population (Nadia) showed working probit kill values of 4.56 and 6.12, respectively (**Figure 3B**). In the case of acetamiprid, the maximum RR value (4.45) was observed in the Hooghly population (**Supplementary Table S11**), wherein the lowest (4 ppm) and highest (400 ppm) tested concentrations resulted in a working probit kill of 4.15 and 5.52 (**Figure 3C**), respectively. Based on the guidelines by World Health Organization (2016) and studies by Mazzarri and Georghiou, 1995 and Yi et al., 2020, the resistance to thiamethoxam and imidacloprid can be considered to exist at a moderate level (i.e., 8.7–9.7), while resistance to acetamiprid was comparatively lower (i.e., 4.45).

Therefore, the bioassay study indicates that the whitefly population from Purulia and Hooghly, consisting of Asia II 7 and Asia II 5 cryptic species populations, respectively, have developed maximum resistance toward the selected neonicotinoids (**Supplementary Table S3**).

Relative Titer of *Arsenophonus* and *Wolbachia* Correlated With Resistance Ratio of Three Neonicotinoid Insecticides

A comparative study involving symbiont titres in different field populations of whitefly revealed varying patterns in their quantitative analysis. The relative titer of P-symbiont (*Portiera*) differed significantly among the experimental whitefly population. Significantly higher members of *Portiera* were observed in the population of Hooghly, followed by the population of Malda and Purulia when compared to the susceptible reference population (Nadia) (**Figure 4A**). The results also revealed varying patterns in titer level of S-endosymbionts, that is, *Arsenophonus*, *Wolbachia,* and *Rickettsia*. A significantly higher abundance of *Arsenophonus* and *Wolbachia* was observed in the population of Purulia, followed by the population of Hooghly and Malda when compared to the reference population

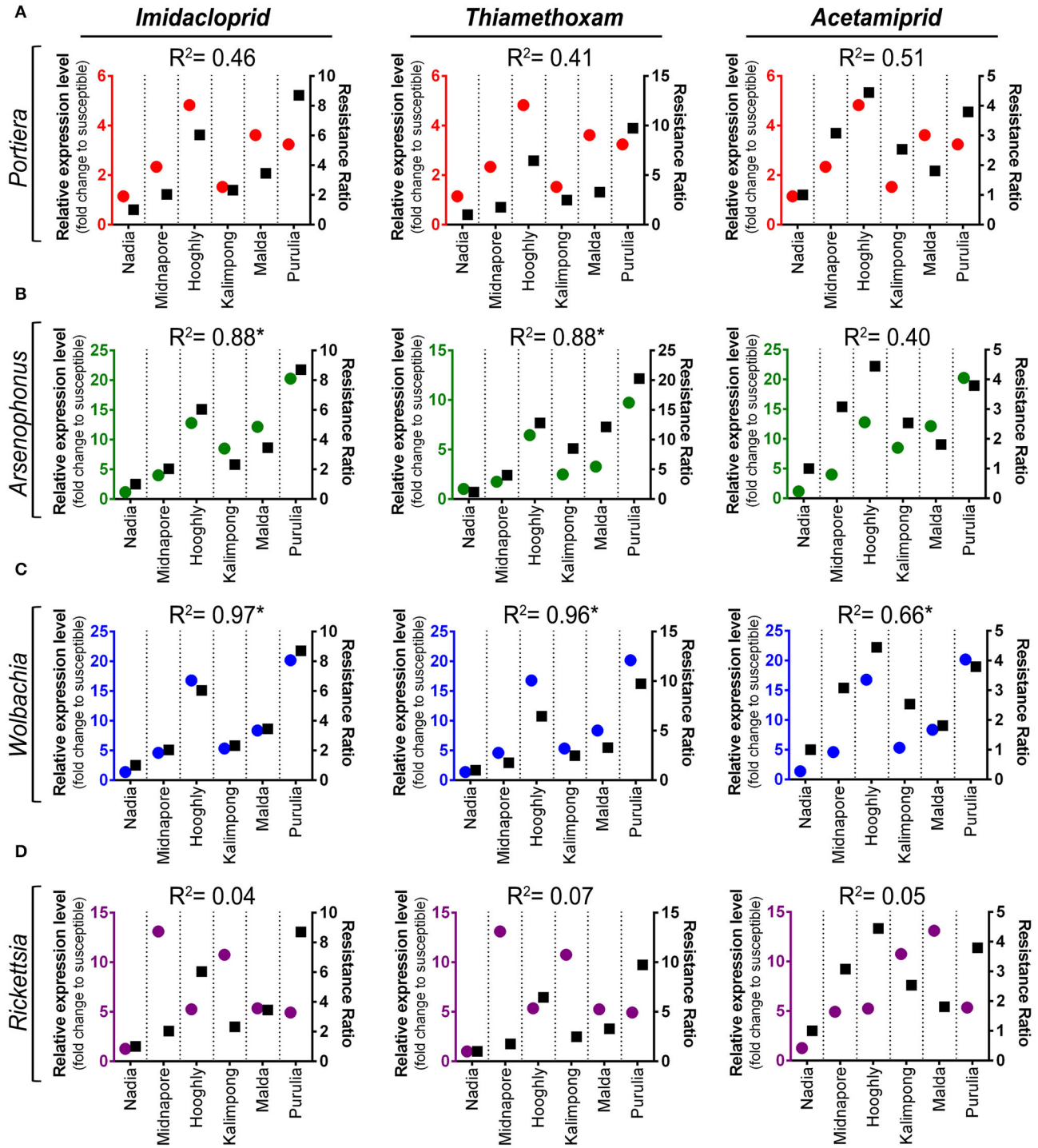

FIGURE 5 | Linear regression analysis between insecticides resistance level and relative symbiont titer of different whitefly populations. Linear regression analysis was used to test for a functional relationship between the resistance level of each insecticide (imidacloprid, thiamethoxam, and acetamiprid) and the mean normalized expression value of each symbiotic bacteria in different whitefly populations: **(A)** *Portiera*, **(B)** *Arsenophonus*, **(C)** *Wolbachia*, and **(D)** *Rickettsia*. Circles in each graph represent the relative titer of each symbiont (marked on the left *Y*-axis), while squares depict the resistance ratio of each insecticide (labeled on the right *Y*-axis).

(**Figures 4B,C**). Contrary to the other symbionts, the maximum titer of *Rickettsia* was observed in the population of Midnapore and Kalimpong (**Figure 4D**).

The correlation coefficient between resistance ratio (RR) values of whitefly field population and relative abundance of symbiont titer is presented in **Figures 5A–D**. The titer

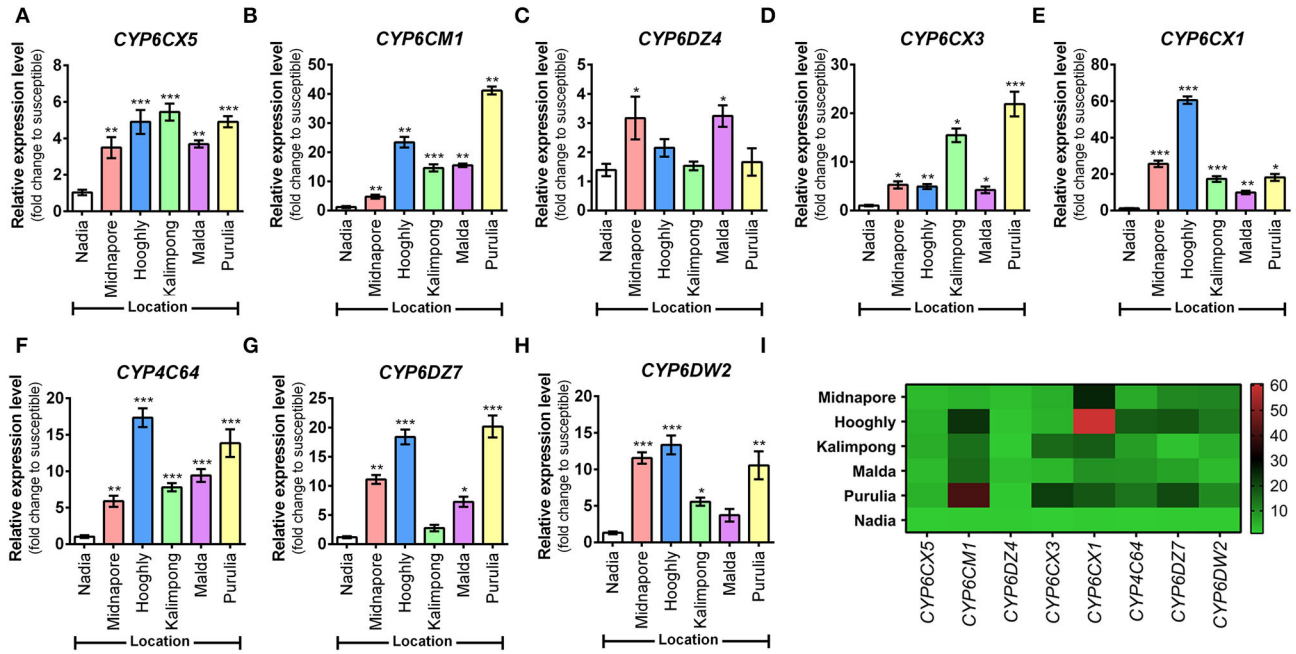

FIGURE 6 | Expression analysis of different cytochrome P450 genes in whitefly (*Bemisia tabaci*) population. Expression profiles of eight P450 genes governing insecticide resistance in whitefly populations (as listed along the *X*-axes). **(A)** CYP6CX5, **(B)** CYP6CM1, **(C)** CYP6DZ4, **(D)** CYP6CX3, **(E)** CYP6CX1, **(F)** CYP4C64, **(G)** CYP6DZ7, and **(H)** CYP6DW2. Relative gene expression was measured by qRT-PCR analysis. Nuclear β-actin has been used as the internal control. The Ct values for tested genes were normalized to the Ct value of actin and calculated relative to a calibrator using the formula $2^{-\Delta\Delta Ct}$. Values represent mean ± SE for three independent replicates. Statistical significance of the experimental sets as compared to the susceptible population has been marked with $^{***}p \leq 0.0001$, $^{**}p \leq 0.001$, and $^{*}p < 0.01$. **(I)** Heatmap represents an overview of the expression level of each gene in a variable whitefly population, with the color gradient provided alongside. Gene expression profiles are represented as a relative expression when compared to the susceptible population, obtained from the qRT-PCR experiment.

level of *Arsenophonus* was significantly correlated with RR of imidacloprid and thiamethoxam, with correlation coefficients of 0.88 ($p = 0.005$) and 0.88 ($p = 0.006$), respectively (**Figure 5B**). Moreover, the resistant ratio of all the three neonicotinoids exhibited a positive correlation with the titer level of *Wolbachia*. The correlation coefficients were 0.97 ($p = <0.001$) for imidacloprid, 0.96 ($p = <0.001$) for thiamethoxam, and 0.65 ($p = 0.050$) for acetamiprid, respectively (**Figure 5C**). The titer level of *Portiera* shows positive but no significant relation with RR among all the treated insecticides.

Upregulation of CYP6DZ7 and CYP4C64 Genes Correlated Well With Resistance Ratio of Neonicotinoid Insecticides

The expression of eight cytochrome P450 genes was compared among five whitefly populations against the susceptible reference population (Nadia), wherein upregulation of all the eight genes was noted at varying degrees. In the case of CYP6CX5, Kalimpong, Purulia, and Hooghly populations showed maximum upregulation (4–5-fold), followed by Malda and Midnapore populations that depicted a 3-fold upregulation (**Figure 6A**). Subsequently, for the CYP6CM1 transcript level, the Purulia population exhibited the highest upregulation (41-fold), followed by Hooghly (23-fold) and Malda (15-fold) (**Figure 6B**). The relative expression of CYP6DZ4 was low in all the populations, with maximum expression observed in the Malda population (3-fold) (**Figure 6C**). Next, for the CYP6CX3 transcript level, the Purulia population exhibited the highest upregulation (21-fold), followed by Kalimpong (15-fold) and Midnapore (5-fold) (**Figure 6D**). Both CYP6CX1 and CYP4C64 transcript levels were maximum for the Hooghly population, with an increase of 60-fold and 17-fold, respectively (**Figures 6E,F**). Lastly, the relative expression of CYP6DZ7 and CYP6DW2 was moderately high in the population of Purulia and Hooghly (20-fold and 18-fold; 10-fold and 13-fold, respectively) (**Figures 6G,H**). Overall, the results show that Purulia and Hooghly populations harbored maximally upregulated insecticide resistance P450 genes.

The correlation coefficient between RR values of the whitefly field population and the relative expression of detoxifying genes (P450s) is presented in **Figures 7A–H**. The expression level of CYP6CM1 significantly correlated with the RR of imidacloprid and thiamethoxam. The correlation coefficients were 0.94 ($p = 0.012$) and 0.95 ($p = <0.001$), respectively (**Figure 7B**). The expression level of both CYP6CX1 and CYP6DW2 genes was positively correlated with the RR of acetamiprid ($R^2 = 0.72$, $p = 0.030$; $R^2 = 0.91$, $p = 0.003$) (**Figures 7E,H**).

Taking together, the RR of all the tested neonicotinoids exhibited a positive correlation with the transcript levels of CYP4C64 and CYP6DZ7 genes (**Figures 7F,G**). The correlation

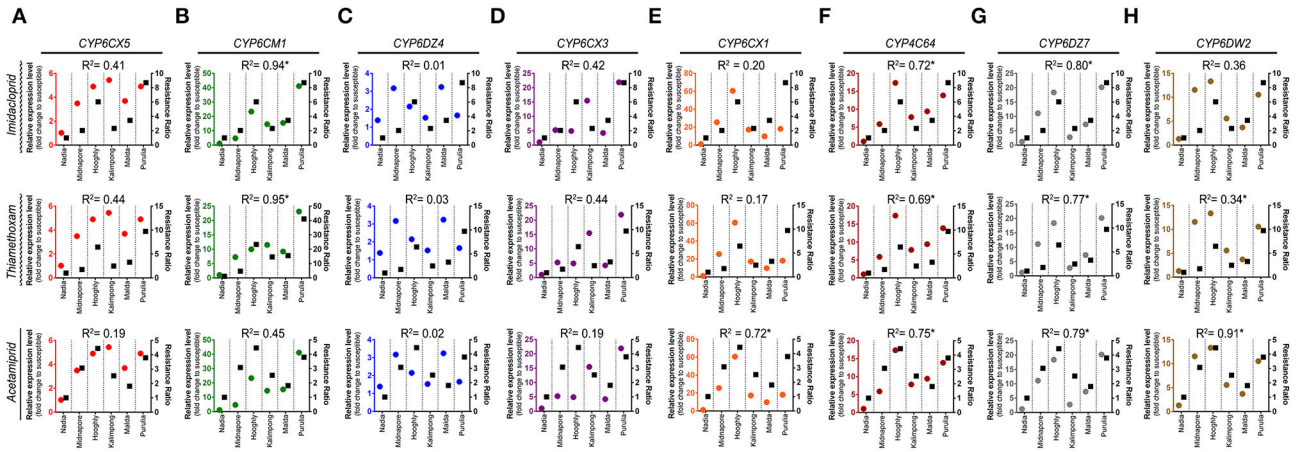

FIGURE 7 | Linear regression analysis between insecticide resistance level and relative expression of insecticide resistance genes (P450s). Linear regression analysis was used to test for a functional relationship between the resistance level of each insecticide (imidacloprid, thiamethoxam, and acetamiprid) and the mean normalized expression value of each P450s gene in different whitefly populations: **(A)** CYP6CX5, **(B)** CYP6CM1, **(C)** CYP6DZ4, **(D)** CYP6CX3, **(E)** CYP6CX1, **(F)** CYP4C64, **(G)** CYP6DZ7, and **(H)** CYP6DW2. Circles in each graph represent the gene expression values (marked on the left *Y*-axis), while squares depict the resistance ratio of each insecticide (labeled on the right *Y*-axis).

coefficients were 0.72 ($p = 0.030$) and 0.80 ($p = 0.015$) for imidacloprid, 0.69 ($p = 0.030$) and 0.77 ($p = 0.020$) for thiamethoxam, and 0.75 ($p = 0.020$) and 0.79 ($p = 0.010$) for acetamiprid, respectively.

DISCUSSION

"Species concept" has been one of the most controversial concepts in biology consistently. This statement holds true for *B. tabaci,* as it is recognized as a complex of cryptic species that are morphologically indistinguishable from one another but genetically diverse (Firdaus et al., 2013; Hadjistylli et al., 2016). The Indian region exhibits an enormous diversity of *B. tabaci* with the presence of 10 cryptic species among the 46 species recorded so far (Rehman et al., 2021). The vast array of genetic groups not only specialize in host plant preference, but also exhibit a diverse dispersal pattern and differential response to pesticides (Pashley et al., 1992; Adamczyk et al., 1997; Barman et al., 2022). In this regard, precise assessment of the genetic identity and insecticide resistance properties is imperative for the development of control strategies.

An extensive survey of whitefly across different regions of Bengal province in India revealed that the pair-wise genetic variation reached up to 20.80%, and the species complex was further diversified into four cryptic species, namely, Asia I, Asia II 5, Asia II 7, and China 3. Of all the reported four genetic groups, Asia I was found to be the major group in the collected whitefly samples. This group was previously reported to be prevalent across Asian countries, including Pakistan, Bangladesh, Malaysia, Singapore, Indonesia, and Cambodia (Dinsdale et al., 2010; Götz and Winter, 2016; Kanakala and Ghanim, 2019). The Asia II cryptic whitefly species is a genetically diverse group consisting of 13 cryptic species, namely, Asia II (1–13) (Kanakala and Ghanim, 2019). Among them, the genetic groups of only Asia II 5 and Asia II 7 were detected in the collected whitefly samples spanning across the Bengal province. Previous reports suggest that Asia II 5 was majorly prevalent in the South Asian countries like Bangladesh, Pakistan, and Nepal (Islam et al., 2018; Khatun et al., 2018; Acharya et al., 2020). In the survey conducted, Asia II 5 was found to be majorly distributed along the southern part of Bengal and associated with a single host crop, that is, eggplant. From a geographical point of view, the close proximity of Bangladesh and Bengal provinces of India might have paved a way for the rapid dispersion of this particular genetic group in India. On the other hand, Asia II 7 was specifically identified in one region, Bagmundi, Purulia, indicating that this cryptic species did not undergo rampant dispersion. The distribution of China 3 was also restricted to only the Birbhum region of Bengal, aligning with the reports of Ellango et al. (2015). Despite the extensive survey, this genetic group did not extend its distribution until now. Keeping in mind the rampant distribution of different cryptic species along with the prevalence of suitable hosts, *B. tabaci* has a high chance of developing adaptive advantage in different regions of the country.

Management of whiteflies is a grave task for farmers and scientists all around the globe, with chemical pesticides being the primary strategy in diverse agricultural systems. After gradual replacement with different groups of insecticides, the neonicotinoids, particularly imidacloprid, are extensively used against *B. tabaci* (Nauen and Denholm, 2005; Barman et al., 2021). Existing field problems, such as poor selection of insecticides and sub-standard application techniques, result in control failures of insecticides against this pest (Peshin and Zhang, 2014; Wang et al., 2020). Several global studies have highlighted the development of resistance in different whitefly populations to different groups of insecticides (Zhao et al., 2020). However, the occurrence of different cryptic forms makes the task further complex due to differential responses

to insecticides. Furthermore, the increasing level of resistance observed in the whitefly population and the rapid evolution of insecticide resistance genes are also a matter of concern. Nonetheless, literature focusing on the susceptibility/resistance status of the whitefly population to insecticides in India is also limited. In this regard, field populations of whitefly surveyed from different geographical locations were tested for their susceptibilities to three commonly used neonicotinoids in these regions. The results revealed that among the three studied insecticides (thiamethoxam, imidacloprid, and acetamiprid), the high susceptibility of the population was recorded toward thiamethoxam. Variation in susceptibility status across different regions can be attributed to the prevalence of different genetic groups. The study data show that the whitefly population from Purulia and Hooghly, comprising Asia II 7 and Asia II 5 cryptic species, recorded higher resistance toward these novel compounds. Several global studies have documented resistance in *B. tabaci* MED and MEAM 1 genetic groups to different groups of insecticides across the continent (Whalon et al., 2013). However, there is limited literature available on the insecticide status of indigenous *B. tabaci* genetic groups in Asia. This study clearly provides the insecticide resistance/susceptibility status of Asian genetic groups like Asia I, Asia II 5, and Asia II 7 against the selected neonicotinoid compounds. As insecticide resistance is regarded by some workers as a major driving force for the selection and establishment of specific *B. tabaci* genetic groups in a region (Horowitz et al., 2005; Barman et al., 2021), there is a need for regular monitoring of insecticide resistance status in diverse *B. tabaci* genetic groups across India. Results from the present survey indicate the dominance of Asia I groups in most of the regions, with Asia II 5 ranking second on the basis of abundance. What is evident in the coming times is that if Asia II 5 or Asia II 7 becomes dominant in these regions, management using neonicotinoids would eventually become difficult. Therefore, further studies were carried out for unraveling the basis of insecticide resistance in different *B. tabaci* field populations, which is necessary for the future management of this pest.

Furthermore, endosymbionts also have an important role to play in protecting their hosts from different environmental stressors, including insecticides (Bhatt et al., 2021). This symbiont-mediated insecticide resistance or susceptibility is highly variable and depends on the species of symbiont and the chemical compound (Liu and Guo, 2019). Hence, the work further focussed on bacterial endosymbiont communities which infect different *B. tabaci* populations across a wide geographical range to gain a detailed understanding of the endosymbiont diversity and their association with insecticide resistance. The profiles of endosymbionts within the different whitefly genetic groups were highly variable. A significant positive association of *Wolbachia* titer was observed with the resistance level of the three test insecticides (imidacloprid, thiamethoxam, and acetamiprid) in different whitefly field populations. Earlier reports opined that the presence of *Wolbachia* increased the resistance of whiteflies to neonicotinoids, such as acetamiprid (Ghanim and Kontsedalov, 2009). On the other hand, *Arsenophonus* also correlated well with the resistance levels of imidacloprid and thiamethoxam. Although the co-existence of *Arsenophonus* with *Rickettsia* symbiont was reported to confer resistance to acetamiprid (Kontsedalov et al., 2008), no such significant correlation between *Rickettsia* titer and insecticide resistance level in whitefly was noted. Such a difference in symbiont performance can be attributed to symbiont species, host genotype, and co-infection with other symbionts (Ghanim and Kontsedalov, 2009; Hoffmann et al., 2015). The network analysis used to compare the genetic variation of secondary symbionts (study samples) with other Asian countries revealed considerable overlap between the haplotypes (Indonesia, Korea, China, Bangladesh, and Pakistan), sometimes with a little variation. These results are clearly suggestive of the fact that the symbionts of whitefly are effectively isolated from other locations and might be in the process of genetic divergence. In contrast, there appear to be significant interactions between the whitefly populations and other distant countries despite the stretches of kilometers between them. The mixing of whitefly populations seems unavoidable due to the migration of nymphs that can occur up to 7 km (Byrne et al., 1996). Hence, this is a source of concern, as it raises the possibility of resistance build up in whiteflies of other countries as well, provided the symbiont dynamics remain the same.

Overexpression and modification of gene encoding members of cytochrome P450, carboxylesterases, and glutathione S-transferases (GSTs) are associated with resistance to different groups of insecticides (Li et al., 2007). In the current study, expression of both *CYP6DZ7* and *CYP4C64* showed a good correlation with the resistance level of imidacloprid, thiamethoxam, and acetamiprid in different whitefly field populations. According to previous reports, expression of *CYP4C64* positively correlated with imidacloprid resistance in whitefly; however, no such correlation was recorded in *CYP6DZ7* (Yang et al., 2013). Possibly, the expression of *CYP6DZ7* imparts resistance to imidacloprid in some whitefly field populations but not in others. As reported by Zhuang et al. (2011), *CYP6CX1* is involved in imidacloprid resistance in both laboratory and field populations of whitefly. Present results revealed a direct correlation of *CYP6CX1* with acetamiprid resistance. Based on the current and previous studies, it can be presumed that *CYP6CX1* is an important gene in conferring resistance to whitefly against several neonicotinoid compounds. Moreover, similar to earlier reports, *CYP6CM1* expression also correlated absolutely well with the resistance level of imidacloprid and thiamethoxam. Therefore, multiple symbiotic interactions with varying gene expression patterns might govern the differential susceptibility of the whitefly population against different test insecticides.

Assembling together all these pieces of information, this research article provides an in-depth notion of the current scenario of different whitefly cryptic species and their susceptibility status toward the selected neonicotinoids. The study further dwells on the infection patterns and role of endosymbionts in imparting insecticide resistance. Studies of symbiont-mediated resistance could provide an interesting prospect to determine biological phenomenona with implications that may extend beyond entomological research and further contribute to a greater understanding of bioremediation,

human–microbiome interactions, pharmacology, etc. The use of neonicotinoid group of insecticides is employed as a major strategy for controlling insects like whiteflies; however, the deep-rooted negative environmental effects of neonicotinoids call for serious attention to some alternative management techniques for this pest. With further development, bioaugmentation of detoxifying bacteria could possibly serve to reduce pesticide residuals in the environment, henceforth improving the health of the ecosystem while eliminating the deleterious effects of these pesticides.

Furthermore, an understanding of different P450 genes and their positive correlation with insecticide resistance in different whitefly populations have also been depicted. Nonetheless, the heterogeneity observed in the collected whitefly population indicates toward the differential response it might show toward the management approaches, which is indeed a matter of concern for scientists and farming communities. A few vital questions that arise on our way stem from the basic evolution of symbiont-mediated insecticide resistance and the precise molecular interactions occurring between symbiont and host genes. Possibly through proper clarification of these vital issues, symbiont-targeted pest management will prove to be an effective control component for the future agricultural community. However, detailed basic work needs to be carried out before the large-scale application of symbiont-targeted pest management.

DATA AVAILABILITY STATEMENT

The original contributions presented in the study are included in the article/**Supplementary Material**, further inquiries can be directed to the corresponding author/s.

AUTHOR CONTRIBUTIONS

Conceptualization: MB and SS. Methodology: MB and HT. Original draft preparation and writing—reviewing and editing the manuscript: SS and GU. Validation: MB and GU. Resources: AS and JT. Investigation: JT and SC. All authors have read and agreed to the published version of the manuscript.

ACKNOWLEDGMENTS

The authors thankfully acknowledge Bidhan Chandra Krishi Viswavidyalaya (ICAR-accredited State Agricultural University) for providing the University Research Scholarship to carry out the research work.

SUPPLEMENTARY MATERIAL

The Supplementary Material for this article can be found online at: https://www.frontiersin.org/articles/10.3389/fmicb.2022.901793/full#supplementary-material

REFERENCES

Abbott, W. S. (1925). A method of computing the effectiveness of an insecticide. *J. Econ. Entomol.* 18, 265–267. doi: 10.1093/jee/18.2.265a

Acharya, R., Shrestha, Y. K., Sharma, S. R., and Lee, K. Y. (2020). Genetic diversity and geographic distribution of *Bemisia tabaci* species complex in Nepal. *J. Asia Pac. Entomol.* 23, 509–515. doi: 10.1016/j.aspen.2020.03.014

Adamczyk, J. J., Holloway, J. W., Leonard, B. R., and Graves, J. B. (1997). Susceptibility of fall armyworm collected from different plant hosts to selected insecticides and transgenic *Bt* cotton. *J. Cotton. Sci.* 1, 21–28.

Ahmad, M., Arif, M. I., and Naveed, M. (2010). Dynamics of resistance to organophosphate and carbamate insecticides in the cotton whitefly *Bemisia tabaci* (Hemiptera: Aleyrodidae) from Pakistan. *J. Pest. Sci.* 83, 409–420. doi: 10.1007/s10340-010-0311-8

Alon, M., Alon, F., Nauen, R., and Morin, S. (2008). Organophosphates' resistance in the B-biotype of *Bemisia tabaci* (Hemiptera: Aleyrodidae) is associated with a point mutation in an ace1-type acetylcholinesterase and overexpression of carboxylesterase. *Insect Biochem. Mol. Biol.* 38, 940–949. doi: 10.1016/j.ibmb.2008.07.007

Barman, M., Samanta, S., Chakraborty, S., Samanta, A., and Tarafdar, J. (2022). Copy number variation of two begomovirus acquired and inoculated by different cryptic species of whitefly, *Bemisia tabaci* in Okra. *PLoS ONE* 17:e0265991. doi: 10.1371/journal.pone.0265991

Barman, M., Samanta, S., Thakur, H., Chakraborty, S., Samanta, A., Ghosh, A., et al. (2021). Effect of neonicotinoids on bacterial symbionts and insecticide-resistant gene in whitefly, *Bemisia tabaci*. *Insects* 12, 742. doi: 10.3390/insects12080742

Basij, M., Talebi, K., Ghadamyari, M., Hosseininaveh, V., and Salami, S. A. (2017). Status of resistance of *Bemisia tabaci* (Hemiptera: Aleyrodidae) to neonicotinoids in Iran and detoxification by cytochrome P450-dependent monooxygenases. *Neotrop. Entomol.* 46, 115–124. doi: 10.1007/s13744-016-0437-3

Bhatt, P., Rene, E. R., Huang, Y., Lin, Z., Pang, S., Zhang, W., et al. (2021). Systems biology analysis of pyrethroid biodegradation in bacteria and its effect on the cellular environment of pests and humans. *J. Environ. Chem. Eng.* 9, 106582. doi: 10.1016/j.jece.2021.106582

Bing, X. L., Yang, J., Zchori-Fen, E., Wang, X. W., and Liu, S. S. (2013). Characterization of a newly discovered symbiont of the whitefly *Bemisia tabaci* (Hemiptera Aleyrodidae). *Appl. Environ. Microbiol.* 72, 569–575. doi: 10.1128/AEM.03030-12

Byrne, D. N., Rathman, R. J., Orum, T. V., and Palumbo, J. C. (1996). Localized migration and dispersal by the sweet potato whitefly, *Bemisia tabaci*. *Oecologia* 105, 320–328. doi: 10.1007/BF00328734

Chiel, E., Gottlieb, Y., Zchori-Fein, E., Mozes-Daube, N., Katzir, N., Inbar, M., et al. (2007). Biotype-dependent secondary symbiont communities in sympatric populations of *Bemisia tabaci*. *Bull. Entomol. Res.* 97, 407–413. doi: 10.1017/S0007485307005159

Daborn, P., Boundy, S., Yen, J., Pittendrigh, B., and ffrench-Constant, R. (2001). DDT resistance in Drosophila correlates with Cyp6g1 over-expression and confers cross-resistance to the neonicotinoid imidacloprid. *Mol. Genet. Genom.* 266, 556–563. doi: 10.1007/s004380100531

De Barro, P. J., Liu, S. S., Boykin, L. M., and Dinsdale, A. B. (2011). *Bemisia tabaci*: a statement of species status. *Annu. Rev. Entomol.* 56, 1–19. doi: 10.1146/annurev-ento-112408-085504

Dinsdale, A., Cook, L., Riginos, C., Buckley, Y. M., and De Barro, P. (2010). Refined global analysis of *Bemisia tabaci* (Hemiptera: Sternorrhyncha: Aleyrodoidea: Aleyrodidae) mitochondrial cytochrome oxidase 1 to identify species level genetic boundaries. *Ann. Entomol. Soc. Am.* 103, 196–208. doi: 10.1603/AN09061

Ellango, R., Singh, S. T., Rana, V. S., Gayatri, P. N., Raina, H., Chaubey, R., et al. (2015). Distribution of *Bemisia tabaci* genetic groups in India. *Environ. Entomol.* 44, 1258–1264. doi: 10.1093/ee/nvv062

Elzaki, M. E. A., Miah, M. A., Wu, M., Zhang, H., Pu, J., Jiang, L., et al. (2017). Imidacloprid is degraded by CYP353D1v2, a cytochrome P450 overexpressed

in a resistant strain of *laodelphax striatellus*. *Pest. Manag. Sci.* 73, 1358–1363. doi: 10.1002/ps.4570

Everett, K. D. E., Thao, M. L., Horn, M., Dyszynski, G. E., and Baumann, P. (2005). Novel chlamydiae in whiteflies and scale insects: endosymbionts 'Candidatus Fritschea bemisiae' strain Falk and 'Candidatus Fritschea eriococci' strain Elm. *Int. J. Syst. Evol. Microbiol.* 55, 1581–1587. doi: 10.1099/ijs.0.63454-0

Excofer, L., and Lischer, H. E. L. (2010). Arlequin suite ver 3.5: a new series of programs to perform population genetics analyses under Linux and Windows. *Mol. Ecol. Resour.* 10, 564–567. doi: 10.1111/j.1755-0998.2010.02847.x

Feyereisen, R. (2011). "Insect CYP genes and P450 enzymes," in *Insect Molecular Biology and Biochemistry*, *1st Edn*. ed L. Gilbert (Amsterdam: Elsevier), 115–128. doi: 10.1016/B978-0-12-384747-8.10008-X

Finney, D. J. (1971). *Probit Analysis*. Cambridge: Cambridge University Press, 333.

Firdaus, S., Vosman, B., Hidayati, N., Jaya, S. E. D., G. F., Visser, R., et al. (2013). The *Bemisia tabaci* species complex: additions from different parts of the world. *Insect Sci.* 20, 723–733. doi: 10.1111/1744-7917.12001

Fu, Y. X. (1997). Statistical tests of neutrality of mutations against population growth, hitchhiking and background selection. *Genetics* 147, 915–925. doi: 10.1093/genetics/147.2.915

Garrood, W. T., Zimmer, C. T., Gorman, K. J., Nauen, R., Bass, C., and Davies, T. G. (2016). Field–evolved resistance to imidacloprid and ethiprole in populations of brown planthopper *Nilaparvata lugens* collected from across south and east Asia. *Pest Manag. Sci.* 72, 140–149. doi: 10.1002/ps.3980

Ghanim, M., and Kontsedalov, S. (2009). Susceptibility to insecticides in the Q biotype of *Bemisia tabaci* is correlated with bacterial symbiont densities. *Pest Manag. Sci.* 65, 939–942. doi: 10.1002/ps.1795

Ghosh, S., Bouvaine, S., and Maruthi, M. N. (2015). Prevalence and genetic diversity of endosymbiotic bacteria infecting cassava whiteflies in Africa. *BMC Microbiol.* 15:93. doi: 10.1186/s12866-015-0425-5

Gottlieb, Y., Ghanim, M., Chiel, E., Gerling, D., Portnoy, V., Steinberg, S., et al. (2006). Identification and localization of a Rickettsia sp. in *Bemisia tabaci* (Homoptera: Aleyrodidae). *Appl. Environ. Microbiol.* 72, 3646–3652. doi: 10.1128/AEM.72.5.3646-3652.2006

Götz, M., and Winter, S. (2016). Diversity of *Bemisia tabaci* in Thailand and Vietnam and indications of species replacement. *J. Asia Pac. Entomol.* 19, 537–543. doi: 10.1016/j.aspen.2016.04.017

Hadjistylli, M., Roderick, G. K., and Brown, J. K. (2016). Global population structure of a worldwide pest and virus vector: genetic diversity and population history of the *Bemisia tabaci* sibling species group. *PLoS ONE* 11:e0165105. doi: 10.1371/journal.pone.0165105

Hoffmann, A. A., Ross, P. A., and Rasic, G. (2015). Wolbachia strains for diseases control: ecological and evolutionary considerations. *Evol. Appl.* 8, 751–768. doi: 10.1111/eva.12286

Horowitz, A. R., Kontsedalov, S., Khasdan, V., and Ishaaya, I. (2005). Biotypes B and Q of *Bemisia tabaci* and their relevance to neonicotinoid and pyriproxyfen resistance. *Arch. Insect Biochem. Physiol.* 58, 216–225. doi: 10.1002/arch.20044

Islam, W., Lin, W., Qasim, M., Islam, S. U., Ali, H., Adnan, M., et al. (2018). A nation-wide genetic survey revealed a complex population structure of *Bemisia tabaci* in Pakistan. *Acta Trop.* 183, 119–125. doi: 10.1016/j.actatropica.2018.04.015

Jones, D. R. (2003). Plant viruses transmitted by whiteflies. *Eur. J. Plant Pathol.* 109, 195–219. doi: 10.1023/A:1022846630513

Kanakala, S., and Ghanim, M. (2019). Global genetic diversity and geographical distribution of *Bemisia tabaci* and its bacterial endosymbionts. *PLoS ONE* 14:e0213946. doi: 10.1371/journal.pone.0213946

Karunker, I., Benting, J., and Lueke, B. (2008). Over-expression of cytochrome P450 CYP6CM1 is associated with high resistance to imidacloprid in the B and Q biotypes of *Bemisia tabaci* (Hemiptera: Aleyrodidae). *Insect Biochem. Mol. Biol.* 38, 634–644 doi: 10.1016/j.ibmb.2008.03.008

Khatun, M. F., Jahan, S. H., Lee, S., and Lee, K. Y. (2018). Genetic diversity and geographic distribution of the *Bemisia tabaci* species complex in Bangladesh. *Acta Trop.* 187, 28–36. doi: 10.1016/j.actatropica.2018.07.021

Kimura, M. (1980). A simple method for estimating evolutionary rates of base substitutions through comparative studies of nucleotide sequences. *J. Mol. Evol.* 16, 111–120. doi: 10.1007/BF01731581

Kontsedalov, S., Zchori-Fein, E., Chiel, E., Gottlieb, Y., Inbar, M., and Ghanim, M. (2008). The presence of Rickettsia is associated with increased susceptibility of *Bemisia tabaci* (Homoptera: Aleyrodidae) to insecticides. *Pest Manag. Sci.* 64, 789–792. doi: 10.1002/ps.1595

Kranthi, K. R., Jadhav, D. R., Kranthi, S., Wanjari, R. R., Ali, S. S., and Russell, D. A. (2002). Insecticide resistance in five major insect pests of cotton in India. *Crop Prot.* 21, 449–460. doi: 10.1016/S0261-2194(01)00131-4

Kumar, S., Stecher, G., Li, M., Knyaz, C., and Tamura, K. (2018). MEGA X: molecular evolutionary genetics analysis across computing platforms. *Mol. Biol. Evol.* 6, 1547–1549. doi: 10.1093/molbev/msy096

Lestari, S. M., Hidayat, P., Hidayat, S. H., Shim, J. K., and Lee, K. Y. (2021). *Bemisia tabaci* in Java, Indonesia: genetic diversity and the relationship with secondary endosymbiotic bacteria. *Symbiosis* 83, 317–333. doi: 10.1007/s13199-021-00752-w

Li, X. C., Schuler, M. A., and Berenbaum, M. R. (2007). Molecular mechanisms of metabolic resistance to synthetic and natural xenobiotics. *Annu. Rev. Entomol.* 52, 231–253. doi: 10.1146/annurev.ento.51.110104.151104

Li, Y., Liu, X., and Guo, H. (2018). Variations in endosymbiont infection between buprofezin-resistant and susceptible strains of *Laodelphax striatellus* (Fallén). *Curr. Microbiol.* 75, 709–715. doi: 10.1007/s00284-018-1436-x

Librado, P., and Rozas, J. (2009). DnaSP v5: a software for comprehensive analysis of DNA polymorphism data. *Bioinforma. Appl. Note.* 25, 1451–1452. doi: 10.1093/bioinformatics/btp187

Liu, X. D., and Guo, H. F. (2019). Importance of endosymbionts Wolbachia and Rickettsia in insect resistance development. *Curr. Opin. Insect. Sci.* 33, 84–90. doi: 10.1016/j.cois.2019.05.003

Livak, K. J., and Schmittgen, T. D. (2001). Analysis of relative gene expression data using real-time quantitative PCR and the $2^{-\Delta\Delta CT}$ method. *Methods* 25, 402–408. doi: 10.1006/meth.2001.1262

Lowe, S., Browne, M., Boudjelas, S., and de Pooter, M. (2000). *100 of the World's Worst Invasive Alien Species a Selection from the Global Invasive Species Database*. Auckland: The Invasive Species Specialist Group (ISSG).

Luo, C., Jones, C. M., and Devine, G. (2010). Insecticide resistance in *Bemisia tabaci* biotype Q (Hemiptera: Aleyrodidae) from China. *Crop Prot.* 29, 429–434. doi: 10.1016/j.cropro.2009.10.001

Ma, D. Y., Gorman, K., and Greg, D. (2007). The biotype and insecticide-resistance status of whiteflies, *Bemisia tabaci* (Hemiptera: Aleyrodidae), invading cropping systems in Xinjiang uygur autonomous region, northwestern China. *Crop Prot.* 26, 612–617. doi: 10.1016/j.cropro.2006.04.027

Mazzarri, M. B., and Georghiou, G. P. (1995). Characterization of resistance to organophosphate, carbamate, and pyrethroid insecticides in field populations of Aedes aegypti from Venezuela. *J. Am. Mosq. Control Assoc.-Mosquito News* 11, 315–322.

Mugerwa, H., Colvin, J., Alicai, T., Omongo, C. A., Kabaalu, R., Visendi, P., et al. (2021). Genetic diversity of whitefly (*Bemisia* spp.) on crop and uncultivated plants in Uganda: implications for the control of this devastating pest species complex in Africa. *J. Pest Sci.* 94, 1307–1330. doi: 10.1007/s10340-021-01355-6

Nauen, R., and Denholm, I. (2005). Resistance of insect pests to neonicotinoid insecticides: current status and future prospects. *Arch. Insect Biochem. Physiol.* 58, 200–215. doi: 10.1002/arch.20043

Nauen, R., Stumpf, N., and Elbert, A. (2002). Toxicological and mechanistic studies on neonicotinoid cross resistance in Q-type *Bemisia tabaci* (Hemiptera: Aleyrodidae). *Pest Manag. Sci.* 58, 868–875. doi: 10.1002/ps.557

Naveen, N. C., Chaubey, R., Kumar, D., Rebijith, K. B., Rajagopal, R., Subrahmanyam, B., et al. (2017). Insecticide resistance status in the whitefly, *Bemisia tabaci* genetic groups Asia-I, Asia-II-1 and Asia-II-7 on the Indian subcontinent. *Sci. Rep.* 7, 1–15. doi: 10.1038/srep40634

Nirgianaki, A., Banks, G. K., Frohlich, D. R., Veneti, Z., Braig, H. R., Miller, T. A., et al. (2003). Wolbachia infections of the whitefly *Bemisia tabaci*. *Curr. Microbiol.* 47, 93–101. doi: 10.1007/s00284-002-3969-1

Pang, S., Lin, Z., Zhang, W., Mishra, S., Bhatt, P., and Chen, S. (2020). Insights into the microbial degradation and biochemical mechanisms of neonicotinoids. *Front. Microbiol.* 11:868. doi: 10.3389/fmicb.2020.00868

Pashley, D. P., Hammond, A. M., and Hardy, T. N. (1992). Reproductive isolating mechanisms in fall armyworm host strains (Lepidoptera: Noctuidae). *Ann. Entomol. Soc. Am.* 85, 400–405. doi: 10.1093/aesa/85.4.400

Peshin, R., and Zhang, W. (2014). "Integrated pest management and pesticide use," in *Integrated Pest Management*, eds D. Pimentel, and R. Peshin (Dordrecht: Springer), 1–46. doi: 10.1007/978-94-007-7796-5_1

Pietri, J. E., and Liang, D. (2018). The links between insect symbionts and insecticide resistance: causal relationships and physiological tradeoffs. *Ann. Entomol. Soc. Am.* 111, 92–97. doi: 10.1093/aesa/say009

Prabhaker, N., Castle, S., and Perring, T. M. (2014). Baseline susceptibility of *Bemisia tabaci* B biotype (Hemiptera: Aleyrodidae) populations from California and Arizona to spirotetramat. *J. Econ. Entomol.* 107, 773–780. doi: 10.1603/EC13429

Rehman, M., Chakraborty, P., Tanti, B., Mandal, B., and Ghosh, A. (2021). Occurrence of a new cryptic species of *Bemisia tabaci* (Hemiptera: Aleyrodidae): an updated record of cryptic diversity in India. *Phytoparasitica* 49, 869–882. doi: 10.1007/s12600-021-00909-9

Sethi, A., and Dilawari, V. K. (2008). Spectrum of insecticide resistance in whitefly from upland cotton in Indian subcontinent. *J. Entomol.* 5, 138–147. doi: 10.3923/je.2008.138.147

Shadmany, M., Omar, D., and Muhamad, R. (2015). Biotype and insecticide resistance status of *Bemisia tabaci* populations from Peninsular Malaysia. *J. Appl. Entomol.* 139, 67–75. doi: 10.1111/jen.12131

Sloan, D. B., and Moran, N. A. (2012). Endosymbiotic bacteria as a source of carotenoids in whiteflies. *Biol. Lett.* 8, 986–989. doi: 10.1098/rsbl.2012.0664

Su, Q., Xie, W., Wang, S. L., Wu, Q. J., Ghanim, M., and Zhang, Y. J. (2014). Location of symbionts in the whitefly *Bemisia tabaci* affects 498 their densities during host development and environmental stress. *PLoS ONE* 9:e91802. doi: 10.1371/journal.pone.0091802

Tajima, F. (1989). Statistical method for testing the neutral mutation hypothesis by DNA polymorphism. *Genetics* 123, 585–595. doi: 10.1093/genetics/123.3.585

Thao, M. L., and Baumann, P. (2004). Evolutionary relationships of primary prokaryotic endosymbionts of whiteflies and their hosts. *Appl. Environ. Microbiol.* 70, 3401–3406. doi: 10.1128/AEM.70.6.3401-3406.2004

Wang, Q., Wang, M. N., Jia, Z. Z., Ahmat, T., Xie, L. J., and Jiang, W. H. (2020). Resistance to neonicotinoid insecticides and expression changes of eighteen cytochrome P450 genes in field populations of *Bemisia tabaci* from Xinjiang, China. *Entomol. Res.* 50, 205–211. doi: 10.1111/1748-5967.12427

Wang, Z. Y., Yan, H. F., and Yang, Y. H. (2010). Biotype and insecticide resistance status of the whitefly *Bemisia tabaci* from China. *Pest Manag. Sci.* 66, 1360–1366. doi: 10.1002/ps.2023

Weeks, A. R., Velten, R., and Stouthamer, R. (2003). Incidence of a new sex-ratiodistorting endosymbiotic bacterium among arthropods. *Proc. Royal Soc.* 270, 1857–1865. doi: 10.1098/rspb.2003.2425

Whalon, M. E., Mota-Sanchez, D., and Hollingworth, R. M. (2013). Gutierrez R. Michigan State University, Arthropod Pesticide Resistance Database. Available online at: http://www.pesticideresistance.com/ (accessed January 5, 2016).

World Health Organization (2016). *Monitoring and Managing Insecticide Resistance in Aedes Mosquito Populations: Interim Guidance for Entomologists*. Available online at: https://apps.who.int/iris/handle/10665/204588 (accessed January 2020).

Yang, X., Xie, W., Wang, S. L., Wu, Q. J., Pan, H. P., Li, R. M., et al. (2013). Two cytochrome P450 genes are involved in imidacloprid resistance in field populations of the whitefly, *Bemisia tabaci*, in China, *Pestic. Biochem. Physiol.* 107, 343–350. doi: 10.1016/j.pestbp.2013.10.002

Yi, T., Lei, L., He, L., Yi, J., Li, L., Dai, L., et al. (2020). Symbiotic fungus affected the asian citrus psyllid (ACP) resistance to imidacloprid and thiamethoxam. *Front. Microbiol.* 11:522164. doi: 10.3389/fmicb.2020.522164

Zchori-Fein, E., Lahav, T., and Freilich, S. (2014). Variations in the identity and complexity of endosymbiont combinations in whitefly hosts. *Front. Microbiol.* 5:310. doi: 10.3389/fmicb.2014.00310

Zhao, Y. X., Huang, J. M., Ni, H., Guo, D., Yang, F. X., Wang, X., et al. (2020). Susceptibility of fall armyworm, *Spodoptera frugiperda* (JE Smmith), to eight insecticides in China, with special reference to lambda-cyhalothrin. *Pestic. Biochem. Physiol.* 168, e104623. doi: 10.1016/j.pestbp.2020.104623

Zhuang, H. M., Wang, K. F., Zheng, L., Wu, Z. J., Miyata, T., and Wu, G. (2011). Identification and characterization of a cytochrome P450 CYP6CX1 putatively associated with insecticide resistance in *Bemisia tabaci*. *Insect Sci.* 18, 484–494. doi: 10.1111/j.1744-7917.2010.01380.x

Conflict of Interest: The authors declare that the research was conducted in the absence of any commercial or financial relationships that could be construed as a potential conflict of interest.

Publisher's Note: All claims expressed in this article are solely those of the authors and do not necessarily represent those of their affiliated organizations, or those of the publisher, the editors and the reviewers. Any product that may be evaluated in this article, or claim that may be made by its manufacturer, is not guaranteed or endorsed by the publisher.

Copyright © 2022 Barman, Samanta, Upadhyaya, Thakur, Chakraborty, Samanta and Tarafdar. This is an open-access article distributed under the terms of the Creative Commons Attribution License (CC BY). The use, distribution or reproduction in other forums is permitted, provided the original author(s) and the copyright owner(s) are credited and that the original publication in this journal is cited, in accordance with accepted academic practice. No use, distribution or reproduction is permitted which does not comply with these terms.

frontiers | Frontiers in Microbiology

TYPE Original Research
PUBLISHED 26 August 2022
DOI 10.3389/fmicb.2022.985852

Check for updates

OPEN ACCESS

EDITED BY
Durgesh K. Jaiswal,
Savitribai Phule Pune University, India

REVIEWED BY
Mohammad Faizan,
Maulana Azad National Urdu University, India
Abhijeet Ghatak,
Bihar Agricultural University, India

*CORRESPONDENCE
Mohammad Danish
danish.botanica@gmail.com

SPECIALTY SECTION
This article was submitted to Microbiotechnology, a section of the journal Frontiers in Microbiology

RECEIVED 04 July 2022
ACCEPTED 15 July 2022
PUBLISHED 26 August 2022

CITATION
Danish M, Shahid M, Ahamad L, Raees K, Atef Hatamleh A, Al-Dosary MA, Mohamed A, Al-Wasel YA, Singh UB and Danish S (2022) Nano-pesticidal potential of *Cassia fistula* (L.) leaf synthesized silver nanoparticles (Ag@*Cf*L-NPs): Deciphering the phytopathogenic inhibition and growth augmentation in *Solanum lycopersicum* (L.). *Front. Microbiol.* 13:985852. doi: 10.3389/fmicb.2022.985852

COPYRIGHT
© 2022 Danish, Shahid, Ahamad, Raees, Atef Hatamleh, Al-Dosary, Mohamed, Al-Wasel, Singh and Danish. This is an open-access article distributed under the terms of the Creative Commons Attribution License (CC BY). The use, distribution or reproduction in other forums is permitted, provided the original author(s) and the copyright owner(s) are credited and that the original publication in this journal is cited, in accordance with accepted academic practice. No use, distribution or reproduction is permitted which does not comply with these terms.

Nano-pesticidal potential of *Cassia fistula* (L.) leaf synthesized silver nanoparticles (Ag@*Cf*L-NPs): Deciphering the phytopathogenic inhibition and growth augmentation in *Solanum lycopersicum* (L.)

Mohammad Danish[1]*, Mohammad Shahid[2,3], Lukman Ahamad[1], Kashif Raees[4], Ashraf Atef Hatamleh[5], Munirah Abdullah Al-Dosary[5], Abdullah Mohamed[6], Yasmeen Abdulrhman Al-Wasel[5], Udai B. Singh[3] and Subhan Danish[7]

[1]Section of Plant Pathology and Nematology, Department of Botany, Aligarh Muslim University, Aligarh, India, [2]Department of Agricultural Microbiology, Faculty of Agricultural Sciences, Aligarh Muslim University, Aligarh, India, [3]Plant-Microbe Interaction and Rhizosphere Biology Lab, ICAR-NBAIM, Mau, India, [4]Department of Chemistry, Chandigarh University, Mohali, India, [5]Department of Botany and Microbiology, College of Science, King Saud University, Riyadh, Saudi Arabia, [6]Research Centre, Future University in Egypt, New Cairo, Egypt, [7]Hainan Key Laboratory for Sustainable Utilization of Tropical Bioresource, College of Tropical Crops, Hainan University, Haikou, China

Plant-based synthesis of silver nanoparticles (Ag-NPs) has emerged as a potential alternative to traditional chemical synthesis methods. In this context, the aim of the present study was to synthesize Ag-NPs from *Cassia fistula* (L.) leaf extract and to evaluate their nano-pesticidal potential against major phyto-pathogens of tomato. From the data, it was found that particle size of spherical *C. fistula* leaf synthesized (Ag@*Cf*L-NPs) varied from 10 to 20 nm, with the average diameter of 16 nm. Ag@*Cf*L-NPs were validated and characterized by UV-visible spectroscopy (surface resonance peak λ_{max} = 430 nm), energy dispersive spectrophotometer (EDX), Fourier transform infrared (FTIR), and X-ray diffraction pattern (XRD), and electron microscopy; scanning electron microscopy (SEM), and transmission electron microscopy (TEM). The FTIR spectra verified the participation of various living molecules (aromatic/aliphatic moieties and proteins) in synthesized Ag@*Cf*L-NPs. The anti-phytopathogenic potential of Ag@*Cf*L-NPs was assessed under *in vitro* conditions. Increasing doses of Ag@*Cf*L-NPs exhibited an inhibitory effect against bacterial pathogen *Pseudomonas syringae* and 400 μg Ag@*Cf*L-NPs ml^{-1} caused a reduction in cellular viability, altered bacterial morphology, and caused cellular death Furthermore, Ag@*Cf*L-NPs reduced exopolysaccharides (EPS) production and biofilm formation by *P. syringae* Additionally, Ag@*Cf*L-NPs showed pronounced antifungal activity against major fungal pathogens. At 400 μg Ag@*Cf*L-NPs ml^{-1}, sensitivity

of tested fungi followed the order: *Fusarium oxysporum* (76%) > *R. solani* (65%) > *Sarocladium* (39%). Furthermore, 400 μg Ag@*Cf*L-NPs ml^{-1} inhibited the egg-hatching and increased larval mortality of *Meloidogyne incognita* by 82 and 65%, respectively, over control. Moreover, pot studies were performed to assess the efficacy of Ag@*Cf*L-NPs to phyto-pathogens using tomato (*Solanum lycopersicum* L.) as a model crop. The applied phyto-pathogens suppressed the biological, physiological, and oxidative-stress responsiveness of tomatoes. However, 100 mg Ag@*Cf*L-NPs kg^{-1} improved overall performance and dramatically increased the root length, dry biomass, total chlorophyll, carotenoid, peroxidase (POD), and phenylalanine ammonia lyase (PAL) activity over pathogens-challenged tomatoes. This study is anticipated to serve as an essential indication for synthesis of efficient nano-control agents, which would aid in the management of fatal phyto-pathogens causing significant losses to agricultural productivity. Overall, our findings imply that Ag@*Cf*L-NPs as nano-pesticides might be used in green agriculture to manage the diseases and promote plant health in a sustainable way.

KEYWORDS

***Cassia fistula*, silver nanoparticles (Ag@*Cf*L-NPs), phytopathogens, nano-pesticides, tomatoes (*Solanum lycopersicum* L.), antioxidant enzymes**

Introduction

Nanotechnology has evolved as a significant and exciting area of research, with distinctive properties and broad applications in fields such as agriculture, food, and medicine (Erci et al., 2018). Metal and metal oxide (MO) nanoparticles (NPs) have been thoroughly researched using science and technology due to their outstanding properties such as the surface area to volume ratio, high diffusion in solution, and so on (Das Purkayastha and Manhar, 2016). As a result of this, Metal and metal oxide nanoparticles have improved the antibacterial capabilities (Ingle et al., 2020). Silver nanoparticles (Ag-NPs) are gaining lot of attention in the research community because of their wide range of applications in microbiology, chemistry, food technology, cell biology, pharmacology, parasitology and so on (Bondarenko et al., 2013; Nour et al., 2019). The physical and chemical properties of silver nanoparticles are determined by their morphology (Bondarenko et al., 2013). Although higher concentration of silver (Ag) are harmful, however, several investigations have shown that lower concentrations of $AgNO_3$ have superior chemical stability, catalytic activity, biocompatibility, with inherent therapeutic potential (Fahimirad et al., 2019). The Ag-NPs have been shown to exhibit the anticancer and antibacterial activity (Haggag et al., 2019). Several approaches, including the sol-gel method, hydrothermal method, chemical vapor deposition, thermal decomposition, microwave-assisted combustion method and others, have been used to synthesize Ag-NPs (Wu et al., 2012). However, while some of these physiochemical approaches are durable and theoretically viable; their large-scale applicability is severely limited due to the use of toxic chemicals, high cost, high energy and time consuming, and difficulties in waste purification. Furthermore, by-products of chemical processes are hazardous to the environment. As a result, there is a rising demand to adopt cost-effective, ecologically safe, and green synthesis techniques that use non-toxic chemicals in nano silver manufacturing methodology. Green synthesis of Ag-NPs employing various microbes, plants, and algae, on the other hand, is a natural, biocompatible, and ecologically friendly method (Aziz et al., 2015). Plant components such as leaves, roots, flowers, fruits, rhizomes, etc., have been effectively used in the synthesis of Ag-NPs (Ahmad et al., 2017; Sumitha et al., 2018). Secondary metabolites found in plants such as alkaloids, amines, proteins, polysaccharides, polyphenols, flavonoids, tannins, terpenoids, ketones, and aldehydes that act as reducing, stabilizing, and capping agents in the conversion of metal ions to metal nanoparticles, resulting in the formation of desirable nanoparticles with predefined properties (Rajan et al., 2015).

Much research has been carried out on the green synthesis of Ag-NPs using plant leaves, however, biosynthesis of Ag-NPs utilizing flower extract demonstrating potential anticancer and antibacterial action has not been extensively investigated. In this context, *Cassia fistula* (L.) is also known as Indian labrum and Golden Shower in English is thought to be an Indian native plant. In Indian literature, it is commonly utilized in the treatment of both common and acute ailments. This

herb is also used in the treatment of hematemesis, pruritus, leukoderma, and diabetes (Alam et al., 1990). The indigenous people of Similia Biosphere Reserve (SBR) use this herb for a variety of ethnomedicinal purposes. The floral extract has antibacterial, antifungal (Duraipandiyan and Ignacimuthu, 2007), antioxidant (Bhalodia et al., 2011), and anti-diabetic properties (Manonmani et al., 2005).

Several biotic (pest and pathogens) and abiotic (temperature, drought, and salinity stress) stresses have detrimental impact on crop yield under changing climatic scenario (Malhi et al., 2021). Since last few decades, agriculture faces a variety of challenges, such as indiscriminate application of synthetic fertilizers, pesticides and other chemical inputs. Due to the inefficient delivery system, there is significant loss of active ingredients (10–75 percent) took place through biodegradation, leaching, and immobilization which ultimately affect the core outcomes (Servin et al., 2015). In addition, disease resistance, toxicity to non-target microbes, and human health risks are also serious problems (Deshpande et al., 2017). To reduce the disease severity with increase in crop production and productivity, an integrated strategy is needed to enhance resistance to biotic and abiotic stresses in plants with maximizing resource use efficiency (He et al., 2016). As a result, there has been a surge in interest in using nanomaterial to create nano-formulations that can replace traditional inputs with higher efficacy, lower input cost, and lower environmental damage (Toksha et al., 2021).

Tomatoes (*Solanum lycopersicum* L.) are the second most valuable crop in the world, yet they are susceptible to several diseases caused by bacteria, fungi, and nematodes (Singh et al., 2017). Tomato root infections are one of the most significant obstacles to profitable tomato cultivation across the world. Soil-dwelling fungus, *Rhizoctonia solani* causes root diseases in different edible crops, including tomatoes. *Pseudomonas syringae*, soil-borne plant pathogenic bacteria cause bacterial speck disease in tomatoes and other crops (Mohammed et al., 2020). The most damaging and destructive diseases of tomatoes are those produced by root-knot nematodes, *Meloidogyne incognita* (Wubie and Temesgen, 2019). This infection reduces the tomato production by 38–56% in India. Root-knot nematodes are the most yield-limiting plant-parasitic nematodes (RKNs; *Meloidogyne* spp.). They are found throughout the world (Jones et al., 2013).

Till date chemical pesticides are used to manage the bacterial, fungal, and nematode infections, however, most of them have detrimental effects on human, animal and soil health. In this perception, the use of biosynthesized Ag-NPs in agriculture is gaining popularity due to their antioxidant and broad range of antibacterial action, as well as their eco-friendly, biocompatible, and cost-effective nature (Danish et al., 2021a). It is thus of great interest to investigate the inhibitory impact of manufactured Ag-NPs against important plant pathogens, which may be employed as a cost-effective, ecologically friendly, and safe technique in the field of nanotechnology. In pot trials, the application of increasing concentration of CuO (copper oxide)nanoparticles dramatically decreased the development of wilt symptoms in *Solanum melongena* (L.) infected by *Verticillium dahliae* and increased the biomass by 64% and Cu content by 32% in roots compared to untreated control plants (Elmer and White, 2016). Looking the importane of diseases, the aim of the present study was to investigate the potential of long-lasting Ag@*Cf*L-NPs (*C. fistula* extract to manufacture a biodegradable, natural product nano-silver with no danger of chemical toxicity) to inhibit the diseases-causing phytopathogenic microbes; *Rhizoctonia solani*, *P. syringae*, and *M. incognita* in tomato by enhancing the growth, photosynthetic attributes, lycopene content and defense responses. The Ag@*Cf*L-NPs were phytogenically synthesized and utilized to assess the anti-microbial activities in both *in vitro* and *in vivo* conditions. The anti-biofilm and anti-exopolysaccharides characteristics, as well as NPs-induced alterations in the morphology and cellular permeability in bacterial pathogens were also assessed. Biological attributes (plant length and dry matter), photosynthetic characteristics and enzymatic activities in tomatoes inoculated with plant pathogens and treated with Ag@*Cf*L-NPs were also assessed.

Materials and methods

Collection and preparation of leaf extract and chemical used in the study

Fresh *Cassia fistula* (L.) leaves were obtained from the Aligarh Muslim University (AMU) campus, India (27°52'N latitude, 78°51'E longitude, and 187.45 m altitude). Taxonomists from the Department of Botany, AMU examined and confirmed the plant species. To eliminate the dust particles, the fresh leaves were properly cleaned with sterilized double deionized water (ddH_2O). The leaves were then carefully macerated using pestle and mortar in sterile ddH_2O to generate a 10% (w/v) leaves broth, which was then heated for a few minutes. After cooling, the resultant extract was filtered through a muslin cloth followed by Whatman No. 1 filter paper before being stored at 4°C. Silver nitrate ($AgNO_3$; Sisco Research Laboratories: SRL, Pvt. Ltd., India) was procured from Sigma-Aldrich, United State.

Synthesis of silver nanoparticles

The silver nanoparticles used in the present study were prepared by using the bio-reduction method of an aqueous solution of $AgNO_3$. The bio-reduction method is among the most reliable and extensively investigated methods for the synthesis of Ag-NPs (Jalal et al., 2016; Qais et al., 2020). Briefly, for the preparation of silver nanoparticles, 25 ml extract of

C. fistula leaf extract was mixed in aqueous solution of $AgNO_3$ (100 ml, 1.0 × 10^{-3} mol dm^{-3}). The mixture was incubated (allowed to react) for 12 h at 25°Ñ with continuous stirring using a magnetic stirrer. The completion of reduction of $AgNO_3$ by the plant extract was indicated by the change in color of the mixture from light green to dark brown. For obtaining silver nanoparticles, the mixture was centrifuged at 15,000 rpm for 20 min to remove any unreacted $AgNO_3$ and plant extract. The nanoparticles obtained were washed thrice with double distilled water followed by washing with ethanol. Finally, the synthesized nanoparticles were dried under a vacuum.

Characterization of silver nanoparticles

The biosynthesized nanoparticles were characterized to confirm their successful synthesis using a UV-visible spectrophotometer (GENESYS 10S UV/VIS, Thermo Fisher Scientific, United States), Scanning electron microscope (SEM; JSM-5600LV, JEOL, Japan), Transmission electron microscope (JEM-2100, JEOL, Japan), X-ray diffractometer (Miniflex II, Rigaku, Japan) equipped with CuKα radiation source (λ = 1.5406 nm), Fourier transform infrared spectrometer (Nicolet iS50, Thermo Fisher Scientific, United States), and Energy-dispersive X-ray spectrometer (JED-2300, JEOL, Japan) following the standard protocols.

Assessment of anti-phytopathogenic properties of *Cassia fistula* leaf synthesized silver nanoparticles (Ag@*Cf*L-NPs)

Anti-bacterial activity against *Pseudomonas syringae*

Collection of bacterial pathogen and assessment of cell viability

Bacterial pathogens *Pseudomonas syringae* were obtained from Section of Plant Pathology, Department of Botany, AMU, Aligarh, India. Bacterial strains was purified by re-culturing on Pseudomonas isolation agar (PIA; HiMedia, Mumbai, India) medium. To determine the potentiality of phytogenically synthesized Ag@*Cf*L-NPs, the vitality of the bacterial strain was determined by growing them in the presence of Ag@*Cf*L-NPs (0–400 μg ml^{-1}) (under *in vitro* conditions) (refer to **Supplementary information section 1.1**).

Effect of Ag@*Cf*L-NPs on surface morphological changes and cellular permeability

The interaction studies for observing morphological changes in the cells of *P. syringae* treated with Ag@*Cf*L-NPs were done by SEM according to previously described methods of Ansari et al. (2014), Shahid and Khan (2018) and Shahid et al. (2019) (refer to **Supplementary information section 1.2**). To assess the effects of synthesized nanohybrid (i.e., Ag@*Cf*L-NPs) on cellular permeability (cell membranes) of the pathogenic isolates, confocal laser scanning microscopy (CLSM) was done (Shahid and Khan, 2018; Khan et al., 2020; Shahid et al., 2021a; Syed et al., 2021) (refer to **Supplementary information section 1.3**).

Effect of Ag@*Cf*L-NPs on biofilm formation

The effect of phytogenically synthesized Ag@*Cf*L-NPs on the biofilm development of *P. syringae* was investigated in a 96-well titer plates (Shahid et al., 2021b). In brief, wells were filled with 200 μl of Luria Bertani (LB; HiMedia, Mumbai, India) broth inoculated with bacterial culture (100 μl) and 0–400 μg Ag@*Cf*L-NPs ml^{-1}. The bacterial cultures without Ag@*Cf*L-NPs were served as a control. The optical density (O.D) was measured using a scanning microplate spectrophotometer at 570 nm and recorded the biofilm development.

Determination of exopolysaccharide in the presence of Ag@*Cf*L-NPs

For the assessment of EPS production, bacterial cells of *P. syringae* were cultured in a liquid culture medium treated with different doses of Ag@*Cf*L-NPs to test the influence of Ag@*Cf*L-NPs on extrapolymeric substances (EPS) produced by bacterial isolates (Ku et al., 2015) (refer to **Supplementary information section 1.4**).

Antifungal activity of Ag@*Cf*L-NPs

Fungal pathogens such as *Fusarium oxysporum*, *Rhizoctonia solani*, and *Sarocladium* sp. were procured from Section of Plant Pathology, Department of Botany, AMU, Aligarh, India. All the fungal phytopathogens was purified by re-culturing on Potato Dextrose agar (PDA; HiMedia, Mumbai, India) medium. The *in vitro* experiments were performed on potato dextrose agar (PDA; HiMedia, Mumbai, India) medium containing different concentrations of Ag@*Cf*L-NPs (0, 25, 50, 100, 200, and 400 μg ml^{-1}). Briefly, 10 ml of Ag@*Cf*L-NPs was taken from each concentration and mixed in 100 ml potato dextrose agar (PDA) media before plating (Petri plates, 90 × 15 mm). Petri plates containing Ag@*Cf*L-NPs were incubated at room temperature for 48 h. Thereafter, the phyto-fungal pathogens such as *Rhizoctonia Solani*, *Fusarium oxysporum*, and *Sarocladium* sp. were inoculated simultaneously at the center of each Petri plate containing Ag@*Cf*L-NPs (agar plugs of uniform size, 5 mm in diameter) and incubated at 28 ± 2°C for 7 days. The Petri plates without Ag@*Cf*L-NPs served as control. After 7 days of incubation, radial growth of fungal mycelium was recorded. All the treatments were performed in three replicates (n = 3). The inhibition of mycelial growth was measured according to the method given by Kaur et al. (2012) and percent inhibition was

calculated using the following equation:

$$\%inhibition = \frac{C - T}{C} \times 100$$

Where,

C = Radial growth of fungi in control plates

T = Radial growth of fungi in treated plates.

Assessment of nematicidal activity of Ag@*Cf*L-NPs

In vitro activity of silver nanoparticles (Ag@*Cf*L-NPs) on hatching and mortality of *Meloidogyne incognita*

For the recovery of root-knot nematodes, infected roots of eggplant (*Solanum melongena* L.) with the root-knot nematode (*M. incognita*) were collected from an eggplant field. Root-knot nematode species *M. incognita* was identified on the basis of the North Carolina differential host test and perennial pattern morphology. The effect of different concentrations (0, 25, 50, 100, 200, and 400 μg ml^{-1}) of Ag@*Cf*L-NPs on egg hatching and mortality of *M. incognita* was studied under *in vitro* conditions. Five (05) egg masses of average sized (collected from eggplant roots) were placed for hatching in small sized (60 × 15 mm) Petri plates containing 10 ml Ag@*Cf*L-NPs solution from each concentration using sterilized forceps and incubated at 25 ± 1°C. Five egg masses placed in 10 ml of ddH_2O were served as control. Each treatment was repeated thrice (n = 3). After 48 h of incubation, the total number of hatched larvae and immobile larvae were counted using a nematode counting dish under a stereoscopic microscope. The death of the juveniles was determined by immersing the immobile larvae in water for 1 h and counting the number of dead larvae.

Effect of Ag@*Cf*L-NPs on phytopathogen-infected tomato crop

Effect of Ag@*Cf*L-NPs on biological attributes of tomato

Efficacy of green-synthesized Ag@*Cf*L-NPs was evaluated in *Solanum lycopersicum* L. (tomato) against root-knot caused by *Meloidogyne incognita*, root rot caused by *Rhizoctonia solani*, and bacterial speck diseases caused by *Pseudomonas syringae*. Tomato seeds were disinfected with four percent sodium hypochlorite (NaOCl; Sisco Research Laboratories: SRL, Pvt. Ltd., India) for 15 min and then washed three times with distilled sterile water. The inoculum of microbial phytopathogens was applied as; *P. syringae* (10^8 CFU ml^{-1}), *R. solani* (50 g mycelial mat), and *M. incognita* (1,000 J_2) (Kaur et al., 2016). To evaluate the disease suppressive and plant growth-promoting effect of Ag@*Cf*L-NPs, the two concentrations (50 and 100 mg kg^{-1}) were used in the tomato experiments (of the two-leaf growth stage). Sterile distilled water (SDW) was used as a negative control. There was eighth different treatments, i.e., (i) Control: water only (negative control), 50 mg Ag@*Cf*L-NPs kg^{-1} only (positive control), 100 mg Ag@*Cf*L-NPs kg^{-1} only (positive control), (ii) Inoculated control: *Meloidogyne incognita* only, *R. solani* only, *P. syringae* only, (iii) *R. solani* + 50 mg Ag@*Cf*L-NPs kg^{-1}, (iv) *M. incognita* + 50 mg Ag@*Cf*L-NPs kg^{-1}, (v) *P. Syringae* + 50 mg Ag@*Cf*L-NPs kg^{-1} (vi) *M. incognita* 100 mg Ag@*Cf*L-NPs kg^{-1}, (vii) *R. solani* + 100 mg Ag@*Cf*L-NPs kg^{-1}, and (viii) *P. syringae* + 100 mg Ag@*Cf*L-NPs kg^{-1}. At 45 days after inoculation (DAI), the pathogen-infected and Ag@*Cf*L-NPs treated tomatoes were harvested and cleaned the roots by removing the adhering peat. The plant growth parameters (root and shoot length, fresh and dry biomass), chlorophyll content, lycopene content, and antioxidant enzymes were estimated. In the case of nematode inoculated plants, the number of galls per root system were enumerated and used to calculate the root-knot index (RKI) and the percentage (%) of root rot per root system was visually inspected. Furthermore, percent disease incidence was assessed from the fungal infected and Ag@*Cf*L-NPs-treated tomato plants.

Chlorophyll pigment and lycopene content estimation

At harvest, from the phytopathogens-inoculated and Ag@*Cf*L-NPs-treated tomato leaf, photosynthetic pigments (total chlorophyll and carotenoid contents) were measured by spectrophotometer (UV-visible spectrophotometer; GENESYS 10S UV/VIS, Thermo Fisher Scientific, United States) following the procedure of MacKinney (1941).

Antioxidant enzymatic activities

Peroxidase (POD) activity was determined by monitoring the absorbance at 470 nm every 20 s using the spectrophotometer (Ramzan et al., 2021). Determination of superoxide dismutase (SOD) activity was performed according to Giannopolitis and Ries (1977), while catalase (CAT) activity was estimated as per methods described by Danish et al. (2021b). The activity of phenylalanine ammonia-lyase (PAL) was spectrophotometrically (UV-visible spectrophotometer; GENESYS 10S UV/VIS, Thermo Fisher Scientific, United States) determined in the plant treated with pathogens and Ag@*Cf*L-NPs as per the method given by Solekha et al. (2020) (Please refer to the respective **Supplementary information sections 2.1** and **2.2** in **Supplementary information**).

Effect of Ag@*Cf*L-NPs on gall formation, root-knot index (RKI), and disease incidence in tomatoes

The *M. incognita* inoculated and Ag@*Cf*L-NPs-treated tomatoes were harvested and the number of galls per plant was visually counted. The size of each gall was measured using a micrometer to determine its maximum length and breadth (in m). With minor modifications, the severity of the disease was measured using the grading scale 0–6 given by Popoola et al. (2015).

Statistical analysis

In vitro and greenhouse studies were carried out in a complete randomized block design (CRBD), and data were analyzed through analysis of variance (ANOVA) at $p < 0.05$ level using the statistical software R. Pearson correlation matrix between variables was performed by XLSTAT.

Results and discussion

Characterization of Ag-NPs

UV-vis spectrophotometric analysis

UV-visible spectroscopy is one of the most reliable methods for the characterization of silver nanoparticles. In Ag-NPs, the conduction band lies very close to the valence band, so the valence band electrons, excited by the photon of the incident light, can easily jump into the conduction band and move freely. The freely moving electrons are responsible for the Surface Plasmon Resonance (SPR), which occurs because of the collective oscillation of electrons in response to the incident light (Zhang et al., 2016; Rezazadeh et al., 2020). A broad absorbance peak was observed at 422 nm for the colloidal solution of Ag@*Cf*L-NPs, which is associated with the SPR band of Ag@*Cf*L-NPs and confirms the stability of NPs (**Figure 1A**).

Transmission electron microscopy (TEM) and scanning electron microscopy (SEM)

To study the surface features of the synthesized NPs, the Ag@*Cf*L-NPs, were characterized using SEM and TEM. The SEM image (**Figures 1B,C**) of Ag@*Cf*L-NPs clearly shows that the shape of the NPs was mostly spherical and some of the Ag@*Cf*L-NPs were oval as well. The SEM images demonstrate the bio-molecule coating of the synthesized Ag@*Cf*L-NPs. This layer confirms the significance of plant extract metabolites in the synthesis and stabilization of Ag@*Cf*L-NPs. These findings are consistent with those of the observation of Oves et al. (2018). Further, to study the topographical and crystallographic characteristics of the NPs TEM imaging was performed. The TEM image of synthesized Ag@*Cf*L-NPs (**Figure 2**) depicts that the NPs vary in size and range between 10 and 20 nm in diameter. Also, the shape of Ag@*Cf*L-NPs observed in the TEM micrograph is following the SEM image, i.e., spherical. This finding was in lined with the results of Danish et al. (2021a).

Energy dispersive X-ray (EDX) analysis

For elemental analysis, the prepared Ag@*Cf*L-NPs were characterized using EDX (**Figure 1**). The result of EDX analysis for synthesized Ag NPs depicts a very high content of Ag (71%) with some O (28%) that may be absorbed on the surface of synthesized Ag@*Cf*L-NPs. This confirmed the existence of the silver element in the synthesized Ag@*Cf*L-NPs.

Fourier transform infrared spectroscopy (FTIR)

The characterization of complicated and particular materials using Fourier Transform Infrared Spectrometry (FTIR) is a difficult assignment for chemists to complete. To study the nature of functional groups present in the Ag@*Cf*L-NPs, the synthesized NPs were characterized using FTIR (**Figure 1E**). The peak observed at 3,447 cm^{-1} is due to the O–H stretching vibrations of the phenol group (Zia et al., 2016). The absorbance peak at 2,942 cm^{-1} is attributed to the C–H stretching vibrations (Manikprabhu and Lingappa, 2013). The stretching vibrations of C = C are observed at 1,634 cm^{-1} (Jyoti et al., 2016). The peaks obtained at 1,492 cm^{-1} and 1,253 cm^{-1} are assigned to C–C stretch and C–N stretch, respectively (Devaraj et al., 2013). And the peak observed at 1,032 cm^{-1} corresponds to the stretching vibrations of the C–OH group (Singh et al., 2014).

X-ray diffraction (XRD)

The analytical technique of X-ray diffraction (XRD) is based on the diffraction of X-rays by matter, particularly crystalline materials. The Ag@*Cf*L-NPs were characterized using XRD to confirm the crystalline nature of the NPs. Four intense peaks were observed in the XRD pattern of Ag@*Cf*L-NPs (**Figure 1F**) at diffraction (2θ) angles of 37.92°, 44.04°, 64.38°, and 77.32°, which corresponds to the planes 111, 200, 220, and 311, respectively (Remya et al., 2015; Sigamoney et al., 2016), indicating the crystalline nature of Ag-NPs (Abbasi et al., 2020). The average crystallite size, calculated with a peak at 2θ = 37.92° using the Debye-Scherrer formula was 14.63 nm.

The anti-phytopathogenic potential of Ag@*Cf*L-NPs

Effect of Ag@*Cf*L-NPs on phytopathogenic bacterium *Pseudomonas syringae*

The growth of bacterial pathogen *Pseudomonas syringae* was hindered by the increasing concentrations Ag@*Cf*L-NPs, which showed a strong antibacterial potential. This study is intriguing from an agronomic standpoint because *P. syringae*, like other bacterial diseases, causes major crop losses in various agriculturally important crops including tomatoes. For example, bacterial speck disease caused by *P. syringae* damages a variety of agricultural products, including tomatoes and tobacco. As a result, breeding of resistant cultivars, cultural practices, and crop rotation are some of the potential traditional measures used to control the negative consequences of *Pseudomonas syringae*.

Growth and viability

The effectiveness of such techniques, on the other hand, has been proven to be highly variable. As a result, the antibacterial activity of Ag@*Cf*L-NPs as demonstrated in this study may be critical in controlling the bacterial phytopathogens. The high surface energy and mobility of nanoparticles are influenced

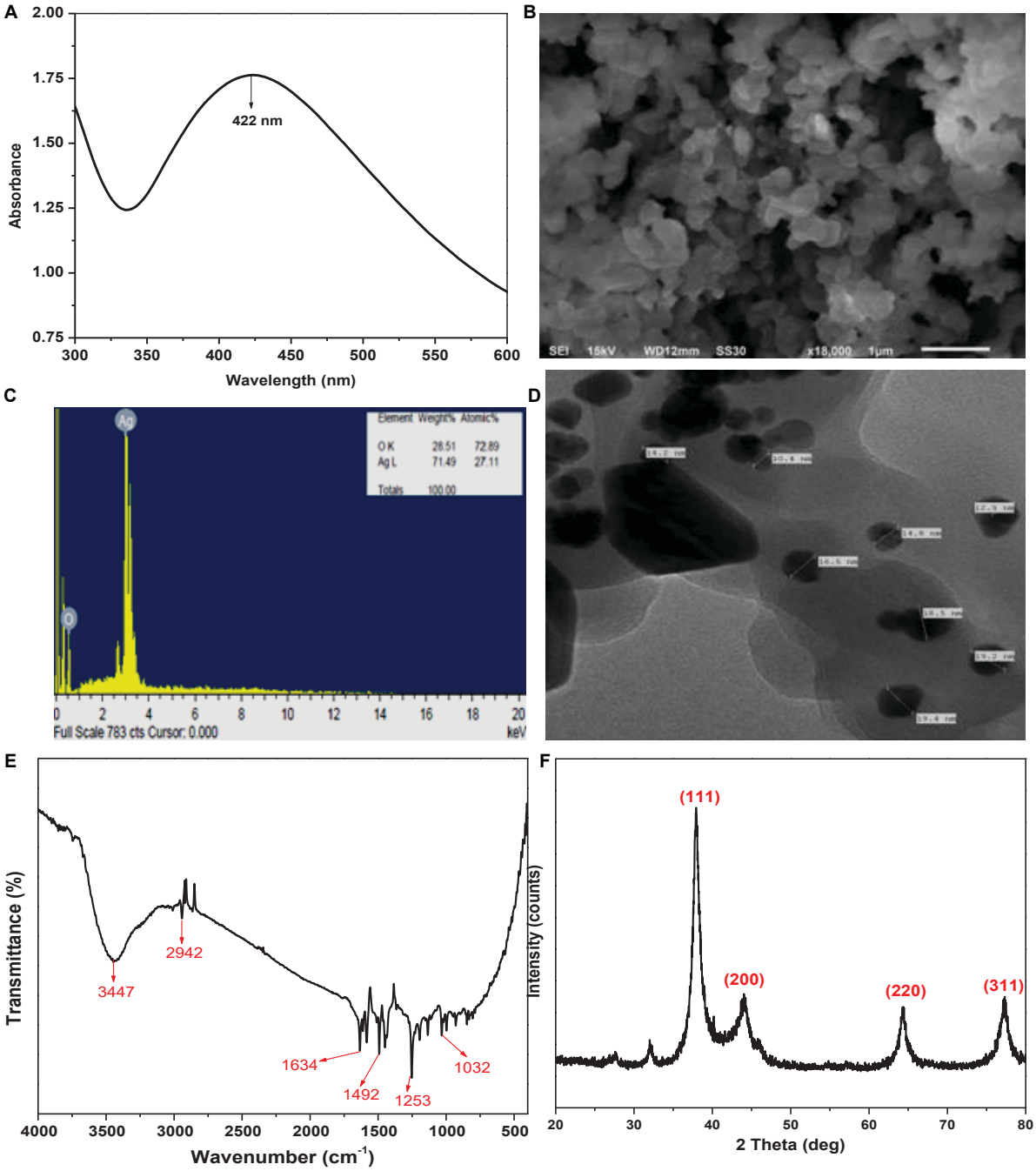

FIGURE 1
Characterization of *Cassia fistula* leaf synthesized silver nanoparticles (Ag@*Cf*L-NPs): UV–vis spectra of Ag@*Cf*L-NPs **(A)**, scanning electron micrographs (SEM) of Ag@*Cf*L-NPs **(B)**, EDX spectrum showing the histogram of wt% of major elements in Ag@*Cf*L-NPs **(C)**, transmission electron micrographs (TEM) of Ag@*Cf*L-NPs **(D)**, FTIR spectrum of Ag@*Cf*L-NPs **(E)** and XRD pattern of powdered Ag@*Cf*L-NPs **(F)**.

by strong contacts between Ag-NPs and the cell wall. The findings of this investigation revealed that Ag@*Cf*L-NPs at various concentrations displayed potent antibacterial action against *Pseudomonas syringae*, with the inhibitory impact increasing as the concentration was raised. The diameter of the inhibitory zones was 12.2 mm in the presence of 400 μg Ag@*Cf*L-NPs ml^{-1}. Previous research has shown that green synthesized Ag-NPs can reduce a variety of bacterial plant diseases, including *Pseudomonas syringae* pv. tomato (Marpu et al., 2017), *Clavibacter michiganensis* subspecies *michiganensis* (Rivas-Cáceres et al., 2018), and *Ralstonia solanacearum* (Chen et al., 2016), which are all in accordance with our

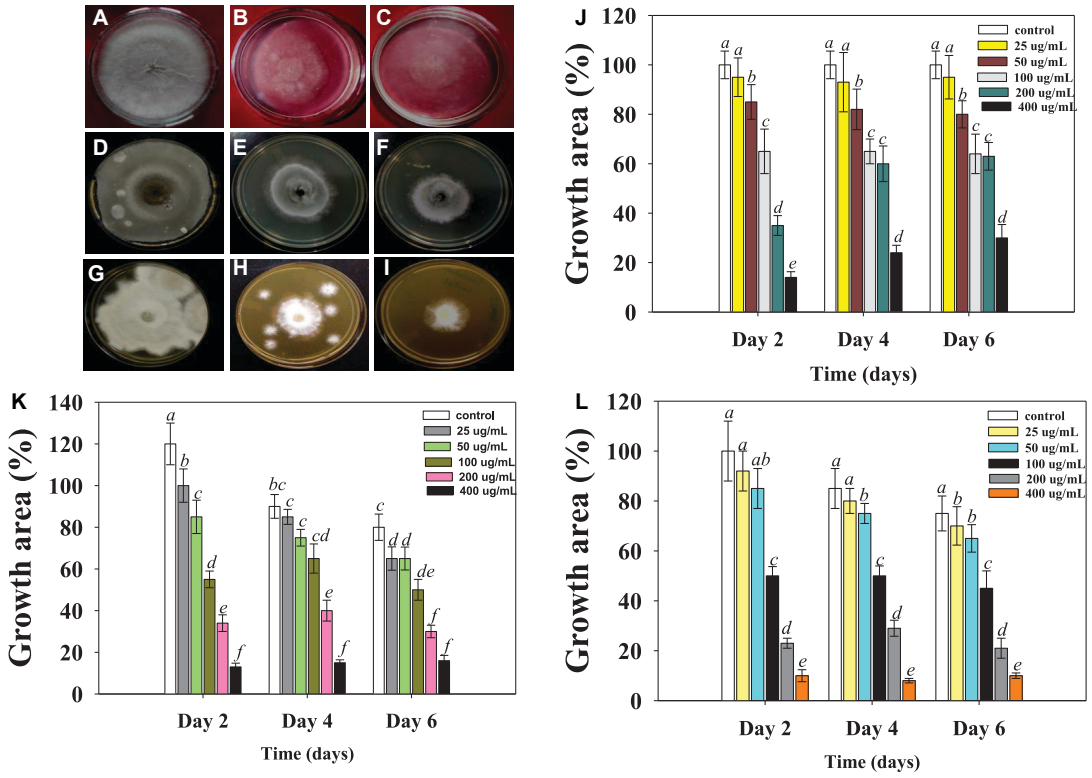

FIGURE 2
Macroscopic examination depicting the Ag@*Cf*L-NPs-induced inhibition in mycelia growth of phytopathogenic fungi; *Rhizoctonia solani*: control **(A)**, treated with 50 **(B)**, 100 μg ml^{-1} Ag@*Cf*L-NPs **(C)**. *Sarocladium* sp.: control **(D)**, treated with 50 **(E)**, 100 μg Ag@*Cf*L-NPs ml^{-1} **(F)**, *Fusarium oxysporum*: control **(G)**, treated with 50 **(H)**, 100 μg ml^{-1} Ag@*Cf*L-NPs **(I)**. In this figures, **(J–L)** represents the bar diagrams showing the numerical data in terms of percentage of growth area as compared to mycelia growth of untreated control done in triplicates (n = 3). Corresponding error bars represents standard deviation (S.D) of three replicates (S.D, n = 3).

findings. Furthermore, the viability of bacterial cells was significantly reduced as the concentration of Ag@*Cf*L-NPs was increased (**Figure 3A**).

Ag@*Cf*L-NPs-induced morphological changes in bacteria

Under a scanning electron microscope (SEM), morpho-structural alterations caused by synthesized Ag@*Cf*L-NPs in *P. syringae* were studied. Bacterial cells with no treatment (control) have smooth cell surfaces and shapes (**Figure 3B**). However, as shown in pictures with yellow arrows and circles, Ag@*Cf*L-NPs-treated cells showed a clear damage to the outer surface, shrinkage, and broken membranes (**Figure 3C**). The peptidoglycan layer of two different bacterial cells differs, resulting in this morphological discrepancy. However, the precise method by which Ag@*Cf*L-NPs inhibit or kill the microorganisms is still unknown. However, other processes cause Ag-NPs to become toxic and eventually contribute to the death of bacterial cells, such as decoupling oxidation, free radical formation, interferences with the respiratory chain of cyt c, interference with the transport chain's components of the microbial electron chain, phosphorous and sulfur compounds, and DNA interactions (Lapresta-Fernández et al., 2012).

Membrane permeability of plant pathogenic bacteria

The qualitative analyses of cell permeability in *P. syringae* were performed using the fluorescently labeled probe propidium iodide (PI). Due to the staining of PI with bacterial DNA, the 400 μg Ag@*Cf*L-NPs ml^{-1} -treated cells looked red against the black background, followed by excitation at 532 nm (**Figures 3D–F**). This is because PI binds to DNA molecules in the membrane-damaged cells (Stiefel et al., 2015). Furthermore, the number of dead cells in Ag@*Cf*L-NPs-treated membrane-impaired bacterial cells was quantified, and it was observed that the number of dead cells increased in a dose-dependent way (**Figure 3G**). The antibacterial properties of nanoparticles are dependent on particle size, stability, and concentration in the growth medium (Azam et al., 2012). The NPs have a stronger reactivity with pathogens because the outer cellular membrane of the bacterial strains has nano-scale pores. As a result of the ROS, the bacterial cell membrane is damaged, allowing the cells

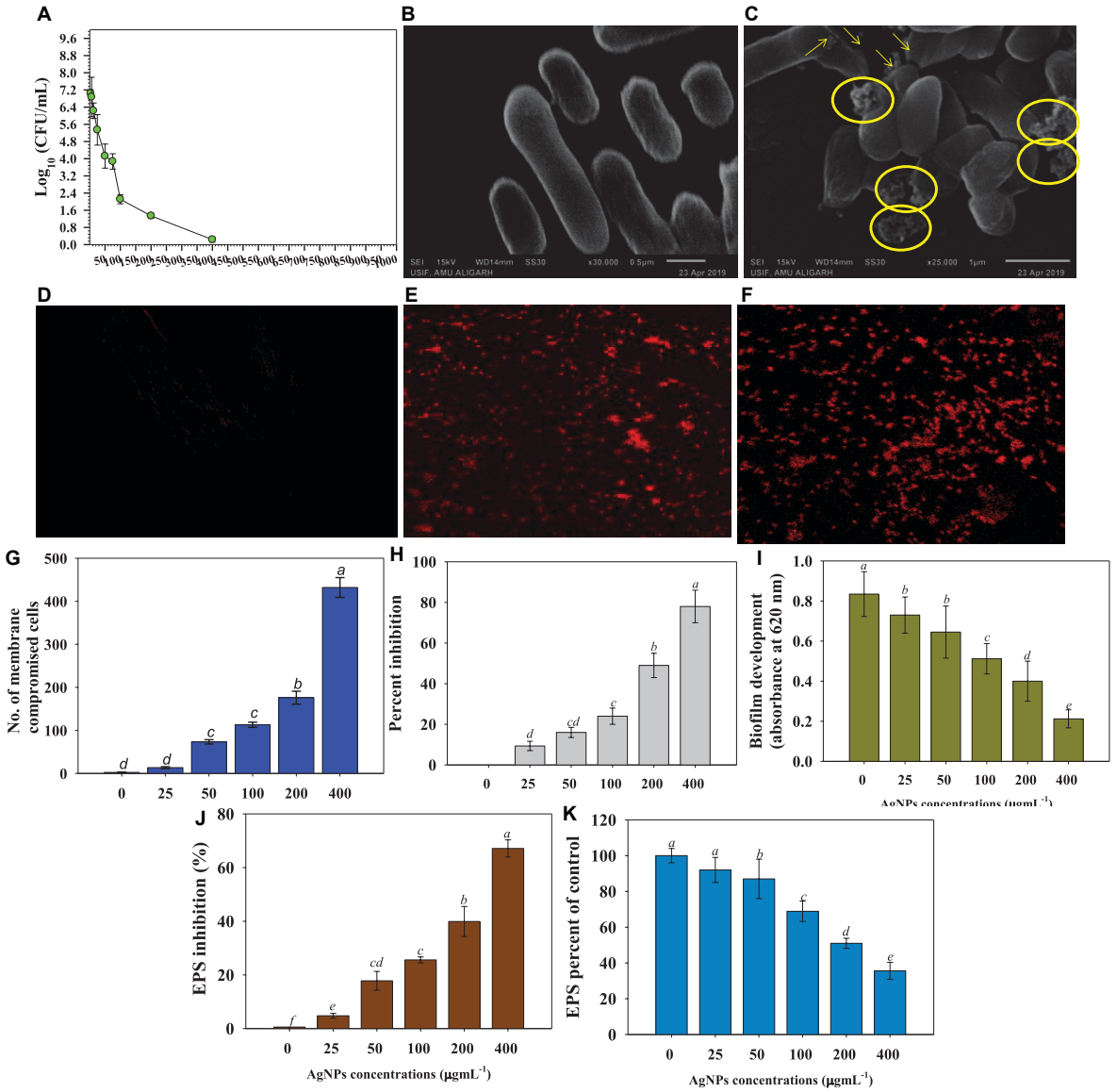

FIGURE 3
Anti-bacterial properties of increasing concentrations of *Cassia fistula* leaf synthesized silver nanoparticles (Ag@*Cf*L-NPs) against soil bacterial pathogen *Pseudomonas syringae*; effect of 0–1,000 μg Ag@*Cf*L-NPs ml^{-1} on CFU count **(A)**, morphological changes: control cells of *P. syringae* **(B)** treated with 100 μg Ag@*Cf*L-NPs ml^{-1} **(C)**, NP-induced cellular permeability: CLSM images of untreated bacterial cells showing no bacterial uptake of propidium iodide **(D)**, treated with 100 μg Ag@*Cf*L-NPs ml^{-1} **(E)** and 200 μg Ag@*Cf*L-NPs ml^{-1} showing the red-colored rod-shaped cells **(F)**, number of membrane compromised cells **(G)**, percent inhibition in bacterial biofilm formation **(H)**, biofilm development in the presence of increasing doses of Ag@*Cf*L-NPs **(I)**, percent inhibition in bacterial EPS **(J)** and EPS percent of control **(K)**. In this figure, bar diagrams represent the mean values of three replicates (n = 3). Corresponding error bars represents standard deviation (S.D) of three replicates (S.D, n = 3).

to absorb PI. Furthermore, the antibacterial effect of Ag@*Cf*L-NPs is principally due to the formation of reactive oxygen species (ROS) such as OH^-, H_2O_2, and O_2.

Biofilm formation and exopolysaccharide production

The results of this investigation showed that at all doses of synthesized Ag@*Cf*L-NPs in this study greatly decreased the biofilm formation ability of *P. syringae*. The Ag@*Cf*L-NPs at concentrations of 200 and 400 μg ml^{-1} caused a greater inhibition in optical density (OD) values, with decreases of 49 and 78%, respectively, over control (Figures 3H,I). Biofilms are bacterial aggregation that may survive in harsh environments and are resistant to the immune system of the host as well as certain chemotherapeutic treatments. Biofilm development protects the bacteria from external stimuli and keeps them

alive, whereas swimming motility permits the plant pathogenic bacteria to easily infiltrate and colonize the host plants (Denny, 2007). As a result, the antibacterial action of Ag@*Cf*L-NP scan be ascribed in part to their prevention of bacterial biofilm formation. The existence of reactive oxygen species (ROS) as a primary inhibitor of biofilm formation was further clarified in the study. As a result, the enhanced generation of extracellular ROS might explain this investigation. Like our study, bio-fabricated AgNPs showed a strong anti-bacterial efficacy and reduced the biofilm formation activity of soil-borne pathogenic bacterium *Xanthomonas oryzae* that causes leaf blight diseases of rice (Mishra et al., 2020). Furthermore, ZnO nanoparticles demonstrated a significant reduction of bacterial growth and biofilm formation against *P. aeruginosa*, as previously reported by Dwivedi et al. (2014). They also identified that reactive oxygen species (ROS) as a key mechanism for ZnO-NP action. With increasing concentrations, Ag@*Cf*L-NPs, the formation of EPS by plant pathogenic bacteria was significantly ($p \leq 0.05$) reduced. The higher rates of synthesized nanomaterial had the maximum toxic effect on EPS. For example, at 400 μg ml^{-1}, Ag@*Cf*L-NPs reduced the EPS formation by 76% over untreated control (**Figures 3J,K**).

Antifungal potential of Ag@*Cf*L-NPs against major fungal pathogens

The antifungal potential of phytogenically synthesized Ag@*Cf*L-NPs was evaluated against major fungal pathogens (*Rhizoctonia solani*, *Sarocladium* sp. and *Fusarium oxysporum*) causing yield losses in edible crops. All the concentrations of synthesized Ag@*Cf*L-NPs had significant ($p \leq 0.05$) inhibitory effect on the growth of tested fungal pathogens (**Supplementary Table 1**). The Ag@*Cf*L-NPs-induced dose-dependent inhibition in mycelial growth of *Rhizoctonia* (**Figures 2A–C**), *Sarocladium* (**Figures 2D–F**), and *Fusarium* (**Figures 2G–I**) were observed which, differed considerably with time. However, no consistent link was found between fungal growth suppression and incubation times. When cultivated on potato dextrose agar (PDA; HiMedia, Mumbai, India) plates supplemented with 400 μg Ag@*Cf*L-NPs ml^{-1}, the growth of *R. solani* was decreased by 65%, 75%, 78% after 2nd, 4th, and 6th days of incubation, respectively (**Figure 2J**). Likewise, at 400 μg Ag@*Cf*L-NPs ml^{-1}, the growth of *F. oxysporum* was inhibited by 24, 56, and 73% at 2nd, 4th, and 6th days of incubation, respectively (**Figure 2K**). It was clear from this study that each concentration of Ag@*Cf*L-NPs had a harmful effect on fungal growth, while at higher concentration (400 μg ml^{-1}), the growth was completely stopped in the tested fungal phytopathogens. Other researchers have also reported that NPs have antifungal properties. ZnO-NPs, for example, hindered the growth of *Botrytis cinerea* and *Penicillium expansum* by deforming the structure of fungal hyphae and stopping the conidial germination and development (He et al., 2011). Likewise, Elgorban et al. (2016) confirmed that varying concentrations of Ag-NPs have antifungal properties against *R. solani* and a strong inhibition was noticed on CDA at different concentrations. The phyto-synthesized Ag-NPs completely inhibited the growth of *R. solani* by increasing lipid peroxidation (ROS generation). It may be the primary cause of toxicity of Ag-NPs in the fungal cell (Kanaujiya et al., 2020). In addition, results showed that cell surfaces of fungal hyphae was distorted. Aside from that, Ag-NPs interfere with the membrane transport processes, such as ion efflux (Rudakiya and Pawar, 2017). The deformed membranes may allow silver ions generated by Ag-NPs to accumulate in the nutritional medium, altering cellular respiration and metabolic processes (Nisar et al., 2019). Another process that negatively affects are lipids, proteins, and nucleic acids due to the generation of intracellular ROS.

Effects of Ag@*Cf*L-NPs on hatching and mortality of root-knot nematode *Meloidogyne incognita*

To assess the nematicidal properties of Ag@*Cf*L-NPs, different concentrations of synthesized Ag-NPs solution (0–400 μg ml^{-1}) were tested on the hatching and mortality of root-knot nematode, *M. incognita*. All the concentrations of Ag-NPs had a significant ($p \leq 0.05$) inhibitory effect on the hatching and mortality of *M. incognita* (**Supplementary Tables 2, 3**). For instance, a reduction of 56, 64, 71, and 82% in egg hatching of *M. incognita* was recorded when treated with 25, 50, 75, and 100 μg Ag@*Cf*L-NPs ml^{-1}, respectively, after 48 h as compared to untreated control (**Figures 4D,E**). The adverse effect encountered might be due to the toxicity of green synthesized Ag@*Cf*L-NPs that inhibited the hatching of *M. incognita*. Similarly, increasing doses of Ag-NPs reduced the egg hatching of *M. javanica* as previously reported by Hamed et al. (2019). The inhibition effect of Ag-NPs was correlated with the physical properties (size, shape, and homogeneity), which may play a crucial role in the cell wall penetration in the eggs followed by dysfunctioning in cells (Jagtap and Bapat, 2013). However, larval mortality of *M. incognita* (2nd stage) was 4.62% in double-distilled water after 48 h. The juvenile mortality of *M. incognita* in Ag-NPs (at 25, 50, 75, and 100 mg/L) was observed to 55.78, 57.89, 60.65, and 65.78%, respectively, after 48 h of the exposure period (**Figures 4F,G**). Microscopic observation revealed that after treatment of 100 and 200 μg Ag@*Cf*L-NPs ml^{-1} to 2nd stage juveniles of *M. incognita* used a remarkable deformation in nematode structure (**Figures 4A–C**). Baronia et al. (2020) observed that direct exposure of Ag-NPs in a solution of water had strong nematicidal potential at low concentration against mortality of *M. graminicola* (J2) irreversibly within 12 h. In a similar study, exposure to Ag-NPs showed cell wall degradation under *in vitro* conditions and ultimately caused mortality of *M. incognita* at different exposure times (Hassan et al., 2016).

Assessing the disease suppressive and growth promotion potential of Ag@*Cf*L-NPs in tomato crop

The Ag@*Cf*L-NPs were drenched in the soil to assess the effectiveness of Ag@*Cf*L-NPs in controlling soil-borne plant pathogenic microbes and plant growth-promoting effects in tomatoes in terms of growth factors and disease development. In the present study, tomatoes were chosen because they are most susceptible to phytopathogens (bacteria, fungi, and nematodes). Fungal pathogens cause severe diseases in different edible crops, including tomatoes. *Pseudomonas syringae*, soil-borne plant pathogenic bacteria cause bacterial speck disease in tomatoes and other crops. The most damaging and destructive diseases of tomatoes are those produced by root-knot nematodes *Meloidogyne incognita*.

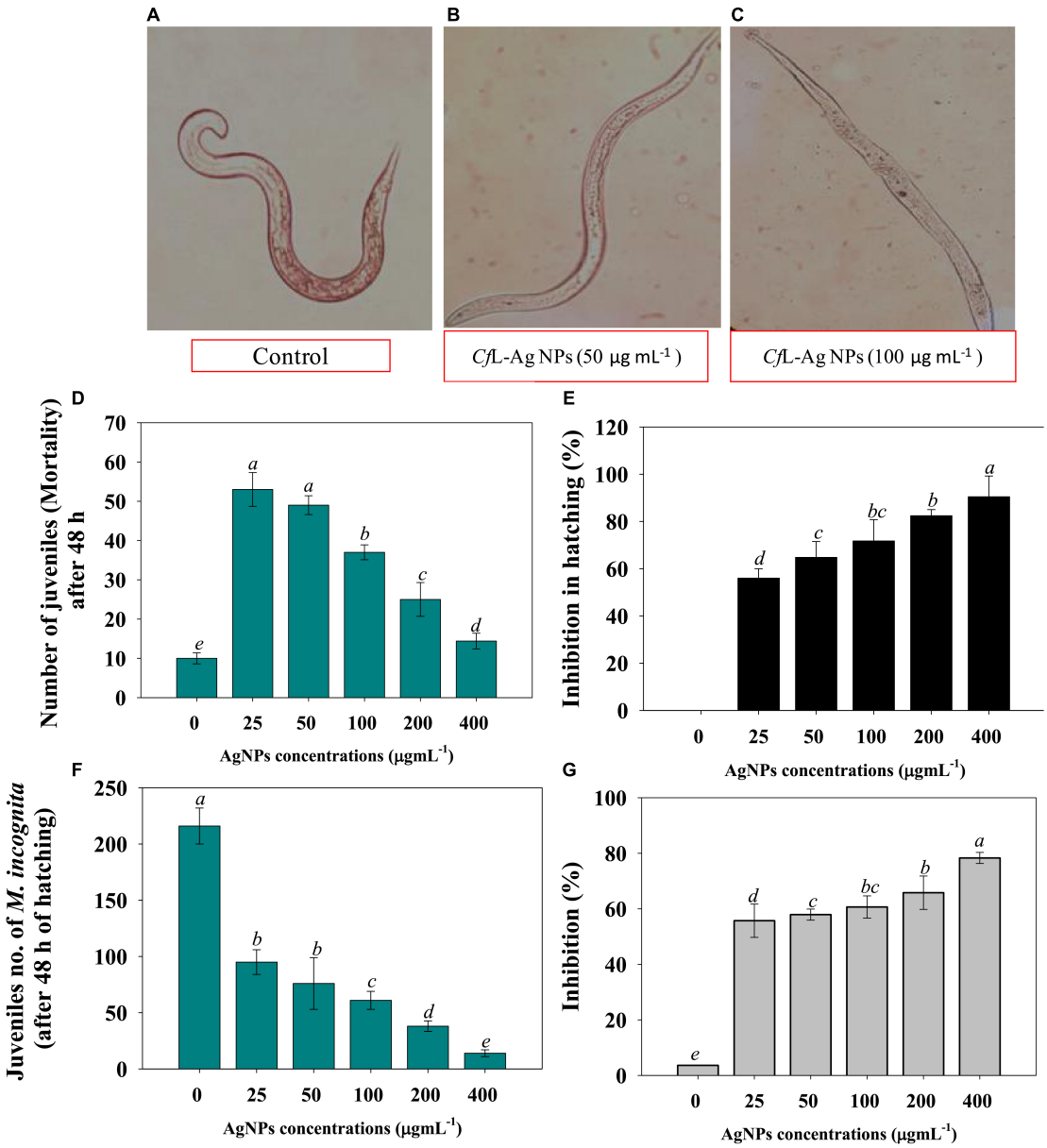

FIGURE 4
(A–C) Represent the microscopic examination of root-knot nematode *Meloidogyne incognita* treated with 0 (control), 50 and 100 µg Ag@*Cf*L-NPs ml^{-1}, respectively. **(D,E)** Shows the effect of Ag@*Cf*L-NP son number of juveniles of *M. incognita* after 48 h of hatching and percent inhibition in hatching, respectively. **(F,G)** Depicts the impact of green-synthesized Ag@*Cf*L-NP son number of juveniles (mortality) after 48 h and inhibition percentage, respectively. In this figure, bar diagrams represents the mean values of three replicates (n = 3). Corresponding error bars represents standard deviation (S.D) of three replicates (S.D, n = 3).

Effect of Ag@*Cf*L-NPs on biological attributes of tomatoes

Under phytopathogen-challenged conditions, the biological parameters of tomatoes were greatly reduced. For instance, dry biomass was reduced by 45, 56, and 67% when tomatoes were infected with *R. solani*, *P. syringae*, and *M. incognita*, respectively. However, findings showed that phytogenically synthesized Ag@*Cf*L-NPs greatly aided the tomato seedling

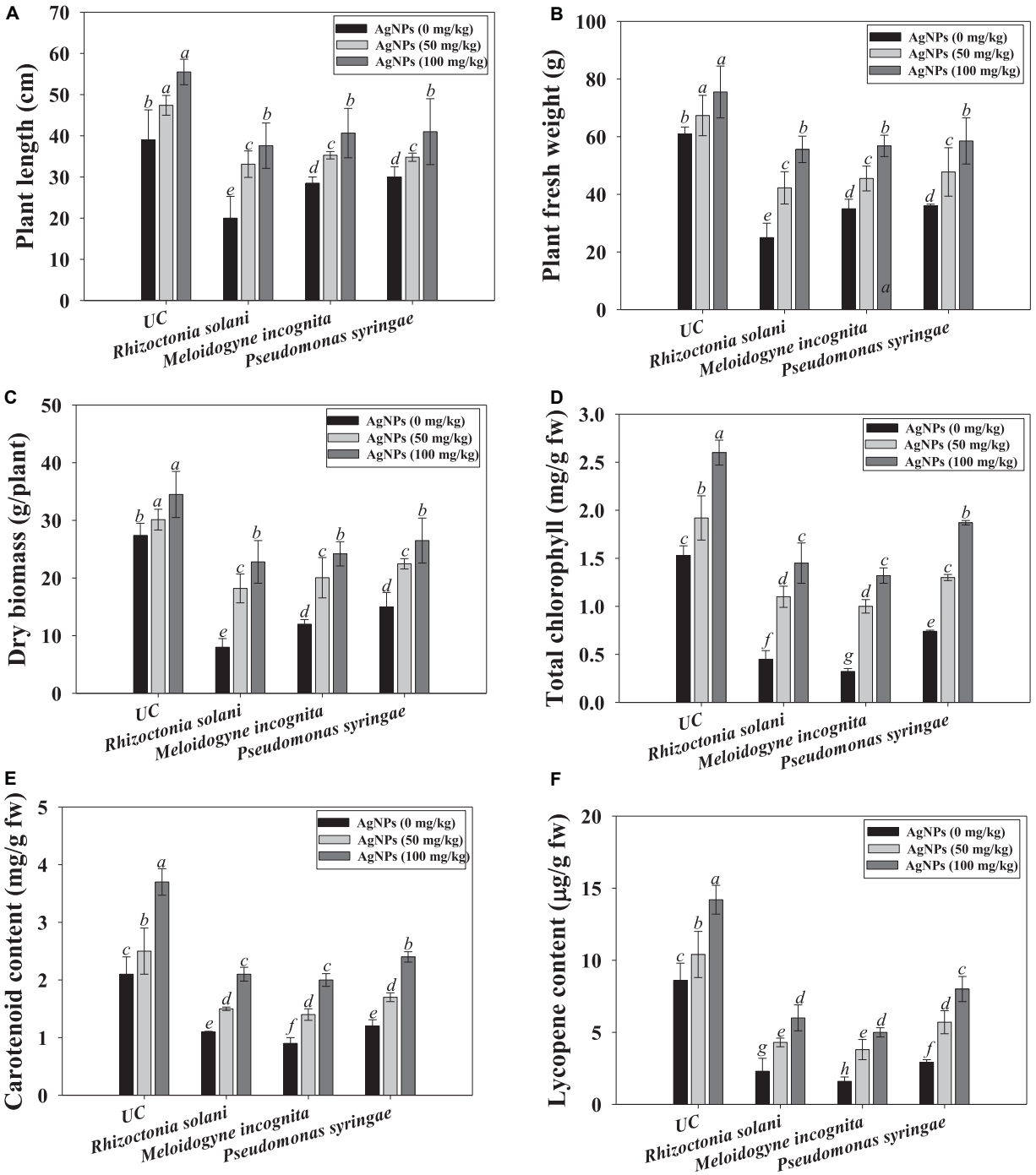

FIGURE 5
Effect of *Cassia fistula* leaf synthesized silver nanoparticles (Ag@*Cf*L-NPs) on biological and physiological parameters of tomato crop cultivated in pot-soils infected with phytopathogens; *R. solani* (fungi), *M. incognita* (root-knot nematodes) and *P. syringae* (bacteria): plant length **(A)**, fresh weight **(B)**, dry biomass **(C)**, total chlorophyll **(D)**, carotenoid content **(E)** and lycopene content **(F)**. In this figure, bar diagrams represents the mean values of three replicates (n = 3). Corresponding error bars represents standard deviation (S.D) of three replicates (S.D, n = 3).

development when compared to the pathogen-inoculated plants. The effects of Ag@*Cf*L-NPs on biological attributes *viz*., growth, length, and dry biomass were varied significantly. For example, at 100 mg Ag@*Cf*L-NPs kg^{-1}, plant length, and dry biomass of tomatoes were greatly increased by 66 and 58%, respectively, over NPs-untreated and pathogen infected plants (**Figures 5A–C**). The green synthesized Ag@*Cf*L-NPs reduced the growth of phytopathogens and improved the growth and biometric parameters of tomatoes cultivated even in pathogen-challenged plants. Previous research has found that green synthesized NPs including Ag-NPs have a favorable influence on plant development, which is consistent with the findings of this study. Plant resilience to stress may be improved by NPs with antioxidant enzyme capabilities, which improve the capacity of plants to scavenge ROS and hence reduce the yield losses (Zhang et al., 2018). In hydroponics studies, Liang et al. (2018) found that the Cos–La nanoparticles greatly improved the development of rice plant by increasing root length and fresh weight and ultimately improve the defense response. Similarly, varied concentrations of Ag-NPs encouraged the growth of tulip plants by raising the leaf greenness index, stomatal conductance, length and fresh weight of roots (Byczyńska et al., 2019).

Photosynthetic pigments and lycopene content

The ability of Ag@*Cf*L-NPs to maintain chlorophyll integrity suggests that following their application, the structure's defense mechanisms and photosynthetic pigments are activated in the tomatoes. The photosynthetic properties of tomato leaf were decreased when plants were grown in soil inoculated with phytopathogenic microbes. However, Ag@*Cf*L-NPs had a considerable and positive impact on the concentration of chlorophyll and carotenoids in tomato leaves. The 100 mg Ag@*Cf*L-NPs kg^{-1} treatment had the highest results in terms of chlorophyll and carotenoid concentration, outperforming control (**Figures 5D,E**).

Lycopene, a carotenoid found naturally in tomatoes, is also responsible for the production of antioxidant molecules. As a result, lycopene-rich meals are extremely healthy. Lycopene content was dramatically reduced when soil pathogenic microbes were inoculated to tomato crops. When Ag@*Cf*L-NPs were used instead of pathogen-infected treatment, the lycopene content of tomato fruit rose significantly. For instance, at 100 mg Ag@*Cf*L-NPs kg^{-1}, lycopene content in tomato fruits was increased by 43, 52, and 38% when applied to soils inoculated with *R. solani*, *P. syringae*, and *M. incognita*, respectively, over NP-untreated but inoculated plants (**Figure 5F**). Similar to our study, *Cassis fistula* leaf synthesized Cu oxide nanoparticles (CuO-CFNPs), improved the lycopene content in tomato fruits raised in soil infected with *Fusarium oxysporum* by inhibiting fungal growth (Ashraf et al., 2021).

Antioxidant enzymatic activity of Ag@*Cf*L-NPs-treated tomato plants

In this work, the synthesized silver nanoparticles (Ag@*Cf*L-NPs) generated a high antioxidant response in tomatoes against pathogen such as *P. syringae*, *R. solani*, and *M. incognita* by lowering their population in the soils and reducing the severity of diseases. The application of Ag@*Cf*L-NPs had a considerable impact on antioxidant enzymatic activities such as superoxide dismutase (SOD), peroxidase (POD), catalase (CAT), and phenylalanine ammonia lyase (PAL) accumulated in root tissues of tomatoes cultivated in phytopathogens-challenged soil system. The treatment of 100 mg Ag@*Cf*L-NPs kg^{-1} was constant, showing that all enzymes had their maximal activity. The enzyme peroxidase (POD) is accountable for controlling the metabolic activity, chlorophyll formation, respiration, substratum oxidation, growth development, and infections in plants (Danish et al., 2021b). POD is known to be involved in lignin production; they help plants defend themselves against infections by strengthening plant cell walls and conveying signals to other cells that are unaffected (Walters, 2011). Superoxide dismutase (SOD) could catalyze the conversion of O_2 to hydrogen peroxide (H_2O_2), providing an initial amount of protection against ROS, but antioxidant enzymes like POD, CAT, and APX were able to limit H_2O_2 build-up to a minimum, keeping plants safe from oxidative stress (Abedi and Pakniyat, 2010). For instance, CAT activity in Ag@*Cf*L-NPs-treated roots, the same findings were reported; treatment with 100 mg Ag@*Cf*L-NPs kg^{-1} was shown to be 61 percent better than control (**Figure 6A**). Additionally, among treatments, the maximum improvement of 47 and 60% in SOD (**Figure 6B**) and POD (**Figure 6C**) were recorded when 100 mg Ag@*Cf*L-NPs kg^{-1} was applied to *Pseudomonas syringae* challenged tomatoes over nanoparticles untreated and pathogen-infected plants. Likewise, phenylalanine ammonia-lyase (PAL) is an enzyme that triggers the plant defense responses in stressful situations; the creation of phenylpropanoid phytoalexins after fungal infection drives the fast production of PAL (MacDonald and D'Cunha, 2007). The Ag@*Cf*L-NPs at 100 mg kg^{-1} showed the maximum PAL activity in tomato plants, outperforming the control by 68% (**Figure 6D**). As a result, it is possible that an increase in PAL activity following the administration of Ag@*Cf*L-NPs. Furthermore, the reaction to antioxidant enzymes is dependent on a variety of parameters, including the kind of NP, the quantity of NPs, and the plant species; yet, the current findings are similar to Ashraf et al. (2021). Likewise, Danish et al. (2021b) observed substantial differences in the level of antioxidant enzymes (APX, POD, SOD, and CAT) in ajwain plants raised in soil exogenously inoculated with Ag-NPs and M. *incognita*.

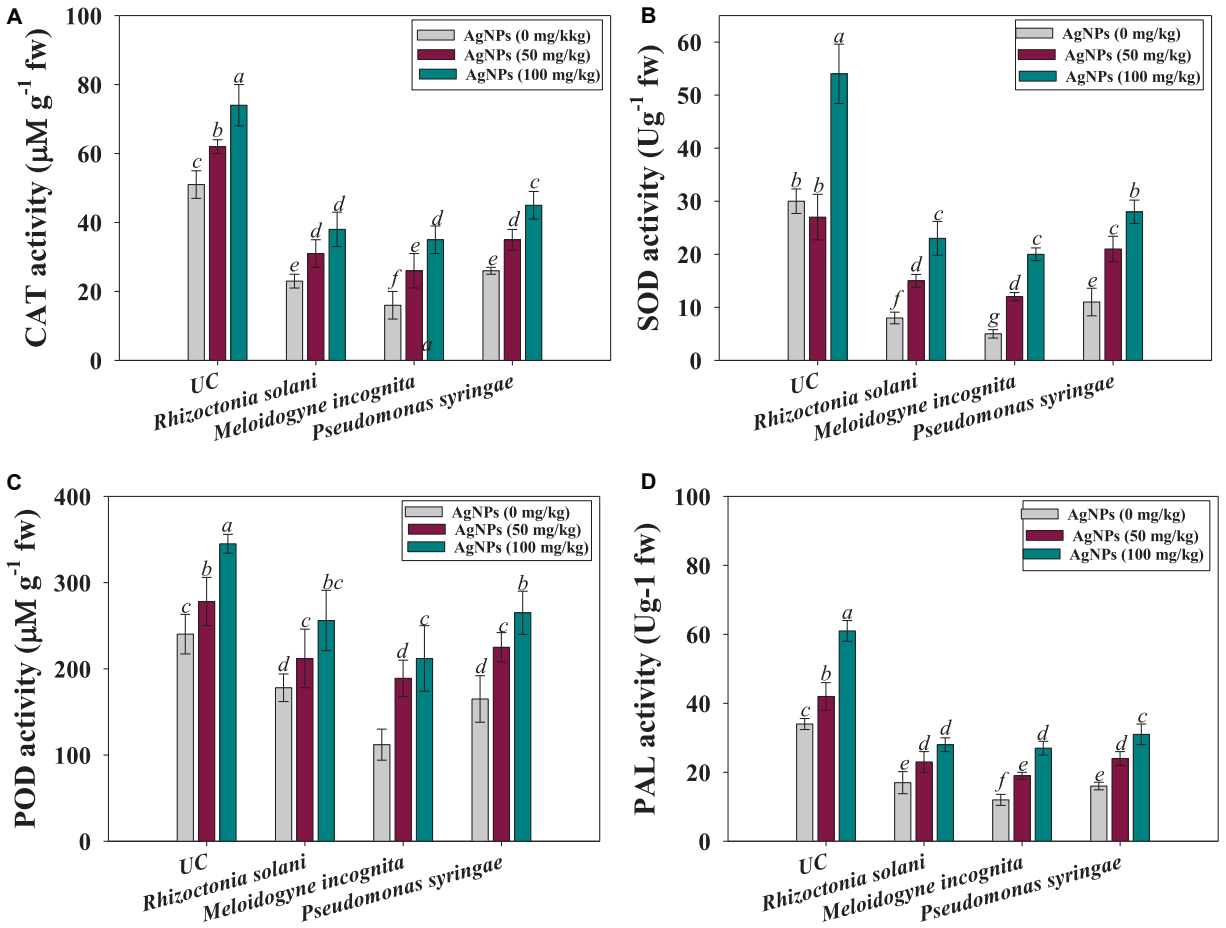

FIGURE 6
Effect of Ag@*Cf*L-NP son antioxidant enzymatic activities in leaf tissues of tomato crop cultivated in pot-soils infected with phytopathogens; *M. incognita* (root-knot nematodes) *P. syringae* (bacteria) and *R. solani* (fungi): catalase; CAT **(A)**, superoxide dismutase; SOD **(B)**, peroxidase; POD **(C)** and phenylalanine ammonia lyase; PAL **(D)**. In this figure, bar diagrams represents the mean values of three replicates (n = 3). Corresponding error bars represents standard deviation (S.D) of three replicates (S.D, n = 3).

Disease attributes (gall formation and disease incidence) in Ag@*Cf*L-NPs-treated tomatoes

Gall development was seen in tomatoes treated with root-knot nematode *M. incognita*. The number of galls was observed to be greatly reduced (76%) when tomatoes were treated with 100 mg Ag@*Cf*L-NPs kg^{-1} as compared to only *M. incognita*-infected plants (**Figures 7A,B**). The action of green synthesized Ag@*Cf*L-NPs, which boosts plant growth and development, was responsible for the decrease in gall number. Likewise, green synthesized Ag-NPs (which had not shown the phytotoxicity) have been reported to reduce the number of galls and suppressed the disease caused by root-knot nematode *M. javanica* in *Solanum melongena* (L.) plants (Abdellatif et al., 2016). In another study, green-synthesized Ag-NPs significantly reduced the disease attributes (galls number, egg masses, and root-knot index) in nematode infected *Solanum Lycopersicum* (L.) and improved the performance of plants (Hassan et al., 2016).

Furthermore, the incidence and severity of disease in tomato seedlings exposed to 50 and 100 mg kg^{-1} of synthesized Ag@*Cf*L-NPs, were evaluated. When compared to plants infected with *F. oxysporum* alone, the highest doses of Ag@*Cf*L-NPs (100 mg kg^{-1}) demonstrated considerable antifungal efficacy against *F. oxysporum*, reducing disease incidence (55% reduction), and disease severity (43% reduction) (**Figures 7C,D**). The primary motivation for using nanomaterials in agriculture practices is to combat diseases, which frequently include compounds with antibacterial capabilities that target soil-borne pathogens. This might be due to a reduction in the ability of pathogenic fungi to produce enzymes and toxins, both of which are necessary for disease development. In field research, Giannousi et al. (2013) found that nano-Cu was more efficient than typical Cu-based formulations that suppressing the development and damage caused by *Phytophthora infestans* in tomato plants.

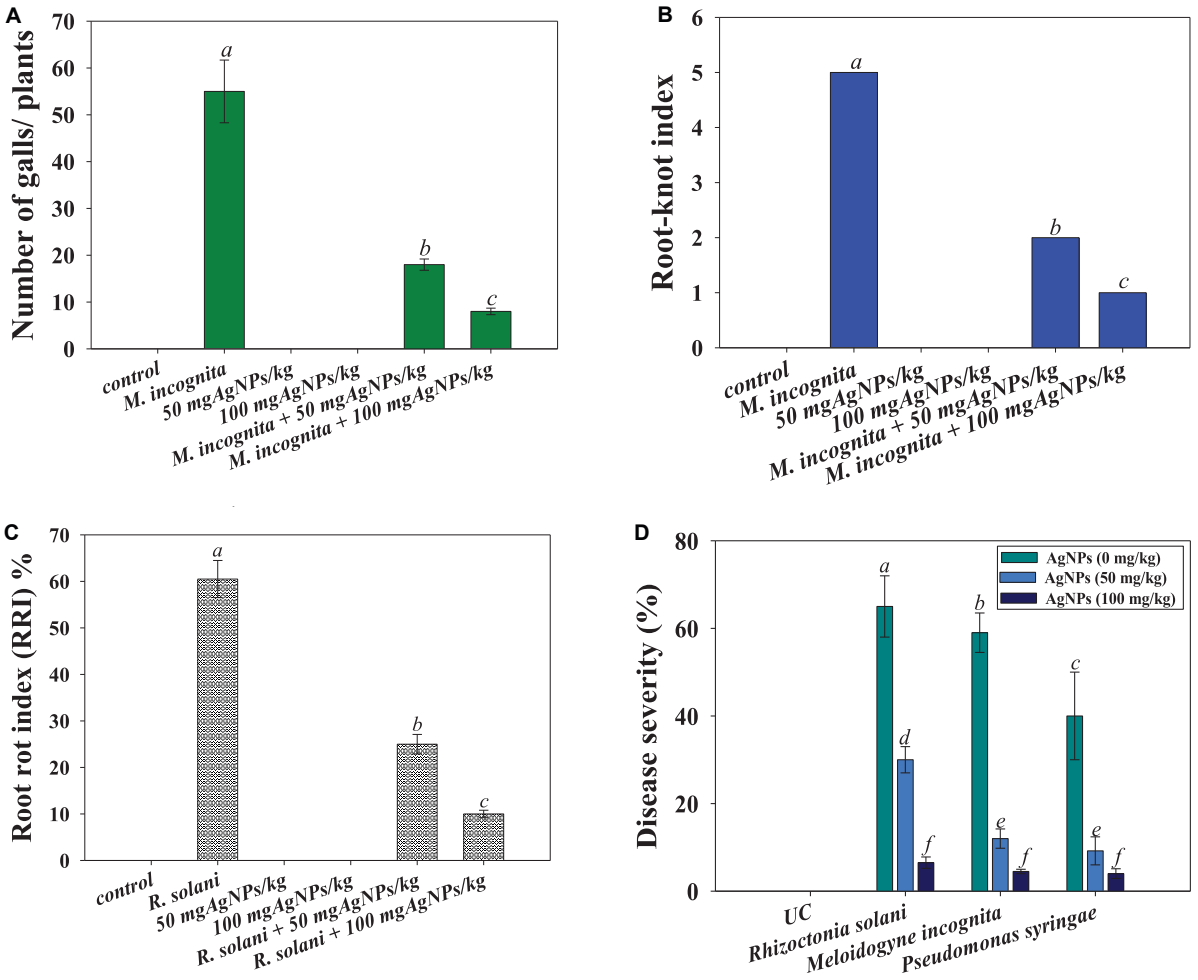

FIGURE 7
Effect of Ag@*Cf*L-NPs on number of galls caused by *M. incognita* **(A)**, root-knot index **(B)**, root-rot index **(C)** and percent disease severity **(D)** in tomato crop cultivated in pot and infected with phytopathogens; *P. syringae*, *M. incognita*, and *R. Solani*. In this figure, bar diagrams represent the mean values of three replicates (n = 3). Corresponding error bars represents standard deviation (SD) of three replicates (S.D, n = 3).

Conclusion

In order to reduce the use of hazardous synthetic chemicals, efficient nano-pesticides that can be synthesized from natural metabolites of plants are critical. We examined and analyzed the anti-phytopathogenic efficacy of phytogenically synthesized Ag@*Cf*L-NPs against *R. solani* (fungi), *P. syringae* (bacteria), and *M. incognita* (root-knot nematode) which adversely affect the growth and yield of agronomically important edible crops. The green synthesized Ag@*Cf*L-NPs represented bactericidal, fungicidal as well as nematicidal activity. Increasing doses of Ag@*Cf*L-NPs inhibited the biofilm formation, impaired membrane integrity, and altered the morphology of *P. syringae*. Furthermore, anti-nematicidal potential of Ag@*Cf*L-NPs displayed as reduction in egg hatching and a considerable increased in larval motility of *M. incognita*. Moreover, when grown in the presence of synthesized Ag@*Cf*L-NPs, micro-morphological characteristics of all tested fungal hyphae were changed. Additionally, nano-pesticidal potential of Ag@*Cf*L-NPs was proved when applied to phytopathogens-challenged tomato crops cultivated in pots. The Ag@*Cf*L-NPs suppressed the disease severity and improved the plant growth, biomass, photosynthetic capacity, lycopene content, and antioxidative properties of tomatoes. As a result of the present study, it appears that Ag@*Cf*L-NPs with sufficient anti-phytopathogenic capability might be utilized as a safe and effective alternative to chemical control measures (synthetic pesticides) for managing phytopathogens that cause significant losses in agricultural productivity in different agro-climatic conditions. However, more research in this area is needed to assess the level of phytotoxicity under field conditions, which must be carried out before recommending the application of nano-based commercial products.

Data availability statement

The original contributions presented in this study are included in the article/**Supplementary material**, further inquiries can be directed to the corresponding author.

Author contributions

MD and LA: conceptualization and investigation. MD, MS, LA, and KR: methodology and writing – original draft preparation. AA and MA-D: validation. MS, MD, and US: formal analysis. MS, US, and YA-W: resources. AM: funding. MS, US, and SD: writing – review and editing and manuscript revision. All authors contributed to the article and approved the submitted version.

Acknowledgments

MD and LA thank the chairperson of the Department of Botany, Aligarh Muslim University, Aligarh, India, for providing the laboratory and other necessary facilities. Sophisticated Instrument Facility (USIF), AMU is designated for TEM and SEM-EDX research, and also we extend our appreciation to the Researchers Supporting Project number (RSP-2021/316) at King Saud University, Riyadh, Saudi Arabia.

Conflict of interest

The authors declare that the research was conducted in the absence of any commercial or financial relationships that could be construed as a potential conflict of interest.

Publisher's note

All claims expressed in this article are solely those of the authors and do not necessarily represent those of their affiliated organizations, or those of the publisher, the editors and the reviewers. Any product that may be evaluated in this article, or claim that may be made by its manufacturer, is not guaranteed or endorsed by the publisher.

Supplementary material

The Supplementary Material for this article can be found online at: https://www.frontiersin.org/articles/10.3389/fmicb.2022.985852/full#supplementary-material

References

Abbasi, B. A., Iqbal, J., Nasir, J. A., Zahra, S. A., Shahbaz, A., Uddin, S., et al. (2020). Environmentally friendly green approach for the fabrication of silver oxide nanoparticles: characterization and diverse biomedical applications. *Microsc. Res. Techn.* 83, 1308–1320. doi: 10.1002/jemt.23522

Abdellatif, K. F., Abdelfattah, R. H., and El-Ansary, M. S. M. (2016). Green nanoparticles engineering on root-knot nematode infecting eggplants and their effect on plant DNA modification. *Iran. J. Biotech.* 14:250. doi: 10.15171/ijb.1309

Abedi, T., and Pakniyat, H. (2010). Antioxidant enzymes changes in response to drought stress in ten cultivars of oilseed rape (*Brassica napus* L.). *Czech J. Genet. Plant Breed.* 46, 27–34. doi: 10.17221/67/2009-CJGPB

Ahmad, A., Wei, Y., Syed, F., Tahir, K., Rehman, A. U., Khan, A., et al. (2017). The effects of bacteria-nanoparticles interface on the antibacterial activity of green synthesized silver nanoparticles. *Microb. Pathol.* 102, 133–142. doi: 10.1016/j.micpath.2016.11.030

Alam, M. M., Siddiqui, M. B., and Husain, W. (1990). Treatment of diabetes through herbal drugs in rural India. *Fitoterapia* 61, 240–242.

Ansari, M. A., Khan, H. M., Khan, A. A., Ahmad, M. K., Mahdi, A. A., Pal, R., et al. (2014). Interaction of silver nanoparticles with *Escherichia coli* and their cell envelope biomolecules. *J. Basic Microbiol.* 54, 905–915. doi: 10.1002/jobm.201300457

Ashraf, H., Anjum, T., Riaz, S., Ahmad, I. S., Irudayaraj, J., Javed, S., et al. (2021). Inhibition mechanism of green-synthesized copper oxide nanoparticles from *Cassia fistula* towards *Fusarium oxysporum* by boosting growth and defense response in tomatoes. *Environ. Sci. Nano* 8, 1729–1748. doi: 10.1039/D0EN01281E

Azam, A., Ahmed, A. S., Oves, M., Khan, M. S., and Memic, A. (2012). Size-dependent antimicrobial properties of CuO nanoparticles against Gram-positive and-negative bacterial strains. *Int. J Nanomed.* 7:3527. doi: 10.2147/IJN.S29020

Aziz, N., Faraz, M., Pandey, R., Shakir, M., Fatma, T., Varma, A., et al. (2015). Facile algae-derived route to biogenic silver nanoparticles: synthesis, antibacterial, and photocatalytic properties. *Langmuir* 31, 11605–11612. doi: 10.1021/acs.langmuir.5b03081

Baronia, R., Kumar, P., Singh, S. P., and Walia, R. K. (2020). Silver nanoparticles as a potential nematicide against. *J. Nematol.* 52, 1–9. doi: 10.21307/jofnem-2020-002

Bhalodia, N. R., Acharya, R. N., and Shukla, V. J. (2011). Evaluation of in vitro Antioxidant Activity of hydroalcoholic seed extratcs of *Cassia fistula* linn. *Free Radic. Antioxid.* 1, 68–76. doi: 10.5530/ax.2011.1.11

Bondarenko, O., Juganson, K., Ivask, A., Kasemets, K., Mortimer, M., and Kahru, A. (2013). Toxicity of Ag, CuO and ZnO nanoparticles to selected environmentally relevant test organisms and mammalian cells in vitro: a critical review. *Arch. Toxicol.* 87, 1181–1200. doi: 10.1007/s00204-013-1079-4

Byczyńska, A., Zawadzińska, A., and Salachna, P. (2019). Silver nanoparticles preplant bulb soaking affects tulip production. *Acta Agric. Scand. B Soil Plant Sci.* 69, 250–256. doi: 10.1080/09064710.2018.1545863

Chen, J., Li, S., Luo, J., Wang, R., and Ding, W. (2016). Enhancement of the antibacterial activity of silver nanoparticles against phytopathogenic bacterium *Ralstonia solanacearum* by stabilization. *J. Nanomaterials* 2016:7135852. doi: 10.1155/2016/7135852

Danish, M., Altaf, M., Robab, M. I., Shahid, M., Manoharadas, S., Hussain, S. A., et al. (2021a). Green synthesized silver nanoparticles mitigate biotic stress induced by Meloidogyne incognita in *Trachyspermum ammi* (L.) by improving growth, biochemical, and antioxidant enzyme activities. *ACS Omega* 6, 11389–11403. doi: 10.1021/acsomega.1c00375

Danish, M., Robab, M. I., Marraiki, N., Shahid, M., Zaghloul, N. S., Nishat, Y., et al. (2021b). Root-knot nematode *Meloidogyne incognita* induced changes in morpho-anatomy and antioxidant enzymes activities in *Trachyspermum ammi*

(L.) plant: a microscopic observation. *Physiol. Mol. Plant Pathol.* 116:101725. doi: 10.1016/j.pmpp.2021.101725

Das Purkayastha, M., and Manhar, A. K. (2016). Nanotechnological applications in food packaging, sensors and bioactive delivery systems. *Nanosci. Food Agric.* 2, 59–128. doi: 10.1007/978-3-319-39306-3_3

Denny, T. (2007). "Plant pathogenic Ralstonia species," in *Plant-Associated Bacteria*, ed. S. S. Gnanamanickam (Dordrecht: Springer), 573–644. doi: 10.1007/978-1-4020-4538-7_16

Deshpande, P., Dapkekar, A., Oak, M. D., Paknikar, K. M., and Rajwade, J. M. (2017). Zinc complexed chitosan/TPP nanoparticles: a promising micronutrient nanocarrier suited for foliar application. *Carbohydr. Polym.* 165, 394–401. doi: 10.1016/j.carbpol.2017.02.061

Devaraj, P., Kumari, P., Aarti, C., and Renganathan, A. (2013). Synthesis and characterization of silver nanoparticles using cannonball leaves and their cytotoxic activity against MCF-7 cell line. *J. Nanotech.* 2013:598328. doi: 10.1155/2013/598328

Duraipandiyan, V., and Ignacimuthu, S. (2007). Antibacterial and antifungal activity of *Cassia fistula* L.: an ethnomedicinal plant. *J. Ethnopharm.* 112, 590–594. doi: 10.1016/j.jep.2007.04.008

Dwivedi, S., Wahab, R., Khan, F., Mishra, Y. K., Musarrat, J., and Al-Khedhairy, A. A. (2014). Reactive oxygen species mediated bacterial biofilm inhibition via zinc oxide nanoparticles and their statistical determination. *PLoS One* 9:e111289. doi: 10.1371/journal.pone.0111289

Elgorban, A. M., El-Samawaty, A. E. R. M., Yassin, M. A., Sayed, S. R., Adil, S. F., Elhindi, K. M., et al. (2016). Antifungal silver nanoparticles: synthesis, characterization and biological evaluation. *Biotechnol. Biotechnol. Equipment* 30, 56–62. doi: 10.1080/13102818.2015.1106339

Elmer, W. H., and White, J. C. (2016). The use of metallic oxide nanoparticles to enhance growth of tomatoes and eggplants in disease infested soil or soilless medium. *Environ. Sci. Nano* 3, 1072–1079. doi: 10.1039/C6EN00146G

Erci, F., Cakir-Koc, R., and Isildak, I. (2018). Green synthesis of silver nanoparticles using *Thymbra spicata* L. var. spicata (zahter) aqueous leaf extract and evaluation of their morphology-dependent antibacterial and cytotoxic activity. *Artif. Cells Nanomed. Biotechnol.* 46, 150–158. doi: 10.1080/21691401.2017.1415917

Fahimirad, S., Ajalloueian, F., and Ghorbanpour, M. (2019). Synthesis and therapeutic potential of silver nanomaterials derived from plant extracts. *Ecotoxicol. Environ. Saf.* 168, 260–278. doi: 10.1016/j.ecoenv.2018.10.017

Giannopolitis, C. N., and Ries, S. K. (1977). Superoxide dismutases: II. Purification and quantitative relationship with water-soluble protein in seedlings. *Plant Physiol.* 59, 315–318. doi: 10.1104/pp.59.2.315

Giannousi, K., Avramidis, I., and Dendrinou-Samara, C. (2013). Synthesis, characterization and evaluation of copper-based nanoparticles as agrochemicals against *Phytophthora infestans*. *RSC Adv.* 3, 21743–21752. doi: 10.1039/c3ra42118j

Haggag, E. G., Elshamy, A. M., Rabeh, M. A., Gabr, N. M., Salem, M., Youssif, K. A., et al. (2019). Antiviral potential of green synthesized silver nanoparticles of *Lampranthus coccineus* and *Malephora lutea*. *Int. J. Nanomed.* 14:6217. doi: 10.2147/IJN.S214171

Hamed, S. M., Hagag, E. S., and El-Raouf, N. A. (2019). Green production of silver nanoparticles, evaluation of their nematicidal activity against Meloidogyne javanica and their impact on growth of faba bean. *Beni Suef Univ. J. Basic Appl. Sci.* 8, 1–12. doi: 10.1186/s43088-019-0010-3

Hassan, M. E., Zawam, H. S., El-Nahas, S. E., and Desoukey, A. F. (2016). Comparison study between silver nanoparticles and two nematicides against Meloidogyne incognita on tomato seedlings. *Plant Path. J.* 15, 144–151. doi: 10.3923/ppj.2016.144.151

He, D. C., Zhan, J. S., and Xie, L. H. (2016). Problems, challenges and future of plant disease management: from an ecological point of view. *J. Integ. Agric.* 15, 705–715. doi: 10.1016/S2095-3119(15)61300-4

He, L., Liu, Y., Mustapha, A., and Lin, M. (2011). Antifungal activity of zinc oxide nanoparticles against *Botrytis cinerea* and *Penicillium expansum*. *Microbiol. Res.* 166, 207–215. doi: 10.1016/j.micres.2010.03.003

Ingle, A. P., Biswas, A., Vanlalveni, C., Lalfakzuala, R., Gupta, I., Ingle, P., et al. (2020). Biogenic synthesis of nanoparticles and their role in the management of plant pathogenic fungi. *Microb. Nanotech.* 8, 135–161. doi: 10.4324/9780429276330-8

Jagtap, U. B., and Bapat, V. A. (2013). Green synthesis of silver nanoparticles using *Artocarpus heterophyllus* Lam. seed extract and its antibacterial activity. *Indus. Crops Products* 46, 132–137. doi: 10.1016/j.indcrop.2013.01.019

Jalal, M., Ansari, M. A., Ali, S. G., Khan, H. M., Eldaif, W. A., and Alrumman, S. A. (2016). Green synthesis of silver nanoparticles using leaf extract of *Cinnamomum tamala* and its antimicrobial activity against clinical isolates of bacteria and fungi. *Int. J. Adv. Res.* 4, 428–440. doi: 10.21474/IJAR01/2412

Jones, J. T., Haegeman, A., Danchin, E. G., Gaur, H. S., Helder, J., Jones, M. G., et al. (2013). Top 10 plant-parasitic nematodes in molecular plant pathology. *Mol. Plant Pathol.* 14, 946–961. doi: 10.1111/mpp.12057

Jyoti, K., Baunthiyal, M., and Singh, A. (2016). Characterization of silver nanoparticles synthesized using *Urtica dioica* Linn. leaves and their synergistic effects with antibiotics. *J. Radiation Res. Appl. Sci.* 9, 217–227. doi: 10.1016/j.jrras.2015.10.002

Kanaujiya, D., Kumar, V., Dwivedi, S. K., and Prasad, G. (2020). Photobiosynthesis of silver nanoparticle using extract of *Aspergillus flavus* CR500: its characterization, antifungal activity and mechanism against *Sclerotium rolfsii* and *Rhizoctonia solani*. *J. Cluster Sci.* 31, 1041–1050. doi: 10.1007/s10876-019-01709-2

Kaur, P., Thakur, R., and Choudhary, A. (2012). An in vitro study of the antifungal activity of silver/chitosan nano-formulations against important seed borne pathogens. *Int. J. Sci. Technol. Res.* 1, 83–86.

Kaur, S., Kang, S. S., Dhillon, N. K., and Sharma, A. (2016). Detection and characterization of Meloidogyne species associated with pepper in Indian Punjab. *Nematropica* 46, 209–220.

Khan, S., Shahid, M., Khan, M. S., Syed, A., Bahkali, A. H., Elgorban, A. M., et al. (2020). Fungicide-tolerant plant growth-promoting rhizobacteria mitigate physiological disruption of white radish caused by fungicides used in the field cultivation. *Int. J. Environ. Res. Public Health* 17:7251. doi: 10.3390/ijerph17197251

Ku, S., You, H. J., Park, M. S., and Ji, G. E. (2015). Effects of ascorbic acid on α-L-arabinofuranosidase and α-L-arabinopyranosidase activities from *Bifidobacterium longum* RD47 and its application to whole cell bioconversion of ginsenoside. *J. Korean Sociol. Appl. Biol. Chem.* 58, 857–865. doi: 10.1007/s13765-015-0113-z

Lapresta-Fernández, A., Fernández, A., and Blasco, J. (2012). Nanoecotoxicity effects of engineered silver and gold nanoparticles in aquatic organisms. *Trends Analytic Chem.* 32, 40–59. doi: 10.1016/j.trac.2011.09.007

Liang, W., Yu, A., Wang, G., Zheng, F., Hu, P., Jia, J., et al. (2018). A novel water-based chitosan-La pesticide nanocarrier enhancing defense responses in rice (*Oryza sativa* L) growth. *Carbohydr. Polym.* 199, 437–444. doi: 10.1016/j.carbpol.2018.07.042

MacDonald, M. J., and D'Cunha, G. B. (2007). A modern view of phenylalanine ammonia lyase. *Biochem. Cell Biol.* 85, 273–282. doi: 10.1139/O07-018

MacKinney, G. (1941). Absorption of light by chlorophyll solutions. *J. Biol. Chem.* 140, 315–322. doi: 10.1016/S0021-9258(18)51320-X

Malhi, G. S., Kaur, M., and Kaushik, P. (2021). Impact of climate change on agriculture and its mitigation strategies: a review. *Sustainable* 13:1318. doi: 10.3390/su13031318

Manikprabhu, D., and Lingappa, K. (2013). Microwave assisted rapid bio-based synthesis of gold nanorods using pigment produced by *Streptomyces coelicolor* klmp33. *Acta Metallurgica Sin.* 26, 613–617. doi: 10.1007/s40195-013-0217-6

Manonmani, G., Bhavapriya, V., Kalpana, S., Govindasamy, S., and Apparanantham, T. (2005). Antioxidant activity of *Cassia fistula* (Linn.) flowers in alloxan induced diabetic rats. *J. Ethnopharma* 97, 39–42. doi: 10.1016/j.jep.2004.09.051

Marpu, S., Kolailat, S. S., Korir, D., Kamras, B. L., Chaturvedi, R., Joseph, A., et al. (2017). Photochemical formation of chitosan-stabilized near-infrared-absorbing silver Nanoworms: a "Green" synthetic strategy and activity on Gram-negative pathogenic bacteria. *J. Colloid Interface Sci.* 507, 437–452. doi: 10.1016/j.jcis.2017.08.009

Mishra, S., Yang, X., Ray, S., Fraceto, L. F., and Singh, H. B. (2020). Antibacterial and biofilm inhibition activity of biofabricated silver nanoparticles against *Xanthomonas oryzae* pv. oryzae causing blight disease of rice instigates disease suppression. *World J. Microbiol. Biotech.* 36, 1–10. doi: 10.1007/s11274-020-02826-1

Mohammed, A. F., Oloyede, A. R., and Odeseye, A. O. (2020). Biological control of bacterial wilt of tomato caused by *Ralstonia solanacearum* using *Pseudomonas* species isolated from the rhizosphere of tomato plants. *Arch. Phytopathol. Plant Protec.* 53, 1–16. doi: 10.1080/03235408.2020.1715756

Nisar, P., Ali, N., Rahman, L., Ali, M., and Shinwari, Z. K. (2019). Antimicrobial activities of biologically synthesized metal nanoparticles: an insight into the mechanism of action. *J. Biol. Inorgan. Chem.* 24, 929–941. doi: 10.1007/s00775-019-01717-7

Nour, S., Baheiraei, N., Imani, R., Khodaei, M., Alizadeh, A., Rabiee, N., et al. (2019). A review of accelerated wound healing approaches: biomaterial-assisted

tissue remodeling. *J. Mater. Sci. Mater. Med.* 30, 1–15. doi: 10.1007/s10856-019-6319-6

Oves, M., Aslam, M., Rauf, M. A., Qayyum, S., Qari, H. A., Khan, M. S., et al. (2018). Antimicrobial and anticancer activities of silver nanoparticles synthesized from the root hair extract of *Phoenix dactylifera*. *Mater. Sci. Eng. C* 89, 429–443. doi: 10.1016/j.msec.2018.03.035

Popoola, A. R., Durosomo, A. H., Afolabi, C. G., and Idehen, E. O. (2015). Regeneration of somaclonal variants of tomato (*Solanum lycopersicum* L.) for resistance to fusarium wilt. *J. Crop Improv.* 29, 636–649. doi: 10.1080/15427528.2015.1066287

Qais, F. A., Shafiq, A., Ahmad, I., Husain, F. M., Khan, R. A., and Hassan, I. (2020). Green synthesis of silver nanoparticles using *Carum copticum*: assessment of its quorum sensing and biofilm inhibitory potential against gram negative bacterial pathogens. *Microb. Pathogol.* 144:104172. doi: 10.1016/j.micpath.2020.104172

Rajan, R., Chandran, K., Harper, S. L., Yun, S. I., and Kalaichelvan, P. T. (2015). Plant extract synthesized silver nanoparticles: an ongoing source of novel biocompatible materials. *Indus. Crops Prod.* 70, 356–373. doi: 10.1016/j.indcrop.2015.03.015

Ramzan, M., Sana, S., Javaid, N., Shah, A. A., Ejaz, S., Malik, W. N., et al. (2021). Mitigation of bacterial spot disease induced biotic stress in *Capsicum annuum* L. cultivars via antioxidant enzymes and isoforms. *Sci. Rep.* 11, 1–10. doi: 10.1038/s41598-021-88797-1

Remya, R. R., Rajasree, S. R., Aranganathan, L., and Suman, T. Y. (2015). An investigation on cytotoxic effect of bioactive AgNPs synthesized using *Cassia fistula* flower extract on breast cancer cell MCF-7. *Biotech. Rep.* 8, 110–115. doi: 10.1016/j.btre.2015.10.004

Rezazadeh, N. H., Buazar, F., and Matroodi, S. (2020). Synergistic effects of combinatorial chitosan and polyphenol biomolecules on enhanced antibacterial activity of biofunctionalized silver nanoparticles. *Sci. Rep.* 10, 1–13. doi: 10.1038/s41598-020-76726-7

Rivas-Cáceres, R. R., Stephano-Hornedo, J. L., Lugo, J., Vaca, R., Del Aguila, P., Yañez-Ocampo, G., et al. (2018). Bactericidal effect of silver nanoparticles against propagation of *Clavibacter michiganensis* infection in *Lycopersicon esculentum* Mill. *Microb. Pathog.* 115, 358–362. doi: 10.1016/j.micpath.2017.12.075

Rudakiya, D. M., and Pawar, K. (2017). Bactericidal potential of silver nanoparticles synthesized using cell-free extract of *Comamonas acidovorans*: in vitro and in silico approaches. *3 Biotech* 7, 1–12. doi: 10.1007/s13205-017-0728-3

Servin, A., Elmer, W., Mukherjee, A., La Torre-Roche, D., Hamdi, H., White, J. C., et al. (2015). A review of the use of engineered nanomaterials to suppress plant disease and enhance crop yield. *J. Nanoparticle Res.* 17, 1–21. doi: 10.1007/s11051-015-2907-7

Shahid, M., and Khan, M. S. (2018). Cellular destruction, phytohormones and growth modulating enzymes production by *Bacillus subtilis* strain BC8 impacted by fungicides. *Pesticide Biochem. Physiol.* 149, 8–19. doi: 10.1016/j.pestbp.2018.05.001

Shahid, M., Manoharadas, S., Altaf, M., and Alrefaei, A. F. (2021a). Organochlorine pesticides negatively influenced the cellular growth, morpho-structure, cell viability, and biofilm-formation and phosphate-solubilization activities of *Enterobacter cloacae* strain EAM 35. *ACS Omega* 6, 5548–5559. doi: 10.1021/acsomega.0c05931

Shahid, M., Manoharadas, S., Chakdar, H., Alrefaei, A. F., Albeshr, M. F., and Almutairi, M. H. (2021b). Biological toxicity assessment of carbamate pesticides using bacterial and plant bioassays: an in-vitro approach. *Chemosphere* 278:130372. doi: 10.1016/j.chemosphere.2021.130372

Shahid, M., Zaidi, A., Ehtram, A., and Khan, M. S. (2019). In vitro investigation to explore the toxicity of different groups of pesticides for an agronomically important rhizosphere isolate *Azotobacter vinelandii*. *Pesticide Biochem. Physiol.* 157, 33–44. doi: 10.1016/j.pestbp.2019.03.006

Sigamoney, M., Shaik, S., Govender, P., and Krishna, S. B. N. (2016). African leafy vegetables as bio-factories for silver nanoparticles: a case study on *Amaranthus dubius* C Mart. Ex Thell. *S. Afr. J. Bot.* 103, 230–240. doi: 10.1016/j.sajb.2015.08.022

Singh, R., Sahu, S. K., and Thangaraj, M. (2014). Biosynthesis of silver nanoparticles by marine invertebrate (polychaete) and assessment of its efficacy against human pathogens. *J. Nanoparticles* 2014:718240. doi: 10.1155/2014/718240

Singh, V. K., Singh, A. K., and Kumar, A. (2017). Disease management of tomato through PGPB: current trends and future perspective. *3 Biotech* 7:255. doi: 10.1007/s13205-017-0896-1

Solekha, R., Susanto, F. A., Joko, T., Nuringtyas, T. R., and Purwestri, Y. A. (2020). Phenylalanine ammonia lyase (PAL) contributes to the resistance of black rice against *Xanthomonas oryzae* pv. oryzae. *J. Plant Pathol.* 102, 359–365. doi: 10.1007/s42161-019-00426-z

Stiefel, P., Schmidt-Emrich, S., Maniura-Weber, K., and Ren, Q. (2015). Critical aspects of using bacterial cell viability assays with the fluorophores SYTO9 and propidium iodide. *BMC Microbiol.* 15:36. doi: 10.1186/s12866-015-0376-x

Sumitha, S., Vasanthi, S., Shalini, S., Chinni, S. V., Gopinath, S. C., Anbu, P., et al. (2018). Phyto-mediated photo catalysed green synthesis of silver nanoparticles using Durio zibethinus seed extract: antimicrobial and cytotoxic activity and photocatalytic applications. *Molecules* 23:3311. doi: 10.3390/molecules23123311

Syed, A., Zeyad, M. T., Shahid, M., Elgorban, A. M., Alkhulaifi, M. M., and Ansari, I. A. (2021). Heavy metals induced modulations in growth, physiology, cellular viability, and biofilm formation of an identified bacterial isolate. *ACS Omega* 6, 25076–25088. doi: 10.1021/acsomega.1c04396

Toksha, B., Sonawale, V. A. M., Vanarase, A., Bornare, D., Tonde, S., Hazra, C., et al. (2021). Nano-fertilizers: a review on synthesis and impact of their use on crop yield and environment. *Environ. Technol. Innov.* 24:101986. doi: 10.1016/j.eti.2021.101986

Walters, D. (2011). *Plant Defense: Warding Off Attack by Pathogens, Herbivores and Parasitic Plants*. Hoboken, NJ: John Wiley & Sons. doi: 10.1002/9781444328547

Wu, T., Shen, H., Sun, L., Cheng, B., Liu, B., and Shen, J. (2012). Facile synthesis of Ag interlayer doped graphene by chemical vapor deposition using polystyrene as solid carbon source. *ACS Appl. Mater. Interfaces* 4, 2041–2047. doi: 10.1021/am300014c

Wubie, M., and Temesgen, Z. (2019). Resistance mechanisms of tomato (*Solanum lycopersicum*) to root-knot nematodes (Meloidogyne species). *J. Plant Breed. Crop Sci.* 11, 33–40. doi: 10.5897/JPBCS2018.0780

Zhang, H., Du, W., Peralta-Videa, J. R., Gardea-Torresdey, J. L., White, J. C., Keller, A., et al. (2018). Metabolomics reveals how cucumber (*Cucumis sativus*) reprograms metabolites to cope with silver ions and silver nanoparticle-induced oxidative stress. *Environ. Sci. Technol.* 52, 8016–8026. doi: 10.1021/acs.est.8b02440

Zhang, X. F., Liu, Z. G., Shen, W., and Gurunathan, S. (2016). Silver nanoparticles: synthesis, characterization, properties, applications, and therapeutic approaches. *Int. J Mol. Sci.* 17:1534. doi: 10.3390/ijms17091534

Zia, F., Ghafoor, N., Iqbal, M., and Mehboob, S. (2016). Green synthesis and characterization of silver nanoparticles using Cydonia oblong seed extract. *Appl. Nanosci.* 6, 1023–1029. doi: 10.1007/s13204-016-0517-z

frontiers | Frontiers in Microbiology

TYPE Original Research
PUBLISHED 08 September 2022
DOI 10.3389/fmicb.2022.998546

Check for updates

OPEN ACCESS

EDITED BY
Avinash Bapurao Ade,
Savitribai Phule Pune University, India

REVIEWED BY
Bilal Ahmed,
Yeungnam University,
South Korea
Akhilesh Yadav,
University of California, Davis,
United States

*CORRESPONDENCE
Murugan Kumar
kumar.m@icar.gov.in;
kumarmic84@gmail.com

†These authors have contributed equally to this work and share first authorship

SPECIALTY SECTION
This article was submitted to Microbiotechnology, a section of the journal Frontiers in Microbiology

RECEIVED 20 July 2022
ACCEPTED 12 August 2022
PUBLISHED 08 September 2022

CITATION
Zeyad MT, Tiwari P, Ansari WA, Kumar SC, Kumar M, Chakdar H, Srivastava AK, Singh UB and Saxena AK (2022) Bio-priming with a consortium of *Streptomyces araujoniae* strains modulates defense response in chickpea against *Fusarium* wilt. *Front. Microbiol.* 13:998546. doi: 10.3389/fmicb.2022.998546

COPYRIGHT
© 2022 Zeyad, Tiwari, Ansari, Kumar, Kumar, Chakdar, Srivastava, Singh and Saxena. This is an open-access article distributed under the terms of the Creative Commons Attribution License (CC BY). The use, distribution or reproduction in other forums is permitted, provided the original author(s) and the copyright owner(s) are credited and that the original publication in this journal is cited, in accordance with accepted academic practice. No use, distribution or reproduction is permitted which does not comply with these terms.

Bio-priming with a consortium of *Streptomyces araujoniae* strains modulates defense response in chickpea against *Fusarium* wilt

Mohammad Tarique Zeyad†, Pushpendra Tiwari†, Waquar Akhter Ansari, Shiv Charan Kumar, Murugan Kumar*, Hillol Chakdar, Alok Kumar Srivastava, Udai B. Singh and Anil Kumar Saxena

ICAR-National Bureau of Agriculturally Important Microorganisms, Mau, Uttar Pradesh, India

Wilt caused by *Fusarium oxysporum* f. sp. *ciceris* (Foc) is one of the major diseases of chickpea affecting the potential yield significantly. Productivity and biotic stress resilience are both improved by the association and interaction of *Streptomyces* spp. with crop plants. In the present study, we evaluated two *Streptomyces araujoniae* strains (TN11 and TN19) for controlling the wilt of chickpea individually and as a consortium. The response of Foc challenged chickpea to inoculation with *S. araujoniae* TN11 and TN19 individually and as a consortium was recorded in terms of changes in physio-biochemical and expression of genes coding superoxide dismutase (SOD), peroxidase, and catalase. Priming with a consortium of TN11 and TN19 reduced the disease severity by 50–58% when challenged with Foc. Consortium primed-challenged plants recorded lower shoot dry weight to fresh weight ratio and root dry weight to fresh weight ratio as compared to challenged non-primed plants. The pathogen-challenged consortium primed plants recorded the highest accumulation of proline and electrolyte leakage. Similarly, total chlorophyll and carotenoids were recorded highest in the consortium treatment. Expression of genes coding SOD, peroxidase, and catalase was up-regulated which corroborated with higher activities of SOD, peroxidase, and catalase in consortium primed-challenged plants as compared to the challenged non-primed plants. Ethyl acetate extracts of TN11 and TN19 inhibited the growth of fungal pathogens *viz.*, *Fusarium oxysporum* f. sp. *ciceris*. *Macrophomina phaseolina, F. udum,* and *Sclerotinia sclerotiarum* by 54–73%. LC–MS analyses of the extracts showed the presence of a variety of antifungal compounds like erucamide and valinomycin in TN11 and valinomycin and dinactin in TN19. These findings suggest that the consortium of two strains of *S. araujoniae* (TN11 and TN19) can modulate defense response in chickpea against wilt and can be explored as a biocontrol strategy.

KEYWORDS

bio-priming, chickpea, consortium, disease alleviation, *Streptomyces araujoniae*

Introduction

Chickpea is an important leguminous crop in India with a 70% share in global production and 71% share in the global area. Although India ranks first in the area under cultivation and total production, the country's productivity (1,063 kg/ha) is much lower compared to many other countries (Lake and Sadras, 2014; Samriti et al., 2020). Lower productivity is attributed to poor adaptation of improved varieties and production technologies by farmers, drought during critical periods of crop growth (Muehe et al., 2019), and a series of biotic stressors like insect pests, and plant diseases (Ankati et al., 2021). Globally, crop growth and production have always been at risk from plant diseases, which obstruct physiological processes like photosynthesis, cell division, water transport, growth, and development. According to estimates, these phytopathogens are responsible for roughly 12.5% of all crop losses worldwide. The fungi are the most harmful phytopathogens, and they can cause 65% loss in plants (Fisher et al., 2012). As per the food and agriculture organization corporate statistical database (FAOSTAT), at the global level, most of the economically important crops are affected by fungi. Numerous fungal diseases have increased in frequency under the current climate change scenario. (Garcia-Solache and Casadevall, 2010). To ensure a steady supply of food for the growing global population, management of these fungal diseases is essential.

Among the different biotic stressors experienced by chickpea during its growth phase, wilt caused by *Fusarium oxysporum* f. sp. *ciceris* (Foc) can lead to high yield loss to complete crop failure under favorable conditions. Foc is both soil-borne and seed-borne and can survive as long as 6 years in the soil even without a susceptible host (Nikam et al., 2007). The use of resistant varieties, one of the most economical and practical solutions for managing fungal diseases, did not result in the successful management of Foc due to the availability of eight pathogenic races (Nikam et al., 2007; Ankati et al., 2021). Other management practices like soil solarization and early sowing have all gone in vain (Ankati et al., 2021). Although some successes have been achieved in controlling this disease using chemical fungicides (Jamil and Ashraf, 2020), the use of chemical fungicides can lead to environmental issues. Under such a scenario it is only pragmatic to look for safe and eco-friendly measures of disease management, i.e., biological control. A variety of commercial formulations based on *Trichoderma* spp. and *Pseudomonas fluorescens* are available in the market to control Foc. There are many reports available on the biocontrol of Foc using different bacterial and fungal agents like *Bacillus* spp. *Pseudomonas* spp. *Trichoderma* spp. *Paenibacillus polymyxa* and non-pathogenic Foc (Jiménez-Díaz et al., 2015). Over the last decade, there is an increased interest in the search for new biocontrol agents with better efficiency, adaptation, and colonization. Due to their diversity and potential to create unique antibiotics, antifungal metabolites, and extracellular enzymes, actinomycetes are the most economically and biotechnologically valuable prokaryotes (Mohite et al., 2019; Savi et al., 2019). Actinomycetes inhabiting various rhizosphere soils have also been reported to produce active biomolecules which promote plant growth like phytohormones, siderophores, iron chelators, and organic acids (Anwar et al., 2016). Various actinomycetes, mainly belonging to the *Streptomyces* genus have been reported as antifungal agents that can prevent the growth of plant pathogenic fungi (Palla et al., 2018). Apart from these, many *Streptomyces* showed antibacterial (Bo et al., 2018), nematicidal (Park et al., 2020), antioxidant, antiviral, and anticancer activities (Fahmy et al., 2022). All these functions are powered by the production and release of hydrolytic enzymes, competition, antibiotic production, and the formation of cyanogenic chemicals. A variety of *Streptomyces* species produce volatile organic compounds (VOCs) with potent antifungal properties (Qi et al., 2019). Due to their potential to synthesize different kinds of antimicrobial compounds, *Streptomyces* spp. can be potential candidates for new biocontrol agents.

Microbial bio-priming, which is an adaptive technique to increase the defense capabilities of plants, results in enhanced resistance/tolerance to stress, and a more exacerbated defense response to stress (Aamir et al., 2019). Defense response of plants against pathogen invasion includes activation of reactive oxygen species (ROS) system, enhanced deposition of suberin and lignin for strengthening of cells at the site of infection, and expression of pathogenesis-related (PR) proteins (Pusztahelyi et al., 2015), which highlights the function of the systemic acquired resistance (SAR) pathway (Gharbi et al., 2017). β-1, 3-glucanases, and endochitinases are two important PR proteins, differentially expressed in many plant species infected by fungal pathogens (Ebrahim et al., 2011; Balasubramanian et al., 2012). The phenylpropanoid pathway is activated in actinobacteria-mediated bio-priming, characterized by the release of numerous antimicrobials. This process not only inhibits the infection and spread of pathogens but also provides tolerance to various abiotic stressors. Numerous studies have shown that treating plants with beneficial microorganisms improves their ability to fend off infections and other abiotic stresses by activating the ROS system (Brotman et al., 2013; Fu et al., 2017). The role of *Streptomyces* spp. mediated bio-priming in Foc-challenged plants concerning signaling pathways and molecular mechanisms has not been explored. Hence the present investigation has been planned to better understand defense signaling, various physio-biochemical alterations, and changes in gene expression due to bio-priming with *Streptomyces araujoniae*.

In our earlier studies on different actinobacterial strains, we reported several species of *Streptomyces* antagonistic against Foc, *F. udum*, *Macrophomina phaseolina,* and *Sclerotium rolfsii*. We selected two strains of *Streptomyces araujoniae* TN11 and TN19 based on their *in vitro* antagonistic potential against the four pathogens. They were explored for their potential as biocontrol agents against Foc

as individuals and as a consortium *via in planta* assays. Additionally, we have analyzed the antifungal compound profile of these two *Streptomyces* strains using liquid chromatography and mass spectrometry (LC–MS).

Materials and methods

Actinobacterial strains and fungal plant pathogens

Two strains of actinobacteria *Streptomyces araujoniae* TN11 (NAIMCC-B-02868) and *S. araujoniae* TN19 (NAIMCC-B-02870) and four phytopathogenic fungi *viz.*, *Macrophomina phaseolina* (NAIMCC-F-01261), *Fusarium oxysporum* f. sp. *ciceris* (NAIMCC-F-02001), *Fusarium udum* (NAIMCC-F-01103), and *Sclerotinia sclerotiorum* (NAIMCC-F-03341) were procured from the National Agriculturally Important Microbial Culture Collection (NAIMCC; WDCM Reg. No. 1060), Mau, India. Actinobacterial strains were revived by growing on starch casein agar (SCA) media (HiMedia, India) for 3–5 days at 30°C. They were chosen from among the 65 strains of actinobacteria (isolated from Tamil Nadu) based on their antagonistic activity against the Foc (data submitted elsewhere). Fungal strains were grown on potato dextrose agar (PDA) media for 3–5 days at 28 ± 2°C.

Pathogen inoculum preparation and pathogenicity test

Fusarium oxysporum f. sp. *ciceris* (Foc) was grown on PDA (Hi-media, India) for 3–5 days at 28 ± 2°C. The fully grown culture was suspended in sterile distilled water; filtered using a muslin cloth to collect the spores. The spore suspension was diluted to contain 10^6 spores per mL (Taylor et al., 2013). A pathogenicity test was conducted to confirm the virulence and to demonstrate the pathogen's participation in the development of vascular wilt disease symptoms. The conventional root dip technique was used to inoculate 20 days old healthy plants (Nirmaladevi et al., 2016). The healthy seedlings of chickpea (Var. Pusa 362) maintained in pots with sterilized soil were gently uprooted from their pots without damaging their root systems, shaken to remove any attached dirt particles, then gently rinsed under sterile water. The apex root part (approximately 1 cm) was trimmed using a sterile scissor and it was dipped in the spore suspension of Foc for 30 min. The treated plants were then planted in small pots (d: 9 cm, surface sterilized with mercuric chloride) containing a 2:1 mixture of sterilized soil and sand. Pots were kept in a greenhouse for L: D:: 16:8 h, with 22–24°C (day) and 16–18°C (night) and humidity of 60%. The symptoms of vascular wilt infection appeared 15–20 days after pathogen inoculation. A parallel control is maintained by dipping the healthy seedlings in sterile distilled water to confirm the vascular wilt infection is only due to the spore suspension of Foc.

Actinobacterial inoculum preparation

Compatibility between TN11 and TN19 was checked on starch casein agar plates and was found compatible. The strains were grown in starch casein broth in an incubator shaker (Jeiotech, Korea) for 5 days at 30°C with continual shaking (120 rpm). After 5 days, the fully grown cultures were subjected to centrifugation at 6000 rpm for 10 min. Cell pellets were then washed with sterile distilled water and resuspended in phosphate buffer (0.1 M, pH-7.0) to a final concentration of Abs >1.0 at 600 nm. A consortium of TN11 and TN19 was prepared by mixing these two actinobacterial suspensions in equal volumes (Chukwuneme et al., 2020).

Pot trial

A pot experiment was performed to evaluate the potential of selected strains as individuals and as a consortium against Foc wilt of chickpea in greenhouse conditions with temperatures 22–24°C (day) and 16–18°C (night) and humidity of 60%. The potting mixture of sand and soil in the ratio of 2:1 was sterilized in an autoclave at 121°C for 1 h, thrice (on three consecutive days). The sterilized potting mixture was then filled in pots (d: 9 cm) at 4 kg/pot. Foc pathogen grown on sterilized sorghum seeds was mixed with the potting mixture at 5 g/kg soil. Fresh and healthy seeds of chickpea (variety Pusa 362) were surface sterilized with 0.1% mercuric chloride for 3 min, followed by treatment with 70% ethanol for 1 min. They were then subjected to washing with sterile distilled water twice and dried under aseptic conditions (Jain et al., 2012). For bio-priming with actinobacterial cultures and their consortium, 15 gm of surface sterilized seeds were soaked in 30 ml of actinobacterial suspension and their consortium for 30 min based on the treatment. The control seeds were soaked in sterilized phosphate buffer for 30 min. Treated seeds were then planted in pots (4 seeds per pot), 48 h after inoculation with the pathogen. A total of five treatments were taken up with five replications each. Treatments include control (no actinobacteria and no Foc), Foc alone (Foc), Foc + TN11, Foc + TN19, Foc + TN11 + TN19 (Foc + consortium of TN11 and TN19). The experiment was carried out up to 50 days after sowing; disease appearance started five weeks after sowing.

Disease severity index

A rater's assessment of the disease severity was used to calculate the disease severity index (DSI), expressed as a percentage (Chiang et al., 2017). The disease severity index is calculated as follows:

$$\mathrm{DSI}(\%) = \left[\mathrm{sum}(c \times s)\right] / \left[(n) \times (\mathrm{md})\right] \times 100.$$

c, class frequency; *s*, score of rating class; *n*, total number of plants; md, maximal disease index.

Morphological parameters

All the parameters were observed 50 days after sowing. Plants were separated from the soil with their roots intact and the shoot length and root length were measured. Parts of the root and shoot were separated, to record the fresh mass of the shoot and root. The dry mass of shoot and root was recorded after drying the plant portions for 48 h at 80°C in an oven. The ratio of dry mass to the fresh mass of root and shoot was estimated (Ansari et al., 2018). Stem width and number of leaves were also recorded.

Relative water content and electrolyte leakage

Relative water content (RWC) and electrolyte leakage (EL) were measured (Khare et al., 2010) and expressed in percentage. Twelve leaf discs were weighed to obtain the fresh mass (F). Leaf discs were then soaked in water for 6 h, surface-dried, and weighed to obtain the turgid mass (T). The soaked leaf discs were then oven-dried for 24 h at 80°C and weighed to get dry mass (D). RWC was calculated using the following formula,

$$\mathrm{RWC} = \left[\left(F - D\right) / \left(T - D\right)\right] \times 100.$$

Ten leaf discs were placed in 30 ml of double-distilled water and kept at 28°C for 4 h. Conductivity was measured after four hours (a). The contents were then autoclaved for 30 min at 121°C and conductivity was measured again (b). The EL was determined using the formula,

$$\mathrm{EL} = \left(a / b\right) \times 100.$$

Hydrogen peroxide, lipid peroxidation, and proline content

For estimation of H_2O_2, 0.2 gm of leaf samples were homogenized in 5 ml of sodium phosphate buffer (50 mM; pH 6.5) and centrifuged for 20 min at 6,000×*g*. Three milliliters of the resultant supernatant was then mixed with 1 ml of titanium sulfate (0.1% w/v) dissolved in 20% H_2SO_4. The mixture was then subjected to centrifugation for 15 min at 6,000×*g*. The supernatant was collected and the absorbance was measured at 410 nm (UV-vis 1601 Shimadzu, Japan). The amount of H_2O_2 was then expressed as μm g^{-1} fresh weight (Jana and Choudhuri, 1981).

For estimation of lipid peroxidation, 0.4 g of leaf tissue was homogenized in four mL trichloroacetic acid reagent comprising 0.1% trichloroacetic acid, 0.5% butylated hydroxytoluene, and 1% polyvinylpyrrolidone. The mixture was subjected to centrifugation for 20 min at 6,000×*g*. The resultant supernatant (2.5 ml) was mixed with 0.5% thiobarbituric acid and 20% trichloroacetic acid and boiled for 30 min. After 30 min the mixture was centrifuged for 20 min at 6,000×*g*. The supernatant's absorbance at 532 nm was measured, and nonspecific turbidity correction was performed by subtracting the absorbance at 600 nm. Lipid peroxidation was expressed as μM malondialdehyde g^{-1} fresh weight (Heath and Packer, 1968).

To measure the proline concentration, leaf samples (0.2 gm) were crushed in 3% sulfosalicylic acid and centrifuged for 10 min at 13,000×*g*. The supernatant (0.5 ml) was incubated at 100°C for 60 min with 0.5 ml each of ninhydrin reagent (freshly prepared) and glacial acetic acid. After 60 min one mL of toluene was added to the mixture and the absorbance was recorded at 520 nm (Bates et al., 1973). The amount of proline was expressed as μg g^{-1} fresh weight.

Photosynthetic pigments

To measure the chlorophyll and carotenoid content, 0.3 g of fresh leaf samples were homogenized in 80% chilled acetone. The mixture was centrifuged for 10 min. at 8000×*g* and the absorbance (UV-vis 1601 Shimadzu, Japan) of the supernatant was recorded at 663 nm (A_{663}), 645 nm (A_{645}), and 470 nm (A_{470}). The following formulae were used to calculate the chlorophyll and carotenoid contents expressed as mg g^{-1} fresh weight,

$$\mathrm{Chlorophyll\ a} = \left[\left(12.7 \times A_{663}\right) - \left(2.69 \times A_{645}\right)\right];$$
$$\mathrm{Chlorophyll\ b} = \left[\left(22.9 \times A_{645}\right) - \left(4.68 \times A_{663}\right)\right];$$
$$\mathrm{Carotenoids} = \left[\left(1{,}000 \times A_{470}\right) - \left(\begin{matrix}3.27 \times \mathrm{Chlorophyll\ a} \\ +\mathrm{Chlorophyll\ b}\end{matrix}\right)\right] / 227.$$

Determination of antioxidant enzyme activity

For superoxide dismutase (SOD) assay fresh leaf sample (0.2 gm) were crushed in 5 ml potassium phosphate buffer (100 mm; pH 7.5) containing EDTA (0.5 mm), Triton X-100 (0.1%) and PVP (2%). The mixture was subjected to centrifugation for 15 min. at 15000 under 4°C. SOD activity was measured from the supernatant in an assay mixture (3 ml) containing sodium carbonate–bicarbonate buffer (50 mm; pH 9.8), EDTA (0.5 mm), and epinephrine (0.6 mm). Absorbance was recorded at 470 nm (UV-vis 1601 Shimadzu, Japan) to record adrenochrome generation (Shah et al., 2001). SOD was expressed as U (mg protein)$^{-1}$.

For catalase activity, fresh leaf sample (0.2 gm) was crushed in 5 ml Tris-NaOH buffer (50 mm; pH 8.0), containing EDTA (0.5 mm), PVP (2%), and Triton X-100 (0.5%). The mixture was subjected to centrifugation for 15 min at 15000 under 4°C. Catalase activity was measured from the supernatant in an assay mixture (1.5 ml) containing 1 ml potassium phosphate buffer (100 mm; pH 7.0), 0.4 ml H_2O_2 (200 mm), and 0.1 ml enzyme extract. Absorbance (UV-vis 1601 Shimadzu, Japan) was recorded at 240 nm (Rai et al., 2012). Catalase activity was expressed as μmol of H_2O_2 oxidized (mg protein)$^{-1}$ min^{-1}.

For Peroxidase (POD) activity fresh leaf samples (0.2 gm) were crushed in five mL of sodium phosphate buffer (60 mm; pH 7.0). The mixture was subjected to centrifugation for 15 min at 15000 rpm under 4°C. POD activity was measured from the supernatant in an assay mixture (2 ml) containing guaiacol (200 µl) H_2O_2 (50 µl), enzyme extract (50 µl) phosphate buffer (1.7 ml). Absorbance (UV-vis 1601 Shimadzu, Japan) was measured at 470 nm (Shah et al., 2001). The activity was expressed as H_2O_2 reduced (mg protein)$^{-1}$ min^{-1}.

RNA extraction and cDNA synthesis

Relative expression of genes coding antioxidant enzymes was determined quantitatively in leaf tissues from all treatments. Total RNA was isolated using TRIZOL reagent (Invitrogen) following the instruction manual. The quality of RNA was confirmed through gel electrophoresis (1.0% agarose gel prepared in DEPC treated water). Nanophotometer (Implen, CA, United States) was also used to evaluate the quantity, purity, and integrity of RNA. cDNA synthesis was carried out from the RNA (1 µg) employing the Iscript™ cDNA synthesis kit (Bio-Rad Laboratories United States) as following the instruction manual.

Real-time quantitative PCR analysis

Quantitative real-time PCR (qRT-PCR) assay was carried out in an iQ5 thermocycler (BioRad Laboratories, United States). PCR reactions were carried out with a reaction mixture containing 2 µl of cDNA template (20 ng), 1 µl each of primers (0.2 µM) of *SOD*, *POD,* and *CAT* (Supplementary Table 1), and 10 µl of iQ-SYBR Green Supermix (Bio-Rad, United States) and an appropriate volume of Milli-Q water to a final volume of 20 µl. The qRT PCR program used was; initial denaturation for 8 min at 95°C followed by 35 cycles of denaturation at 95°C for 20 s, annealing at 60°C for 30 s, and extension at 72°C for 30 s. ACTIN (chickpea) gene was used as a reference because of its constant and steady expression (Karkute et al., 2019). The Δ^{Ct} value was calculated by subtracting the Ct values of the housekeeping gene (ACTIN) from the target gene. The relative quantification was examined using Livak and Schmittgen's (2001) $2^{-\Delta\Delta CT}$ method. The Ct value concerning the transcript level of the ACTIN gene was then normalized as an internal control.

Cell-free extracts of actinobacteria and their antifungal assay

Actinobacterial strains were grown as broth culture in starch casein broth for preparation of mother culture. One liter of broth culture is raised with 5% mother inoculum and grown with continuous agitation at 120 rpm for 10 days at 30°C. After incubation was complete, the obtained culture broth was centrifuged at 8000 rpm for 20 min at 4°C. The supernatant was collected and metabolites were extracted with an equal volume of different organic solvents *viz.*, ethyl acetate, n-hexane, and dimethyl sulfoxide (SRL, India). After extraction, excess solvents were evaporated in a rotary vacuum evaporator (Hahnshin, Korea) and the resultant metabolites were dissolved in the respective solvents to a final volume of 2 ml. Cell-free extracts (supernatant) were collected and subjected to antagonistic activity against the pathogenic fungi by amending the extracts at 1% in the growth media just before plating. Metabolites extracted using different solvents were tested for their ability to control selected phytopathogenic fungi by employing the well diffusion assay. The assay is carried out on a media containing PDA and SCA in the ratio of 1:1. From a fully grown fresh culture, 6 mm fungal discs were placed in the center of PDA/SCA media plates. Wells (d: 4 mm) were made in the plates at four places on the plate around the fungus disc. Solvent extracts (20 µl) were placed in each well with solvent as the negative control. The plates were incubated at 28 ± 2°C for 3–5 days. Growth inhibition of fungal pathogen was recorded regularly. The percent growth inhibition of pathogen was recorded for both cell-free extracts and organic solvent extracts (Shahid et al., 2021).

LC–MS analysis of ethyl acetate extract

Liquid chromatography-mass spectrometry was carried out at Central Instrumentation Facility, South Campus, Delhi University (DU), India. The metabolites were identified using Thermo Fisher Scientific Compound Discoverer 2.2. The data were analyzed, and it was used to predict chemical formulae and identify the peaks. mZCloud; an Advanced Mass Spectral Database[1] and Chemspider database[2] were used (Shahid et al., 2021).

Statistical analysis

The experimental data were analyzed by One-Way analysis of variance (ANOVA) using SPSS software (V-16). Duncan's Multiple Range Test (DMRT) at $p < 0.05$ was used to further examine treatments and rank them. Analyzed data were presented as mean ± SE.

Results

Chickpeas disease control

The disease severity index (DSI) was calculated as a measure of disease control in different treatments. DSI of Foc, Foc + TN11, Foc + TN19, and Foc + TN11 + TN19, treated plants were 100, 50, 44.44 and 41.66%, respectively. Hence, disease severity is reduced

1 https://www.mzcloud.org/
2 http://www.chemspider.com

TABLE 1 Shoot length, root length, plant height, stem width, and the number of leaves of chickpea plants under unprimed control, Foc challenged, Foc challenged + TN11 primed, Foc challenged + TN19 primed, and Foc challenged + TN11+TN19 primed, conditions.

Treatment	Shoot length (cm)	Root length (cm)	Plant height (cm)	Stem width (cm)	No. of leaves
Control	30.0 ± 2.28^{b}	5.03 ± 0.28^{a}	35.0 ± 4.29^{ab}	1.92 ± 0.09^{b}	793 ± 64.2^{ab}
Foc only	22.4 ± 1.73^{d}	3.82 ± 0.21^{c}	26.2 ± 1.35^{c}	1.54 ± 0.04^{d}	572 ± 28.9^{d}
Foc + TN11	28.2 ± 1.54^{bc}	4.94 ± 0.33^{a}	33.1 ± 1.85^{b}	1.81 ± 0.17^{c}	712 ± 23.4^{c}
Foc + TN19	28.5 ± 0.95^{bc}	4.71 ± 0.49^{ab}	33.2 ± 1.62^{b}	1.83 ± 0.13^{c}	588 ± 47.3^{d}
Foc + TN11 + TN19	33.5 ± 1.69^{a}	5.13 ± 0.24^{a}	38.3 ± 1.55^{a}	2.13 ± 0.11^{a}	812 ± 39.1^{a}

The data are the mean of three replicates ± standard error, within each column, values followed by the same letter are not significantly different ($p \leq 0.05$) according to Duncan's multiple range test.

TABLE 2 Shoot fresh weight (SFW), shoot dry weight (SDW), root fresh weight (RFW), root dry weight (RDW), SDW/SFW ratio, RDW/RFW ratio, relative water content (RWC), and electrolyte leakage (EL), of chickpea plants under unprimed control, Foc challenged, Foc challenged + TN11 primed, Foc challenged + TN19 primed, and Foc challenged + TN11+TN19 primed, conditions.

Treatment	SFW (gm)	SDW (gm)	RFW (gm)	RDW (gm)	SDW/SFW	RDW/RFW	RWC (%)	EL (%)
Control	12.8 ± 0.883^{a}	3.42 ± 0.283^{a}	1.5 ± 0.08^{c}	0.319 ± 0.022^{b}	0.267 ± 0.012^{b}	0.213 ± 0.014^{b}	70.59 ± 6.32^{ab}	30.77 ± 2.68^{cd}
Foc only	2.2 ± 0.112^{e}	0.915 ± 0.091^{d}	0.7 ± 0.05^{f}	0.256 ± 0.011^{c}	0.416 ± 0.024^{a}	0.366 ± 0.029^{a}	50.10 ± 3.82^{e}	61.79 ± 6.72^{a}
Foc + TN11	6.5 ± 0.273^{d}	2.56 ± 0.133^{b}	1.8 ± 0.11^{b}	0.319 ± 0.025^{b}	0.394 ± 0.029^{a}	0.177 ± 0.014^{c}	60.63 ± 2.46^{d}	38.46 ± 1.68^{b}
Foc + TN19	7.8 ± 0.521^{bc}	2.32 ± 0.114^{bc}	0.8 ± 0.03^{e}	0.165 ± 0.011^{d}	0.297 ± 0.025^{b}	0.206 ± 0.007^{b}	67.90 ± 5.78^{bc}	38.89 ± 2.23 ^{b}
Foc + TN11 + TN19	8.3 ± 0.392^{b}	2.17 ± 0.153^{c}	3.8 ± 0.24^{a}	0.627 ± 0.041^{a}	0.261 ± 0.017^{b}	0.165 ± 0.009^{d}	74.11 ± 8.24^{a}	33.33 ± 1.88^{c}

The data are mean of three replicates ± standard error, within each column, values followed by the same letter are not significantly different ($p \leq 0.05$) according to Duncan's multiple range test.

by 50, 55.56, and 58.33% by priming with TN11, TN19, and the consortium of TN11 + TN19 respectively.

Growth promotion

Priming chickpea seeds with *S. araujoniae* strains individually and as a consortium resulted in the profuse growth of the chickpea plants in the presence of pathogens, exhibiting a significant increase in the morphological attributes *viz.*, shoot and root length, plant height, the thickness of stem, and the number of leaves. Effects of different treatments on the shoot and root length, plant height, stem width, and the number of leaves are presented in Table 1. In the presence of the Foc challenge, priming chickpea seeds with the consortium of TN11 + TN19 recorded the highest values for shoot length, root length, plant height, stem width, and the number of leaves while Foc challenged plants without any priming exhibited the lowest values. Priming with individual strains of *S. araujoniae* also showed a significant increase in shoot and root length, plant height, stem width, and the number of leaves over the unprimed Foc challenged plants. But the values recorded were lower than that of the consortium treatment.

Effects of different treatments on the shoot and root fresh weight, shoot and root dry weight, and the ratio of dry to fresh weight of shoot and root are presented in Table 2. They are found to show significant differences among the treatments. In Foc challenged treatments priming with consortium has shown the highest values of shoot fresh weight, root fresh weight, and root dry weight while priming with TN11 recorded the highest shoot dry weight. The ratio of dry to fresh weight of shoot was highest in unprimed Foc challenged plants (0.416) followed by Foc + TN11 (0.394), although both treatments are statistically at par, while it was least in Foc + TN11 + TN19 and at par with Foc + TN19 and control (non-challenged and unprimed) treatments. Similarly, the ratio of dry to fresh weight of root was again highest in unprimed Foc challenged plants (0.366), while it was least in Foc + TN11 + TN19 (0.165).

Relative water content and electrolyte leakage

Significant variation among the treatments was observed for RWC and EL (Table 2). RWC was highest in Foc challenged plants receiving priming with the consortium of TN11 + TN19 (74.11%) followed by control plants (unprimed and non-challenged), while the lowest RWC was recorded in Foc challenged unprimed plants (50.10%). EL was highest in unprimed Foc challenged plants (61.79%) followed by Foc challenged plants primed with TN19 (38.89%), Foc challenged plants primed with TN11 (38.46%) and Foc challenged plants primed with the consortium of TN11 + TN19 (33.33%). Among Foc challenged plants treatments primed with TN11 + TN19 recorded the lowest EL which is statistically on par with control plants.

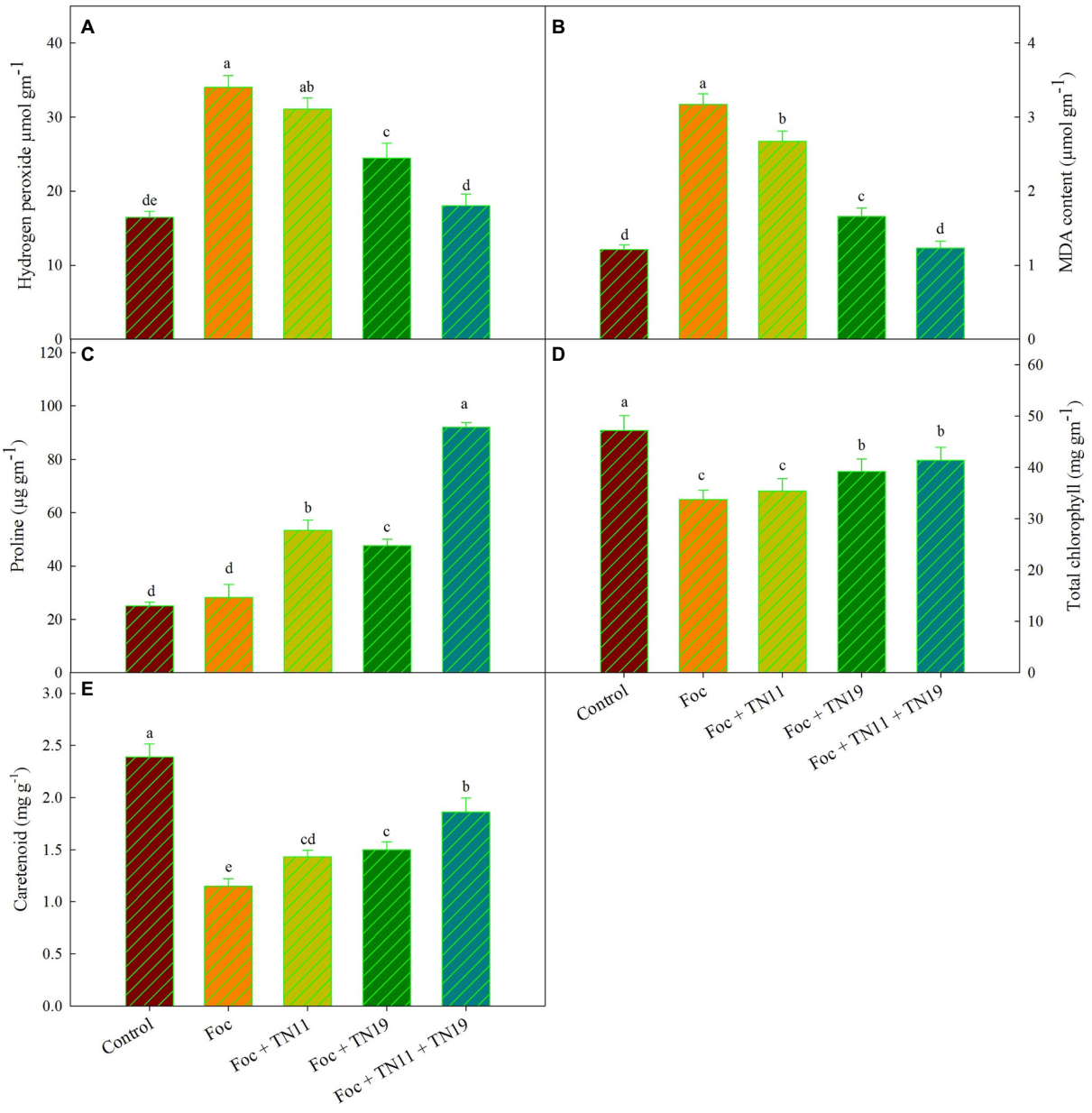

FIGURE 1
(A) Hydrogen peroxide, **(B)** lipid peroxidation (MDA content), **(C)** proline, **(D)** total chlorophyll, **(E)** carotenoids, in chickpea leaves under unprimed control, Foc challenged, Foc challenged + TN11 primed, Foc challenged + TN19 primed, and Foc challenged + TN11+TN19 primed conditions. The data are the mean of three replicates ± standard error, within each graph, values followed by the same letter are not significantly different ($p \leq 0.05$) according to Duncan's multiple range test.

Quantitative estimation of hydrogen peroxide, lipid peroxidation, and proline

The amount of H_2O_2 generation was recorded significantly higher in Foc challenged plants and reduced in Foc challenged plants receiving priming with TN11, TN19, and the consortium of TN11 and TN19. Among the Foc challenged plants treatments primed with the consortium of TN11 + TN19 recorded the lowest accumulation of H_2O_2 (Figure 1A). There was 47.02% reduced accumulation of H_2O_2 in Foc challenged plants receiving consortium of TN11 + TN19 compared to unprimed plants.

Lipid peroxidation was quantified in terms of MDA generation. MDA was significantly higher in Foc challenged plants (3.17 µmol g^{-1} (FM)) followed by Foc + TN11 (2.67 µmol g^{-1} (FM)), Foc + TN19 (1.66 µmol g^{-1} (FM)) and Foc + TN11 + TN19 (1.23 µmol g^{-1} (FM)). MDA generation in Foc + TN11 + TN19 was statistically on par with control treatment that did not receive any pathogen and priming. Compared to Foc challenged plants, the percent reduction in MDA generation was 15.78, 47.64, and

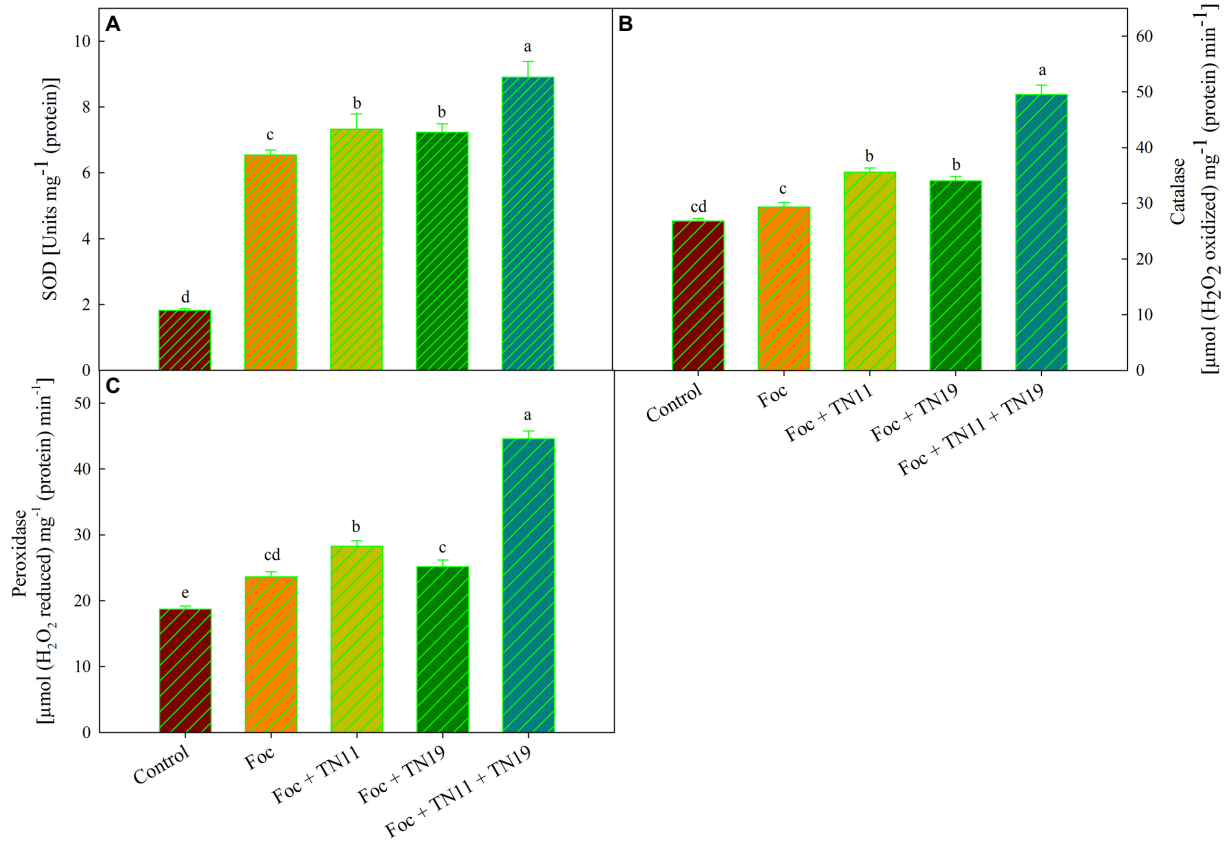

FIGURE 2
(A) Superoxide dismutase (SOD), **(B)** catalase (CAT), **(C)** peroxidase (POD), in chickpea leaves under unprimed control, Foc challenged, Foc challenged + TN11 primed, Foc challenged + TN19 primed, and Foc challenged + TN11+TN19 primed. The data are the mean of three replicates ± standard error, within each graph, values followed by the same letter are not significantly different ($p \leq 0.05$) according to Duncan's multiple range test.

61.20%, respectively in Foc challenged plants primed with TN11, TN19, and the consortium of TN11 and TN19 (Figure 1B).

Similarly, accumulation of proline was highest (92.07 μg^{-1} FM) in Foc + TN11 + TN19 followed by Foc + TN11 (53.42 μg^{-1} FM), Foc + TN19 (47.67 μg^{-1} FM) and Foc challenged plants (28.20). Proline accumulation in Foc + TN11 + TN19 was statistically on par with control plants (Figure 1C). Compared to Foc challenged plants percent increase in proline accumulation was 89.43, 69.04, and 226.5%, respectively in Foc challenged plants primed with TN11, TN19, and the consortium of TN11 and TN19 (Figure 1C).

Photosynthetic pigments

Total chlorophyll content in leaves of all the treatments along with control was recorded, and it was found maximum (47.23 $mg\,g^{-1}$) in control unprimed plants, followed by Foc + TN11 + TN19 (41.37 $mg\,g^{-1}$), Foc + TN19 (39.23 $mg\,g^{-1}$), Foc + TN11 (35.42 $mg\,g^{-1}$) and Foc challenged plants (33.73 $mg\,g^{-1}$). A non-significant difference in total chlorophyll content was recorded between Foc challenged plants and Foc challenged plants primed with TN11 (Figure 1D). Carotenoid content was maximum (2.39 $mg\,g^{-1}$) in control unprimed plants, while it was lowest (1.15 $mg\,g^{-1}$) in Foc challenged plants (Figure 1E). Compared to Foc challenged plants percent increase in carotenoid content was of 61.74% in Foc + TN11 + TN19.

Antioxidative enzymes

SOD, POD, and CAT activity

SOD activity was maximum (8.9 U mg^{-1} (protein)) in Foc + TN11 + TN19 treated plants, while it was 7.3 U mg^{-1} (protein) and 7.2 U mg^{-1} (protein) and 6.54 U mg^{-1} (protein) in Foc + TN11 and Foc + TN19 and Foc challenged plants, respectively (Figure 2A). CAT activity was minimum; 29.33 µmol (H_2O_2 reduced) min^{-1} mg^{-1} (protein) in Foc challenged plants, and a significant increase in catalase activity was recorded in all the treatments receiving priming. CAT activity recorded in Foc + TN11, Foc + TN19, and Foc + TN11 + TN19, respectively, were 1.21-, 1.16- and 1.69-folds of the same in Foc challenged

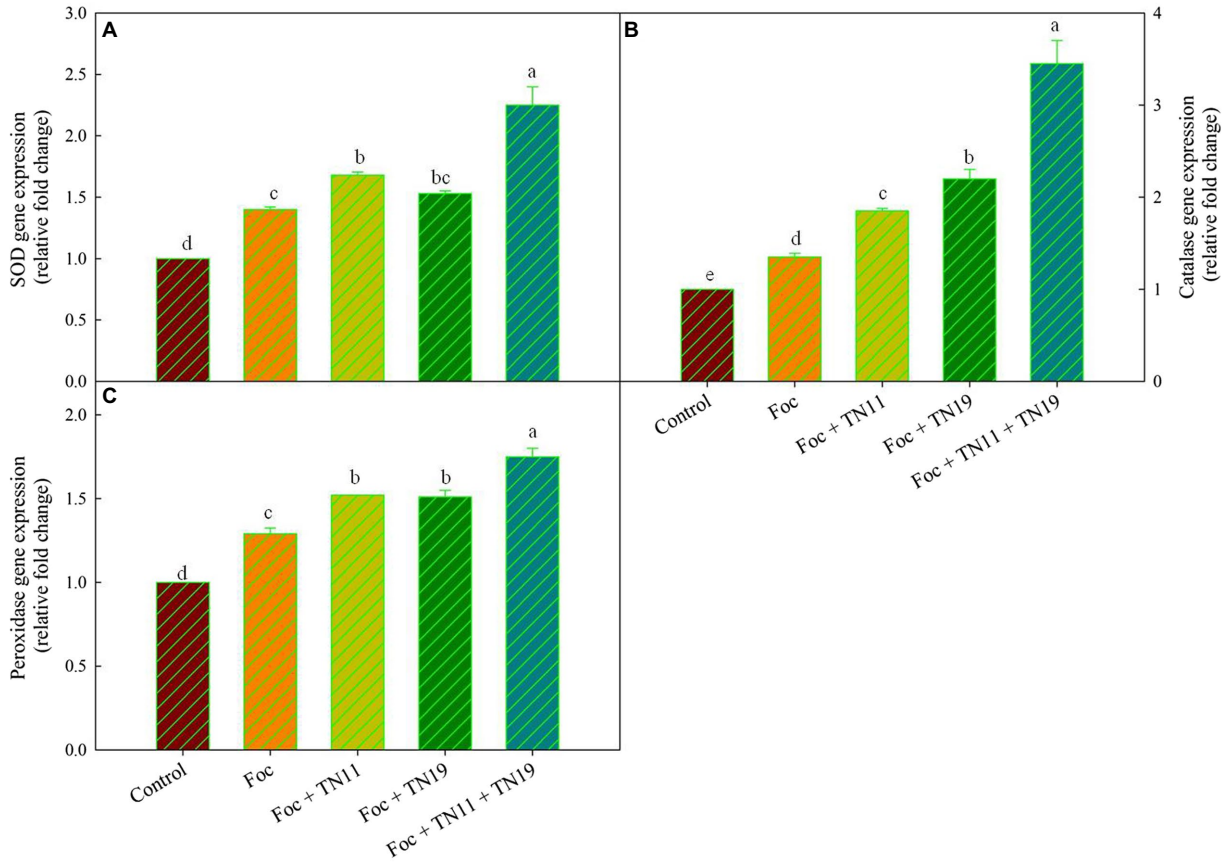

FIGURE 3
Relative expression of **(A)** superoxide dismutase (SOD), **(B)** catalase (CAT), **(C)** peroxidase (POD), gene in chickpea leaves under unprimed control, Foc challenged, Foc challenged + TN11 primed, Foc challenged + TN19 primed, and Foc challenged + TN11+TN19 primed, conditions. The data are the mean of three replicates ± standard error, within each graph, values followed by the same letter are not significantly different ($p \leq 0.05$) according to Duncan's multiple range test.

unprimed plants (Figure 2B). Similarly, POD activity of Foc + TN11, Foc + TN19 and Foc + TN11 + TN19, respectively were 1.20-, 1.06- and 1.89-folds, the same recorded in Foc challenged unprimed plants (Figure 2C).

Gene expression analysis

It was found that an upregulated expression of *SOD*, *POD*, and *CAT* gene was recorded in Foc + TN11, Foc + TN19, and Foc + TN11 + TN19 treatments (Figure 3). Compared to control 1.40-, 1.68-, 1.53-, and 2.25- folds enhanced SOD expression were recorded in Foc, Foc + TN11, Foc + TN19 and Foc + TN11 + TN19 treatments, respectively. CAT expression profile was 1.35-, 1.85-, 2.20-, and 3.45- folds in Foc, Foc + TN11, Foc + TN19, and Foc + TN11 + TN19 treatments, respectively as compared to control. Similarly, POD expression in Foc, Foc + TN11, Foc + TN19, and Foc + TN11 + TN19 treatments, respectively, were 1.29-, 1.52-, 1.51-, and 1.75-folds as compared to control.

Effect of cell-free extracts and ethyl acetate extracts on fungal pathogens

Cell-free extract of *S. araujoniae* strains TN11 and TN19 were tested against all the four pathogens employing amendment with media at 1%. The highest growth inhibition of cell-free extract of TN11 was observed against *F. oxysporum* (45.55%), followed by *F. udum* (41.93%), *S. sclerotiorum* (38.33%), and *M. phaseolina* (33.33%). Similarly, cell-free extract of TN19 inhibited the growth of *F. udum*, *M. phaseolina*, *F. oxysporum*, and *S. sclerotiorum* by 45.45, 45, 44.9, and 38.3%, respectively.

Metabolites extracted using different solvents ethyl acetate, n-hexane, and dimethyl sulfoxide were tested against all the four selected phytopathogens. Results revealed that extracts obtained using ethyl acetate were able to control the growth of all the pathogens tested while the extracts obtained using the other two solvents were not found to control the growth of any phytopathogen. Ethyl acetate extract of *S. araujoniae* TN11 showed the highest antagonistic activity in *S. sclerotiorum* (73.01%), followed by *M. phaseolina* (69.84%), *F. udum* (63.15%),

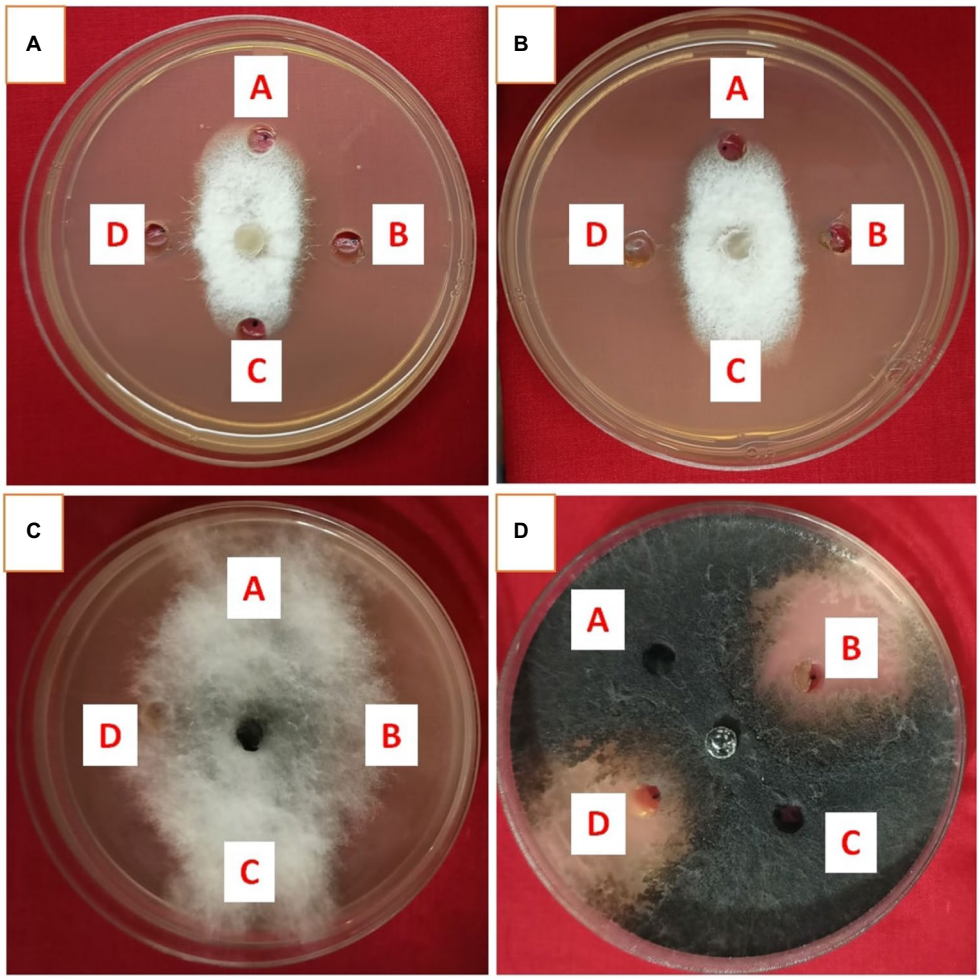

FIGURE 4
Antifungal activity of ethyl acetate extract of *Streptomyces araujoniae* TN11 in well diffusion assay against fungal pathogens *Fusarium udum* **(A)**, *Fusarium oxysporum* **(B)**, *Macrophomina phaseolina* **(C)** and *Sclerotinia sclerotiorum* **(D)**. Well A=Control, C=solvent control, B and D=ethyl acetate extract (20μl).

and *F. oxysporum* (59.1%), while the extracts of *S. araujoniae* TN19 showed maximum antagonistic effect (60%) against *M. phaseolina* followed by *F. udum* (57.14%), *S. sclerotiorum* (57.14%), and *F. oxysporum* (54.54%; Figures 4–7).

LC–MS of ethyl acetate extracts of *Streptomyces araujoniae* TN11 and TN19

Metabolites of *S. araujoniae* TN11 and TN19 extracted in ethyl acetate were subjected to LC–MS analyses. A total of more than 10 thousand compounds were detected through LC–MS in the ethyl acetate extracts of each strain. Ten major compounds detected in the extract with known antifungal properties are presented in Tables 3, 4. Erucamide was the most dominant antifungal compound found, followed by dinactin and valinomycin in the extracts of TN11. The extracts of TN19 showed 2-Octadecylfuran as the most dominant antifungal compound followed by valinomycin and dinactin. LC–MS studies revealed that *S. araujoniae* TN11 and TN19 produced a combination of antifungal compounds capable of inhibiting the development of several phytopathogenic fungi.

Discussion

Fungal phytopathogens pose a significant threat to agriculture, as they cause a variety of plant diseases (Sharma and Manhas, 2020) that cause severe damage, resulting in lower productivity. According to the food and agriculture organization, averting fungal diseases in five major crops, including maize, wheat, rice, potato, and soybean would be able to additionally feed 8.5% of the world's population (Fisher et al., 2012). Fungal plant pathogens like *Sclerotinia*, *Fusarium*, *Macrophomina*, *Sarocladium, Rhizoctonia*, and *Aspergillus* have been found to cause several dreaded diseases

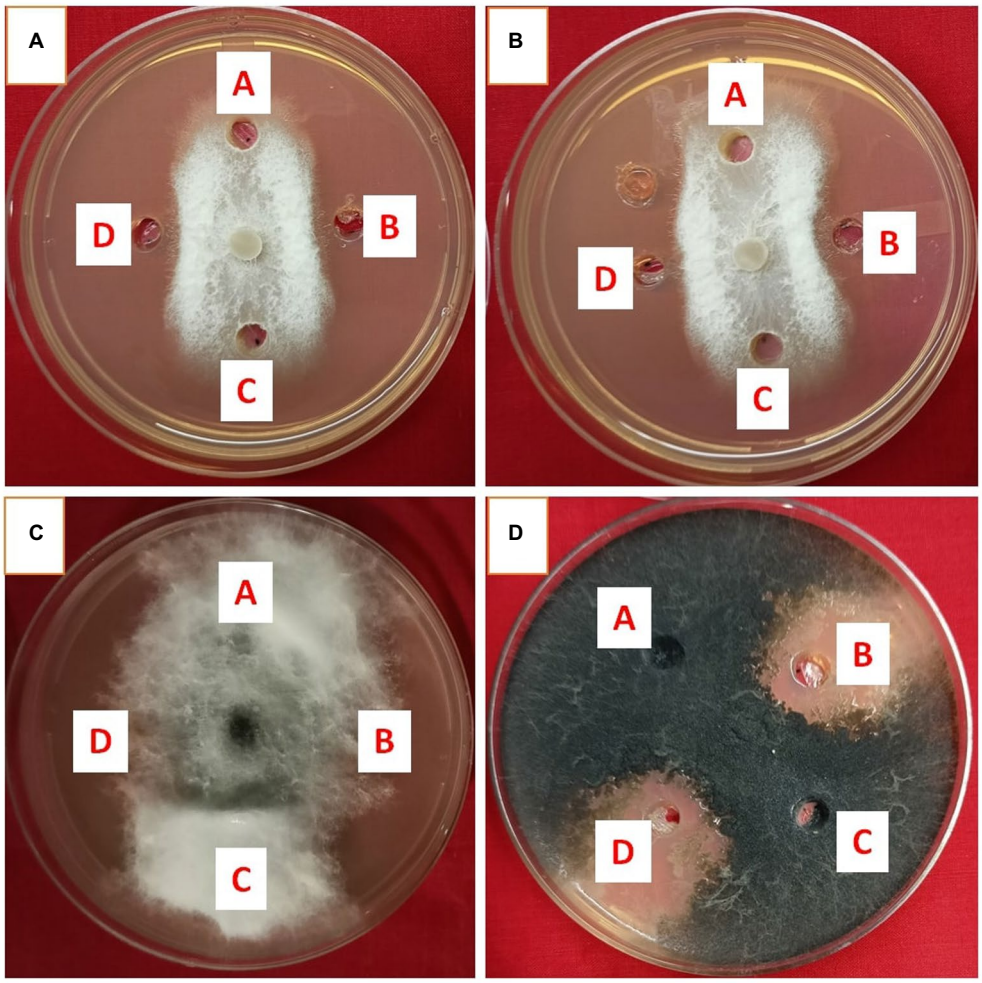

FIGURE 5
Antifungal activity of ethyl acetate extract of *Streptomyces araujoniae* TN19 in well diffusion assay against fungal pathogens *Fusarium oxysporum* **(A)**, *Fusarium udum* **(B)**, *Macrophomina phaseolina* **(C)** and *Sclerotinia sclerotiorum* **(D)**. Well A=Control, C=solvent control, B and D=ethyl acetate extract (20μl).

in many food, feed, and cash crops (Derbyshire and Denton-Giles, 2016; Hassan et al., 2021).

The *Fusarium oxysporum* f. sp. *ciceris* (Foc) that causes chickpea wilt was first discovered in India in 1918 and is currently widespread in many nations. The pathogen exhibits a wide range of cultural traits and pathogenicity with as many as eight pathogenic races identified (Ankati et al., 2021). Yield losses range from 10 to 100% depending on the vulnerability of the variety and the agroclimatic conditions (Chand and Khirbat, 2009). Overuse of chemical fungicides for control of plant diseases is a very common practice in most developing nations which drastically affects the ecosystem and health. Generally, chemical pesticides persist in the environment and devastate the useful soil microbes that have plant growth-promoting traits and maintain the fertility of the soil. Microbes and their secondary metabolites are more eco-friendly and are sustainable alternatives to insecticides and herbicides. Actinomycetes are widely known among microbes for the production of secondary metabolites with antimicrobial properties (Shahid et al., 2021). More than 70% of the well-recognized secondary metabolites are products of actinomycetes; among them over 10,000 bioactive compounds have been reported from *Streptomyces* alone. *Streptomyces* sp. displayed a broad range of antagonistic activity against numerous fungal pathogens, which include *Fusarium oxysporum*, *Rhizoctonia solani*, *Colletotrichum gloeosporioides*, *Botrytis cinerea*, *Cochliobolus miyabeanus*, and *Pyricularia oryzae*. Recently Ankati et al. (2021) reported *Streptomyces griseus* strains (CAI-24, CAI-121, and CAI-127), *Streptomyces coelicolor* KAI-90, and *Streptomyces africanus* KAI-32 with properties of biocontrol against Foc mediated wilt and plant growth promotion in chickpea. Screening of effective antagonistic actinomycetes is essential for the development of various biocontrol agents; *Streptomyces* sp. SCA3-4 demonstrated wide antifungal potential against 13 fungal pathogens (Qi et al., 2019). Sarika et al. (2021) reported the antibacterial and antifungal activity of *Streptomyces felleus* BHPL-KSKU5 isolated from a coal mine in Telangana (India). In the present study ethyl acetate

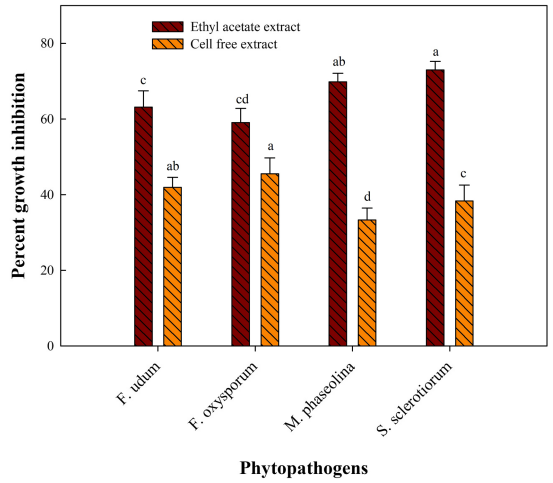

FIGURE 6
Antifungal activity (% inhibition) of *Streptomyces araujoniae* TN11 metabolites extracted in ethyl acetate and cell-free extract against different fungal pathogens. The data are the mean of three replicates ± standard error, within each graph, values followed by the same letter are not significantly different ($p \leq 0.05$) according to Duncan's multiple range test.

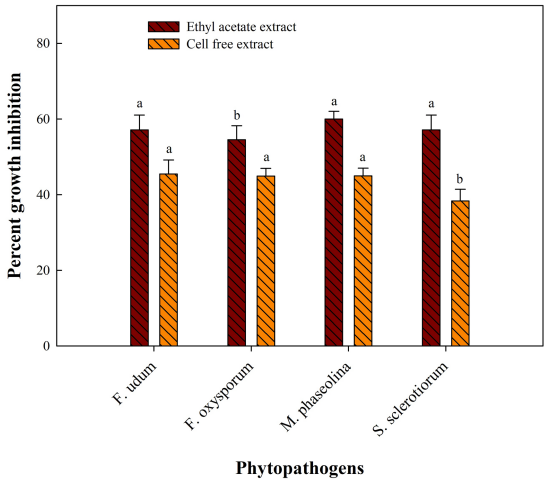

FIGURE 7
Antifungal activity (% inhibition) of *Streptomyces araujoniae* TN19 metabolites extracted in ethyl acetate and cell-free extract against different fungal pathogens. The data are the mean of three replicates ± standard error, within each graph, values followed by the same letter are not significantly different ($p \leq 0.05$) according to Duncan's multiple range test.

TABLE 3 List of some bioactive molecules with reported antifungal activity identified through LC–MS analyses of ethyl acetate extracts of *Streptomyces araujoniae* (TN11).

Sl. no.	Metabolites	Molecular formula	Retention time (min)	Peak area (%)	Activity against fungal pathogens	References
1	Erucamide	$C_{22}H_{43}NO$	26.321	7.970	*Fusarium oxysporum* f. sp. *cubense*	Qi et al., 2022
2	Dinactin	$C_{42}H_{68}O_{12}$	24.447	3.920	*Colletotrichum gloeosporioides*, *Colletotrichum musae*, *Botryodiplodia theobromae*, *F. oxysporum* f. sp. *cubense*, *Magnaporthe oryzae*, *Alternaria solani*	Islam et al., 2016; Zhang et al., 2020
3	Valinomycin	$C_{54}H_{90}N_6O_{18}$	25.429	2.736	*Botrytis cinerea*, *Rhizoctonia solani*	Park et al., 2008; Jeon et al., 2019
4	4-Aminobenzoic acid	$C_7H_7NO_2$	4.943	0.726	*M. oryzae*, *R. solani*, *Sclerotinia sclerotiorum*	Laborda et al., 2018
5	Docosanamide	$C_{22}H_{45}NO$	28.152	0.246	*C. gloeosporioides*, *B. cinerea*, *Colletotrichum acutatum*, *R. solani*	Vázquez-Fuentes et al., 2021
6	3-BHA	$C_{11}H_{16}O_2$	1.194	0.294	*Aspergillus niger*, *Aspergillus oryzae*	Tabti et al., 2014
7	Tramadol	$C_{16}H_{25}NO_2$	12.598	0.279	*Candida albicans*, *Tricophyton rubrum*	Kathwate and Karuppayil (2016)
8	(4aR,5R,6R,8aR)-2-(6,10-Dimethyl-2-undecanyl)-5,8a-dimethyldecahydro-6-isoquinolinol	$C_{24}H_{47}NO$	28.151	0.259	*Candida krusei*	Dos Reis et al., 2019
9	Maltol	C_6H_6O3	0.990	0.097	*Phytophthora capsici*, *Bursaphelenchus xylophilus*	Tian et al., 2020
10	Caryophyllene oxide	$C_{15}H_{24}O$	10.907	0.093	*Fusarium moniliforme*, *R. solani*, *Helminthosporium oryzae* and *A. solani*	Huang et al., 2019; Jassal et al., 2021

BHA-Butylated hydroxyanisole.

extracts of the strains, *Streptomyces araujoniae* TN11 and TN19 showed antagonistic activity against *M. phaseolina*, *F. oxysporum*, *F. udum*, and *S. sclerotiorum* fungal pathogens. Similarly, *Streptomyces* sp. M4 isolated from soil (Punjab, India) and secondary metabolites extracted in ethyl acetate showed antifungal activity against various pathogens like *Botrytis cinerea*, *Fusarium* spp., *Cladosporium herbarum*, *Colletotrichum* spp., and *Alternaria* spp. (Sharma and Manhas, 2020).

TABLE 4 List of some bioactive molecules with reported antifungal activity identified through LC–MS analyses of ethyl acetate extracts of *Streptomyces araujoniae* (TN19).

Sl. no.	Metabolites	Molecular formula	Retention time (min)	Peak area (%)	Activity against fungal pathogens	References
1	2-Octadecylfuran	$C_{22}H_{40}O$	26.302	7.998	*C. albicans*, *A. niger*	El-Sayed et al., 2020
2	Valinomycin	$C_{54}H_{90}N_6O_{18}$	25.402	3.887	*B. cinerea*, *R. solani*,	Park et al., 2008; Jeon et al., 2019
3	Dinactin	$C_{42}H_{68}O_{12}$	24.370	1.560	*C. gloeosporioides*, *C. musae*, *B. theobromae*, *F. oxysporum* f. sp. *cubense*, *M. oryzae*, *A. solani*	Islam et al., 2016; Zhang et al., 2020
4	4-Aminobenzoic acid	$C_7H_7NO_2$	4.851	1.310	*M. oryzae*, *R. solani*, *S. sclerotiorum*	Laborda et al., 2018
5	Diethylene glycol	$C_4H_{10}O_3$	0.809	0.564	*C. albicans*, *C. glabrata*, *C. krusei*, *C. parapsilosis*, *A. flavus*, *A. nidulans*, *A. terreus*	Chandrika et al., 2016
6	3-BHA	$C_{11}H_{16}O_2$	1.194	0.402	*A. niger*, *A. oryzae*	Tabti et al., 2014
7	Docosanamide	$C_{22}H_{45}NO$	28.170	0.275	*C. gloeosporioides*, *B. cinerea*, *C. acutatum*, *Fusarium* sp., *R. solani*	Vázquez-Fuentes et al., 2021
8	10-Undecenoic acid	$C_{11}H_{20}O_2$	9.855	0.32530	*C. albicans*	Shi et al., 2016
9	Bengamide Z	$C_{18}H_{32}N_2O_7$	11.533	0.261	*C. albicans*	Jamison et al., 2019
10	TBHQ	$C_{10}H_{14}O_2$	0.968	0.186	*Fusarium*, *Penicillium* and *Aspergillus*	Thompson (1992)

BHA-Butylated hydroxyanisole; TBHQ-tert-Butylhydroquinone.

Plants are constantly subjected to diverse abiotic and biotic stressors in their natural environment. However, they show a high level of phenotypic flexibility and adaptability, which is defined by the plant's genome, to respond to such stimuli (Aamir et al., 2017). By engaging complex, synergistic, and/or antagonistic signaling networks plants respond effectively to such stressors (Pandey and Somssich, 2009). Microorganisms that support plant growth and biocontrol pests have become secure substitutes for chemical pesticides. Several bacterial and fungal antagonists have been discovered for the biological control of *Fusarium* wilt in chickpea like *Trichoderma* spp., *Pseudomonas* spp., *Bacillus* spp., isolates of non-pathogenic *Fusarium oxysporum,* and *Streptomyces* spp. (Jiménez-Díaz et al., 2015; Ankati et al., 2021). The genus *Streptomyces* shows great promise for fostering plant growth and defending plants from several diseases. A variety of bacterial and fungal phytopathogens can be effectively controlled by *Streptomyces araujoniae* and their metabolites (Silva et al., 2014). In our present study bio-priming with *Streptomyces araujoniae* strains, TN11 and TN19 reduce the disease development by Foc in chickpea (variety Pusa 362) as suggested by the disease severity index.

Reduction in disease development may be attributed to antifungal compounds produced by TN11 and TN19. Antagonism of *Streptomyces* spp. against fungi is generally mediated *via* the synthesis of antimicrobial secondary metabolites, the release of lytic and cell wall disintegrating enzymes, and competition for resources (Baz et al., 2012). The synthesis of antimicrobial compounds by the genus *Streptomyces* has previously been documented and has been the subject of extensive research in recent years (Santoyo et al., 2021). *Streptomyces* species generate a variety of bioactive compounds with antibacterial properties. For instance, *S. padanus* PMS-702 synthesizes the polyene macrolide antibiotic fungichromin, which exhibits strong antagonistic properties against many phytopathogenic fungi (Fan et al., 2019). Hyphae development in *Alternaria brassicicola* was restricted by 6-prenylindole; a compound produced by *Streptomyces* sp. TP-A0595 (Singh and Dubey, 2018). In the present study, through LC–MS we identified 10 major compounds produced by TN11 and TN19 with reported antifungal properties. Erucamide, dinactin, valinomycin, and strophanthidol were major compounds identified in the TN11 strain with peak areas, of 7.97, 3.92, 2.74, and 2.39%, respectively. Similarly, the TN19 strain had predominantly valinomycin (3.89%), dinactin (1.56%), and 4-aminobenzoic acid (1.31%). Earlier Qi et al. (2022) and Xie et al. (2021), reported antifungal properties of Erucamide. Antifungal properties of dinactin have been reported against various fungi like *Pestolotiopsis mangiferae*, *Neoscytalidium dimidiatum*, *Fusarium dimerum*, *Magnaporthe oryzae*, *Alternaria solani*, *Fusarium* oxysporum f.sp. *cubense*, *Colletotrichum gloeosporioides*, and *Colletotrichum musae* (Islam et al., 2016; Zhang et al., 2020). Similarly, Jeon et al. (2019), observed antifungal activities of valinomycin against *Botrytis cinerea*, *Rhizoctonia solani*, and *C. gloeosporioides*. The findings of our study demonstrated the antifungal properties of TN11 and TN19 strains and suggest their implementation as biocontrol agents.

The effect of bio-priming in controlling the disease is more pronounced in consortium treatment as compared to individual treatments. The synergistic effect of the consortium of TN11 and TN19 might be due to the complementation of the antifungal compounds produced by them individually. Earlier synergistic effects of different consortia on various crops have been reviewed by Santoyo et al. (Santoyo et al., 2021). Bio-priming with TN11 and TN19 also improved plant growth in presence of the Foc challenge. Like the reduction in disease development, a synergistic effect by the consortium is shown in plant growth parameters too.

As compared to individual strains' treatment consortium treatment resulted in a more pronounced enhancement of plant growth. Such enhanced performance by consortium over the individual strain treatments has been reported by Singh et al. (Singh et al., 2014). For commercial applications, the microbial consortium has been suggested as a sustainable method for improving plant health and growth (Kofoworola et al., 2016). Better plant growth parameters observed in the presence of Foc challenge for treatments receiving priming with TN11, and TN19 individually and as a consortium suggest that these strains reduce the negative effect of the pathogen on plants. *Streptomyces* spp. being a member of the rhizospheric microbial community got the ability to act as a plant growth promoter (Dias et al., 2017). Plant pathogens causing wilt hinders the transport of water within the plants thereby lowering RWC and inducing membrane damage; membrane damage in turn leads to increased EL (Rodrigues et al., 2018). In the present study, the application of the TN11 and TN19 strains results in significantly increased RWC and reduced EL by reducing disease severity; similar results were reported in maize and groundnut (Ghorai et al., 2015; Fazal and Bano, 2016) using different species of *Pseudomonas*.

When exposed to oxidative stress, plants produce H_2O_2 which plays a double function, as it may result in programmed cell death, but it can also serve as a quick signal to activate antioxidant defense responses (Gullner et al., 2018). In Foc + TN11, Foc + TN19, and Foc + TN11 + TN19 treated plants, H_2O_2 accumulations were lower compared to pathogen treated plants, signifying a feeble balance between H_2O_2 scavenging and H_2O_2 generation. The increased MDA concentration in the leaf is considered an oxidative stress indicator responsible for cellular damage (Lata et al., 2011). The reduction in MDA contents due to the Foc + TN11, Foc + TN19, and Foc + TN11 + TN19 treatment suggests it can reduce the peroxidation of plasma lemma under pathogen infection to shield the leaf cell membrane from damage. Similar results were reported in tomato plants inoculated with *Bacillus cereus* AR156 (Wang et al., 2013), in maize inoculated with *Pseudomonas putida* (Nosheen and Bano, 2014), and in rice inoculated with *P. fluorescens, P. jessenii,* and *P. synxantha* (Gusain et al., 2015). Proline protects plant cells from damage by acting as both an osmotic agent and a scavenger of reactive oxygen species (Liu et al., 2011). In the present study, proline level rises in Foc + TN11, Foc + TN19, and Foc + TN11 + TN19 treated plants. The elevated levels of proline within infected plant tissues can be interpreted as a host reaction to protect against stresses caused by pathogens (Rodrigues et al., 2018). Chlorophyll and carotenoids are two important leaf pigments that act as a physiological status to evaluate the performance of photosynthetic machinery under stress conditions either biotic or abiotic (Ansari et al., 2019). Biotic stress frequently causes leaves to exhibit chlorosis and necrosis because it reduces the number of chloroplasts and breaks down chlorophyll (Dinis et al., 2011), which was observed in the current study too. Chlorophyll and carotenoid content declined significantly in Foc challenged plants; the reduction was lower in Foc challenged plants primed with TN11, TN19, and TN11 + TN19.

All plants treated with Foc and the combination of Foc and TN11, TN19 showed differential SOD activity compared to the control unprimed plants. Foc challenged plants and Foc + TN11, Foc + TN19, Foc + TN11 + TN19, treated plants showed higher SOD activity compared to control plants. Plants have evolved a variety of defense mechanisms to cope with pathogen challenges, among them mechanism of ROS accumulation is the most significant which includes SOD accumulation (Aamir et al., 2019). Peroxidase is recognized as a major pathogen-related protein (PR-protein) or defense protein that participates in multiple physiological adaptations of plants against biotic stresses. Salla et al. (2016) reported that plants treated with *Streptomyces* as a biocontrol agent, exhibiting *Fusarium* wilt showed increased peroxidase activity in cucumber (Zhao et al., 2012). The antioxidant defense system of plants includes peroxidase and CAT, which scavenges ROS to quench the negative effects of stressors (Das and Roychoudhury, 2014). In this study, the combination of Foc + TN11, Foc + TN19, and Foc + TN11 + TN19, induces catalase activity compared to the control. Nikoo et al. (2014) demonstrated that *Pseudomonas fluorescens* treatment induces systemic resistance in tomatoes through defense-related enzymes POD and CAT. They demonstrated increased activity of POD and CAT due to inoculation of *P. fluorescens* and treatment with elicitors as compared to the activities of POD and CAT in plants treated with pathogen alone. Similar findings were also reported by Ankati et al. (2021), in chickpea plants after *Streptomyces* consortium treatment.

Enhanced expression of genes like *SOD*, *CAT,* and *POD* results in diminished ROS activity, which stimulates the activation of the different signaling cascades. In our study, like increased enzyme activity of SOD, CAT, and POD, enhanced expression of their respective genes was observed, and it was maximum in *Streptomyces araujoniae* consortium treated plants. Similarly, Mastouri et al. (2012) reported an enhanced expression of *SOD*, *CAT*, and *POD* genes because of *T. harzianum* treatment in tomatoes. Aamir et al. (2019), reported enhanced expression of these genes in tomato plants after bio-priming with *T. erinaceum*.

Conclusion

The present study has shown that the application of *Streptomyces araujoniae* strains individually and as a consortium reduces wilt severity in chickpea plants. Reduction in disease development is supported by the production of antifungal metabolites at a higher level by TN11 and TN19. The results on disease development, plant growth parameters, physiological and biochemical parameters, and gene expression studies suggest that the consortium of TN11 and TN19 can act as an efficient biocontrol tool against chickpea wilt caused by Foc.

Data availability statement

The original contributions presented in the study are included in the article/Supplementary material, further inquiries can be directed to the corresponding author.

Author contributions

MK and ASa conceived the idea and planned the experiments. MZ, PT, WA, and SK performed the experiments. WA, MZ, and PT analyzed the data. WA, MK, and MZ wrote the manuscript. MK, HC, ASr, ASa, and US checked the final draft of the manuscript. All authors contributed to the article and approved the submitted version.

Funding

Indian Soil Microbiome Project, funded by ICAR-NBAIM, Mau, India.

Acknowledgments

Authors express sincere gratitude to the Director ICAR-NBAIM, for providing the infrastructure facility. Authors are thankful to NAIMCC, Mau, India, for providing the cultures. Authors are highly thankful to Sarvesh Pratap Kashyap for helping in the gene expression study.

Conflict of interest

The authors declare that the research was conducted in the absence of any commercial or financial relationships that could be construed as a potential conflict of interest.

Publisher's note

All claims expressed in this article are solely those of the authors and do not necessarily represent those of their affiliated organizations, or those of the publisher, the editors and the reviewers. Any product that may be evaluated in this article, or claim that may be made by its manufacturer, is not guaranteed or endorsed by the publisher.

Supplementary material

The Supplementary material for this article can be found online at: https://www.frontiersin.org/articles/10.3389/fmicb.2022.998546/full#supplementary-material

References

Aamir, M., Singh, V. K., Meena, M., Upadhyay, R. S., Gupta, V. K., and Singh, S. (2017). Structural and functional insights into WRKY3 and WRKY4 transcription factors to unravel the WRKY–DNA (W-Box) complex interaction in tomato (*Solanum lycopersicum* L.). A computational approach. *Front. Plant Sci.* 8:819. doi: 10.3389/fpls.2017.00819

Aamir, M., Kashyap, S. P., Zehra, A., Dubey, M. K., Singh, V. K., Ansari, W. A., et al. (2019). *Trichoderma erinaceum* bio-priming modulates the WRKYs defense programming in tomato against the *Fusarium oxysporum* f. sp. *lycopersici* (Fol) challenged condition. *Front. Plant Sci.* 10:911. doi: 10.3389/fpls.2019.00911

Ankati, S., Srinivas, V., Pratyusha, S., and Gopalakrishnan, S. (2021). *Streptomyces* consortia-mediated plant defense against *Fusarium* wilt and plant growth-promotion in chickpea. *Microb. Pathog.* 157:104961. doi: 10.1016/j.micpath.2021.104961

Ansari, W. A., Atri, N., Pandey, M., Singh, A. K., Singh, B., and Pandey, S. (2019). Influence of drought stress on morphological, physiological and biochemical attributes of plants: a review. *Biosci. Biotechnol. Res. Asia* 16, 697–709. doi: 10.13005/bbra/2785

Ansari, W. A., Atri, N., Singh, B., Kumar, P., and Pandey, S. (2018). Morpho-physiological and biochemical responses of muskmelon genotypes to different degree of water deficit. *Photosynthetica* 56, 1019–1030. doi: 10.1007/s11099-018-0821-9

Anwar, S., Ali, B., and Sajid, I. (2016). Screening of rhizospheric actinomycetes for various in-vitro and in-vivo plant growth promoting (PGP) traits and for agroactive compounds. *Front. Microbiol.* 7:1334. doi: 10.3389/fmicb.2016.01334

Balasubramanian, V., Vashisht, D., Cletus, J., and Sakthivel, N. (2012). Plant β-1, 3-glucanases: their biological functions and transgenic expression against phytopathogenic fungi. *Biotechnol. Lett.* 34, 1983–1990. doi: 10.1007/s10529-012-1012-6

Bates, L. S., Waldren, R. P., and Teare, I. D. (1973). Rapid determination of free proline for water-stress studies. *Plant Soil* 39, 205–207. doi: 10.1007/BF00018060

Baz, M., Lahbabi, D., Samri, S., Val, F., Hamelin, G., Madore, I., et al. (2012). Control of potato soft rot caused by *Pectobacterium carotovorum* and *Pectobacterium atrosepticum* by *Moroccan actinobacteria* isolates. *World J. Microbiol. Biotechnol.* 28, 303–311. doi: 10.1007/s11274-011-0820-5

Bo, S. T., Xu, Z. F., Yang, L., Cheng, P., Tan, R. X., Jiao, R. H., et al. (2018). Structure and biosynthesis of mayamycin B, a new polyketide with antibacterial activity from *Streptomyces* sp. 120454. *J. Antibiot.* 71, 601–605. doi: 10.1038/s41429-018-0039-x

Brotman, Y., Landau, U., Cuadros-Inostroza, A., Takayuki, T., Fernie, A. R., Chet, I., et al. (2013). *Trichoderma*-plant root colonization: escaping early plant defense responses and activation of the antioxidant machinery for saline stress tolerance. *PLoS Pathog.* 9. doi: 10.1371/journal.ppat.1003221

Chand, H., and Khirbat, S. K. (2009). Chickpea wilt and its management: A review. *Agric. Rev.* 30, 1–12.

Chandrika, N. T., Shrestha, S. K., Ngo, H. X., and Garneau-Tsodikova, S. (2016). Synthesis and investigation of novel benzimidazole derivatives as antifungal agents. *Bioorg. Med. Chem.* 24, 3680–3686. doi: 10.1016/j.bmc.2016.06.010

Chiang, K. S., Liu, H. I., and Bock, C. H. (2017). A discussion on disease severity index values. Part I: warning on inherent errors and suggestions to maximise accuracy. *Ann. Appl. Biol.* 171, 139–154. doi: 10.1111/aab.12362

Chukwuneme, C. F., Babalola, O. O., Kutu, F. R., and Ojuederie, O. B. (2020). Characterization of actinomycetes isolates for plant growth promoting traits and their effects on drought tolerance in maize. *J. Plant Interact.* 15, 93–105. doi: 10.1080/17429145.2020.1752833

Das, K., and Roychoudhury, A. (2014). Reactive oxygen species (ROS) and response of antioxidants as ROS-scavengers during environmental stress in plants. *Front. Environ. Sci.* 2:53. doi: 10.3389/fenvs.2014.00053

Derbyshire, M. C., and Denton-Giles, M. (2016). The control of sclerotinia stem rot on oilseed rape (*Brassica napus*): current practices and future opportunities. *Plant Pathol.* 65, 859–877. doi: 10.1111/ppa.12517

Dias, M. P., Bastos, M. S., Xavier, V. B., Cassel, E., Astarita, L. V., and Santarém, E. R. (2017). Plant growth and resistance promoted by *Streptomyces* spp. in tomato. *Plant Physiol. Biochem.* 118, 479–493. doi: 10.1016/j.plaphy.2017.07.017

Dinis, L. T., Peixoto, F., Zhang, C., Martins, L., Costa, R., and Gomes-Laranjo, J. (2011). Physiological and biochemical changes in resistant and sensitive chestnut (*Castanea*) plantlets after inoculation with *Phytophthora cinnamomi*. *Physiol. Mol. Plant Pathol.* 75, 146–156. doi: 10.1016/j.pmpp.2011.04.003

Dos Reis, C. M., da Rosa, B. V., da Rosa, G. P., do Carmo, G., Morandini, L. M. B., Ugalde, G. A., et al. (2019). Antifungal and antibacterial activity of extracts produced from *Diaporthe schini*. *J. Biotechnol.* 294, 30–37. doi: 10.1016/j.jbiotec.2019.01.022

Ebrahim, S., Usha, K., and Singh, B. (2011). Pathogenesis related (PR) proteins in plant defense mechanism. *Sci. Against Microb. Pathog.* 2, 1043–1054.

El-Sayed, S. E., Abdelaziz, N. A., El-Housseiny, G. S., and Aboshanab, K. M. (2020). Octadecyl 3-(3, 5-di-tert-butyl-4-hydroxyphenyl) propanoate, an antifungal metabolite of *Alcaligenes faecalis* strain MT332429 optimized through response surface methodology. *Appl. Microbiol. Biotechnol.* 104, 10755–10768. doi: 10.1007/s00253-020-10962-9

Fahmy, S. A., Nematallah, K. A., Mahdy, N. K., El-Askary, H. I., Meselhy, M. R., and El-Said Azzazy, H. M. (2022). Enhanced antioxidant, antiviral, and anticancer activities of the extract of fermented egyptian rice bran complexed with hydroxypropyl-β-cyclodextrin. *ACS Omega* 7, 19545–19554. doi: 10.1021/acsomega.2c01281

Fan, Y. T., Chung, K. R., and Huang, J. W. (2019). Fungichromin production by *Streptomyces padanus* PMS-702 for controlling cucumber downy mildew. *Plant Pathol. J.* 35, 341–350. doi: 10.5423/PPJ.OA.03.2019.0057

Fazal, A., and Bano, A. (2016). Role of plant growth-promoting rhizobacteria (PGPR), biochar, and chemical fertilizer under salinity stress. *Commun. Soil Sci. Plant Anal.* 47, 1985–1993. doi: 10.1080/00103624.2016.1216562

Fisher, M. C., Henk, D., Briggs, C. J., Brownstein, J. S., Madoff, L. C., McCraw, S. L., et al. (2012). Emerging fungal threats to animal, plant and ecosystem health. *Nature* 484, 186–194. doi: 10.1038/nature10947

Fu, Y., Gao, H., Li, H., Qin, Y., Tang, W., Lu, J., et al. (2017). Change of growth promotion and disease resistant of wheat seedling by application of biocontrol bacterium *Pseudochrobactrum kiredjianiae* A4 under simulated microgravity. *Acta Astronaut.* 139, 222–227. doi: 10.1016/j.actaastro.2017.06.022

Garcia-Solache, M. A., and Casadevall, A. (2010). Global warming will bring new fungal diseases for mammals. *MBio* 1, e00061–e00010. doi: 10.1128/mBio.00061-10

Gharbi, Y., Barkallah, M., Bouazizi, E., Gdoura, R., and Triki, M. A. (2017). Differential biochemical and physiological responses of two olive cultivars differing by their susceptibility to the hemibiotrophic pathogen *Verticillium dahliae*. *Physiol. Mol. Plant Pathol.* 97, 30–39. doi: 10.1016/j.pmpp.2016.12.001

Ghorai, S., Pal, K. K., and Dey, R. (2015). Alleviation of salinity stress in groundnut by application of PGPR. *Int. Res. J. Eng. Technol.* 2, 742–750.

Gullner, G., Komives, T., Király, L., and Schröder, P. (2018). Glutathione S-transferase enzymes in plant-pathogen interactions. *Front. Plant Sci.* 9:1836. doi: 10.3389/fpls.2018.01836

Gusain, Y. S., Singh, U. S., and Sharma, A. K. (2015). Bacterial mediated amelioration of drought stress in drought tolerant and susceptible cultivars of rice (*Oryza sativa* L.). African. *J. Biotechnol.* 14, 764–773. doi: 10.5897/AJB2015.14405

Hassan, H. S., Mohamed, A. A., Feleafel, M. N., Salem, M. Z., Ali, H. M., Akrami, M., et al. (2021). Natural plant extracts and microbial antagonists to control fungal pathogens and improve the productivity of zucchini (*Cucurbita pepo* L.) *In Vitro* and in greenhouse. *Horticulturae* 7:470. doi: 10.3390/horticulturae7110470

Heath, R. L., and Packer, L. (1968). Photoperoxidation in isolated chloroplasts: I. Kinetics and stoichiometry of fatty acid peroxidation. *Arch. Biochem. Biophys.* 125, 189–198. doi: 10.1016/0003-9861(68)90654-1

Huang, X., Chen, S. Y., Zhang, Y., Wang, Y. H., Zhang, X., Bi, Z. Y., et al. (2019). Chemical composition and antifungal activity of essential oils from three *Artemisia* species against *Alternaria solani*. *J. Essent. Oil Bear. Plants* 22, 1581–1592. doi: 10.1080/0972060X.2019.1708812

Islam, M., Laatsch, H., and Von Tiedemann, A. (2016). Inhibitory effects of macrotetrolides from *Streptomyces* spp. on zoosporogenesis and motility of peronosporomycete zoospores are likely linked with enhanced ATPase activity in mitochondria. *Front. Microbiol.* 7:1824. doi: 10.3389/fmicb.2016.01824

Jain, A., Singh, S., Kumar, S. B., and Bahadur, S. H. (2012). Microbial consortium–mediated reprogramming of defence network in pea to enhance tolerance against *Sclerotinia sclerotiorum*. *J. Appl. Microbiol.* 112, 537–550. doi: 10.1111/j.1365-2672.2011.05220.x

Jamil, A., and Ashraf, S. (2020). Utilization of chemical fungicides in managing the wilt disease of chickpea caused by *Fusarium oxysporum* f. sp. *ciceri*. *Arch. Phytopathol. Pflanzenschutz.* 53, 876–898. doi: 10.1080/03235408.2020.1803705

Jamison, M. T., Wang, X., Cheng, T., and Molinski, T. F. (2019). Synergistic anti-Candida activity of bengazole A in the presence of bengamide A. *Mar. Drugs* 17:102. doi: 10.3390/md17020102

Jana, S., and Choudhuri, M. A. (1981). Glycolate metabolism of three submersed aquatic angiosperms: effect of heavy metals. *Aquat. Bot.* 11, 67–77. doi: 10.1016/0304-3770(81)90047-4

Jassal, K., Kaushal, S., Rashmi, and Rani, R. (2021). Antifungal potential of guava (*Psidium guajava*) leaves essential oil, major compounds: beta-caryophyllene and caryophyllene oxide. *Arch. Phytopathol. Pflanzenschut.* 54, 2034–2050. doi: 10.1080/03235408.2021.1968287

Jeon, C. W., Kim, D. R., and Kwak, Y. S. (2019). Valinomycin, produced by *Streptomyces* sp. S8, a key antifungal metabolite in large patch disease suppressiveness. *World J. Microbiol. Biotechnol.* 35, 128–110. doi: 10.1007/s11274-019-2704-z

Jiménez-Díaz, R. M., Castillo, P., del Mar Jiménez-Gasco, M., Landa, B. B., and Navas-Cortés, J. A. (2015). *Fusarium* wilt of chickpeas: biology, ecology and management. *Crop Prot.* 73, 16–27. doi: 10.1016/j.cropro.2015.02.023

Karkute, S. G., Krishna, R., Ansari, W. A., Singh, B., Singh, P. M., Singh, M., et al. (2019). Heterologous expression of the *AtDREB1A* gene in tomato confers tolerance to chilling stress. *Biol. Plant.* 63, 268–277. doi: 10.32615/bp.2019.031

Kathwate, G. H., and Karuppayil, S. M. (2016). Tramadol, an opioid receptor agonist: an inhibitor of growth, morphogenesis, and biofilm formation in the human pathogen, *Candida albicans*. *Assay Drug Dev. Technol.* 14, 567–572. doi: 10.1089/adt.2016.760

Khare, N., Goyary, D., Singh, N. K., Shah, P., Rathore, M., Anandhan, S., et al. (2010). Transgenic tomato cv. Pusa Uphar expressing a bacterial mannitol-1-phosphate dehydrogenase gene confers abiotic stress tolerance. *Plant Cell Tiss. Organ. Cult.* 103, 267–277. doi: 10.1007/s11240-010-9776-7

Kofoworola, A. A., Oluwambe, T. M., Oluwagbemiga, A. P., and Mobolaji, O. T. (2016). Screening of indigenous plant growth-promoting bacterial strains for enhancing growth of tomato (*Lycopersicon esculentum* Mill.) in Nigeria. *J. Global Agric. Ecol.* 6, 127–135.

Laborda, P., Zhao, Y., Ling, J., Hou, R., and Liu, F. (2018). Production of antifungal p-aminobenzoic acid in Lysobacter antibioticus OH13. *J. Agric. Food Chem.* 66, 630–636. doi: 10.1021/acs.jafc.7b05084

Lake, L., and Sadras, V. O. (2014). The critical period for yield determination in chickpea (*Cicer arietinum* L.). *Field Crops Res.* 168, 1–7. doi: 10.1016/j.fcr.2014.08.003

Lata, C., Jha, S., Dixit, V., Sreenivasulu, N., and Prasad, M. (2011). Differential antioxidative responses to dehydration-induced oxidative stress in core set of foxtail millet cultivars [*Setaria italica* (L.)]. *Protoplasma* 248, 817–828. doi: 10.1007/s00709-010-0257-y

Liu, C., Zhao, L., and Yu, G. (2011). The dominant glutamic acid metabolic flux to produce γ-amino butyric acid over proline in *Nicotiana tabacum* leaves under water stress relates to its significant role in antioxidant activity. *J. Integ. Plant Biol.* 53, 608–618. doi: 10.1111/j.1744-7909.2011.01049.x

Livak, K. J., and Schmittgen, T. D. (2001). Analysis of relative gene expression data using real-time quantitative PCR and the $2^{-\Delta\Delta CT}$ method. *Methods* 25, 402–408. doi: 10.1006/meth.2001.1262

Mastouri, F., Björkman, T., and Harman, G. E. (2012). *Trichoderma harzianum* enhances antioxidant defense of tomato seedlings and resistance to water deficit. *Mol. Plant Microbe Interact.* 25, 1264–1271. doi: 10.1094/MPMI-09-11-0240

Mohite, O. S., Weber, T., Kim, H. U., and Lee, S. Y. (2019). Genome-scale metabolic reconstruction of actinomycetes for antibiotics production. *Biotechnol. J.* 14:1800377. doi: 10.1002/biot.201800377

Muehe, E. M., Wang, T., Kerl, C. F., Planer-Friedrich, B., and Fendorf, S. (2019). Rice production threatened by coupled stresses of climate and soil arsenic. *Nat. Commun.* 10, 4985–4910. doi: 10.1038/s41467-019-12946-4

Nikam, P. S., Jagtap, G. P., and Sontakke, P. L. (2007). Management of chickpea wilt caused by *Fusarium oxysporium* f. sp. *ciceri*. *Afr. J. Agric. Res.* 2, 692–697.

Nikoo, F. S., Sahebani, N., Aminian, H., Mokhtarnejad, L., and Ghaderi, R. (2014). Induction of systemic resistance and defense-related enzymes in tomato plants using *Pseudomonas fluorescens* CHAO and salicylic acid against root-knot nematode *Meloidogyne javanica*. *J. Plant Prot. Res.* 54, 383–389. doi: 10.2478/jppr-2014-0057

Nirmaladevi, D., Venkataramana, M., Srivastava, R. K., Uppalapati, S. R., Gupta, V. K., Yli-Mattila, T., et al. (2016). Molecular phylogeny, pathogenicity and toxigenicity of *Fusarium oxysporum* f. sp. *lycopersici*. *Sci. Rep.* 6, 1–14. doi: 10.1038/srep21367

Nosheen, A., and Bano, A. (2014). Potential of plant growth promoting rhizobacteria and chemical fertilizers on soil enzymes and plant growth. *Pak. J. Bot.* 46, 1521–1530.

Palla, M. S., Guntuku, G. S., Muthyala, M. K. K., Pingali, S., and Sahu, P. K. (2018). Isolation and molecular characterization of antifungal metabolite producing actinomycete from mangrove soil. *Biodiver. J. Biol. Div.* 7, 250–256. doi: 10.1016/j.bjbas.2018.02.006

Pandey, S. P., and Somssich, I. E. (2009). The role of WRKY transcription factors in plant immunity. *Plant Physiol.* 150, 1648–1655. doi: 10.1104/pp.109.138990

Park, E. J., Jang, H. J., Park, C. S., Lee, S. J., Lee, S., Kim, K. H., et al. (2020). Evaluation of nematicidal activity of *Streptomyces yatensis* KRA-28 against

Meloidogyne incognita. *J. Microbiol. Biotechnol.* 30, 700–707. doi: 10.4014/jmb.1908.08038

Park, C. N., Lee, J. M., Lee, D. H., and Kim, B. S. (2008). Antifungal activity of valinomycin, a peptide antibiotic produced by *Streptomyces* sp. strain M10 antagonistic to *Botrytis cinerea*. *J. Microbiol. Biotechnol.* 18, 880–884.

Pusztahelyi, T., Holb, I. J., and Pócsi, I. (2015). Secondary metabolites in fungus-plant interactions. *Front. Plant Sci.* 6:573. doi: 10.3389/fpls.2015.00573

Qi, D., Zou, L., Zhou, D., Chen, Y., Gao, Z., Feng, R., et al. (2019). Taxonomy and broad-spectrum antifungal activity of *Streptomyces* sp. SCA3-4 isolated from rhizosphere soil of *Opuntia stricta*. *Front. Plant Sci.* 10:1390. doi: 10.3389/fmicb.2019.01390

Qi, D., Zou, L., Zhou, D., Zhang, M., Wei, Y., Li, K., et al. (2022). Biocontrol potential and antifungal mechanism of a novel *Streptomyces sichuanensis* against *Fusarium oxysporum* f. sp. *cubense* tropical race 4 in vitro and in vivo. *Appl. Microbiol. Biotechnol.* 106, 1633–1649. doi: 10.1007/s00253-022-11788-3

Rai, A. C., Singh, M., and Shah, K. (2012). Effect of water withdrawal on formation of free radical, proline accumulation and activities of antioxidant enzymes in ZAT12-transformed transgenic tomato plants. *Plant Physiol. Biochem.* 61, 108–114. doi: 10.1016/j.plaphy.2012.09.010

Rodrigues, F. A., Einhardt, A. M., Oliveira, L. M., and Dias, C. S. (2018). Physiological and biochemical changes in plants infected by pathogens. VIII Simpósio Sobre Atualidades em Fitopatologia: Ferramentas Moleculares Aplicadas à Fitopatologia, 46.

Salla, T. D., Astarita, L. V., and Santarém, E. R. (2016). Defense responses in plants of eucalyptus elicited by *Streptomyces* and challenged with *Botrytis cinerea*. *Planta* 243, 1055–1070. doi: 10.1007/s00425-015-2460-8

Samriti, S. S., Sharma, R., and Pathania, A. (2020). Trends in area, production, productivity and trade of chickpeas in India. *Econ. Aff.* 65, 261–265. doi: 10.46852/0424-2513.2.2020.19

Santoyo, G., Guzmán-Guzmán, P., Parra-Cota, F. I., Santos-Villalobos, S. D. L., Orozco-Mosqueda, M. D. C., and Glick, B. R. (2021). Plant growth stimulation by microbial consortia. *Agronomy* 11:219. doi: 10.3390/agronomy11020219

Sarika, K., Sampath, G., Govindarajan, R. K., Ameen, F., Alwakeel, S., Al Gwaiz, H. I., et al. (2021). Antimicrobial and antifungal activity of soil actinomycetes isolated from coal mine sites. *Saudi J. Biol. Sci.* 28, 3553–3558. doi: 10.1016/j.sjbs.2021.03.029

Savi, D. C., Shaaban, K. A., Gos, F. M., Thorson, J. S., Glienke, C., and Rohr, J. (2019). Secondary metabolites produced by *microbacterium* sp. LGMB471 with antifungal activity against the phytopathogen *Phyllosticta citricarpa*. *Folia Microbiol.* 64, 453–460. doi: 10.1007/s12223-018-00668-x

Shah, K., Kumar, R. G., Verma, S., and Dubey, R. S. (2001). Effect of cadmium on lipid peroxidation, superoxide anion generation and activities of antioxidant enzymes in growing rice seedlings. *Plant Sci.* 161, 1135–1144. doi: 10.1016/S0168-9452(01)00517-9

Shahid, M., Singh, B. N., Verma, S., Choudhary, P., Das, S., Chakdar, H., et al. (2021). Bioactive antifungal metabolites produced by *Streptomyces amritsarensis* V31 help to control diverse phytopathogenic fungi. *Braz. J. Microbiol.* 52, 1687–1699. doi: 10.1007/s42770-021-00625-w

Sharma, M., and Manhas, R. K. (2020). Purification and characterization of salvianolic acid B from *Streptomyces* sp. M4 possessing antifungal activity against fungal phytopathogens. *Microbiol. Res.* 237:126478. doi: 10.1016/j.micres.2020.126478

Shi, D., Zhao, Y., Yan, H., Fu, H., Shen, Y., Lu, G., et al. (2016). Antifungal effects of undecylenic acid on the biofilm formation of *Candida albicans*. *Int. J. Pharmacol. Ther.* 54, 343–353. doi: 10.5414/CP202460

Silva, L. J., Crevelin, E. J., Souza, W. R., Moraes, L. A. B., Melo, I. S., and Zucchi, T. D. (2014). *Streptomyces araujoniae* produces a multiantibiotic complex with ionophoric properties to control *Botrytis cinerea*. *Phytopathology* 104, 1298–1305. doi: 10.1094/PHYTO-11-13-0327-R

Singh, R., and Dubey, A. K. (2018). Diversity and applications of endophytic actinobacteria of plants in special and other ecological niches. *Front. Microbiol.* 9:1767. doi: 10.3389/fmicb.2018.01767

Singh, A., Jain, A., Sarma, B. K., Upadhyay, R. S., and Singh, H. B. (2014). Rhizosphere competent microbial consortium mediates rapid changes in phenolic profiles in chickpea during *Sclerotium rolfsii* infection. *Microbiol. Res.* 169, 353–360. doi: 10.1016/j.micres.2013.09.014

Tabti, L., Dib, M. E. A., Gaouar, N., Samira, B., and Tabti, B. (2014). Antioxidant and antifungal activity of extracts of the aerial parts of *Thymus capitatus* (L.) *Hoffmanns* against four phytopathogenic fungi of *Citrus sinensis*. *Jundishapur J. Nat. Pharm. Prod.* 9, 49–54. doi: 10.17795/jjnpp-13972

Taylor, A., Vagany, V., Barbara, D. J., Thomas, B., Pink, D. A. C., Jones, J. E., et al. (2013). Identification of differential resistance to six *Fusarium oxysporum* f. sp. *cepae* isolates in commercial onion cultivars through the development of a rapid seedling assay. *Plant Pathol.* 62, 103–111. doi: 10.1111/j.1365-3059.2012.02624.x

Thompson, D. P. (1992). Inhibition of mycelial growth of mycotoxigenic fungi by phenolic antioxidants. *Mycologia* 84, 791–793. doi: 10.1080/00275514.1992.12026206

Tian, Y. E., Sun, D., Yang, J. M., Che, Z. P., Liu, S. M., Lin, X. M., et al. (2020). Synthesis of sulfonate derivatives of maltol and their biological activity against *Phytophthora capsici* and *Bursaphelenchus xylophilus in vitro*. *J. Asian Nat. Prod. Res.* 22, 578–587. doi: 10.1016/j.micres.2013.09.014

Vázquez-Fuentes, S., Pelagio-Flores, R., López-Bucio, J., Torres-Gavilán, A., Campos-García, J., de la Cruz, H. R., et al. (2021). N-vanillyl-octanamide represses growth of fungal phytopathogens in vitro and confers postharvest protection in tomato and avocado fruits against fungal-induced decay. *Protoplasma* 258, 729–741. doi: 10.1016/j.micres.2013.09.014

Wang, C., Wang, Z., Qiao, X., Li, Z., Li, F., Chen, M., et al. (2013). Antifungal activity of volatile organic compounds from *Streptomyces alboflavus* TD-1. *FEMS Microbiol. Lett.* 341, 45–51. doi: 10.1111/1574-6968.12088

Xie, Y., Peng, Q., Ji, Y., Xie, A., Yang, L., Mu, S., et al. (2021). Isolation and identification of antibacterial bioactive compounds from *Bacillus megaterium* L2. *Front. Microbiol.* 12:645484. doi: 10.3389/fmicb.2021.645484

Zhang, K., Gu, L., Zhang, Y., Liu, Z., and Li, X. (2020). Dinactin from a new producer, *Streptomyces badius* gz-8, and its antifungal activity against the rubber anthracnose fungus *Colletotrichum gloeosporioides*. *Microbiol. Res.* 240:126548. doi: 10.1016/j.micres.2020.126548

Zhao, S., Du, C. M., and Tian, C. Y. (2012). Suppression of *Fusarium oxysporum* and induced resistance of plants involved in the biocontrol of *Cucumber Fusarium* Wilt by *Streptomyces bikiniensis* HD-087. *World J. Microbiol. Biotechnol.* 28, 2919–2927. doi: 10.1007/s11274-012-1102-6

frontiers | Frontiers in Microbiology

TYPE Original Research
PUBLISHED 15 September 2022
DOI 10.3389/fmicb.2022.924407

Check for updates

OPEN ACCESS

EDITED BY
Durgesh K. Jaiswal,
Savitribai Phule Pune University, India

REVIEWED BY
Anukool Vaishnav,
Agroscope, Switzerland
Savita Singh,
Babu Shivnath Agrawal College, India

*CORRESPONDENCE
Shiva Dhar
drsdmishra@gmail.com
Mahendra Vikram Singh Rajawat
rajawat.mvs@gmail.com

†These authors have contributed equally to this work

SPECIALTY SECTION
This article was submitted to Microbiotechnology, a section of the journal Frontiers in Microbiology

RECEIVED 20 April 2022
ACCEPTED 28 June 2022
PUBLISHED 15 September 2022

CITATION
Gupta G, Dhar S, Kumar A, Choudhary AK, Dass A, Sharma VK, Shukla L, Upadhyay PK, Das A, Jinger D, Rajpoot SK, Sannagoudar MS, Kumar A, Bhupenchandra I, Tyagi V, Joshi E, Kumar K, Dwivedi P and Rajawat MVS (2022) Microbes-mediated integrated nutrient management for improved rhizo-modulation, pigeonpea productivity, and soil bio-fertility in a semi-arid agro-ecology. *Front. Microbiol.* 13:924407. doi: 10.3389/fmicb.2022.924407

COPYRIGHT
© 2022 Gupta, Dhar, Kumar, Choudhary, Dass, Sharma, Shukla, Upadhyay, Das, Jinger, Rajpoot, Sannagoudar, Kumar, Bhupenchandra, Tyagi, Joshi, Kumar, Dwivedi and Rajawat. This is an open-access article distributed under the terms of the Creative Commons Attribution License (CC BY). The use, distribution or reproduction in other forums is permitted, provided the original author(s) and the copyright owner(s) are credited and that the original publication in this journal is cited, in accordance with accepted academic practice. No use, distribution or reproduction is permitted which does not comply with these terms.

Microbes-mediated integrated nutrient management for improved rhizo-modulation, pigeonpea productivity, and soil bio-fertility in a semi-arid agro-ecology

Gaurendra Gupta[1†], Shiva Dhar[2*], Adarsh Kumar[3†], Anil K. Choudhary[2,4], Anchal Dass[2], V. K. Sharma[5], Livleen Shukla[6], P. K. Upadhyay[2], Anup Das[7], Dinesh Jinger[8], Sudhir Kumar Rajpoot[9], Manjanagouda S. Sannagoudar[1], Amit Kumar[10], Ingudam Bhupenchandra[11], Vishal Tyagi[12], Ekta Joshi[13], Kamlesh Kumar[2,14], Padmanabh Dwivedi[15] and Mahendra Vikram Singh Rajawat[3*]

[1]Indian Grassland and Fodder Research Institute, Indian Council of Agricultural Research, Jhansi, India, [2]Division of Agronomy, Indian Agricultural Research Institute, Indian Council of Agricultural Research, New Delhi, India, [3]National Bureau of Agriculturally Important Microorganisms, Indian Council of Agricultural Research, Mau, India, [4]Central Potato Research Institute, Indian Council of Agricultural Research, Shimla, India, [5]Division of SSAC, Indian Agricultural Research Institute, Indian Council of Agricultural Research, New Delhi, India, [6]Division of Microbiology, Indian Agricultural Research Institute, Indian Council of Agricultural Research, New Delhi, India, [7]Research Complex for NEH Region, Tripura Centre, Indian Council of Agricultural Research, Lembucherra, India, [8]Indian Institute of Soil and Water Conservation, Research Centre, Indian Council of Agricultural Research, Vasad, India, [9]Institute of Agricultural Sciences, Banaras Hindu University, Varanasi, India, [10]ICAR RC for NEH Region, Sikkim Centre, Gangtok, India, [11]ICAR–Krishi Vigyan Kendra, ICAR RC for NEH Region, Manipur Centre, Tamenglong, India, [12]Indian Institute of Seed Science, Indian Council of Agricultural Research, Mau, India, [13]Rajmata Vijayaraje Scindia Krishi Vishwa Vidyalaya, Gwalior, India, [14]Indian Institute of Farming Systems Research, Indian Council of Agricultural Research, Meerut, India, [15]Department of Plant Physiology, Institute of Agricultural Sciences, Banaras Hindu University, Varanasi, India

Excessive dependence on chemical fertilizers and ignorance to organic and microbial inputs under intensive cropping systems are the basic components of contemporary agriculture, which evolves several sustainability issues, such as degraded soil health and sub-optimal crop productivity. This scenario urges for integrated nutrient management approaches, such as microbes-mediated integrated plant nutrition for curtailing the high doses as chemical fertilizers. Rationally, experiment has been conducted in pigeonpea at ICAR-IARI, New Delhi, with the aim of identifying the appropriate nutrient management technique involving microbial and organic nutrient sources for improved rhizo-modulation, crop productivity, and soil bio-fertility. The randomized block-designed experiment consisted nine treatments *viz*. Control, Recommended dose of fertilizers (RDF), RDF+ Microbial inoculants (MI), Vermicompost (VC), Farm Yard Manure (FYM),

Leaf Compost (LC), VC + MI, FYM + MI, and LC + MI. *Rhizobium* spp., *Pseudomonas* spp., *Bacillus* spp., and *Frateuria aurantia* were used as seed-inoculating microbes. The results indicated the significant response of integration following the trend VC + MI > FYM + MI > LC + MI > RDF + MI for various plant shoot-root growth attributes and soil microbial and enzymatic properties. FYM + MI significantly improved the water-stable aggregates (22%), mean weight diameter (1.13 mm), and geometric mean diameter (0.93 mm), soil organic carbon (SOC), SOC stock, and SOC sequestration. The chemical properties *viz*. available N, P, and K were significantly improved with VC + MI. The study summarizes that FYM + MI could result in better soil physico-chemical and biological properties and shoot-root development; however; VC + MI could improve available nutrients in the soil and may enhance the growth of pigeonpea more effectively. The outcomes of the study are postulated as a viable and alternative solution for excessive chemical fertilizer-based nutrient management and would also promote the microbial consortia and organic manures-based agro-industries. This would add to the goal of sustainable agricultural development by producing quality crop produce, maintaining agro-biodiversity and making the soils fertile and healthy that would be a "gift to the society."

KEYWORDS

crop growth, microbial inoculants, nutrient management, pigeonpea, soil health, root growth

Introduction

With the ever-growing population, scarcity of arable lands, and resources alongside multiple environmental pressure, the need to focus on efficient natural resources management in agriculture for food security and sustainability is one of the biggest challenges for researchers and farming community (Meena et al., 2021). To meet this challenge, environment-unfriendly agricultural chemicals, such as fertilizers, have played a significant role in green revolution and are even, today, commonly recommended to outwit nutrient deficiencies of the soils (Kumar et al., 2018a). The use of agro chemicals has been a major factor in improving crop production; however, it causes severe deterioration in soil health and quality and thus poses a negative impact on crop production sustainability and environmental safety (Nelson et al., 2019). Besides this, fertility exhaustive cereal-based cropping systems are also having serious implications on sustainability of the agro-eco system (Gupta et al., 2018, 2020; Tanveer et al., 2019). The disruption of microbial diversity and, consequently, the bio-fertility, owing to the inappropriate nutrient management strategy, has become a concern for optimum soil health and plant growth (Fernández-Romero et al., 2016; Patra et al., 2016). In this context, the role of naturally abundant but functionally unexplored microorganisms, such as nitrogen fixing, phosphorus, and potash solubilizing microbial inoculants, along with their synergic integration with other organic sources of nutrients, such as bulky manures under a fertility augmentative legume crop, is crucial and offers a unique opportunity for balancing soil fertility, maintaining soil health, improving plant growth and profitable crop production in a sustainable way (Kumar et al., 2015; Gupta et al., 2020; Bhakar et al., 2021).

The determination of soil health and quality parameters, along with assessing the influence on the plant root-shoot growth attributes, is an important aspect of assessing a soil-plant management technique; and their precise estimates are essential to judge the impact of any soil fertility management experiment on the agricultural productivity and sustainability (Allen et al., 2011; Thapa et al., 2017; Bünemann et al., 2018; Nath et al., 2018; Miner et al., 2020).

Imbalanced fertilizer use and mismanagement of crop residue *via* burning and removal from the field are still in practice under cereal-cereal cropping systems (Kannan et al., 2013; Kumar et al., 2018a; Kumar S. et al., 2021), which cause soil and environmental pollution, nutrient mining, multi-nutrient deficiency, losses in soil bio-fertility, the reduction in partial factor productivity, loss of agri-biodiversity, and, ultimately, poor soil health and sub-optimal crop production (Bastida et al., 2006; Mahetele and Kushwaha, 2011). Considering

these negative implications on agro-ecology, the need for reduced and balanced fertilizer applications, along with crop diversification, is felt more essential than ever before (Thapa et al., 2017; Kumar et al., 2018a). "Legumes in crop rotation" are considered as an effective and much-needed approach to diversifying problematic cropping systems, (CS) such as rice-wheat CS (Ghosh et al., 2020). In this regard, pigeonpea, by virtue of its superior physiological and agronomical traits, makes it hardy and adaptive, has emerged as the best alternate in the *kharif* season in India to replace the rice crop, which is nutrient and water exhaustive for semiarid agro-ecosystem (Fernández-Romero et al., 2016). Besides, integrated nutrient management (INM) for balanced nutrition is also proved worthy (Jinger et al., 2020, 2021) and much-needed strategy under present circumstances and scenarios of semiarid regions of India (Song et al., 2015; Singh et al., 2019, 2020b). The practice of high, rather balanced, input application does not need fulensue in the growth of the agriculture sector with sustainability point of view, especially in respect of optimized crop production and resource use (Mahetele and Kushwaha, 2011); whereas, soil with good health and quality driven by balanced input management would be helpful to produce higher crop production in a sustainable manner under varied agro-climatic conditions (Congreves et al., 2015). In this view, microbial inoculants and organic manure-based INM technique could minimize the undesirable repercussions, resulting from cultivation of exhaustive crops, intensive cultivation, and imbalanced use of fertilizers followed through the restriction on use of organic manures and microbial inoculants (Samal et al., 2017).

Nowadays, microbial inoculants cultures are considered as a key component of plant nutrient management and fertility restoration that enhance soil microbial health, maintain soil fertility, improve crop growth and productivity thus make a contribution to sustainable agro-ecosystems (Harish et al., 2022; Kumar et al., 2022). It is a component that aggregates an expansion of microbes-based bio-products primarily, whose bioactivities are vital to stimulate and enhance the biological functions of intricate soil-microbe-plant continuum (Singh et al., 2019). The combined use of mineral, organic, and microbial resources is an emerging researchable area that targets to develop and design coherent microbes-based techniques, which are highly amicable with inorganic and organic inputs, with positive impacts on soil, crops, and environment (Gupta et al., 2020). Integration of microbial inoculants, along with chemical fertilizers and organic resources of nutrients, could improve soil health, plant growth, and thus sustain the soil and crop productivity (Singh et al., 2018, 2020a, 2021). Microbial inoculants-based nutrient management is a sustainable and eco-friendly strategy since it uses available forms of organic and inorganic nutrients to develop healthy environmental conditions and economically viable crop production systems, besides their plant growth-promoting (PGP) ability (Dhandayuthapani et al., 2015; Gupta et al., 2020). Despite its utmost importance, very meager research reports are available that advocate direct evidence of linking greater soil organic matter (SOM) resulting from microbial inoculants and manure-based INM to increase the soil health, root development and growth of crops, and much work remains to be done to find out the impact of such INM practices with respect to soil-plant relationship (Gupta et al., 2020, 2018; Lal, 2020). The exploration of microbial inoculants and organic manure-based technique is also believed to have the impact on the agro-industry by promoting the microbial inoculants culture-based agri-startups and organic manure-based agri-business. Outcomes of the study are also expected to solve the problem of crop residue and animal bi-products management in form of its use as manure for soil health and fertility augmentation. Overall, the study has the linkage with the various concurrent intangible ecological and social aspects apart from measurable impact on agro-biodiversity and production sustainability. Considering the rational, the study with an objective of assessing the influence of microbes mediated integrated nutrient management on root-shoot growth-promoting ability, soil health, rhizosphere modulation, and growth parameters of pigeonpea was conducted to bring an appropriate and biologically viable and integrated recommendation for efficient nutrient management for enhanced crop production besides maintaining soil fertility and health.

Materials and methods

Experiment allocation, agro-climate, and soil characteristics

The 2-year field experimentation on a fixed site was done at ICAR-Indian Agricultural Research Institute, New Delhi (28.38°N Latitude, 77.09°E Longitude, 229 m Altitude) during *kharif* 2016 and *kharif* 2017. The climate of the experimental site is semiarid type and subtropical in nature; hot winds prevail during the summer season and severe cold during the winter season. Mean maximum temperature during the period of crop cultivation was 34.3 and 33.5°C; mean minimum temperature, 22.8 and 22.1°C; total rainfall was 665.8 and 707.4 mm during 2016 and 2017, respectively. Average annual pan evaporation was recorded as about 850 mm. The details of meteorological observations throughout the field experimentation period (*Kharif*, 2016 and *Kharif*, 2017) are depicted in **Figure 1**. The soil of the research experiment site was alluvial, sandy clay loam in texture, low in SOC content (0.40%) and available nitrogen (164.5 kg ha^{-1}), medium in available phosphorus (14.5 kg ha^{-1}), high in available potassium (292.5 kg ha^{-1}), and slightly alkaline in reaction. The physical, chemical, and

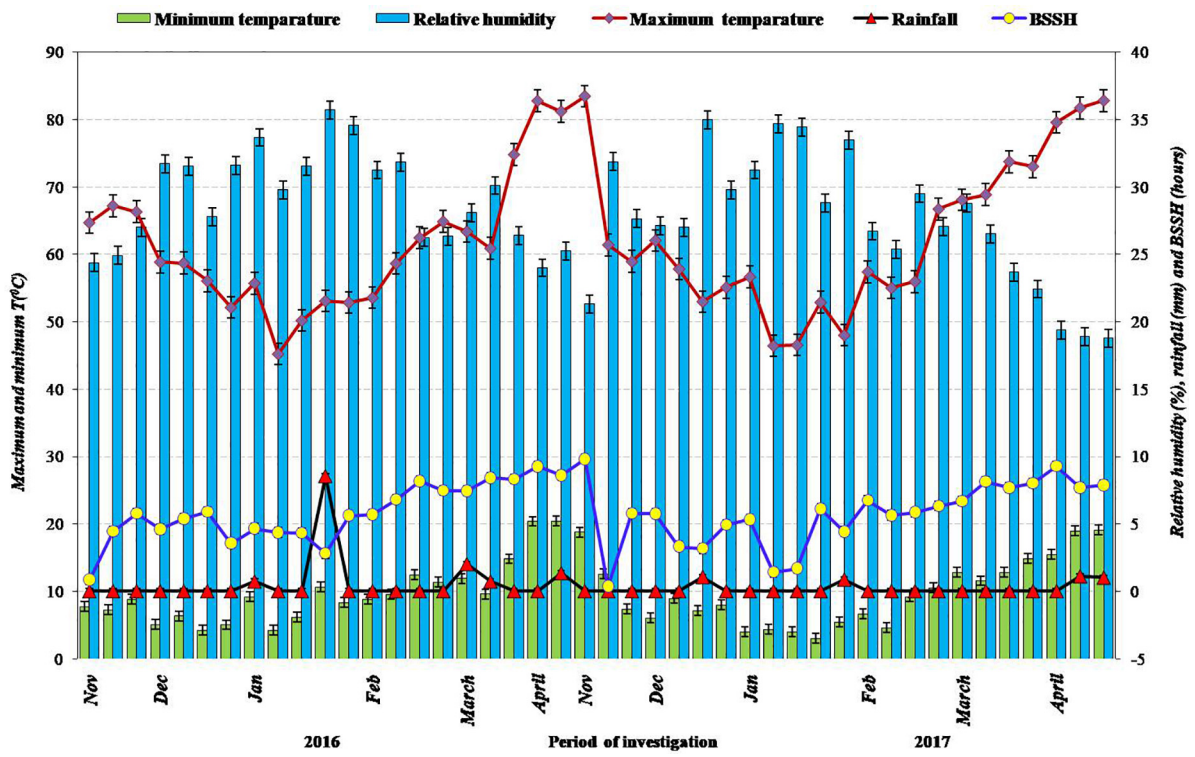

FIGURE 1
Meteorological data during the period of investigation during 2016 and 2017, respectively.

biological characteristics of soil analyzed from the initial soil test are described in Table 1.

Experimental treatments and design

The present study was designed in randomized block design (RBD) replicated three times and consisted of nine treatments of nutrient management, *viz*. Control, recommended dosage of fertilizers (RDF, 30: 60: 40 kg NPK ha^{-1}), RDF+ microbial inoculants (MI), Vermicompost (VC), Farm Yard Manure (FYM), Leaf Compost (LC), VC + MI, FYM + MI, and LC + MI. The details of treatments under experimentation are depicted in Table 2.

Microbial inoculants and organic manures

The *Rhizobium leguminosarum* as nitrogen-fixing inoculants, phosphorus-solubilizing bacteria (PSB) (*Pseudomonas striata, Pseudomonas putida, Bacillus megaterium,* and *Bacillus subtilis*) as phosphorus-solubilizing microbial inoculants, and *Frateuria aurantia* and *Bacillus mucilagenosus* as potassium solubilizers were used for seed inoculation. Seed treatment with *Rhizobium* and PSB was done at the rate of 250-g carrier-based culture 10^{-1} kg seed and K-solubilizing microbes (liquid-based formulation) at the rate of 50-ml culture 10^{-1} kg seeds. The slurry method of seed treatment was used for proper mixing of microbial inoculants culture and seeds. After the mixing, the seed was allowed to dry in a cool and shady area before sowing. Organic manures used under the experiment were vermicompost, FYM, and leaf compost. These manures were analyzed for their nutrient concentration, which is presented in Table 3.

Crop management

The seeds of pigeonpea variety Pusa-991 (an early maturing short duration variety, which fits well under pigeonpea-wheat cropping system of IGP) were seeded at 60 cm (row-row) × 20 cm (plant-plant). Seed sowing was done manually at the depth of 5 cm by using a 15-kg ha^{-1} seed rate. At the stage of field preparation, the fertilizer inputs (30:60:40 kg N, P_2O_5, and K_2O ha^{-1}), FYM (5 t ha^{-1}), VC (5 t ha^{-1}), and LC (5 t ha^{-1}) were applied as per treatment protocol. NPK fertilizers were applied as the basal through urea, diammonium phosphate (DAP) and muriate of potash (MoP), respectively. A total of three irrigations were scheduled at the branching,

TABLE 1 Physico-chemical and biological properties of the experimental field (initial value).

SN	Particulars	Values		References
		2016	2017	
I	Mechanical analysis			
	Sand (%)	63.28	63.40	Bouyoucos, 1962
	Silt (%)	12.24	12.26	
	Clay (%)	24.48	24.34	
	Textural class	Sandy clay loam		
II	Physical Properties			
	Bulk density (Mg m^{-3})	1.58	1.56	Piper, 1966
	Water stable aggregates (%)	11.5	11.0	Yoder, 1936; Bouyoucos, 1962
III	Chemical properties			
	Soil organic carbon (%)	0.39	0.40	Jackson, 1973
	Available N (kg ha^{-1})	164.5	166.5	Subbiah and Asija, 1956
	Available P (kg ha^{-1})	14.5	14.8	Olsen et al., 1954
	Available K (kg ha^{-1})	292.0	292.0	Jackson, 1973
	pH (1:2.5, soil: water)	7.8	7.8	Jackson, 1973
	Electrical conductivity (EC, dsm^{-1})	0.40	0.39	Jackson, 1973
IV	Biological properties			
	Microbial biomass carbon (MBC, mg kg^{-1} soil)	102.5	112.0	Nunan et al., 1998
	Dehydrogenase activity (DHA, µg TPF g^{-1} soil day^{-1})	105.5	118.0	Casida et al., 1964
	Alkaline phosphatase activity (APA, µg PNP g^{-1} soil hr^{-1})	46.2	50.3	Tabatabai and Bremner, 1969
	Acetylene reduction activity (ARA, n moles ethylene $gram^{-1}$ soil hr^{-1})	13.5	16.8	Rakshit et al., 2018
	Total polysaccharides (mg kg^{-1} soil)	266.5	270.8	Acton et al., 1963

flowering, and pod-filling stages. The preliminary use of pendimethalin 30 EC @.9 kg ha^{-1}, along with one manual weeding at 30 DAS, was practiced for the management of weed in crops. Dimethoate 30 EC (Rogor) at the rate of 250-ml a.i. ha^{-1} (0.025%) and monocrotophos at the rate of 300-ml a.i. ha^{-1} (0.03%) were introduced as spray to control insect-pests of the crop. Zineb (0.2%) was applied at 60 DAS to control fungal diseases like the leaf spot. The crop was harvested when seeds became relatively hard, having 75–80% moisture. The harvested produce from the net plot area was sundried for 4–5 days; after that, bundle weight was recorded. Pullman thresher was used for threshing and seed cleaning.

TABLE 2 Treatment details of the experiment.

T_1	Control	T_6	LC (5 t ha^{-1})
T_2	RDF (30:60:40 kg N:P:K ha^{-1})	T_7	VC (5 t ha^{-1}) + MI
T_3	RDF + Microbial inoculants (MI)	T_8	FYM (5 t ha^{-1}) + MI
T_4	VC (5 t ha^{-1})	T_9	LC (5 t ha^{-1}) + MI
T_5	FYM (5 t ha^{-1})		

Data recording and analysis

Crop growth parameters

Growth parameters were observed and recorded as per standard methodology and protocols. Plant height was taken from the base region to the tip of the longest branch at 30, 60, and 90 days after sowing (DAS) and at the maturity stage.

TABLE 3 Chemical composition of FYM, vermicompost, and leaf compost used in the experiment.

Nutrient content	FYM		Vermicompost		Leaf compost	
	2016	2017	2016	2017	2016	2017
Total N (%)	0.52	0.57	1.48	1.45	0.40	0.40
Available P (%)	0.20	0.25	0.51	0.47	0.15	0.16
Available K (%)	0.55	0.56	1.37	1.40	0.45	0.44
Fe (mg kg^{-1})	1700	1730	2024	1991	1400	1350
Zn (mg kg^{-1})	107.5	104.2	100.2	99.6	85.5	95.5
Mn (mg kg^{-1})	341.7	354.2	370.1	354.8	320.5	332.5
Cu (mg kg^{-1})	15.8	16.2	17.7	18.1	15.0	15.5

The plant dry matter accumulation (DMA) was noted at a regular interval of 30, 60, and 90 DAS and at the maturity stage. For this purpose, the harvesting of plants of a 0.5-m continuous row length area was done at different growth stages. The observations on number of the branches plant^{-1} were recorded by counting the five tagged plants of each plot at maturity. Then, the average was calculated and value expressed as a number of the branches plant^{-1}. After measuring the leaf area, these plants were kept for sun-drying and then oven-drying at 65°C till the constant weight was achieved. Finally, DMA value was expressed as g plant^{-1}. The leaf area of randomly selected five plants from each experimental plot was noted at the 30-, 60-, and 90-DAS stage using the leaf area meter. Then, the average was calculated, and the final value of the leaf area was expressed in the cm^2 plant^{-1}. Leaf area index (LAI) was worked out by dividing value of the leaf area with the ground area using the following standard formula:

$$\text{Leaf area index (LAI)} = \text{Leaf area(sq.cm)/Land area (sq.cm)}$$

The mean crop growth rate of the crop was estimated using the following formula:

$$\text{CGR} = \left(\frac{W_2 - W_1}{T_2 - T_1}\right)\left(\frac{1}{S}\right)$$

where

W_1 and W_2 represent dry weight (g) at time T_1 and T_2, respectively

T_2- T_1 represent the interval of time (days)

S is the value of the land area (m^{-2}) as occupied by crop plants

CGR of the crop expressed as g m^{-2} of the land area day^{-1}.

Soil health parameters

Soil physical parameters *viz.,* Bulk density (BD), water stable aggregates (WSA), mean weight diameter (MWD), and geometric mean diameter (GMD) were recorded at the beginning and the end of the crop cycle. The sample for measuring field BD was collected by the core sampler of Piper (1966) from the randomly selected 3–4 areas of each experimental plot. The distribution of aggregate size was measured using approximately 250-g oven dried soil, and the remaining portion of soil was air-dried at the room temperature. Then, the material was passed through a 2-mm sieve in order to determine aggregate particle size distribution, following the Bouyoucos Hydrometer Method (Bouyoucos, 1962). The wet-sieving method was used for the estimation of the size distribution of WSA (Yoder, 1936). The GMD and MWD of soil aggregates were measured, with the method outlined by Kemper and Rosenau (1986). For separating the 4- to 8-mm aggregates from the bulk soil, the dry-sieving technique was used. During this process, the rupture of aggregates is common; hence, to prevent a sudden rupture, 50 g of aggregates was placed on the first sieve and moistened gently from below. Then, the set of sieves was shaken in water for about 10 min at the oscillations rate of 30 min^{-1}. Now, after correction for sand content, the settled soil on each sieve was utilized for calculating the MWD of the WSA. The percentage weight of aggregates retained on sieves (>0.25-mm diameter) was noted as WSA. The calculation of WSA was worked out as per the following equation:

$$MWD = \sum_{i=1}^{n} \overline{Xi}Wi$$

$$GMD = \exp\left[\sum_{i=1}^{n} \log \overline{xi}wi/m\right]$$

where, 'Xi' represents the mean fraction diameter, 'i' is the aggregate diameter fraction, 'Wi' is the proportion of total sample weight in that particular fraction, and 'm' is the total sample mass.

$$\text{Distribution of water stable aggregates (\%)} = \frac{\text{(Aggregates weight in each size group)}}{\text{(Total weight of soil)}} \times 100$$

Soil chemical characteristics (initial and end of the experiment) were estimated from collected soil samples from the depth of 0–15 cm of the soil profile. Soil reaction (pH) was analyzed in aqueous extract of soil and de-ionized water using the soil:water ratio as 1:2.5. The collected soil samples were air-dried and organic carbon (OC was measured by following the procedure described by Walkley and Black (Jackson, 1973). Available nutrients (N, P, and K) were estimated by soil sample collection from the depth of 0–15 cm of the soil profile from the experimental plot at the initial stage and the end of each experiment. The samples for N, P, and K analyses were air-dried, grounded, and allowed to pass through a 2-mm mesh sieve. The available N was analyzed through the alkaline potassium permanganate ($KMnO_4$) procedure as described by Subbiah and Asija (1956) and the value expressed as kg ha^{-1}. The available P status in soil was measured by following the Olsen's method (Olsen et al., 1954) and expressed as kg ha^{-1}. Available K was measured from the neutral ammonium acetate extraction method of Jackson (1973) and expressed as kg ha^{-1}. On the basis of primary data (SOC and BD values), the SOC stock, the build-up rate, and the sequestration rate were calculated (Lenka et al., 2013; Paul et al., 2016; Yadav et al., 2018). The following formula has been used for calculating SOC stock and the rate of sequestration:

$$\text{SOC stock (Mg/ha)} = \frac{\text{SOC} \times \text{Bulk density (Mega g /cubic m)} \times \text{Soil depth (m)} \times 10000}{100}$$

The rate of soil carbon sequestration (Mg C ha^{-1} year^{-1}) for the 2 years of the experimental period was estimated as a change

in the soil organic carbon (SOC) stock (Mg ha^{-1}) divided by the experiment duration (year).

$$\text{Soil C sequestration rate} = \frac{\text{SOC (final)} - \text{SOC (initial)}}{\text{Duration of experiment}}$$

The biological properties of soil were estimated by collecting the samples from the depth of 0–15 cm of the soil profile using the tube augur at the crop stage of 50% flowering (75 days after sowing). The gentle sieving by the use of a 4-mm mesh sieve was done to remove plant roots, stones, and large organic contents. After sieving, the field moist samples were subjected to pass by the use of a 2-mm sieve and laid in at 4°C until used for the estimation of soil microbial biomass carbon and activities of enzymes (dehydrogenase and alkaline phosphatase). Soil microbial biomass carbon (SMBC), dehydrogenase activity (DHA), and alkaline phosphatase activity (APA) in soil samples were measured by following the method described by Casida et al. (1964), Tabatabai and Bremner (1969), and Nunan et al. (1998) respectively. The brief methodology for the estimation of soil microbial parameters is as follows:

For the determination of SMBC (mg kg^{-1} soil), a 5-g soil sample was fumigated with chloroform and then incubation for 24 h. After the incubation process, the evaporation of chloroform was done at 50°C in Bio-chemical oxygen demand (BOD) by opening the tube caps for 20–24 h. After the process of evaporation, 70 ml of 0.5-M potassium sulfate (K_2SO_4) was added in samples and shaken for 30 min, followed by settle down. Final supernatant liquid was subjected for the measurement of absorbance. The final value of SMBC was worked out from the following formula:

$$\text{SMBC (mg per kg soil)} = \text{Fumigated soil organic carbon} - \text{Unfumigated soil organic carbon} \times 17.5 \times 15487$$

For the estimation of DHA (μg TPF g^{-1} soil day^{-1}), saturation of 6.0 g of the soil sample was done with 1.0-ml Tri phenyl tetrazolium chloride (TTC) by adding 0.1-g calcium carbonate ($CaCO_3$) and incubated for a day; then, methanol (10 ml) was added, and the sample tube was shaken for about 1.0 min followed by filtration to obtain supernatant liquid. The absorbance reading of the supernatant liquid was taken by the Spectrophotometer at the wavelength of 485 nm. The final calculation was worked out with the following equation:

$$\text{DHA (μgTPF/g soil)/day)} = \text{Soil weight (g)} \times \text{Concentration} \times \text{Dilution factor}$$

Alkaline phosphatase activity (μg p-nitro phenol g^{-1} soil hr^{-1}) was determined by estimating *p*-nitrophenol (PNP) as relinquished by incubation of a 1-g soil sample with 0.25-ml toluene, a 4-ml universal buffer, and a 1 ml of a 5-mM substrate at 37°C for 1 h. The content of *p*-nitro phenol in the sample was estimated from the Spectrophotometer at the wavelength of 440 nm.

For the measurement acetylene reduction activity in soil, estimation of ethylene (index of nitrogenase activity) with gas chromatography was done (Rakshit et al., 2018). The ARA values are expressed as moles of ethylene produced g^{-1} soil hr^{-1}. For this purpose, a 2-m long Porapak-R stainless steel column and a flame ionization detector were used for the estimation of gas samples on Gas Chromatograph (GC) of Hewlett Packard 5890 series II. The column temperature was maintained at 100°C, and the injector and detector temperature were maintained at 110°C. A gas flow rate of 35-ml min^{-1} of N_2 was served as carrier gas.

$$\text{Soil Acetylene Reduction Activity (ARA)} = 0.1653 \times \text{x} \times \text{(conc. by G.C.)}$$

The total polysaccharides content of soils as affected through different treatments was analyzed following the method as described by Acton et al. (1963). For the colorimetric measurement of the carbohydrate content in soil, 10 g of soil was disseminated in 10 ml of.5-N NaOH for 10 min in a Waring blender, moved in Erlenmeyer flasks by addition of 60-milliliter NaOH, and shaken for 3 h. The soil suspension was then maintained with the concentrated hydrochloric acid (HCI) up to a pH value of 2–3, and the fulvic acids were isolated from the humic acids and soil colloids by centrifugation process. The proportion of humic acids and soil colloids remaining in the centrifuged tube was then washed with the acidified water made by adding 10-ml concentrated HCI in 400-ml H_2O. The process of centrifugation was done again, and the supernatant liquid was summed to the previous extract. The fulvic acids supernatant was then diluted to volume where two volumes of acetone were mixed to one volume of an aliquot of solution. The supernatant solution, after centrifuging, comprised the acetone soluble fraction. The removal of acetone was done by evaporation up to dryness using a steam bath, and the residues dissolved in water. The precipitated flocculent known as microbial gum was redissolved in 0.5 A/NaOH, and also volume was maintained. The fractions of organic matter were hydrolyzed through sufficient H_2SO_4 to provide a solution equivalent to 100 ml of 3 N H_2SO_4. Polysaccharide constituents were then estimated with anthrone.

Root properties

For the measurement of root properties, samples of plant roots were collected from the third row of the cultivated crop at the flowering stage of the 50% (75 days after sowing) stage. For the purpose, a root auger measuring an 8-cm diameter

and 15-cm length (core volume = 754.28 cm^3) was utilized for root sampling up to the depth of 0–30 cm of the soil profile. The core ring of auger was maintained at the base level of the stem at the center. By gradually loosening the soil, the roots were collected. To prevent loss of finer roots while washing, the remaining soil adhered on roots was removed by gentle washing and placing the roots on sieve containers and immediately kept for refrigeration at 4°C. The root parameters, such as root length and the root surface area, were estimated from a computer-based RHIZO device scanner, which scans and analyzes the images using WIN-RHIZO software. These values were further used for calculating the root length density (RLD), root surface density (RSD), and root volume density (RVD) on the basis of unit soil volume in a cubic centimeter (cc). After the scanning, the root samples were subjected to drying at 60°C for 2 days for obtaining root dry weight (RDW). Number of nodules per plant was recorded by selecting five plants randomly at the flowering and maturity stage from the rows subjected for sampling from each plot. Nodules detached from the roots and the number of nodules were measured from each plant and expressed as the number of the nodules $plant^{-1}$.

Statistical analysis and data visualization

All the experimental data for various characters were statistically studied through the ANOVA method as described by Panse and Sukhatme (1985). The comparison of treatment means was made by the least significant difference (LSD) test at the probability level of $p < 0.05$ (Steel et al., 1997). The significance of treatment response was analyzed with the help of the 'F' (variance) test, and significance of difference was analyzed and critical difference (CD) or LSD calculated by using formula:

$$\text{LSD or CD} = \sqrt{\frac{2\ \text{MSE} \times \text{t at 5\% significance level}}{\text{n}}}$$

where 'MSE' is the mean square error, 'n' is the number of observations, 't' is the value of percentage point of 't' distribution for error degrees of freedom at the 5% level of significance.

Pearson correlation coefficient and multivariate analysis

Pearson correlation coefficient analysis was carried out to understand the association between diverse soil physical, chemical, and biological parameters. The R software (version 3.5.1) was used to perform Pearson correlation coefficient analysis. Two chemometric approaches *viz*. principal component analysis (PCA) and agglomerative hierarchical clustering (AHC) were used, resorting to SPSS of version 22. The cluster analysis (CA) was done, which supports in grouping the objects (cases) into classes (clusters) and depends on relative similarities within a class and dissimilarities between different classes. The findings of cluster analysis help in the interpretation of data and indicating the pattern and were presented as the heat map (Vega et al., 1998). A heat map represents two-dimensional illustration of data where values are analyzed by colors, which deliver the visual information. The heat map sorts the rows, and columns depend on the hierarchical clustering/cluster analysis. The colors will then be apportioned to the soil properties to represent the values. Principal component analysis (PCA) is a multivariate technique, which analyzes the data through various inter-correlated and quantified dependent variables to find out the abstract of the significant information from the data to represent it as a set of novel orthogonal variables referred to as principal components (PC), and to show the configuration of relationship among the observations and the variables (Mishra et al., 2017). For clarity in interpretation, data were resorted to Varimax orthogonal rotation.

Results and discussion

Plant growth and yield of pigeonpea

Effect of microbial-inoculants (MI)-mediated nutrient management on plant height of pigeonpea was not established significant at 30 DAS; however, it showed significance at 60 and 90 DAS and at the maturity stage (**Table 4**). Significantly higher plants height of pigeonpea at 60 and 90 DAS and the harvest stage were recorded with VC + MI treatment, which remained at par with the FYM + MI and LC + MI. Plant height at 60 and 90 DAS, and the harvest stage did not vary significantly with the application of RDF + MI over sole RDF. Among the organic sources, VC recorded higher plant height followed by FYM and LC under both treated and sole application. The DMA was significantly affected because of various treatments during 60 and 90 DAS and at the harvest stage, whereas, at 30 DAS, it was non-significant (**Table 4**). The effect of inoculation with organic resources was substantial over sole organic resources. However, the application of RDF + MI and sole RDF did not differ significantly with respect to DMA at 60 and 90 DAS and at the harvest stage. DMA with VC + MI application at 60 and 90 DAS and the harvest stage was at par with the use of FYM + MI and LC + MI. The DMA was higher in VC over FYM and LC. Significantly higher DMA was recorded with VC + MI over FYM + MI and LC + MI. Branches per plant of pigeonpea were influenced significantly due to the bio-inoculation of the crop with microbial inoculants (**Table 4**). The higher number of branches per plant (23.3) was noted with the use of VC + MI, which was at par with branching with FYM + MI. Inoculation of pigeonpea with MI was observed more effective when applied along with organic nutrient sources; however, integration of MI with RDF was found ineffective to enhance the branching significantly. The advantage of integrating MI with nutrient sources was to the tune of 47.9, 41.3, 25.9, and 2.5% for LC + MI,

TABLE 4 Influence of microbial inoculants-mediated nutrient management on crop growth parameters (mean of 2-year data) of pigeonpea.

Treatments*	Plant height (cm)			DMA (g plant^{-1})			Branches plant^{-1}	LAI			CGR (g plant^{-1} day^{-1})		
	30 DAS	60 DAS	90 DAS	Maturity	30 DAS	60 DAS	90 DAS	Maturity	At 50% flowering (75 DAS)	30 DAS	60 DAS	90 DAS	0-30 DAS	30-60 DAS	60-90 DAS
Control	36.3	87.3^{d}	107.2^{d}	114.3^{d}	4.0	10.2^{e}	35.5^{e}	46.8^{e}	12.0^{f}	0.32	0.94^{d}	2.02^{d}	1.11	1.76^{e}	7.0^{c}
RDF	38.3	98.5^{c}	119.6^{c}	131.1^{c}	4.6	12.1^{d}	40.5^{d}	54.0^{d}	16.2^{d}	0.33	1.10^{c}	2.26^{c}	1.28	2.10^{de}	8.0^{bc}
RDF + MI	38.9	100.3^{c}	120.9^{c}	133.7^{c}	4.7	12.4^{d}	40.8^{d}	55.2^{d}	16.6^{d}	0.35	1.12^{c}	2.28^{c}	1.30	2.19^{d}	8.0^{bc}
VC	38.2	107.8^{b}	131.2^{b}	145.9^{b}	4.3	14.0^{c}	44.4^{c}	59.8^{c}	18.5^{c}	0.35	1.23^{b}	2.50^{b}	1.20	2.82^{c}	8.7^{ab}
FYM	37.2	97.7^{c}	118.5^{c}	130.6^{c}	4.2	12.2^{d}	40.0^{d}	53.3^{d}	15.5^{de}	0.32	1.05^{c}	2.24^{c}	1.16	2.25^{d}	7.8^{bc}
LC	37.0	95.6^{c}	115.8^{c}	127.7^{c}	4.2	11.8^{d}	39.3^{d}	52.3^{d}	14.0^{e}	0.35	1.05^{c}	2.23^{c}	1.15	2.18^{d}	7.6^{c}
VC + MI	39.0	119.4^{a}	146.3^{a}	165.1^{a}	4.8	17.3^{a}	50.5^{a}	70.8^{a}	23.3^{a}	0.37	1.37^{a}	2.77^{a}	1.32	3.69^{a}	9.5^{a}
FYM + MI	39.3	117.0^{a}	143.8^{a}	162.9^{a}	4.7	15.8^{b}	47.7^{b}	65.2^{b}	21.9^{ab}	0.35	1.36^{a}	2.74^{a}	1.30	3.23^{ab}	9.2^{a}
LC + MI	38.5	115.7^{a}	141.5^{a}	157.8^{a}	4.8	15.5^{b}	47.4^{b}	64.7^{b}	20.7^{b}	0.34	1.33^{a}	2.72^{a}	1.33	3.16^{bc}	9.1^{a}
SEm±	1.1	1.8	2.6	3.5	0.3	0.3	0.8	1.3	0.6	0.01	0.03	0.06	0.07	0.13	0.4
LSD (P = 0.05)	NS	5.3	7.7	10.4	NS	1.0	2.5	4.0	1.7	NS	0.09	0.19	NS	0.40	1.1

Values in the same column followed by different letters are significantly different at $p < 0.05$ according to Duncan's multiple-range test for separation of means.
*Refer to Table 2 for treatment description.

FYM + MI, VC + MI, and RDF + MI, respectively. LAI of pigeonpea was significantly affected due to MI-mediated nutrient management during 60 and 90 DAS, whereas, at 30 DAS, the effect was non-significant during both years (Table 4). Significantly, higher LAI at 60 and 90 DAS was found in RDF + MI; however, it was at par with the sole use of RDF. Higher LAI was measured with VC + MI application at 60 and 90 DAS and at the harvest stage, which was at par with the LAI under FYM + MI and LC + MI treatment during both years. Among the organic sources of nutrients, VC has resulted in the highest LAI, followed by FYM and LC under both treated and sole application.

Effect of various MI-mediated nutrient management practices on crop growth rate ($\overline{CGR}$) was significant during 30–60 and 60–90 DAS (Table 4). Maximum $\overline{CGR}$ was recorded with VC + MI application at 30–60 and 60–90 DAS, which was at par with the FYM + MI and LC + MI. Significantly higher $\overline{CGR}$ was measured in inoculated organic sources of nutrients. Growth attributes *viz.* plant height, DMA, Branching, LAI, and $\overline{CGR}$, were established significantly better under MI-treated organic resources over sole organic resources of nutrients, which might be because of their PGP ability, meager competition for growth factors, high root growth, better soil aeration and microbial activity, and available nutrients in the long run might be responsible for superior growth attributes of the plant (Dhandayuthapani et al., 2015). The maximum value of growth attributes under VC + MI over other manures supports the fact of its nutrient richness (Table 3). In comparison to chemical fertilizers, vermicompost promotes biological fertility of soil through accessing resources (dissolved organic carbon and dissolved organic nitrogen) and environment for better microbial growth (Zhang et al., 2012). Hence, the higher contents of available nutrients and favorable microbial properties under VC + MI might have resulted in higher growth attributes over other manures (Song et al., 2015). The effectiveness of integrating microbial agents and vermicompost to replace for regular chemical fertilization practices is proved (Song et al., 2015). Improvement in growth attributes under inoculated VC treatment over sole VC and other inoculated manures was due to the better nutrient management through the integrated use of microbial-inoculants, which raised the availability of major nutrients to plants, which further result in elevation of biochemical and physiological processes *viz.*, energy transfer reactions, root development, and photosynthesis, which allowed the crop to grow to their full potential (Shete et al., 2010; Kumar et al., 2015; Zeyad et al., 2021; Sharma et al., 2022).

Root growth and development

The MI-mediated nutrient management significantly affected the root length (RL) and RLD (Table 5). The influence of inoculation with RDF was non-significant over sole RDF,

TABLE 5 Influence of microbial inoculants-mediated nutrient management on rhizospheric attributes (mean of 2-year data) of pigeonpea.

Treatments*	Root length (cm)	Root length density (cm cc^{-1})	Root dry weight (g)	Root surface density (cm^2 cc^{-1})	Root volume density (cm^3 cc^{-1})	Root nodules (no.)	
						Flowering	Maturity
Control	34.1^{f}	34.2^{d}	22.7^{f}	23.1_{f}	9.4^{f}	12.6^{f}	6.5^{f}
RDF	37.8^{e}	37.9^{c}	28.7^{e}	26.8^{e}	11.3^{ef}	19.2^{cd}	8.4^{e}
RDF + MI	40.0^{d}	39.7^{c}	32.4^{d}	29.6^{de}	11.9^{def}	23.8^{b}	15.3^{b}
VC	38.4^{de}	38.6^{c}	30.4^{de}	28.9^{de}	13.7^{bcd}	16.5^{e}	8.7^{e}
FYM	43.9^{c}	44.0^{b}	37.9^{c}	34.9^{c}	15.1^{abc}	20.0^{cd}	11.4^{d}
LC	38.9^{de}	39.0^{c}	31.4^{de}	30.2^{d}	$12.9b^{cde}$	17.8^{de}	11.2^{d}
VC + MI	44.8^{bc}	45.3^{ab}	39.2^{bc}	37.4^{bc}	15.2^{ab}	20.3^{c}	13.6^{c}
FYM + MI	47.5^{a}	48.0^{a}	41.5^{a}	40.7^{a}	16.1^{a}	26.3^{a}	18^{a}
LC + MI	45.9^{b}	46.6^{ab}	40.2^{b}	38.8^{ab}	14.0^{cde}	26.0^{ab}	17.4^{a}
SEm±	1.1	1.0	1.5	1.0	0.6	0.76	0.57
LSD ($P = 0.05$)	3.2	3.0	4.4	3.1	1.8	2.28	1.72

Values in the same column followed by different letters are significantly different at $p < 0.05$ according to Duncan's multiple-range test for separation of means.
*Refer to Table 2 for treatment description.

while organic sources, along with MI, had significant effect over sole use of organic sources of nutrients. FYM caused higher RL followed by LC and VC under both MI-treated and sole applications. FYM + MI showed the highest RL and RLD, which was at par with LC + MI, as well as sole FYM. Inoculation response was seen higher with LC + MI (18%), followed by 16.7, 8.2, and 5.8%, with VC + MI, FYM + MI, and RDF + MI, respectively. RDW was noted to be influenced significantly when the organic as well as inorganic nutrient sources were integrated with MI cultures (Table 5). However, the response of integration was higher (29%) with VC + MI, followed by LC + MI (28%), RDF + MI (12.9%), and FYM + MI (9.5%), although the FYM + MI recorded the highest (41.5 g) RDW, and this was at par by the use of LC + MI and FYM + MI. RSD was recorded to be influenced significantly when the organic, as well as inorganic nutrient sources, were integrated with MI cultures (Table 5). However, the response of integration was higher (29.4%) with VC + MI, followed by LC + MI (28.5%), FYM + MI (16.6%) and RDF + MI (10.5%), although the FYM + MI observed the highest RSD (40.8 cm^2cc^{-1}), and it was at par with LC + MI and FYM + MI. The RSD was ranked as FYM + MI ≈ LC + MI > VC + MI ≈ LC ≈ FYM > VC > RDF + MI ≈ RDF > control. RVD was enhanced with the integration of MI with the organic and inorganic nutrient sources; however, this effect was not significant (Table 5). Among the organic combinations, FYM + MI recorded the highest (16.1 cm^3 cc^{-1}) and LC + MI the lowest value (14.1 cm^3 cc^{-1}) of RVD and VC + MI as intermediate (15.2 cm^3 cc^{-1}). Number of the nodules $plant^{-1}$ was measured at the maximum flowering and maturity stage of the pigeonpea crop, and it was noticed that MI-mediated nutrient management practices significantly influenced the nodulation (Table 5). Organic sources of nutrients, especially FYM, resulted in a higher number of root nodules when applied as sole or in combination with MI. However, LC (sole), as well as LC + MI performed at par with FYM + MI, while VC (sole), as well as VC + MI could not perform statistically at par with FYM and LC. Integration effect of MI with various nutrient sources on nodulation was 46.1, 31.5, 24, and 23% higher with LC, FYM, RDF, and VC, respectively, at the flowering stage, while, at the maturity, it followed the trend as RDF + MI (82.1%) > FYM + MI (57.9%) > VC + MI (56.3) and LC + MI (55.4%).

The resultant favorable rhizospheric attributes with the application of FYM followed by VC > LC > RDF under both inoculated and un-inoculated treatments might be due to the better soil properties, especially, SOC, WSA, water holding capacity, lower BD, higher porosity, and higher microbial activity, which created easiness for the proper development of roots (Dar et al., 2017; Singh et al., 2020a; Kumar et al., 2022). Another reason for higher root development under FYM + MI might be the accelerated production of PGP and root growth-promoting hormones by microbial inoculants, such as IAA, phosphatase, and ACC deaminase (Helman et al., 2012). According to a report, there was a significant improvement in root volume (62%), root weight (74%), root length (54%), and root area (75%) due to MI inoculation (Mäder et al., 2011; Kumar et al., 2015). Improvement in rooting characteristics under bulky organic manures may also be due to the synergistic effect of certain microbes that enable organic manures to mineralize quickly and release plant nutrients in a balanced and quick manner (Gupta et al., 2020). FYM, being rich in organic carbon, provides favorable growth conditions for plant growth-promoting rhizobacteria (PGPR), which shows a symbiotic

TABLE 6 Influence of microbial inoculants-mediated nutrient management on soil physical, chemical, and biological properties (at the end of the 2-year experiment).

Treatments*	Soil physical properties				Soil chemical properties				Soil biological properties (During flowering stage, 70 DAS)				
	BD (Mg m^{-3})	WSA (%)	MWD (mm)	GMD (mm)	Available N (kg ha^{-1})	Available P (kg ha^{-1})	Available K (kg ha^{-1})	OC (%)	DHA activity (µg TPF g^{-1} soil day^{-1})	APA activity (µg p-nitro phenol g^{-1} soil hr^{-1})	SMBC (mg kg^{-1} soil)	ARA (n moles ethylene $gram^{-1}$ soil hr^{-1})	Polysaccharides (mg kg^{-1} soil)
Control	1.59	10.7^{g}	0.59^{d}	0.48^{e}	161.7^{b}	10.7^{c}	276.5^{d}	0.40	110.3^{e}	54.7^{e}	117.3^{e}	18.4^{e}	315.0^{f}
RDF	1.59	16.7^{d}	0.74^{cd}	0.56^{e}	165.0^{b}	16.7^{b}	325.3^{bc}	0.42	132.3^{d}	72.1^{d}	141.5^{d}	21.6^{de}	338.3^{e}
RDF + MI	1.58	17.3^{c}	0.84^{bcd}	0.68^{d}	167.3^{b}	17.3^{b}	335.5^{abc}	0.43	136.7^{d}	78.3^{d}	146.1^{cd}	22.9^{cd}	368.3^{cd}
VC	1.56	15.3^{f}	0.89^{abc}	0.77^{cd}	187.3^{a}	20.3^{a}	334.7^{abc}	0.45	156.4^{c}	92.7^{c}	160.6^{c}	23.6^{cd}	367.6^{d}
FYM	1.54	20.3^{b}	1.03^{ab}	0.82^{abc}	182.0^{a}	16.7^{b}	325.5^{bc}	0.46	180.3^{b}	111.7^{b}	193.1^{b}	25.1^{bc}	383.0^{c}
LC	1.55	16.7^{d}	0.99^{abc}	0.74^{cd}	181.0^{a}	15.3^{b}	321.4^{c}	0.45	176.4^{b}	107.1^{b}	188.5^{b}	23.9^{cd}	370.6^{cd}
VC + MI	1.54	16.0^{e}	1.11^{a}	0.90^{ab}	191.0^{a}	22.0^{a}	346.5^{a}	0.46	183.3^{b}	113.7^{b}	197.3^{b}	24.7^{bcd}	400.6^{b}
FYM + MI	1.53	22.0^{a}	1.13^{a}	0.93^{a}	183.0^{a}	17.0^{b}	340.6^{ab}	0.46	208.1^{a}	132.3^{a}	222.3^{a}	29.5^{a}	419.0^{a}
LC + MI	1.54	17.0^{cd}	1.00^{ab}	0.80^{bc}	186.0^{a}	16.0^{b}	335.0^{abc}	0.45	203.7^{a}	128.1^{a}	217.0^{a}	27.6^{ab}	405.3^{ab}
SEm±	0.03	0.21	0.09	0.04	4.2	1.0	6.0	0.03	6.1	4.6	5.9	1.1	3.9
LSD ($P = 0.05$)	NS	0.64	0.26	0.11	12.4	3.0	18.1	NS	18.2	13.7	17.6	3.4	15.8

Values in the same column followed by different letters are significantly different at $p < 0.05$ according to Duncan's multiple-range test for separation of means.
*Refer to Table 2 for treatment description.

10.3389/fmicb.2022.924407

TABLE 7 Correlation coefficient (r)* matrix between soil physical, chemical, and biological properties.

	MWD	GMD	BD	WSA	OC	N	P	K	DH	APA	MBC	ARA	POLY
MWD	***1***	***0.933***	***−0.867***	**0.681**	***0.898***	***0.895***	**0.591**	***0.737***	***0.942***	***0.95***	***0.941***	***0.868***	***0.938***
GMD	***0.933***	***1***	**−0.672**	**0.682**	***0.813***	***0.883***	***0.753***	***0.839***	***0.865***	***0.879***	***0.854***	***0.863***	***0.943***
BD	***−0.867***	**−0.672**	***1***	**−0.568**	***−0.791***	***−0.702***	−0.192	−0.405	***−0.887***	***−0.883***	***−0.906***	***−0.742***	***−0.779***
WSA	**0.681**	**0.682**	**−0.568**	***1***	0.473	0.408	0.36	**0.68**	***0.715***	***0.726***	***0.722***	***0.828***	***0.752***
OC	***0.898***	***0.813***	***−0.791***	0.473	***1***	***0.951***	0.473	***0.522***	***0.869***	***0.871***	***0.849***	***0.738***	***0.771***
N	***0.895***	***0.883***	***−0.702***	0.408	***0.951***	***1***	**0.683**	**0.667**	***0.825***	***0.832***	***0.804***	***0.705***	***0.796***
P	**0.591**	***0.753***	−0.192	0.36	0.473	**0.683**	***1***	***0.864***	0.41	0.432	0.393	0.421	**0.56**
K	***0.737***	***0.839***	−0.405	**0.68**	***0.522***	**0.667**	***0.864***	***1***	**0.667**	**0.684**	**0.659**	***0.737***	***0.801***
DH	***0.942***	***0.865***	***−0.887***	***0.715***	***0.869***	***0.825***	0.41	**0.667**	***1***	***0.999***	***0.998***	***0.952***	***0.948***
APA	***0.95***	***0.879***	***−0.883***	***0.726***	***0.871***	***0.832***	0.432	**0.684**	***0.999***	***1***	***0.997***	***0.955***	***0.957***
MBC	***0.941***	***0.854***	***−0.906***	***0.722***	***0.849***	***0.804***	0.393	**0.659**	***0.998***	***0.997***	***1***	***0.947***	***0.947***
ARA	***0.868***	***0.863***	***−0.742***	***0.828***	***0.738***	***0.705***	0.421	***0.737***	***0.952***	***0.955***	***0.947***	***1***	***0.958***
POLY	***0.938***	***0.943***	***−0.779***	***0.752***	***0.771***	***0.796***	**0.56**	***0.801***	***0.948***	***0.957***	***0.947***	***0.958***	***1***

The correlation coefficient (r) values are significantly positive at $p < 0.01$ (Boldfaced italics) and $p < 0.05$ (Bold) levels of probability (two-tailed).
Boldfaced yellow italics and bold blue-colored fonts indicate significantly negative correlation at $p < 0.01$ and $p < 0.05$ levels of probability (two-tailed).
*Correlation coefficient (r) values correspond directly to the color code from (decrease) green to yellow and red, respectively.
MWD, mean weight diameter; GMD, geometric mean diameter; BD, bulk density; WSA, water stable aggregates; OC, organic carbon; N, nitrogen; P, phosphorus; K, potassium; DH, dehydrogenase; APA, alkaline phosphatase activity; MBC, microbial biomass carbon; ARA, acetylene reduction activity, POLY, total polysaccharides.

relationship with plant roots and enables them to uptake more nutrients and water that ultimately helps in the optimum development of the root rhizosphere (Paramesh et al., 2020; Kumar A. et al., 2021). FYM, along with microbial inoculants, increases organic carbon, available nutrients, soil biological properties *viz*., dehydrogenase activity and improved microbial population (Kumar A. et al., 2021; Kumar S. et al., 2021), which becomes the reason for the enhanced root nodulation and root growth attributes (Singh et al., 2020b, 2021). Inoculated organic treatments increase the porosity of soil, which results in an improvement in root growth and raises soil biological/microbial activities, which enhance oxygen/air availability in the region of plant roots (Dar et al., 2017).

Soil physical properties

The effect of MI-based nutrient management along with organic sources or RDF on BD of soil was non-significant ($p < 0.05$) (**Table 6**). However, a slight reduction in BD was observed in plots applied with organic manures. A maximum reduction in the value of BD was found over the initial value of 1.58 g cc^{-1} in the FYM + MI treatment, while the least influence was recorded in the control plot. The efficacy of organic nutrient management practices in improving BD can be ranked as FYM > LC > VC. Soil aggregation expressed in terms of percentage of geometric mean diameter (GMD), mean weight diameter (MWD), and water-stable aggregates (WSA) is presented in **Table 6**. Significantly ($p < 0.05$), the higher WSA (22.0%), MWD (1.13 mm), and GMD (0.93 mm) were recorded in treatment FYM + MI. The effect of inoculation with microbial inoculants was significant ($p < 0.05$) in the case of RDF, FYM, VC; however, inoculation with LC was non-significantly effective. The extent of this improvement in WSA under inoculated treatments over the sole application was 7.7, 4.4, and 3.5% for FYM, VC, and RDF, respectively; in MWD: 8.8, 19.8, and 11.2%; in GMD: 11.8, 14.4, and 17.6%, respectively. Improvement in aggregates stability under LC + MI application was found to be inefficient. Significant improvement in WSA, MWD, and GMD under MI-mediated organic combinations, especially FYM + MI, might be due to a favorable impact on soil aeration as a result of proper rhizosphere development (Kumar S. et al., 2021) and optimum microbial activity (Singh et al., 2017; Kumar et al., 2018b; Kumar A. et al., 2021). The enhanced level of organic matter under organic treatments also played an important role in raising soil physical health (Nandapure et al., 2011), as is evident from the correlation matrix (**Table 7**) and the heat map analysis (**Figure 2**), which indicates a strong relationship between soil properties. Another reason for the improvement of soil physical properties under FYM + MI could be due to maintained soil-plant-water relationship in a better way as a result of proper root development and soil aggregation (Kumar et al., 2015; Graham et al., 2017; Singh et al., 2020b; Bhakar et al., 2021; Kumar A. et al., 2021). Accordingly, soils managed with organic manure, along with MI, tend to have more stable soil aggregates in comparison to inorganic fertilizers and MI combinations (Babu et al., 2015).

Soil chemical properties

The observations on available-N status in soil revealed that integration of microbial inoculants with organic and inorganic sources of plant nutrients was ineffective for showing a significant response on the status of available nitrogen in

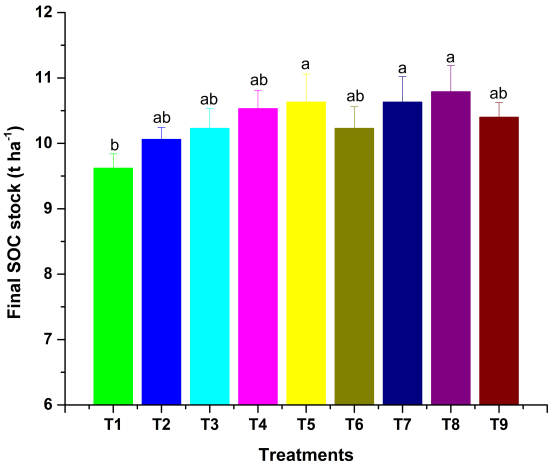

FIGURE 2
Final SOC stock as influenced by MI-mediated nutrient management. Different letters in alphabetical orders in figure are generally assigned to indicate the significantly different values at $p < 0.05$ according to Duncan's multiple-range test for separation of means.

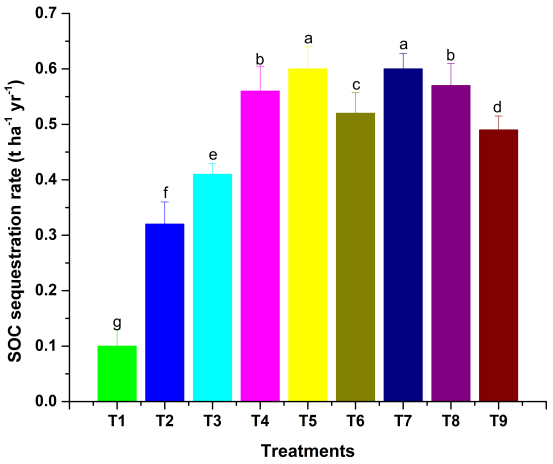

FIGURE 3
The SOC seq. rate as influenced by MI-mediated nutrient management. Different letters in alphabetical orders in figure are generally assigned to indicate the significantly different values at $p < 0.05$ according to Duncan's multiple-range test for separation of means.

soil (Table 6). However, sole and integrated organic sources were significantly effective for impacting available nitrogen in soil positively. The extent of additional nitrogen added by the application of organic sources, along with MI, as compared to RDF + MI was 12.4% higher with VC + MI, 8.1% with FYM + MI and 10.1% with LC + MI. Hence, this indicates that integration of MI with organic sources is significantly advantageous as compared to integration with chemical fertilizers. In comparison to sole application, the integration influence of RDF + MI, VC + MI, and LC + MI was higher to the tune of 1.4, 1.9, and 2.7%, respectively; however, FYM + MI was lesser effective by 0.5%. Available P status in soil was significantly ($p < 0.05$) affected by organic nutrient sources over inorganic sources (Table 6). The addition of available P in soil was analyzed to be higher with the use of VC + MI, and this was significantly higher than FYM + MI, LC + MI, RDF + MI, RDF, FYM, and LC; however, it was non-significant with sole VC application. The quantity of available P added in soil under VC + MI was 21.4% higher than RDF + MI; however, FYM + MI and LC + MI have added a lesser amount of available N in soil by -1.8% and -8.1%, respectively. In comparison to sole application, integration effect of RDF + MI, VC + MI, FYM + MI, and LC + MI was higher to the tune of 3.5, 7.7, 1.8, and 4.4%, respectively, with respect to available soil P. Status of available K in the soil at the end of a 2-year experiment was established significantly ($p < 0.05$) higher (Table 6) over the initial value (Table 1) under all the nutrient management treatments except control. Among the various MI-based combinations of nutrient management, application of VC + MI resulted in a significantly higher level of available K (346 kg ha^{-1}) in comparison to FYM, LC, and RDF; however, it was at par with available K status under VC, FYM + MI, RDF + MI, and LC + MI treatment. The response of integration of MI with different nutrient sources over the sole application was higher with FYM + MI (4.4%), followed by LC + MI (4.2%), VC + MI (3.5%), and RDF + MI (3%). The non-significant deviation was observed due to MI-mediated nutrient management on SOC (Table 6). However, a relatively higher amount of SOC was added to the soil with the use of organic resources of nutrients over inorganic sources. Among the organic sources, FYM added a relatively higher amount of SOC in the soil when applied sole as well as in combination with MI. The SOC stock (Mg ha^{-1}) was also observed higher under inoculated manure treatments (Figure 2). The trend of estimated final SOC stock was observed in the order of FYM + MI > FYM = VC + MI > VC > LC + MI > LC > RDF + MI > RDF > control. Observations in Figure 2 revealed that inoculation of crops with MI influenced the SOC stock; however, marginal improvement was noticed when manures or fertilizers were applied in combination. The SOC sequestration rate (t ha^{-1} yr^{-1}) also showed almost similar findings (Figure 3).

The improvement in the level of available NPK under VC + MI application might be due to enhanced nutrient release as a result of microbes-mediated accelerated decomposition and mineralization of inoculated manure (Kuotsu et al., 2014; Gupta et al., 2020). Application of inoculated manure proved to encourage and sustain soil health by raising the SOC, available NPK status, and uptake of nutrients by plants by reducing the BD of soil (Tiwari et al., 2011; Kumar et al., 2015, 2018a; Kumar S. et al., 2021). SOC, SOC Stock, and the SOC sequestration rate were found to be influenced in a non-significant way, following the mechanism of soil buffering capacity, which shows that a soil resists the changes in its properties up to a certain period, owing to the buffering ability

(Yigini and Panagos, 2016). Hence, this 2-year experiment was not sufficient enough to cause a significant effect on SOC; however, a slight improvement was definitely noted under organic combinations, which might be due to the higher addition of SOM and optimum mineralization of this SOM under the microbial-rich environment in root rhizosphere (Snapp et al., 1998; Tiwari et al., 2011; Thapa et al., 2017).

Soil biological properties

Bio-inoculation of pigeonpea seeds with MI culture of N, P, and K, along with the treatment of organic manures (FYM, VC, LC), improved the dehydrogenase enzyme activity (μg TPF g^{-1} soil day^{-1}) in soil, significantly; however, RDF + MI was non-significantly effective to influence dehydrogenase activity over the sole RDF (**Table 6**). The trend of dehydrogenase activity under various treatments was FYM + MI ≈ LC + MI > VC + MI ≈ LC ≈ FYM > VC > RDF + MI ≈ RDF > control. However, the increment of this positive influence due to bio-inoculation of nutrient sources over the sole application was to the tune of 17.2, 15.5, 15.4, and 3.3% under VC + MI, LC + MI, FYM + MI, and RDF + MI, respectively. Hence, it can be reported that MI with organic manures may affect the activity of dehydrogenase enzymes in soil significantly. Alkaline phosphatase activity of soil was also influenced significantly when the pigeonpea crop was inoculated with microbial strains of N, P, and K fixers and solubilizers (**Table 6**). Among the various MI-based nutrient management practices, use of FYM + MI resulted in higher activity (132.3 μg p-nitro phenol g^{-1} soil hr^{-1}) of alkaline phosphatase enzyme in soil; however, LC + MI also exhibited almost similar value (128.1 μg p-nitro phenol g^{-1} soil hr^{-1}). The trend of influence on alkaline phosphatase activity under the experimentation was seen in the order of FYM + MI ≈ LC + MI > VC + MI ≈ LC ≈ FYM > VC > RDF + MI ≈ RDF > control. However, the augmentation of this positive impact under integrated treatment over the sole application was to the tune of 22.7, 19.6, 18.4, and 8.6% under VC + MI, LC + MI, FYM + MI, and RDF + MI, respectively. SMBC content in soil was affected significantly ($p < 0.05$) due to MI-mediated nutrient management (**Table 6**). Among various treatments, application of FYM + MI resulted in higher SMBC (222.3 mg kg^{-1} soil), which was at par with SMBC content of 217.-mg kg^{-1} soil under LC + MI application. The ranking of impact on SMBC under the experimentation was in the order of FYM + MI ≈ LC + MI > VC + MI ≈ LC ≈ FYM > VC > RDF + MI ≈ RDF > control. However, the incremental effect of inoculation was noted as 22.9, 15.1, 15.1, and 3.3% under VC + MI, LC + MI, FYM + MI, and RDF + MI, respectively, over the sole application of these nutrient sources, which profound that inoculation of microbial strains with organics may be more advantageous over the inorganic when SMBC is concerned. Acetylene reduction activity of soil was estimated in the range of 18.4–29.5 n moles ethylene $gram^{-1}$ soil hr^{-1}. The higher value of ARA (29.5 n moles ethylene $gram^{-1}$ soil hr^{-1}) was measured by the combined use of FYM + MI, which was found higher significantly ($p < 0.05$) than ARA under the remaining treatments. The order of influence was noted as FYM + MI > LC + MI > FYM > VC + MI > VC ≈ RDF + MI ≈ RDF > control. The advantage of integrating MI with nutrient sources was to the tune of 17.5, 15.5, 6.0, and 4.7% for FYM + MI, LC + MI, RDF + MI, and VC + MI, respectively. This inferred that ARA activity response was highest with FYM + MI and lowest with VC + MI application. MI-mediated nutrient management practices affected the total polysaccharides content in soil significantly (**Table 6**). The highest value (419 mg kg^{-1} soil) of total polysaccharides was measured by the use of FYM + MI, which was significantly ($p < 0.05$) higher than others. The sequence of influence due to the imposition of different treatments was noted in the order of FYM + MI > LC + MI > VC + MI > LC ≈ RDF + MI ≈ VC ≈ RDF + MI > RDF > control. The improvement of integrating MI with nutrient sources was to the tune of 9.4, 9.4, 9. and 8.9% for FYM + MI, LC + MI, RDF + MI, and VC + MI, respectively.

The resulted trend of soil microbial parameters *viz.* dehydrogenase, alkaline phosphatase, SMBC, acetylene reduction activity, and the total polysaccharides level followed the order as FYM > LC > VC with and without MI, and these might be due to the improvement in soil-water relationship, enhanced addition of nutrients and organic carbon through microbes-mediated-accelerated decomposition of FYM (Samal et al., 2017; Ghosh et al., 2020). Inoculated manures enhance SOC and available moisture in the soil, which improves microbial health of the soil as microbial health is positively correlated with enhanced soil moisture status and organic carbon content in soil (Almeida et al., 2011). Organic manures promote the soil MBC and enzyme activities as compared to mineral fertilizers (Babu et al., 2020b). The soil phosphatase activity is recorded to enhance in rhizosphere by 2–3 times under inoculated treatments as that of un-inoculated soil (Gong et al., 2009). Enhancement in soil biological properties by adding the inoculated organic manures was due to higher population and activity of soil microbes and accelerated mineralization of organic manures, coupled with better soil physical parameters, such as BD and soil aggregation (Bongiorno et al., 2019). The inhibitory effect on enzyme activity was found with higher levels of RDF, which may be due to interference of nitrate, which serves as a substitute electron acceptor, ensuing in the drop down of enzyme activity (Babu et al., 2020a). The application of organic sources of nutrients increased organic carbon status in soil, and it acts as a substrate for microorganisms and also increased the availability of nutrients required for growth of microorganisms, resulting in higher microbial activity and, in turn, corresponded with

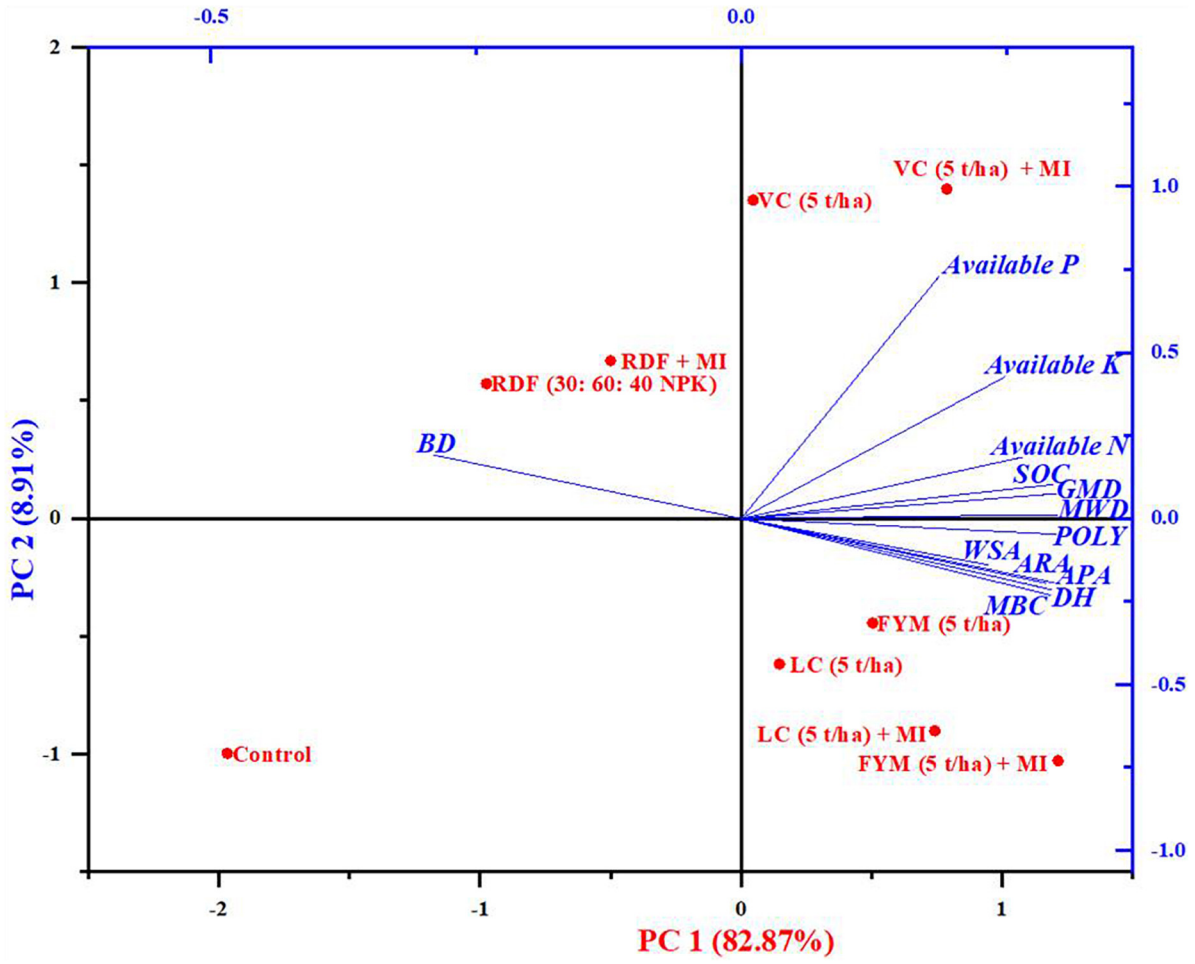

FIGURE 4
The two-dimensional graphical biplot showing both the loading and the scoreplot of soil physical, chemical, and biological properties.

higher SMBC and population counts in soil (Mäder et al., 2011). Increased soil enzymatic activities under inoculated organic manures application might be due to improvement in microbial population, which increased soil enzyme activities and thereby soil health (Kumar S. et al., 2021).

Correlation coefficient (*r*) matrix between soil physical, chemical, and biological characteristics

The univariate Pearson's correlation coefficient (*r*) matrix (**Table 7**) indicated that physico-chemical and biological properties of soil were found to be significant and positively correlated among them. The MWD was substantially and positively correlated among physico-chemical and biological characteristics of soil; however, it had a highly substantial negatively correlated ($p < 0.01$ and $r = -0.867$) with BD. The GMD exhibited a substantial negatively correlated ($p < 0.01$ and $r = -0.672$) with BD; however, it showed a positive correlation with the rest of the parameters. BD displayed a highly significant negative correlation ($p < 0.01$) among physic-chemical and biological properties, while the correlation with WSA displayed a substantial negative correlation ($p < 0.05$). WSA noticed a significant correlation with the following descending order ARA > POLY > APA > MBC > OC > DH > K. Organic carbon recorded a highly significant positive correlation ($p < 0.01$) with these parameters in descending order N > APA > Poly > DH > MBC > ARA > K > P. N noticed a highly significant negative correlation ($p < 0.01$) with K, DH, APC, MBC, ARA, and POLY and a significant positive correlation ($p < 0.05$) with P. P also recorded a significant positive correlation with K ($p < 0.01$ and $r = 0.864$) and POLY ($p < 0.05$ and $r = 0.560$), while K was significantly correlated ($p < 0.01$) with DH, APA, MBA, ARA, and POLY ($p < 0.05$) biological properties. DH exhibited a substantial positive correlation ($p < 0.01$) with APA, MBC, ARA, and POLY. Similarly, APA displayed a substantial positive correlation

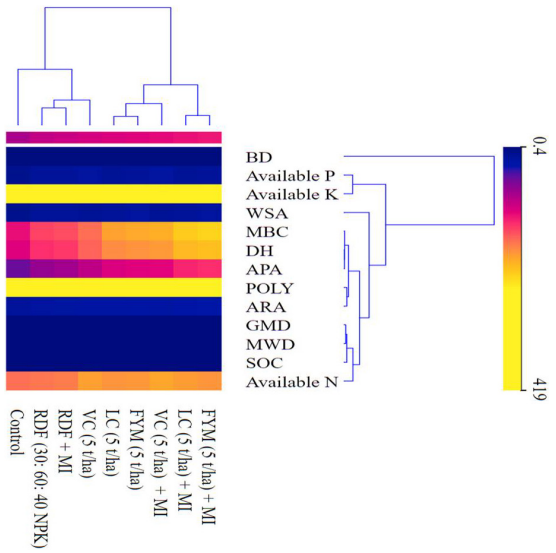

FIGURE 5
The heat map depicting the clustering of soil physical, chemical, and biological properties. MWD, mean weight diameter; GMD, geometric mean diameter; BD, bulk density; WSA, water stable aggregates; OC, organic carbon; N, nitrogen; P, phosphorus; K, potassium; DH, dehydrogenase; APA, alkaline phosphatase activity; MBC, microbial biomass carbon; ARA, acetylene reduction activity; POLY, total polysaccharides.

($p < 0.01$) with MBC, ARA, and POLY. MBC was positively and substantially correlated ($p < 0.01$) with ARA and POLY. ARA also displayed a substantial positive correlation ($p < 0.01$ and $r = 0.958$) with POLY.

Principal component analysis of physical, chemical, and biological properties

The results based on principal component analysis conducted on the physical, chemical, and biological characteristics of soil extracted two dominant principal components: PC1 and PC2, accounting for 79.20 and 10.30% variability, which explained up to 90% of the total variability (Figure 4). The biplot (Figure 4) depicted both factors loading of physical, chemical, and biological characteristics of soil (Blue color) and the score of treatment (Red color). The loading plot of the biplot (Figure 4) displayed that PC1 had large positive loadings on MBC, which was closely followed by DH, APA, ARA, and POLY, which belong to soil biological properties; however, it shows negative loading on BD. Furthermore, these parameters are strictly correlated to each other as the angle amid the variables of 0 or 1,800 divulges a correlation of 1 or -1, respectively (Kohler and Luniak, 2005). Similarly, PC 2 also exerted strong positive loading on P, K, and N, and negative loading on BD again. In respect of the scoreplot of the biplot (Figure 4), it can be seen that treatments, including VC + MI, occupied the Ist quadrant of the score plot and significantly influenced the component of PC2 (P, K, N, SOC, MWD), which were dominantly soil chemical and physical characteristics. Similarly, in the second quadrant, the treatments RDF + MI and RDF affected the BD of soil; however, the control plot (third quadrant) did not have any substantial impact on any parameters of soil. Interestingly, in the fourth quadrant, the treatments, including FYM (5 t ha^{-1}), LC, LC + MI, and FYM + MI, substantially affected most components of PC1 *viz.*, soil biological properties, comprising of MBC, DH, ARA, and POLY (Figure 4).

Heat map depicting the clustering of chemical, physical, and biological properties

The heatmap generated (Figure 5) displayed the soil properties vertically and treatments horizontally wherein three dominant clusters were formed. The 1st cluster consists of primary nutrients P and K, while the 2nd cluster consists of soil biological properties (MBC, DHA, APA, POLY, ARA). Similarly, the 3rd cluster encompasses root characters (RSD, RLD, RL, RDW, and RVD) and, finally, a pair of soil physical properties (GMD and MWD) and soil chemical properties (OC and N). BD was the only soil physical parameter that formed a discrete outlier without clustering with any other parameters under investigation, as it had a negative correlation with them.

Conclusion

The need of integrated and balanced nutrient management was a rational for the experiment "microbes-mediated integrated nutrient management for improved rhizo-modulation, pigeonpea productivity, and soil bio-fertility in a semiarid agro-ecology." The holistic findings concluded that the integration of certain N fixing, P, and K, solubilizing microbial inoculants along with organic manures could have significant impact on the crop growth, root development, and soil health parameters. A significant response of integration of MI with organic manures was assessed, following the trend VC + MI > FYM + MI > LC + MI > RDF + MI for plant shoot-root growth attributes and soil chemical health and bio-fertility. FYM + MI were exceptionally superior with respect to the soil physical health. Such findings were much better or at par with the results RDF + MI, which establish a base for the replacement of the chemical fertilizers in pigeonpea cultivation under pigeonpea-wheat crop rotation. Besides a solution for overuse of chemical fertilizers, study outcomes are also believed to solve the problem of crop residues and animal bi-products management by promoting the microbial consortia and organic manures-based agro-industries, which are basic to the microbial inoculants and organic manure-based INM. This

way, outcomes of the study would add to the goal of sustainable agricultural development by producing quality crop produce, maintaining agro-biodiversity and making the soils healthy, fertile, and productive.

Data availability statement

The raw data supporting the conclusions of this article will be made available by the corresponding author.

Author contributions

GG, SD, MR, AcD, VS, and LS: conceptualization. GG, AdK, VS, DJ, LS, KK, SR, and PU: methodology. GG, IB, DJ, SD, MR, AmK, KK, and MS: formal analysis. GG, AdK, AuD, DJ, AC, and SD: investigation. SD, LS, VS, and AcD: resources. GG, SD, IB, DJ, AmK, and MS: data curation. GG, AmK, IB, DJ, AC, SR, and PU: writing–original draft. SD, AcD, SR, PU, PD, MR, VT, and EJ: suggestions, editing, and reviewing the manuscript. All authors read and agreed to the published version of the manuscript.

Funding

The authors acknowledge ICAR-Indian Agricultural Research Institute, New Delhi, India, for providing the necessary funding and laboratory facilities required for conducting the study.

Conflict of interest

The authors declare that the research was conducted in the absence of any commercial or financial relationships that could be construed as a potential conflict of interest.

Publisher's note

All claims expressed in this article are solely those of the authors and do not necessarily represent those of their affiliated organizations, or those of the publisher, the editors and the reviewers. Any product that may be evaluated in this article, or claim that may be made by its manufacturer, is not guaranteed or endorsed by the publisher.

References

Acton, C., Paul, E., and Rennie, D. (1963). Measurement of the polysaccharide content of soils. *Can. J. Soil Sci.* 43, 141–150. doi: 10.4141/cjss63-017

Allen, D. E., Singh, B. P., and Dalal, R. C. (2011). "Soil health indicators under climate change: a review of current knowledge," in *Soil Health and Climate Change. Soil Biology*, eds B. Singh, A. Cowie, and K. Chan (Berlin: Springer). doi: 10.1007/978-3-642-20256-8_2

Almeida, D. D. O., Klauberg Filho, O., Almeida, H. C., Gebler, L., and Felipe, A. F. (2011). Soil microbial biomass under mulch types in an integrated apple orchard from Southern Brazil. *Sci. Agric.* 68, 217–222. doi: 10.1590/S0103-90162011000200012

Babu, S., Singh, R., Avasthe, R., Yadav, G. S., Das, A., Singh, V. K., et al. (2020b). Impact of land configuration and organic nutrient management on productivity, quality and soil properties under baby corn in Eastern Himalayas. *Sci. Rep.* 10, 1–14. doi: 10.1038/s41598-020-73072-6

Babu, S., Mohapatra, K., Yadav, G. S., Lal, R., Singh, R., Avasthe, R., et al. (2020a). Soil carbon dynamics in diverse organic land use systems in North Eastern Himalayan ecosystem of India. *Catena* 194:104785. doi: 10.1016/j.catena.2020.104785

Babu, S., Prasanna, R., Bidyarani, N., Nain, L., and Shivay, Y. S. (2015). Synergistic action of PGP agents and Rhizobium spp. for improved plant growth, nutrient mobilization and yields in different leguminous crops. *Biocatal. Agric. Biotechnol.* 4, 456–464. doi: 10.1016/j.bcab.2015.09.004

Bastida, F., Moreno, J. L., Hernandez, T., and García, C. (2006). Microbiological degradation index of soils in a semiarid climate. *Soil Biol. Biochem.* 38, 3463–3473. doi: 10.1016/j.soilbio.2006.06.001

Bhakar, A., Singh, M., Kumar, S., Kumar, D., Meena, B., Meena, V., et al. (2021). Enhancing root traits and quality of sorghum and guar through mixed cropping and nutrient management. *Indian J. Agric. Sci.* 91, 99–104.

Bongiorno, G., Bünemann, E. K., Oguejiofor, C. U., Meier, J., Gort, G., Comans, R., et al. (2019). Sensitivity of labile carbon fractions to tillage and organic matter management and their potential as comprehensive soil quality indicators across pedoclimatic conditions in Europe. *Ecol. Indic.* 99, 38–50. doi: 10.1016/j.ecolind.2018.12.008

Bouyoucos, G. J. (1962). Hydrometer method improved for making particle size analyses of soils. *Agronomy* 54, 464–465. doi: 10.2134/agronj1962.00021962005400050028x

Bünemann, E. K., Bongiorno, G., Bai, Z., Creamer, R. E., De Deyn, G., de Goede, R., et al. (2018). Soil quality–A critical review. *Soil Biol. Biochem.* 120, 105–125. doi: 10.1016/j.soilbio.2018.01.030

Casida, L. Jr., Klein, D. A., and Santoro, T. (1964). Soil dehydrogenase activity. *Soil Sci.* 98, 371–376. doi: 10.1097/00010694-196412000-00004

Congreves, K., Hayes, A., Verhallen, E., and Van Eerd, L. (2015). Long-term impact of tillage and crop rotation on soil health at four temperate agroecosystems. *Soil Tillage Res.* 152, 17–28. doi: 10.1016/j.still.2015.03.012

Dar, S., Mishra, D., Zahida, R., and Afshana, B. (2017). Hydrogel: to enhance crop productivity per unit available water under moisture stress agriculture. *Bull. Env. Pharmacol. Life Sci.* 6, 129–135.

Dhandayuthapani, U. N., Vimalendran, L., and Latha, K. (2015). Growth, yield and biological indices of medium duration pigeonpea (*Cajanus cajan* L.) influenced by intercrop and different plant population. *Bioscan* 10, 303–307.

Fernández-Romero, M., Parras-Alcántara, L., Lozano-García, B., Clark, J., and Collins, C. (2016). Soil quality assessment based on carbon stratification index in different olive grove management practices in Mediterranean areas. *Catena* 137, 449–458. doi: 10.1016/j.catena.2015.10.019

Ghosh, D., Brahmachari, K., Skalicky, M., Hossain, A., Sarkar, S., Dinda, N. K., et al. (2020). Nutrients supplementation through organic manures influence the growth of weeds and maize productivity. *Molecules* 25:4924. doi: 10.3390/molecules25214924

Gong, W., Yan, X., Wang, J., Hu, T., and Gong, Y. (2009). Long-term manure and fertilizer effects on soil organic matter fractions and microbes under a wheat–maize cropping system in northern China. *Geoderma* 149, 318–324. doi: 10.1016/j.geoderma.2008.12.010

Graham, R. F., Wortman, S. E., and Pittelkow, C. M. (2017). Comparison of organic and integrated nutrient management strategies for reducing soil N_2O emissions. *Sustainability* 9:510. doi: 10.3390/su9040510

Gupta, G., Dhar, S., Dass, A., Sharma, V. K., Shukla, L., Singh, R., et al. (2020). Assessment of bio-inoculants-mediated nutrient management in terms of productivity, profitability and nutrient harvest index of pigeon pea–wheat cropping system in India. *J. Plant Nutr.* 43, 2911–2928. doi: 10.1080/01904167.2020.1806302

Gupta, G., Dhar, S., Dass, A., Sharma, V. K., Singh, R. K., Kumar, A., et al. (2018). Influence of bio-inoculant mediated organic nutrient management on productivity and profitability on pigeonpea (*Cajanu cajan*) in a semi-arid agroecology. *Indian J. Agric. Sci.* 88, 1600–1605.

Harish, M. N., Choudhary, A. K., Kumar, S., Dass, A., Singh, V. K., Sharma, V. K., et al. (2022). Double zero tillage and foliar phosphorus fertilization coupled with microbial inoculants enhance maize productivity and quality in a maize–wheat rotation. *Sci. Rep.* 12, 1–23. doi: 10.1038/s41598-022-07148-w

Helman, Y., Burdman, S., and Okon, Y. (2012). "Plant growth promotion by rhizosphere bacteria through direct effects," in *Beneficial microorganisms in Multicellular Life Forms*, eds E. Rosenberg and U. Gophna (Heidelberg: Springer), 89–103. doi: 10.1007/978-3-642-21680-0_6

Jackson, M. (1973). *Soil Chemical Analysis*. New Delhi: Pentice hall of India Pvt, Ltd, 151–154.

Jinger, D., Dhar, S., Dass, A., Sharma, V. K., Paramesh, V., Parihar, M., et al. (2021). Co-fertilization of Silicon and Phosphorus Influences the Dry Matter Accumulation, Grain Yield, Nutrient Uptake, and Nutrient-Use Efficiencies of Aerobic Rice. *Silicon* 14, 4683–4697. doi: 10.1007/s12633-021-01239-5

Jinger, D., Dhar, S., Dass, A., Sharma, V. K., Shukla, L., Parihar, M., et al. (2020). Crop productivity, grain quality, water use efficiency, and soil enzyme activity as influenced by silicon and phosphorus application in aerobic rice (*Oryza sativa*). *Commun. Soil Sci. Plant Anal.* 51, 2147–2162. doi: 10.1080/00103624.2020.1812629

Kannan, R. L., Dhivya, M., Abinaya, D., Krishna, R. L., and Krishnakumar, S. (2013). Effect of integrated nutrient management on soil fertility and productivity in maize. *Bull. Environ. Pharmacol. Life Sci.* 2, 61–67.

Kemper, W., and Rosenau, R. (1986). "Aggregate stability and size distribution," in *Methods of Soil Analysis. Part 1. Physical and Mineralogical Methods-Agronomy Monograph no. 9*, 2nd Edn, ed. A. Klute (Madison: American Society of Agronomy and Soil Science Society of America), 425–442. doi: 10.2136/sssabookser5.1.2ed.c17

Kohler, U., and Luniak, M. (2005). Data inspection using biplots. *Stata J.* 5, 208–223. doi: 10.1177/1536867X0500500206

Kumar, A., Jha, M. N., Singh, D., Pathak, D., and Rajawat, M. V. S. (2021). Prospecting catabolic diversity of microbial strains for developing microbial consortia and their synergistic effect on Lentil (*Lens esculenta*) growth, yield and iron biofortification. *Arch. Microbiol.* 203, 4913–4928. doi: 10.1007/s00203-021-02446-9

Kumar, A., Rana, K. S., Choudhary, A. K., Bana, R. S., Sharma, V. K., Gupta, G., et al. (2022). Sole-or Dual-Crop Basis Residue Mulching and Zn Fertilization Lead to Improved Productivity, Rhizo-modulation and Soil Health in Zero-Tilled Pigeonpea–Wheat Cropping System. *J. Soil Sci. Plant Nutr.* 22, 1193–1214. doi: 10.1007/s42729-021-00723-6

Kumar, S., Dhar, S., Barthakur, S., Chandrakala, M., Meena, S. K. L., Meena, L., et al. (2018a). Effect of integrated potassium management on soil biological properties and yields of corn under corn-wheat cropping system. *Int. J. Curr. Microbiol. App. Sci.* 7, 1855–1866. doi: 10.20546/ijcmas.2018.712.217

Kumar, S., Dhar, S., Barthakur, S., Kumar, S., Mondal, B., Kumar, D., et al. (2018b). Integrated K Management Exhibit a Key Role in Potassium Uptake Transporter (ZmKUP) Expression to Improve Growth and Yield of Corn. *Int. J. Curr. Microbiol. App. Sci.* 7, 1867–1887. doi: 10.20546/ijcmas.2018.712.218

Kumar, S., Dhar, S., Barthakur, S., Rajawat, M. V. S., Kochewad, S. A., Kumar, S., et al. (2021). Farmyard Manure as K-Fertilizer Modulates Soil Biological Activities and Yield of Wheat Using the Integrated Fertilization Approach. *Front. Environ. Sci.* 9:764489. doi: 10.3389/fenvs.2021.764489

Kumar, S., Dhar, S., Om, H., and Meena, R. L. (2015). Enhanced root traits and productivity of maize (Zea mays) and wheat (*Triticum aestivum*) in maize-wheat cropping system through integrated potassium management. *Indian J. Agric. Sci.* 85, 251–255.

Kuotsu, K., Munda, G., Das, A., and Verma, B. (2014). Soil health as affected by altered land configuration and conservation tillage in a groundnut (Arachis hypogaea)-toria (Brassica campestris var. toria) cropping system. *Indian J. Agric. Sci.* 84, 241–247.

Lal, R. (2020). Soil organic matter content and crop yield. *J. Soil Water Conserv.* 75, 27A–32A. doi: 10.2489/jswc.75.2.27A

Lenka, N. K., Sudhishri, S., Dass, A., Choudhury, P., Lenka, S., and Patnaik, U. (2013). Soil carbon sequestration as affected by slope aspect under restoration treatments of a degraded alfisol in the Indian sub-tropics. *Geoderma* 204, 102–110. doi: 10.1016/j.geoderma.2013.04.009

Mäder, P., Kaiser, F., Adholeya, A., Singh, R., Uppal, H. S., Sharma, A. K., et al. (2011). Inoculation of root microorganisms for sustainable wheat–rice and wheat–black gram rotations in India. *Soil Biol. Biochem.* 43, 609–619. doi: 10.1016/j.soilbio.2010.11.031

Mahetele, D., and Kushwaha, H. (2011). Productivity and profitability of pigeonpea as influenced by FYM, PSB and phosphorus fertilization under rainfed condition. *J. Food Legumes* 24, 72–74.

Meena, A., Karwal, M., and Raghavendra, K. J. (2021). Sustainable and climate smart agriculture: challenges and opportunities in indian perspective. *Agriallis: e-newletter* 3, 47–57.

Miner, G. L., Delgado, J. A., Ippolito, J. A., and Stewart, C. E. (2020). Soil health management practices and crop productivity. *Agric. Environ. Lett.* 5:e20023. doi: 10.1002/ael2.20023

Mishra, S., Srakar, U., Taraphder, S., Datta, S., Swain, D., and Saikhom, R. (2017). Multivariate statistical data analysis-principal component analysis (PCA). *Int. J. Livest. Res.* 7, 60–78.

Nandapure, S., Sonune, B., Gabhane, V., Katkar, R., and Patil, R. (2011). Long term effects of integrated nutrient management on soil physical properties and crop productivity in sorghum-wheat cropping sequence in a vertisol. *Indian J. Agric. Res.* 45, 336–340.

Nath, A. J., Brahma, B., Sileshi, G. W., and Das, A. K. (2018). Impact of land use changes on the storage of soil organic carbon in active and recalcitrant pools in a humid tropical region of India. *Sci. Total Environ.* 624, 908–917. doi: 10.1016/j.scitotenv.2017.12.199

Nelson, A. R. L. E., Ravichandran, K., and Antony, U. (2019). The impact of the Green Revolution on indigenous crops of India. *J. Ethn. Foods* 6, 1–10. doi: 10.1186/s42779-019-0011-9

Nunan, N., Morgan, M., and Herlihy, M. (1998). Ultraviolet absorbance (280 nm) of compounds released from soil during chloroform fumigation as an estimate of the microbial biomass. *Soil Biol. Biochem.* 30, 1599–1603. doi: 10.1016/S0038-0717(97)00226-5

Olsen, S. R., Watanabe, F. S., Cosper, H. R., Larson, W., and Nelson, L. (1954). Residual phosphorus availability in long-time rotations on calcareous soils. *Soil Sci.* 78, 141–152. doi: 10.1097/00010694-195408000-00008

Panse, V. G., and Sukhatme, P. V. (1985). *Statistical Methods for Agricultural Workers*. New Delhi: Indian Council of Agricultural Research.

Paramesh, V., Sreekanth, G. B., Chakurkar, E., Chethan Kumar, H., Gokuldas, P., Manohara, K. K., et al. (2020). Ecosystem network analysis in a smallholder integrated crop–livestock system for coastal lowland situation in tropical humid conditions of India. *Sustainability* 12:5017. doi: 10.3390/su12125017

Patra, S., Mishra, P., Mahapatra, S., and Mithun, S. (2016). Modelling impacts of chemical fertilizer on agricultural production: a case study on Hooghly district, West Bengal, India. *Model. Earth Syst. Environ.* 2, 1–11. doi: 10.1007/s40808-016-0223-6

Paul, J., Choudhary, A. K., Sharma, S., Bohra, M., Dixit, A., and Kumar, P. (2016). Potato production through bio-resources: long-term effects on tuber productivity, quality, carbon sequestration and soil health in temperate Himalayas. *Sci. Hortic.* 213, 152–163. doi: 10.1016/j.scienta.2016.10.022

Piper, C. (1966). *Soil and Plant Analysis, Hans. Pub*. Bombay: Asian Ed, 368–374.

Rakshit, R., Das, A., Padbhushan, R., Sharma, R. P., and Kumar, S. (2018). Assessment of soil quality and identification of parameters influencing system yield under long-term fertilizer trial. *J. Indian Soc. Soil Sci.* 66, 166–171. doi: 10.5958/0974-0228.2018.00021.X

Samal, S., Rao, K., Poonia, S., Kumar, R., Mishra, J., Prakash, V., et al. (2017). Evaluation of long-term conservation agriculture and crop intensification in rice-wheat rotation of Indo-Gangetic Plains of South Asia: carbon dynamics and productivity. *Eur. J. Agron.* 90, 198–208. doi: 10.1016/j.eja.2017.08.006

Sharma, B., Singh, B. N., Dwivedi, P., and Rajawat, M. V. S. (2022). Interference of climate change on plant-microbe interaction: present and future prospects. *Front. Agron.* 3:725804. doi: 10.3389/fagro.2021.725804

Shete, P., Adhav, S., and Kushare, Y. (2010). Response of rabi greengram (*Vigna radiata* L.) to land configuration and inorganic fertilizer with and without FYM. *Int. J. Plant Sci.* 5, 498–501.

Singh, B. N., Rajawat, M. V. S., Hidangmayum, A., Ansari, W. A., Singh, D., Zeyad, M. T., et al. (2019). "Importance and utilization of plant-beneficial rhizobacteria in agriculture," in *Microbial Interventions in Agriculture and Environment*, eds D. Singh and R. Prabha (Singapore: Springer), 171–187. doi: 10.1007/978-981-32-9084-6_8

Singh, D., Prasanna, R., Sharma, V., Rajawat, M. V. S., Nishanth, S., and Saxena, A. K. (2020b). "Prospecting plant–microbe interactions for enhancing nutrient

availability and grain biofortification," in *Wheat and Barley Grain Biofortification*, eds O. P. Gupta, V. Pandey, S. Narwal, P. Sharma, S. Ram, and G. P. Singh (Amsterdam: Elsevier), 203–228. doi: 10.1016/B978-0-12-818444-8.00008-0

Singh, D., Geat, N., Rajawat, M. V. S., Prasanna, R., and Saxena, A. K. (2020a). Performance of low and high Fe accumulator wheat genotypes grown on soils with low or high available Fe and endophyte inoculation. *Acta Physiol. Plant* 42, 1–13. doi: 10.1007/s11738-019-2997-4

Singh, D., Geat, N., Rajawat, M. V. S., Prasanna, R., Kar, A., Singh, A. M., et al. (2018). Prospecting endophytes from different Fe or Zn accumulating wheat genotypes for their influence as inoculants on plant growth, yield, and micronutrient content. *Ann. Microbiol.* 68, 815–833. doi: 10.1007/s13213-018-1388-1

Singh, D., Rajawat, M. V. S., Kaushik, R., Prasanna, R., and Saxena, A. K. (2017). Beneficial role of endophytes in biofortification of Zn in wheat genotypes varying in nutrient use efficiency grown in soils sufficient and deficient in Zn. *Plant Soil* 416, 107–116. doi: 10.1007/s11104-017-3189-x

Singh, D., Thapa, S., Geat, N., Mehriya, M. L., and Rajawat, M. V. S. (2021). "Biofertilizers: Mechanisms and application," in *Biofertilizers Advances ib Bio-inoculants*, eds A. Rakshit, V. S. Meena, M. Parihar, H. B. Singh, and A. K. Singh (Amsterdam: Elsevier), 151–166. doi: 10.1016/B978-0-12-821667-5.00024-5

Snapp, S. S., Mafongoya, P., and Waddington, S. (1998). Organic matter technologies for integrated nutrient management in smallholder cropping systems of southern Africa. *Agric. Ecosyst. Environ.* 71, 185–200. doi: 10.1016/S0167-8809(98)00140-6

Song, X., Liu, M., Wu, D., Griffiths, B. S., Jiao, J., Li, H., et al. (2015). Interaction matters: synergy between vermicompost and PGPR agents improves soil quality, crop quality and crop yield in the field. *Appl. Soil Ecol.* 89, 25–34. doi: 10.1016/j.apsoil.2015.01.005

Steel, R. G., Torrie, J. H., and Dicky, D. A. (1997). *Principles and Procedures of Statistics: a Biometrical Approach*, 3rd Edn. New York, NY: McGraw-Hill, Inc., Book Co.

Subbiah, B., and Asija, G. (1956). A rapid procedure for the estimation of available nitrogen in soils. *Curr. Sci.* 25, 259–260.

Tabatabai, M. A., and Bremner, J. M. (1969). Use of p-nitrophenyl phosphate for assay of soil phosphatase activity. *Soil Biol. Biochem.* 1, 301–307. doi: 10.1016/0038-0717(69)90012-1

Tanveer, A., Ikram, R. M., and Ali, H. H. (2019). "Crop Rotation: Principles and Practices," in *Agronomic Crops*, ed. M. Hasanuzzaman (Singapore: Springer), 1–12. doi: 10.1007/978-981-32-9783-8_1

Thapa, S., Prasanna, R., Ranjan, K., Velmourougane, K., and Ramakrishnan, B. (2017). Nutrients and host attributes modulate the abundance and functional traits of phyllosphere microbiome in rice. *Microbiol. Res.* 204, 55–64. doi: 10.1016/j.micres.2017.07.007

Tiwari, D., Sharma, B., and Singh, V. (2011). Effect of integrated nutrient management in pigeonpea based intercropping system. *J. Food Legumes* 24, 304–309.

Vega, M., Pardo, R., Barrado, E., and Debán, L. (1998). Assessment of seasonal and polluting effects on the quality of river water by exploratory data analysis. *Water Res.* 32, 3581–3592. doi: 10.1016/S0043-1354(98)00138-9

Yadav, G. S., Das, A., Lal, R., Babu, S., Meena, R. S., Saha, P., et al. (2018). Energy budget and carbon footprint in a no-till and mulch based rice–mustard cropping system. *J. Clean. Prod.* 191, 144–157. doi: 10.1016/j.jclepro.2018.04.173

Yigini, Y., and Panagos, P. (2016). Assessment of soil organic carbon stocks under future climate and land cover changes in Europe. *Sci. Total Environ.* 557, 838–850. doi: 10.1016/j.scitotenv.2016.03.085

Yoder, R. E. (1936). A direct method of aggregate analysis of soils and a study of the physical nature of erosion losses. *Agron. J.* 28, 337–351. doi: 10.2134/agronj1936.00021962002800050001x

Zeyad, M. T., Rajawat, M. V. S., Kumar, M., Malik, A., Anas, M., Ansari, W. A., et al. (2021). "Role of Microorganisms in Plant Adaptation Towards Climate Change for Sustainable Agriculture," in *Microbiomes and the Global Climate Change*, eds S. A. Lone and A. Malik (Singapore: Springer), 247–266. doi: 10.1007/978-981-33-4508-9_14

Zhang, Q.-C., Shamsi, I. H., Xu, D.-T., Wang, G.-H., Lin, X.-Y., Jilani, G., et al. (2012). Chemical fertilizer and organic manure inputs in soil exhibit a vice versa pattern of microbial community structure. *Appl. Soil Ecol.* 57, 1–8. doi: 10.1016/j.apsoil.2012.02.012

frontiers | Frontiers in Microbiology

TYPE Original Research
PUBLISHED 04 October 2022
DOI 10.3389/fmicb.2022.975421

Check for updates

OPEN ACCESS

EDITED BY
Eric Altermann,
Massey University,
New Zealand

REVIEWED BY
Jian Zha,
Shaanxi University of Science and Technology, China
Xinwei Jiang,
Jinan University,
China

*CORRESPONDENCE
Chang-ye Hui
hcy_sypu@hotmail.com

SPECIALTY SECTION
This article was submitted to Microbiotechnology, a section of the journal Frontiers in Microbiology

RECEIVED 22 June 2022
ACCEPTED 21 September 2022
PUBLISHED 04 October 2022

CITATION
Guo Y, Huang Z-l, Zhu D-l, Hu S-y, Li H and Hui C-y (2022) Anthocyanin biosynthetic pathway switched by metalloregulator PbrR to enable a biosensor for the detection of lead toxicity.
Front. Microbiol. 13:975421.
doi: 10.3389/fmicb.2022.975421

COPYRIGHT
© 2022 Guo, Huang, Zhu, Hu, Li and Hui. This is an open-access article distributed under the terms of the Creative Commons Attribution License (CC BY). The use, distribution or reproduction in other forums is permitted, provided the original author(s) and the copyright owner(s) are credited and that the original publication in this journal is cited, in accordance with accepted academic practice. No use, distribution or reproduction is permitted which does not comply with these terms.

Anthocyanin biosynthetic pathway switched by metalloregulator PbrR to enable a biosensor for the detection of lead toxicity

Yan Guo[1], Zhen-lie Huang[2], De-long Zhu[3,4], Shun-yu Hu[1,2], Han Li[4,5] and Chang-ye Hui[4]*

[1]National Key Clinical Specialty of Occupational Diseases, Shenzhen Prevention and Treatment Center for Occupational Diseases, Shenzhen, China, [2]Department of Toxicology, School of Public Health, Southern Medical University, Guangzhou, China, [3]School of Public Health, Guangdong Medical University, Dongguan, China, [4]Department of Pathology and Toxicology, Shenzhen Prevention and Treatment Center for Occupational Diseases, Shenzhen, China, [5]College of Lab Medicine, Hebei North University, Zhangjiakou, China

Environmental lead pollution mainly caused by previous anthropogenic activities continuously threatens human health. The determination of bioavailable lead is of great significance to predict its ecological risk. Bacterial biosensors using visual pigments as output signals have been demonstrated to have great potential in developing minimal-equipment biosensors for environmental pollutant detection. In this study, the biosynthesis pathway of anthocyanin was heterogeneously reconstructed under the control of the PbrR-based Pb(II) sensory element in *Escherichia coli*. The resultant metabolic engineered biosensor with colored anthocyanin derivatives as the visual signal selectively responded to concentrations as low as 0.012μM Pb(II), which is lower than the detection limit of traditional fluorescent protein-based biosensors. A good linear dose–response pattern in a wide Pb(II) concentration range (0.012–3.125 μM) was observed. The color deepening of culture was recognized to the naked eye in Pb(II) concentrations ranging from 0 to 200 μM. Importantly, the response of metabolic engineered biosensors toward Pb(II) was not significantly interfered with by organic and inorganic ingredients in environmental water samples. Our findings show that the metabolic engineering of natural colorants has great potential in developing visual, sensitive, and low-cost bacterial biosensors for the detection and determination of pollutant heavy metals.

KEYWORDS

bacterial biosensor, anthocyanin biosynthesis, environmental lead, bioavailability, ecotoxic effect

Introduction

Lead (Pb), one of the toxic heavy metals, is a globally prevalent inorganic pollutant that persistently threatens human health (Pourrut et al., 2011). Various instrumental methods such as graphite furnace atomic absorption spectrometry (GFAAS) and inductively coupled plasma mass spectrometry (ICP-MS) are widely used to monitor environmental heavy metals including Pb (USEPA, 2016). However, the information about its bioavailability and ecotoxicity is usually missing in these applications, which is of predictive value for the assessment of its health risk (Hui et al., 2021b).

To address the shortcomings of traditional instrumental methods in determining the bioavailable, bioaccessible, and toxic fractions of heavy metals, some biological devices, especially whole-cell biosensors, have been continuously developed (Kim et al., 2018; Gupta et al., 2019). Based on Pb(II)-responsive metalloregulator PbrR, programmed bacteria could selectively respond to bioavailable Pb(II) with fluorescent proteins and beta-galactosidase as the output signals (Wei et al., 2014; Bereza-Malcolm et al., 2016; Guo et al., 2019; Hui et al., 2020b). However, these whole-cell biosensors failed in the field detection of Pb(II) because the readout of fluorescent and enzymatic signals is highly dependent on the complex instruments. Employment of visual signals has provided an alternative to developing mini-equipment bacterial biosensors responsive to heavy metal pollutions such as Cu(II) (Chen et al., 2017), Cd(II) (Hui et al., 2022a,c), and Hg(II) (Guo et al., 2021a). These pigment-based biosensors have shown more excellent biosensing characteristics than traditional reporters-based biosensors for Cd(II) and Hg(II; Zhang et al., 2021; Guo et al., 2021b; Hui et al., 2021c, 2022b). In our previous studies, bacterial biosensors using blue indigoidine (Hui et al., 2021a), navy violacein (Hui et al., 2020a), and purple deoxyviolacein (Hui et al., 2022d) as the biosensing signals have been successfully developed to detect bioavailable Pb(II). The detection limits of three biosensors had been demonstrated to be lower than the criteria for maximum concentration (CMC) for Pb in freshwater (0.31 μM) recommended by the United States Environmental Protection Agency (USEPA) (USEPA, 2016). The detection limit of the whole-cell biosensors using indigoidine and deoxyviolacein as the visual signals was even lower than the national primary drinking water standard (0.072 μM) recommended by USEPA (USEPA, 2009). Due to the rapid development of metabolic engineering and synthetic biology, heterologous biosynthesis of rainbow colorants had been realized in programmed bacteria (Yang et al., 2020, 2021). The development of novel bacterial biosensors using colorful pigments as visual reporters would provide us with more biological devices for the sensitive detection of toxic heavy metals in different applications.

Anthocyanins are red, purple, or blue water-soluble pigments found in terrestrial plants, which belong to the family of polyphenolic compounds (Yan et al., 2005). Their anti-oxidative, anti-cancer, anti-inflammatory, and cardioprotective properties have attracted much attention to the reconstruction of their biosynthetic metabolic pathways (Yan et al., 2008). In the study, two key biosynthetic enzymes were employed to reconstruct the biosynthetic metabolic pathway flux toward anthocyanin, which is designed to be triggered by Pb(II)-responsive metalloregulator PbrR. Engineered bacterial biosensors selectively responded to bioavailable Pb(II) at the nanomolar level by secreting colored anthocyanidin derivatives (CACD) with maximum absorption at 428 nm into the culture. Importantly, the CACD-based whole-cell biosensor was validated in detecting bioavailable and toxic Pb(II) existing in both experimental and environmental samples. Compared with traditional fluorescent reporters-based or enzymatic reporters-based whole-cell biosensors, metabolic engineering of natural colorants was shown to have the potential to be employed as the visual reporter to develop a low-cost, mini-equipment biosensor for heavy metals. The sole cost of culture medium and consumable material is negligible, and only an incubator and a microplate reader are the necessary instruments.

Materials and methods

Bacterial strains, plasmids, and agents

The vectors, bacterial host, and engineered bacterium involved in this study are listed in Supplementary Table S1. *Escherichia coli* (*E. coli*) TOP10 was used as the bacterial host for the gene cloning and biosensing tests. The engineered bacterium was cultured at 37°C in Luria-Bertani (LB) broth containing 1% tryptone, 0.5% yeast extract, and 1% sodium chloride supplemented with 50 μg/ml ampicillin. Reagents for molecular cloning were obtained from Sangon Biotech (Shanghai, China). The recombinant constructs were all verified by DNA sequencing (Sangon Biotech). (+)-catechin was purchased from Sigma-Aldrich (St Louis, MO, United States), dissolved in ethanol to achieve a final concentration of 125 mM, and stored in the dark at 4°C. Cadmium chloride, lead nitrate, zinc sulfate, and mercuric chloride are of analytical grade and purchased from Sigma-Aldrich (St Louis, MO, United States). Stock solutions of metal salts were freshly prepared and filtered through a 0.22 μM filter before the experiments.

Genetic assembly of pigment-based biosensor

To reconstruct the anthocyanin biosynthetic module, a bicistronic genetic fragment encoding two open reading frames (ORFs) designated as 3-*O*-glycosyltransferase originating from *Arabidopsis thaliana* (Genbank: AY072325) and anthocyanidin synthase originating from *Petunia hybrid* (Genbank: P51092) was artificially synthesized by Sangon Biotech according to the *E. coli* codon preference (Supplementary Figure S1). The synthetic anthocyanin biosynthetic cassette was PCR amplified from the vector pT-3GT-ANS and inserted into the *Nde*I and *Sac*I sites of

pPpbr-vio to generate pPb-CACD, which is designed as a bioavailable Pb(II) biosensing construct with the CACD as the output signals. The resultant pPb-CACD was used for transformation into *E. coli* TOP10 competent cells. Whole-cell biosensors TOP10/pPb-CACD were selected on LB agar plates containing 50 μg/ml ampicillin.

Characterization of Pb(II)-driven color signal from the pigment-based biosensor

To obtain the Pb(II)-induced water-soluble pigment, overnight LB culture of TOP10/pPb-CACD was diluted 1:100 in fresh LB medium supplemented with or without 1 mM catechin. Engineered TOP10/pPb-CACD was then induced with 50 μM Pb(II) overnight (about 15 h) at 37°C with shaking at 250 rpm. The cell-free culture supernatants were prepared by centrifugation at 8000 g for 1 min, pipetted into a 96-well microplate, and scanned in a microplate reader (BioTek Epoch, United States). A 300–750 nm scanning wavelength range with an interval of 2 nm was set.

Detection selectivity assay

To evaluate the detection selectivity of engineered bacterium, TOP10/pPb-CACD preserved in 20% glycerol was diluted 1:100 in fresh LB medium supplemented with 1 mM catechin. Stock solutions of Cd(II), Pb(II), Zn(II), and Hg(II) were then added to the cultures at a final concentration of 0, 1.25, 2.5, 5, 10, and 20 μM, followed by incubation overnight at 37°C with shaking at 250 rpm. Aliquots of 100 μl culture and cell-free supernatant were pipetted into a 96-well microplate and determined at 600 nm and 428 nm for bacterial density and color signal, respectively.

Detection sensitivity assay

To study the dose–response relationship of engineered bacterium toward increased concentrations of Pb(II), TOP10/pPb-CACD preserved in 20% glycerol was diluted 1:100 in fresh LB medium supplemented with 1 mM catechin, and exposed to 200, 100, 50, 25, 12.5, 6.25, 3.125, 1.56, 0.78, 0.39, 0.195, 0.098, 0.049, 0.024, 0.012, 0.006, and 0 μM Pb(II) using a double dilution method as described previously (Hui et al., 2022b). After incubation overnight at 37°C with shaking at 250 rpm, bacterial density and color signal were measured as described above.

Detection of bioavailable Pb(II) in environmental water samples

To validate the capability of an engineered bacterium to sense the soluble, bioaccessible, and bioavailable Pb(II) in environmental water samples, recombinant TOP10/pPb-CACD preserved in 20% glycerol was diluted 1:100 in fresh LB medium prepared with purified water, tap water from our laboratory, and surface water from two downtown parks as described previously (Hui et al., 2022a,c,d). The cultures were supplemented with 1 mM catechin, spiked with 25, 12.5, 6.25, 3.125, 1.56, 0.78, 0.39, and 0 μM Pb(II) in a double dilution method, and then followed by incubation overnight at 37°C with shaking at 250 rpm, bacterial density and color signal were measured as described above.

Results and discussion

Design of Pb(II)-responsive bacterial biosensor based on the anthocyanin biosynthetic pathway

The construction scheme and molecular mechanism of the whole-cell biosensor based on the anthocyanidin biosynthesis which is switched by bioavailable Pb(II) are summarized in Figure 1. Anthocyanidins, as valuable natural colorants, have always attracted intense attention due to their beneficial health effects (Yan et al., 2008). Their biosynthesis pathways have been extensively investigated (Yang et al., 2021). Two key enzymes including anthocyanidin synthase (ANS) and 3-*O*-glycosyltransferase (3GT) are essential in the biosynthesis of the anthocyanin cyanidin 3-O-glucoside (C3G; Yan et al., 2005). The improved production of C3G has been achieved by using a bicistronic 3GT-ANS expression cassette (Lim et al., 2015). The same bicistronic genetic module was employed as a reporter module under the control of the Pb(II) sensory element in the present study. Upon exposure to bioavailable Pb(II), metabolic engineered bacterial biosensors are expected to secrete water-soluble colorants into the culture supernatant by triggering the transcription of the bicistronic pigment biosynthesis genes (Figure 1).

Anthocyanins are relatively stable under acidic conditions and rapidly break down under neutral conditions (Tsuda et al., 2005). Significant degradation of C3G was previously observed at pH 7.0. However, C3G was stable at pH 5.0 or lower (Yan et al., 2008). The pH value of the culture was maintained at about 7.0 in the present study, which was suitable for the growth of a bacterial biosensor. However, the product C3G was demonstrated to degrade severely in the current condition. As shown in Figure 2, the visible absorption spectra of 50 mM Pb(II)-induced culture supernatant containing CACD showed maximum absorption at 428 nm, which was different from the maximum absorption of the red-colored C3G at 512 nm reported previously (Lim et al., 2015). HPLC was usually used for product analysis of fermentation samples for pigment production. Residual anthocyanidin could be conveniently identified by retention times and UV absorption spectra (Yan et al., 2008). However, there are few studies about the identification of its degradation products. We infer that the anthocyanin is seriously degraded through the change of color

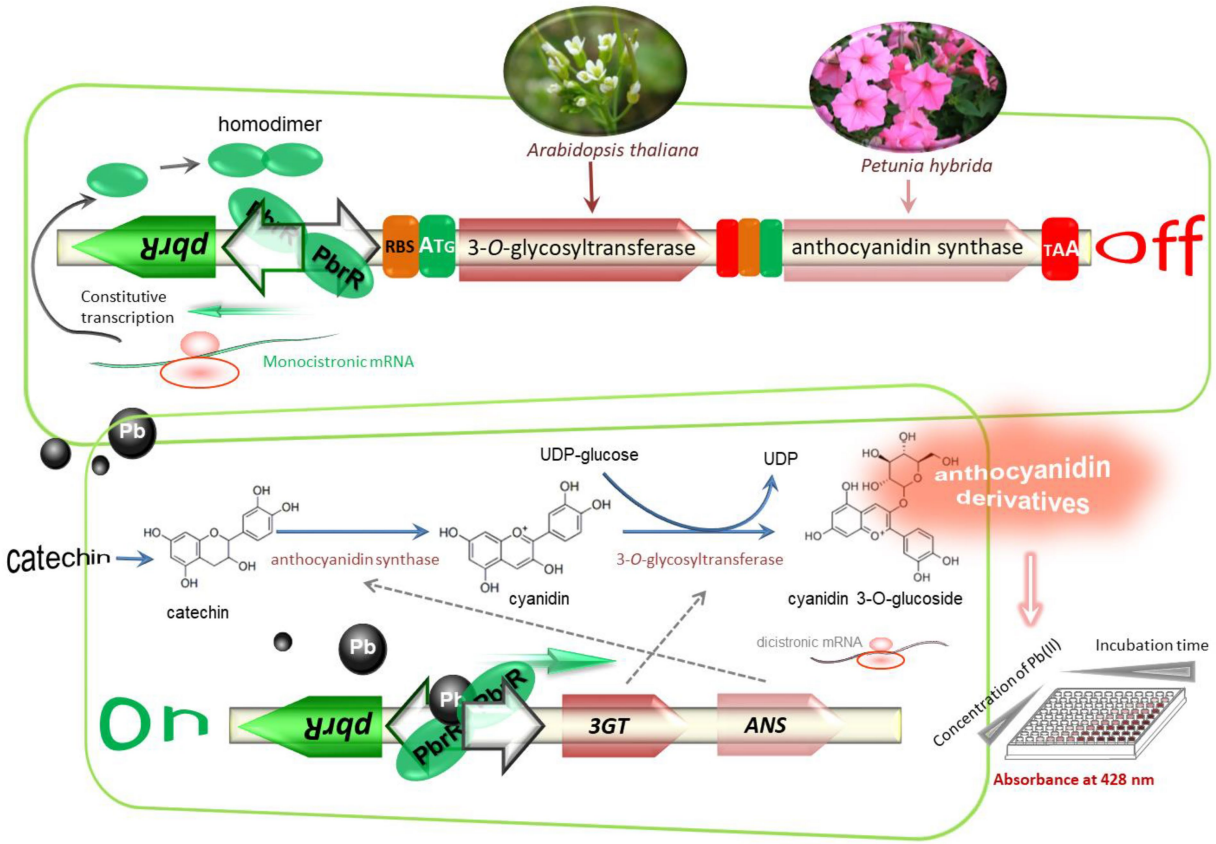

FIGURE 1
Reconstruction of the anthocyanidin biosynthetic pathway under the control of Pb(II)-responsive genetic element. The anthocyanidin biosynthesis genes cluster was artificially synthesized and inserted downstream of the divergent *pbr* promote to assemble Pb(II) biosensing construct. Anthocyanidin synthase originating from *Petunia hybrida* and 3-*O*-glycosyltransferase originating from *Arabidopsis thaliana* are expected to be transcribed and translated as a bicistronic unit when the metabolically engineered bacterium is exposed to bioavailable Pb(II). The anthocyanidin cyanidin 3-O-Glucoside is biosynthesized by catalyzing the production of cyanidin from the substrate catechin by ANS and transferring a glucose group to cyanidin to yield C3G by 3GT. Water-soluble CACD will be secreted by biosensor cells and quantitatively measured at 428 nm in a 96-well microplate.

and the migration of maximum absorption wavelength. This conclusion needs to be further identified by reliable measurements such as HPLC-MS in future studies. Thus, the CACD-derived signal was determined at 428 nm instead of 512 nm in the following study.

The cascade amplification effect of enzymatic reporters made whole-cell biosensors using enzyme-based reporters such as luciferase and beta-galactosidase are more sensitive than fluorescent proteins-based biosensors (Hui et al., 2021b). Because a small amount of expressed enzymes can overproduce visible amounts of pigment (McNerney et al., 2019), the continuous biosynthesis of reporter pigments with the extension of heavy metals induction time was commonly observed in previously developed pigment-based biosensors (Guo et al., 2021a; Hui et al., 2022a,d). The continuous production accompanied by the degradation of C3G was also observed in Pb(II)-induced TOP10/pPb-CACD grown in a regular LB medium (at pH 7.0). However, the dose–response relation became less obvious to the naked eye with the extension of induction time (Supplementary Figure S2A). Furthermore, continuous deepening of the color was also observed when Pb(II)-induced culture was placed at 37°C (Supplementary Figure S2B). To exclude the influence of the biosensor cells containing anthocyanin biosynthetic enzymes, the stability of cell-free culture supernatant was investigated at both acidic and neutral pH (Supplementary Figure S3). No color change was observed in acidic culture supernatant and the result demonstrated that anthocyanin compounds are stable at acidic pH which is consistent with previous reports (Springob et al., 2003; Yan et al., 2008). Taking this into consideration, a constant incubation time (15 h) followed by an immediate measurement was used in the following study to obtain the colorimetric signal of CACD.

To avoid spontaneous chemical degradation of red C3G in a fermentation culture, a two-step fermentation strategy is deserved to be developed in the future study. High biomass was first obtained by growing biosensor cells in a regular medium at neutral pH and then exposed to toxic Pb(II) in a modified medium at acidic pH to reduce the degradation of reporter C3G.

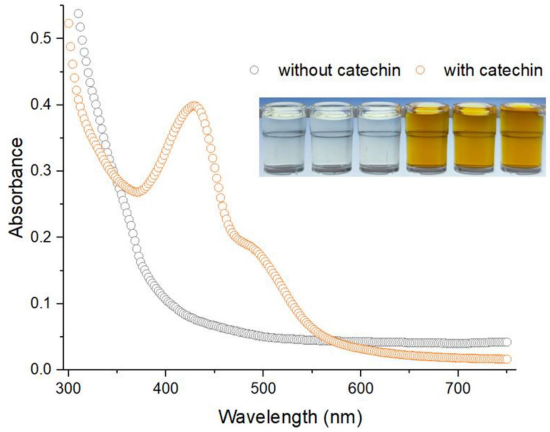

FIGURE 2
The visible absorption spectrum of water-soluble CACD generated from Pb(II)-induced TOP10/pPb-CACD. The inset shows the cell-free culture supernatants of 50 mM Pb(II)-induced TOP10/pPb-CACD supplemented with or without 1 mM catechin. The maximum absorption peak of secreted CACD is located at around 428 nm. Data are representative of three independent tests with similar results.

Selective response of the metabolic engineered bacterial biosensor

MerR-like transcriptional regulators do not distinguish chemically related group 12 metals well (Caguiat et al., 1999; Hakkila et al., 2011). The weak nonspecific responses of MerR-family metalloregulators toward metals especially group 12 members were found in Pb(II)-responsive PbrR (Bereza-Malcolm et al., 2016), Cd(II)-responsive CadR (Hui et al., 2022b), Cd(II)-responsive CadC (Hui et al., 2021c), Zn(II)-responsive ZntR (Kang et al., 2018), and so on. A slight cross-response of metabolic engineered biosensor toward Hg(II) was found in this study. No significant growth inhibition led by toxic Hg(II) was observed at 5 μM or less (Figure 3A) and an enhanced response to 1.25 and 2.5 μM Hg(II) was observed in Figure 3B. Importantly, a dose-dependent response toward Pb(II) was preliminary verified at concentrations of Pb(II) ranging from 0 to 20 μM (Figure 3B). Furthermore, the color of Pb(II)-induced cultures gradually deepened which was recognizable to the naked eye (Figure 3C).

The response selectivity of the bacterial biosensor using PbrR as the sensory element was demonstrated to be determined by the inherent characteristics of native PbrR (Chen et al., 2005). However, the optimizations of gene circuits (Cai et al., 2018; Jia et al., 2018), the directed evolution of metalloregulators (Cai et al., 2022), and the combined use of several metal sensory elements (Hui et al., 2022b) have been demonstrated to improve the performance of a whole-cell biosensor toward chemically-similar metals. Although the novel pigment-based actuator developed in this study did not contribute to improving the metal selectivity of whole-cell biosensors, the combination of pigment reporter with a modified metal sensory module is expected to improve the biosensing properties including metal selectivity in the future study.

Response properties of metabolic engineered bacterial biosensor toward Pb(II)

To further study the dose–response relationship, metabolic engineered TOP10/pPb-CACD was exposed to systematically varied concentrations of Pb(II). Due to the low cytotoxic activity of Pb(II), the bacterial concentration did not show a decreasing trend (Figure 4A). Recombinant TOP10/pPb-CACD was demonstrated to respond to concentrations as low as 0.012 μM Pb(II) using a colorimetric method (Figure 4B). The detection limit of this biosensor is lower than the CMC for Pb in freshwater (0.31 μM) and the primary drinking water standard (0.072 μM) recommended by USEPA (USEPA, 2009, 2016). The result showed that this metabolically engineered biosensor was expected to detect toxic Pb(II) in the ecosystem to early warn acute toxicity in aquatic organisms. However, the detection limit of the PbrR-based bacterial biosensor using the fluorescent protein as a reporter was increased to 0.97 μM (Bereza-Malcolm et al., 2016).

The whole dose–response of TOP10/pPb-CACD toward Pb(II) was shown in Figure 4C, which was similar to that of the previously constructed PbrR-based bacterial biosensor with the blue pigment indigoidine as the output signal (Hui et al., 2021a). The CACD-derived signal was significantly increased from 0 to 12.5 μM and gradually stabilized from 25 to 200 μM (Figure 4C). The constant expression of PbrR is attributed to the regulation of the natural *pbr* promoter (Borremans et al., 2001). Before the metal binding sites of PbrR were saturated with Pb(II), the transcription of pigment biosynthetic enzymes would continuously improve with the increased Pb(II) concentration, and it led to the increased pigment signal until the metal binding sites of PbrR were saturated with excess Pb(II) (Hui et al., 2022d). Interestingly, the Pb(II) concentration ($\log_2$ scale) and the absorbance of CACD could be well fitted by a linear regression relation within a wide Pb(II) concentration range between 0.012 and 3.125 μM (Figure 4D). Importantly, the gradual color deepening of Pb(II)-induced culture was easily recognized by the naked eye independent of any instruments (Figure 4E).

The performance of metabolic engineered bacterial biosensor in monitoring bioavailable Pb(II) in environmental samples

A simple protocol for the determination of bioavailable Pb(II) using this metabolically engineered biosensor was drawn up based on the above findings (Figure 5A). The culture system is first prepared using up to 90% of lead polluted environmental water samples to be tested, inoculation with the bacterial biosensor,

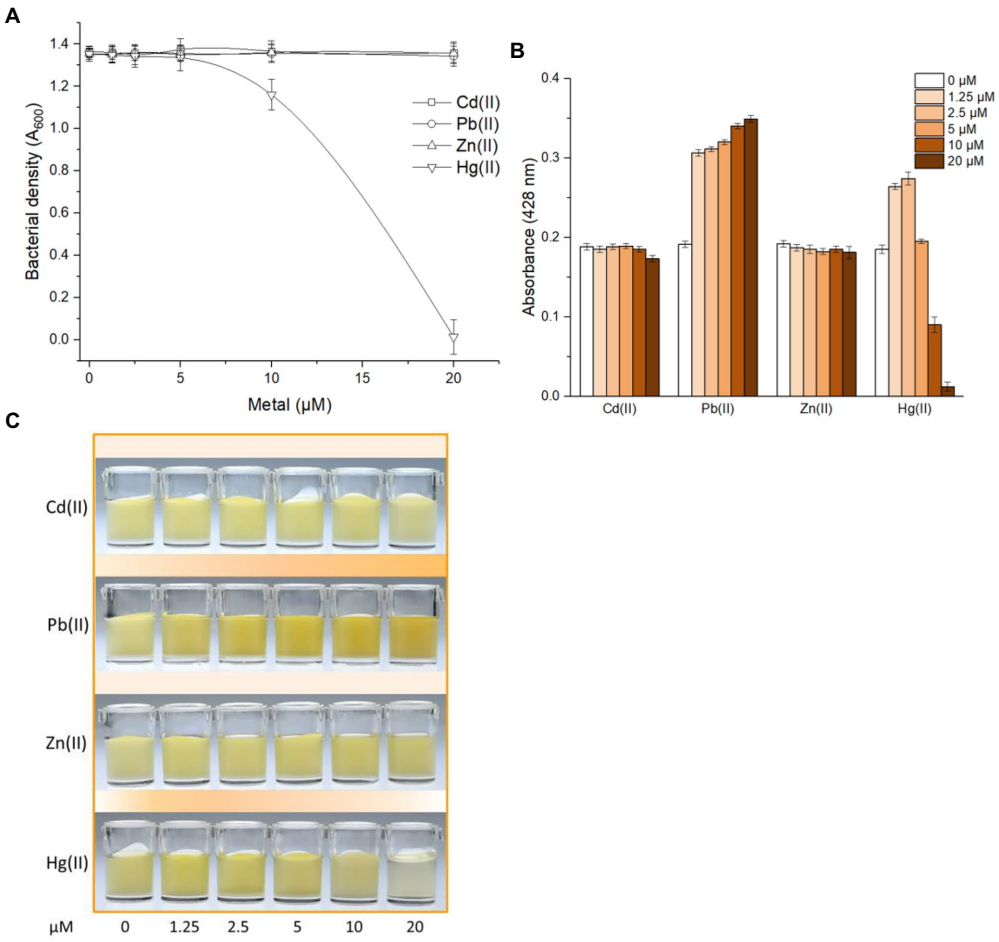

FIGURE 3
Differential responses of TOP10/pPb-CACD toward various metal ions. TOP10/pPb-CACD was inoculated into fresh LB medium supplemented with 1 mM catechin and exposed to increased concentrations of Cd(II), Pb(II), Zn(II), or Hg(II). After culture at 37°C overnight, bacterial cell densities **(A)** and pigment signal **(B)** was measured at 600 nm and 428 nm, respectively. Data represent the average of three independent assays with similar results and error bars represent standard deviations. Data shown are mean±SD (n = 3). A representative picture of induced cultures **(C)** was chosen from three independent tests with similar results.

followed by incubation at 37°C for 15 h in a constant temperature shaker. The CACD-derived signal is then measured at 428 nm using a microplate reader after a simple centrifugation step. The whole test can be finished within one day.

The capability of a novel biosensor in detecting toxic heavy metals in environmental water samples is important for evaluating its potential application in the real world. Environmental surface water was collected from two downtown parks and the sampling sites were shown in Figure 5B. Total Pb in collected tap water and two kinds of environmental surface water was detected using the ICP-MS and demonstrated to be below the detection limit (0.145 nM). Artificially contaminated environmental samples were usually used when no heavy metals polluted environmental sample was available (Kumar et al., 2017; Hui et al., 2022c). In this study, freshly prepared culture systems using different water samples were artificially contaminated by spiking with different concentrations of soluble Pb(II), inoculated with TOP10/pPb-CACD, and incubated overnight at 37°C. The four culture systems were maintained at about neutral pH during the whole process. As expected, the response patterns showed a striking similarity in the dose–response curves among all four groups, and the relative standard deviations were all below 3.3 (Figure 5C).

Many factors including the pH value, hardness, and dissolved organic matter (DOM) in the aquatic system can affect the speciation of heavy metals, which is vital for their bioavailability and ecotoxic effects (Ryan et al., 2009). However, the inorganic ions and DOM existing in the natural aquatic system only exerted a slight influence on the Pb(II)-responsive property of TOP10/pPb-CACD, which is similar to previously developed pigment-based biosensors (Guo et al., 2021a; Hui et al., 2022a,c).

Different from dithizone colorimetry, this biosensing technique has obvious advantages in sensitivity and specificity. Compared with high-precision instruments such as atomic absorption spectrometry and ICP-MS, low selectivity, and low sensitivity can also be improved by modifying Pb(II) sensory

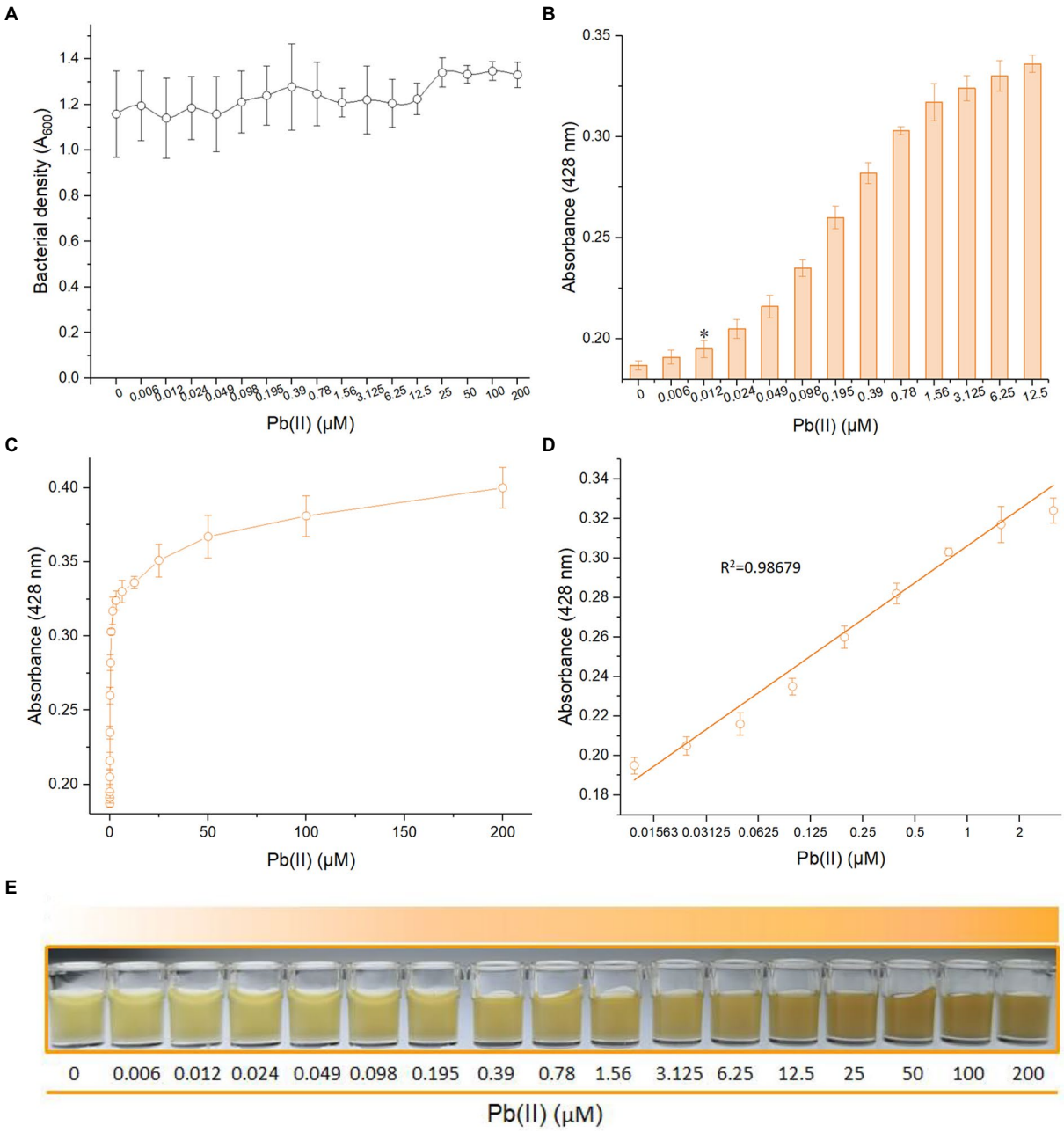

FIGURE 4
Response of TOP10/pPb-CACD to increased concentrations of Pb(II). TOP10/pPb-CACD was inoculated into fresh LB medium supplemented with 1 mM catechin and induced with increased concentrations of Pb(II) at 37°C overnight. The cell-free culture supernatants containing CACD were prepared and detected by visible light absorbance at 428 nm. **(A)** Bacterial densities of TOP10/pPb-CACD exposed to different concentrations of Pb(II). **(B)** The detection sensitivity of TOP10/pPb-CACD. Data represent the average of three independent assays with similar results. Error bars represent standard deviations. The asterisk represents the limit of detection, which is adopted as the lowest concentration of Pb(II) that triggered a significant increase of absorbance value at 428 nm (background +3 × SD). **(C)** The dose–response curve with Pb(II) concentration ranges from 0 to 200μM. **(D)** Regression analysis of the relationship of pigment-based signal and the Pb(II) concentrations ranging from 0.012 to 3.125 μM. The *x*-axis displays the Pb(II) concentration on the $\log_2$ scale. Data shown are mean±SD (n =3). **(E)** A representative picture of the cultures induced with increased concentrations of Pb(II).

module and genetic circuits in the future study. Importantly, monitoring of bioaccessible, bioavailable, and toxic Pb(II) is essential in predicting its ecotoxicity and health risk, which makes the whole-cell biosensor become a powerful supplement to above traditional methods. In summary, our study shows that a metabolic engineered bacterial biosensor has the potential to become a low-cost, portable, and user-friendly biological device for detecting environmental Pb(II).

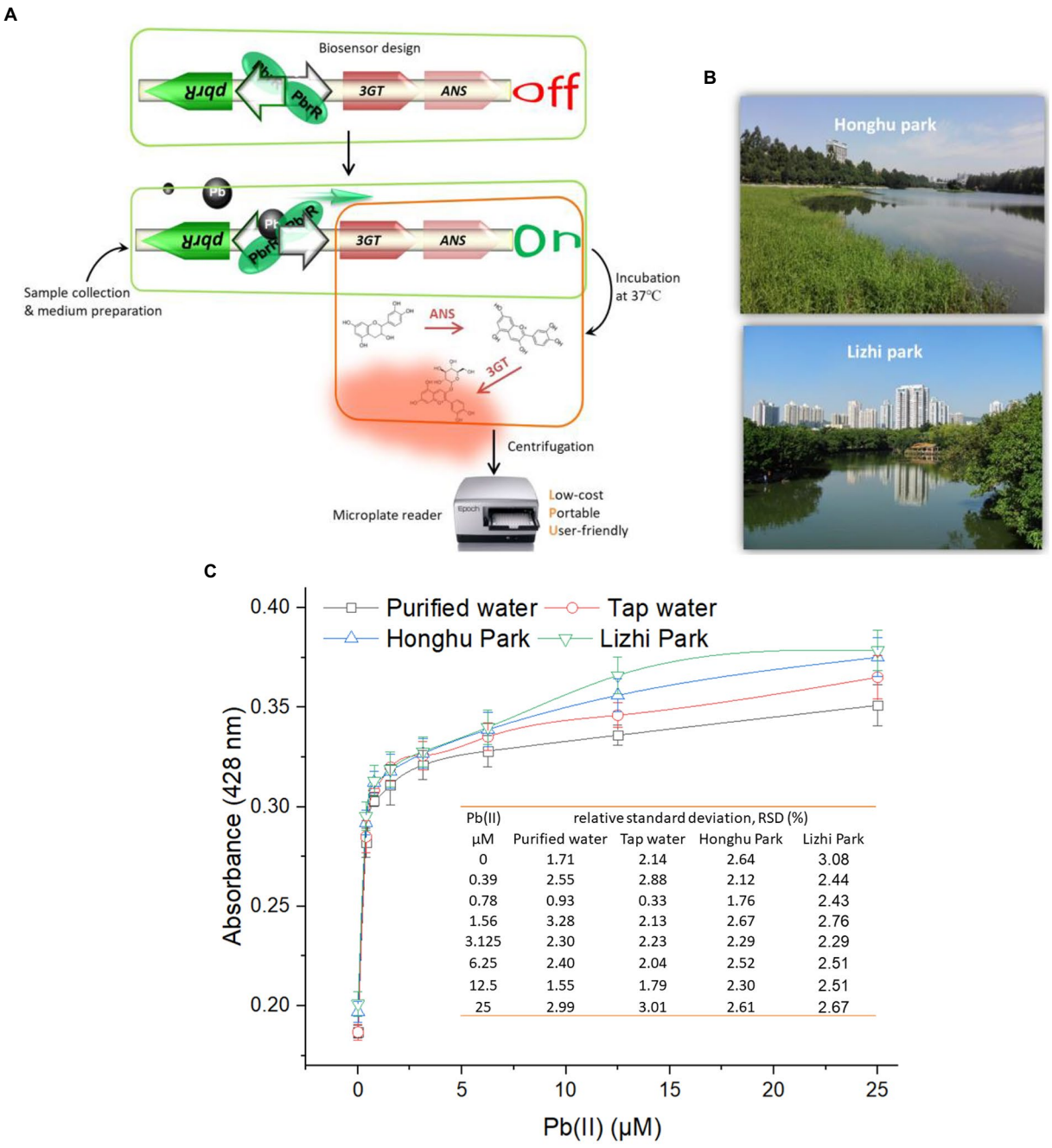

Pb(II)	relative standard deviation, RSD (%)			
μM	Purified water	Tap water	Honghu Park	Lizhi Park
0	1.71	2.14	2.64	3.08
0.39	2.55	2.88	2.12	2.44
0.78	0.93	0.33	1.76	2.43
1.56	3.28	2.13	2.67	2.76
3.125	2.30	2.23	2.29	2.29
6.25	2.40	2.04	2.52	2.51
12.5	1.55	1.79	2.30	2.51
25	2.99	3.01	2.61	2.67

FIGURE 5
Detection of bioavailable Pb(II) in environmental samples using TOP10/pPb-CACD. **(A)** The detailed protocol for the field measurement. The capability of TOP10/pPb-CACD was validated in determining bioaccessible Pb(II) in environmental samples using a three-step colorimetric method. Surface water was collected from two downtown parks in Shenzhen city, South China **(B)**. TOP10/pPb-CACD was inoculated into fresh LB medium prepared with four different water samples and supplemented with 1 mM catechin. Different concentrations of Pb(II) were spiked into the culture system. After culturing at 37°C overnight, the cell-free culture supernatants containing CACD were prepared and determined at 428 nm **(C)**. Data shown are mean±SD (n = 3). The inset table shows the relative standard deviation (RSD) of pigment derived signal.

Conclusion

Limited attempts have been made to assemble heavy metal whole-cell biosensors using the natural pigment synthesis pathway. In this study, the Pb(II)-responsive metabolic flow toward anthocyanin enabled a minimal-equipment whole-cell biosensor. The resultant CACD could be quantitatively determined at 428 nm in a colorimetric method. The metabolically engineered biosensor selectively responded to Pb(II), the detection limit was 0.012 μM, and the quantitative detection range was

0.012–3.125 μM. The colorimetric bacterial biosensor was validated in detecting bioavailable Pb(II) in artificially polluted environmental water samples. Our study shows that bacterial biosensor modified by metabolic engineering is promising for environmental monitoring of heavy metal pollution sensitively and visually.

Data availability statement

The original contributions presented in the study are included in the article/Supplementary material, further inquiries can be directed to the corresponding author.

Author contributions

C-yH and YG designed the experimental protocol. C-yH drafted the manuscript. D-lZ, S-yH, and HL carried out the majority of the study. YG and Z-lH analyzed the data. All authors contributed to the article and approved the submitted version.

Funding

This work was supported by the National Natural Science Foundation of China (82073517), the Natural Science Foundation of Guangdong Province (2019A1515011989 and 2021A1515012472), the Science and Technology Program of Shenzhen (JCYJ20180306170237563, JCYJ20190808175205480, and KCXFZ20201221173602007), Shenzhen Key Medical Discipline Construction Fund (SZXK068), and Shenzhen Fund for Guangdong Provincial High-level Clinical Key Specialties (SZGSP015).

Conflict of interest

The authors declare that the research was conducted in the absence of any commercial or financial relationships that could be construed as a potential conflict of interest.

Publisher's note

All claims expressed in this article are solely those of the authors and do not necessarily represent those of their affiliated organizations, or those of the publisher, the editors and the reviewers. Any product that may be evaluated in this article, or claim that may be made by its manufacturer, is not guaranteed or endorsed by the publisher.

Supplementary material

The Supplementary material for this article can be found online at: https://www.frontiersin.org/articles/10.3389/fmicb.2022.975421/full#supplementary-material

References

Bereza-Malcolm, L., Aracic, S., and Franks, A. E. (2016). Development and application of a synthetically-derived lead biosensor construct for use in gram-negative bacteria. *Sensors* 16:16. doi: 10.3390/s16122174

Borremans, B., Hobman, J. L., Provoost, A., Brown, N. L., and Van Der Lelie, D. (2001). Cloning and functional analysis of the *pbr* lead resistance determinant of *Ralstonia metallidurans* CH34. *J. Bacteriol.* 183, 5651–5658. doi: 10.1128/JB.183.19.5651-5658.2001

Caguiat, J. J., Watson, A. L., and Summers, A. O. (1999). Cd(II)-responsive and constitutive mutants implicate a novel domain in MerR. *J. Bacteriol.* 181, 3462–3471. doi: 10.1128/JB.181.11.3462-3471.1999

Cai, S., Shen, Y., Zou, Y., Sun, P., Wei, W., Zhao, J., et al. (2018). Engineering highly sensitive whole-cell mercury biosensors based on positive feedback loops from quorum-sensing systems. *Analyst* 143, 630–634. doi: 10.1039/C7AN00587C

Cai, Y., Zhu, K., Shen, L., Ma, J., Bao, L., Chen, D., et al. (2022). Evolved biosensor with high sensitivity and specificity for measuring cadmium in actual environmental samples. *Environ. Sci. Technol.* 56, 10062–10071. doi: 10.1021/acs.est.2c00627

Chen, P., Greenberg, B., Taghavi, S., Romano, C., Van Der Lelie, D., and He, C. (2005). An exceptionally selective lead(II)-regulatory protein from *Ralstonia metallidurans*: development of a fluorescent lead(II) probe. *Angew. Chem. Int. Ed. Engl.* 44, 2715–2719. doi: 10.1002/anie.200462443

Chen, P.-H., Lin, C., Guo, K.-H., and Yeh, Y.-C. (2017). Development of a pigment-based whole-cell biosensor for the analysis of environmental copper. *RSC Adv.* 7, 29302–29305. doi: 10.1039/C7RA03778C

Guo, Y., Hui, C. Y., Liu, L., Chen, M. P., and Huang, H. Y. (2021a). Development of a bioavailable hg(II) sensing system based on MerR-regulated visual pigment biosynthesis. *Sci. Rep.* 11:13516. doi: 10.1038/s41598-021-92878-6

Guo, Y., Hui, C. Y., Liu, L., Zheng, H. Q., and Wu, H. M. (2019). Improved monitoring of low-level transcription in *Escherichia coli* by a beta-galactosidase alpha-complementation system. *Front. Microbiol.* 10:1454. doi: 10.3389/fmicb.2019.01454

Guo, Y., Hui, C. Y., Zhang, N. X., Liu, L., Li, H., and Zheng, H. J. (2021b). Development of cadmium multiple-signal biosensing and bioadsorption systems based on artificial *cad* operons. *Front. Bioeng. Biotechnol.* 9:585617. doi: 10.3389/fbioe.2021.585617

Gupta, N., Renugopalakrishnan, V., Liepmann, D., Paulmurugan, R., and Malhotra, B. D. (2019). Cell-based biosensors: recent trends, challenges and future perspectives. *Biosens. Bioelectron.* 141:111435. doi: 10.1016/j.bios.2019.111435

Hakkila, K. M., Nikander, P. A., Junttila, S. M., Lamminmaki, U. J., and Virta, M. P. (2011). Cd-specific mutants of mercury-sensing regulatory protein MerR, generated by directed evolution. *Appl. Environ. Microbiol.* 77, 6215–6224. doi: 10.1128/AEM.00662-11

Hui, C. Y., Guo, Y., Gao, C. X., Li, H., Lin, Y. R., Yun, J. P., et al. (2022a). A tailored Indigoidine-based whole-cell biosensor for detecting toxic cadmium in environmental water samples, 102511. *Environ. Technol. Innov.* doi: 10.1016/j.eti.2022.102511

Hui, C. Y., Guo, Y., Li, H., Chen, Y. T., and Yi, J. (2022b). Differential detection of bioavailable mercury and cadmium based on a robust dual-sensing bacterial biosensor. *Front. Microbiol.* 13:846524. doi: 10.3389/fmicb.2022.846524

Hui, C. Y., Guo, Y., Li, H., Gao, C. X., and Yi, J. (2022c). Detection of environmental pollutant cadmium in water using a visual bacterial biosensor. *Sci. Rep.* 12:6898. doi: 10.1038/s41598-022-11051-9

Hui, C. Y., Guo, Y., Li, L. M., Liu, L., Chen, Y. T., Yi, J., et al. (2021a). Indigoidine biosynthesis triggered by the heavy metal-responsive transcription regulator: a visual whole-cell biosensor. *Appl. Microbiol. Biotechnol.* 105, 6087–6102. doi: 10.1007/s00253-021-11441-5

Hui, C. Y., Guo, Y., Liu, L., and Yi, J. (2021b). Recent advances in bacterial biosensing and bioremediation of cadmium pollution: a mini-review. *World J. Microbiol. Biotechnol.* 38:9.

Hui, C. Y., Guo, Y., Liu, L., Zhang, N. X., Gao, C. X., Yang, X. Q., et al. (2020a). Genetic control of violacein biosynthesis to enable a pigment-based whole-cell lead biosensor. *RSC Adv.* 10, 28106–28113. doi: 10.1039/D0RA04815A

Hui, C. Y., Guo, Y., Liu, L., Zheng, H. Q., Gao, C. X., and Zhang, W. (2020b). Construction of a RFP-lacZalpha bicistronic reporter system and its application in lead biosensing. *PLoS One* 15:e0228456. doi: 10.1371/journal.pone.0228456

Hui, C. Y., Guo, Y., Wu, J., Liu, L., Yang, X. Q., Guo, X., et al. (2021c). Detection of bioavailable cadmium by double-color fluorescence based on a dual-sensing bioreporter system. *Front. Microbiol.* 12:696195. doi: 10.3389/fmicb.2021.696195

Hui, C. Y., Guo, Y., Zhu, D. L., Li, L. M., Yi, J., and Zhang, N. X. (2022d). Metabolic engineering of the violacein biosynthetic pathway toward a low-cost, minimal-equipment lead biosensor. *Biosens. Bioelectron.* 214:114531. doi: 10.1016/j.bios.2022.114531

Jia, X., Zhao, T., Liu, Y., Bu, R., and Wu, K. (2018). Gene circuit engineering to improve the performance of a whole-cell lead biosensor. *FEMS Microbiol. Lett.* 365, 1–8. doi: 10.1093/femsle/fny157

Kang, Y., Lee, W., Jang, G., Kim, B. G., and Yoon, Y. (2018). Modulating the sensing properties of *Escherichia* coli-based bioreporters for cadmium and mercury. *Appl. Microbiol. Biotechnol.* 102, 4863–4872. doi: 10.1007/s00253-018-8960-2

Kim, H. J., Jeong, H., and Lee, S. J. (2018). Synthetic biology for microbial heavy metal biosensors. *Anal. Bioanal. Chem.* 410, 1191–1203. doi: 10.1007/s00216-017-0751-6

Kumar, S., Verma, N., and Singh, A. K. (2017). Development of cadmium specific recombinant biosensor and its application in milk samples. *Sensors Actuators B Chem.* 240, 248–254. doi: 10.1016/j.snb.2016.08.160

Lim, C. G., Wong, L., Bhan, N., Dvora, H., Xu, P., Venkiteswaran, S., et al. (2015). Development of a recombinant *Escherichia coli* strain for overproduction of the plant pigment anthocyanin. *Appl. Environ. Microbiol.* 81, 6276–6284. doi: 10.1128/AEM.01448-15

McNerney, M. P., Michel, C. L., Kishore, K., Standeven, J., and Styczynski, M. P. (2019). Dynamic and tunable metabolite control for robust minimal-equipment assessment of serum zinc. *Nat. Commun.* 10:5514. doi: 10.1038/s41467-019-13454-1

Pourrut, B., Shahid, M., Dumat, C., Winterton, P., and Pinelli, E. (2011). Lead uptake, toxicity, and detoxification in plants. *Rev. Environ. Contam. Toxicol.* 213, 113–136. doi: 10.1007/978-1-4419-9860-6_4

Ryan, A. C., Tomasso, J. R., and Klaine, S. J. (2009). Influence of pH, hardness, dissolved organic carbon concentration, and dissolved organic matter source on the acute toxicity of copper to Daphnia magna in soft waters: implications for the biotic ligand model. *Environ. Toxicol. Chem.* 28, 1663–1670. doi: 10.1897/08-361.1

Springob, K., Nakajima, J., Yamazaki, M., and Saito, K. (2003). Recent advances in the biosynthesis and accumulation of anthocyanins. *Nat. Prod. Rep.* 20, 288–303. doi: 10.1039/b109542k

Tsuda, T., Ueno, Y., Kojo, H., Yoshikawa, T., and Osawa, T. (2005). Gene expression profile of isolated rat adipocytes treated with anthocyanins. *Biochim. Biophys. Acta* 1733, 137–147. doi: 10.1016/j.bbalip.2004.12.014

USEPA (2009). "*National Primary Drinking Water Regulations*". United States: USEPA.

USEPA (2016). "*National Recommended Water Quality Criteria*". United States: USEPA.

Wei, W., Liu, X., Sun, P., Wang, X., Zhu, H., Hong, M., et al. (2014). Simple whole-cell biodetection and bioremediation of heavy metals based on an engineered lead-specific operon. *Environ. Sci. Technol.* 48, 3363–3371. doi: 10.1021/es4046567

Yan, Y., Chemler, J., Huang, L., Martens, S., and Koffas, M. A. (2005). Metabolic engineering of anthocyanin biosynthesis in *Escherichia coli*. *Appl. Environ. Microbiol.* 71, 3617–3623. doi: 10.1128/AEM.71.7.3617-3623.2005

Yan, Y., Li, Z., and Koffas, M. A. (2008). High-yield anthocyanin biosynthesis in engineered *Escherichia coli*. *Biotechnol. Bioeng.* 100, 126–140. doi: 10.1002/bit.21721

Yang, D., Park, S. Y., and Lee, S. Y. (2021). Production of rainbow colorants by metabolically engineered *Escherichia coli*. *Adv. Sci.* 8:e2100743. doi: 10.1002/advs.202100743

Yang, D., Park, S. Y., Park, Y. S., Eun, H., and Lee, S. Y. (2020). Metabolic engineering of *Escherichia coli* for natural product biosynthesis. *Trends Biotechnol.* 38, 745–765. doi: 10.1016/j.tibtech.2019.11.007

Zhang, N. X., Guo, Y., Li, H., Yang, X. Q., Gao, C. X., and Hui, C. Y. (2021). Versatile artificial mer operons in *Escherichia coli* towards whole cell biosensing and adsorption of mercury. *PLoS One* 16:e0252190. doi: 10.1371/journal.pone.0252190

frontiers | Frontiers in Microbiology

TYPE Original Research
PUBLISHED 13 October 2022
DOI 10.3389/fmicb.2022.1006609

Check for updates

OPEN ACCESS

EDITED BY
Durgesh K. Jaiswal,
Savitribai Phule Pune University, India

REVIEWED BY
Yongtao Zhu,
Minnesota State University, Mankato, United States
Liang Shen,
Anhui Normal University, China

*CORRESPONDENCE
Ines Krohn
ines.krohn@uni-hamburg.de

SPECIALTY SECTION
This article was submitted to Microbiotechnology, a section of the journal Frontiers in Microbiology

RECEIVED 29 July 2022
ACCEPTED 21 September 2022
PUBLISHED 13 October 2022

CITATION
Astafyeva Y, Gurschke M, Streit WR and Krohn I (2022) Interplay between the microalgae *Micrasterias radians* and its symbiont *Dyadobacter* sp. HH091. *Front. Microbiol.* 13:1006609. doi: 10.3389/fmicb.2022.1006609

COPYRIGHT
© 2022 Astafyeva, Gurschke, Streit and Krohn. This is an open-access article distributed under the terms of the Creative Commons Attribution License (CC BY). The use, distribution or reproduction in other forums is permitted, provided the original author(s) and the copyright owner(s) are credited and that the original publication in this journal is cited, in accordance with accepted academic practice. No use, distribution or reproduction is permitted which does not comply with these terms.

Interplay between the microalgae *Micrasterias radians* and its symbiont *Dyadobacter* sp. HH091

Yekaterina Astafyeva, Marno Gurschke, Wolfgang R. Streit and Ines Krohn*

Department of Microbiology and Biotechnology, Biocenter Klein Flottbek, University of Hamburg, Hamburg, Germany

Based on previous research, related to detailed insight into mutualistic collaboration of microalga and its microbiome, we established an artificial plant-bacteria system of the microalga *Micrasterias radians* MZCH 672 and the bacterial isolate *Dyadobacter* sp. HH091. The bacteria, affiliated with the phylum Bacteroidota, strongly stimulated growth of the microalga when it was added to axenic algal cultures. For further advances, we studied the isolate HH091 and its interaction with the microalga *M. radians* using transcriptome and extensive genome analyses. The genome of HH091 contains predicted polysaccharide utilizing gene clusters co-working with the type IX secretion system (T9SS) and conceivably involved in the algae-bacteria liaison. Here, we focus on characterizing the mechanism of T9SS, implementing the attachment and invasion of microalga by *Dyadobacter* sp. HH091. Omics analysis exposed T9SS genes: *gldK*, *gldL*, *gldM*, *gldN*, *sprA*, *sprE*, *sprF*, *sprT*, *porU* and *porV*. Besides, *gld* genes not considered as the T9SS components but required for gliding motility and protein secretion (*gldA*, *gldB*, *gldD*, *gldF*, *gldG*, *gldH*, *gldI*, *gldJ*), were also identified at this analysis. A first model of T9SS apparatus of *Dyadobacter* was proposed in a course of this research. Using the combination of fluorescence labeling of *Dyadobacter* sp. HH091, we examined the bacterial colonisation and penetration into the cell wall of the algal host *M. radians* MZCH 672.

KEYWORDS

***Dyadobacter* sp. HH091, *Micrasterias radians*, microalgaebacteria interaction, synthetic early plant-bacteria system, symbiotic relations**

Introduction

Algae and bacteria synergistically collaborate with each other, influence ecosystems, and represent various modes of interactions between organisms (Ramanan et al., 2016). The positive effect of bacteria on algal growth in the field of biotechnology, has changed the main concept of a mere contamination of algal cultures, considering bacteria as an important driver in this interaction (Lee et al., 2015; Shen and Benner, 2018). Strong

associations between microalgae and bacteria have resulted in the evolution of a complex network of these cross-kingdom interactions and narrow specialization of different organisms (Krohn et al., 2013; Krohn-Molt et al., 2017; Cirri and Pohnert, 2019; Astafyeva et al., 2022).

Nowadays, it is recognized that the potential of the interactions between microalgae and microorganisms, determined by special applicability in aquaculture, aims to improve algal biomass production and to enrich this biomass with compounds of biotechnological interest such as lipids, carbohydrates, and pigments. The algal microenvironment may be altered by bacteria in ways that stimulate algal functions. The general bacterial attributes that may profit the interaction with microalgae, and which might affect their growth and photosynthetic activity, include adhesion, clumping factor, motility, chemotaxis, different secretion systems, quorum sensing and quenching systems, and synthesis of growth promoters (Luo and Moran, 2014; Brameyer et al., 2015; Shen and Benner, 2018; Astafyeva et al., 2022).

Previous research of microalgae-and photobioreactors-associated biofilm bacteria, identified that the majority of the observed microorganisms were affiliated with α-Proteobacteriota, β-Proteobacteriota, and Bacteroidota (Mouget et al., 1995; Davies et al., 1998; Krohn et al., 2013; Whitman et al., 2018). Further investigations have characterized the biotic interaction of microalgae and bacteria using metagenomic, transcriptomic, and proteomic approaches. In this research the microbiomes of microalga have been sequenced, and various bacterial strains affiliated with the algae have been isolated to answer, if the associated microbiota is specific for the microalgae and which role individual bacterial taxa play (Krohn-Molt et al., 2017). Thereby it was observed that effector molecules known from plant–microbe interactions as inducers for the innate immunity are already of relevance at this evolutionary early plant-microbiome level. Key genes involved in plant–microbe interactions were mostly affiliated with different mechanisms, including vitamin biosynthesis, transport and secretion systems, signal transduction, carbohydrate and lipid modification. The metatranscriptome analysis indicated that the transcriptionally most active bacteria, with respect to key genes commonly involved in plant–microbe interactions, in the microbiome of the *Chlorella* (Trebouxiophyceae), *Scenedesmus* (Chlorophyceae) and *Micrasterias* (Zygnematophyceae) belong to the phylum of the α-Proteobacteriota and Bacteroidota (Krohn-Molt et al., 2017).

Recent studies unveiled tight associations of microalga *Scenedesmus quadricauda* and bacteria using metatranscriptomic analysis, including physiological investigations, microscopy observations, photosynthetic activity measurements and flow cytometry. The crucial key features of overall plant-bacteria interaction covered different mechanisms with the involvement of transport and secretion systems (e.g., T6SS, T9SS), quorum quenching proteins (QQ), leucine-rich repeat proteins and enzymes (LRR) related to bacterial reactive oxygen species (ROS) tolerance, as well as the biosynthesis of vitamins (B_1, B_2, B_5, B_6 B_7, B_9 and B_{12}). The metatranscriptome analysis demonstrated that within the microbiota of *S. quadricauda* the dominant species were affiliated with the genera of *Variovorax*, *Porphyrobacter* and *Dyadobacter*. Experimental and transcriptome-based evidences implied that within this multispecies interaction *Dyadobacter* was a key to alga growth and fitness, and is highly adopted to live in the phycosphere (Astafyeva et al., 2022).

Within this framework, we addressed the following questions in the current study. Which role do secretion systems play in these remarkable interactions? Is a direct cell-to-cell contact between the interaction partners required and what influence does bacterial QS have? To answer these questions, we used fluorescence labeling of bacteria and 4′-6-diamidino-2-phenylindole (DAPI) staining with confocal microscopy to determine the physical association of microalga cells with the *Dyadobacter* isolate HH091. Further, to get a deeper insight in this fascinating synthetic bacteria-microalgae model system, we have characterized the interactions of the isolate *Dyadobacter* sp. HH091 (Astafyeva et al., 2022), with the microalga *M. radians* MZCH 672 using transcriptome and genome analyses. These data expand our understanding of species-species interactions and identify several genes involved in the molecular basis of bacteria-alga interactions that can serve as an established synthetic plant-bacteria system. Therefore, the genome and metabolic potential of the bacterium *Dyadobacter* sp. HH091 is of particular interest in understanding bacteria-algae interactions.

Materials and methods

Microorganisms used in this study and cultivation media

Micrasterias radians MZCH 672 was obtained from the Microalgae and Zygnematophyceae Collection Hamburg (*MZCH*) and cultivated in WHM medium (Stein, 1973) at 20 ± 1°C and 100 ± 10 µmol photons m^{-2} s^{-1} with a 14/10-h light/dark period. To maintain the axenity of the algal culture, *M. radians* was treated with the antibiotic cocktail: penicillin G, streptomycin sulfate and gentamycin sulfate (100/25/25 mg/l) (Droop, 1967; Andersen, 2005; Lee et al., 2015; Astafyeva et al., 2022).

Dyadobacter sp. HH091 was isolated previously from a laboratory culture of *S. quadricauda* MZCH 10104 (Krohn-Molt et al., 2017; Astafyeva et al. 2022). The isolate was routinely grown in 5 ml of tryptone yeast extract salts (TYES) broth (Reasoner and Geldreich, 1985; Holt, 1993), at 22°C for 3–4 days at 200 rpm.

Analysis of the flexirubin pigments in *Dyadobacter* sp. HH091

We experimentally validate the production of flexirubin by *Dyadobacter* sp. HH091 by exposing them to 50 µl 10 M KOH, which resulted in a change from yellow to orange/red

if flexirubin pigments were present, followed by a neutralization step with 42 µl 12 M HCl, which resulted in a return to yellow pigmentation.

Co-culturing procedure and conditions

Micrasterias radians MZCH 672 and *Dyadobacter* sp. HH091 were co-cultured in WHM medium at 20 ± 1°C and 100 ± 10 µmol photons m^{-2} s^{-1} with a 14/10 h light/dark period over a time period of 12 days. Therefore, 1 ml of *M. radians* was treated with an antibiotic cocktail of penicillin G, streptomycin sulfate and gentamycin sulfate in 50 ml of WHM medium to remove all bacteria. The antibiotic treatment was performed for 1 day. Afterwards, the microalga was centrifuged (5,000 rpm, 10 min) and washed two times with 1 ml WHM medium and finally resuspended in 50 ml of medium, where it was grown for 20 days. At the start of the experiment, each flask contained 50 ml of WHM, *M. radians* (OD_{750nm} = 0.007) and *Dyadobacter* sp. (OD_{600nm} = 0.05).

Dyadobacter sp. HH091 transformation

The strain HH091 was transformed with modified plasmid pBBR1MCS-5-eGFP by electroporation according to standard methods, which resulted in bright green fluorescent colonies as observed by fluorescence microscopy (Sambrook and Russell, 2001). The plasmid contains the broad-host-range vector pBBR1MCS-5, providing a gentamycin resistance and the expression of GFP. Gentamycin was applied at 100 µg/ml, and the bacteria were grown as described previously (Droop, 1967; Andersen, 2005; Lee et al., 2015; Astafyeva et al., 2022).

Confocal laser scanning microscopy

Dyadobacter sp. HH091 expressing eGFP was co-cultured with *M. radians* MZCH 672 and studied using a confocal laser scanning microscope (CLSM) Axio Observer.Z1/7 LSM 800 (Carl Zeiss Microscopy GmbH, Jena, Germany), which also included Z-Stack microscope techniques. The analysis of the CLSM images were done with ZEN software (version 2.3; Carl Zeiss Microscopy GmbH). DAPI staining procedure was used in microscopy investigations as described previously (Astafyeva et al., 2022). Modifications included the treatment with TrueVIEW Autofluorescence Quenching Kit (Vector Labs, SP-8400), which was employed to enhance staining and to lower the autofluorescence of chlorophyll of the microalga. Background autofluorescence occurring in the 600–700 nm range, makes it impossible to detect the bacteria transformed with plasmids expressing fluorescent proteins. The TrueVIEW Quencher is an aqueous solution of a hydrophilic molecule, which binds to chlorophyll electrostatically and lowers the fluorescence (Karpishin, 2018).

Bacterial RNA isolation and sequencing

Dyadobacter sp. HH091 cells, separated by dialysing bags (Roth, Germany), were co-cultured with microalga for 1 week. Then bacterial cells were subsequently harvested, treated with RNAlater (Sigma, Germany) and frozen at −80°C. The samples were processed by Eurofins (Constance, Germany), where the RNA was isolated and assessed for QC. The RNA Integrity Number (RIN) for all samples was ≥8. Strand-specific cDNA library preparation from polyA enriched RNA (150 bp mean read length) and RNA sequencing was performed using the genome sequencer Illumina HiSeq technology in NovaSeq 6000 S4 PE150 XP sequencing mode. For further analysis fastq-files were provided.

Bacterial RNA data analysis

RNA-seq analysis was performed using PATRIC, the Pathosystems Resource Integration Center.[1] Trim Galore 0.6.5dev was used to remove adapters (Phred quality score below 20) (Krueger, 2012). RNA-Seq data was processed by the tuxedo strategy (Trapnell et al., 2012). All genes were selected with|log2 (fold change)| ≥ 1,5. The differentially expressed genes (DEGs) dataset was collected and used for further analysis. The volcano plot of the distribution of all DEGs was generated using A Shiny app ggVolcanoR (Mullan et al., 2021).

Carbohydrate-active enzymes were screened through local Blastp search in the database of carbohydrate-active enzymes (CAZymes).[2] The database compiles categories of enzymes that act on carbohydrates, e.g., glycoside hydro-lases (GHs), polysaccharide lyases (PLs), glycosyltransferases (GTs) (Levasseur et al., 2013). Domain guided annotation based on conserved domains in *Dyadobacter* sp. HH091 was performed within the STRING database (Szklarczyk et al., 2021).

Sequences obtained and GenBank submissions

RNA sequences obtained for this study were submitted to the European Nucleotide Archive (ENA). They are publicly available under accession PRJEB54772. Assembly of the *Dyadobacter* sp. HH091 genome is available *via* IMG/MER[3] using the IMG ID 2842103827.

1 www.patricbrc.org
2 www.cazy.org
3 https://img.jgi.doe.gov

Results

Symbiont *Dyadobacter* sp. HH091 attached to the surface of *Micrasterias radians* MZCH 672

Based on our previous research, we were intrigued to examine the bacterial colonisation of the microalga *M. radians* MZCH 672. CLSM was used to observe the interaction process between *Dyadobacter* sp. HH091 and *M. radians*. The co-culture of *M. radians* with *Dyadobacter* sp. expressing eGFP are shown in Figure 1. In addition, Z-Stack microscopy was employed to generate a more detailed and higher resolution image of the microalgal contact site with its symbiont. Our results showed, that symbiotic bacterial cells were found in close proximity of the alga after 1 day of incubation (Figure 1A). More nearby contacts were identified *via* CLSM between the host microalga and its symbiont on the third day of incubation (Figure 1B). At Figure 1A bacterial cells are found close to algal cells, while Figure 1B demonstrates the penetration of the symbiont into its host's cell wall. These experiments revealed the presence of direct contacts between *M. radians* and symbiotic *Dyadobacter* sp. HH091 cells through their surrounding and tight interaction, promising the mutual exchange of various substances between the two partners.

We examined co-cultures of HH091 grown together with *M. radians* and compared its relative growth performance with the antibiotic-treated algal control cultures over a time period of 20 days (Supplementary Figure S1). To identify the difference in the growth of algal cultures (with and without HH091) we used the optical density measurement (Supplementary Figure S1). In these tests first hints of visible difference were observed after 3–4 days.

RNA seq identifies active genes for host-symbiont interaction pathways

Transcriptome analysis was applied to indicate highly active genes involved into bacteria-algal interaction. In total, we obtained 43 million (mio) reads of bacteria data after trimming. The data are the result of three replicates with each replicate producing between 4 and 8 mio reads (Supplementary Table S1). The RNAseq data covered a significant portion of the bacterial genome and the affiliated pathways. During data preprocessing low quality transcripts were filtered, resulting in 1,530 genes to be studied (Supplementary Table S2). RNA-Seq analysis was performed using the Tuxedo strategy, the heatmap (Figure 2) was generated using the Expression Import Service of the Pathosystems Resource Integration Center, PATRIC, the absolute value of $\log_2$ Ratio > 1.5 (Kim et al., 2013, 2015; McClure et al., 2013).

The expression levels of the DEGs response of *Dyadobacter* sp. HH091 in co-culture with *M. radians* are depicted in the heatmap (Figure 2). The heatmap reflects the expression of genes affiliated with overall mechanisms described in categories. The highest number of transcripts belongs to carbohydrate transport and metabolism, inorganic ion transport and metabolism, signal

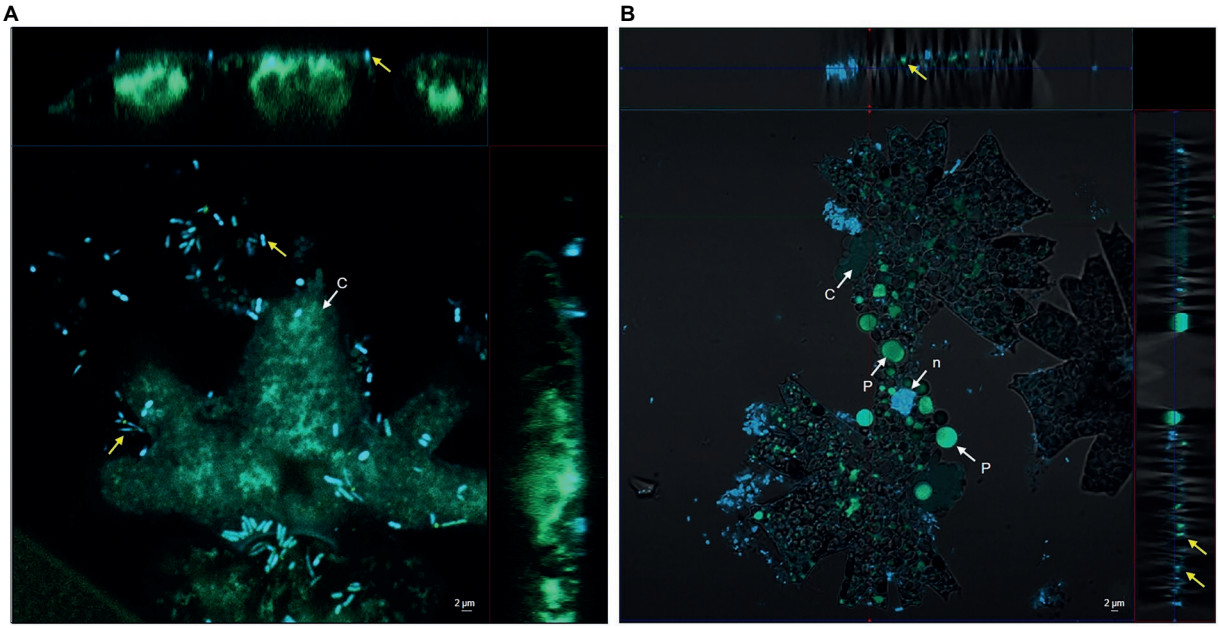

FIGURE 1
Confocal microscope including Z-Stack images of *Dyadobacter* sp. HH091 expressing eGFP (yellow arrows) found in a close proximity to *Micrasterias radians* MZCH 672. Autofluorescence Quenching Kit was used to lower the autofluorescence of chlorophyll of the microalga. Structures: c chloroplast, n nuclear region, p pyrenoid. Scale bar=2µm in each micrograph. **(A)** First day of incubation. **(B)** Third day of incubation.

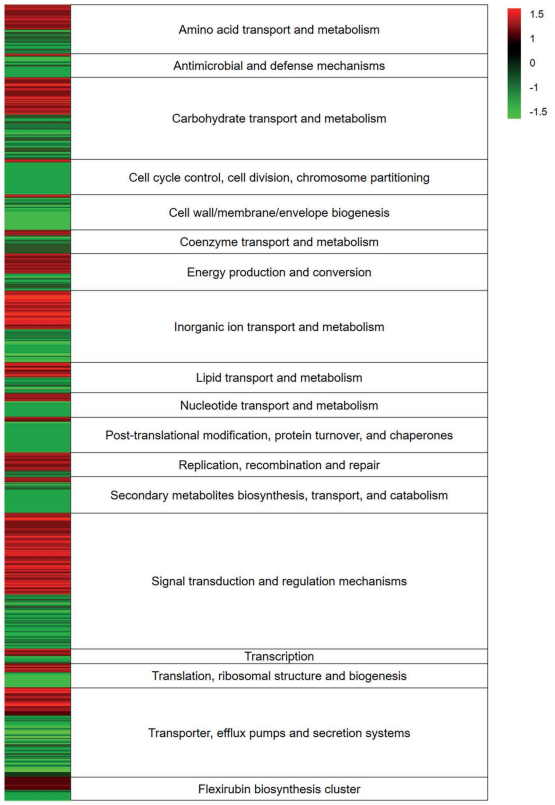

FIGURE 2
Heatmap of expression levels of differentially expressed genes (DEGs) response of *Dyadobacter* sp. HH091 in co-culture with *Micrasterias radians*. RNA-Seq analysis was performed using the Tuxedo strategy, the heatmap was generated using the Expression Import Service of the Pathosystems Resource Integration Center, PATRIC, the absolute value of log2 Ratio>1.5. Color key: up-regulated genes, down-regulated genes.

transduction and regulation mechanisms, and transporter, efflux pumps and secretion systems.

The distribution of gene expression between *Dyadobacter* sp. HH091 co-cultured with *M. radians* and control samples is represented by the volcano plot (Figure 3A). The volcano plot was constructed to compare the two groups using ggVolcanoR. A total of 1,530 differentially expressed genes (DEGs) were identified from the dataset (Figure 3A). Among them, 612 and 918 genes were up-regulated and downregulated, respectively, between two groups according to their $\log_2$FC and *p*-values. Function profile of the DEGs in *Dyadobacter* sp. HH091 is shown in Figure 3B. The studying of the transcriptome of the strain HH091 co-cultured with its microalgal host unveiled the multifaceted combination of mechanisms required for and/or affiliated with T9SS, as well as T9SS cargo proteins, Sus proteins (SusC and SusD), TonB-dependent receptors, cAMP-binding proteins, oxidoreductases, aminotransferases, cytochrome c, numerous transcriptional regulators, including LuxR solos, and flexirubin biosynthesis. The highest number of up-regulated genes belongs to T9SS cargo proteins (42), transcriptional regulators (56), Sus proteins (SusC (10) and SusD (6)), permeases (14), and oxidoreductases (13). Most down-regulated genes are related to oxidoreductases (11), T9SS cargo proteins (24), SusC (10) and SusD proteins (14), T9SS components and Gld proteins (35), permeases (16), and transcriptional regulators (20). Intriguingly, flexirubin biosynthesis mechanism involved 13 up-regulated and 4 down-regulated genes.

Transcriptome analysis indicated highly active genes of T9SS mechanism and flexirubin biosynthesis cluster

By a combination of comparative genome and transcriptome analyses we identified a cluster of genes presumably involved in flexirubin biosynthesis, which was performed using the STRING database (Szklarczyk et al., 2021). This cluster includes two genes, *darA* and *darB*, with likely roles in flexirubin synthesis, and other genes that could be involved in localization of flexirubin pigments (Supplementary Table S3). The flexirubin biosynthesis cluster of *Dyadobacter* sp. HH091 consists of the *dar* operon and a neighboring gene encoding LuxR solo (NarL/FixJ). NarL/FixJ shares 46% identity and 47% similarity with the LuxR solo PluR of *Photorhabdus luminescens* (Brameyer et al., 2015). In *P. luminescens* PluR performs as a LuxR-type receptor serving for QS. Based on these observations we proposed the model of flexirubin/dialkylresorcinol (DAR) biosynthesis in HH091, which consists of QS circuit genes possibly up-regulating several mechanisms like T9SS, gliding motility and protein secretion (Figure 4). These QS circuit genes are found to be adjacent to T9SS genes, genes affiliated with gliding motility and protein secretion (genes coding for gliding motility-associated-like proteins, T9SS type A sorting domain-containing proteins, chitin binding proteins, peptidoglycan-associated proteins, and PorT family protein).

Additional studying of homologs showed the presence of these genes in the representative genomes of the phylum Bacteriodota *Flavobacterium johnsoniae*, *Flavobacterium psychrophilum* (McBride et al., 2009) and *Chitinophaga pinensis* (Schöner et al., 2014), and among the members of the phylum Proteobacteriota *Photorhabdus asymbiotica* (Brameyer et al., 2015) and *Pseudomonas aurantiaca* (Nowak-Thompson et al., 2003). Responsible for flexirubin biosynthesis, genes *darA* and *darB* are similar to *F. johnsoniae*, which were previously identified to be engaged in biosynthesis of 2-hexyl-5-propyl-alkylresorcinol (McBride et al., 2009). In addition to *darA* and *darB*, other genes in this cluster are predicted to encode enzymes involved in lipid synthesis and some of these enzymes likely have roles in flexirubin synthesis (Supplementary Table S3). This cluster includes numerous genes, such as acyl carrier protein, (3-oxoacyl)-acyl carrier protein synthase, acyl-CoA thioester hydrolase, histidine ammonia-lyase, 1-acyl-sn-glycerol-3-phosphate acyltransferase, beta-ketoacyl synthases, and beta-hydroxyacyl-(acyl carrier protein) dehydratase, including several

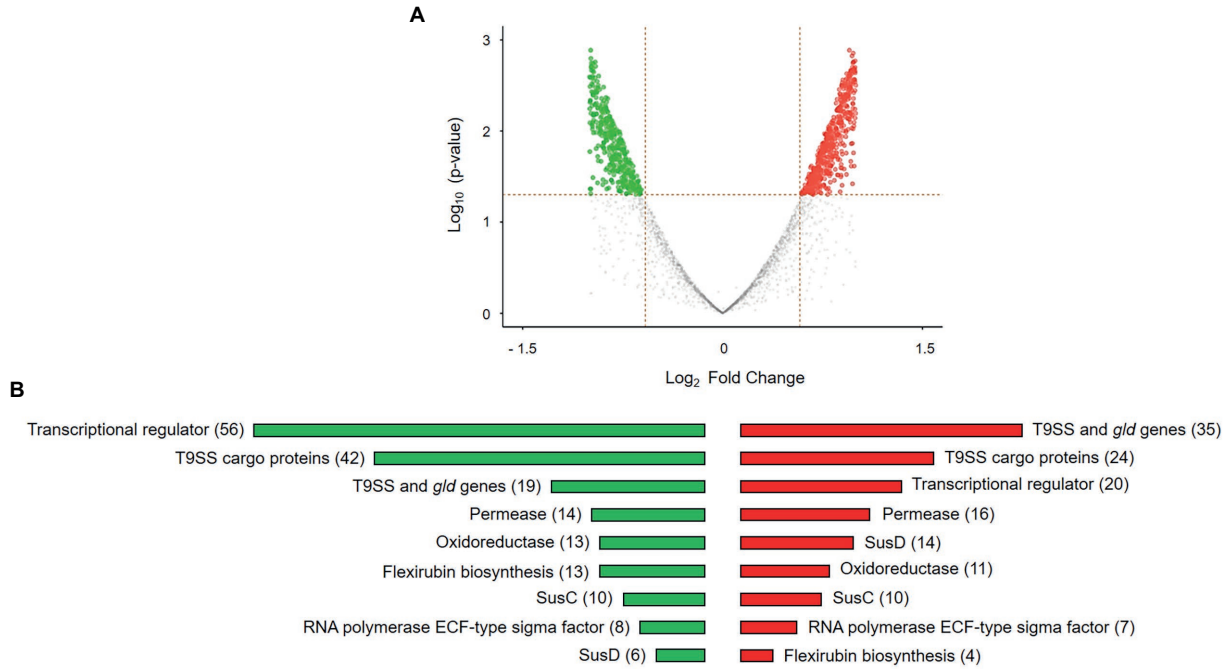

FIGURE 3
DEGs in *Dyadobacter* sp. HH091 co-cultured with *M. radians* MZCH 672 compared with control dataset. **(A)** Volcano plot is highlighting the DEGs in Dyadobacter sp. x-axis: log2, large-scale fold changes; y-axis: −log10 of the value of p showing the statistical significance. Each point corresponds to one gene. The points above the vertical and horizontal dotted lines represent log2FC≥0.58 and value of $p<0.05$. A volcano plot was generated using A Shiny app ggVolcanoR. **(B)** Function profile of differentially expressed genes (DEGs) in *Dyadobacter* sp. HH091 is presenting the groups of highly active genes. Total number of genes are shown in brackets. Color key: up-regulated genes, down-regulated genes.

ABC-2-type transporters known to be entangled in the localization of flexirubin (McBride et al., 2009).

Experimental identification and validation of flexirubin confirmed its production by *Dyadobacter* sp. HH091 (Supplementary Figure S2). Cells were photographed before treatment (I), after exposure to 50 µl of 10 M KOH (II), and after exposure to KOH followed by exposure to 42 µl 12 M HCl (III). Flexirubin-positive cells were yellow at neutral pH (I and III) and orange/red under alkaline conditions (II).

Proposed model of T9SS in *Dyadobacter* sp.

Highly active genes within this transcriptome belong to T9SS mechanism and gliding motility (Supplementary Table S4). Overall, 18 genes (*gldA*, *gldB*, *gldD*, *gldF*, *gldG*, *gldH*, *gldI*, *gldJ*, *gldK*, *gldL*, *gldM*, *gldN*, *sprA*, *sprE*, *sprF*, *sprT*, *porU* and *porV*), required for gliding motility and protein secretion, and/or involved in T9SS (Hunnicutt and Mcbride, 2000; McBride and Braun, 2004; Braun et al., 2005; Lauber et al., 2018; McBride, 2019; Hennell James et al., 2021; Trivedi et al. 2022; Veith et al., 2022), were identified among DEGs (Supplementary Table S2).

Besides that, a high number of transcripts was observed among genes responsible for polysaccharides utilization. That can also elucidate the up-regulation of genes coding for T9SS, while in commensal and environmental bacteroidotal species the T9SS is characteristically used to secrete enzymes that enable the organisms to utilize complex polysaccharides as a carbon source (Veith et al., 2013; Hennell et al., 2021).

Among up-regulated genes we identified different GHs and cell surface glycan-binding lipoproteins, known to be involved into plant and algal cell wall degradation mechanisms (Giovannoni et al., 2020). That included cellulose-degrading endoglucanases, hemicellulose-degrading xylosidases, pectin degradation proteins, starch-degrading enzymes, β-glucuronyl hydrolases, SusC and SusD family cell surface glycan-binding lipoproteins (Supplementary Table S2).

Being concentrated on the components of T9SS, we identified highly active genes by transcriptome analysis of the strain HH091 co-cultured with its microalgal host. Domain guided annotation is based on conserved domains detected by STRING analysis of *Dyadobacter* sp. HH091 primary sequences against the genome of *Flavobacterium* spp. (Supplementary Table S4). Based on this analysis and previous researches (McBride and Zhu, 2013; Veith et al., 2013; Astafyeva et al., 2022), we proposed a model of T9SS including gliding motility proteins in *Dyadobacter* sp. HH091 (Figure 5). Intriguingly, genes, transcribing for the Gld motor proteins, were mostly down-regulated (*gldKLMN*), while genes coding for gliding motility-associated ABC transporter ATP-binding proteins were up-regulated. The transcriptome analysis suggests an explanation for this finding, because the symbiont possibly uses the T9SS not only for gliding motility, but

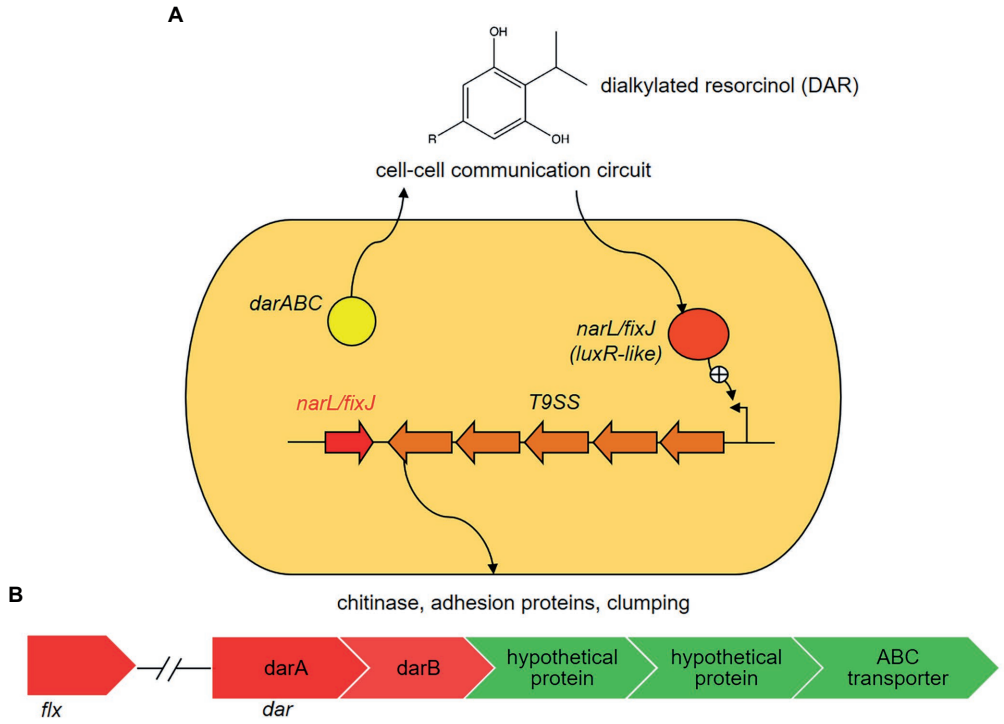

FIGURE 4
Proposed model of flexirubin or dialkylresorcinol (DARs) biosynthesis in *Dyadobacter* sp. HH091. In the proposed model, *Dyadobacter* sp. HH091 communicates *via* DARs and represents a novel quorum sensing (QS) circuit (Brameyer et al., 2015). It consists of the *dar* operon and a neighboring gene encoding a *luxR* solo (*narL/fixJ*). NarL/FixJ shares 46% identity and 47% similarity with the LuxR solo PluR of *P. luminescens* (IMG 2597490348), LuxR-type receptor serving for QS. The proposed QS circuit genes, adjacent to T9SS genes, genes affiliated with gliding motility and protein secretion, possibly upregulates several mechanisms, including T9SS, gliding motility and protein secretion. **(A)** Expression levels of DEGs involved into flexirubin biosynthesis: *dar* and *flx* clusters, and transport systems (ATP binding cassettes (ABC) and hypothetical proteins). Color key: up-regulated genes, down-regulated genes. **(B)** Expression levels of differentially expressed genes (DEGs) involved into flexirubin biosynthesis: *dar* and *flx* clusters, and transport systems (ATP binding cassettes (ABC)-transporters and hypothetical proteins).

also for the secretion of other proteins. Recent results by McBride and Saiki showed that nonmotile bacteroidotal members, such as *P. gingivalis*, *B. fragilis*, *B. thetaiotaomicron*, *B. vulgatus*, *P. distasonis*, and *Salinibacter ruber*, have homologs of genes, that have functions essential for protein secretion, but not for motility (Saiki and Konishi, 2007; McBride et al., 2009). Figure 5 represents a model of the T9SS including proteins required for gliding motility and/or protein secretion of *Dyadobacter* sp. HH091. This model includes the T9SS category (GldK, GldL, GldM, GldN, SprA, SprE, SprF, SprT, PorU, PorV), multiple PorXY-SigP signalling system components, and further Gld proteins (GldA, GldB, GldD, GldF, GldG, GldH, GldI, GldJ).

Most of the *gld* and T9SS genes are found to be adjacent to genes coding for proteins, involved into biosynthesis of glycosyltransferases, cell surface proteins, lipoprotein export proteins, as well as antibacterials, adhesion factors, microcolonization development, and EPS production. Interestingly, the up-regulated adjacent genes are also affiliated with cargo proteins of the T9SS. T9SS cargoes possess a conserved C-terminal domain (CTD) and an N-terminal signal peptide, and carry a CTD as a secretion signal, which is cleaved and replaced with anionic lipopolysaccharide by transpeptidation for extracellular anchorage to the outer membrane (OM) (Kulkarni et al., 2017; Mizgalska et al., 2021, 22; Gorasia et al., 2022). In this research, DEGs covered 42 up-regulated and 24 down-regulated genes affiliated with T9SS cargo proteins (Supplementary Table S5).

Along this detailed dataset investigation, the high activity of genes related to secretion systems and other entangled mechanisms underline the ability of *Dyadobacter* to perform the interaction with microalga and enable its dominance in many diverse environments.

Discussion

The most comprehensive and fundamental understanding of microbial metabolic pathways in a multispecies system, as well as symbiotic and competitive interactions, is required to provide scientific and theoretical bases for the interaction mechanisms between microalgae and other microorganisms. The presented results promote not only the development of effective methods for simultaneous cultivation of algae, they also encourage the increasing the efficiency of microalgal biomass growth and associated production of valuable compounds.

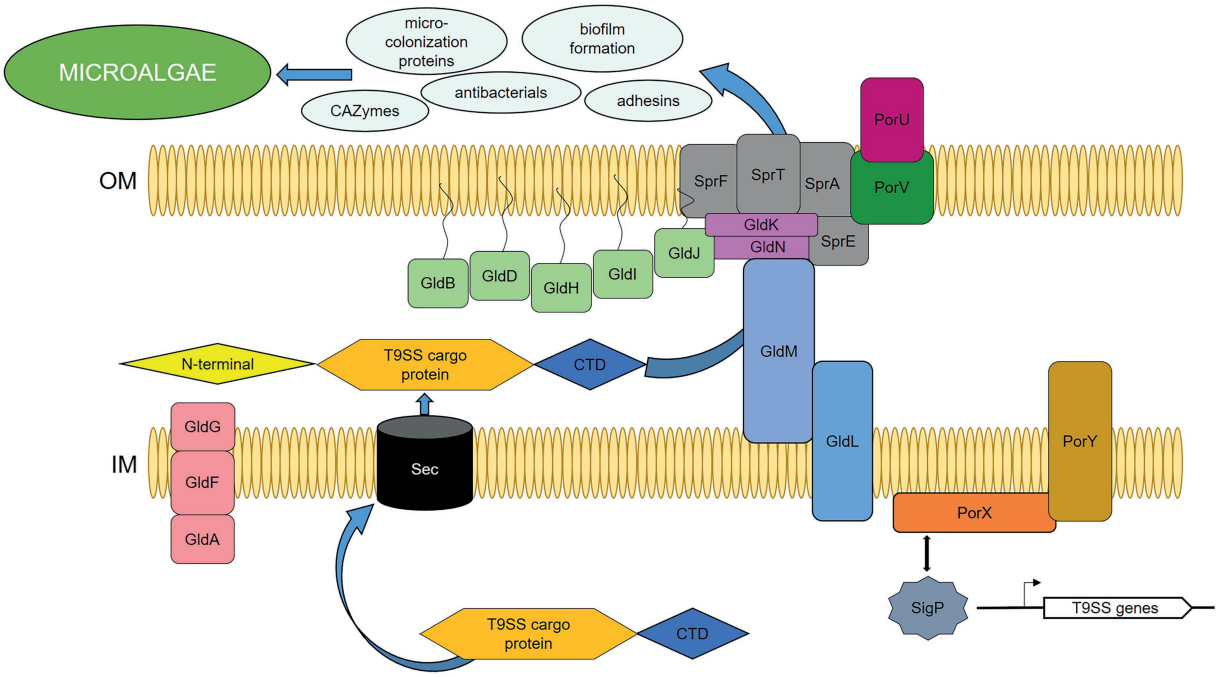

FIGURE 5
Proposed model of T9SS in *Dyadobacter* sp. HH091, serving as the secretion system of cargo-proteins. PorXY-SigP signalling system upregulates several components: T9SS category (GldK, GldL, GldM, GldN, SprA, SprE, SprF, SprT, PorU, PorV), and further Gld proteins (GldA, GldB, GldD, GldF, GldG, GldH, GldI, GldJ). C-terminal domain (CTD), N-terminal signal peptide (N-terminal), outer membrane (OM), inner membrane (IM).

Flexirubin biosynthesis conceivably involved into microalgae-bacteria interaction

Our transcriptome analysis of *Dyadobacter* sp. HH091 co-cultured with microalga *M. radians* revealed highly active genes affiliated with the cluster of flexirubin biosynthesis. This cluster includes *darA* and *darB genes*, homologs of *F. johnsoniae* UW101 (McBride et al., 2009) and *C. pinensis* (Schöner et al., 2014).

Flexirubin is a pigment consisting of a ω-(4-hydroxyphenyl)-polyene carboxylic acid chromophore, esterified with a 2,5-dialkylresorcinol (DAR), also known as novel and widespread bacterial signalling molecule (Nowak-Thompson et al., 2003; Abt et al., 2011; Schöner et al., 2014). Genes coding for the biosynthesis of these pigments are found in many bacteroidotal genomes, including *Flavobacterium psychrophilum, Flavobacterium johnsoniae* (McBride et al., 2009), *Leadbetterella byssophila (Abt et al., 2011), Chryseobacterium artocarpi* (Venil et al., 2016), *Chryseobacterium rhizoplanae* sp. nov. (Kämpfer et al., 2015), *Flavobacterium maris* sp. nov. (Romanenko et al., 2015), and *Flavobacterium tilapiae* sp. nov. (Chen et al., 2013). Homologs of *darA*, a dialkylresorcinol condensing enzyme, and *darB*, a 3-oxoacyl-[acyl-carrier-protein] synthase III protein, were previously identified using bioinformatics tools within the genome analysis of our model organism *Dyadobacter* sp. HH091 (Astafyeva et al., 2022).

Another interesting point, is that on the plant-bacteria interaction model, flexirubin also performs as free radical scavenging antioxidant protecting from the attack of free radicals (Combes and Finet, 1997; Schöner et al., 2015). The antioxidant potential *via* hydrogen donating ability of flexirubin has been shown through the assessment using different assays such as radical scavenging activities, lipid peroxide inhibition and ferrous chelating ability (Mogadem et al., 2021). Several studies show that microalgae produce reactive oxygen species (ROS) to get an advantage in the competition for resources against other algae, be a way to prevent fouling bacteria, and act as a signalling mechanism between cells (Marshall et al., 2005). Furthermore, ROS, such as superoxide (O_2^-), hydrogen peroxide (H_2O_2), and hydroxyl radical (•OH), are thought to be produced as antibacterial agents and involved in oxidation or reduction of necessary or toxic metals (Palenik et al., 1987). Former investigation of microalga *Micrasterias* spp., demonstrated that ROS are constantly generated as by-products of general metabolic cellular pathways and can be over-produced in response to stress (Darehshouri and Lütz-Meindl, 2010; Lütz-Meindl, 2016; Felhofer et al., 2021). Our results indicate, that *Dyadobacter* sp. HH091 uses flexirubin hybrid pigments to protect itself from ROS produced by microalga, which explains this interaction, making it possible for microalgal symbiont to have a tight contact with its host.

T9SS tangled in the symbiotic interactions of *Dyadobacter* with microalgae

The presence of different secretion systems suggests that *Dyadobacter* sp. HH091 and microalgae possess a signal exchange system allowing establishment and maintenance of a symbiosis that includes adhesion factors, microcolonization development, EPS production, and biofilm formation factors, which are important for the institution of a successful symbiosis. Previously, a comprehensive set of cell surface-associated proteins required for host cell invasion was described for other bacterial model organisms (Foster et al., 2014; Kusch and Engelmann, 2014; Hecker et al., 2018). All of these mechanisms express particular cocktails of factors that facilitate niche adaptation that include cell-host attachment, microcolonization and biofilm formation. Genes coding for the cell surface-associated proteins and secretion systems are mainly up-regulated in *Dyadobacter* sp. HH091, expecting them to be crucial for the microcolonization process because they establish interaction with the host. Cell-host interaction and adhesion factors, as well as microcolonization development, and biofilm formation succeed to a closely interaction and an exchange of growth-promoting substances between the symbiont and microalga.

Surface exposed proteins that are covalently or non-covalently bound to the cell surface and proteins are secreted into the extracellular matrix using different secretion mechanisms (Dreisbach et al., 2010; Ythier et al., 2012; Solis et al., 2014; Hecker et al., 2018). Secreted proteins accommodate the majority of virulence factors, enzymes required for nutrient acquisition or cell spreading, immune evasion proteins that can bypass the immune system or interfere with components of the complement system and many others. Overall, secretion systems are known to transport effector proteins into the cytosol of eukaryotic cells that allows the direct communication and modification of the host cells, additionally suppressing any activity of competitive microorganisms (Wooldridge, 2009). *Dyadobacter* sp. HH091 has many unique features together with the complex of different secretion systems, which are available to arbitrate secretion of proteins across the outer membrane, including T9SS, a complex translocon found only in some species of the Bacteroidota phylum (Lasica et al., 2017; Astafyeva et al., 2022).

A complex translocon of T9SS, including *gld* and *spr* genes, and *porXY-sigP* signalling system components, are proposed to serve as the secretion system of cargo-proteins. The T9SS cargo proteins have a conserved C-terminal domain (CTD) that enables them pass *via* T9SS and an N-terminal signal peptide that guides T9SS cargo proteins through the Sec system (Veith et al., 2013; Kulkarni et al., 2017). The CTD signal has been identified to be of two types, type A and type B (Kulkarni et al., 2017; Gorasia et al., 2020). Subsequent to the early *Dyadobacter* genome studies (Astafyeva et al., 2022), high activity of T9SS cargo proteins has been observed at this transcriptome analysis as well. It resulted in 48 up-regulated and 24 down-regulated genes, affiliated with T9SS cargo proteins of both types (Supplementary Table S5).

gldA, gldF and *gldG* encode components of an ATP-binding cassette (ABC) transporter that is required for motility and/or for the protein secretion (Agarwal et al., 1997; Hunnicutt et al., 2002). Genes encoding lipoproteins required for gliding (*gldB*, *gldD*, *gldH*, *gldI*, and *gldJ*) have also been identified (Hunnicutt and Mcbride, 2000; Hunnicutt and McBride, 2001; McBride and Braun, 2004; Braun and McBride, 2005). GldK, GldL, GldM, and GldN are each required for efficient motility and chitin utilization, indicating that Gld proteins may function in both gliding and chitin utilization (Braun et al., 2005). SprA is required for secretion of SprB and RemA and utilization of chitin (Nelson et al., 2007). In *F. johnsoniae*, SprA has been identified as the major translocon protein of T9SS, and it is hypothesized that SprA of *Dyadobacter* sp. HH091 can also have the same function (Lauber et al., 2018). Down-regulated gene coding for SprF is known to be essential for the secretion of SprB to the cell surface, but is not required for the secretion of extracellular chitinase (Rhodes et al., 2011). That also gives a hint that the symbiont possibly utilizes T9SS for the secretion of other proteins and not only involved in gliding motility.

Polysaccharide utilization is a crucial aspect of microalgae-bacteria interaction

T9SS is known to be tangled in the secretion of polysaccharide utilization proteins (Braun et al., 2005; Kharade and McBride, 2014). Previously, it was shown that the major chitinase (ChiA) in *F. johnsoniae* is fully secreted from the cell in soluble form by T9SS and is essential for chitin degradation (McBride and Zhu, 2013; Kharade and McBride, 2014; Larsbrink et al., 2016).

Based on genome and transcriptome analyses, presumably, *Dyadobacter* sp. HH091 has a complex of carbohydrate utilization domains for digestion of microalgae cell wall hemicelluloses, such as cellulose, xylan or mannan fibrils, and extensive matrix polysaccharides. Numerous carbohydrate-active enzymes predicted to encode GHs and esterases that could be involved in the degradation of microalgal cell wall hemicelluloses were highly active within transcriptome datasets (Supplementary Table S2). In addition, candidates like xylanases, β-xylosidases, arabinofuranosidases, and beta-glucuronidases involved in xylan digestion, β-mannosidases involved in mannan digestion, and candidate β-glycosidases and endoglucanase that could be involved in xyloglucan digestion were also identified.

Data obtained from transcriptome analysis allows to better understand the nature of the involvement of bacterial polysaccharide utilization genes into bacteria-algae liaison. In our previous study, we observed that the genome of given symbiont possesses a wide assortment of CAZymes predicted to breach algal cell wall (Astafyeva et al., 2022). Deep

investigation of transcriptome datasets unveiled the presence of these genes among DEGs. We observed that a significant number of genes (82) identified belonging to functions vital for carbohydrate transport and metabolism, including different GHs families, which are known to be involved into plant polysaccharides degradation (Kumar et al., 2017). For example, many up-regulated transcripts are affiliated with genes responsible for biosynthesis of GH5, GH13, GH25, GH30 and GH43 families enzymes, which function as effectors with roles in the degradation of plant polysaccharides (Rovenich et al., 2016; Snelders et al., 2018). These enzymes are known for acting as cellulose-degrading (Chang et al., 2016), starch-degrading (DeBoy et al., 2008), and catalysing hemicellulose and removing xyloses from xyloglucan (Glass et al., 2013; Bradley et al., 2022). Additionally, it was uncovered that genes affiliated with the synthesis of GH88 CAZyme, utilizing polysaccharide lyase activity to degrade pectins (Cantarel et al., 2009), was also up-regulated. Another highly active genes, coding for xylose isomerases, belong to CAZyme family GH43 that generally display specificity for arabinose-containing substrates. These gene combination reflects the competence of the symbiont to utilize starch and the complex of arabinan side-chains of pectin-rich cell walls as important nutrients (Ha et al., 2005; DeBoy et al., 2008).

Overall, our transcriptome analysis clearly showed, that bacteria can profit through the degradation of algal polysaccharides, while microalgae are being supplied with the repertoire of growth-promoting substances. The results of this research will serve as an efficient tool in further investigations of symbiotic microalgal–bacteria interactions. The remarkable benefit of a co-cultivation of microalgae and bacteria will have commercial and environmental positive impacts into the microalgal cultivation in the future.

Data availability statement

The datasets presented in this study can be found in online repositories. The names of the repository/repositories and accession number(s) can be found at: Genbank, ON237360.

Author contributions

YA and IK contributed to experimental design, lab work of metatranscriptomic, bioinformatics, and physiological analytical approaches, and writing of the research article. YA contributed to lab work of metatranscriptomic approaches and to assembly of metatranscriptomic datasets and bioinformatics approaches. MG and YA contributed to lab work of microscopic and analytical approaches. WS and IK contributed to general experimental design and writing of the research article. All authors contributed to the article and approved the submitted version.

Funding

This work was in part supported by the DAAD, and the BMBF programs MarBioTech (FKZ 031A565) and AquaHealth (FKZ 031B0945C).

Acknowledgments

The authors would like to thank the members of the "MZCH" for helpful discussion and for providing the microalgae samples. We also thank the Bioinformatics Core at the University Medical Center Hamburg-Eppendorf for excellent technical support, and help during the transcriptomic data analysis.

Conflict of interest

The authors declare that the research was conducted in the absence of any commercial or financial relationships that could be construed as a potential conflict of interest.

Publisher's note

All claims expressed in this article are solely those of the authors and do not necessarily represent those of their affiliated organizations, or those of the publisher, the editors and the reviewers. Any product that may be evaluated in this article, or claim that may be made by its manufacturer, is not guaranteed or endorsed by the publisher.

Supplementary material

The Supplementary material for this article can be found online at: https://www.frontiersin.org/articles/10.3389/fmicb.2022.1006609/full#supplementary-material

SUPPLEMENTARY FIGURE S1
Growth measurement (OD 750nm) of *Micrasterias radians* MZCH 672 in co-culture with the strain *Dyadobacter* sp. HH091. Increased growth rate (OD 750nm) can be observed in the co-culture with HH091 compared to the antibiotic-treated *M. radians* culture.

SUPPLEMENTARY FIGURE S2
Identification and validation of flexirubin pigments. Analysis of *Dyadobacter* sp. HH091, Maribacter dokdonemsis (yellow-pigment control, no flexirubin identified, Yoon et al., 2005), and Escherichia coli DH5α (negative control) strains for the presence of flexirubin pigments. Cells were photographed before treatment (I), after exposure to 50 µL of 10 M KOH (II), and after exposure to KOH followed by exposure to 42µL 12 M HCl (III). Flexirubin-positive cells were yellow at neutral pH (I and III) and orange/red under alkaline conditions (II).

SUPPLEMENTARY TABLE S2
Differentially expressed genes (DEGs) of transcriptome dataset of *Dyadobacter* sp. HH091 co-cultured with *M. radians*.

SUPPLEMENTARY TABLE S5
Differently expressed genes (DEGs) coding for the T9SS cargo proteins.

References

Abt, B., Teshima, H., Lucas, S., Lapidus, A., Del Rio, T. G., Nolan, M., et al. (2011). Complete genome sequence of Leadbetterella byssophila type strain (4M15). *Stand. Genomic Sci.* 4, 2–12. doi: 10.4056/sigs.1413518

Agarwal, S., Hunnicutt, D. W., and McBride, M. J. (1997). Cloning and characterization of the Flavobacterium johnsoniae (Cytophaga johnsonae) gliding motility gene, gldA. *Proc. Natl. Acad. Sci. U. S. A.* 94, 12139–12144. doi: 10.1073/pnas.94.22.12139

Andersen, R. A. (2005). *Algal Culturing Techniques*. College Park, MD: Phycological Society of America.

Astafyeva, Y., Gurschke, M., Qi, M., Bergmann, L., Indenbirken, D., de Grahl, I., et al. (2022). Microalgae and bacteria interaction—Evidence for division of diligence in the alga microbiota. *Microbiol. Spectr.* (in press).

Bradley, E. L., Ökmen, B., Doehlemann, G., Henrissat, B., Bradshaw, R. E., and Mesarich, C. H. (2022). Secreted glycoside hydrolase proteins as effectors and invasion patterns of plant-associated fungi and oomycetes. *Front. Plant Sci.* 13:853106. doi: 10.3389/fpls.2022.853106

Brameyer, S., Kresovic, D., Bode, H. B., and Heermann, R. (2015). Dialkylresorcinols as bacterial signalling molecules. *Proc. Natl. Acad. Sci. U. S. A.* 112, 572–577. doi: 10.1073/pnas.1417685112

Braun, T. F., Khubbar, M. K., Saffarini, D. A., and McBride, M. J. (2005). Flavobacterium johnsoniae gliding motility genes identified by mariner mutagenesis. *J. Bacteriol.* 187, 6943–6952. doi: 10.1128/JB.187.20.6943-6952.2005

Braun, T. F., and McBride, M. J. (2005). Flavobacterium johnsoniae GldJ is a lipoprotein that is required for gliding motility. *J. Bacteriol.* 187, 2628–2637. doi: 10.1128/JB.187.8.2628-2637.2005

Cantarel, B. L., Coutinho, P. M., Rancurel, C., Bernard, T., Lombard, V., and Henrissat, B. (2009). The carbohydrate-active EnZymes database (CAZy): an expert resource for Glycogenomics. *Nucleic Acids Res.* 37, D233–D238. doi: 10.1093/nar/gkn663

Chang, H.-X., Yendrek, C. R., Caetano-Anolles, G., and Hartman, G. L. (2016). Genomic characterization of plant cell wall degrading enzymes and in silico analysis of xylanses and polygalacturonases of fusarium virguliforme. *BMC Microbiol.* 16:147. doi: 10.1186/s12866-016-0761-0

Chen, W.-M., Huang, W.-C., Young, C.-C., and Sheu, S.-Y. (2013). Flavobacterium tilapiae sp. nov., isolated from a freshwater pond, and emended descriptions of Flavobacterium defluvii and Flavobacterium johnsoniae. *Int. J. Syst. Evol. Microbiol.* 63, 827–834. doi: 10.1099/ijs.0.041178-0

Cirri, E., and Pohnert, G. (2019). Algae–bacteria interactions that balance the planktonic microbiome. *New Phytol.* 223, 100–106. doi: 10.1111/nph.15765

Combes, S., and Finet, J. P. (1997). A simple synthesis of the natural 2,5-Dialkylresorcinol free radical scavenger antioxidant: Resorstatin. *Synth. Commun.* 27, 3769–3778. doi: 10.1080/00397919708007301

Darehshouri, A., and Lütz-Meindl, U. (2010). H_2O_2 localization in the green alga Micrasterias after salt and osmotic stress by TEM-coupled electron energy loss spectroscopy. *Protoplasma* 239, 49–56. doi: 10.1007/s00709-009-0081-4

Davies, D. G., Parsek, M. R., Pearson, J. P., Iglewski, B. H., Costerton, J. W., and Greenberg, E. P. (1998). The involvement of cell-to-cell signals in the development of a bacterial biofilm. *Science* 280, 295–298. doi: 10.1126/science.280.5361.295

DeBoy, R. T., Mongodin, E. F., Fouts, D. E., Tailford, L. E., Khouri, H., Emerson, J. B., et al. (2008). Insights into plant cell wall degradation from the genome sequence of the soil bacterium Cellvibrio japonicus. *J. Bacteriol.* 190, 5455–5463. doi: 10.1128/JB.01701-07

Dreisbach, A., Hempel, K., Buist, G., Hecker, M., Becher, D., and van Dijl, J. M. (2010). Profiling the surfacome of Staphylococcus aureus. *Proteomics* 10, 3082–3096. doi: 10.1002/pmic.201000062

Droop, M. R. (1967). A procedure for routine purification of algal cultures with antibiotics. *Br. Phycol. Bull.* 3, 295–297. doi: 10.1080/00071616700650171

Felhofer, M., Mayr, K., Lütz-Meindl, U., and Gierlinger, N. (2021). Raman imaging of Micrasterias: new insights into shape formation. *Protoplasma* 258, 1323–1334. doi: 10.1007/s00709-021-01685-3

Foster, T. J., Geoghegan, J. A., Ganesh, V. K., and Höök, M. (2014). Adhesion, invasion and evasion: the many functions of the surface proteins of Staphylococcus aureus. *Nat. Rev. Microbiol.* 12, 49–62. doi: 10.1038/nrmicro3161

Gorasia, D. G., Lunar Silva, I., Butler, C. A., Chabalier, M., Doan, T., Cascales, E., et al. (2022). Protein Interactome analysis of the type IX secretion system identifies PorW as the missing link between the PorK/N ring complex and the Sov Translocon. *Microbiol. Spectr.* 10:e0160221. doi: 10.1128/spectrum.01602-21

Giovannoni, M., Gramegna, G., Benedetti, M., and Mattei, B. (2020). Industrial use of Cell Wall degrading enzymes: the fine line between production strategy and economic feasibility. *Front. Bioeng. Biotechnol.* 8:356. doi: 10.3389/fbioe.2020.00356

Glass, N. L., Schmoll, M., Cate, J. H. D., and Coradetti, S. (2013). Plant cell wall deconstruction by ascomycete fungi. *Annu. Rev. Microbiol.* 67, 477–498. doi: 10.1146/annurev-micro-092611-150044

Gorasia, D. G., Veith, P. D., and Reynolds, E. C. (2020). The type IX secretion system: advances in structure, function and organisation. *Microorganisms* 8:1173. doi: 10.3390/microorganisms8081173

Ha, M. A., Viëtor, R. J., Jardine, G. D., Apperley, D. C., and Jarvis, M. C. (2005). Conformation and mobility of the arabinan and galactan side-chains of pectin. *Phytochemistry* 66, 1817–1824. doi: 10.1016/j.phytochem.2005.06.001

Hecker, M., Mäder, U., and Völker, U. (2018). From the genome sequence via the proteome to cell physiology—Pathoproteomics and pathophysiology of Staphylococcus aureus. *Int. J. Med. Microbiol. IJMM* 308, 545–557. doi: 10.1016/j.ijmm.2018.01.002

Hennell, J. R., Deme, J. C., Kjær, A., Alcock, F., Silale, A., Lauber, F., et al. (2021). Structure and mechanism of the proton-driven motor that powers type 9 secretion and gliding motility. *Nat. Microbiol.* 6, 221–233. doi: 10.1038/s41564-020-00823-6

Holt, R. A. (1993). "Bacterial cold-water disease," in *Bacterial Diseases of Fish*, (Blackwell Sci. Publ.), 3–22.

Hunnicutt, D. W., Kempf, M. J., and McBride, M. J. (2002). Mutations in Flavobacterium johnsoniae gldF and gldG disrupt gliding motility and interfere with membrane localization of GldA. *J. Bacteriol.* 184, 2370–2378. doi: 10.1128/JB.184.9.2370-2378.2002

Hunnicutt, D. W., and Mcbride, M. J. (2000). Cloning and characterization of the Flavobacterium johnsoniae gliding-motility genes gldB and gldC. *J. Bacteriol.* 182, 911–918. doi: 10.1128/JB.182.4.911-918.2000

Hunnicutt, D. W., and McBride, M. J. (2001). Cloning and characterization of the Flavobacterium johnsoniae gliding motility genes gldD and gldE. *J. Bacteriol.* 183, 4167–4175. doi: 10.1128/JB.183.14.4167-4175.2001

Kämpfer, P., McInroy, J. A., and Glaeser, S. P. (2015). Chryseobacterium rhizoplanae sp. nov., isolated from the rhizoplane environment. *Antonie Van Leeuwenhoek* 107, 533–538. doi: 10.1007/s10482-014-0349-3

Karpishin, T. (2018). Reducing tissue autofluorescence. *Genet. Eng. Biotechnol. News* 38, 16–17. doi: 10.1089/gen.38.05.05

Kharade, S. S., and McBride, M. J. (2014). Flavobacterium johnsoniae chitinase ChiA is required for chitin utilization and is secreted by the type IX secretion system. *J. Bacteriol.* 196, 961–970. doi: 10.1128/JB.01170-13

Kim, D., Langmead, B., and Salzberg, S. L. (2015). HISAT: a fast spliced aligner with low memory requirements. *Nat. Methods* 12, 357–360. doi: 10.1038/nmeth.3317

Kim, D., Pertea, G., Trapnell, C., Pimentel, H., Kelley, R., and Salzberg, S. L. (2013). TopHat2: accurate alignment of transcriptomes in the presence of insertions, deletions and gene fusions. *Genome Biol.* 14:R36. doi: 10.1186/gb-2013-14-4-r36

Krohn-Molt, I., Alawi, M., Förstner, K. U., Wiegandt, A., Burkhardt, L., Indenbirken, D., et al. (2017). Insights into microalga and bacteria interactions of selected Phycosphere biofilms using metagenomic, transcriptomic, and proteomic approaches. *Front. Microbiol.* 8:1941. doi: 10.3389/fmicb.2017.01941

Krohn, I., Wemheuer, B., Alawi, M., Poehlein, A., Güllert, S., Schmeisser, C., et al. (2013). Metagenome survey of a multispecies and alga-associated biofilm revealed key elements of bacterial-algal interactions in Photobioreactors. *Appl. Environ. Microbiol.* 79, 6196–6206. doi: 10.1128/AEM.01641-13

Krueger, F. (2012). Trim galore: a wrapper tool around Cutadapt and FastQC to consistently apply quality and adapter trimming to FastQ files, with some extra functionality for MspI-digested RRBS-type (reduced representation Bisufite-Seq) libraries. Available at: http://www.bioinformatics.babraham.ac.uk/projects/trim_galore/

Kulkarni, S. S., Zhu, Y., Brendel, C. J., and McBride, M. J. (2017). Diverse C-terminal sequences involved in Flavobacterium johnsoniae protein secretion. *J. Bacteriol.* 199:e00884-16. doi: 10.1128/JB.00884-16

Kumar, A., Pandey, V., Singh, M., Pandey, D., Saharan, M. S., and Marla, S. S. (2017). Draft genome sequence of Karnal bunt pathogen (Tilletia indica) of wheat provides insights into the pathogenic mechanisms of quarantined fungus. *PLoS One* 12:e0171323. doi: 10.1371/journal.pone.0171323

Kusch, H., and Engelmann, S. (2014). Secrets of the secretome in Staphylococcus aureus. *Int. J. Med. Microbiol.* 304, 133–141. doi: 10.1016/j.ijmm.2013.11.005

Larsbrink, J., Zhu, Y., Kharade, S. S., Kwiatkowski, K. J., Eijsink, V. G., Koropatkin, N. M., et al. (2016). A polysaccharide utilization locus from Flavobacterium johnsoniae enables conversion of recalcitrant chitin. *Biotechnol. Biofuels* 9:260. doi: 10.1186/s13068-016-0674-z

Lasica, A. M., Ksiazek, M., Madej, M., and Potempa, J. (2017). The type IX secretion system (T9SS): highlights and recent insights into its structure and function. *Front. Cell. Infect. Microbiol.* 7:215. doi: 10.3389/fcimb.2017.00215

Lauber, F., Deme, J. C., Lea, S. M., and Berks, B. C. (2018). Type 9 secretion system structures reveal a new protein transport mechanism. *Nature* 564, 77–82. doi: 10.1038/s41586-018-0693-y

Lee, H. G., Shin, S. Y., Jin, L., Yoo, C., Srivastava, A., La, H. J., et al. (2015). Establishment and maintenance of an axenic culture of Ettlia sp. using a species-specific approach. *Biotechnol. Bioprocess Eng.* 20, 1056–1063. doi: 10.1007/s12257-015-0289-4

Levasseur, A., Drula, E., Lombard, V., Coutinho, P. M., and Henrissat, B. (2013). Expansion of the enzymatic repertoire of the CAZy database to integrate auxiliary redox enzymes. *Biotechnol. Biofuels* 6:41. doi: 10.1186/1754-6834-6-41

Luo, H., and Moran, M. A. (2014). Evolutionary ecology of the marine Roseobacter clade. *Microbiol. Mol. Biol.Rev. MMBR* 78, 573–587. doi: 10.1128/MMBR.00020-14

Lütz-Meindl, U. (2016). Micrasterias as a model system in plant cell biology. *Front. Plant Sci.* 7:999. doi: 10.3389/fpls.2016.00999

Marshall, J.-A., de Salas, M., Oda, T., and Hallegraeff, G. (2005). Superoxide production by marine microalgae. *Mar. Biol.* 147, 533–540. doi: 10.1007/s00227-005-1596-7

McBride, M. J., and Braun, T. F. (2004). GldI is a lipoprotein that is required for Flavobacterium johnsoniae gliding motility and chitin utilization. *J. Bacteriol.* 186, 2295–2302. doi: 10.1128/JB.186.8.2295-2302.2004

McBride, M. J., Xie, G., Martens, E. C., Lapidus, A., Henrissat, B., Rhodes, R. G., et al. (2009). Novel features of the polysaccharide-digesting gliding bacterium Flavobacterium johnsoniae as revealed by genome sequence analysis. *Appl. Environ. Microbiol.* 75, 6864–6875. doi: 10.1128/AEM.01495-09

McBride, M. J., and Zhu, Y. (2013). Gliding motility and Por secretion system genes are widespread among members of the phylum Bacteroidetes. *J. Bacteriol.* 195, 270–278. doi: 10.1128/JB.01962-12

McBride, M. J. (2019). Bacteroidetes gliding motility and the type IX secretion system. *Microbiol. Spectr.* 7:7.1.15. doi: 10.1128/microbiolspec.PSIB-0002-2018

McClure, R., Balasubramanian, D., Sun, Y., Bobrovskyy, M., Sumby, P., Genco, C. A., et al. (2013). Computational analysis of bacterial RNA-Seq data. *Nucleic Acids Res.* 41:e140. doi: 10.1093/nar/gkt444

Mizgalska, D., Goulas, T., Rodríguez-Banqueri, A., Veillard, F., Madej, M., Małecka, E., et al. (2021). Intermolecular latency regulates the essential C-terminal signal peptidase and sortase of the Porphyromonas gingivalis type-IX secretion system. *Proc. Natl. Acad. Sci. U. S. A.* 118:e2103573118. doi: 10.1073/pnas.2103573118

Mogadem, A., Almamary, M. A., Mahat, N. A., Jemon, K., Ahmad, W. A., and Ali, I. (2021). Antioxidant activity evaluation of FlexirubinType pigment from Chryseobacterium artocarpi CECT 8497 and related docking study. *Molecules* 26:979. doi: 10.3390/molecules26040979

Mouget, J.-L., Dakhama, A., Lavoie, M. C., and de la Noüe, J. (1995). Algal growth enhancement by bacteria: is consumption of photosynthetic oxygen involved? *FEMS Microbiol. Ecol.* 18, 35–43. doi: 10.1016/0168-6496(95)00038-C

Mullan, K. A., Bramberger, L. M., Munday, P. R., Goncalves, G., Revote, J., Mifsud, N. A., et al. (2021). ggVolcanoR: a shiny app for customizable visualization of differential expression datasets. *Comput. Struct. Biotechnol. J.* 19, 5735–5740. doi: 10.1016/j.csbj.2021.10.020

Nelson, S. S., Glocka, P. P., Agarwal, S., Grimm, D. P., and McBride, M. J. (2007). Flavobacterium johnsoniae SprA is a cell surface protein involved in gliding motility. *J. Bacteriol.* 189, 7145–7150. doi: 10.1128/JB.00892-07

Nowak-Thompson, B., Hammer, P. E., Hill, D. S., Stafford, J., Torkewitz, N., Gaffney, T. D., et al. (2003). 2,5-Dialkylresorcinol biosynthesis in Pseudomonas aurantiaca: novel head-to-head condensation of two fatty acid-derived precursors. *J. Bacteriol.* 185, 860–869. doi: 10.1128/JB.185.3.860-869.2003

Palenik, B., Zafiriou, O. C., and Morel, F. M. M. (1987). Hydrogen peroxide production by a marine phytoplankter1. *Limnol. Oceanogr.* 32, 1365–1369. doi: 10.4319/lo.1987.32.6.1365

Ramanan, R., Kim, B.-H., Cho, D.-H., Oh, H.-M., and Kim, H.-S. (2016). Algae–bacteria interactions: evolution, ecology and emerging applications. *Biotechnol. Adv.* 34, 14–29. doi: 10.1016/j.biotechadv.2015.12.003

Reasoner, D. J., and Geldreich, E. E. (1985). A new medium for the enumeration and subculture of bacteria from potable water. *Appl. Environ. Microbiol.* 49, 1–7. doi: 10.1128/aem.49.1.1-7.1985

Rhodes, R. G., Samarasam, M. N., Van Groll, E. J., and McBride, M. J. (2011). Mutations in Flavobacterium johnsoniae sprE result in defects in gliding motility and protein secretion. *J. Bacteriol.* 193, 5322–5327. doi: 10.1128/JB.05480-11

Romanenko, L. A., Tanaka, N., Svetashev, V. I., Kurilenko, V. V., and Mikhailov, V. V. (2015). Flavobacterium maris sp. nov. isolated from shallow sediments of the sea of Japan. *Arch. Microbiol.* 197, 941–947. doi: 10.1007/s00203-015-1128-x

Rovenich, H., Zuccaro, A., and Thomma, B. P. H. J. (2016). Convergent evolution of filamentous microbes towards evasion of glycan-triggered immunity. *New Phytol.* 212, 896–901. doi: 10.1111/nph.14064

Saiki, K., and Konishi, K. (2007). Identification of a Porphyromonas gingivalis novel protein Sov required for the secretion of Gingipains. *Microbiol. Immunol.* 51, 483–491. doi: 10.1111/j.1348-0421.2007.tb03936.x

Sambrook, J. F., and Russell, D. (2001). *Molecular Cloning: A Laboratory Manual (3-Volume Set). Vol. 1. 3rd Edn*. New York: Cold Spring Harbor Laboratory Press.

Schöner, T. A., Fuchs, S. W., Schönau, C., and Bode, H. B. (2014). Initiation of the flexirubin biosynthesis in Chitinophaga pinensis. *Microb. Biotechnol.* 7, 232–241. doi: 10.1111/1751-7915.12110

Schöner, T. A., Kresovic, D., and Bode, H. B. (2015). Biosynthesis and function of bacterial dialkylresorcinol compounds. *Appl. Microbiol. Biotechnol.* 99, 8323–8328. doi: 10.1007/s00253-015-6905-6

Shen, Y., and Benner, R. (2018). Mixing it up in the ocean carbon cycle and the removal of refractory dissolved organic carbon. *Sci. Rep.* 8:2542. doi: 10.1038/s41598-018-20857-5

Snelders, N. C., Kettles, G. J., Rudd, J. J., and Thomma, B. P. H. J. (2018). Plant pathogen effector proteins as manipulators of host microbiomes? *Mol. Plant Pathol.* 19, 257–259. doi: 10.1111/mpp.12628

Solis, N., Parker, B. L., Kwong, S. M., Robinson, G., Firth, N., and Cordwell, S. J. (2014). Staphylococcus aureus surface proteins involved in adaptation to oxacillin identified using a novel cell shaving approach. *J. Proteome Res.* 13, 2954–2972. doi: 10.1021/pr500107p

Stein, J. R. (1973). *Handbook of Phycological Methods: Culture Methods and Growth Measurements*. Cambridge: Cambridge University Press), 56–60.

Szklarczyk, D., Gable, A. L., Nastou, K. C., Lyon, D., Kirsch, R., Pyysalo, S., et al. (2021). The STRING database in 2021: customizable protein-protein networks, and functional characterization of user-uploaded gene/measurement sets. *Nucleic Acids Res.* 49, D605–D612. doi: 10.1093/nar/gkaa1074

Trapnell, C., Roberts, A., Goff, L., Pertea, G., Kim, D., Kelley, D. R., et al. (2012). Differential gene and transcript expression analysis of RNA-seq experiments with TopHat and cufflinks. *Nat. Protoc.* 7, 562–578. doi: 10.1038/nprot.2012.016

Trivedi, A., Gosai, J., Nakane, D., and Shrivastava, A. (2022). Design principles of the rotary type 9 secretion system. *Front. Microbiol.* 13:845563. doi: 10.3389/fmicb.2022.845563

Veith, P. D., Nor Muhammad, N. A., Dashper, S. G., Likić, V. A., Gorasia, D. G., Chen, D., et al. (2013). Protein substrates of a novel secretion system are numerous in the Bacteroidetes phylum and have in common a cleavable C-terminal secretion signal, extensive post-translational modification, and cell-surface attachment. *J. Proteome Res.* 12, 4449–4461. doi: 10.1021/pr400487b

Veith, P. D., Glew, M. D., Gorasia, D. G., Cascales, E., and Reynolds, E. C. (2022). The type IX secretion system and its role in bacterial function and pathogenesis. *J. Dent. Res.* 101, 374–383. doi: 10.1177/00220345211051599

Venil, C. K., Sathishkumar, P., Malathi, M., Usha, R., Jayakumar, R., Yusoff, A. R. M., et al. (2016). Synthesis of flexirubin-mediated silver nanoparticles using Chryseobacterium artocarpi CECT 8497 and investigation of its anticancer activity. *Mater. Sci. Eng. C* 59, 228–234. doi: 10.1016/j.msec.2015.10.019

Whitman, T., Neurath, R., Perera, A., Chu-Jacoby, I., Ning, D., Zhou, J., et al. (2018). Microbial community assembly differs across minerals in a rhizosphere microcosm. *Environ. Microbiol.* 20, 4444–4460. doi: 10.1111/1462-2920.14366

Wooldridge, K. (ed.) (2009). *Bacterial Secreted Proteins*. Centre for Biomolecular Sciences, University of Nottingham, UK: Caister Academic Press.

Yoon, J. H., Kang, S. J., Lee, S. Y., Lee, C. H., and Oh, T. K. (2005). Maribacter dokdonensis sp. nov., isolated from sea water off a Korean island, Dokdo. *Int. J. Syst. Evol. Microbiol.* 55, 2051–2055. doi: 10.1099/ijs.0.63777-0

Ythier, M., Resch, G., Waridel, P., Panchaud, A., Gfeller, A., Majcherczyk, P., et al. (2012). Proteomic and transcriptomic profiling of Staphylococcus aureus surface LPXTG-proteins: correlation with agr genotypes and adherence phenotypes. *Mol. Cell. Proteomics MCP* 11, 1123–1139. doi: 10.1074/mcp.M111.014191

frontiers | Frontiers in Microbiology

TYPE Original Research
PUBLISHED 21 October 2022
DOI 10.3389/fmicb.2022.965968

Check for updates

OPEN ACCESS

EDITED BY
Tarun Belwal,
Zhejiang University,
China

REVIEWED BY
Weiwen Zhang,
Tianjin University,
China
Jianping Yu,
National Renewable Energy Laboratory (DOE), United States
Chunpeng Wan,
Jiangxi Agricultural University, China

*CORRESPONDENCE
Maurycy Daroch
m.daroch@pkusz.edu.cn

†PRESENT ADDRESS
Sadaf Riaz,
Department of Neuroscience,
University of Connecticut School of Medicine, Farmington, CT, United States

SPECIALTY SECTION
This article was submitted to Microbiotechnology, a section of the journal Frontiers in Microbiology

RECEIVED 10 June 2022
ACCEPTED 23 September 2022
PUBLISHED 21 October 2022

CITATION
Cui Y, Rasul F, Jiang Y, Zhong Y, Zhang S, Boruta T, Riaz S and Daroch M (2022) Construction of an artificial consortium of *Escherichia coli* and cyanobacteria for clean indirect production of volatile platform hydrocarbons from CO_2. *Front. Microbiol.* 13:965968. doi: 10.3389/fmicb.2022.965968

COPYRIGHT
© 2022 Cui, Rasul, Jiang, Zhong, Zhang, Boruta, Riaz and Daroch. This is an open-access article distributed under the terms of the Creative Commons Attribution License (CC BY). The use, distribution or reproduction in other forums is permitted, provided the original author(s) and the copyright owner(s) are credited and that the original publication in this journal is cited, in accordance with accepted academic practice. No use, distribution or reproduction is permitted which does not comply with these terms.

Construction of an artificial consortium of *Escherichia coli* and cyanobacteria for clean indirect production of volatile platform hydrocarbons from CO_2

Yixuan Cui[1], Faiz Rasul[1], Ying Jiang[1], Yuqing Zhong[1], Shanfa Zhang[1], Tomasz Boruta[2], Sadaf Riaz[1†] and Maurycy Daroch[1*]

[1]School of Environment and Energy, Peking University Shenzhen Graduate School, Shenzhen, China, [2]Department of Bioprocess Engineering, Faculty of Process and Environmental Engineering, Lodz University of Technology, Lodz, Poland

Ethylene and isoprene are essential platform chemicals necessary to produce polymers and materials. However, their current production methods based on fossil fuels are not very efficient and result in significant environmental pollution. For a successful transition more sustainable economic model, producing these key polymeric building blocks from renewable and sustainable resources such as biomass or CO_2 is essential. Here, inspired by the symbiotic relationship of natural microbial communities, artificial consortia composed of *E. coli* strains producing volatile platform chemicals: ethylene and isoprene and two strains of cyanobacteria phototrophically synthesizing and exporting sucrose to feed these heterotrophs were developed. Disaccharide produced by transgenic cyanobacteria was used as a carbon and electron shuttle between the two community components. The *E. coli cscB* gene responsible for sucrose transport was inserted into two cyanobacterial strains, *Thermosynechococcus elongatus* PKUAC-SCTE542 and *Synechococcus elongatus* PCC7942, resulting in a maximal sucrose yield of 0.14 and 0.07 g/L, respectively. These organisms were co-cultured with *E. coli* BL21 expressing ethylene-forming enzyme or isoprene synthase and successfully synthesized volatile hydrocarbons. Productivity parameters of these co-cultures were higher than respective transgenic cultures of *E. coli* grown individually at similar sucrose concentrations, highlighting the positive impact of the artificial consortia on the production of these platform chemicals.

KEYWORDS

ethylene, isoprene, cyanobacteria, co-culture, sucrose, microbial community

Introduction

Platform chemicals, defined as essential chemical building blocks serving as precursors to numerous secondary chemicals and materials are essential components of our economy. Ethylene and isoprene are platform chemicals with conjugated double bonds and the primary substrates for the production of many polymers such as synthetic rubber and resins (Easterbrook and Allen, 1987; Deepak et al., 2019). With the advance of industrialization, the demand for basic industrial materials is rising. At present, these two substances are mainly produced from petroleum raw materials, such as natural gas, naphtha, diesel, and heavy oil, which are obtained by petroleum fractionation and petroleum cracking (Valenzuela et al., 2008; Zhang et al., 2020). These methods result in significant carbon dioxide emissions and environmental polluting by-products. Therefore, it is a hot research field to seek a cleaner production method. With biosynthesis technology, the production of these by-products is avoided, and the harm to the environment is reduced. Studies have shown that the two volatile platform hydrocarbons, ethylene, and isoprene, can be produced through biological systems using their corresponding synthases and associated, native biosynthetic pathways. Isoprene in *E. coli* can be synthesized from dimethylallyl pyrophosphate (DMAPP) precursor generated by a native methylerythritol 4-phosphate (MEP) pathway using heterologously expressed isoprene synthase (IspS; Kuzuyama, 2002). Ethylene can, in principle, be synthesized in *E. coli* from methionine by NADH: Fe(II)EDTA oxidoreductase or from α-ketoglutaric acid (AKG) by the ethylene-forming enzyme (Efe; Kazuhiro et al., 1991). The first pathway requires ammonia limitation (C/N = 20) conditions, which is not suitable for the growth of *E. coli* or cyanobacteria; therefore, the pathway utilizing Efe is more optimal (Ishihara et al., 1995). Both precursors, DMAPP and AKG, are readily available in *E. coli,* making it a suitable cell factory for producing these metabolites.

Inspired by the symbiotic relationship of microbial communities in nature (Beliaev et al., 2014), researchers designed and simulated the symbiosis system with artificial substance exchange pathways (Brenner et al., 2008) and gradually developed synthetic consortia between the same microbial species (such as co-culture of multiple *E. coli* strains; Zhang et al., 2022), heterotrophic microbial consortia (such as co-culture of *E. coli* and fungi; Minty et al., 2012), or autotrophic-heterotrophic consortia (such as co-culture of cyanobacteria and heterotrophic *Streptomyces* or *E. coli*; Li et al., 2017; Weiss et al., 2017) and used them in pollution abatement and product biosynthesis (Hays et al., 2016). Studies show that this method avoids the frequent issues caused by some microbial contamination and other undesirable factors associated with cultivating a single strain in large volumes (Gavrilescu and Chisti, 2005; Venkata Mohan and Venkateswar Reddy, 2013). In this way, a variety of functional genes are expressed in different strains and work separately to avoid interaction between gene expression, which strengthens the core characteristics of each microbial strain, reducing the metabolic load of each bacterial chassis and is suitable for completing multiple complex tasks at the same time (Song et al., 2014; Ma et al., 2019).

Among the bioproduction-oriented synthetic consortia that have been designed and characterized so far (reviewed by Diender et al., 2021; Mittermeier et al., 2022), the co-cultures involving a model photosynthetic bacterium *Synechococcus elongatus* are primary examples of CO_2-utilizing microbial platforms. Since the foundational work performed a decade ago (Ducat et al., 2012), the concept has been progressively developed. Sucrose-secreting *S. elongatus* was used in co-culture to support the growth of the several accompanying heterotrophic species (*Bacillus subtilis*, *Saccharomyces cerevisiae*, or *Escherichia coli*; Hays et al., 2016); and used for the production of an industrially relevant bioplastic polyhydroxybutyrate (PHB) in conjunction with *Halomonas boliviensis* (Weiss et al., 2017). Another polyhydroxyalkanoates production study explored the coupling of sucrose exporting *S. elongatus* with *Pseudomonas putida* (Löwe et al., 2017). More recently, the possibility of light-driven 3-hydroxypropionic acid production by the co-culture system composed of *S. elongatus* and *E. coli* was demonstrated (Hays et al., 2016). The same pair of organisms with different genetic modifications has been recently used to produce isoprene (Liu et al., 2021). All these studies shared the idea of designing the synthetic co-culture system capable of converting the photosynthetically produced sugar into high-value target molecules of biotechnological importance (Weiss et al., 2017). Furthermore, the stability of light-driven co-cultures can be improved by using hydrogel systems to ensure the space-efficient structure of the consortium (Gao et al., 2022). As the consortia-related methodological toolbox continues to expand (Ma et al., 2022; Singh and Ducat, 2022), the importance of the "phototroph + heterotroph" designs based on the conversion of CO_2 to organic chemicals can be expected to grow.

Cyanobacteria are photosynthetic autotrophs with higher carbon fixation efficiency than plants (Wang et al., 2008). With a relatively simple genetic background, easy cultivation, and fast growth rates (Cheali et al., 2016), they are suitable microbial cell factories that avoid competition for land with food cultivation (Quintana et al., 2011). With the discovery of natural transformation (Kondo et al., 1994), electrotransformation (Thiel and Poo, 1989), and conjugation (Thiel and Peter Wolk, 1987) methods of plasmid uptake by the cyanobacterial cells, the existing barriers to importing target genes to cyanobacteria were eliminated, and the research on transgenic cyanobacteria is gradually increased. At present, research on cyanobacterial cell factories has covered many fields, such as the synthesis of high-value products and renewable compounds, carbon or nitrogen fixation, etc. (Choi et al., 2020; Tarawat et al., 2020; Mukherjee et al., 2021; Watanabe and Horiike, 2021). Cyanobacteria can synthesize sucrose, storage, and osmo-protective compound using triose phosphates, ATP, and electron equivalents generated during photosynthesis and native enzymes, including sucrose synthase (SPS; Huber and Huber, 1992). Although sucrose is not as common carbon

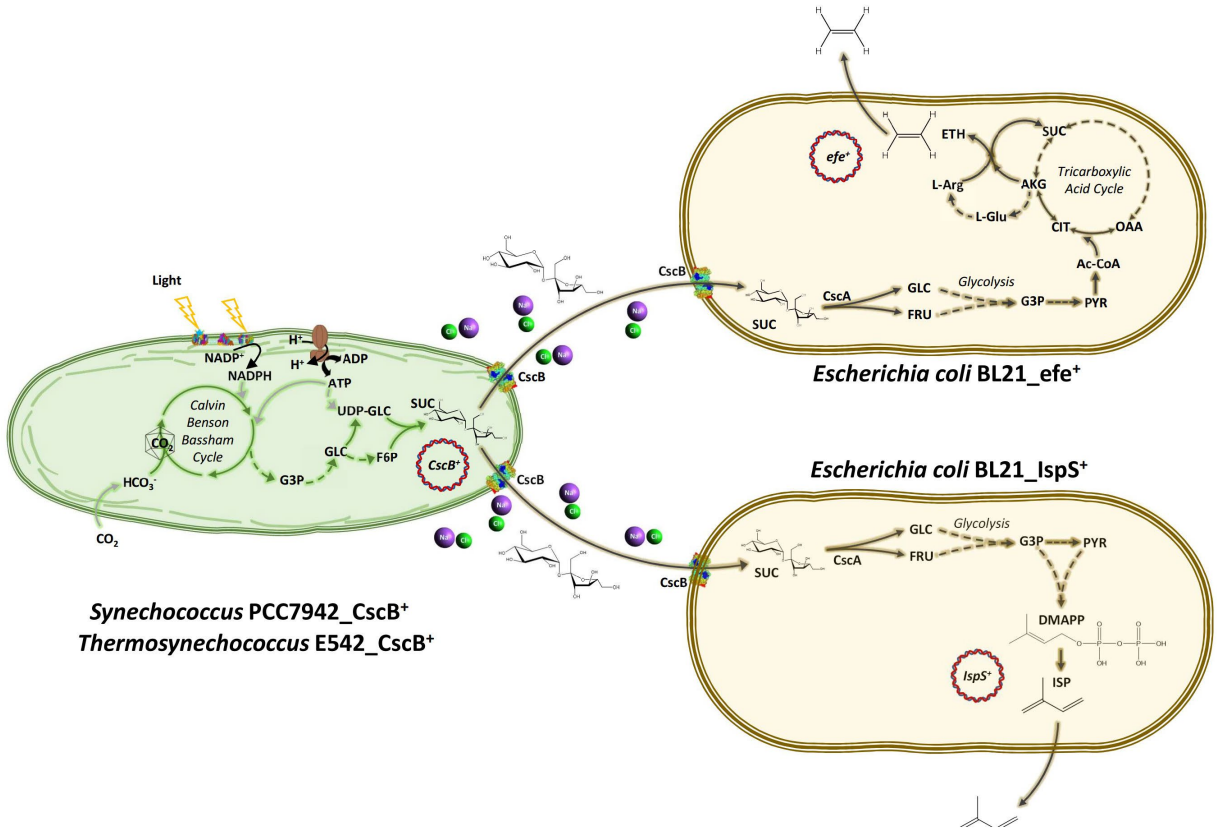

FIGURE 1
Schematic diagram of the artificial consortium system used in this study. *Thermosynechococcus* E542 and *Synechococcus* PCC7942 engineered to secrete sucrose under osmotic stress to support the growth of transgenic *Escherichia coli* strains capable of the synthesis of ethylene or isoprene. CO_2, carbon dioxide; HCO_3^-, bicarbonate; G3P, glyceraldehyde 3-phosphate; GLC, glucose; FRU, fructose; PYR, pyruvate; UDP-Glc, uridine diphosphate glucose; F6P, fructose 6-phosphate; SUC, sucrose; Ac-CoA, acetyl CoA; CIT, citrate; AKG, alpha ketoglutarate; SUC, succinate; OAA, oxaloacetate; L-Glu, glutamate; L-Arg, L-Arginine; ETH, ethylene; DMAPP, dimethylallyl pyrophosphate; ISP, isoprene; ATP, adenosine triphosphate; ADP, adenosine diphosphate; $NADP^+$, oxidized nicotinamide adenine dinucleotide phosphate; NADPH, reduced nicotinamide adenine dinucleotide phosphate; CscB, sucrose permease; CscA, sucrose hydrolase; IspS, isoprene synthase; and efe, ethylene forming enzyme.

source for *E. coli* as glucose, it has been found that about 50% of wild-type *E. coli* can utilize it (Holt et al., 1994). Under low carbohydrate conditions, the chromosomally coded sucrose catabolism genes—*csc,* namely *cscA*, *cscB,* and *cscK* are expressed in many *E. coli* strains K-12, BL21, O157:H7, and EC3132 (Hayashi et al., 2001; Jahreis et al., 2002). The imported sucrose is further broken down to glucose and fructose using CscA and metabolized as carbon and energy sources through glycolysis (Figure 1). Sucrose permease, sucrose: proton transporter encoded by the *cscB* gene, is a large proton symport system with 12 transmembrane helixes and three overlapping substrate specificities (Bockmann et al., 1992; Figure 1). It belongs to the oligosaccharide/H^+ cotransporter subfamily in the Major Facilitator Superfamily (MFS; Marger and Saier, 1993), similar to LacY, and both can catalyze the oligosaccharide/H^+ cotransport across the plasma membrane. Substrate specificity of CscB is to the fructofuranosyl ring of sucrose allows for sucrose, fructose, and lactulose, but not glucopyranosyl moiety to be metabolized (Sugihara et al., 2011). This makes sucrose a good intermediate for carbon and energy transfer between different members of an artificial community.

Some microorganisms can synthesize and secrete sucrose as an osmolyte when cultivated in excessive concentrations of salts (Hagemann, 2011). Exploration of this phenomenon in cyanobacteria enables continuous production of sucrose that exceeds the productivity of sugarcane, sugar beet, and other traditional sugar crops (Han and Watson, 1992). On this basis, cyanobacteria can be engineered to express sucrose permease, *CscB*, to secrete the disaccharide to the growth medium, and support the growth of *E. coli* in the absence of other carbon sources (Hays et al., 2016). For example, the sucrose yield of *Synechocystis* sp. PCC 6803 (3.13 mg/L/h) under 600 mM NaCl stress can be achieved by overexpressing genes related to sucrose synthesis and downstream sucrose metabolism (*sps*, *spp*, and *ugp* genes; Du et al., 2013). Meanwhile, *E. coli cscB* gene expression in *Synechococcus elongatus* PCC 7942 resulted in a yield of 36.1 mg/L/h (Ducat et al., 2012). Zhang et al. (2020) pointed out that sucrose derived from cyanobacteria may be considered an

attractive renewable feedstock to produce chemicals. However, its separation and purification generate considerable costs. These costs can be eliminated by employing the microbial consortium involving a cyanobacterium that provides photosynthetically produced sucrose to *E. coli*, which in turn serves as a producer of the target chemical.

In this study, artificial consortia consisting of cyanobacteria: *Thermosynechococcus elongatus* PKUAC-SCTE542 (subsequently, E542), *Synechococcus elongatus* PCC7942 (subsequently, PCC7942) in conjunction with *E. coli* BL21 expressing either IspS or Efe were constructed to produce volatile platform hydrocarbons indirectly from CO_2. In this system, cyanobacteria overexpressing the *E. coli cscB* gene under the control of a light-driven promoter produced and exported sucrose into the medium. The second component of the consortium, *E. coli* engineered with ethylene-forming enzyme gene *efe*, or isoprene synthetase gene *ispS*, can use sucrose in the medium and produce volatile platform hydrocarbons.

Materials and methods

Plasmid construction

All the strains used in this study are listed in Table 1. All plasmids (Supplementary Table 1) were created using oligonucleotides summarized in Supplementary Table 2. The polymerase chain reaction was performed using Phanta Max 2x (Vazyme, China) according to the manufacturer's recommendations. Constructs were assembled using ligase-independent ClonExpress II One Step Cloning Kit (Vazyme, China) using the manufacturer's guidelines, propagated in *E. coli* DH5α, and sequence verified by Sanger sequencing. The ethylene-forming enzyme (*efe*) of *Pseudomonas syringae pv. Phaseolicola* (AF101058.1) and isoprene synthetase (*ispS*) from *E. globulus* (BAF02831) were synthesized commercially at BGI WRITE (Beijing, China). After PCR amplification with their respective primers (Supplementary Table 2), both genes were separately cloned into the bacterial expression plasmid pBAD_LIC_cloning vector (8A) linearized with EcoRV essentially as described earlier (Cui et al., 2022; Cui and Daroch, 2022). The plasmids were propagated under 50 μg/ml ampicillin selection, and both enzymes were expressed under arabinose promoter (*araBAD*) with 0.2% arabinose.

The self-replicative plasmid expressing *cscB* gene (pLJD31) was created using a five-way assembly of the following fragments. The backbone and antibiotic resistance gene promoters were amplified from pAM5057 using MDLJCSTR224 and MDLJCSTR225, and MDLJCSTR500 and MDLJCSTR501, respectively. Plasmid pAM5057 was a gift from Susan Golden (Addgene plasmid # 120085; http://n2t.net/addgene:120085; RRID:Addgene_120,085). The kanamycin resistance gene was amplified from pETM11_Saz_CA (Hou et al., 2019) based on pETM11 backbone (EMBL Heidelberg) using MDLJCSTR120 and MDLJCSTR161. Light-driven promoter PsbA* along with the RBSV33 of *Synechocystis* PCC6803 (Wang et al., 2018) were custom synthesized at BGI WRITE (Beijing, China) and amplified using primer pair MDLJCSTR502 and MDLJCSTR136. The *cscB* gene expressing sucrose permease was amplified from *E. coli* DH5α using MDLJCSTR226 and MDLJCSTR227. The resultant plasmid pLJD31 was used for the transformation of E542.

The integrative plasmid expressing *cscB* gene was created using a three-step procedure. First, the plasmid pLJD50 was constructed based on pAM2991 backbone targeting the Neutral Site I of PCC7942 genome. The backbone was amplified with MDLJCSTR290 and MDLJCSTR291 primer pair. The plasmid pAM2991 was a gift from Susan Golden (Addgene plasmid # 40248; http://n2t.net/addgene:40248; RRID:Addgene_40,248; Ivleva et al., 2005). The antibiotic resistance promoter P_{amp}, spectinomycin resistance gene, the light-driven promoter of PCC7942, multiple cloning site, RBS, and terminator were amplified from pETS1 plasmid (Liang et al., 2019) using primer pair MDLJCSTR282 and MDLJCSTR228. Second, from pLJD50 vector a kanamycin-containing derivative pLJD51 was generated using a two-way assembly of PCR products amplified with primer pair MDLJCSTR207-MDLJCSTR289, and MDLJCSTR161-MDLJCSTR162. Finally, pLJD51 was linearized with MDLJCSTR319 and MDLJCSTR320 pair and assembled with *cscB* PCR product amplified with MDLJCSTR381 MDLJCSTR382 pair from the gDNA of *E. coli* DH5α. The resultant plasmid pLJD32 was used to transform PCC7942.

Recombinant strains construction

The modified plasmids with *efe* (pBAD-*efe*) or *IspS* (pBAD-*IspS*) were transformed to *E. coli* BL21 to produce ethylene or

TABLE 1 Strains used in the study.

Strains	Genotype	Source
DH5α	F^- *φ80 lacZ ΔM15 Δ(lacZYA-argF)U169 endA1 recA1 hsdR17* (r_k^-, m_k^+) *supE44* λ^- *thi-1 gyrA96 relA1 phoA*	From ktsm-life
BL21(DE3)	F^- *ompT hsdS*($r_B^-m_B^-$) *gal dcm*(DE3)	From ktsm-life
Conjugation helper strain	*E. coli* HB101 harboring pRL443 and pRL623	Zhang et al. (2020)
Thermosynechococcus elongatus PKUAC-SCTE542	Thermophilic cyanobacteria collected from the hot springs in Ganzi area, Sichuan, China	Tang et al. (2018) and Liang et al. (2019)
Synechococcus elongatus PCC 7942	*Synechococcus elongatus* PCC 7942 wild type	PCC Collection

isoprene. The *cscB* containing plasmid (pLJD31) was transformed into E542 through the conjugation *via E. coli* HB101 harboring pRL443 and pRL623 (Thiel and Peter Wolk, 1987) and *E. coli* DH5α carrying the pLJD31 plasmids, respectively. Meanwhile, the pLJD32 was transformed into PCC7942 using the recently optimized protocol (Riaz et al., 2022).

Culture conditions

Two co-culture media, Co-BG11 and M9-BG11, were tested to establish synthetic consortia between *E. coli* BL21 and E542 and PCC 7942. The Co-BG11 medium was prepared as described earlier (Zhang et al., 2020). In short, the medium was based on a conventional BG-11 medium and modified with the supplementation of 150 mM NaCl, 4 mM NH_4Cl, and 3 g/L 2-[[1,3-dihydroxy-2-(hydroxymethyl) propan-2-yl] amino] ethanesulfonic acid (TES) to support the growth of *E. coli*. In addition, NaCl was also added to induce stress in cyanobacterial strains for sucrose production and secretion. The second co-culture medium, M9-BG11 was designed based on regular BG-11 and M9 minimal media optimal for cyanobacteria and *E. coli*. The original BG11 medium (Stanier et al., 1971) was supplemented with 6 g/L K_2HPO_4, 3 g/L KH_2PO_4, 150 mM NaCl, 1 g/L NH_4Cl, 0.12 g/L $MgSO_4$, 0.014 g/L $CaCl_2$, and 0.001 g/L vitamin B1. In the consortia of ethylene, 0.2 g/l $FeSO_4$ was supplemented.

For cloning and precultures, *E. coli* cells were routinely grown in liquid LB medium in a shaking incubator (HZQ-X300C, Yiheng, Shanghai, China) at 180 rpm or LB agar (solid) plates at 37°C. Further, 50 μg/ml of ampicillin was added to maintain plasmids, and 0.2% arabinose was used to induce the expression of *efe* and *IspS* genes.

Cyanobacteria were cultivated in BG11 medium in an illuminated shaking incubator (Jintan Jingda Instruments TS-2112B) under constant illumination with white light at 2000 LUX (~36 $\mu mol\, m^{-2}\, s^{-1}$) at 180 rpm at 37°C for PCC7942 and 45°C for E542. In addition, the medium was supplemented with 50 μg/ml of kanamycin to maintain the plasmids and genomic integration.

Before establishing synthetic consortia, cyanobacteria grown in the exponential phase were diluted into one of the two co-culture media (Co-BG11 and M9-BG11) at a cell density of $OD_{750} \approx 0.15$ (corresponding to 9×10^6 cells/ml) and grown at 37°C (PCC7942) or 45°C (E542) for 48 h to reach the cell density of OD_{730} of 0.3. The *E. coli* BL21 cells were preincubated in the M9 medium supplemented with antibiotic and 2 g/L sucrose instead of glucose for 12 h. Later, the cells were collected by centrifugation, washed twice with deionized water, and inoculated into the 15 ml cyanobacterial culture described above to the final cell density of $OD_{600} = 0.1–0.2$ (corresponding to $1 \times 10^7–2 \times 10^7$ cells/ml). After adding arabinose to the concentration of 0.2%, the co-culture was incubated at 30°C for 48 h to produce ethylene or isoprene.

Quantification of cells

For pure cultures of cyanobacteria and *E. coli*, cell density was measured at OD_{730} and OD_{600} with an EPOCH microplate reader (BIOTEK, United States). For the co-culture, the cell number of *E. coli* was calculated by counting colony-forming units (CFU) in LB plate after 14 h of incubation at 37°C, and the cell number of cyanobacteria was counted by Countstar-IC1000 Cell Analyzer (Ruiyu, China).

Real-time RT-PCR analysis

Approximately 1.5–2 ml *E. coli* culture at $OD_{600} = 0.4–0.6$ was collected by centrifugation at 4°C, 8,000 rpm for 3 min to isolate RNA with Total RNA kit I (Omega Bio-Tec, United States) to compare the mRNA levels of sucrose catabolism genes (*cscB*, *cscA*, and *cscK*) and *efe* or *IspS* gene in M9 media supplemented with 2 g/L sucrose or conventional LB media. The reference gene for *E. coli* RT-qPCR is 16S rRNA. In the case of cyanobacteria, approximately 50–100 ml cultured cells were centrifugated at 4°C 8,000 rpm for 15 min to isolate total RNA to verify the mRNA levels of *cscB* gene in engineered strains. The reference gene for E542 is an "analysis fragment" from the literature at positions "2,985–3,144" of CP032152, and *purl* was used for PCC7942 (Riaz et al., 2021). The total RNA of *E. coli* was isolated with Total RNA kit I (Omega Bio-Tech, United States), while the total RNA of cyanobacterial was isolated with Trizol Reagent (Invitrogen, United States; Chomczynski and Sacchi, 2006). PrimeScript™ RT reagent Kit with gDNA Eraser (Takara, Japan) was used to remove the gDNA and reverse transcribe RNA to cDNA. The RT-qPCR reaction mix was prepared with TB Green Premix Ex Taq II (TaKaRa) in a QuantStudio 5 real-time system (ABI, United States). All the primers used for RT-qPCR analysis are given in Supplementary Table 2.

Quantification of ethylene production

The ethylene production in the gas phase was performed in a 60 ml sealed bottle headspace with 15 ml cyanobacterial-*E. coli* co-culture essentially as described before (Cui et al., 2022). In short, 1 ml air sample was injected into Agilent Technology 6850 GC FID with Porapak Q 3 M × 1/8 column to measure the concentration of ethylene. Three biological replicates were prepared to measure ethylene production, while one was maintained to determine the cellular density (CFU or OD). Ethylene production was defined as the amount (1 μmol) of ethylene produced by 10^{11} cells. The ethylene production per day was calculated as follows:

$$\text{Ethylene production} = \frac{C \cdot Va}{22.4\,\mu L / \mu mol \cdot 1{,}000 \cdot N \cdot T}$$

C: concentration of ethylene in the bottle, measured by GC (ppm); *V*a: gas volume in the bottle (mL); *N*: cell number; and *T*: reaction time (day).

Quantification of isoprene production

Isoprene production in the gas phase was analyzed in a headspace of a 60 ml sealed bottle with 15 ml co-cultured cells, as described before (Cui and Daroch, 2022). Briefly, toluene was injected into the bottle to absorb isoprene and incubated overnight at 4°C to condense the isoprene. The Agilent Technology 6850 N-5975 GC–MS with HP-5MS 5% Phenyl Methyl Siloxa column was used to measure the isoprene concentration. Different gradient volumes of liquid isoprene were added to the bottle and detected with GC–MS to make the standard curve. Three replicas for each strain were prepared to measure isoprene, while one replica was used for the cell density measurement (CFU or OD). The efficiency of isoprene production was calculated as follows:

$$\text{Isoprene production} = \frac{W}{68.11\frac{\mu g}{\mu mol}\cdot N\cdot T}$$

W: the content of isoprene in the bottle (μg); *N*: cell number; and *T*: reaction time (day).

Quantification of extracellular sucrose content

The 20 ml cyanobacterial culture supernatants grown under NaCl stress were collected and concentrated ten times to 2 ml at 65°C. The concentrated sucrose solution was hydrolyzed with 2 ml 6 mol/l HCl for 10 min at 100°C, then pH was adjusted to 9, and ddH_2O was added to the final volume of 10 ml. Subsequently, 0.8 ml of this liquid was mixed with 0.6 ml DNS detection reagent (Casmart, China) and boiled for 5 min at 100°C. The sucrose concentration was determined at OD_{520} against the standard curve prepared for known concentrations of sucrose treated under the same conditions (Miller, 1959).

Results

Growth and sucrose secretion of cyanobacterial cells

Growth parameters and gene expression analysis of sucrose-producing cyanobacteria

E542 and PCC7942 were engineered to secrete sucrose by expressing the sucrose permease encoding gene *cscB* under the light-driven promoters (Supplementary Figure 1) and the kanamycin resistance gene. The plasmids were transferred into the cyanobacteria E542 and PCC7942 using conjugation and natural transformation, respectively. The insertion of *cscB* gene and sucrose secretion did not significantly affect the growth of cyanobacteria under their optimal growth conditions (Supplementary Figure 2). As is shown in RT-qPCR results (Table 2), the *cscB* gene was successfully transcribed in engineered strains. The mRNA expression levels of the cells grown under constant illumination were 8.01 and 7.22 fold higher than the reference for PCC7942 and E542, respectively.

Sucrose secretion of engineered strains

The cells of E542_*cscB*$^+$ and PCC7942_ *cscB*$^+$ were cultured from an initial OD_{730} = 0.1–0.13 at 45°C (E542) or 37°C (PCC7942). Their growth and sucrose secretion was monitored for 3.5 and 7.5 days, as shown in Figure 2. Compared with the wild-type strains (WT), the sucrose yield of the engineered strains increased when cultivated under the same culture conditions. Compared with the yield in the dark environment and in the culture environment without NaCl, the sucrose yield of the engineered strains significantly increased under 150 mM NaCl with light. The sucrose yield in E542_*cscB*$^+$ reached 0.073 g/L (0.234 g/L/OD_{730}) and 0.136 g/L (0.221 g/L/OD_{730}) after 3.5 and 7.5 days, respectively, and the secretion efficiency remained at about 0.02 g/L/day. However, sucrose yield in PCC7942_*cscB*$^+$ was 0.054 g/L (0.226 g/L/OD_{730}) and 0.075 g/L (0.166 g/L/OD_{730}) after 3.5 and 7.5 days, respectively. The yield decreased slightly under long-term culture, and the maximum secretion efficiency was about 0.015 g/L/day. The secretion efficiency is lower than the recent study with *Synechococcus elongatus* UTEX 2973 cultured in BG11 + 150 mM NaCl (~0.1 g/L/day, ~0.59 g/L/OD_{730} for 3 days; Zhang et al., 2020) and the other studies with PCC7942 and *lac* promoter in other media (0.05–0.3 g/L/day for 2–4 days, total production is 0.156–0.625 g/L, 0.07–0.25 g/L/OD_{730}; Hays et al., 2016; Li et al., 2017). The carbon allocation ratio analysis shows an interesting difference between both transgenic cyanobacteria. Examination of the PCC7942_ *cscB*$^+$ indicates that sucrose secretion at dark remains relatively stable, which, combined with low biomass production, yields relatively high carbon partitioning to sucrose (Figures 2A–C). A different effect is observed in E542_*cscB*$^+$ where the dry weight upon transfer to dark conditions remains stable and sucrose secretion almost halts, resulting in very low sucrose to biomass ratio. Conversely, prolonged incubation at saline illuminated conditions results in low biomass accumulation and maximal sucrose productivity and carbon partitioning to sucrose significantly exceeding 1, indicating the majority of the

TABLE 2 Relative gene expression levels of *cscB* in engineered strains.

	delta–delta Ct value (ΔΔCt)				Fold change ($2^{-\Delta\Delta Ct}$)
	1	2	3	Average	
PCC7942_*cscB*$^+$	2.36	3.60	3.04	3.00	8.01
E542_ *cscB*$^+$	2.00	3.63	2.93	2.85	7.22

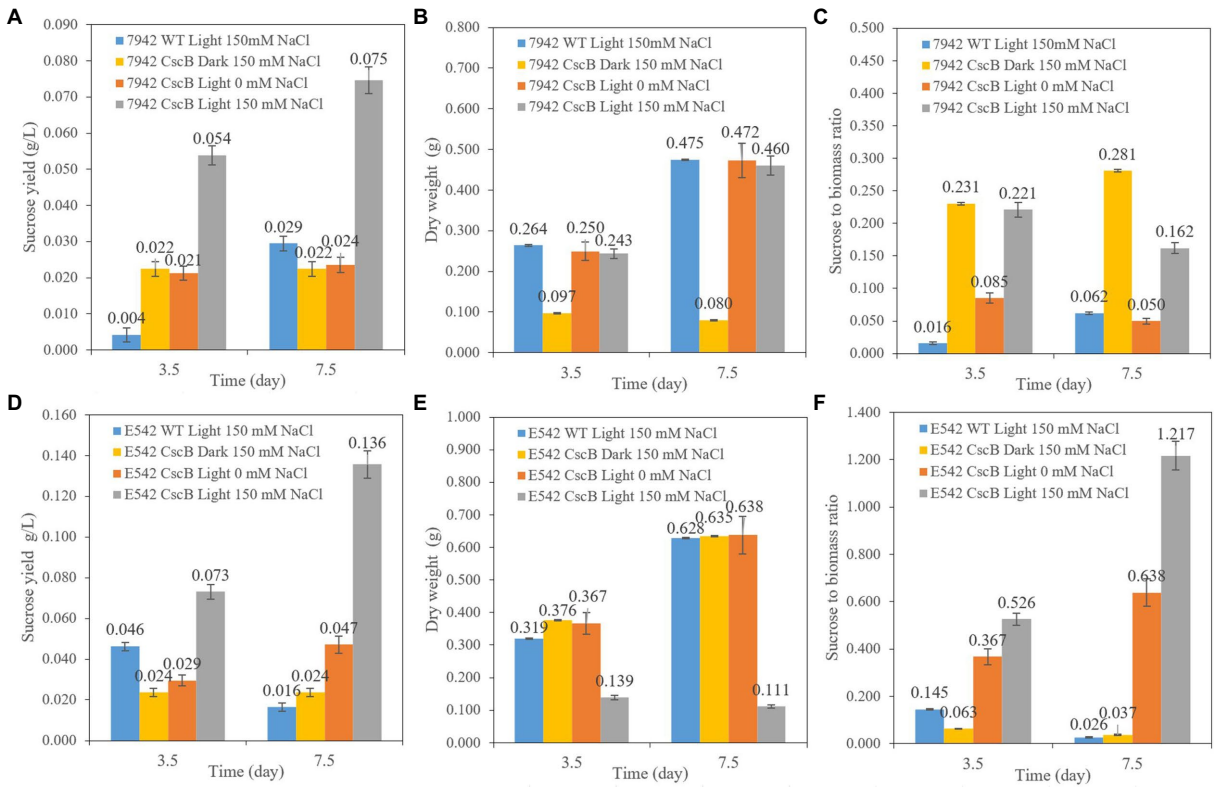

FIGURE 2
The comparison of sucrose yield of the PCC7942_*cscB*$^+$ **(A)**, E542_*cscB*$^+$ **(D)**, accumulated dry weight **(B,E)**, and sucrose to biomass ratio **(C,F)** grown under different light and osmotic pressure in BG11 growth medium. Height of the bars shows the mean of three independent experiments with error bars representing SD from measurements.

flux being directed toward sucrose secretion. Similar results have been obtained before (Ducat et al., 2012), indicating that a high stress level is required to maximize sucrose production.

Both the strain and the constructs may influence the sucrose production of the transgenic cells and the sucrose secretion efficiency. Besides, cell density may be a factor affecting sucrose secretion yield. If the sucrose secretion efficiency of single cells is the same, a lower growth rate and cell density may lead to a lower sucrose yield per liter cell culture.

The two engineered strains were cultured at different temperatures (30, 37, and 45°C), and samples were taken at 3.5 and 7.5 days to measure and compare the sucrose content in the culture medium and the growth of the strains (Figure 3). At 30°C, E542_*cscB*$^+$ grows slowly (Figure 3B), and the sucrose yield (0.053 g/L for 3.5 days; 0.040 g/L for 7.5 days; Figure 3A) was also lower, while the sucrose yield of PCC7942_*cscB*$^+$ (0.057 g/L for 3.5 days; 0.085 g/L for 7.5 days) was better at this temperature. At 37°C, both strains could grow well, and the 0.094 g/L sucrose yield of E542_*cscB*$^+$ for 7.5 days was better than 0.067 g/L of PCC7942_*cscB*$^+$. At 45°C, the E542 grew well, and the sucrose yield was the highest (0.136 g/L for 7.5 days), while PCC7942 died gradually due to poor tolerance to high temperature. Consequently, no sucrose was secreted by PCC7942_*cscB*$^+$ at 7.5 days. The changes in sucrose yield were consistent with the changes in cell density during this process. Sucrose yield was higher when cells grew well and lowered at lower growth rates. Therefore, the temperature significantly affected the sucrose secretion by the engineered strains by impacting their sucrose biosynthesis, growth, or both. Since sucrose biosynthesis in cyanobacteria strains was not artificially regulated in this experiment, the biosynthesis mainly came from the overflow of the photosynthate produced, and the efficiency may be biased toward strains' respective optimal growth temperatures (Warr et al., 1985). Longer cultivation of the co-culture exceeding 10 days resulted in the cell growth approaching a plateau, probably due to decreased cell viability and saturation of sucrose secretion capacity of the community.

Growth of BL21_*efe*$^+$ and BL21_*lspS*$^+$ in the co-culture medium and gene expression

Growth of *Escherichia coli* strains in the co-culture medium

To ensure the suitability of selected co-culture growth media for the cultivation of engineered *E. coli* strains and sucrose uptake; the two transgenic strains were cultured in derivatives of sucrose-containing media to choose the optimal composition for

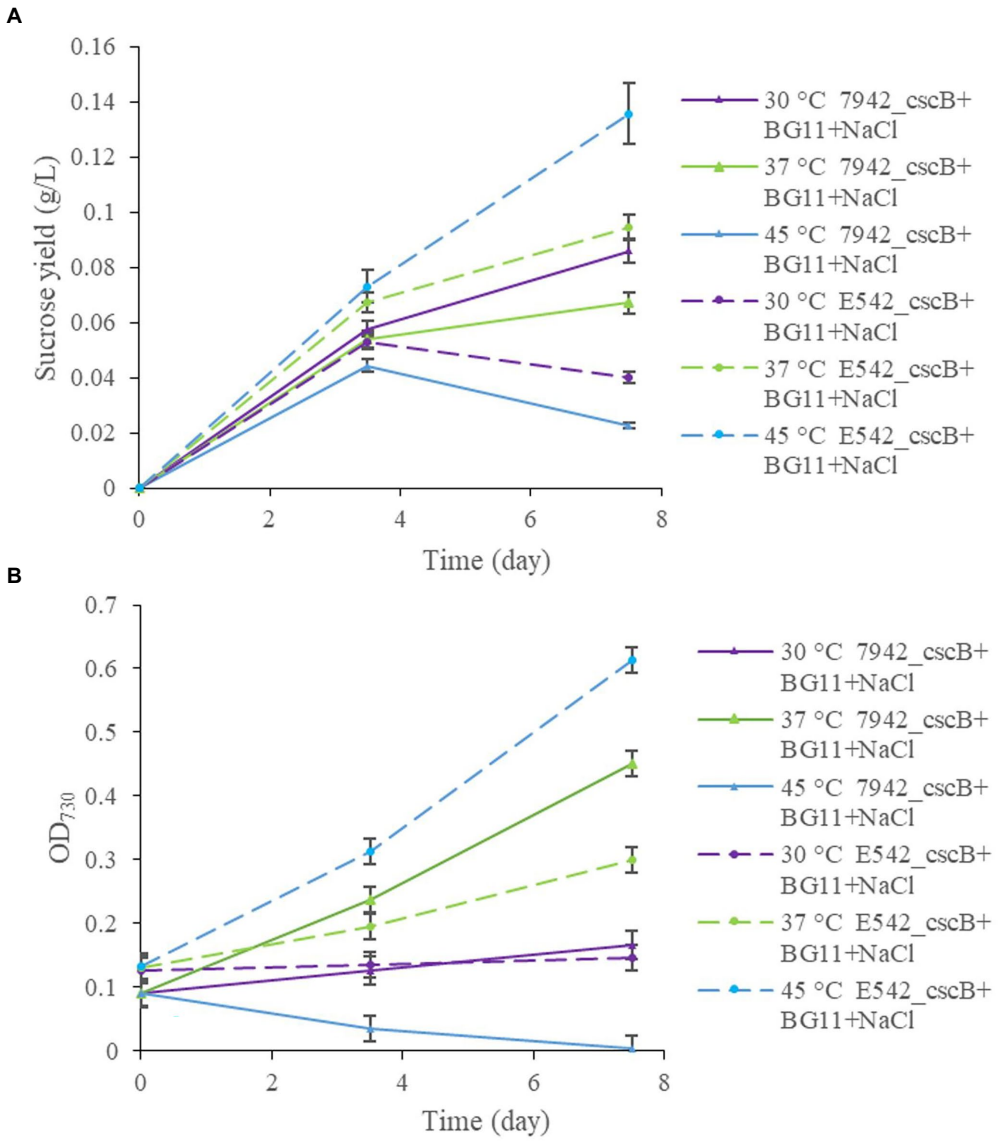

FIGURE 3
The comparison of sucrose yield **(A)**, and growth curve **(B)**, of engineered E542_*cscB*⁺ and 7,942_*cscB*⁺ strains at different temperatures grown in BG-11 medium under salt stress. Distribution of the data points shows the mean of three independent experiments with error bars representing SD from measurements.

co-culture studies. Previous studies showed that *E. coli* ATCC#9637 Δ*cscR* strain required about 1.2 g/L sucrose to grow well (that varied depending on other elements of the growth medium; Hays et al., 2016), while the sucrose yield achieved by the transgenic cyanobacteria typically does not reach this level. Therefore, in the preliminary experiment designed to determine the initial cultivation conditions, the co-culture environment was simulated by adding sucrose to the final concentration of 0.2 and 2 g/L in both of the co-culture media, i.e., co-BG11 and M9-BG11. The experiment was performed at 30 and 37°C (Supplementary Figure 3). Results showed the good growth of engineered *E. coli* BL21_*Efe_PS* at 37°C when 2 g/L sucrose was added to each of the co-culture media, while the growth at 30°C was much poorer, with the final cell density of $OD_{600} = 0.4$, markedly lower than other conditions tested (Supplementary Figure 3). This may be due to the high energy consumption of the cells at low temperature, and sucrose being gradually consumed during 96 h of cultivation and insufficient to provide sufficient carbon and energy for the rapid proliferation of *E. coli*. The lower concentration (0.2 g/L) of sucrose in the medium significantly inhibited the growth of *E. coli*.

Gene expression of *Escherichia coli* BL21_efe⁺ and BL21_IspS⁺ in sucrose-containing medium

The expression of sucrose metabolism-related genes (*cscA*, *cscB*, and *cscK*) and the volatile platform hydrocarbon synthase

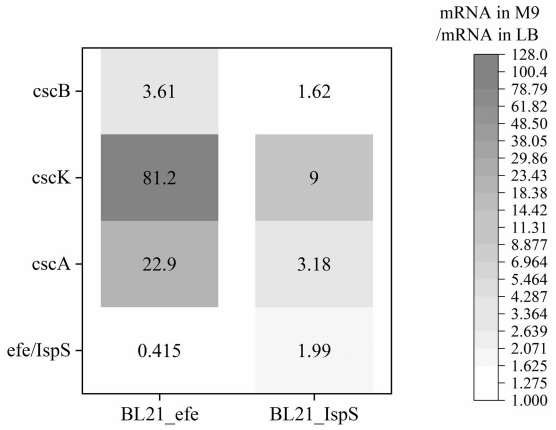

FIGURE 4
Changes of gene expression of BL21_*efe-PS* and BL21_*IspS_EG*$^+$ in the cultures with sucrose as the sole carbon source calculated using the relevant ratio of the mRNA value in the M9 medium to the mRNA value in the LB with $2^{-\Delta\Delta CT}$ method (Livak and Schmittgen, 2001).

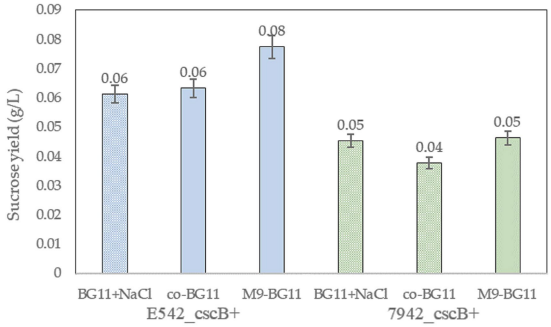

FIGURE 5
The comparison of sucrose yield of the engineered strains of E542_*cscB*$^+$ and PCC7942_*cscB*$^+$ in different co-culture media during 48-h long cultivation. Height of the bars shows the mean of three independent experiments with error bars representing SD from measurements.

genes (*efe* and *IspS*) in engineered *E. coli* strains cultured with sucrose as the sole carbon source was studied. After BL21_*efe_PS*$^+$ and BL21_*IspS_EG*$^+$ strains were cultured to OD_{600} = 0.4–0.6 in LB and M9 medium (glucose in M9 medium was replaced with 2 g/L sucrose), 0.2% arabinose was added to induce the expression. After induction at 30°C for 5 h, total RNA was extracted and detected. mRNA levels of the two strains in the M9 medium containing sucrose were compared with those in the LB medium (Figure 4). As shown in Figure 4, the RNA transcription levels of sucrose hydrolase gene *cscA* and fructokinase gene *cscK* increased significantly in the BL21_*efe*$^+$ and BL21_*IspS*$^+$, while the increase for sucrose permease gene *cscB* was not significant, indicating sufficient sucrose flux. In the two strains, the transcription of all *csc* genes in BL21_*IspS_EG*$^+$ was significantly lower than that of BL21_*efe_PS*$^+$. This may be related to the different synthesis pathways of their precursors in *E. coli* (Figure 1). In *E. coli*, the main precursors of ethylene synthesis are α-ketoglutaric acid and arginine. Arginine is an amino acid, which can be obtained directly from tryptone in LB medium, while α-ketoglutaric acid is synthesized by the TCA cycle (Li et al., 2006; Xiao et al., 2016). Acetyl-CoA, an essential node in the TCA cycle, can be derived from glycolysis and the decomposition of fatty acids and amino acids; meanwhile, it is also a building block for synthesizing these compounds (Han et al., 2001; Luo et al., 2014). In LB medium, raw materials such as amino acids are abundant, but the carbohydrate content is low, so presumably lower portion of acetyl-CoA is synthesized from glycolysis. However, in an M9 medium supplemented with sucrose, amino acids and other building blocks are likely to be limiting. Presumably, the resultant metabolism depends primarily on glycolysis to synthesize acetyl-CoA and, ultimately α-ketoglutaric acid, amino acids, and other essential substances to keep the cells alive. Therefore, the transcription and expression of related genes (*csc* genes) were likely to be increased under the increased metabolic requirements of glycolysis. However, since the synthesis of α -ketoglutaric acid was lower, the supply of arginine was limited; consequently, the ethylene synthesis could also be limited by the availability of precursors. On the contrary, the precursors of isoprene synthesis in this *E. coli* strain are pyruvate and glyceraldehyde-3-phosphate, both directly linked to glycolysis, and *csc* series genes may have been expressed in LB medium. Compared with the LB medium, precursors can be directly synthesized from sucrose available in the M9 medium, and the increase in precursor supply was conducive to the synthesis of isoprene and promoted the transcription of related genes.

Growth of engineered cyanobacteria in co-culture media

The addition of arabinose and extra ions to the co-culture media may affect the growth of cyanobacteria. E542_*cscB*$^+$ and PCC7942_*cscB*$^+$ were cultured in BG11 and the two co-culture media to explore these effects. Cyanobacteria can grow normally in both co-culture media, but the growth in the co-BG11 medium was somewhat slower (Supplementary Figure 4). Meanwhile, the addition of 0.2% arabinose had no significant effect on the growth of the strains. The sucrose yield in different media was tested to explore the sucrose secretion capacity of engineered strains in the co-culture system (Figure 5). The culture was started with OD_{730} = 0.15 and the sucrose yield of the strains cultured at their optimal growth temperatures for 2 days was detected. As shown in Figure 5, the sucrose yield of E542_*cscB*$^+$ was higher than that of PCC7942_*cscB*$^+$ in all media; this was consistent with the prior results of measurement for sucrose secretion by other transgenic cyanobacteria. Both the OD_{730} and sucrose yield in the M9-BG11 medium was higher than that of the co-BG11 medium (Figure 5; Supplementary Figure 4), indicating its more optimal composition for this task.

TABLE 3 Ethylene and isoprene production in consortium system.

	Ethylene production			Isoprene production		
	Production (μmol/L)	Production (μmol/10^{11} cells)	V (μmol/10^{11} cells/day)	Production (μmol/L)	Production (μmol/10^{11} cells)	V (μmol/10^{11} cells/day)
PCC7942 Co-BG11	16.94 ± 1.80	112.97	56.48	TLTD	/	/
PCC7942 M9-BG11	43.82 ± 8.42	219.08	109.54	0.75 ± 0.05	3.74	1.87
E542 Co- BG11	10.60 ± 1.96	70.64	35.32	TLTD	/	/
E542 M9-BG11	52.71 ± 0.18	263.55	131.77	0.39 ± 0.01	1.94	0.97
Co-BG11 + 0.05 g/L sucrose (only *E. coli*)	17.81 ± 1.85	59.37	29.69	TLTD	/	/
M9-BG11 + 0.05 g/L sucrose (only *E. coli*)	25.78 ± 0.96	64.47	32.23	0.34 ± 0.06	1.66	0.83
Co-BG11 + 2 g/L sucrose (only *E. coli*)	73.93 ± 5.26	164.30	82.15	0.38 ± 0.05	1.25	0.64
M9-BG11 + 2 g/L sucrose (only *E. coli*)	89.16 ± 2.98	139.31	69.65	1.67 ± 0.10	2.57	1.29
LB (Cui et al., 2022; Cui and Daroch, 2022)	794.07 ± 23.82	2908.7	13961.8	0.97 ± 0.09	0.97	1.94

TLTD, Too low to detect (below 0.2 μmol/L).

Production of volatile platform hydrocarbons in artificial consortium systems

Based on the literature and previous studies (Cui et al., 2022; Cui and Daroch, 2022), ethylene synthase and isoprene synthase were expressed well when the induced temperature was lower than the growth temperature of *E. coli* (37°C), and both proteins were prone to inclusion body formation at high temperature. In analyzing sucrose secretion by cyanobacteria above, engineered PCC7942 performed better at 30 and 37°C. Meanwhile, E542 secreted little sucrose at 30°C due to the poor growth parameters of the strain at this temperature. To compensate for those drawbacks, sucrose secretion during co-culture could be enhanced by increasing initial cell density. Based on the productivity data per cell, these lower growth rates may have better channeled the available cellular resources for sucrose production. Therefore, 30°C was selected as the reaction condition for co-cultures. Before that, cells were cultured separately to maintain good initial activity and density.

The artificial consortium systems of engineered strains of cyanobacteria E542_*cscB*$^+$ and PCC7942_*cscB*$^+$ with engineered strains of *E. coli* BL21_*efe_PS*$^+$ were established at co-BG11 medium and M9-BG11 media. After culturing for 48 h at 30°C, ethylene was detected by the GC. At the same time, the number of *E. coli* cells in the co-culture system was calculated by the CFU. The results of ethylene productivity are shown in Table 3. *Escherichia coli* BL21_*efe_PS*$^+$ was cultured in the co-culture medium supplemented with 2 g/L sucrose without cyanobacteria as the control group.

During the co-culture process, *E. coli* cell density was stable at the level of 1.5×10^7–2×10^7/ml and cyanobacteria grew normally in the system. The ratio of cyanobacteria and *E coli* cells was from 8.3 (15×10^7 cyanobacteria per milliliter/1.8×10^7 *E.coli* per milliliter, at the beginning) to 10.6 (20×10^7 vs. 1.89×10^7, after 1 day) then 12.5 (25×10^7 vs. 2.0×10^7, after 2 days) in consortium with M9-BG11. While the ratio was from 8.2 (15×10^7 cyanobacteria per milliliter/1.83×10^7 *E.coli* per milliliter, at the beginning) to 10.2 (19×10^7 vs. 1.86×10^7, after 1 day), and then 11.5 (22×10^7 vs. 1.92×10^7, after 2 days) in the consortium with Co-BG11. No other species was observed under microscopy.

The ethylene production was observed in all consortia, but the ethylene production was lower than that of the individual *E. coli* strain grown in LB (794.07 μmol/L for 5 h), or in the two co-culture media with 2 g/L sucrose (70.93 and 89.16 μmol/L for 48 h). In the studies that utilized *E. coli* as a single producer, the ethylene production level was 6–500 μmol/L/h in the strains with different vectors (Digiacomo et al., 2014; Eckert et al., 2014). In PCC7942, the productivity of ~20 μmol/L/h was recorded with psbAI promoter (Takahama et al., 2003) and ~6.25 μmol/L/h was recorded with *trc* promoter (Carbonell et al., 2019), while in the engineered strain of *Synechocystis* PCC 6803 the levels of 12–42 μmol/L/h were observed (Lee et al., 2015; Veetil et al., 2017; Wang et al., 2018). The comparison shows that the E542 strain and M9-BG11 medium combination had the highest ethylene yield, 52.71 μmol/L culture for 2 days, among the conditions tested. Combined with sucrose secretion and the growth of *E. coli*, inadequate nutrition leading to low cell density and low metabolic efficiency may be the reason for sub-par productivity. It is worth mentioning here that the approach of submerged cultivation is not the only one reported for ethylene bioproduction. A system based on cyanobacterial biofilms was designed to achieve a 2.2-fold increase in the ethylene production yield compared to the cell suspension (Vajravel et al., 2020).

The consortium systems of cyanobacteria and *E. coli* for isoprene production were constructed in the same media and conditions as for ethylene production. Isoprene concentration was detected by GC after culturing for 48 h. At the same time, the number of *E. coli* cells in the co-culture system was calculated by CFU. The results of isoprene productivity are shown in Table 3. In three instances, the isoprene productivity of the consortium was lower than the sensitivity of the assay, i.e., 0.2 μmol/L. The control group of *E. coli* BL21_IspS_EG$^+$ was cultured in the co-culture medium supplemented with 2 g/L sucrose without cyanobacteria.

The change in cell ratio was similar in the ethylene co-culture system. The comparison shows that the PCC7942 strain and M9-BG11 medium combination had the highest isoprene yield, 0.75 μmol/L culture for 48 h, among the conditions tested. Compared with the production per liter of individual BL21_*IspS_EG*$^+$ cell culture under carbon saturation, the isoprene production per liter of cell culture in each co-culture system also decreased, but not significantly. Especially, isoprene production per cell was especially stable, suggesting that the decrease resulted from lower sucrose availability. The isoprene production of individual strains expressing *IspS* gene in the other studies was 0.4–1.25 mg/L *E. coli* for 18 h in M9 media (Zurbriggen et al., 2012) and 3–7 mg/L *S. elongatus* PCC 7942 for 72 h in BG-11 containing 100 mM $NaHCO_3$ (Gao et al., 2016). Notably, it was demonstrated that the *S. elongatus* + *E. coli* co-cultivation system could provide isoprene titers as high as 0.4 g/L (Liu et al., 2021). The promoter, source of the synthase, and host organism may be reasons for the yield difference. It is also worth optimizing the ratio of the cyanobacteria and *E. coli* for more stable production and operates on higher cellular densities to improve the production per liter of cell culture (Zhao et al., 2011). Designing an effective inoculation approach may lead to considerable enhancement in terms of isoprene titers; however, it also affects the time required to reach satisfactory product levels in S. *elongatus* + *E. coli* co-cultures (Liu et al., 2021).

When the individual strain BL21_*efe_PS*$^+$ and BL21_*IspS_EG*$^+$ was cultured in co-culture media with 0.05 g/L sucrose (the sucrose yield of cyanobacteria in 2 days), the production of volatile platform hydrocarbons was lower than that of the consortium. Therefore, there are two possible explanations for these results. First, the gradual sucrose secretion during the co-culturing improved the yield of isoprene, and the consumption of sucrose by *E. coli* may allow the cyanobacteria to secrete more sucrose. Alternatively, cyanobacteria natively produce and secrete other than carbohydrates metabolites that can be metabolized by *E. coli*. Moreover, the higher availability of oxygen thanks to the oxygen evolution reaction can also have a positive impact on the co-culture system when compared with the sucrose supplementation study.

When the individual *E. coli* strain was cultured in consortium media with sufficient sucrose (2 g/L), the production of individual strain BL21_*efe_PS*$^+$ in co-culture media supplemented with 2 g/L sucrose was 73.93 μmol/L (Co-BG11) and 89.16 μmol/L (M9-BG11), and the production of individual strain BL21_*IspS_EG*$^+$ in co-culture mediums supplemented with 2 g/L sucrose is 0.38 μmol/L (Co-BG11) and 0.67 μmol/L (M9-BG11). In other words, *E. coli* can produce 37–45 μmol ethylene or 0.19–0.34 μmol isoprene with 1 g of sucrose, which was also used as the energy and carbon source. Cells grew better with sufficient sucrose (the final cell density is $OD_{600} = 0.6$ with 2 g/L sucrose while cell density is $OD_{600} = 0.2$ in the consortium system), and the production of ethylene and isoprene per liter culture was higher than that of the consortium system, but the production per cell had little difference. On the one hand, sucrose secreted by cyanobacteria in the co-culture system may be mainly used to produce volatile platform hydrocarbons with a high utilization rate; on the other hand, *E. coli* cells hardly grew with limited sucrose resulting in lower total production per liter culture.

Discussion

Sucrose yield in this study was 0.14 g/L (E542_*cscB*$^+$) and 0.07 g/L (PCC7942_*cscB*$^+$; Figure 2). This yield is lower than in previous studies (Hays et al., 2016; Li et al., 2017; Zhang et al., 2020), and it may be influenced by the strain, constructs, and, importantly, the lack of external inorganic carbon supply in the form of highly concentrated CO_2 or bicarbonate. Consequently, the growth parameters under salt stress in this study are inferior to many of those presented earlier. For example, it took 10 more days to grow from $OD_{730} = 0.05$ to $OD_{730} = 0.8$ (Supplementary Figure 2) under a light intensity of ~36 $\mu Em^{-2}s^{-1}$ in BG11 with 150 mM NaCl and no CO_2 supplementation than it did in other studies. For instance, PCC7942 cells incubated at 35°C, 2% CO_2, 150 rpm, ~65 $\mu Em^{-2}s^{-1}$ light intensity, grew to $OD_{750} = 1$ in 7 days in BG11 containing 150 mM NaCl (Ducat et al., 2012). Elsewhere, cell density of $OD_{750} = 3$ was achieved in 3 days in Co-BG11 (106 mM NaCl and other ions), 35°C, 2% CO_2, 150 rpm, and initial cell density $OD_{750} = 0.25$ (Hays et al., 2016). All of these indicate that light intensity and CO_2 supplementation are crucial for faster growth and are significant factors to improve the sucrose secretion efficiency and to provide more sucrose to *E. coli* in the consortium system.

Two kinds of co-culture media were compared for the cell growth, gene expression, and production of volatile hydrocarbon. The results showed that when sucrose was served as the only carbon source, sucrose utilization-related genes (*csc* series genes) showed an obvious upward transcription to provide energy for cell growth, and the volatile platform hydrocarbons could be successfully expressed (Figure 4, Supplementary Figure 3). The transgenic cyanobacterial cells exhibited satisfactory growth and sucrose secretion in both growth media, and its performance in M9-BG11 medium was superior to that in Co-BG11 (Figure 5, Supplementary Figure 4). In the consortium system, both ethylene and isoprene were synthesized, and the maximum yields were 52.71 μmol/l (ethylene production) and 0.75 μmol/l (isoprene production), respectively (Tables 2, 3).

Compared to the productivity in the LB medium, ethylene and isoprene yield per liter of cell culture for individual *E. coli* strain, decreased in the co-culture medium supplemented with 2 g/L sucrose. It may be caused by the inhibition of cell growth and metabolism due to incomplete sucrose utilization. In many studies utilizing sucrose as a shuttle molecule in the consortium, *csc* series genes were artificially regulated (overexpressed *cscA*, *cscB*, and *cscK*, deleted gene for sucrose catabolism operon repressor *cscR* etc.) to improve sucrose utilization in *E. coli* (Weiss et al., 2017; Zhang et al., 2020). It may be worth exploring similar strategies in the future to improve the performance of consortia in the production of volatile hydrocarbons. Under the conditions tested in this study, the consortium producing isoprene showed better yields than that for ethylene production. The result was consistent with the results of RT-qPCR describing gene transcription under sucrose utilization

(*IspS* gene mRNA level increased, while *efe* gene mRNA level decreased) caused by different synthesis pathways for the two platform hydrocarbons in *E. coli* (Figure 1). Arginine and α-ketoglutaric acid are the precursors of ethylene synthesis. In LB medium, arginine can be obtained directly from tryptone present in the medium. Meanwhile, sufficient protein and other energy sources can produce enough acetyl-CoA to drive the synthesis of α-ketoglutaric acid. However, in the co-culture medium, sucrose was used as the sole carbon source, which made acetyl-CoA synthesis dependent on glycolysis and simultaneously exploited for amino acid synthesis and other important metabolic pathways, resulting in a decrease of flux to α-ketoglutaric acid. Lower precursor availability resulted in a significant decrease in ethylene synthesis. In contrast, isoprene precursors in *E. coli* BL21 are synthesized *via* the MEP pathway from pyruvate and glyceraldehyde-3-phosphate, mainly derived from glycolysis. Compared with the LB medium, the co-culture system directly provided sucrose to *E. coli*., which was beneficial to the synthesis of isoprene, but not ethylene.

Conclusion

In this study, artificial consortia comprising *E. coli* and cyanobacteria, using sucrose as carbon and electron shuttle, for the production of volatile hydrocarbons were successfully constructed. The *cscB* gene was successfully expressed in both cyanobacterial strains. The results showed that the sucrose yield of the strains was 0.14 g/L (E542_*cscB*$^+$) and 0.07 g/L (PCC7942_*cscB*$^+$) under their respective growth temperatures, similar to other studies that did not utilize carbon dioxide supplementation but lower compared to the studies that applied high light and external CO_2 supplementation. This suggests that sucrose production by cyanobacteria expressing the sucrose transporter is typically carbon limited and an increased flux toward the secreted carbon can be generated using higher inorganic carbon loads and fine-tuning electron supply from the photosystem for carbon fixation and biosynthesis of sucrose. The growth parameters and gene expression of both engineered members of the artificial community were compared and analyzed, suggesting different metabolic responses of the community members depending on the type of product being synthesized. Various combinations of the consortia cultivation parameters were tested and the maximal yields of hydrocarbon production were achieved using 52.71 μmol/L for ethylene in M9-BG11 with E542 and 0.75 μmol/L for isoprene in M9-BG11 with PCC7942. The productivity of co-culture systems was similar to or superior to pure cultures containing an equivalent carbon source, showing the consortium partners' positive effect on producing these platform chemicals. However, from the applicative point of view, there is still a significant productivity gap that will allow these systems to replace fossil-derived volatile platform chemicals. The areas that could further improve the productivity of such a system include optimization of carbon and light supply, enhanced cellular concentrations, and in the longer scheme formation of hierarchical structures in which different community members could be arranged to facilitate the transfer of carbon between community members.

Data availability statement

The original contributions presented in the study are included in the article/Supplementary material, further inquiries can be directed to the corresponding author.

Author contributions

YC: conceptualization, methodology, validation, formal analysis, investigation, data curation, writing—original draft, writing—review and editing, and visualization. FR: methodology, validation, investigation, data curation, writing—review and editing, and supervision. YJ and YZ: investigation and data curation. SZ: supervision and project administration. TB: resources, validation, formal analysis, writing—review and editing, and visualization. SR: methodology and supervision. MD: conceptualization, methodology, resources, validation, formal analysis, investigation, data curation, writing—original draft, writing—review and editing, visualization, supervision, project administration, and funding acquisition. All authors contributed to the article and approved the submitted version.

Funding

This research was funded by Shenzhen Fundamental Research Program (GXWD20201231165807007-20200806170221001).

Conflict of interest

The authors declare that the research was conducted in the absence of any commercial or financial relationships that could be construed as a potential conflict of interest.

Publisher's note

All claims expressed in this article are solely those of the authors and do not necessarily represent those of their affiliated organizations, or those of the publisher, the editors and the reviewers. Any product that may be evaluated in this article, or claim that may be made by its manufacturer, is not guaranteed or endorsed by the publisher.

Supplementary material

The Supplementary material for this article can be found online at: https://www.frontiersin.org/articles/10.3389/fmicb.2022.965968/full#supplementary-material

References

Beliaev, A. S., Romine, M. F., Serres, M., Bernstein, H. C., Linggi, B. E., Markillie, L. M., et al. (2014). Inference of interactions in cyanobacterial-heterotrophic co-cultures via transcriptome sequencing. *ISME J.* 8, 2243–2255. doi: 10.1038/ismej.2014.69

Bockmann, J., Heuel, H., and Lengeler, J. W. (1992). Characterization of a chromosomally encoded, non-PTS metabolic pathway for sucrose utilization in *Escherichia coli* EC3132. *Mol. Gen. Genet. MGG* 235, 22–32. doi: 10.1007/BF00286177

Brenner, K., You, L., and Arnold, F. H. (2008). Engineering microbial consortia: a new frontier in synthetic biology. *Trends Biotechnol.* 26, 483–489. doi: 10.1016/j.tibtech.2008.05.004

Carbonell, V., Vuorio, E., Aro, E.-M., and Kallio, P. (2019). Enhanced stable production of ethylene in photosynthetic cyanobacterium *Synechococcus elongatus* PCC 7942. *World J. Microbiol. Biotechnol.* 35:77. doi: 10.1007/s11274-019-2652-7

Cheali, P., Posada, J. A., Gernaey, K. V., and Sin, G. (2016). Economic risk analysis and critical comparison of optimal biorefinery concepts. *Biofuels Bioprod. Biorefin.* 10, 435–445. doi: 10.1002/bbb.1654

Choi, Y.-N., Lee, J., Kim, J., and Park, J. (2020). Acetyl-CoA-derived biofuel and biochemical production in cyanobacteria: a mini review. *J. Appl. Phycol.* 32, 1643–1653. doi: 10.1007/s10811-020-02128-x

Chomczynski, P., and Sacchi, N. (2006). The single-step method of RNA isolation by acid guanidinium thiocyanate–phenol–chloroform extraction: twenty-something years on. *Nat. Protoc.* 1, 581–585. doi: 10.1038/nprot.2006.83

Cui, Y., and Daroch, M. (2022). "Clean synthesis of isoprene with six *E. coli* engineering strains" in The 2022 International Conference on Energy, Resources, Environment and Chemical Engineering. (China), 2, 322, 329.

Cui, Y., Jiang, Y., Xiao, M., Munir, M. Z., Riaz, S., Rasul, F., et al. (2022). Discovery of five new ethylene-forming enzymes for clean production of ethylene in *E. coli*. *Int. J. Mol. Sci.* 23:4500. doi: 10.3390/ijms23094500

Deepak, V. D., Mahmud, I., and Gauthier, M. (2019). Synthesis of carboxylated derivatives of poly(isobutylene-co-isoprene) by azide–alkyne "click" chemistry. *Polym. J.* 51, 327–335. doi: 10.1038/s41428-018-0130-y

Diender, M., Parera Olm, I., and Sousa, D. Z. (2021). Synthetic co-cultures: novel avenues for bio-based processes. *Curr. Opin. Biotechnol.* 67, 72–79. doi: 10.1016/j.copbio.2021.01.006

Digiacomo, F., Girelli, G., Aor, B., Marchioretti, C., Pedrotti, M., Perli, T., et al. (2014). Ethylene-producing bacteria that ripen fruit. *ACS Synth. Biol.* 3, 935–938. doi: 10.1021/sb5000077

Du, W., Liang, F., Duan, Y., Tan, X., and Lu, X. (2013). Exploring the photosynthetic production capacity of sucrose by cyanobacteria. *Metab. Eng.* 19, 17–25. doi: 10.1016/j.ymben.2013.05.001

Ducat, D. C., Avelar-Rivas, J. A., Way, J. C., and Silver, P. A. (2012). Rerouting carbon flux to enhance photosynthetic productivity. *Appl. Environ. Microbiol.* 78, 2660–2668. doi: 10.1128/aem.07901-11

Easterbrook, E. K., and Allen, R. D. (1987). "Ethylene-Propylene Rubber," in *Rubber Technology.* ed. M. Morton (Dordrecht: Springer), 260–283.

Eckert, C., Xu, W., Xiong, W., Lynch, S., Ungerer, J., Tao, L., et al. (2014). Ethylene-forming enzyme and bioethylene production. *Biotechnol. Biofuels* 7:33. doi: 10.1186/1754-6834-7-33

Gao, X., Gao, F., Liu, D., Hao, Z., Nie, X., and Yang, C. (2016). Engineering the methylerythritol phosphate pathway in cyanobacteria for photosynthetic isoprene production from CO_2. *Energy Environ. Sci.* 9, 1400–1411. doi: 10.1039/C5EE03102H

Gao, H., Manishimwe, C., Yang, L., Wang, H., Jiang, Y., Jiang, W., et al. (2022). Applications of synthetic light-driven microbial consortia for biochemicals production. *Bioresour. Technol.* 351:126954. doi: 10.1016/j.biortech.2022.126954

Gavrilescu, M., and Chisti, Y. (2005). Biotechnology—a sustainable alternative for chemical industry. *Biotechnol. Adv.* 23, 471–499. doi: 10.1016/j.biotechadv.2005.03.004

Hagemann, M. (2011). Molecular biology of cyanobacterial salt acclimation. *FEMS Microbiol. Rev.* 35, 87–123. doi: 10.1111/j.1574-6976.2010.00234.x

Han, Y. W., and Watson, M. A. (1992). Production of microbial Levan from sucrose, sugarcane juice and beet molasses. *J. Ind. Microbiol.* 9, 257–260. doi: 10.1007/BF01569633

Han, M. J., Yoon, S. S., and Lee, S. Y. (2001). Proteome analysis of metabolically engineered *Escherichia coli* producing poly(3-hydroxybutyrate). *J. Bacteriol.* 183, 301–308. doi: 10.1128/jb.183.1.301-308.2001

Hayashi, T., Makino, K., Ohnishi, M., Kurokawa, K., Ishii, K., Yokoyama, K., et al. (2001). Complete genome sequence of enterohemorrhagic *Escherichia coli* O157:H7 and genomic comparison with a laboratory strain K-12. *DNA Res.* 8, 11–22. doi: 10.1093/dnares/8.1.11

Hays, S., Yan, L., Silver, P., and Ducat, D. (2016). Synthetic photosynthetic consortia define interactions leading to robustness and photoproduction. *J. Biol. Eng.* 11:4. doi: 10.1186/s13036-017-0048-5

Holt, J. H., Krieg, N. R., Sneath, P. H. A., Staley, J. T., and Williams, S. T. (1994). *Bergey's Manual of Determinative Bacteriology. 9th Edn.* Baltimore: Williams and Wilikins, 786-788.

Hou, J., Xingkang, L., Kaczmarek, M., Chen, P., Li, K., Jin, P., et al. (2019). Accelerated CO_2 hydration with thermostable *Sulfurihydrogenibium azorense* carbonic anhydrase-chitin binding domain fusion protein immobilised on chitin support. *Int. J. Mol. Sci.* 20:1494. doi: 10.3390/ijms20061494

Huber, S. C., and Huber, J. L. (1992). Role of sucrose-phosphate synthase in sucrose metabolism in leaves. *Plant Physiol.* 99, 1275–1278. doi: 10.1104/pp.99.4.1275

Ishihara, K., Matsuoka, M., Inoue, Y., Tanase, S., Ogawa, T., and Fukuda, H. (1995). Overexpression and in vitro reconstitution of the ethylene-forming enzyme from *pseudomonas syringae*. *J. Ferment. Bioeng.* 79, 205–211. doi: 10.1016/0922-338X(95)90604-X

Ivleva, N. B., Bramlett, M. R., Lindahl, P. A., and Golden, S. S. (2005). LdpA: a component of the circadian clock senses redox state of the cell. *EMBO J.* 24, 1202–1210. doi: 10.1038/sj.emboj.7600606

Jahreis, K., Bentler, L., Bockmann, J., Hans, S., Meyer, A., Siepelmeyer, J., et al. (2002). Adaptation of sucrose metabolism in the Escherichia coli wild-type strain EC3132. *J. Bacteriol.* 184, 5307–5316. doi: 10.1128/JB.184.19.5307-5316.2002

Kazuhiro, N., Ogawa, T., Fujii, T., Tazaki, M., Tanase, S., Morino, Y., et al. (1991). Purification and properties of an ethylene-forming enzyme from *pseudomonas syringae* pv. *Phaseolicola* PK2. *J. Gen. Microbiol.* 137, 2281–2286. doi: 10.1099/00221287-137-10-2281

Kondo, T., Tsinoremas Nicholas, F., Golden Susan, S., Johnson Carl, H., Kutsuna, S., and Ishiura, M. (1994). Circadian clock mutants of cyanobacteria. *Science* 266, 1233–1236. doi: 10.1126/science.7973706

Kuzuyama, T. (2002). Mevalonate and nonmevalonate pathways for the biosynthesis of isoprene units. *Biosci. Biotechnol. Biochem.* 66, 1619–1627. doi: 10.1271/bbb.66.1619

Lee, T.-C., Xiong, W., Paddock, T., Carrieri, D., Chang, I.-F., Chiu, H.-F., et al. (2015). Engineered xylose utilization enhances bio-products productivity in the cyanobacterium *Synechocystis* sp. PCC 6803. *Metab. Eng.* 30, 179–189. doi: 10.1016/j.ymben.2015.06.002

Li, M., Ho, P. Y., Yao, S., and Shimizu, K. (2006). Effect of sucA or sucC gene knockout on the metabolism in *Escherichia coli* based on gene expressions, enzyme activities, intracellular metabolite concentrations and metabolic fluxes by 13C-labeling experiments. *Biochem. Eng. J.* 30, 286–296. doi: 10.1016/j.bej.2006.05.011

Li, T., Li, C.-T., Butler, K., Hays, S. G., Guarnieri, M. T., Oyler, G. A., et al. (2017). Mimicking lichens: incorporation of yeast strains together with sucrose-secreting cyanobacteria improves survival, growth, ROS removal, and lipid production in a stable mutualistic co-culture production platform. *Biotechnol. Biofuels* 10:55. doi: 10.1186/s13068-017-0736-x

Liang, Y., Tang, J., Luo, Y., Kaczmarek, M., Xingkang, L., and Daroch, M. (2019). *Thermosynechococcus* as a thermophilic photosynthetic microbial cell factory for CO_2 utilisation. *Bioresour. Technol.* 278, 255–265. doi: 10.1016/j.biortech.2019.01.089

Liu, H., Cao, Y., Guo, J., Xu, X., Long, Q., Song, L., et al. (2021). Study on the isoprene-producing co-culture system of *Synechococcus elongates–Escherichia coli* through omics analysis. *Microb. Cell Factories* 20:6. doi: 10.1186/s12934-020-01498-8

Livak, K. J., and Schmittgen, T. (2001). Analysis of relative gene expression data using real-time quantitative PCR and the 2-DDCt method. *Methods* 25, 402–408. doi: 10.1006/meth.2001.1262

Löwe, H., Hobmeier, K., Moos, M., Kremling, A., and Pflüger-Grau, K. (2017). Photoautotrophic production of polyhydroxyalkanoates in a synthetic mixed culture of *Synechococcus elongatus* cscB and *Pseudomonas putida cscAB*. *Biotechnol. Biofuels* 10:190. doi: 10.1186/s13068-017-0875-0

Luo, Y., Zhang, T., and Wu, H. (2014). The transport and mediation mechanisms of the common sugars in *Escherichia coli*. *Biotechnol. Adv.* 32, 905–919. doi: 10.1016/j.biotechadv.2014.04.009

Ma, J., Guo, T., Ren, M., Chen, L., Song, X., and Zhang, W. (2022). Cross-feeding between cyanobacterium *Synechococcus* and *Escherichia coli* in an artificial autotrophic–heterotrophic co-culture system revealed by integrated omics analysis. *Biotechnol. Biofuels Bioproducts* 15:69. doi: 10.1186/s13068-022-02163-5

Ma, W., Liu, Y., Lv, X., Li, J., Du, G., and Liu, L. (2019). Combinatorial pathway enzyme engineering and host engineering overcomes pyruvate overflow and enhances overproduction of N-acetylglucosamine in *Bacillus subtilis*. *Microb. Cell Factories* 18:1. doi: 10.1186/s12934-018-1049-x

Marger, M. D., and Saier, M. H. (1993). A major superfamily of transmembrane facilitators that catalyse uniport, symport and antiport. *Trends Biochem. Sci.* 18, 13–20. doi: 10.1016/0968-0004(93)90081-W

Miller, G. L. (1959). Use of Dinitrosalicylic acid reagent for determination of reducing sugar. *Anal. Chem.* 31, 426–428. doi: 10.1021/ac60147a030

Minty, J., Singer, M., Bae, C. H., Ahn, J. H., Foster, C., Liao, J., et al. (2012). "Design and construction of synthetic fungi-bacteria consortia for direct production of isobutanol from cellulosic feedstocks."

Mittermeier, F., Bäumler, M., Arulrajah, P., García Lima, J. de. J., Hauke, S., Stock, A., et al. (2022). Artificial microbial consortia for bioproduction processes. *Eng. Life Sci.* doi: 10.1002/elsc.202100152

Mukherjee, A., Sarkar, D., and Sasmal, S. (2021). A review of green synthesis of metal nanoparticles using algae. *Front. Microbiol.* 12:693899. doi: 10.3389/fmicb.2021.693899

Quintana, N., Van der Kooy, F., Van de Rhee, M. D., Voshol, G. P., and Verpoorte, R. (2011). Renewable energy from cyanobacteria: energy production optimization by metabolic pathway engineering. *Appl. Microbiol. Biotechnol.* 91, 471–490. doi: 10.1007/s00253-011-3394-0

Riaz, S., Jiang, Y., Xiao, M., You, D., Klepacz-Smolka, A., Rasul, F., et al. (2022). Generation of miniploid cells and improved natural transformation procedure for a model cyanobacterium *Synechococcus elongatus* PCC 7942. *Front. Microbiol.* 13:959043. doi: 10.3389/fmicb.2022.959043

Riaz, S., Xiao, M., Chen, P., Li, M., Cui, Y., and Daroch, M. (2021). Genome copy number of a thermophilic cyanobacterium *Thermosynechococcus elongatus* E542 is controlled by growth phase and nutrient availability. *Appl. Environ. Microbiol.* 87:e02993-20. doi: 10.1128/AEM.02993-20

Singh, A. K., and Ducat, D. C. (2022). Generation of stable, light-driven co-cultures of cyanobacteria with heterotrophic microbes. *Methods Mol. Biol.* 2379, 277–291. doi: 10.1007/978-1-0716-1791-5_16

Song, H., Ding, M. Z., Jia, X. Q., Ma, Q., and Yuan, Y. J. (2014). Synthetic microbial consortia: from systematic analysis to construction and applications. *Chem. Soc. Rev.* 43, 6954–6981. doi: 10.1039/c4cs00114a

Stanier, R., Kunisawa, R., Mandel, M., and Cohen-Bazire, G. (1971). Purification and properties of unicellular blue-green algae (order *Chroococcales*). *Bacteriol. Rev.* 35, 171–205. doi: 10.1128/BR.35.2.171-205.1971

Sugihara, J., Smirnova, I., Kasho, V., and Kaback, H. R. (2011). Sugar recognition by CscB and LacY. *Biochemistry* 50, 11009–11014. doi: 10.1021/bi201592y

Takahama, K., Matsuoka, M., Kazuhiro, N., and Ogawa, T. (2003). Construction and analysis of a recombinant cyanobacterium expressing a chromosomally inserted gene for an ethylene-forming enzyme at the psbAI locus. *J. Biosci. Bioeng.* 95, 302–305. doi: 10.1016/S1389-1723(03)80034-8

Tang, J., Jiang, D., Luo, Y., Liang, Y., Li, L., Shah, M. M. R., et al. (2018). Potential new genera of cyanobacterial strains isolated from thermal springs of western Sichuan, China. *Algal Res.* 31, 14–20. doi: 10.1016/j.algal.2018.01.008

Tarawat, S., Incharoensakdi, A., and Monshupanee, T. (2020). Cyanobacterial production of poly(3-hydroxybutyrate-co-3-hydroxyvalerate) from carbon dioxide or a single organic substrate: improved polymer elongation with an extremely high 3-hydroxyvalerate mole proportion. *J. Appl. Phycol.* 32, 1095–1102. doi: 10.1007/s10811-020-02040-4

Thiel, T., and Peter Wolk, C. (1987). "Conjugal transfer of plasmids to cyanobacteria," in *Methods in Enzymology*. eds. R. Wu and L. Grossman (Waltham, MA: Academic Press), 232–243.

Thiel, T., and Poo, H. (1989). Transformation of a filamentous cyanobacterium by electroporation. *J. Bacteriol.* 171, 5743–5746. doi: 10.1128/jb.171.10.5743-5746.1989

Vajravel, S., Sirin, S., Kosourov, S., and Allahverdiyeva, Y. (2020). Towards sustainable ethylene production with cyanobacterial artificial biofilms. *RSC Green Chem.* 22, 6404–6414. doi: 10.1039/d0gc01830a

Valenzuela, R., Asperilla, J., and Cortés Corberán, V. (2008). Isoprene and C5 olefins production by oxidative dehydrogenation of Isopentane†. *Ind. Eng. Chem. Res.* 47, 8037–8042. doi: 10.1021/ie800756p

Veetil, V. P., Angermayr, S. A., and Hellingwerf, K. J. (2017). Ethylene production with engineered *Synechocystis sp*. PCC 6803 strains. *Microb. Cell Factories* 16:34. doi: 10.1186/s12934-017-0645-5

Venkata Mohan, S., and Venkateswar Reddy, M. (2013). Optimization of critical factors to enhance polyhydroxyalkanoates (PHA) synthesis by mixed culture using Taguchi design of experimental methodology. *Bioresour. Technol.* 128, 409–416. doi: 10.1016/j.biortech.2012.10.037

Wang, B., Eckert, C., Maness, P.-C., and Yu, J. (2018). A genetic toolbox for modulating the expression of heterologous genes in the cyanobacterium *Synechocystis* sp. PCC 6803. *ACS Synth. Biol.* 7, 276–286. doi: 10.1021/acssynbio.7b00297

Wang, B., Li, Y., Wu, N., and Lan, C. Q. (2008). CO2 bio-mitigation using microalgae. *Appl. Microbiol. Biotechnol.* 79, 707–718. doi: 10.1007/s00253-008-1518-y

Warr, S., Reed, R., and Stewart, W. (1985). Carbohydrate accumulation in osmotically stressed cyanobacteria (blue-green algae): interactions of temperature and salinity. *New Phytol.* 100, 285–292. doi: 10.1111/j.1469-8137.1985.tb02779.x

Watanabe, T., and Horiike, T. (2021). The evolution of molybdenum dependent Nitrogenase in cyanobacteria. *Biology* 10:329. doi: 10.3390/biology10040329

Weiss, T. L., Young, E. J., and Ducat, D. C. (2017). A synthetic, light-driven consortium of cyanobacteria and heterotrophic bacteria enables stable polyhydroxybutyrate production. *Metab. Eng.* 44, 236–245. doi: 10.1016/j.ymben.2017.10.009

Xiao, D., Zeng, L., Yao, K., Kong, X., Wu, G., and Yin, Y. (2016). The glutamine-alpha-ketoglutarate (AKG) metabolism and its nutritional implications. *Amino Acids* 48, 2067–2080. doi: 10.1007/s00726-016-2254-8

Zhang, L., Chen, L., Diao, J., Song, X., Shi, M., and Zhang, W. (2020). Construction and analysis of an artificial consortium based on the fast-growing cyanobacterium *Synechococcus elongatus* UTEX 2973 to produce the platform chemical 3-hydroxypropionic acid from CO2. *Biotechnol. Biofuels* 13:82. doi: 10.1186/s13068-020-01720-0

Zhang, G., Yang, X., Zhao, Z., Xu, T., and Jia, X. (2022). Artificial consortium of three *E. coli* BL21 strains with synergistic functional modules for complete phenanthrene degradation. *ACS Synth. Biol.* 11, 162–175. doi: 10.1021/acssynbio.1c00349

Zhao, Y., Yang, J., Qin, B., Li, Y., Sun, Y., Su, S., et al. (2011). Biosynthesis of isoprene in *Escherichia coli* via methylerythritol phosphate (MEP) pathway. *Appl. Microbiol. Biotechnol.* 90, 1915–1922. doi: 10.1007/s00253-011-3199-1

Zurbriggen, A., Kirst, H., and Melis, A. (2012). Isoprene production via the Mevalonic acid pathway in *Escherichia coli* (bacteria). *Bioenergy Res.* 5, 814–828. doi: 10.1007/s12155-012-9192-4

frontiers | Frontiers in Microbiology

TYPE Original Research
PUBLISHED 02 November 2022
DOI 10.3389/fmicb.2022.994847

Check for updates

OPEN ACCESS

EDITED BY
Durgesh K. Jaiswal,
Savitribai Phule Pune University, India

REVIEWED BY
Abhijeet Ghatak,
Bihar Agricultural University, India
Laith Khalil Tawfeeq Al-Ani,
Universiti Sains Malaysia, Malaysia

*CORRESPONDENCE
Vellaichamy Mageshwaran
mageshbioiari@gmail.com;
mageshwaran.v@icar.gov.in
Udai B. Singh
udaiars.nbaim@gmail.com

SPECIALTY SECTION
This article was submitted to Microbiotechnology, a section of the journal Frontiers in Microbiology

RECEIVED 15 July 2022
ACCEPTED 14 September 2022
PUBLISHED 02 November 2022

CITATION
Mageshwaran V, Gupta R, Singh S, Sahu PK, Singh UB, Chakdar H, Bagul SY, Paul S and Singh HV (2022) Endophytic *Bacillus subtilis* antagonize soil-borne fungal pathogens and suppress wilt complex disease in chickpea plants (*Cicer arietinum* L.). *Front. Microbiol.* 13:994847. doi: 10.3389/fmicb.2022.994847

COPYRIGHT
© 2022 Mageshwaran, Gupta, Singh, Sahu, Singh, Chakdar, Bagul, Paul and Singh. This is an open-access article distributed under the terms of the Creative Commons Attribution License (CC BY). The use, distribution or reproduction in other forums is permitted, provided the original author(s) and the copyright owner(s) are credited and that the original publication in this journal is cited, in accordance with accepted academic practice. No use, distribution or reproduction is permitted which does not comply with these terms.

Endophytic *Bacillus subtilis* antagonize soil-borne fungal pathogens and suppress wilt complex disease in chickpea plants (*Cicer arietinum* L.)

Vellaichamy Mageshwaran[1]*, Rishabh Gupta[1], Shailendra Singh[2], Pramod K. Sahu[2], Udai B. Singh[2]*, Hillol Chakdar[1], Samadhan Y. Bagul[3], Surinder Paul[1] and Harsh V. Singh[2]

[1]Microbial Technology Lab, ICAR-National Bureau of Agriculturally Important Microorganisms, Maunath Bhanjan, Uttar Pradesh, India, [2]Plant-Microbe Interaction and Rhizosphere Biology Lab, ICAR-National Bureau of Agriculturally Important Microorganisms, Maunath Bhanjan, Uttar Pradesh, India, [3]ICAR-Directorate of Medicinal and Aromatic Plants Research, Anand, Gujarat, India

The present study aimed to identify potential endophytic bacteria antagonistic against three soil-borne fungal pathogens, *Rhizoctonia solani, Sclerotium rolfsii,* and *Fusarium oxysporum* f.sp. *ciceri* causing root rot, collar rot, and fungal wilt diseases in chickpea plants, respectively. A total of 255 bacterial endophytes were isolated from the leaves, stems, and roots of seven different crop plants (chickpea, tomato, wheat, berseem, mustard, potato, and green pea). The dual culture-based screening for antifungal properties indicated that three endophytic isolates had strong inhibition (>50%) against all three pathogens tested. Based on morphological, biochemical, and molecular characterization, the selected isolates (TRO4, CLO5, and PLO3) were identified as different strains of *Bacillus subtilis*. The bacterial endophytes (TRO4 and CLO5) were positive for plant growth promoting (PGP) traits *viz.*, ammonia, siderophore, and indole-3-acetic acid (IAA) production. The bio-efficacy of the endophytes (TRO4, CLO5, and PLO3) was tested by an *in planta* trial in chickpea pre-challenged with *R. solani, S. rolfsii,* and *F. oxysporum* f.sp. *ciceri*. The *B. subtilis* strains TRO4 and CLO5 were found to be effective in reducing percent disease incidence ($p \leq 0.05$) and enhancing plant growth parameters. The different root parameters *viz.* root length (mm), surface area (cm^2), root diameter (mm), and root volume (cm^3) were significantly ($p \leq 0.05$) increased in TRO4 and CLO5 inoculated chickpea plants. Confocal Scanning Laser Microscopy showed heavy colonization of bacteria in the roots of endophyte-inoculated chickpea plants. The inoculation of endophytic *Bacillus subtilis* strains TRO4 and CLO5 in chickpea plants through seed biopriming reduced the accumulation of superoxide, enhanced the plant defense enzymes, and induced the expression of Pathogenesis-Related (PR) genes. Semi-quantitative analysis of defense-related genes showed differential activation of PR genes (*60srp* and *IFR*) by endophyte inoculation. The results of the present study reveal the antagonistic potential of *B. subtilis* strains TRO4 and CLO5 against three major soil-borne fungal pathogens and their ability to suppress wilt complex disease in chickpea plants. This is the first report on the simultaneous

suppression of three major soil-borne fungal pathogens causing wilt complex in chickpea plants by endophytic *B. subtilis* strains.

KEYWORDS

antagonism, bacterial endophytes, *Bacillus subtilis*, chickpea (*Cicer arietinum* L.), fungal pathogens, ISR, seed biopriming, wilt complex

Introduction

Chickpea (*Cicer arietinum* L.) is the major food legume grown in south Asia. Globally, it is the third largest legume crop grown after common bean and field pea (Mula et al., 2011). Chickpea has been grown in the area of 14.56 million ha with a productivity of 970 kg ha^{-1}. India is the largest producer with 65% of the global production. The other major chickpea-producing countries are Pakistan, Turkey, Iran, Myanmar, Australia, Ethiopia, Canada, Mexico, and Iraq. It is a major pulse crop in India with a share of 46% followed by Pigeonpea, Urd bean, Mung bean, Lentil, Pea, and others (Merga and Haji, 2019). In general, chickpea production is largely affected by five important soil-borne phytopathogens that cause wilt and root rot complex in chickpea plants. Among them, fusarium wilt, dry root rot, wet root rot, black root rot, and collar rot are most important and caused by *Fusarium oxysporum* f.sp. *ciceri*, *Rhizoctonia bataticola*, *R. solani*, *F. solani*, and *Sclerotium rolfsii*, respectively (Beniwal et al., 1992). The soil-borne plant pathogenic fungi *viz.*, *F. oxysporum*, *S. rolfsii*, and *R. solani* have a wide host range, occur in combination, and cause severe disease complex symptoms which in turn lead to great worldwide economic losses every year (Rudresh et al., 2005; Senthilkumar et al., 2009). *R. solani* causes root rot in chickpea/sugar beet, bare patch in cereals, black scurf in potatoes, and sheath blight in rice. They infect the lower root and stem of the plant (Anderson, 1982). However, *Sclerotium rolfsii* causes collar rot disease in chickpea, watermelon, pepper, tomato, sweet potato, onion, and groundnut. They infect the host in the early stages of crop growth. White threads of mycelial growth in a fan shape pattern on the stem and plant leaves are a sign of this disease (Aycock, 1966; Sahu et al., 2019). *Fusarium oxysporum* f.sp. *ciceri* is a soil-borne pathogen and causes wilt disease in chickpea plants. It is a devastating disease and can cause a yield loss of 10–100% in chickpea depending on the aggressiveness of fungal inoculum, virulence, and environmental conditions. The pathogen is a facultative saprophyte and can survive in soil or crop residues as chlamydospores for up to 6 years (Agrios, 2005). The unique symptoms are the drooping of the petioles, rachis, and leaves, and internal discoloration (browning) of xylem vessels (Jendoubi et al., 2017).

Management of the wilt complex is largely dependent on the use of toxic chemical fungicides. These chemicals are toxic to non-target flora and fauna in the soil ecosystem (Singh et al., 2016). Further, the residual impact of these toxic chemicals on the health of animals, humans, and the environment. The breeding of resistant cultivars is one of the safer alternatives and to date, some cultivars are available with moderate resistance to either of these pathogens. However, the availability of suitable donor parents with a high degree of resistant genes/quantitative trait loci and the transfer of these traits to agronomically important cultivars is a great challenge for plant breeders (Singh et al., 2016). Looking at the importance of the crops and the problem therein, biological control of these notorious pathogens is a viable and sustainable management option as chemical fungicides harm the environment and human health (Sarma et al., 2015; Singh et al., 2020a). In the recent past, several researchers have reported that plant growth promoting rhizobacteria (PGPR) mediates modulation of systemic resistance against wilt and root rot pathogens in many crops including chickpea (Rudresh et al., 2005; Zaim et al., 2016; Bekkar et al., 2018; Kumari and Khanna, 2019). Besides PGPRs, bacterial endophytes are a group of bacteria that have a special ability to colonize and reside inside the plants and protect the host plant from biotic and abiotic stresses (Ziedan, 2006; Sahu et al., 2020, 2021; Singh et al., 2021). Among the plant parts, the roots are considered the major entry point of microorganisms and have the highest frequency of colonization of endophytic bacteria. Bacterial endophytes colonize the same niche as plant pathogens and suppress the pathogen through various mechanisms such as the production of hydrogen cyanide (HCN), siderophore, hydrolytic enzymes, antibiotics, and induction of systemic resistance (Sahu et al., 2020; Singh et al., 2020a,b). Further, they support plant growth through the production of phytohormones, solubilizing nutrients, and nitrogen fixation (Ryan et al., 2007; Senthilkumar et al., 2009). Thus, bacterial endophytes could be used as an efficient bio-control agent against potential soil-borne pathogens as they provide localized protection to the host plant. Beneficial bacteria living inside the plant interact with the host and fight against different phytopathogens (Sahu et al., 2019, 2020). These microorganisms either produce broad-spectrum biotic stimuli or directly interact with the pathogens during the infection and/or invasion process and thereby enhance the physiological state of defense, known in general as induced systemic resistance. The induction of systemic resistance is categorized as (i) induced systemic resistance (ISR) and (ii) systemic acquired resistance (SAR). ISR occurs when plants' intrinsic defense mechanisms are triggered in response to biotic threats (Pineda et al., 2013; Sahu et al., 2020; Singh et al., 2020a). In general, during host-pathogen interaction, microbial inoculants activate the various defense

enzymes (PPO, POX, GLU, CHI, and PAL) and several other pathways/cascades responsible for systemic resistance in plants such as phenylpropanoid, MAPKs, and jasmonate, (Harman et al., 2004; Harman, 2011; Sahu et al., 2020; Singh et al., 2020a). Reduction in the disease severity and enhanced up-regulation and bioaccumulation of defensive enzymes triggered by the combined inoculation of *Bacillus atrophaeus*, *B. subtilis*, and *Burkholderia cepacia* exhibited a direct bio-control and ISR in the suppression of vascular disease in tomato crops (Shanmugam and Kanoujia, 2011). Although the isolation of bacterial endophytes and their antagonist property against fungal pathogens have been reported so far (Souza et al., 2014; Gond et al., 2015; Zhao et al., 2015), there is no report on the bio-control of pathogens involved in wilt complex disease in chickpea using bacterial endophytes. Looking at the importance of root diseases especially, wilt complex in chickpea and endophytes with antimicrobial properties, it is the need of the hour to explore the potential of endophytes for the management of wilt complex in chickpea. It is hypothesized that bacterial endophytes provide localized and systemic protection against invasion of soilborne fungal pathogens, Therefore, the present investigation was aimed to identify bacterial endophytes showing strong antagonism against multiple plant pathogenic fungi, *R. solani, S. rolfsii,* and *F. oxysporum* f.sp. *ciceri* and bio-control of wilt complex disease caused by these pathogens in chickpea using selected potential endophytes.

Materials and methods

Collection of plant samples

The whole plant samples (chickpea, tomato, wheat, berseem, mustard, potato, and green pea) were collected from different agricultural farms in a village, Onhaich, which is situated at nearby ICAR-National Bureau of Agriculturally Important Microorganisms (NBAIM), Mau, Uttar Pradesh, India (25°53′30”N; 83°28′46″ E). The sampling was done in the month of January 2020. The crops were of local commercial cultivars and were approximately 20–30 days old during sample collection. The plant parts *viz.*, roots, stems, and leaves were separated and washed carefully in running tap water. Thereafter, the clean samples were used immediately for the isolation of bacterial endophytes.

Microorganisms

The test fungal pathogens, *R. solani*, *S. rolfsii* were obtained from the Plant-Microbe Interaction Laboratory and Rhizosphere Biology Lab, ICAR-NBAIM, Kushmaur, whereas *F. oxysporum* f.sp. *ciceri* (NAIMCC-F-02214) was obtained from the National Agriculturally Important Microbial Culture Collection (NAIMCC), ICAR-NBAIM, Kushmaur. The fungal cultures were grown on the Petri plates containing potato dextrose agar (PDA, HiMedia Pvt. Ltd., Mumbai, India) at 28 ± 2°C till complete growth. The full-grown fungal cultures were preserved at 4°C till further use.

Isolation of bacterial endophytes

The roots, stems, and leaves (1 g each) were cleaned in running water to remove adhering particles. The endophytic bacterial strains were isolated from different plant samples using the protocols described by Sahu et al. (2020) with slight modifications. Briefly, the plant parts were surface sterilized with 70% ethanol for 30 s in the case of the leaves, 1 min for the stems, and 2 min for the roots, and all were subsequently washed with sterile water thrice. Thereafter, the plant parts were surface sterilized with 2% sodium hypochlorite for 30 s in the case of the leaves, 1 min for the stems, and 1.5 min for the roots. To ascertain the successful sterilization, the representative surface sterilized plant parts were placed at the center of nutrient agar (NA, HiMedia Pvt. Ltd., Mumbai, India) plates and incubated at 30°C for 48 h to observe the presence or absence of microbial growth on the plant surface. The surface sterilized samples were cut into small pieces and crushed along with 10 ml of 0.8% saline water in a sterile pestle and mortar. The dilutions (10^{-1}, 10^{-2}, and 10^{-3}) of the samples were made using 0.8% saline water. Each dilution of the sample (0.1 ml) was spread over NA, potato dextrose agar (PDA), R-2A, and Luria Bertani agar (LBA, HiMedia Pvt. Ltd., Mumbai, India) plates to obtain the endophytic bacteria diversity. The composition (g/L) of R-2A agar medium used as follows: Enzymatic digest of casein – 0.25; Enzymatic digest of animal tissue – 0.25; Acid hydrolysate of casein – 0.5; Yeast extract – 0.5; Glucose – 0.5; Starch soluble – 0.5; Dipotassium phosphate – 0.3; Magnesium sulfate heptahydrate – 0.05; Sodium pyruvate – 0.3; Agar-15. The plates were incubated at 30°C for 24 h. After incubation, the bacterial colonies with distinct colony morphology were subcultured on NA plates to obtain pure colonies. The pure cultures were maintained in the refrigerator at 4°C until further use.

Selection of potential antagonist(s)

During isolation, 255 bacterial isolates were obtained from different plant samples used in the present study. These isolates were preliminarily screened for antagonistic activity against fungal pathogens, *R. solani*, *S. rolfsii*, and *F. oxysporum* using a dual culture plate assay (Singh et al., 2016). Briefly, the fungal disc (5 mm diameter) was made by unplugging the fully grown fungal pathogens in PDA plates using the flame sterilized cork borer. The fungal disc was kept at the center of a fresh PDA plate and the bacterial endophytes to be tested were streaked on side of the Petri plate. The inoculated plates were kept for incubation at 28 ± 2°C for 7 days. After 7 days of incubation, the plates were observed for

any inhibitory zones. The bacterial endophytes showing strong inhibition (>5 mm radius of zone of inhibition) against all the test fungal pathogens were selected for further characterization.

Morphological and biochemical characterization of the selected bacterial endophytes

The morphological and biochemical characterization of the selected bacterial endophytes (TRO4, CLO5, and PLO3) was performed using standard protocols. To designate the strain number, the following rule was adopted: the first letter stands for the crop type (T-Tomato; C-Chickpea; P-Potato), the second letter stands for plant part (R-Root; L-Leaf) and the third letter stands for the place the crop was grown (O – Onhaich). The morphological parameters such as colony characteristics, Gram staining, and endospore staining and the biochemical characteristics such as catalase, oxidase, nitrate reductase, starch hydrolysis, Methyl Red Voges Proskaeur (MR-VP), indole production, citrate utilization, urease production, and hydrogen sulfide production were assessed according to Dubey and Maheswari (2008).

Evaluation of growth characteristics

The growth characteristics of the selected endophytes (TRO4, CLO5, and PLO3), such as specific growth rate and generation time, were determined according to Mageshwaran et al. (2014). Each bacterial culture was inoculated in a nutrient broth (1X) in 5 wells of 96-well microtitre plates and incubated for 72 h at 30°C in a growth kinetics chamber (Bioscreen C, Clover Scientific Pvt. Ltd., New Delhi) and the absorbance at 600 nm was recorded at 1-h intervals.

Characterization of selected strains for PGP traits

The PGP traits such as ammonia production, mineral solubilization (phosphate, potassium, and zinc), siderophore production, and hydrogen cyanide (HCN) were assessed in the selected strains. The selected bacterial isolates grown in a nutrient broth for 24 h were characterized for PGP traits qualitatively using the methods as described by Sharma et al. (2016) with slight modification (Singh et al., 2016).

Quantitative determination of antifungal property by dual culture assay

The selected bacterial endophytic isolates (TRO4, CLO5, and PLO3) were evaluated quantitatively for antifungal properties. The fungal disc was kept at the center of a fresh PDA plate and the selected bacterial endophyte was streaked (co-inoculate) on both sides of the Petri plates equidistant from the disc and incubated at 28 ± 2°C for 48 h. The inhibition percentage was calculated using the formula: inhibition of mycelial growth percentage = (A-B)/A × 100, where A is the diameter of mycelial growth of the fungal pathogen in the control plate, B is the diameter of mycelial growth of the fungal pathogen in the dual culture plate.

Molecular characterization of selected bacterial endophytes based on 16s rRNA gene sequencing

Bacterial endophytes were grown in NB at 28 ± 2°C for 24 h, centrifuged, and the pellets were separated. The pellets were used for DNA extraction. Genomic DNA of bacterial endophytes was extracted using Nucleopore gDNA Fungal Bacterial mini kit (Genetix Biotech Asia Pvt. Ltd., India, NB-7006 D) following the manufacturer protocols. To identify the selected bacterial endophytic isolates at the species level, PCR amplification of the 16s rRNA gene was done using the GoTaq Green master mix (M/s Promega, United States). The primer pair used in the PCR was: forward primer 27 F(AGA GTT TGA TCC TGG CTC AG) and reverse primer 1,492 R (TAC GGT TAC CTT GTT ACG ACT; GeNei, India). The PCR amplification for 16s rRNA (35 cycles) was done using a thermocycler (PeqSTAR, VWR, United States) and the PCR conditions were as follows: heat lid temperature 110°C, initial denaturation temperature 94°C for 4 min, denaturation temperature 94°C for 30 s, annealing temperature 52°C for 45 s, extension temperature 72°C for 90 s, and final extension temperature 72°C for 10 min. The PCR product was run in 1.2% agarose gel electrophoresis along with a 1 kb DNA ladder (Thermo Fisher Scientific, United States). The intact DNA band visible near 1,500 bp was cut with the help of a sterile scalpel blade and transferred into a 2 ml centrifuge tube. The 16s rRNA amplicons were purified with the help of a DNA purification kit (Nucleopore, Genetix Biotech Asia (P) Ltd., New Delhi). The purified 16s rRNA was sequenced using a 16 capillary ABI sequencer (ABI prism 3130XL) and sequence quality was checked using FinchTV software. The contigs were made using Bioedit software. The 16s rDNA sequences were BLAST in the NCBI database to obtain the identity of the cultures by finding the closest related species.

In vivo evaluation of selected endophytes for growth and antagonism against wilt complex disease in chickpea

The shortlisted endophytic *Bacillus subtilis* strains (TRO4, CLO5, and PLO3) were further evaluated for growth and

antagonism against wilt complex disease in chickpea plants. The present investigation was based on previous baseline studies which confirmed the suppression of pathogens by the selected endophytes. Pot culture experiments were conducted from October to December 2020 (winter season) at ICAR-NBAIM, Mau.

Preparation of inoculum

The inoculum of fungal pathogens was developed by inoculating the mother culture in a flask containing the autoclaved (two times) sand and maize grains at 8:1 (w/w) according to Rudresh et al. (2005) with a slight modification in that maize grains were used in place of sorghum. The inoculated flasks were incubated for 2 weeks at 28 ± 2°C and used for inoculating soil. The inoculum of endophytic bacteria was prepared by inoculating the culture (from agar plates) to the flask containing 100 ml of sterilized nutrient broth (1X) and incubated for 24 h under shaking conditions (125 rpm) at 28 ± 2°C. The colony-forming unit of the inoculum was calculated as 1×10^8 CFU ml^{-1}.

Experimental set-up

The experimental soil was collected from the agricultural farm, ICAR-NBAIM, Mau. The physicochemical properties of the soil used in the experiment were pH (8.0), electrical conductivity (0.81 dS/m), and organic carbon (0.39%). The experimental soil was moistened and autoclaved twice at 12 h intervals. Clean plastic pots (9 × 15 cm) were three-quarters filled with sterile soil. Each pot contained 2 kg of sterile soil. The fungal inoculum (10 g) with a colony-forming unit of 1.25×10^4 CFU g^{-1} was added to the pots and mixed properly. The inoculated pots were incubated for 10 days to develop and establish the fungal inoculum in the pots containing experimental soil (Rudresh et al., 2005). Seed priming with endophytes was done by suspending the surface sterilized chickpea seeds (susceptible cv. JG 62) in endophytes inoculum for 30 min according to Singh et al. (2021). Five seeds were sown in each pot.

Three sets of experiments were conducted to evaluate the biocontrol efficacy of bacterial endophytes against three soil-borne pathogens. The first set of experiments consisted of treatments to evaluate the biocontrol against *R. solani,* while the second set of experiments consists of treatments to evaluate the biocontrol against *S. rolfsii* and the third set of experiments consists of treatments to evaluate the biocontrol against *F. oxysporum* f.sp. *ciceri* (Table 1). A negative control [Uninoculated (UC)] was maintained in which neither pathogen nor endophyte was inoculated. Plants were irrigated with Jenson's liquid nutrient medium (Senthilkumar et al., 2009) once a week for 45 days. Five replications were maintained for each treatment. The experiment was conducted in a completely randomized design (CRD).

Further, the best performing endophytic *Bacillus subtilis* strains, TRO4 and CLO5 were evaluated for the induction of ISR in chickpea plants. There were three sets of experiments to evaluate the induction of ISR by bacterial endophytes in chickpea plants pre-challenged with soil-borne fungal pathogens. Each set of experiments consists of five treatments. For all the experiments, a negative control (Uninoculated (UC)) in which neither pathogen nor endophyte was inoculated. The resistant cultivar (RC; var. Avrodhi) was taken as a standard check. The first set of experiments consists of treatments pre-challenged with *R. solani*-A1 positive control (inoculated with *R. solani* alone), A2 inoculated with *B. subtilis* TRO4 + *R. solani* and A3 inoculated with *B. subtilis* CLO5 + *R. solani*. The second set of experiments consists of treatments to evaluate the biocontrol of *S. rolfsii-B1* positive control (inoculated with *S. rolfsii* alone), B2 inoculated with *B. subtilis* TRO4 + *S. rolfsii*, and B3 inoculated with *B. subtilis* CLO5 + *S. rolfsii*. The third set of experiments consists of treatments to evaluate the biocontrol of *F. oxysporum* f.sp. *ciceri* – C1 positive control (inoculated with. *F. oxysporum* f.sp. *ciceri* alone), C2 inoculated with *B. subtilis* TRO4 + *F. oxysporum* f.sp. *ciceri*, and C3 inoculated with *B. subtilis* CLO5 + *F. oxysporum* f.sp. *ciceri*. Five replications were maintained for each treatment. The experiment was conducted in a completely randomized design (CRD).

TABLE 1 Treatments detail.

S. No.	Treatments		
	Set-1: *R. solani*	**Set-2: *S. rolfsii***	**Set-3: *F. oxysporum* f.sp. *ciceri***
1.	A1: positive control (inoculated with *R. solani* alone)	B1: positive control (inoculated with *S. rolfsii* alone)	C1: positive control (inoculated with. *F. oxysporum* f.sp. *ciceri* alone)
2.	A2: inoculated with *B. subtilis* TRO4 + *R. solani*	B2: inoculated with *B. subtilis* TRO4 + *S. rolfsii*	C2: inoculated with *B. subtilis* TRO4 + *F. oxysporum* f.sp. *ciceri*
3.	A3: inoculated with *B. subtilis* CLO5 + *R. solani*	B3: inoculated with *B. subtilis* CLO5 + *S. rolfsii*	C3: inoculated with *B. subtilis* CLO5 + *F. oxysporum* f.sp.*ciceri*
4.	A4: inoculated with *B. subtilis* PLO3 + *R. solani*	B4: inoculated with *B. subtilis* PLO3 + *S. rolfsii*	C4: inoculated with *B. subtilis* PLO3 + *F. oxysporum* f.sp. *ciceri*
5.	A5: Carbendazim at 2 g/kg of seeds + *R. solani* (chemical control).	B5: Carbendazim at 2 g/kg of seeds + *S. rolfsii* (chemical control)	C5: Carbendazim at 2 g/kg of seeds + *F. oxysporum* f.sp. *ciceri* (chemical control)

Assessment of disease incidence and plant growth

Germination (%) was recorded 7 days after sowing. The plants were observed for the appearance of disease symptoms at 15, 30, and 45 days after sowing (DAS). A numerical disease rating was assigned as follows: 0-healthy seedlings; 1-brown lesions on collar/root region; 3-stunted growth; 4-dead plants with completely dried leaves. Mean Disease Rate (MDR) and Percentage Disease Incidence (PDI) of germinated plants were calculated according to the formula described by Senthilkumar et al. (2009) as given here.

$$\mathrm{MDR} = \left[(a*0)+(b*1)+(c*2)+(d*3)+(e*4)\right] / (a+b+c+d+e)$$

where *a*, *b*, *c*, *d*, and *e* are the number of plants with a disease rating of 0, 1, 2, 3, and 4, respectively.

$$\mathrm{PDI} = \frac{\mathrm{MDR}*100}{4(\text{maximum grade})}$$

At 45 DAS, the plants were uprooted and the roots were washed using slow-running tap water and the observations such as plant height (cm), the number of branches per plant, and dry weight of plant biomass (after drying in an oven at 60°C for 6 h) were recorded using standard protocols.

Analysis of root morphology

Forty-five days after sowing, chickpea plants from three replicates of all the treatments were uprooted and washed, and cleaned roots were used to study the root architecture. The root parameters such as root length (mm), surface area (cm^2), the average diameter (mm), and root volume (cm^3) were determined using a Hewlett Packard scanner and analyzed using the WinRHIZO V. 2002\u00B0C software (Regent Instruments Inc. Ltd. Quebec, Canada) according to Singh et al. (2017).

Confocal scanning laser microscopic analysis

A separate experimental trial was conducted under gnotobiotic conditions to evaluate the colonization potential of bacterial endophytes in chickpea plants. The colonization pattern of *B. subtilis* strains TRO4 and CLO5 in 45-day-old chickpea roots was examined under the Confocal Scanning Laser Microscope (CSLM; Nikon Eclipse 90i). Freshly collected roots were stained with LIVE/DEAD™ BacLight bacterial viability stain (Invitrogen, United States) to localize the colonization of inoculated bacteria as described by Sahu et al. (2019). The colonization was compared with control plant roots with similar optical adjustments. The images were processed using NIS Element 3.2.3 software (Nikon, Japan).

In vivo evaluation of bacterial endophytes on induction of ISR in chickpea

Effect of endophytes inoculation on the accumulation of superoxide radicals

The accumulation of superoxide radicals (O^{2-}) in the leaf was visualized under a stereomicroscope after staining with nitroblue tetrazolium (NBT) as described by Sahu et al. (2019). The leaves collected from chickpea plants pre-challenged with *R. solani* after 45 DAS were stained with NBT and the formation of blue color formazan was taken as an indication of superoxide accumulation.

Effect of endophytes inoculation on plant defense-related enzymes

To evaluate the effect of endophytes inoculation on ISR in chickpea plants, defense-related enzymes *viz.*, phenylalanine ammonia-lyase (PAL) and peroxidase (PO) were assayed (Sadasivam and Manickam, 1996). For estimation of PAL activity, a leaf tissue sample (0.5 g) was extracted in 4 ml of 0.2 M borate buffer (pH 8.7) with 1.4 mM β-mercaptoethanol. Enzyme extract (200 µl) was added with 500 µl borate buffer, 1 ml of 0.1 M L-phenylalanine, and 1.3 ml of distilled water. The mixture was incubated at 32°C for 30 min and the reaction was terminated by adding 500 µl of Trichloroacetic acid. The activity was measured at 290 nm and expressed in µmole of *trans*-cinnamic acid g^{-1} fresh weight. For the estimation of PO activity, 0.5 g of leaf tissue was extracted in 4 ml of 50 mM phosphate buffer. Enzyme extract (200 µl) was added with 3 ml of 50 mM phosphate buffer, 0.5 ml of 20 mM guaiacol, and 300 µl of 12.3 mM H_2O_2. The absorbance was measured at 436 nm.

Effect of endophytes inoculation on the expression of PR genes

The expression of PR genes (*60srp* and *IFR*) was studied using the semi-quantitative reverse transcriptase PCR (semi-q RT-PCR) along with the housekeeping gene CHS, CAC and GADPH. The pathogen was inoculated and plants were raised as described in section 2.9. Total RNA isolation, cDNA synthesis, and PCR amplification of housekeeping and PR genes were performed according to Sahu et al. (2019). The primer sequences for PCR amplification of defense-related chickpea genes are given in Supplementary Table 3.

Statistical analysis

The data collected in this study were analyzed in a completely randomized design (CRD) using a one-way analysis of variance

(ANOVA; WASP.1; ICAR research complex, Goa). For all analyses, the differences were considered to be significant at $p \leq 0.05$.

Results

Assessment of bacterial endophytes for antagonistic activity and PGP traits under *in vitro* conditions

In the present study, an attempt was made to isolate bacterial endophytes from surface-sterilized plant parts of seven different crop plants. The successful sterilization of plant parts was ascertained by the absence of any microbial growth in the surface-sterilized plant part kept on NA medium (data not shown). In total, 255 bacterial endophytes were isolated from different plant parts (stems, leaves, and roots) of the collected plant samples. Among the crop plants, the greatest number of isolates was obtained from wheat (54), followed by chickpea (49), berseem (41), potato (40), tomato (30), mustard (27), and green pea (14). Among the plant parts, the greater number of isolates was obtained from the roots (91), followed by the stems (84), and leaves (80; Table 2). All the isolated bacterial endophytes were subject to screening for antifungal properties against all three pathogens on a dual plate culture assay. The number of isolates showing inhibition against *R. solani*, *S. rolfsii*, and *F. oxysporum* f.sp. *ciceri*, individually, and all three pathogens simultaneously, were 55, 45, 16, and 16, respectively. Out of which, the number of isolates showing inhibition of more than a 5 mm radius was 16, 15, 6, and 3, each pathogen and all three, respectively (Table 2). The three bacterial isolates showing inhibition (>5 mm radius) against all three test fungal pathogens were considered for further experiments.

Thus, out of 255 bacterial isolates, 3 isolates (TRO4, CLO5, and PLO3) showed strong antagonism against all three fungal pathogens, *R. solani*, *S. rolfsii*, and *F. oxysporum* f.sp. *ciceri*. The biochemical characterization showed that all three selected bacterial endophytes were positive for Gram staining, endospore staining, catalase, oxidase, nitrate reductase, starch hydrolysis, Voges-Proskauer, and citrate utilization while they were negative for methyl red, indole, urease, and H_2S production test. Morphologically, the colonies were a cream color, rough, circular, entire surface, and opaque (results not shown). The results of morphological and biochemical characterization showed the selected bacterial endophytes

TABLE 2 Screening of bacterial endophytes against soil-borne fungal pathogens.

Crop	Plant part	No. of total isolates	Number of isolates antagonistic against			
			R. solani	*S. rolfsii*	*F. oxysporum* f.sp. *ciceri*	All the three pathogens
Chickpea	Leaf	15	06 (02)	05 (02)	03 (01)	03 (01)
	Stem	19	09 (02)	–	–	–
	Root	15	01	–	–	–
Tomato	Leaf	08	03 (03)	01	01 (01)	01
	Stem	16	–	02	–	–
	Root	06	03 (02)	04 (02)	03 (02)	03 (01)
Wheat	Leaf	09	–	03	–	–
	Stem	13	04	02	02	02
	Root	32	03	03 (01)	02	02
Berseem	Leaf	15	06	02	01	01
	Stem	10	05 (03)	04 (04)	–	–
	Root	16	03	02	–	–
Mustard	Leaf	12	1	–	–	–
	Stem	08	–	01	–	–
	Root	07	02 (01)	03 (02)	02	02
Potato	Leaf	14	02 (02)	03(02)	02(02)	02(01)
	Stem	17	01	02	–	–
	Root	09	06 (01)	02	–	–
Green pea	Leaf	07	–	06 (02)	–	–
	Stem	01	–	–	–	–
	Root	06	–	–	–	–
Total		255	55 (16)	45 (15)	16 (06)	16 (03)

The value in the brackets shows the number of isolates showing strong inhibition (>5 mm radius of zone of inhibition) against the pathogen.

belong to *Bacillus* sp. The specific growth rate (μ) of the endophytes was 0.38 (h^{-1}) for TRO4 and CLO5 and 0.43 (h^{-1}) for PLO3. The molecular characterization of 16s rRNA sequences and identification based on the closest related species obtained from the NCBI database revealed that the selected bacterial endophytes belong to different strains of *B. subtilis* (Table 3). The 16s rRNA sequences were submitted to the NCBI database and the GenBank accession numbers were obtained for bacterial endophytes (Table 3). The bacterial endophytes (TRO4, CLO5, and PLO3) were submitted to the National Agriculturally Important Microbial Culture Collection (NAIMCC), Mau, India, and the accession numbers were obtained (Table 3).

The endophytic *B. subtilis* strains (TRO4, CLO5, and PLO3) were assessed for their antagonistic property by evaluating the inhibition of fungal growth percentage using a dual culture assay and various plant growth promoting characteristics. All the selected endophytes showed more than 50% inhibition of the tested pathogens in a dual plate assay. The bacterial endophytes (CLO5 and PLO3) showed a higher inhibition percentage (64.3%) against *R. solani*, whereas TRO4 had a higher inhibition percentage (83.8 and 70.9%) against *S. rolfsii* and *F. oxysporum* f.sp. *ciceri,* respectively (Table 4). The qualitative determination of plant growth-promoting traits showed that all the selected endophytes were positive for ammonia and siderophore production. The bacterial endophytes, TRO4 and CLO5 were positive for IAA production. All the selected endophytes were negative for mineral solubilization (phosphate, potassium, and zinc), chitinase activity, and HCN production. The antifungal activity of TRO4 and CLO5 against all three fungal pathogens tested is depicted in Figure 1.

Bio-efficacy of endophytes on growth and antagonism against wilt complex

A pot culture experiment was conducted in the winter season from November–December, 2020 to evaluate the effect of seed priming with bacterial endophytes on plant growth and the suppression of wilt complex disease in chickpea plants. Three sets of experiments (one set for each pathogen) were conducted to evaluate the ability of the chickpea plants to suppress root rot caused by *R. solani*, collar rot caused by *S. rolfsii,* and wilt caused by *F. oxysporum* f.sp. *ciceri* using bacterial endophytic strains (TRO4, CLO5, and PLO3). The plant growth characteristics such as plant height, dry plant biomass, and the number of branches per plant were recorded at 45 DAS. Germination percentage was recorded at 10 DAS. The disease incidence was recorded at 15, 30, and 45 DAS. The results on the effect of bacterial endophytes on germination percentage, percent disease incidence, and dry plant biomass (g $plant^{-1}$) at 45 DAS are given in Figure 2. The MDR and PDI recorded at 15, 30, and 45 days are given in Supplementary Table 1. The effect of bacterial endophytes on plant height and the number of branches per plant is given in Supplementary Table 2. The suppression of soil-borne fungal pathogens by bacterial endophytes (TRO4 and CLO5) in chickpea plants (45 days old) is pictorially depicted in Figure 3.

Rhizoctonia solani pre-challenged soil

Germination percentage was higher in the bacterial endophytes (TRO4 and CLO5) treated seeds (100%) followed by the chemical (Carbendazim at 2 g kg^{-1} of seeds) treated seeds (93.3%). While the germination percentage was lower in the PLO3-treated seeds (10). The dry plant biomass (g $plant^{-1}$) was higher (1.46) in the PLO3-treated seeds and lower in the uninoculated control (0.74). The plant height (cm) was higher in

TABLE 3 Molecular characterization of the selected bacterial endophytes based on 16s rRNA gene sequence analysis.

Isolate	GenBank accession number	Closest related species	% of similarity	Query size (base pair)	NAIMCC accession no.
TRO4	MW888880	*Bacillus subtilis* strain SEGB1 (MN565269.1)	100	1,396	B-02794
CLO5	MW888882	*Bacillus subtilis* strain soil G2B (MT641205.1)	100	1,405	B-02790
PLO3	MW888883	*Bacillus subtilis* sub sp. stercosis (MN704443.1)	100	1,401	B-02792

TABLE 4 Antifungal properties and PGP of selected bacterial endophytes.

Isolate	% of inhibition			Plant Growth Promoting traits							
	Rhizoctonia solani	*Sclerotium rolfsii*	*Fusarium oxysporum*	I	II	III	IV	V	VI	VII	VIII
TRO4	58.9	83.8	70.9	+	–	–	–	+	–	–	+
CLO5	64.3	73.3	69.2	+	–	–	–	+	–	–	+
PLO3	64.3	62.9	66.5	+	–	–	–	+	–	–	–

Ammonia production (I), Phosphate solubilization (II), Potassium solubilization (III), Zinc solubilization (IV), Siderophore Production (V), HCN production (VI), Chitinase production (VII), IAA production (XIII). The (+) and (–) signs indicate positive and negative for PGP traits, respectively.

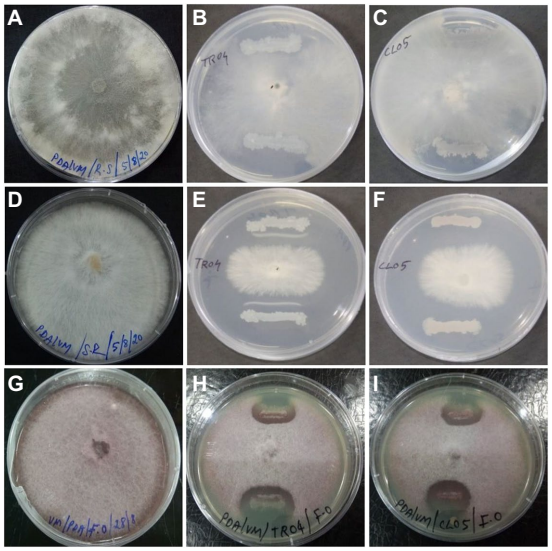

FIGURE 1
Antagonistic property of endophytic *Bacillus subtilis* strains TRO4 and CLO5 against soil-borne fungal pathogens. **(A)** *R. solani* control, **(B)** *R. solani* vs. TRO4, **(C)** *R. solani* vs. CLO5, **(D)** *S. rolfsii* control, **(E)** *S. rolfsii* vs. TRO4, **(F)** *S. rolfsii* vs. CLO5, **(G)** *F. oxysporum* control, **(H)** *F. oxysporum* vs. TRO4, **(I)** *F. oxysporum* vs. CLO5.

the TRO4-treated seeds (57.4) and lower in the uninoculated control (40.7). The number of branches per plant varied between 2.5 to 3.0 among the treatments. The MDR and PDI were not recorded from 0 up to 30 DAS as there were no symptoms occurring during this period. At 45 DAS, the PDI was recorded higher in the positive control (13.75) and lower in the PLO3-treated seeds (0.5; Figures 2B, 3A). The PDI of the TRO4 and CLO5 treatments were significantly ($p \leq 0.05$) lower than the positive control.

Sclerotium rolfsii pre-challenged soil

In general, the germination percentage was lower in *S. rolfsii* pre-challenged soil. The maximum germination percentage was observed in TRO4-treated seeds (80) and the minimum germination percentage was observed in PLO3-treated seeds (40). The dry plant biomass (g plant^{-1}) was higher in the TRO4 treatment (1.32) and lower in the positive control (only pathogen; 0.61). The plant height (cm) was higher in the TRO4-treated seeds (53.8) and lower in the uninoculated control (40.7). The number of branches per plant was higher in TRO4 and CLO5 treated seeds (3.0) and lower in PLO3-treated seeds (2.0). The collar rot disease incidence occurred during the initial stages of plant growth. At 15 DAS, the PDI was higher in the PLO3-treated seeds (37.5) and lower in the TRO4-treated seeds (5). There was no occurrence of disease recorded in the uninoculated control. At 30 DAS, PDI was higher in the PLO3-treated seeds (82.5) and lower in the Carbendazim-treated seeds (10.5). As recorded at 15 DAS, there was no occurrence of disease in the uninoculated control. At 45 DAS, PDI was higher in the PLO3-treated seeds (82.5) and lower in the TRO4-treated seeds (23; $p \leq 0.05$; Figures 2B, 3B). The PDI recorded in the positive control was 58.25.

F. oxysporum f.sp. *ciceri* pre-challenged soil

The germination percentage was recorded higher in Carbendazim treated seeds (100) followed by TRO4 treated seeds (93.3) and lower in CLO5 and PLO3 treated seeds (60). The dry plant biomass (g/plant) was recorded higher in the endophytes (TRO4, CLO5, and PLO3) treated seeds compared to the uninoculated control and positive control. The plant height (cm) was recorded higher in the CLO5-treated seeds (51.0) and lower in the uninoculated control (40.7). The number of branches per plant was higher in the CLO5-treated seeds (3.5) and lower in Carbendazim-treated seeds (2.7). At 15 DAS, the PDI was higher in the PLO3-treated seeds (33.3) as compared to the positive control (1.75). No symptoms occurred in the TRO4, CLO5, and uninoculated treatments. Similarly, at 30 DAS, no symptoms occurred in the TRO4, CLO5, and uninoculated treatments whereas a higher PDI was recorded in the PLO3-treated seeds (49.25) as compared to the chemical control (0.5). At 45 DAS, PDI was higher in the PLO3-treated seeds (49.25) and lower in the TRO4-treated seeds (7.5; $p \leq 0.05$; Figures 2B, 3C). The PDI recorded in the positive control (only pathogen) was 20.75.

Effect of endophytic *Bacillus subtilis* strains on root growth of chickpea

The effect of inoculation of endophytic *B. subtilis* strains on root growth parameters of chickpea plants pre-challenged with soil-borne fungal pathogens was evaluated. The different root growth parameters estimated were root length (mm), surface area (cm^2), root diameter (mm), and root volume (cm^3). The results are given in Table 5.

Rhizoctonia solani pre-challenged soil

In soil pre-challenged with *R. solani*, the root length (mm) was significantly higher (1056.7) in the TRO4-inoculated seeds followed by the CLO5-treated seeds (750) and lower in the uninoculated negative control (156.3). The root surface area (cm^2) was higher in the TRO4-treated seeds (39.4) followed by the CLO5-treated seeds (31.2) and lower in the uninoculated negative control (17.9). However, the root diameter (mm) was found higher in the uninoculated negative control (0.58) and lower in the positive control (0.45). The root volume (cm^3) was recorded higher in the TRO4-treated seeds (1.47) followed by the CLO5-treated seeds (1.27) and lower in the uninoculated control (0.55).

Sclerotium rolfsii pre-challenged soil

In soil pre-challenged with *S. rolfsii*, the root length (mm) was recorded higher in the TRO4-treated seeds (860) followed by the CLO5-treated seeds (500) and lower in the uninoculated control (156.3). The root surface area (cm^2) was found higher in the CLO5-treated seeds (38.1) followed by the carbendazim-treated

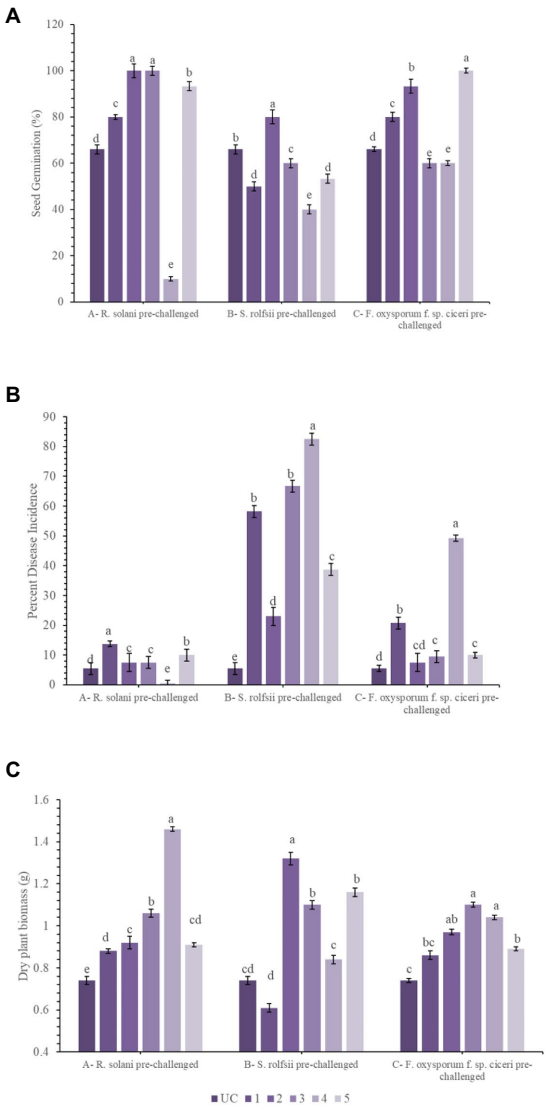

FIGURE 2
Effect of endophytes inoculation on plant growth and disease incidence in chickpea [**A**, Seed Germination (%); **B**, Percent Disease Incidence; **C**, Dry plant biomass (g)]. Treatment details: UC-Uninoculated (negative control which is not inoculated with a pathogen or bacterial strain). A1, B1, C1 – Positive control of *R. solani*, *S. rolfsii,* and *F. oxysporum* f. sp. *ciceri*, respectively in which only pathogen inoculated. A2, B2, C2-Respective pathogen + *B. subtilis* strain TRO4 inoculated. A3, B3, C3-Respective pathogen + B. *subtilis* strain CLO5 inoculated. A4, B4, C4-Respective pathogen + *B. subtilis* strain PLO3 inoculated. A5, B5, C5-Chemical control (Respective pathogen + Carbendazim at 2g per kg of seed). The PDI was calculated based on the number of plants germinated. Data are mean (n=5) and vertical bars represent standard deviation.

seeds (28.3) and lower in the uninoculated control (17.9). The root diameter (mm) was found higher in the TRO4-treated seeds (0.61) followed by the uninoculated control (0.58) and lower in the positive control (0.41). The root volume (cm^3) was recorded higher in the TRO4-treated seeds (2.03) followed by the carbendazim-treated seeds (1.7) and lower in the positive control (0.39).

Fusarium oxysporum f.sp. *ciceri* pre-challenged soil

In soil pre-challenged with *F. oxysporum* f.sp. *ciceri*, the root length (mm) was higher in the TRO4-treated seeds (1010) followed by the CLO5-treated seeds (690) and lower in the uninoculated control (156.3). The root surface area (cm^2) was higher in the TRO4-treated seeds (37.1) followed by the CLO5-treated seeds (34.3) and lower in the uninoculated control (17.9). The root diameter (mm) was higher in the CLO5-treated seeds (0.59) and the uninoculated control (0.58), whereas, root diameter was recorded lower in the positive control (0.49). The root volume (cm^3) was recorded higher in the TRO4-treated seeds (2.3) followed by the CLO5-treated seeds (1.5) and lower in the uninoculated control (0.55).

Confocal scanning laser microscopic analysis of endophytic colonization

The colonization studies using confocal scanning laser microscopy indicated that root tissues of chickpea plants inoculated with bacterial endophytes (TRO4 and CLO5) produced more signals as compared to the uninoculated control (Figure 4). Confocal microphotograph clearly indicated that the endophyte TRO4 primarily produced micro-aggregates, while CLO5 produced macro-aggregates on the root surface (Figures 4B,C, respectively).

Effect of endophytic *Bacillus subtilis* strains on induction of ISR in chickpea

The effect of inoculation with endophytic *B. subtilis* strains on the induction of ISR in chickpea plants pre-challenged with soil-borne fungal pathogens was evaluated. The different ISR parameters estimated were the accumulation of superoxide radicals, plant defense enzymes, and the up-regulation of defense-related genes.

Accumulation of superoxide radicals

Superoxide (O^{2-}) accumulation in chickpea leaves was found to vary among the treatments (Figure 5). The visualization of superoxide accumulation in *R. solani* pre-challenged treatments under stereomicroscope is given in Figure 6. NBT staining revealed that the positive control plants (only pathogen challenged) had the highest accumulation of superoxide. The negative control plants had the least accumulation since there was no pathogen inoculation and thus the generation of oxidative stress was also low. Reduced superoxide accumulation was observed in chickpea plants treated with endophytes, TRO4 followed by CLO5.

FIGURE 3
Effect of bacterial endophytes on suppression of root wilt complex disease in chickpea plants (**A**, *R. solani* pre-challenged; **B**, *S. rolfsii* pre-challenged; **C**, *F. oxysporum* f. sp. *ciceri* pre-challenged). Treatment details: UC-Uninoculated (negative control which is not inoculated with a pathogen or bacterial strain). A1, B1, C1 – Positive control of *R. solani*, *S. rolfsii,* and *F. oxysporum* f. sp. *ciceri*, respectively in which only pathogen inoculated. A2, B2, C2 – Respective pathogen + *B. subtilis* strain TRO4 inoculated. A3, B3, C3 – Respective pathogen + *B. subtilis* strain CLO5 inoculated. The age of the plant under observation was 45days after sowing.

Plant defense enzymes

The analysis of defense enzymes Peroxidase (PO) and Phenylalanine Ammonia-Lyase (PAL) in chickpea leaves showed an increased level of enzyme activity in the endophyte-inoculated plants pre-challenged with soil-borne fungal pathogens than the positive control (only pathogen challenged; Figure 7). The highest activity of PAL (4513; µmol TCA g^{-1} of fresh weight) was recorded in the CLO5-treated chickpea plants pre-challenged with *F. oxysporum* f.sp. *ciceri* while the lowest activity (3537) was observed in the uninoculated plants (negative control). Similarly, the highest PO activity (7.09; units g^{-1} of fresh weight) was observed in the CLO5-treated chickpea plants pre-challenged with *S. rolfsii* while the lowest activity (4.64) was observed in the *F. oxysporum* f.sp. *ciceri* pre-challenged plants.

Up-regulation of defense-related genes

Semi-quantitative RT-PCR analysis of defense-related genes was performed using gene-specific oligonucleotides in endophytes-inoculated and pathogen-challenged chickpea plants (cv. JG-62; Figure 8). A resistant cultivar (var. avrodhi) was used as a standard check. The expression of PR genes, *60srp* (gene for 60s ribosomal protein), and *IFR* (Isoflavone reductase) were studied with the normalization of *CAC* (Clathrin adaptor complexes medium subunit family protein). The stable expression of the housekeeping gene, *CAC,* was noticed in all the treatments. The results showed the expression of the *60srp* gene was highest in endophyte-inoculated and pathogen-inoculated plants than in pathogen-alone and resistant cultivars. The expression of the *60srp* gene was higher in the CLO5-inoculated and plants challenged with *F. oxysporum* f.sp. *ciceri*. In general, the expression level of the *IFR* gene was higher in endophyte-inoculated and pathogen-challenged plants. The increase in expression of the IFR gene was noticed in the CLO5-inoculated plants and plants challenged with *F. oxysporum* f.sp. *ciceri*.

Discussion

The irrational use of chemical fungicides in agriculture causes serious health problems to humans and animals along with irreparable deleterious effects on the environment. Researchers worldwide have undertaken research on environmentally friendly agents as an alternative to toxic chemical fungicides. Biocontrol is one of the strategies for the eco-friendly management of crop diseases. It uses naturally occurring bio-agents such as viruses, bacteria, fungi, algae, insects, etc., to control crop diseases and pests, and endophytes are one of them (Bacon and White, 2000). Bacterial endophytes are a group of bacteria that reside inside the root, stem, leaves, and other parts of a plant. They are potential bio-agents as they provide localized protection to the host plant against the invasion of pathogenic fungi and bacteria (Sahu et al., 2020; Singh et al., 2020a). They produce antimicrobial compounds, provide systemic resistance to the host plant and improve plant growth by solubilizing the mineral nutrients (phosphorus, potassium, zinc etc.), fixing atmospheric nitrogen, producing siderophore, IAA, etc. (Ryan et al., 2007). Previously, several attempts have been made to isolate bacterial endophytes from different crops such as Rice, Maize, Peanut, Banana, Soybean, Medicinal crops, etc. (Souza et al., 2014; Gond et al., 2015; Zhao et al., 2015). In the present study, we have identified three potential bacterial endophytes (TRO4, CLO5, and PLO3) out of

TABLE 5 Effect of bacterial endophytes inoculation on root parameters of chickpea challenged with soil-borne fungal pathogens.

Treatments	Root length (mm)	Surface area (cm^2)	Average root dia (mm)	Root volume (cm^3)
R. solani pre-challenged				
UC	156.3^{e}	17.9^{c}	0.58^{a}	0.55^{c}
A1	317.0^{d}	21.2^{c}	0.45^{c}	0.63^{c}
A2	1056.7^{a}	39.4^{a}	0.54^{a}	1.47^{a}
A3	750.0^{b}	31.2^{b}	0.57^{a}	1.27^{ab}
A4	403.7^{c}	29.8^{b}	0.51^{b}	1.07^{b}
A5	736.7^{b}	27.0^{b}	0.56^{ab}	1.0^{b}
CD (0.05%)	66.77	5.37	0.05	0.275
CV	6.58	10.85	5.48	15.49
S. rolfsii pre-challenged				
UC	156.3^{f}	17.9^{c}	0.58^{ab}	0.55^{d}
B1	310.0^{e}	18.7^{c}	0.41^{d}	0.39^{d}
B2	860.0^{a}	38.1^{a}	0.61^{a}	2.03^{a}
B3	500.0^{b}	26.3^{b}	0.53^{bc}	1.0^{c}
B4	432.0^{d}	19.2^{c}	0.53^{bc}	0.9^{c}
B5	463.0^{c}	28.3^{b}	0.51^{c}	1.7^{b}
CD (0.05%)	24.13	2.15	0.05	0.24
CV	2.99	4.89	5.5	12.48
F. oxysporum f.sp. *ciceri* pre-challenged				
UC	156.3^{e}	17.9^{e}	0.58^{ab}	0.55^{d}
C1	278.7^{d}	18.5^{e}	0.49^{c}	0.9^{c}
C2	1010.0^{a}	37.1^{a}	0.57^{ab}	2.3^{a}
C3	690.0^{b}	34.3^{b}	0.59^{a}	1.5^{b}
C4	465.7^{c}	28.5^{c}	0.52^{bc}	1.3^{b}
C5	420.6^{c}	23.6^{d}	0.58^{ab}	0.9^{c}
CD (0.05%)	57.69	2.38	0.06	0.33
CV	6.44	5.04	6.29	14.82

Treatment details: UC – Uninoculated (negative control). A1, B1, C1 – Positive control of *R. solani*, *S. rolfsii* and *F. oxysporum* f.sp. *ciceri*, respectively. A2, B2, C2 – Respective pathogen + *B. subtilis* strain TRO4 inoculated. A3, B3, C3 – Respective pathogen + *B. subtilis* strain CLO5 inoculated. A4, B4, C4 – Respective pathogen + *B. subtilis* strain PLO3 inoculated. A5, B5, C5 – Chemical control (Respective pathogen + Carbendazim @ 2 g per kg of seed). The treatment with the same superscript within a column does not differ significantly at $p = 0.05$.

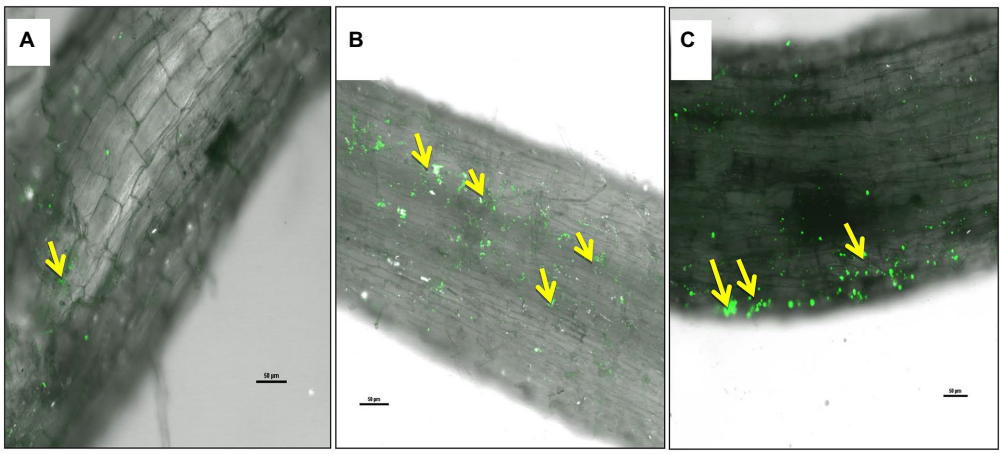

FIGURE 4
Confocal Scanning Laser Microscopic images indicating colonization of bacterial endophytes in chickpea roots using LIVE/DEAD™BacLight™ Bacterial viability staining, yellow arrows indicating endophytic colonization in the roots. **(A)** Uninoculated control root, **(B)** *B. subtilis* TRO4 inoculated root, **(C)** *B. subtilis* CLO5 inoculated root.

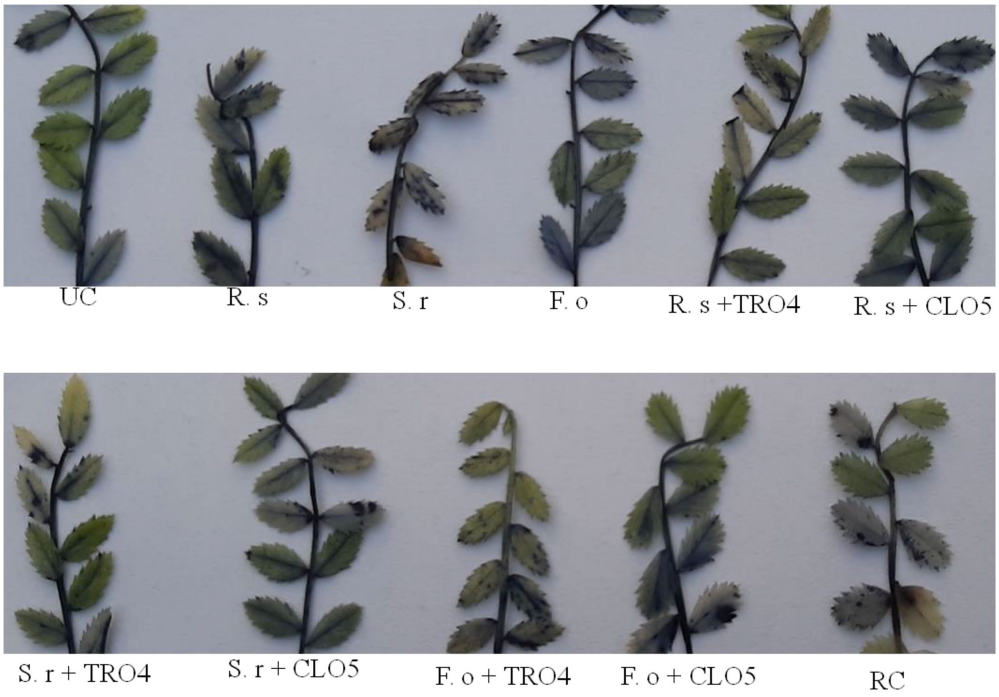

FIGURE 5
Effect of bacterial endophytes on the accumulation of superoxide radicals in chickpea leaves. UC, Un-inoculated control in which neither pathogen nor bacterial strain inoculated; R.s, *Rhizoctonia solani*; S.r, *Sclerotium rolfsii*; F. o, *Fusarium oxysporum* f. sp. *ciceri*; RC, Resistant cultivar.

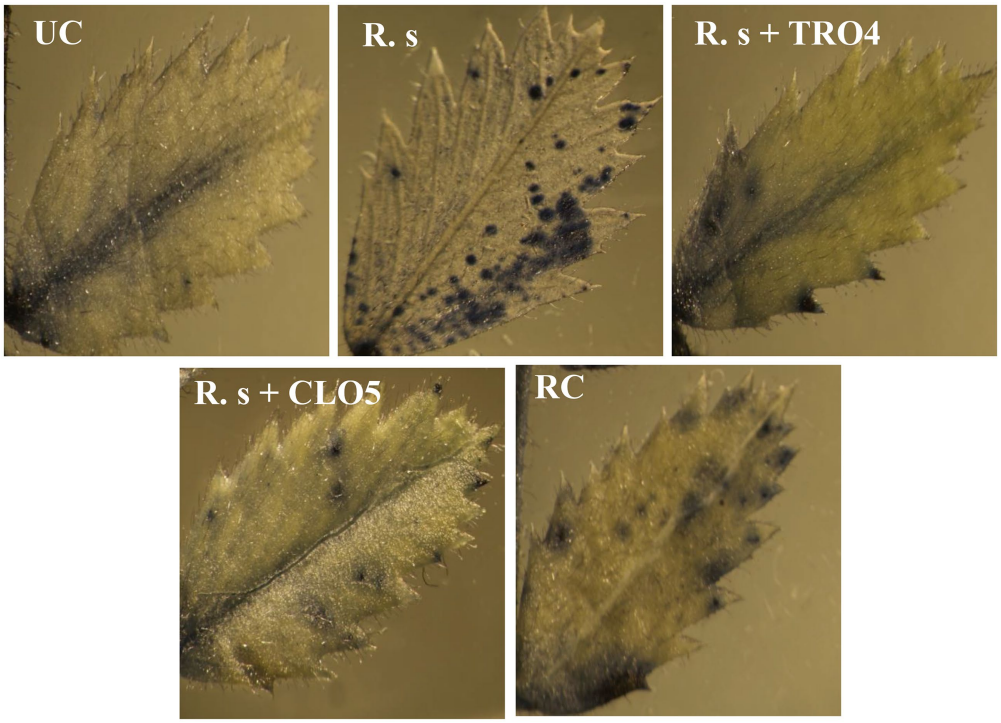

FIGURE 6
Visualization of accumulation of superoxide radicals in chickpea leaves under a stereomicroscope. UC, Un-inoculated control in which neither pathogen nor bacterial strain inoculated; R.s, *Rhizoctonia solani*; S.r, *Sclerotium rolfsii*; F. o, *Fusarium oxysporum* f. sp. *ciceri*; RC, Resistant cultivar.

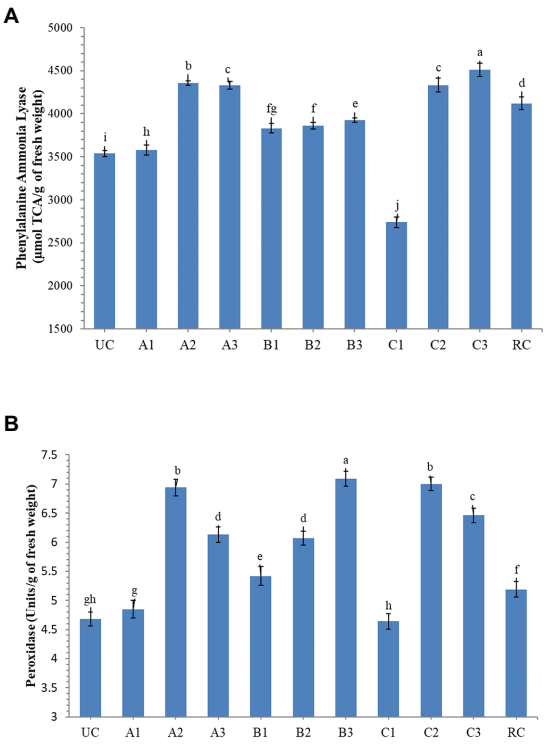

FIGURE 7
Effect of bacterial endophytes inoculation on plant defense enzymes of chickpea challenged with soil-borne fungal pathogens. **(A)** Phenylalanine Ammonia Lyase; **(B)** Peroxidase. Treatment details: UC-Uninoculated (negative control which is not inoculated with a pathogen or bacterial strain). A1, B1, C1 – Positive control of *R. solani*, *S. rolfsii*, and *F. oxysporum* f. sp. *ciceri*, respectively in which only pathogen inoculated. A2, B2, C2 – Respective pathogen + *B. subtilis* strain TRO4 inoculated. A3, B3, C3 – Respective pathogen + *B. subtilis* strain CLO5 inoculated. RC, Resistant cultivar. Data are mean (n =5) and vertical bars represent standard deviation.

255, based on the screening of antagonistic activity against all the three fungal pathogens (*R. solani*, *S. rolfsii*, and *F. oxysporum* f.sp. *ciceri*). The molecular identification of these three endophytes revealed that they are different strains of *Bacillus subtilis*. The results are in agreement with the previous reports where most of the potential bacterial endophytes as a biocontrol agent were identified as *Bacillus* and *Pseudomonas* irrespective of the crops used for isolation (Sun et al., 2013; Chen et al., 2014; Zhao et al., 2015; Kumar et al., 2016; Vinodkumar et al., 2017). In a similar study, the inhibition percentage of soil-borne fungal pathogens by potent bacterial endophytes was 50 to 70% (Sahu et al., 2019). The endophytic *Bacillus subtilis* has also been reported in other studies for the control of *Fusarium* and other plant pathogens through the production of diffusible and volatile inhibitory compounds (Hazarika et al., 2019). The usefulness of endophytic *Bacillus subtilis* was also proven in the biocontrol of take-all disease in wheat in which the bacterium was found to have endophytic colonization and disintegrate the cytoplasm of the fungal pathogen (Chung et al., 2008; Liu et al., 2009).

The biocontrol efficacy of selected bacterial endophytes against the wilt complex disease in chickpea plants was evaluated under pot culture conditions in soil pre-challenged with fungal pathogens, i.e., *R. solani*, *S. rolfsii*, and *F. oxysporum* f.sp. *ciceri*. The results revealed that the incidence of collar rot caused by *S. rolfsii* occurred in the initial stage whereas the incidences of root rot caused by *R. solani* and fungal wilt caused by *F. oxysporum* f.sp. *ciceri* occurred at later stages. A similar observation was made in the evaluation of *Trichoderma* in suppressing wilt complex disease in chickpea plants (Rudresh et al., 2005). The results of the pot experiment showed that the chickpea plants inoculated with bacterial endophytes (TRO4 and CLO5) had a lower PDI as compared to pathogen alone (positive control; Figures 2, 3). Similarly, the vigor, plant growth characteristics, and germination percentage in chickpea plants were higher in TRO4 and CLO5 treated seeds. Similar results on the effectiveness of bacterial endophytes in increasing the germination percentage, vigor, and plant growth characteristics were reported in tomato plants challenged with *S. rolfsii* (Sahu et al., 2019) and rice plants challenged with *R. solani* (Sahu et al., 2020). In a similar experiment, the disease control percentage (60–65) of wilt complex in chickpea plants was recorded in seeds treated with *T. viride* at 8 g kg^{-1} or soil applied with *T. harzianum* (Kaur and Mukhopadhyay, 1992; Rajput et al., 2010). The different root growth parameters, root length (mm), surface area (cm^2), root diameter (mm), and root volume (cm^3) were significantly ($p \leq 0.05$) improved in TRO4 and CLO5 inoculated chickpea plants. The improved root growth parameters provide the host plant resistance against the invasion of soil-borne fungal pathogens. These results are in agreement with Singh et al. (2017) where inoculation with zinc solubilizing bacteria, *B. subtilis* DS-178 and *Arthrobacter* sp. DS – 179, improved the root growth parameters in wheat.

Bacterial endophytes able to successfully colonize the plant tissue could impart protection from biotic and abiotic stresses to the host plants. The analysis of the root tissue of chickpea plants using confocal microscopy revealed that the endophytic *B. subtilis* strains TRO4 and CLO5 inoculated plants produced more signals than the control. The uninoculated control plants also showed weak signals which might be due to their native endophytes (Figure 4). Following the dye system used for staining bacteria (Boulos et al., 1999), the intensity of the signals is proportional to the bacterial cells colonizing the root tissue which indicates successful colonization of the bacterial endophytes in the plant roots. The results are in agreement with other researchers (Sahu et al., 2020). The induction of systemic resistance in chickpea plants pre-challenged with soil-borne fungal pathogens by seed priming with bacterial endophytes was evaluated. Bacterial endophytes stimulate the expression of PR genes and phenol content and increase the activity of PR proteins such as PO, PPO, PAL, chitinases, lipoxygenases, and glucanases in the host plant as a defense mechanism to suppress the pathogenic effect (Zaim et al., 2016; Bekkar et al., 2018; Kumari and Khanna, 2019). In the

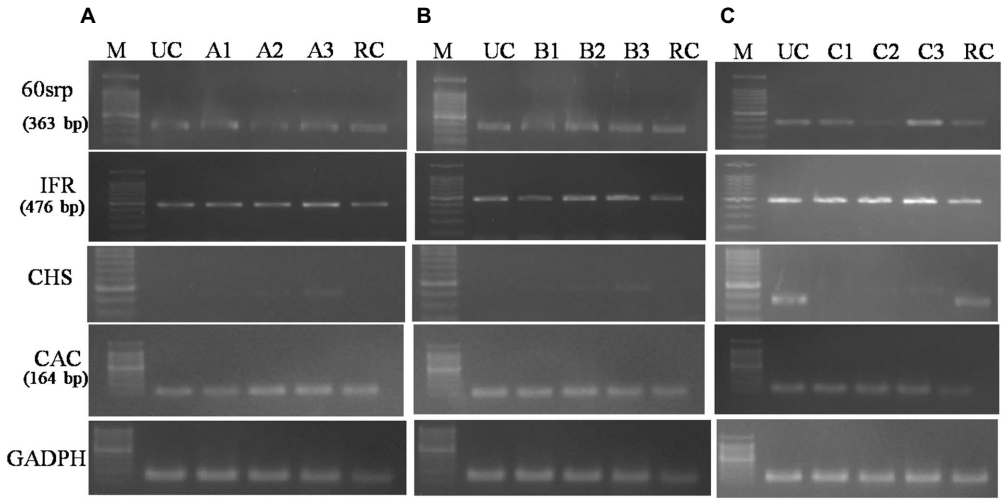

FIGURE 8
Effect of bacterial endophytes inoculation on expression of PR genes (**A**, *R. solani* pre-challenged; **B**, *S. rolfsii* pre-challenged; **C**, *F. oxysporum* f. sp. *ciceri* pre-challenged) Treatment details: UC-Uninoculated (negative control in which neither pathogen nor bacterial strain inoculated). A1, B1, C1 – Positive control of *R. solani*, *S. rolfsii,* and *F. oxysporum* f. sp. *ciceri*, respectively in which only pathogen inoculated. A2, B2, C2 – Respective pathogen + *B. subtilis* strain TRO4 inoculated. A3, B3, C3 – Respective pathogen + *B. subtilis* strain CLO5 inoculated. RC, Resistant cultivar.

present study, we examined the accumulation of superoxide radicals, defense-related enzymes (PO and PAL), and the up-regulation of defense-related genes (*60srp* and *IFR*) to evaluate bacterial endophytes for the induction of systemic resistance in chickpea plants pre-challenged with soil-borne fungal pathogens.

Reactive oxygen species (ROS), i.e., $^1O_2$, O^{2-}, H_2O_2, and OH^-, are generated as signaling molecules in biotic and abiotic stressed plants and an excess amount of these ROS is deleterious to plant growth (Czarnocka and Karpiński, 2018). The antioxidant machinery of plants keeps the levels of superoxide and other ROS under control. There are reports of endophytes supplementing enzymatic and non-enzymatic antioxidant production in the host plants (Sahu et al., 2019, 2020). The reduced accumulation in TRO4 and CLO5 inoculated treatments indicate protective effects against superoxide accumulation at deleterious levels under biotic stress conditions (Figures 5, 6). Bacterial endophytes are able to induce the expression of defense-related enzymes such as PAL, PO, polyphenol oxidases (PPO), and phenols in the host plant to enable defense against invading pathogens. The activity of defense enzymes PAL and PO were higher in the CLO5-treated plants than in the positive control (pathogen alone; Figure 7). In a similar study, chickpea plants pre-challenged with *F. oxysporum* f.sp. *ciceri* and inoculated with the isolates of antagonistic rhizobacteria (Ps 45 and Ba1a) along with native *Mesorhizobium* exhibited the highest activity of PAL, PO, and PPO compared to fungicide treatment and the positive control (pathogen alone; Kumari and Khanna, 2019; Malviya et al., 2020). PAL and PO are the key enzymes of phenylpropanoid pathways. PAL is a key/primary enzyme of the phenylpropanoid pathway which catalyzes the formation of intermediate metabolites such as cinnamic acid, p-coumaric acid, caffeic acid, ferulic acids, and gallic acid which ultimately leads to cell wall lignification and thickening (Lopez and Hernández, 2014). Phenylpropanoids are one of the important cascades activated during host-pathogen interaction. They regulate a wide range of physiological processes inside the plant cells and modulate the expression of key genes in the plants, inducing ISR and SAR against biotic stresses across the plant species (Singh A. et al., 2013; Singh U. B. et al., 2013; Lopez and Hernández, 2014). Our results are in accordance with the findings of Harman et al. (2004) and Singh et al. (2013), who observed that the inoculation of plants with *T. harzianum*, *B. amyloliquefaciens,* and other PGPRs induced cascades relating to plant defense and the up-regulation of enzymes over a period of time. In general, PAL and PO elicit several downstream processes leading to defense responses characterized by the inhibition of growth of invading fungi through phytoalexin formation, callose deposition, cell wall lignifications, synthesis of antimicrobial secondary metabolites, and pathogenesis-related (PR) proteins (Harman et al., 2004; Lopez and Hernández, 2014). Cell wall lignification renders the plant more resistant to pathogen attack (Tiwari et al., 2011; Jain et al., 2012; Lopez and Hernández, 2014). The bacterial inoculants induce the expression of PR genes in the host plant to overcome the deleterious effects of biotic stress caused by the invading pathogens. In our study, we observed the up-regulation of expression of PR genes in endophytes inoculated plants. According to Reddy et al. (2016), the genes *UCP* and *G6PD* were stably expressed while *TIP41* and *CAC* were found to be highly stable in the chickpea genotypes. In this study, *CAC* was chosen as the housekeeping gene and used for normalization. The expression of the PR genes (*60srp* and *IFR*) was noticed to be highly up-regulated in chickpea plants pre-challenged with *F. oxysporum* f.sp. *ciceri* and bio-primed with CLO5 compared to the resistant check and positive control (pathogen alone). These observations clearly indicated the protection afforded to host plants by bacterial

endophytes under pathogenic stressed conditions (Figure 8). Similar observations were made by Gurjar et al. (2012). The present study revealed the up-regulation of defense-related genes and the over-expression of PR proteins in chickpea plants bio-primed with bacterial endophytes and their role in combating pathogenesis in the host plants under biotic stress conditions. Overall, the results suggested that the application of TRO4 and CLO5 not only helps control wilt complex disease but also increased plant growth, as well as enhances the systemic resistance of chickpea plants against plant pathogens causing wilt complex.

Conclusion

The bacterial endophytes isolated in the study were found to have potential biocontrol activity. *In-vitro* experiments indicated three promising isolates have antagonistic activity against all three soil-borne fungal pathogens (*R. solani, S. rolfsii,* and *F. oxysporum* f.sp. *ciceri*). The *in-planta* assay revealed that TRO4 and CLO5 treated seeds had improved plant growth and reduced disease incidence percentage of wilt complex disease in chickpea plants. The current study provides insight into the possibilities of using potential endophytes for managing wilt complex disease in chickpea plants. Such an approach would be an eco-friendly means to manage wilt disease and would also contribute to the maintenance of plant and soil health.

Data availability statement

The datasets presented in this study can be found in online repositories. The names of the repository/repositories and accession number(s) can be found in the article/ Supplementary material.

Author contributions

VM: conceptualization and writing-original draft preparation. VM, PS, and US: methodology. HS: validation. VM, HC, and SB: formal analysis. RG and SS: investigation. HS: resources. PS and SP: writing-review and editing. All authors contributed to the article and approved the submitted version.

Funding

The funding received from ICAR-NBAIM, Mau, Uttar Pradesh, India to carry out the present study is acknowledged.

Acknowledgments

The authors sincerely thank Anil K. Saxena, Former Director, ICAR-NBAIM for guidance and support. The authors gratefully acknowledge the Indian Council of Agricultural Research, Ministry of Agriculture and Farmers Welfare, Government of India, for providing financial support for the study.

Conflict of interest

The authors declare that the research was conducted in the absence of any commercial or financial relationships that could be construed as a potential conflict of interest.

Publisher's note

All claims expressed in this article are solely those of the authors and do not necessarily represent those of their affiliated organizations, or those of the publisher, the editors and the reviewers. Any product that may be evaluated in this article, or claim that may be made by its manufacturer, is not guaranteed or endorsed by the publisher.

Supplementary material

The Supplementary material for this article can be found online at: https://www.frontiersin.org/articles/10.3389/fmicb.2022.994847/full#supplementary-material

References

Agrios, G.N. (2005). *Plant Pathology*, *5th Edn*, Amsterdam: Elsevier Academic Press.

Anderson, N. A. (1982). The genetics and pathology of *Rhizoctonia solani*. *Annu. Rev. Phytopathol.* 20, 329–347. doi: 10.1146/annurev.py.20.090182.001553

Aycock, R. (1966). Stem rot and other diseases caused by *Sclerotium rolfsii*. *NC Agric. Exp. Stn. Tech. Bull.* 174:202.

Bacon, C.W., and White, J.F. (2000). *Microbial Endophytes.* Published by Marcel Decker Inc., New York, USA

Bekkar, A. A., Zaim, S., and Belabid, L. (2018). Induction of systemic resistance in chickpea against *Fusarium* wilt by *Bacillus* strains. *Arch. Phytopathol. Pflanzenschutz.* doi: 10.1080/03235408.2018.1438819

Beniwal, S. P. S., Ahmed, S., and Gorfu, D. (1992). Wilt/root rot diseases in chickpea in Ethiopia. *Trop. Pest Manag.* 38, 48–51. doi: 10.1080/09670879209371644

Boulos, L., Prevost, M., Barbeau, B., Coallier, J., and Desjardins, R. (1999). LIVE/DEAD® BacLight™: application of a new rapid staining method for direct enumeration of viable and total bacteria in drinking water. *J. Microbiol. Methods* 37, 77–86. doi: 10.1016/S0167-7012(99)00048-2

Chen, T., Chen, Z., Ma, G. H., Du, B. H., Shen, B., Ding, Y. Q., et al. (2014). Diversity and potential application of endophytic bacteria in ginger. *Genet. Mol. Res.* 13, 4918–4931. doi: 10.4238/2014.July.4.6

Chung, B. S., Aslam, Z., Kim, S. W., Kim, G. G., Kang, H. S., Ahn, J. W., et al. (2008). A bacterial endophyte, *Pseudomonas brassicacearum* YC 5480, isolated from the root of Artemisia sp. producing antifungal and phytotoxic compounds. *Plant Pathol. J.* 24, 461–468. doi: 10.5423/PPJ.2008.24.4.461

Czarnocka, W., and Karpiński, S. (2018). Friend or foe? Reactive oxygen species production, scavenging and signaling in plant response to environmental

stresses. *Free Radic. Biol. Med.* 122, 4–20. doi: 10.1016/j.freeradbiomed.2018.01.011

Dubey, R.C., and Maheswari, D.K. (2008). *Practical Microbiology*. S. Chand & Company Ltd., New Delhi.

Gond, S. K., Bergen, M. S., Torres, M. S., and White, J. F. Jr. (2015). Endophytic *Bacillus* spp. produce antifungal lipopeptides and induce host defence gene expression in maize. *Microbiol. Res.* 172, 79–87. doi: 10.1016/j.micres.2014.11.004

Gurjar, S. G., Giri, A. P., and Gupta, V. S. (2012). Gene expression profiling during wilting in chickpea caused by *Fusarium oxysporum* f.sp. *ciceri*. *Am. J. Plant Sci.* 03, 190–201. doi: 10.4236/ajps.2012.32023

Harman, G. E. (2011). Multifunctional fungal plant symbionts: new tools to enhance plant growth and productivity. *New Phytol.* 189, 647–649. doi: 10.1111/j.1469-8137.2010.03614.x

Harman, G. E., Howell, C. R., Viterbo, A., Chet, I., and Lorito, M. (2004). *Trichoderma* species-opportunistic: avirulent plant symbionts. *Nat. Rev. Microbiol.* 2, 43–56. doi: 10.1038/nrmicro797

Hazarika, D. J., Goswami, G., Gautom, T., Parveen, A., Das, P., Barooah, M., et al. (2019). Lipopeptide mediated biocontrol activity of endophytic *Bacillus subtilis* against fungal phytopathogens. *BMC Microbiol.* 19:71. doi: 10.1186/s12866-019-1440-8

Jain, A., Singh, S., Sarma, B. K., and Singh, H. B. (2012). Microbial consortium-mediated reprogramming of defence network in pea to enhance tolerance against *Sclerotinia sclerotiorum*. *J. Appl. Microbiol.* 112, 537–550. doi: 10.1111/j.1365-2672.2011.05220.x

Jendoubi, W., Bouhadida, M., Boukteb, A., Beji, M., and Kharrat, M. (2017). Fusarium wilt affecting chickpea crop. *Agriculture* 7:23. doi: 10.3390/agriculture7030023

Kaur, N. P., and Mukhopadhyay, A. N. (1992). Integrated control of chickpea wilt complex by *Trichoderma* and chemical methods in India. *Trop. Pest Manag.* 38, 372–375. doi: 10.1080/09670879209371730

Kumar, A., Singh, R., Yadav, A., Giri, D. D., Singh, P. K., and Pandey, K. D. (2016). Isolation and characterization of bacterial endophytes of *Curcuma longa* L.3. *Biotech* 6, 1–8. doi: 10.1007/s13205-015-0313-6

Kumari, S., and Khanna, V. (2019). Induction of systemic resistance in chickpea (*Cicer arietinum* L.) against *Fusarium oxysporum* f.sp. *ciceris* by antagonistic rhizobacteria in assistance with native *Mesorhizobium*. *Curr. Microbiol.* 77, 85–98. doi: 10.1007/s00284-019-01805-6

Liu, B., Qiao, H., Huang, L., Buchenauer, H., Han, Q., Kang, Z., et al. (2009). Biological control of take-all in wheat by endophytic *Bacillus subtilis* E1R-j and potential mode of action. *Biol. Control* 49, 277–285. doi: 10.1016/j.biocontrol.2009.02.007

Lopez, O. V., and Hernández, G. (2014). Phenyl propanoids as master regulators:state of the art and perspectives in common bean (*Phaseolus vulgaris*). *Front. Plant Sci.* 5:336. doi: 10.3389/fpls.2014.00336

Mageshwaran, V., Inmann, F. I. I. I., and Holmes, L. D. (2014). Growth kinetics of *Bacillus subtilis* in lignocellulosic carbon sources. *Int. J. Microbiol. Res.* 6, 570–574.

Malviya, D., Singh, U. B., Singh, S., Sahu, P. K., Pandiyan, K., Kashyap, A. S., et al. (2020). "Microbial interactions in the rhizosphere contributing crop resilience to biotic and abiotic stresses" in *Rhizosphere Microbes: Soil and Plant Fuction*. eds. S. K. Sharma, U. B. Singh, P. K. Sahu, H. V. Singh and P. K. Sharma (Singapore: Springer), 1–33.

Merga, B., and Haji, J. (2019). Economic importance of chickpea: production, value and world trade. *Cogent Food Agric.* 5:1615718. doi: 10.1080/23311932.2019.1615718

Mula, M.G., Gonzales, F.R., Mula, R.P., Gaur, P.M., Gonzales, I.C., Dar, W.D., et al. (2011). *Chickpea (Garbanzos): An Emerging Crop for the Rainfed and Dryland Areas of the Philippines. Information Bulletin No. 88* Patancheru, India: International Crops Research Institute for the Semi-Arid Tropics, pp. 84.

Pineda, A., Dicke, M., Pieterse, C. M., and Pozo, M. J. (2013). Beneficial microbes in a changing environment: are they always helping plants to deal with insects? *Funct. Ecol.* 27, 574–586. doi: 10.1111/1365-2435.12050

Rajput, V. A., Konde, S. A., and Thakur, M. R. (2010). Evaluation of bio-agents against chickpea wilt complex. *J. Soils Crops* 20, 155–158.

Reddy, D. S., Bhatnagar-Mathur, P., Reddy, P. S., Sri Cindhuri, K., Sivaji Ganesh, A., and Sharma, K. K. (2016). Identification and validation of reference genes and their impact on normalized gene expression studies across cultivated and wild *Cicer* species. *PLoS One* 11:e0148451. doi: 10.1371/journal.pone.0148451

Rudresh, D. L., Shivprakash, M. K., and Prasad, R. D. (2005). Potential of *Trichoderma* spp. as biocontrol agents of pathogens involved in wilt complex of chickpea (*Cicer arietinum* L.). *J. Biol. Control.* 19, 157–166.

Ryan, R. P., Germaine, K., Franks, A., Ryan, D. J., and Dowling, D. N. (2007). Bacterial endophytes: recent developments and applications. *FEMS Microbiol. Lett.* 278, 1–9. doi: 10.1111/j.1574-6968.2007.00918.x

Sadasivam, S., and Manickam, A. (1996). *Biochemical Methods*. New Age International (P) Ltd., New Delhi, India, pp. 256. doi: 10.18641/jbc/19/2/40331

Sahu, P. K., Singh, S., Gupta, A. R., Gupta, A., Singh, U. B., Manzar, N., et al. (2020). Endophytic bacilli from medicinal-aromatic perennial holy basil (*Ocimum tenuiflorum* L.) modulate plant growth promotion and induced systemic resistance against *Rhizoctonia solani* in rice (*Oryza sativa* L.). *Biol. Control* 150:104353. doi: 10.1016/j.biocontrol.2020.104353

Sahu, P. K., Singh, S., Gupta, A., Singh, U. B., Brahmaprakash, G. P., and Saxena, A. K. (2019). Antagonistic potential of bacterial endophytes and induction of systemic resistance against collar rot pathogen *Sclerotium rolfsii* in tomato. *Biol. Control* 137:104014. doi: 10.1016/j.biocontrol.2019.104014

Sahu, P. K., Singh, S., Singh, U. B., Chakdar, H., Sharma, P. K., Sarma, B. K., et al. (2021). Inter-Genera Colonization of Ocimum tenuiflorum Endophytes in Tomato and Their Complementary Effects on Na^+/K^+ Balance, Oxidative Stress Regulation, and Root Architecture Under Elevated Soil Salinity. *Front. Microbiol.* 12:744733. doi: 10.3389/fmicb.2021.744733

Sarma, B. K., Yadav, S. K., Singh, S., and Singh, H. B. (2015). Microbial consortium-mediated plant defense against phytopathogens: readdressing for enhancing efficacy. *Soil Biol. Biochem.* 87, 25–33. doi: 10.1016/j.soilbio.2015.04.001

Senthilkumar, M., Swarnalakshmi, K., Govindasamy, V., Lee, Y. K., and Annapurna, K. (2009). Biocontrol potential of soybean bacterial endophytes against charcoal rot fungus, *Rhizoctonia bataticola*. *Curr. Microbiol.* 58, 288–293. doi: 10.1007/s00284-008-9329-z

Shanmugam, V., and Kanoujia, N. (2011). Biological management of vascular wilt of tomato caused by *fusarium oxysporum* f. sp. *lycospersici* by plant growth-promoting rhizobacterial mixture. *Biol. Control* 57, 85–93. doi: 10.1016/j.biocontrol.2011.02.001

Sharma, S. K., Vaisnav, A., Singh, M., Kumar, R., and Yadav, R. C. (2016). "Functional characterization of bacteria" in *Microbial Culture Handling and Maintenance: A Training Manual* (Kushmaur: ICAR-NBAIM), 61–66.

Singh, A., Jain, A., Sarma, B. K., Upadhyay, R. S., and Singh, H. B. (2013). Rhizosphere microbes facilitate redox homeostasis in *Cicer arietinum* against biotic stress. *Ann. Appl. Biol.* 163, 33–46. doi: 10.1111/aab.12030

Singh, U. B., Malviya, D., Wasiullah, S., Singh, S., Pradhan, J. K., Singh, B. P., et al. (2016). Bio-protective microbial agents from rhizosphere eco-systems trigger plant defense responses provide protection against sheath blight disease in Rice (*Oryza sativa* L.). *Microbiol. Res.* 192, 300–312. doi: 10.1016/j.micres.2016.08.007

Singh, D., Rajawat, M. V. S., Kaushik, R., Prasanna, R., and Saxena, A. K. (2017). Beneficial role of endophytes in biofortification of Zn in wheat genotypes varying nutrient use efficiency grown in soils sufficient and deficient in Zn. *Plant Soil* 416, 107–116. doi: 10.1007/s11104-017-3189-x

Singh, U. B., Sahu, A., Sahu, N., Singh, R. K., Singh, R., Dinesh, K., et al. (2013). Nematophagous fungi: *Catenaria anguillulae* and *Dactylaria brochopaga* from seed galls as potential biocontrol agents of *Anguina tritici* and *Meloidogyne graminicola* in wheat (*Triticum aestivum* L.). *Biol. Control* 67, 475–482. doi: 10.1016/j.biocontrol.2013.10.002

Singh, S., Singh, U. B., Malviya, D., Paul, S., Sahu, P. K., Trivedi, M., et al. (2020a). Seed biopriming with microbial inoculant triggers local and systemic defense responses against *Rhizoctonia solani* causing banded leaf and sheath blight in maize (*Zea mays* L.). *Ijerph* 17:1396. doi: 10.3390/ijerph17041396

Singh, S., Singh, U. B., Trivdi, M., Malviya, D., Sahu, P. K., Roy, M., et al. (2021). Restructuring the cellular responses: connecting microbial intervention with ecological fitness and adaptiveness to the maize (*Zea mays* L.) grown in saline-sodic soil. *Front. Microbiol.* 11:568325. doi: 10.3389/fmicb.2020.568325

Singh, S., Singh, U. B., Trivedi, M., Sahu, P. K., Paul, S., Paul, D., et al. (2020b). Seed biopriming with salt-tolerant endophytic *Pseudomonas geniculata* modulated biochemical responses provide ecological fitness in maize (*Zea mays* L.) grown in saline sodic soil. *Ijerph* 17:253. doi: 10.3390/ijerph17010253

Souza, A., Cruz, J. C., Sousa, N. R., Procópio, A. R. L., and Silva, G. F. (2014). Endophytic bacteria from banana cultivars and their antifungal activity. *Genet. Mol. Res.* 13, 8661–8670. doi: 10.4238/2014.October.27.6

Sun, H., Yan, H., Qing, X., Renyuan, Y., and Yongqiang, T. (2013). Isolation, characterization, and antimicrobial activity of endophytic bacteria from *Polygonum cuspidatum*. *African J. Microbiol. Res.* 7, 1496–1504. doi: 10.5897/AJMR12.899

Tiwari, S., Singh, P., Tiwari, R., Meena, K. K., Yandigeri, M., Singh, D. P., et al. (2011). Salt-tolerant rhizobacteria-mediated induced tolerance in wheat (*Triticum aestivum*) and chemical diversity in rhizosphere enhance plant growth. *Biol. Fertil. Soils* 47, 907–916. doi: 10.1007/s00374-011-0598-5

Vinodkumar, S., Nakkeeran, S., Renukadevi, P., and Malathi, V. G. (2017). Biocontrol potentials of antimicrobial peptide producing *bacillus* species: multifaceted antagonists for the management of stem rot of carnation caused by *Sclerotinia sclerotiorum*. *Front. Microbiol.* 8, 1–13. doi: 10.3389/fmicb.2017.00446

Zaim, S., Belabid, L., Bayaa, B., and Bekkar, A. A. (2016). "Biological control of chickpea fusarium wilts using rhizobacteria "PGPR"" in *Microbial-Mediated Induced Systemic Resistance in Plants*. eds. D. K. Choudhary and A. Verma (Singapore: Springer)

Zhao, L., Xu, Y., Lai, X.-H., Shan, C., Deng, Z., and Ji, Y. (2015). Screening and characterization of endophytic *Bacillus* and *Paenibacillus* strains from medicinal plant *Lonicera japonica* for use as potential plant growth promoters. *Brazilian J. Microbiol.* 46, 977–989. doi: 10.1590/S1517-838246420140024

Ziedan, E. H. E. (2006). Manipulating endophytic bacteria for biological control to soil borne diseases of peanut. *J. Appl. Sci. Res.* 2, 467–502.

frontiers | Frontiers in Microbiology

TYPE Original Research
PUBLISHED 22 December 2022
DOI 10.3389/fmicb.2022.1064013

Check for updates

OPEN ACCESS

EDITED BY
Durgesh K. Jaiswal,
Savitribai Phule Pune University, India

REVIEWED BY
Liya Liang,
Dalian University of Technology, China
Yujia Jiang,
Nanjing Tech University, China

*CORRESPONDENCE
Maria Suarez-Diez
✉ maria.suarezdiez@wur.nl

†These authors have contributed equally to this work

SPECIALTY SECTION
This article was submitted to Microbiotechnology, a section of the journal Frontiers in Microbiology

RECEIVED 07 October 2022
ACCEPTED 05 December 2022
PUBLISHED 22 December 2022

CITATION
Benito-Vaquerizo S, Nouse N, Schaap PJ, Hugenholtz J, Brul S, López-Contreras AM, Martins dos Santos VAP and Suarez-Diez M (2022) Model-driven approach for the production of butyrate from CO_2/H_2 by a novel co-culture of *C. autoethanogenum* and *C. beijerinckii*. *Front. Microbiol.* 13:1064013. doi: 10.3389/fmicb.2022.1064013

COPYRIGHT
© 2022 Benito-Vaquerizo, Nouse, Schaap, Hugenholtz, Brul, López-Contreras, Martins dos Santos and Suarez-Diez. This is an open-access article distributed under the terms of the Creative Commons Attribution License (CC BY). The use, distribution or reproduction in other forums is permitted, provided the original author(s) and the copyright owner(s) are credited and that the original publication in this journal is cited, in accordance with accepted academic practice. No use, distribution or reproduction is permitted which does not comply with these terms.

Model-driven approach for the production of butyrate from CO_2/H_2 by a novel co-culture of *C. autoethanogenum* and *C. beijerinckii*

Sara Benito-Vaquerizo[1†], Niels Nouse[2†], Peter J. Schaap[1,3], Jeroen Hugenholtz[2], Stanley Brul[2], Ana M. López-Contreras[4], Vitor A. P. Martins dos Santos[5,6] and Maria Suarez-Diez[1*]

[1]Laboratory of Systems and Synthetic Biology, Wageningen University and Research, Wageningen, Netherlands, [2]Molecular Biology and Microbial Food Safety, University of Amsterdam, Amsterdam, Netherlands, [3]UNLOCK Large Scale Infrastructure for Microbial Communities, Wageningen University and Research and Delft University of Technology, Wageningen, Netherlands, [4]Wageningen Food and Biobased Research, Wageningen University and Research, Wageningen, Netherlands, [5]Bioprocess Engineering, Wageningen University and Research, Wageningen, Netherlands, [6]LifeGlimmer GmbH, Berlin, Germany

One-carbon (C1) compounds are promising feedstocks for the sustainable production of commodity chemicals. CO_2 is a particularly advantageous C1-feedstock since it is an unwanted industrial off-gas that can be converted into valuable products while reducing its atmospheric levels. Acetogens are microorganisms that can grow on CO_2/H_2 gas mixtures and syngas converting these substrates into ethanol and acetate. Co-cultivation of acetogens with other microbial species that can further process such products, can expand the variety of products to, for example, medium chain fatty acids (MCFA) and longer chain alcohols. Solventogens are microorganisms known to produce MCFA and alcohols *via* the acetone-butanol-ethanol (ABE) fermentation in which acetate is a key metabolite. Thus, co-cultivation of an acetogen and a solventogen in a consortium provides a potential platform to produce valuable chemicals from CO_2. In this study, metabolic modeling was implemented to design a new co-culture of an acetogen and a solventogen to produce butyrate from CO_2/H_2 mixtures. The model-driven approach suggested the ability of the studied solventogenic species to grow on lactate/glycerol with acetate as co-substrate. This ability was confirmed experimentally by cultivation of *Clostridium beijerinckii* on these substrates in batch serum bottles and subsequently in pH-controlled bioreactors. Community modeling also suggested that a novel microbial consortium consisting of the acetogen *Clostridium autoethanogenum*, and the solventogen *C. beijerinckii* would be feasible and stable. On the basis of this prediction, a co-culture was experimentally established. *C. autoethanogenum* grew on CO_2/H_2 producing acetate and traces of ethanol. Acetate was in turn, consumed by *C. beijerinckii* together with lactate, producing butyrate. These results show that community modeling of metabolism is a valuable tool to guide the design of microbial consortia for the tailored production of chemicals from renewable resources.

KEYWORDS

microbial communities, *Clostridium autoethanogenum*, *Clostridium beijerinckii*, constraint-based metabolic modeling, CO_2, H_2, lactate, butyrate

1. Introduction

The energy crisis and the effects of climate change have emphasized the need to accelerate the transition toward a circular bio-based economy (Gottinger et al., 2020). Current circular approaches focus on the application of microbial conversion to convert low-value carbon feedstocks, such as biomass waste streams, into commodity chemicals (Casau et al., 2022). Recalcitrant lignocellulosic biomass can be pretreated and hydrolyzed into sugars (Loow et al., 2016) or gasified to produce synthesis gas (syngas), a one-carbon (C1) feedstock consisting of a mixture of CO, CO_2 and H_2 (Richardson et al., 2015). In addition, C1-rich industrial waste gases from steel and thermal power plants can be directly used as microbial feedstocks (Hwang et al., 2020). In this regard, CO_2 is an advantageous one-carbon feedstock (C1) since it can be obtained from natural and industrial sources, and can be converted into valuable products reducing the release of contaminant gases to the environment.

Acetogens are strict anaerobes that can grow on CO_2/H_2 and syngas as their sole carbon source using the Wood-Ljungdahl metabolic pathway (Ragsdale and Pierce, 2008; Bertsch and Müller, 2015). Acetogenic fermentation of C1 gases leads mainly to the production of acetate and ethanol, as well as, 2,3-butanediol or lactate (Köpke et al., 2014; Valgepea et al., 2018), and the production of ethanol has been commercialized recently (Marcellin et al., 2016; Bae et al., 2022). Acetogens that grow autotrophically on these slightly soluble gases are energy limited and produce a constrained product spectrum and low product titers. This can be overcome by exploring alternative strategies, such as mixotrophic growth or co-cultivation (Lee et al., 2022).

Solventogenic Clostridia have been widely applied to ferment sugars into mixtures of the solvents acetone, butanol, and ethanol (ABE) (Tracy et al., 2012) or in some cases isopropanol, butanol, ethanol (IBE) (Yang et al., 2016). These fermentations consist of an acidogenic phase followed by a solventogenic phase. During acidogenesis, solventogens produce carboxylic acids (mainly acetate and butyrate), and CO_2 and H_2. Accumulation of carboxylic acids and the concomitant lowering of the pH trigger solventogenesis during which solventogens reduce the carboxylic acids into solvents (Liao et al., 2015).

Cross-feeding strategies have been used to establish synthetic microbial communities that produce a wider product range (Diender et al., 2016, 2019; Du et al., 2020; Moreira et al., 2021). Therefore, co-cultivation of an acetogen and a solventogen has the potential to overcome the drawbacks associated to acetogens by increasing the product spectrum. Charubin and Papoutsakis (2019) recently established a co-culture of the solventogen *Clostridium acetobutylicum* and the acetogen *Clostridium ljungdahlii*. In this setup, glucose was metabolized by *C. acetobutylicum* to butanol, ethanol, acetone, acetoin, CO_2, and H_2. Subsequently, CO_2 and H_2 were fixed, and acetone and acetoin were reduced to isopropanol and 2,3-butanediol, respectively, by *C. ljungdahlii*.

Acetate is one of the most abundant products in acetogens (Bengelsdorf et al., 2018), and while solventogenic strains cannot grow on acetate as sole carbon source, they can reassimilate acetate and convert it into carboxylic acids such as butyrate, or solvents when glucose is used as co-substrate (Monot et al., 1982; Kuit et al., 2012; Diallo et al., 2021). Therefore, in a co-culture of acetogens/solventogens on CO_2/H_2, butyrate could be produced as main product. Butyrate is a valuable product as it is used in many commercial applications, as a solvent, cosmetic, food, animal feed, or as a precursor of pharmaceuticals (Dwidar et al., 2012; Brändle et al., 2016).

In this study, we followed a model-driven approach to find an alternative route for production of butyrate. We produced butyrate from CO_2 using a co-culture of two strains, one acetogen producing acetate from CO_2/H_2, and one solventogenic strain that co-metabolized acetate with an alternative carbon source into butyrate. To select the solventogenic strain, we systematically assessed growth on several carbon sources using the genome-scale metabolic models (GEMs) of *C. acetobutylicum* and *Clostridium beijerinckii*. The most promising carbon sources were experimentally tested and validated. On the basis thereof, we constructed a community model of *Clostridium autoethanogenum* and *C. beijerinckii*, and qualitatively assessed the fermentation of CO_2/H_2 and the new carbon source through scenario simulations. Model predictions guided the experimental work and led to the successful establishment of this new co-culture.

2. Materials and methods

2.1. GEM availability and curation

The GEM of *C. autoethanogenum* DSM 10061, iCLAU786 (Valgepea et al., 2017) was downloaded in sbml and table format and used without modification.

The GEM of *C. acetobutylicum* ATCC 824, iCac802 (Dash et al., 2014) was downloaded in sbml and table format, and modified as follows: Two reactions were defined as reversible: ATP:3-phospho-D-glycerate 1-phosphotransferase (with model identifier R0239), and Hydrogenase (R1563). Formate dehydrogenase (R1562) was removed since it was not found in the genome of *C. acetobutylicum*. Three new reactions were added in the model: Pyruvate transport (pyrt),

Abbreviations: ABE, acetone, butanol and ethanol; C1-feedstock, one-carbon feedstock; cFBA, community flux balance analysis; FBA, flux balance analysis; GEM, genome-scale metabolic model; HPLC, high-performance liquid chromatography; IBE, isopropanol, butanol, and ethanol; LDH, lactate dehydrogenase; MCFA, medium-chain fatty acid; OD, optical density; Syngas, synthesis gas.

Pyruvate exchange (EX_PYR_e), and glycerol kinase (R0426), the latter reaction was found to be present in the genome of *C. acetobutylicum* (EC 2.7.1.30; locus tag: CAC1321). Finally, we replaced the ethanol transport reaction (R1708), expressed as a proton (H^+) symport reaction, by a diffusion transport reaction. The modified version of the model (iCac803) is available at: https://gitlab.com/wurssb/Modelling/coculture_cacb.

The GEM of *C. beijerinckii* NCIMB 8052, iCM925 (Milne et al., 2011) was downloaded in sbml and table format and modified as follows: Ferredoxin-NAD^+ reductase (FDXNRx) and ferredoxin-$NADP^+$ reductase (FDXNRy) reactions were removed, and Na^+-translocating ferredoxin:NAD^+ oxidoreductase (Rnf) complex and electron-bifurcating, ferredoxin-dependent transhydrogenase (Nfn) complex, were added to the model. Transport of hydrogen reaction (Habc) was replaced by the ATPase reaction (ATPase). The EC number and genes of (*S*)-3-Hydroxybutanoyl-CoA:$NADP^+$ oxidoreductase reaction (HACD1y) were modified and the EC numbers of butyryl-CoA dehydrogenase (ACOAD1) and 3-hydroxybutyryl-CoA dehydrogenase (HACD1x) as well. Finally, the reduced ferredoxin:dinitrogen oxidoreductase (ATP-hydrolyzing) reaction (DNOR) was stoichiometrically balanced. The updated version of the model (iCM943) is available in the git repository.

2.2. *In-silico* carbon source screening in *C. acetobutylicum* and *C. beijerinckii*

We systematically assessed growth capabilities on the updated versions of the GEMs of *C. acetobutylicum* and *C. beijerinckii* on a wide range of carbon sources. Model simulations were done using COBRApy, version 0.15.4 (Ebrahim et al., 2013), and Python 3.9. Growth capabilities were assessed using Flux Balance Analysis (FBA). The biomass synthesis reaction (termed "Biomass" or "biomass" in the respective *C. acetobutylicum* and *C. beijerinckii* models), was defined as the objective function for maximization. Growth was considered when the growth rate was higher than 0.0001 h^{-1}. For each assessed carbon source, the maximum uptake (corresponding to minus the lower bound of the associated exchange reaction denoted "EX_xx") was constrained to 20 mmol g_{DW}^{-1} h^{-1}, and the minimum uptake (corresponding to minus the upper bound of the associated exchange reaction) was constrained to 0.1 mmol g_{DW}^{-1} h^{-1}. In addition, uptake of small metabolites and ions was allowed by setting the lower bound of the corresponding exchange reaction to −1,000 as described in the corresponding script in the git repository.

2.3. Co-culture GEM reconstruction

A compartmentalized co-culture model of *C. autoethanogenum* and *C. beijerinckii* was obtained by combining single species models iCLAU786 (Valgepea et al., 2017) and iCM943 (Milne et al., 2011), following a previous approach (Benito-Vaquerizo et al., 2020). In this approach, each species is considered a single compartment. The compartment associated with *C. autoethanogenum* was defined as "cytosol_ca" and the compartment associated with *C. beijerinckii* was defined as "cytosol." Intracellular metabolites were assigned to their respective compartment and the flag "_ca" was added to the identifier of metabolites belonging to "cytosol_ca" to distinguish them from the *C. beijerinckii* metabolites. In addition, the combined model included an extracellular compartment, defined as "extracellular," common to both species. Metabolites in this compartment are either secreted, metabolized, or exchanged by both species, and separated from metabolites present in the cellular compartments by adding the "_e" flag to the identifier. All extracellular metabolites follow the same naming system (namespace) for both species. Therefore, the same namespace was applied to metabolites secreted by both species. All metabolites present in both intracellular compartments and the extracellular compartment can be exchanged between species if favored by the directionality. Interchanged metabolites are assumed to be first transported into the extracellular compartment, before taken up by the other species using the corresponding exchange reaction. The co-culture GEM contains one biomass synthesis reaction per species, termed "biomass_auto" and "biomass_beije" for *C. autoethanogenum* and *C. beijerinckii*, respectively. Additionally, the model contains a community biomass synthesis reaction ("Community_biomass"), which incorporates the biomass of *C. autoethanogenum* and *C. beijerinckii* in the form of metabolite "biomass_ca" and metabolite "biomass," respectively. The combined model incorporates a transport reaction of butyrate ("BUTex_au") from the extracellular compartment to the intracellular compartment of *C. autoethanogenum*, and the reaction to produce butyraldehyde from butyrate ("buttobuta") in *C. autoethanogenum*. In addition, we incorporated the transport reaction of acetone ("ACETONE_ca") from the extracellular compartment to the intracellular compartment of *C. autoethanogenum*; an alcohol dehydrogenase to convert acetone into isopropanol ("ISOBIO"); a transport reaction of isopropanol from the intracellular compartment of *C. autoethanogenum* to the extracellular compartment ("ISOPRO_ca"), and an exchange reaction of isopropanol ("EX_IPRO_e").

The final three-compartment co-culture model was translated into SBML level 3 version 1 (see git repository).

2.4. Co-culture modeling framework

Co-culture model simulations were carried out using a previously described modeling framework (Benito-Vaquerizo et al., 2020), similar to SteadyCom (Chan et al., 2017), and based

on Community FBA (cFBA) (Khandelwal et al., 2013). Specific fluxes (mmol g_{DW}^{-1} h^{-1}) were substituted by environmental fluxes (mmol l^{-1} h^{-1}), and thus, the biomass synthesis reaction of each species was changed accordingly accounting for the growth rate and biomass of each species (g_{DW} l^{-1} h^{-1}). The relative contribution of each species to the community biomass was calculated from the total biomass of the community and the species ratio.

2.5. Co-culture model simulations

In this study, we simulated hypothetical scenarios varying biomass species ratios, growth rates, and substrates environmental fluxes to explore the feasible solution space of the co-culture. We selected a community biomass of 0.22 g_{DW} l^{-1} based on the average value measured for a similar co-culture of *C. autoethanogenum* and *Clostridium kluyveri* on syngas (Diender et al., 2019). The biomass of each species was calculated based on the indicated species ratio and the community biomass. The biomass of each species was multiplied by the indicated growth rate, and the value was used to constrain the flux through the biomass synthesis reaction of each species. We assessed conditions with *C. autoethanogenum*–*C. beijerinckii* ratios ranging from 0.1–0.9 to 0.9–0.1, and growth rates from 0.005 to 0.1 h^{-1}. For this exploratory analysis, we assumed equal growth rates for each species and steady-state. For each condition, we fixed the uptake rate of CO_2 and H_2 to 5 mmol l^{-1} h^{-1} or to 2.5 mmol l^{-1} h^{-1}, covering values found in literature for a similar co-culture (Diender et al., 2019). The maximum lactate uptake rate was constrained to 2.5 or 5 mmol l^{-1} h^{-1} and a minimum uptake rate of 0.1 mmol l^{-1} h^{-1} was imposed. We defined the community biomass reaction ("Community_biomass") as the objective function and we performed FBA to assess the feasibility of each condition. For a selected number of feasible conditions, the solution space and the set of fluxes compatible with the measured constraints were sampled using the *sample* function in the flux_analysis submodule of COBRApy. Presented results show the average and standard deviation based on 5,000 iterations generated at each condition (git repository).

2.6. Bacterial strains

The laboratory strains *C. beijerinckii* NCIMB 8052 and *C. acetobutylicum* ATCC 824 were stored as spore suspensions in 20% glycerol at −20°C. Spores of *C. beijerinckii* and *C. acetobutylicum* were heat-activated for 1 min at 95°C and 10 min at 70°C, respectively, before inoculation. *C. autoethanogenum* DSM 10061 was kindly provided by Professor Diana Z. Sousa from the Laboratory of Microbiology, Wageningen University and Research, Wageningen, the Netherlands, and was stored as vegetative cells suspended in 25% glycerol buffered with phosphate and reduced with Ti(III)citrate under anoxic conditions at −80°C.

2.7. Experimental carbon source screening of *C. acetobutylicum* and *C. beijerinckii*

Cultures were prepared in serum bottles containing CM2 medium consisting of the following components: 2.5 g l^{-1} yeast extract (Duchefa Biochemie), 1.0 g l^{-1} KH_2PO_4 (Fischer Scientific), 0.61 g l^{-1} K_2HPO_4 (Sigma-Aldrich), 1 g l^{-1} $MgSO_4 \cdot 7H_2O$ (Roth), 2.9 g l^{-1} ammonium acetate (USB), 0.10 g l^{-1} 4-aminobenzoic acid (Duchefa Biochemie), 6.6 mg l^{-1} $Fe(II)SO_4 \cdot 7H_2O$ (Sigma-Aldrich), and 0.5 mg l^{-1} Na-resazurin (Sigma-Aldrich). Acetic acid (Sigma-Aldrich), L-lactic acid (∼90%, Merck), ethanol (Merck) and glycerol (Sigma-Aldrich) were added to final concentrations of 40 mM. pH was set to pH 6.1–6.2 with KOH and/or HCl. Media were made anoxic with N_2(g) and autoclaved. D-Glucose was made anoxic and autoclaved separately and added to a final concentration of 40 mM. Media were inoculated with 4% (v/v) culture made from heat-activated spore suspension grown overnight at 37°C in CM2 medium supplemented with 40 g l^{-1} D-glucose (Duchefa Biochemie). Cultures were incubated at 37°C and sampled at t_0 and after 4 d. Cell density was measured as optical density at 600 nm (OD_{600}), extracellular metabolites were analyzed with high-performance liquid chromatography (HPLC) as described in Section 2.9, and pH was measured. Acetate co-assimilation was determined by calculating the fraction of the total converted carbon coming from consumed acetate.

2.8. Cultivation experiments in pH-controlled bioreactors

pH-controlled bioreactor experiments were performed in a working volume of 2 l in Infors HT Labfors 5 bioreactors (Infors HT, Switzerland). The stirrer, set at 150 rpm, consisted of at equidistance from top to bottom a pitch-blade and two Rushton impellers. Temperature was controlled at 37°C and pH at pH 5.5 ± 0.1 using 3 M KOH and 2 M H_3PO_4. Foaming was controlled with Antifoam 204 (Sigma-Aldrich). 2.9 g l^{-1} ammonium acetate in the CM2 medium was replaced by 2.5 g l^{-1} ammonium sulfate (Merck). 0.75 g l^{-1} anoxic and sterilized L-cysteine HCl · H_2O (Merck) was added after autoclaving.

In pH-controlled batch fermentations of *C. beijerinckii* growing on different concentrations of acetate and lactate, the adapted CM2 medium was supplemented with acetic acid and L-lactic acid prior to autoclaving. 10 ml min^{-1} N_2(g) was flushed across the head space to keep anoxic

conditions. Reactors were inoculated with 1% (v/v) *C. beijerinckii* culture growing overnight at 37°C in CM2 medium supplemented with 20 g l^{-1} D-glucose and 0.75 g l^{-1} L-cysteine HCl.H_2O. Cultures were sampled at regular time intervals for analysis of cell density, extracellular metabolites, and morphology with phase-contrast microscopy. The overall stoichiometry was calculated by scaling the difference of the concentrations of the main extracellular metabolites between t_0 and t_{end} to the difference in the measured lactate concentration.

In pH-controlled fed-batch co-cultivation experiments of *C. autoethanogenum* and *C. beijerinckii*, reactors were equipped with sinter spargers to flush 40 ml min^{-1} H_2(g) and 10 ml min^{-1} CO_2(g) through the medium. At t_0, reactors were inoculated with <1% (v/v) *C. autoethanogenum* culture growing at 37°C in CM2 medium supplemented with 10 g l^{-1} D-fructose (VWR Chemicals) and 0.75 g l^{-1} L-cysteine HCl.H_2O. After establishment of growth and acetate production by *C. autoethanogenum*, reactors were inoculated with <1% (v/v) *C. beijerinckii* culture growing overnight at 37 °C in CM2 medium supplemented with 20 g l^{-1} D-glucose and 0.75 g l^{-1} L-cysteine HCl.H_2O. Furthermore, the continuous L-lactic acid feed was started. Cultures were sampled at regular time intervals for analysis of cell density, extracellular metabolites, and morphology with phase-contrast microscopy. Theoretical acetate production from CO_2 was calculated for each time point after the start of the L-lactic acid feed as follows: The amount of lactate converted was calculated from the difference in the amount of lactate fed and calculated amount of lactate remaining in the reactor. The conversion of lactate *via* pyruvate yields the intermediate metabolite acetyl-CoA and CO_2 in a 1:1 ratio. The fraction of the amount of carbon from lactate available for the formation of products was subtracted from the amount of carbon present in the produced (iso)butyrate to obtain a theoretical amount of carbon coming from a difference source than lactate, i.e., from converted acetate. This theoretical amount of converted acetate was added to the calculated amount of acetate in the reactor to get a theoretical amount of acetate produced from CO_2. Subsequently, the stoichiometry for the production of (iso)butyrate from lactate and acetate was calculated by scaling the difference of (iso)butyrate produced, theoretical acetate converted, and lactate converted between t_0 and the selected time points to lactate converted.

2.9. Analysis of extracellular metabolites

Concentrations of acetate, acetone, butanol, (iso)butyrate, ethanol, fructose, glycerol, glucose, and lactate were analyzed with HPLC. Supernatant was mixed with an equal volume of 1 M H_2SO_4 with 30 mM 4-methylpentanoic or 100 mM pentanoic acid as internal standard. This was filtered through a 0.2 μm regenerated cellulose filter followed by analysis on a Waters HPLC system with a Shodex KC-811 column at 65°C, 1 ml/min 3 mM H_2SO_4 mobile phase, and a refractive index and UV detector.

3. Results

Figure 1 shows the steps for the model-driven approach followed to establish a novel co-culture of *C. autoethanogenum* and *C. beijerinckii* for the production of butyrate from CO_2/H_2. GEMs of solventogens were used to evaluate candidate species and possible carbon sources. After the experimental validation of the model predictions, the co-culture was successfully established.

3.1. Updated GEMs of *C. autoethanogenum*, *C. acetobutylicum*, and *C. beijerinckii*

The GEM of *C. autoethanogenum*, iCLAU786 was used as the original version (Valgepea et al., 2017) with no modification. The updated version of the GEM of *C. acetobutylicum*, iCac803 (Dash et al., 2014), had 1,254 reactions, 1,465 reactions, and 803 genes, and the GEM of *C. beijerinckii*, iCM943 (Milne et al., 2011), had 881 metabolites, 941 reactions, and 943 genes.

Regarding the GEM of *C. beijerinckii*, we included the Na^+-translocating ferredoxin:NAD^+ oxidoreductase (Rnf) complex (EC 7.2.1.2) in the model of *C. beijerinckii*. Rnf is formed by the following gene cluster: rnfC, rnfD, rnfG, rnfE, rnfA, rnfB, (locus_tag: Cbei_2449, Cbei_2450, Cbei_2451, Cbei_2452, Cbei_2453, and Cbei_2454, respectively). Additionally, we have identified an electron-bifurcating, ferredoxin-dependent transhydrogenase (Nfn) complex that catalyzes NADH-dependent reduced Ferredoxin:$NADP^+$ oxidoreductase activity in *C. beijerinckii*. The Nfn complex has two subunits: NAD(P)-binding subunit, and a glutamate synthase subunit. These two subunits showed 56–79% identity with the Nfn subunits of *C. kluyveri*, *C. autoethanogenum*, *C. difficile* (Kremp et al., 2020), and of the recently annotated *Anaerotignum neopropionicum* (Benito-Vaquerizo et al., 2020), forming two possible complexes: (Cbei_2182 and Cbei_2183) or (Cbei_0661 and Cbei_0662). To our knowledge, this is the first time the Nfn complex is reported in *C. beijerinckii* NCIMB 8052. Ferredoxin NAD^+ reductase (EC 1.18.1.3) is not found in the genome of *C. beijerinckii*, and the ferredoxin $NADP^+$ reductase (EC 1.18.1.2) showed lower percentage identity to the FNR of *C. acetobutylicum*, and thus, we hypothesized that the former FNR corresponds to the NADP-binding subunit of the Nfn complex.

10.3389/fmicb.2022.1064013

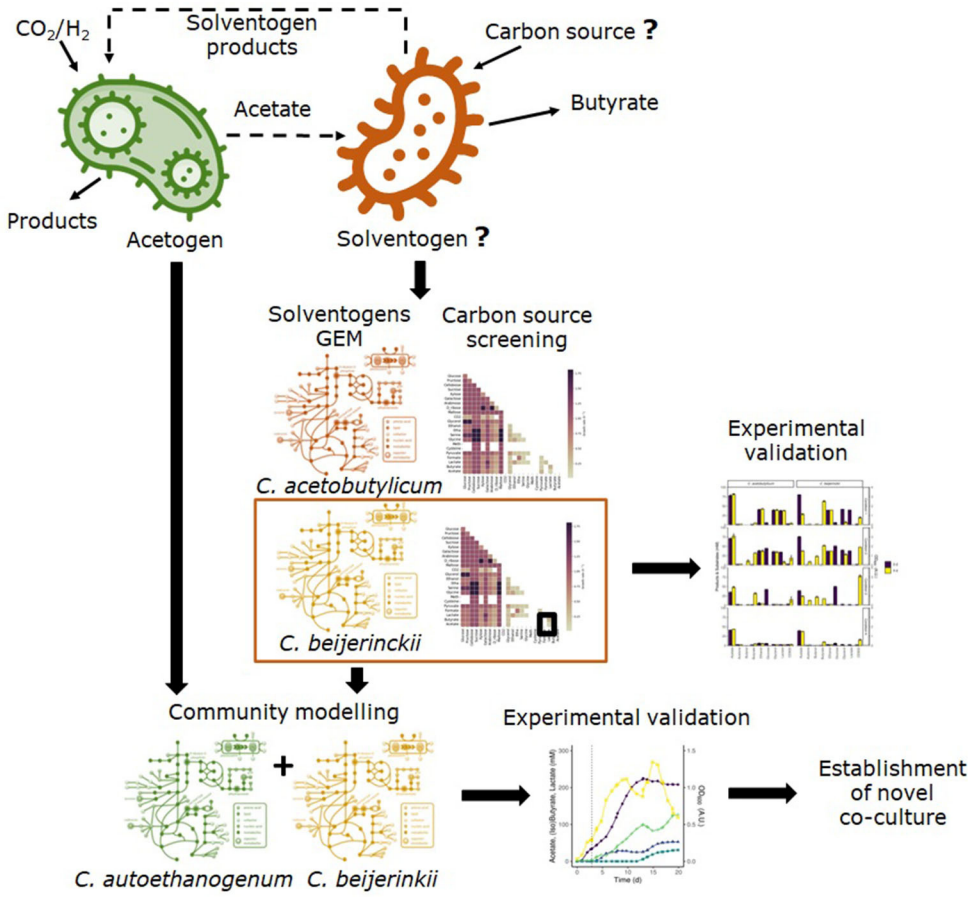

FIGURE 1
Overview of the followed methodology to establish a co-culture of an acetogen and a solventogen to produce butyrate from CO_2/H_2. We used genome-scale metabolic models of two solventogens to assess growth on several carbon sources and to find the alternative carbon source that sustained growth on the solventogen with acetate. The predicted carbon sources were experimentally validated and growth was confirmed in one of the solventogens. After that, we assessed the feasibility of the co-culture of the acetogen *C. autoethanogenum* and the selected solventogen using community modeling, and finally, the co-culture was experimentally established.

3.2. *In-silico* carbon source screening of *C. acetobutylicum* and *C. beijerinckii*

We explored growth on 25 carbon sources individually and pairs of these carbon sources with one another in the model of *C. acetobutylicum* (Figure 2).

Growth was predicted on sugars, glycerol, lactate, serine, and pyruvate as single carbon sources, reaching the highest growth rates on cellobiose, sucrose and maltose. As expected, acetate did not sustain growth as the sole carbon source and neither was sustained on acetone, succinate, acetoin (not shown here). Pairwise combinations of most carbon sources that led to growth as single carbon source, also led to growth in combination with an alternative carbon source. However, L-methione, L-cysteine and CO_2 did not show growth in combination with carbon sources that sustained growth alone since the model was forced to uptake a minimum amount of each carbon source, leading in some cases, to infeasible solutions. The highest growth rates were obtained with cellobiose, sucrose or maltose in combination with serine, glycine or ethanolamine; the combination of glucose or fructose with glycerol, and xylose, or arabinose with ribose. Interestingly, acetate, in combination with lactate or glycerol, could sustain growth in *C. acetobutylicum*, as previously described for other solventogens (Diez-Gonzalez et al., 1995; Kumar et al., 2022).

Additionally, we assessed growth on glucose, glycerol, ethanol, formate, butyrate, lactate, and acetate in the model of *C. beijerinckii* (Figure 3). As observed for *C. acetobutylicum*, *C. beijerinckii* only sustained growth on glucose, glycerol, and lactate as single carbon sources. Pairwise combinations of the latter carbon sources sustained growth in combination with the rest of carbon sources. The highest growth rates were obtained with glucose in combination with glycerol or lactate. Here, acetate with lactate or glycerol also sustained growth,

10.3389/fmicb.2022.1064013

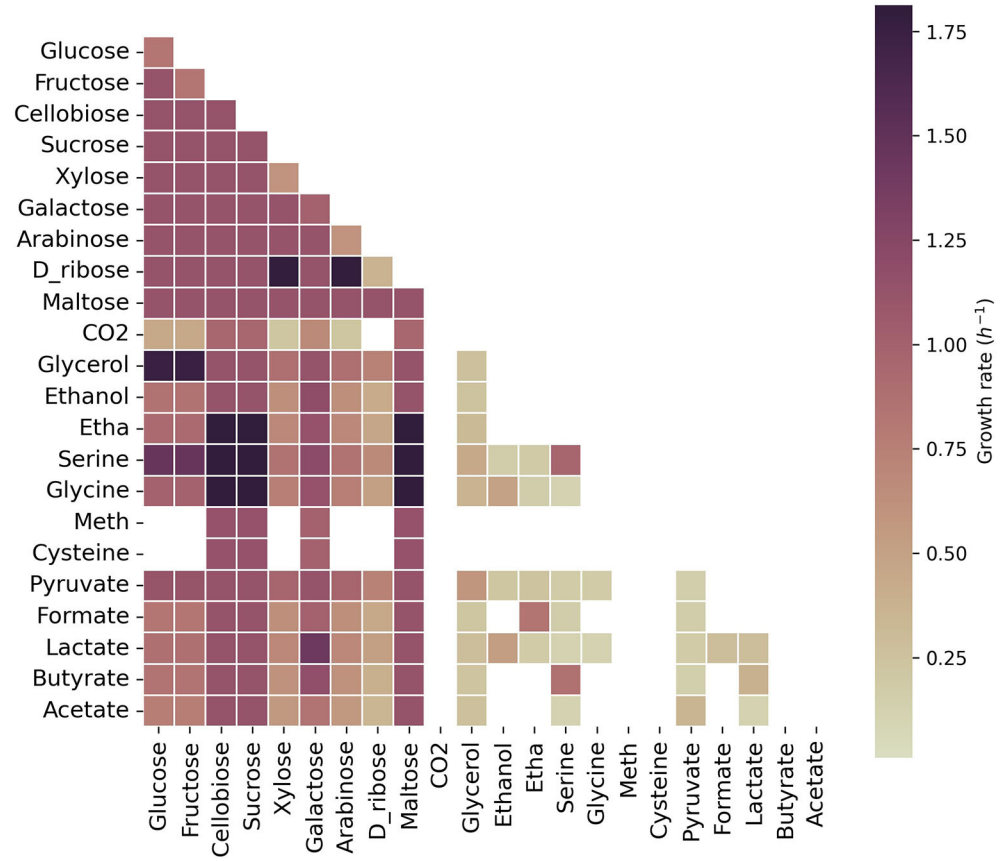

FIGURE 2
Growth capabilities predicted for *C. acetobutylicum*. The color scale shows growth rates in h^{-1}. Squares on the diagonal correspond to single carbon sources. Squares below the diagonal correspond to the combination of the carbon source presented on the x-axis with the carbon source presented on the y-axis. Non-colored squares show that no growth was predicted for the specified carbon source(s). Meth, methionine; Etha, ethanolamine. The maximum uptake rate for each carbon source was set to 20 mmol g_{DW}^{-1} h^{-1} and the minimum to 0.1 mmol g_{DW}^{-1} h^{-1}.

being the growth rate higher with addition of acetate in both scenarios.

3.3. Growth of *C. acetobutylicum* and *C. beijerinckii* on lactate and acetate

The substrate space provided by the model was used in an initial screening to assess growth and co-assimilation of acetate on various carbon sources by the solventogens *C. acetobutylicum* and *C. beijerinckii* (Figure 4). On all assessed carbon sources *C. beijerinckii* grew to higher cell densities after 4 days than *C. acetobutylicum*, which is known to produce autolysins toward the end of the exponential growth phase (Croux et al., 1992). As predicted by the models (Figures 2, 3), neither strain grew on acetate alone (Figure 4; Condition 4), as both strains only converted the residual metabolites from the inoculum, i.e., glucose. This showed the need for an additional carbon source to co-assimilate acetate. Contrary to the model predictions (Figure 2), *C. acetobutylicum* did not grow on acetate with lactate, glycerol and ethanol as co-substrates under the tested conditions. However, the model predictions for *C. beijerinckii* (Figure 3) were confirmed, and acetate was co-assimilated using all lactate and part of the glycerol into butyrate (Figure 4; Condition 1). Both solventogens further reduced butyrate to butanol with the addition of glucose (Figure 4; Condition 2). The fraction of carbon coming from acetate in the products produced by *C. beijerinckii* was not improved by the addition of glucose to the medium, and was highest in the medium containing only acetate, ethanol, glycerol, and lactate (Figure 4; Condition 1–3, Supplementary Table 1).

Growth of *C. beijerinckii* on lactate and acetate was further explored in a bioreactor at a controlled pH of 5.5 (Supplementary Figure 1). This pH is close to the optimal pH of *C. autoethanogenum* (Abrini et al., 1994), and acid re-assimilation and ABE production in *C. beijerinckii* (Diallo et al., 2020, 2021). Butyrate was the most abundant product and

10.3389/fmicb.2022.1064013

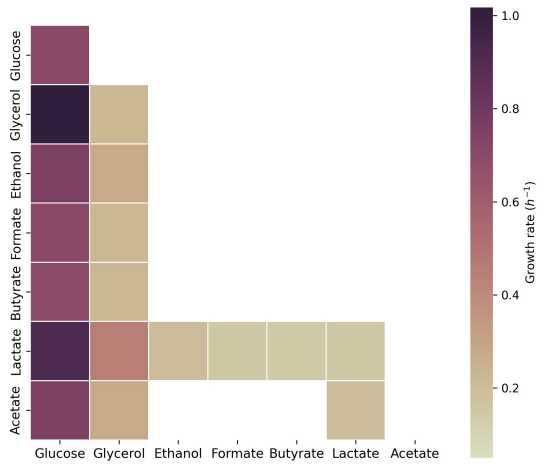

FIGURE 3
Growth capabilities predicted for *C. beijerinckii*. The color scale shows growth rates in h^{-1}. Squares on the diagonal correspond to single carbon sources. Squares below the diagonal correspond to the combination of the carbon source presented on the x-axis with the carbon source presented on the y-axis. Non-colored squares show that no growth was predicted for the specified carbon source(s). The maximum uptake rate for each carbon source was set to 20 mmol g_{DW}^{-1} h^{-1} and the minimum to 0.1 mmol g_{DW}^{-1} h^{-1}.

the stoichiometry was as follows: consumption of one mol lactate and 0.4–0.5 mol acetate produced 0.6–0.7 mol butyrate. This was similar to the stoichiometry reported for *Clostridium saccharobutylicum* NCP 262, previously known as *Clostridium acetobutylicum* P262 (Keis et al., 2001), growing on lactate and acetate (Diez-Gonzalez et al., 1995).

The screening of the solventogens *C. acetobutylicum* and *C. beijerinckii* on various carbon sources showed that the combination of *C. beijerinckii* and lactate was most promising for the re-assimilation of acetate produced from CO_2/H_2 by *C. autoethanogenum* in a future co-culture.

3.4. Fermentation of lactate and acetate by *C. beijerinckii*

In *C. beijerinckii*, lactate is oxidized to pyruvate *via* NAD-independent L-lactate dehydrogenase (EC 1.1.1.27) encoded by the following isoenzymes: Cbei_4072, Cbei_4903, or Cbei_2789 (Figure 5). Pyruvate is decarboxylated to acetyl-CoA *via* pyruvate:ferredoxin oxidoreductase (PFOR; EC 1.2.7.10, encoded by Cbei_1853, Cbei_4318, or Cbei_1458), generating reduced ferredoxin and CO_2. Model predictions showed that reduced ferredoxin is partly spent to produce H_2 and oxidized ferredoxin *via* ferredoxin hydrogenase (EC 1.12.7.2, Cbei_0327, Cbei_4000, or Cbei_3796), and partly spent to regenerate oxidized ferredoxin and NADH *via* the Rnf complex (EC 7.2.1.2, Cbei_2449-55), translocating Na^+/H^+ (Patakova et al., 2019). The Rnf complex is coupled to an ATPase (EC 7.1.2.2) encoded by the cluster Cbei_0412 to Cbei_0419, that pumps in Na^+/H^+ for energy generation.

Model predictions suggested that acetate is converted into acetyl phosphate (acetyl-P) investing ATP by acetate kinase (EC 2.7.2.1, Cbei_1165), and acetyl-P is converted into acetyl-CoA *via* phosphate acetyltransferase (EC 2.3.1.8, Cbei_3402 or Cbei_1164). As previously mentioned, *C. beijerinckii* produces butyrate *via* acetyl-CoA (Chen and Blaschek, 1999). First, two acetyl-CoA molecules are converted into one acetoacetyl-CoA by acetoacetyl-CoA thiolase (EC 2.3.1.9, Cbei_0411 or Cbei_3630). Acetoacetyl-CoA is reduced to 3-hydroxybutyryl-CoA *via* (*S*)-3-Hydroxybutanoyl-CoA:NAD^+ oxidoreductase (EC 1.1.1.157, Cbei_0325) or *via* NAD(P)-dependent acetoacetyl-CoA reductase (EC 1.1.1.36, Cbei_5834). Then, 3-hydroxybutyryl-CoA is converted into crotonyl-CoA by 3-hydroxybutyryl-CoA dehydratase (EC 4.2.1.55, Cbei_2034 or Cbei_4544). Crotonyl-CoA is reduced *via* the butyryl-CoA dehydrogenase/electron-transferring flavoprotein complex (Bcd-EtfAB) producing reduced ferredoxin. Two complete clusters were identified in the genome: Cbei_0322 (Bcd), Cbei_0323 (EtfB), and Cbei_0324 (EtfA) or Cbei_2035 (Bcd), Cbei_2036 (EtfB) and Cbei_2037 (EtfA). An acyl-CoA dehydrogenase (Acd) showed 79.4% similarity with the Bcd subunit of *C. acetobutylicum* ATCC 824. Butyrate can be produced from butyryl-CoA *via* two routes in *C. beijerinckii*. The first route is a linear pathway in which butyryl-CoA is first converted into butyryl phosphate *via* butanoyl-CoA:phosphate butanoyltransferase (Ptb; EC 2.3.1.19, Cbei_0203). Butyryl phosphate is then converted into butyrate producing ATP *via* butyrate kinase (Buk; EC 2.7.2.7, Cbei_0204). The second route is catalyzed by a butyryl-CoA-acetoacetate CoA-transferase (EC 2.8.3.9, Cbei_2654 or Cbei_2653 or Cbei_3834 or Cbei_3833 or Cbei_4614 or Cbei_4612), where the CoA moiety of butyryl-CoA is transferred to acetate producing acetyl-CoA and butyrate. However, model predictions showed that butyrate is mostly produced generating ATP *via* Ptb and Buk.

3.5. Community model simulations of *C. autoethanogenum* and *C. beijerinckii* for the fermentation of CO_2/H_2 and lactate

The GEM of the co-culture consisted of 2,005 metabolites, 2,107 reactions, and 1,659 genes. Community model simulations supported the co-existence of the co-culture of *C. autoethanogenum* and *C. beijerinckii* for the fermentation of CO_2/H_2 and lactate in a wide range of growth rate and species ratio combinations.

10.3389/fmicb.2022.1064013

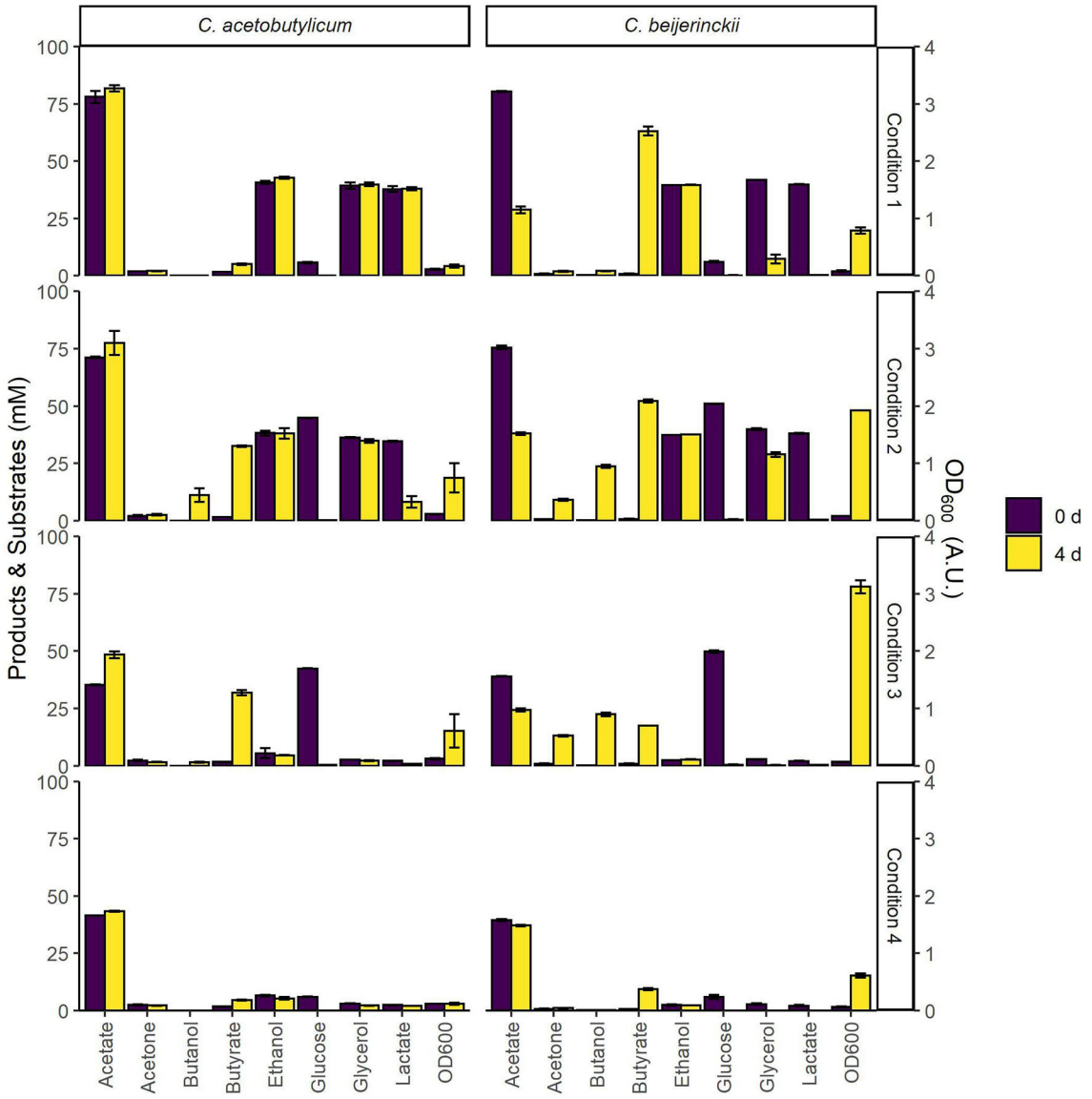

FIGURE 4
Initial screening of *C. beijerinckii* and *C. acetobutylicum* for growth on various combinations of carbon sources. The bars indicate substrate and product concentrations, and cell density at the time of inoculation and after 4 days. CM2 medium, containing 38 mM acetate, was supplemented with 40 mM of each of the various carbon sources as follows: Condition 1: acetic acid, ethanol, glycerol, and L-lactic acid; Condition 2: acetic acid, ethanol, glycerol, L-lactic acid and glucose; Condition 3: glucose. Condition 4: none. Error bars show standard deviations between two cultures inoculated with the same inoculum.

Figure 6 shows the feasible solution space for multiple combinations of species ratios, growth rates, CO_2, H_2, and lactate feeds. When the maximum uptake rate of lactate is 2.5 mmol l^{-1} h^{-1} (Figure 6; green figures), the feasibility of the co-culture becomes more limited. In these conditions, the co-culture is only feasible at low growth rates (<0.02 h^{-1}) for all species ratios, and feasible at higher growth rates (up to 0.07 h^{-1}) when *C. autoethanogenum* and *C. beijerinckii* are similarly present in the community for CO_2/H_2 feed ratio of 0.5. The co-culture is infeasible in all conditions when the CO_2/H_2 feed ratio is 2, and only feasible when the presence of *C. autoethanogenum* is low and the CO_2/H_2 feed ratio is 1. The range of feasible solutions becomes wider when the lactate feed rate is 5 mmol l^{-1} h^{-1}. When *C. autoethanogenum* and *C. beijerinckii* are equally present in the community, the co-culture can be established with all explored growth rates, except when the CO_2/H_2 feed ratio is 2, that is only feasible up to 0.04 h^{-1}. Again, only at lower

10.3389/fmicb.2022.1064013

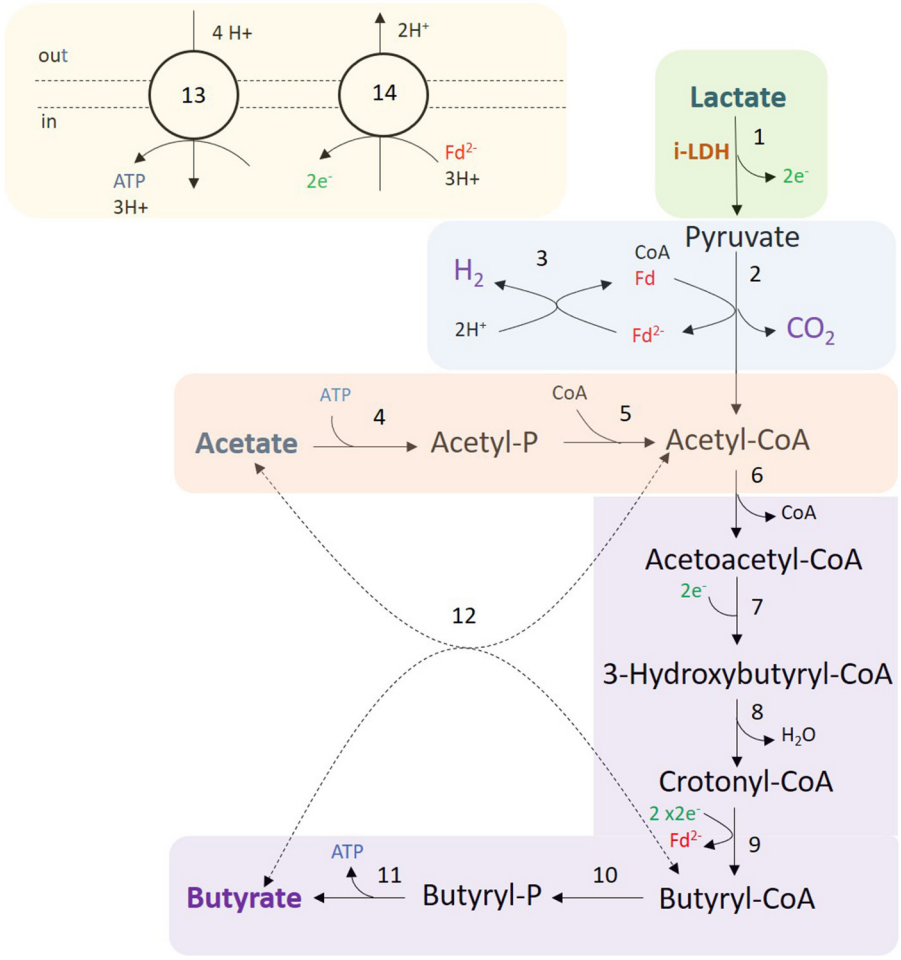

FIGURE 5
Fermentation of lactate and acetate by *C. beijerinckii*. Colored areas correspond to the following modules: lactate oxidation (green); H_2, CO_2, and acetyl-CoA production (blue); acetate consumption (red); butyrate production (purple); and redox cofactor regeneration, and ATPase (yellow). Numbers in reactions correspond to the following enzymes and reaction identifiers in the model: 1, NAD-independent L-lactate dehydrogenase (LDH_L); 2, pyruvate:ferredoxin oxidoreductase (POR4); 3, Ferredoxin hydrogenase (FDXNH); 4, acetate kinase (ACK); 5, phosphate acetyltransferase (PTA); 6, Acetoacetyl-CoA thiolase (ACACT1); 7, (*S*)-3-Hydroxybutanoyl-CoA:NAD^+ oxidoreductase or NAD(P)-dependent acetoacetyl-CoA reductase (HACD1x or HACD1y); 8, 3-hydroxybutyryl-CoA dehydratase (3HBCD); 9, Butyryl-CoA dehydrogenase/electron-transferring flavoprotein complex (Bcd-EtfAB) (ACOAD1); 10, Butanoyl-CoA:phosphate butanoyltransferase (BCOPBT); 11, Butyrate kinase (BUTK); 12, Butyryl-CoA-acetoacetate CoA-transferase (COAT2); 13, ATPase (ATPase); 14, Na^+-translocating ferredoxin:NAD^+ oxidoreductase complex (Rnf). Dashed lines (reaction 12) indicate that the reaction might not be the main pathway.

growth rates ($<0.02\ h^{-1}$), the co-culture is feasible for all tested species ratios.

Figure 7 shows the steady-state consumption and production rates observed in co-culture compared to the consumption and production rates associated to *C. autoethanogenum* or *C. beijerinckii*. Part of the acetate produced by *C. autoethanogenum* is taken up by *C. beijerinckii* since the steady-state production rates in the co-culture are lower than the production rates of *C. autoethanogenum*. The fermentation of acetate and lactate leads to the production of butyrate in *C. beijerinckii*. A small amount of butyrate is reassimilated by *C. autoethanogenum* and by *C. beijerinckii* and converted into butanol (not shown). Furthermore, ethanol is being produced in smaller amounts by *C. autoethanogenum* and *C. beijerinckii*. Model predictions also showed an exchange of CO_2 and H_2 from *C. beijerinckii* to *C. autoethanogenum*. *C. beijerinckii* produces CO_2 and H_2 that are taken up by *C. autoethanogenum*, since the flux through *C. autoethanogenum* is higher than the flux through the exchange reaction in the co-culture. Model predictions suggested that acetate consumption by *C. beijerinckii* varied depending on the lactate feed rate, being lower when the lactate feed rate was higher than 2.5 mmol l^{-1} h^{-1} ($\approx$ 5 mmol l^{-1} h^{-1}). A higher lactate feed rate also led to more CO_2 and H_2 produced by *C. beijerinckii*, and thus, to more

10.3389/fmicb.2022.1064013

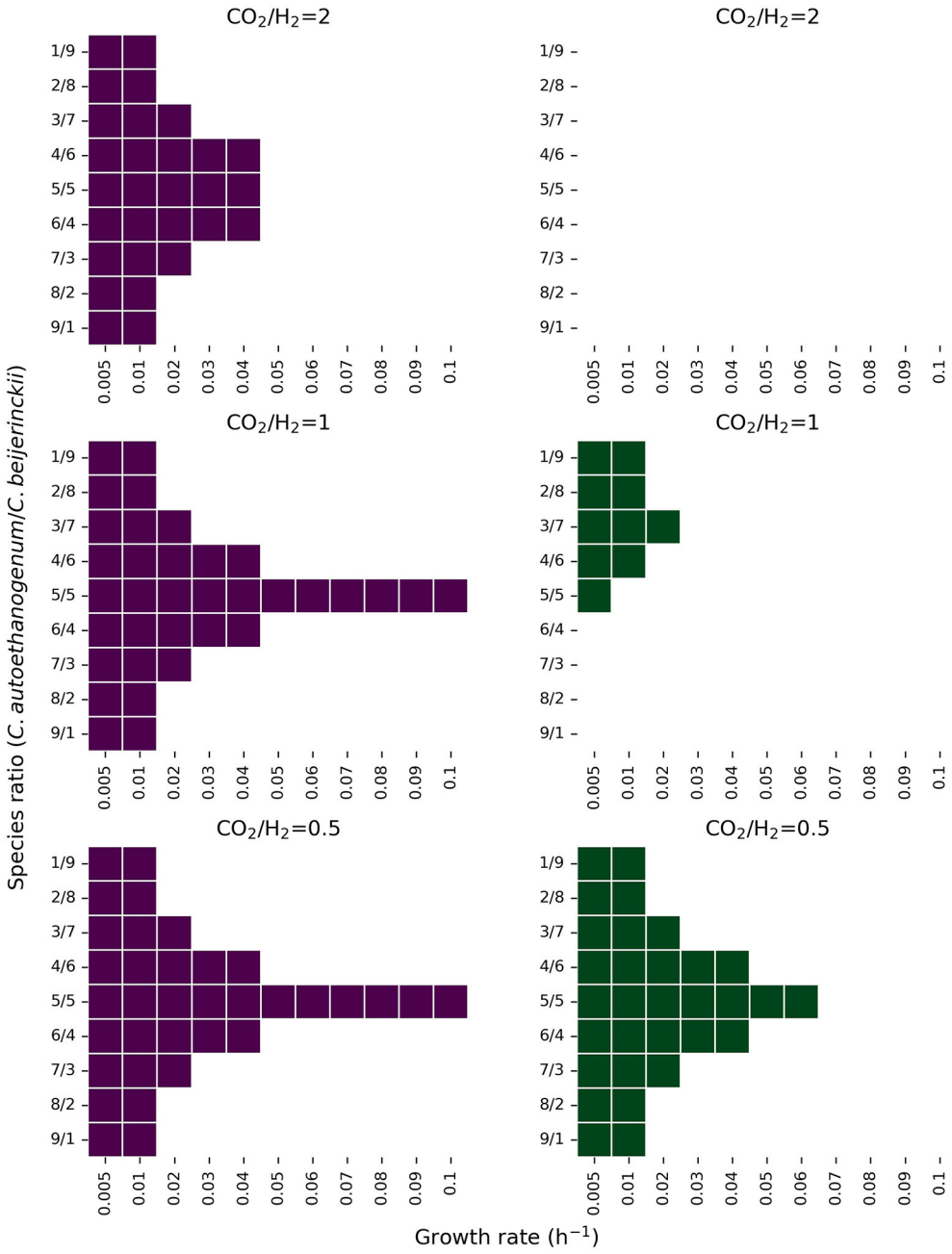

FIGURE 6
Feasible solution space of the co-culture of *C. autoethanogenum* and *C. beijerinckii* for several species ratio and growth rate combinations under different CO_2, H_2, and lactate feed rates. The y-axis shows the biomass species ratio of *C. autoethanogenum*/*C. beijerinckii* and the x-axis shows the growth rate in h^{-1}. Colored areas indicate feasible solutions predicted by the model. Figures in purple and green show results when the lactate feed rate is set to a maximum of 5 mmol l^{-1} h^{-1}, and 2.5 mmol l^{-1} h^{-1}, respectively. Predictions shown on the first row were obtained with a CO_2 and H_2 feed rate of 5, and 2.5 mmol l^{-1} h^{-1}, respectively. Predictions shown on the second row were obtained with a CO_2 and H_2 feed rate of 5 mmol l^{-1} h^{-1}, and on the third row, with a CO_2 and H_2 feed rate of 2.5, and 5 mmol l^{-1} h^{-1}, respectively.

gases being recirculated and consumed by *C. autoethanogenum* producing more acetate (git repository).

Furthermore, we observed traces of formate, 2,3-butanediol, acetone, isopropanol, and butanol (see git repository).

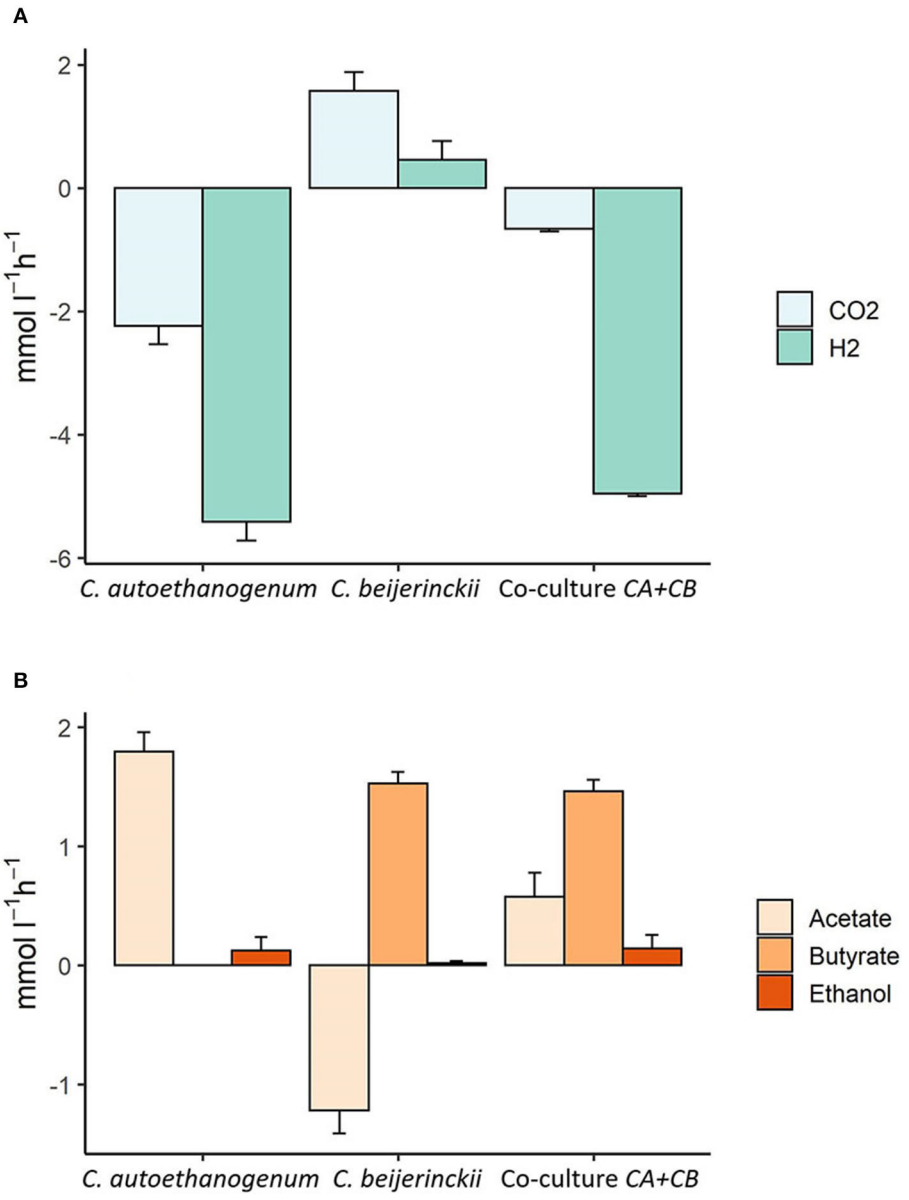

FIGURE 7
Steady-state production and consumption rates of the main substrates and products predicted by the community model of *C. autoethanogenum* and *C. beijerinckii*. The x-axis shows the species associated to the illustrated fluxes. The y-axis shows uptake (negative) or production (positive) fluxes in mmol l^{-1} h^{-1}. **(A)** Shows CO_2 and H_2 production or consumption rates, and **(B)** shows the production or uptake of acetate, butyrate, and ethanol. Modeled uptake and production rates are shown for *C. autoethanogenum*, *C. beijerinckii* and for the co-culture of *C. autoethanogenum* and *C. beijerinckii* (Co-culture *CA+CB*), respectively. Growth rate was set to 0.02 h^{-1}; biomass species ratio was set to 1:1; maximum and minimum lactate uptake rate was set to 2.5 and 0.1 mmol l^{-1} h^{-1}, and the maximum and minimum uptake of CO_2 and H_2 were set to 5 and 0.5 mmol l^{-1} h^{-1}, respectively.

3.6. Fed-batch fermentation of CO_2/H_2 and lactate by the novel co-culture of *C. autoethanogenum* and *C. beijerinckii*

Production of butyrate from CO_2/H_2 and the co-substrate lactate by the modeled co-culture of *C. autoethanogenum* and *C. beijerinckii* was experimentally verified with two biologically independent pH-controlled fed-batch fermentations (Figure 8 and Supplementary Figure 2). Both fermentations showed similar trends in biomass production and metabolites profiles. Below, the results are described for the fermentation shown in Figure 8. Initially, *C. autoethanogenum* was grown

10.3389/fmicb.2022.1064013

solely on a continuous CO_2/H_2 feed, and after 3 d, the OD_{600} had reached a value of 0.29 and the acetate concentration a value of 34 mM. This acetate concentration was considered sufficient to support *C. beijerinckii*. *C. beijerinckii* was added and the L-lactic acid feed was started. The rate of the L-lactic acid feed was set lower than the rate of acetate production from CO_2/H_2 by *C. autoethanogenum* to prevent complete depletion of acetate. Upon inoculation with *C. beijerinckii* and the start of the L-lactic acid feed, a continued growth phase was observed till 10 d in which butyrate was produced up to 28 mM.

A theoretical acetate production from CO_2 was calculated from which the corresponding stoichiometry for butyrate production at each time point was calculated (Supplementary Figure 2). Between 4 and 7 d, during butyrate production in the first growth phase, for each mol of consumed lactate, 0.2–1 mol acetate was reassimilated, and 0.5–0.6 mol butyrate was produced.

The drop in cell density observed between 10 and 13 d could be explained by the accumulation of biomass observed at the reactor wall above the fermentation medium from 6 d onward (data not shown). No production of butyrate was observed in this period and microscope observations showed that the consortium consisted almost entirely of vegetative cells (data not shown). These cells could not be assigned to either species as the morphologies of *C. autoethanogenum* and *C. beijerinckii* could not be clearly distinguished. As a result, the species ratio in the co-culture was not determined experimentally. In future studies, the species ratio could be obtained from transcriptomic (Benito-Vaquerizo et al., 2020), amplicon (Ibarbalz et al., 2014), or qPCR data (Charubin and Papoutsakis, 2019).

After this adaptation period, a second growth phase was observed between 13 and 15 d coinciding with a larger fraction of sporulating cells in the culture and the co-production of butyrate and isobutyrate to final concentrations of 53 and 31 mM, respectively. While measured in both replicates (Figure 8 and Supplementary Figure 2), the production of isobutyrate by the consortium was not predicted by the models, and will be further investigated in a follow-up research. The calculated stoichiometry indicated a shift toward the conversion of lactate during this second growth and production phase (Supplementary Figure 2).

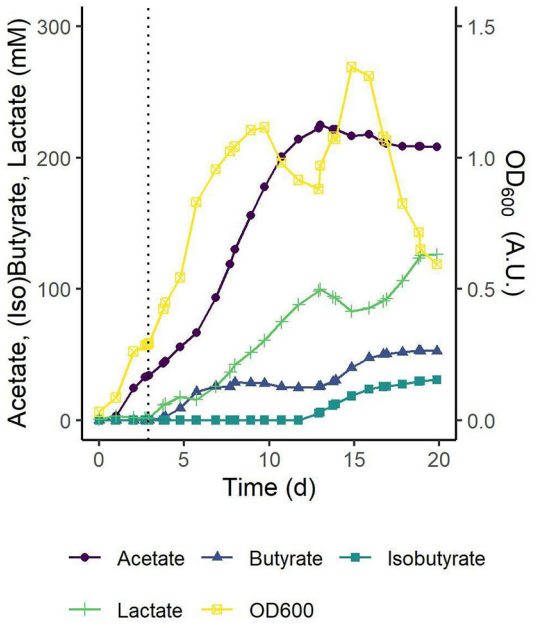

FIGURE 8
pH-controlled fed-batch fermentation of the *C. autoethanogenum*–*C. beijerinckii* co-culture on 1:4 CO_2/H_2 with an L-lactic acid feed. Concentrations of the main substrates, products, and cell density are shown. At t_0 cultures were inoculated with *C. autoethanogenum*. The dotted black line marks inoculation with *C. beijerinckii* and the start of the L-lactic acid feed. L-lactic acid was fed at a rate of 3 ml d^{-1} till 19 d. Traces of ethanol (3–8 d, max. 4.6 mM at 7 d and 13–20 d, max. 5.6 mM at 20 d), butanol (14–20 d, max. 3.1 mM at 20 d) and glucose from the *C. beijerinckii* inoculum (<1 mM at 3 d) were detected. pH was controlled at pH 5.5 ± 0.1. Results of a single biological replicate are shown here and the results of a second independent biological replicate are shown in Supplementary Figure 2.

3.7. Analysis of substrate consumption and product formation by the co-culture model

C. autoethanogenum takes-up CO_2 and H_2 through the Wood-Ljungdahl pathway, where H_2 is used as an electron donor for CO_2 reduction to acetyl-CoA (Figure 9). Acetyl-CoA is mainly converted into acetate producing ATP, and ethanol. In addition, traces of 2,3-butanediol, formate and lactate were predicted by the model (not shown here). Part of the acetate was in turn taken-up by *C. beijerinckii* together with the external lactate feed, following the metabolism described in Section 3.3. Ethanol was produced by *C. autoethanogenum* and by *C. beijerinckii*, as observed in the experiments. Model simulations suggested the production of butyrate, CO_2 and H_2 by *C. beijerinckii*, and traces of acetone and butanol. We observed that most of the CO_2 and H_2 produced by *C. beijerinckii* was metabolized by *C. autoethanogenum* (Figure 8). Furthermore, we observed traces of isopropanol formed from the conversion of the assimilated acetone by *C. autoethanogenum* through an alcohol dehydrogenase. The community model suggested that butanol was produced by *C. beijerinckii* and by *C. autoethanogenum* (Figure 9). As Diender et al. (2016) already observed, butyrate could be exchanged between *C. beijerinckii* and *C. autoethanogenum*, and converted into butanol by an alcohol dehydrogenase and the aldehyde ferredoxin oxidoreductase.

In addition, the model predicts traces of formate and lactate produced by *C. autoethanogenum* being assimilated by *C. beijerinckii* (not shown here).

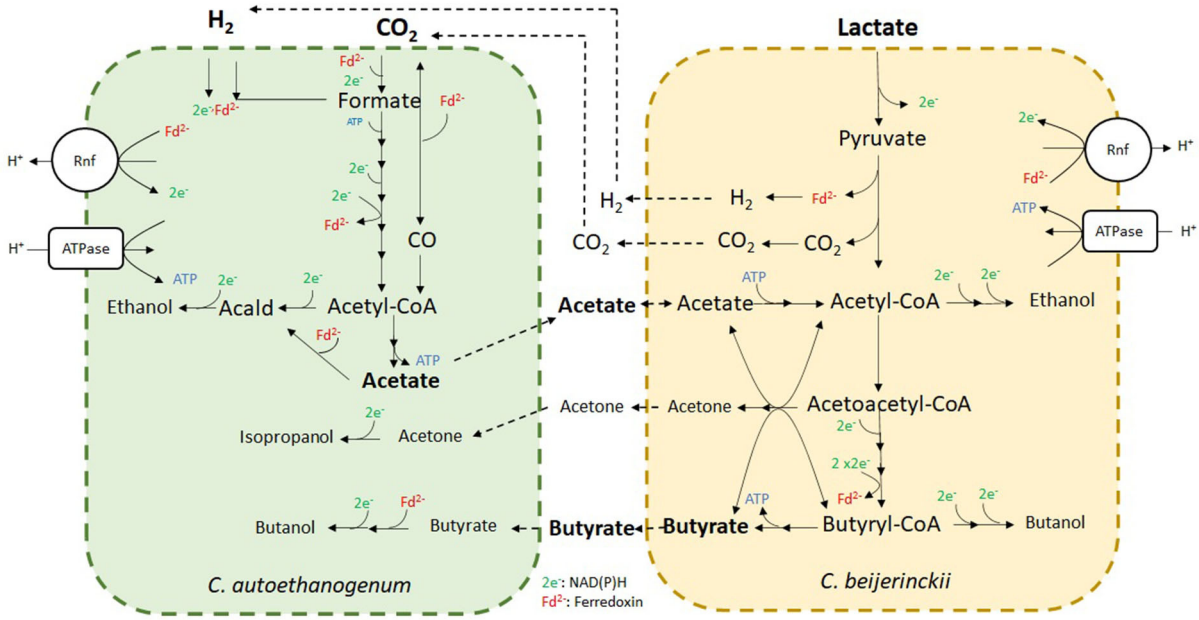

FIGURE 9
Fermentation of CO_2/H_2 and lactate by the novel co-culture of *C. autoethanogenum* and *C. beijerinckii*. Metabolites in bold indicate substrates and main products. Metabolites in smaller letter size indicate minor products. Arrows indicate the flux direction. Dashed lines display transport reactions of metabolites from the extracellular compartment to the intracellular compartment of the indicated microbe, and *vice versa*.

Supplementary Figure 3 represents the metabolic profile of the novel co-culture with glucose, instead of lactate, as additional carbon source. As observed in Figure 4, the addition of glucose would lead to an increase of ABE production by *C. beijerinckii*, since there are more reducing equivalents when glucose is converted to pyruvate. Acetate would still be the main product in *C. autoethanogenum* and ethanol would be produced in minor amounts. Part of the acetate could be metabolized by *C. beijerinckii*, but also produced together with butyrate during the acidogenic phase. Once the pH drops enough, the acids could be partly reassimilated during solventogensis to produce solvents. Acetone and butyrate could be partly taken up by *C. autoethanogenum* producing isopropanol and more butanol. Possibly, part of the CO_2 and H_2 produced by *C. beijerinckii* would be consumed by *C. autoethanogenum* as described for the co-culture growing on lactate.

4. Discussion

GEMs are mathematical representations of the metabolism and have been successfully employed to gain insights into metabolic capabilities of single species (Milne et al., 2011; Dash et al., 2014; Valgepea et al., 2017; Gu et al., 2019; Benito-Vaquerizo et al., 2022), and to elucidate possible strategies to optimize the performance of microorganism(s) in mono- and co-cultivation (Kim et al., 2019; Benito-Vaquerizo et al., 2020; Foster et al., 2021; García-Jiménez et al., 2021). In this study, the use of constrained-based modeling has been key to design an alternative way to produce butyrate from CO_2/H_2 and lactate. We have proven the capacity of *C. beijerinckii* NCIMB 8052 to grow on lactate and acetate as the sole carbon and energy source. Moved by the need to upcycle sustainable feedstocks, we have used this new found capacity of *C. beijerinckii* to established a novel synthetic co-culture of *C. autoethanogenum* and *C. beijerinckii* for the fermentation of CO_2/H_2 and lactate into butyrate.

The use of lactate as alternative carbon source by *C. beijerinckii* as co-substrate with acetate creates new possibilities for the production of butyrate. Acetate is the most abundant product of gas fermentation, and therefore, has an essential role in the establishment of the co-culture. Lactate is a minor fermentation product of acetogens grown on syngas or CO_2/H_2 (Valgepea et al., 2018; Im et al., 2022), but a major fermentation product of acetogens grown on sugars (Drake and Daniel, 2004). Acetogens could be engineered toward autotrophic lactate production from CO_2/H_2 (Mook et al., 2022) or syngas, thereby facilitating butyrate production in co-cultivation with *C. beijerinckii* without the need of adding an additional carbon source. Alternatively, lactate can be obtained from other sources, such as side-streams from the dairy industry (Sar et al., 2022), spoiled agri-food products (Xu et al., 2020), ensiled

agricultural biomass (Chen et al., 2007), and fermented grass (Sakarika et al., 2022).

C. beijerinckii has wide physiological versatility, which makes this microbe an ideal candidate to produce butyrate in a co-culture. However, butyrate production could also be achieved by the co-cultivation of an acetogen with a butyrate producing species, such as *Clostridium butyricum*, whose ability to grow on lactate and acetate was also proved recently (Detman et al., 2019).

Additionally, the use of the newly established co-culture could increase carbon recycling and electron transport, since model predictions indicated that CO_2 and H_2 produced by *C. beijerinckii* were almost fully reassimilated by *C. autoethanogenum* (Figure 7), which reduces the carbon footprint. Incorporation of an organism able to produce H_2 needed for CO_2 assimilation is interesting to consider for future approaches. Besides solventogenic Clostridia, other anaerobic bacterial species have been described that produce H_2 from the fermentation of sugars at high yields (Show et al., 2012). This opens up new alternatives for more efficient co-cultures without the need of external H_2.

Model predictions showed slow growth on lactate and acetate by *C. acetobutylicum*. However, this was not confirmed by experiments in which lactate was not consumed, and acetate was produced rather than consumed (Figure 4; condition 1). Diez-Gonzalez et al. (1995) showed growth on lactate and acetate in the solventogen *C. saccharobutylicum* NCP 262. They analyzed extracts of cells grown on lactate and acetate and observed NAD-dependent lactate dehydrogenase (d-LDH) as well as NAD-independent lactate dehydrogenase (i-LDH) activity. d-LDH regulated the conversion of pyruvate to lactate and required fructose-1,6-biphosphate to be active (Freier and Gottschalk, 1987; Diez-Gonzalez et al., 1995). i-LDH regulated the conversion of lactate to pyruvate (Figure 5) and had double the activity over d-LDH. In addition, i-LDH activity decreased fourfold when glucose was added to cultures growing on lactate and acetate. However, lactate was only converted by *C. acetobutylicum* ATCC 824 when glucose was added (Figure 4; Condition 2) suggesting that i-LDH from *C. acetobutylicum* ATCC 824 is activated by glucose. Interestingly, the LDH of *C. beijerinckii* NCIMB 8052 and *C. acetobutylicum* ATCC 824 showed 87.7 and 57% similarity with the LDH of *C. saccharobutylicum* NCP 262, respectively. Keis et al. (2001) showed that *C. saccharobutylicum* NCP 262 is more similar to *C. beijerinckii* NCIMB 8052 than to *C. acetobutylicum* ATCC 824. Therefore, we hypothesize that *C. beijerinckii* has an i-LDH activity comparable to *C. saccharobutylicum*, whereas i-LDH activity in *C. acetobutylicum* ATCC 824 is regulated differently.

Model predictions showed a high production of butyrate, acetate, and traces of ethanol, acetone, butanol, isopropanol, 2,3-butanediol, and formate. Fed-batch experiments also showed butyrate and acetate as major fermentations products, and ethanol and butanol as minor fermentation products. Charubin and Papoutsakis (2019) observed production of 2,3-butanediol from the assimilation by *C. ljungdahlii* of the acetoin produced by *C. acetobutylicum*. However, acetolactate decarboxylase was only annotated in the genome of *C. autoethanogenum* and not in the genome of *C. beijerinckii* (Siemerink et al., 2014), and thus, acetoin could not be produced by the solventogen. Lactate degradation results in less NAD(P)H available, and therefore, the production of solvents is lower compared to the standard ABE fermentation on sugars (Sreekumar et al., 2015; Charubin and Papoutsakis, 2019). In contrast, the co-culture in our study has a relatively high butyrate production (up to 53 mM). Furthermore, mono-culture experiments on lactate and acetate in our study produced higher concentrations of butyrate (up to 42 mM) than the reported co-assimilation of glycerol and acetate by *C. beijerinckii* (≈20 mM) (Kumar et al., 2022), and than the co-assimilation of lactate and acetate by *C. saccharobutylicum* (Diez-Gonzalez et al., 1995) (≈20 mM).

Model predictions indicated that *C. beijerinckii* could grow on lactate as the sole carbon and energy source, as was recently observed (Schwalm et al., 2019). However, the growth rate was improved by the addition of acetate (Figure 3), as was previously shown (Diez-Gonzalez et al., 1995). The addition of acetate favors lactate uptake, since the acetyl-CoA pool increases with addition of acetate as co-substrate, and thus, more acetyl-CoA would be converted into butyrate producing more ATP. Co-culture fed-batch experiments showed, however, accumulation of acetate in the fermentation broth. This showed that not all acetate produced by *C. autoethanogenum* was consumed by *C. beijerinckii*, as indicated by the model, and possibly that some acetate could also be produced by *C. beijerinckii*.

We should note that the deployed modeling approach predicts steady-state production or consumption rates, and thus, we cannot compare the results quantitatively with bioreactor data, which consist of concentrations over time. Instead, our study should be seen as an exploratory study assessing the feasibility of the co-culture. Future optimization of this co-culture could integrate current experimental data and relative abundance of species into dynamic modeling approaches to gain better insights into the concentration profiles over time. These results show that community modeling of metabolism is a valuable tool to guide the design of microbial consortia for the tailored production of important chemicals from renewable resources. It thereby expands the space of options to possibly accelerate the transition to a biobased economy.

5. Conclusion

Genome-scale metabolic modeling helped identifying the ability of *C. beijerinckii* to co-metabolize acetate and lactate for the production of butyrate. This ability was experimentally verified in batch serum bottles and pH-controlled batch bioreactor fermentations. A community

model of *C. autoethanogenum* and *C. beijerinckii* was then constructed to assess the feasibility of the co-culture to produce butyrate from CO_2/H_2 and lactate. Community modeling predicted the feasibility of the co-culture in several conditions and the interactions between species, especially, the exchange of acetate. Following model predictions, the co-culture of *C. autoethanogenum* and *C. beijerinckii* was established in pH-controlled fed-batch fermentations. The main products were acetate, butyrate and the newly identified metabolite, isobutyrate. Our study shows the strength of a model-driven approach to explore the high metabolic flexibility of clostridial species for the production of chemicals from renewable sources.

Data availability statement

The original contributions presented in the study are included in the article/Supplementary material, further inquiries can be directed to the corresponding author.

Author contributions

SB-V and NN conceived and designed the study and drafted the manuscript. SB-V constructed the models and performed model simulations and data analysis. NN performed the experiments and data analysis. MS-D, AML-C, JH, SB, PS, and VM conceived, designed, and supervised the research. MS-D, VM, JH, and AML-C acquired project funding. All authors reviewed and edited the study. All authors read and approved the content of the submitted version.

Funding

The research leading to these results has received funding from the Netherlands Science Foundation (NWO) under the programme Closed Cycles (Project no. ALWGK.2016.029) and the Netherlands Ministry of Education, Culture and Science under the Gravitation Grant no. 024.002.002. AML-C received funding from the European Union's Horizon 2020 research and innovation programme under Grant Agreement no. 761042 (BIOCON-CO2).

Acknowledgments

We thank Dr. Truus de Vrije and Hetty van der Wal for their help with the experiments and Professor Diana Z. Sousa for the fruitful discussions.

Conflict of interest

VM has interests in LifeGlimmer. JH has interests in NoPalm Ingredients BV.

The remaining authors declare that the research was conducted in the absence of any commercial or financial relationships that could be construed as a potential conflict of interest.

Publisher's note

All claims expressed in this article are solely those of the authors and do not necessarily represent those of their affiliated organizations, or those of the publisher, the editors and the reviewers. Any product that may be evaluated in this article, or claim that may be made by its manufacturer, is not guaranteed or endorsed by the publisher.

Supplementary material

The Supplementary Material for this article can be found online at: https://www.frontiersin.org/articles/10.3389/fmicb.2022.1064013/full#supplementary-material

References

Abrini, J., Naveau, H., and Nyns, E. J. (1994). *Clostridium autoethanogenum*, sp. nov., an anaerobic bacterium that produces ethanol from carbon monoxide. *Arch. Microbiol.* 161, 345–351. doi: 10.1007/BF00303591

Bae, J., Song, Y., Lee, H., Shin, J., Jin, S., Kang, S., et al. (2022). Valorization of C1 gases to value-added chemicals using acetogenic biocatalysts. *Chem. Eng. J.* 428:131325. doi: 10.1016/j.cej.2021.131325

Bengelsdorf, F. R., Beck, M. H., Erz, C., Hoffmeister, S., Karl, M. M., Riegler, P., et al. (2018). Bacterial anaerobic synthesis gas (syngas) and CO_2H_2 fermentation. *Adv. Appl. Microbiol.* 103, 143–221. doi: 10.1016/bs.aambs.2018.01.002

Benito-Vaquerizo, S., Diender, M., Parera Olm, I., Martins dos Santos, V. A., Schaap, P. J., Sousa, D. Z., et al. (2020). Modeling a co-culture of *Clostridium autoethanogenum* and *Clostridium kluyveri* to increase syngas conversion to medium-chain fatty-acids. *Comput. Struct. Biotechnol. J.* 18, 3255–3266. doi: 10.1101/2020.06.23.167189

Benito-Vaquerizo, S., Olm, I. P., de Vroet, T., Schaap, P. J., Sousa, D. Z., dos Santos, V. A. M., and Suarez-Diez, M. (2022). Genome-scale metabolic modelling enables deciphering ethanol metabolism *via* the acrylate pathway in the propionate-producer *Anaerotignum neopropionicum*. *Microb. Cell Fact.* 21, 1–18. doi: 10.1186/s12934-022-01841-1

Bertsch, J., and Müller, V. (2015). Bioenergetic constraints for conversion of syngas to biofuels in acetogenic bacteria. *Biotechnol. Biofuels* 8, 1–12. doi: 10.1186/s13068-015-0393-x

Brändle, J., Domig, K. J., and Kneifel, W. (2016). Relevance and analysis of butyric acid producing clostridia in milk and cheese. *Food Control* 67, 96–113. doi: 10.1016/j.foodcont.2016.02.038

Casau, M., Dias, M. F., Matias, J. C., and Nunes, L. J. (2022). Residual biomass: a comprehensive review on the importance, uses and potential in a circular bioeconomy approach. *Resources* 11:35. doi: 10.3390/resources11040035

Chan, S. H. J., Simons, M. N., and Maranas, C. D. (2017). Steadycom: predicting microbial abundances while ensuring community stability. *PLoS Comput. Biol.* 13:e1005539. doi: 10.1371/journal.pcbi.1005539

Charubin, K., and Papoutsakis, E. T. (2019). Direct cell-to-cell exchange of matter in a synthetic *Clostridium syntrophy* enables CO_2 fixation, superior metabolite yields, and an expanded metabolic space. *Metab. Eng.* 52, 9–19. doi: 10.1016/j.ymben.2018.10.006

Chen, C. K., and Blaschek, H. P. (1999). Effect of acetate on molecular and physiological aspects of *Clostridium beijerinckii* NCIMB 8052 solvent production and strain degeneration. *Appl. Environ. Microbiol.* 65, 499–505. doi: 10.1128/AEM.65.2.499-505.1999

Chen, Y., Sharma-Shivappa, R. R., and Chen, C. (2007). Ensiling agricultural residues for bioethanol production. *Appl. Biochem. Biotechnol.* 143, 80–92. doi: 10.1007/s12010-007-0030-7

Croux, C., Canard, B., Goma, G., and Soucaille, P. (1992). Autolysis of *Clostridium acetobutylicum* ATCC 824. *J. Gen. Microbiol.* 138, 861–869. doi: 10.1099/00221287-138-5-861

Dash, S., Mueller, T. J., Venkataramanan, K. P., Papoutsakis, E. T., and Maranas, C. D. (2014). Capturing the response of *Clostridium acetobutylicum* to chemical stressors using a regulated genome-scale metabolic model. *Biotechnol. Biofuels* 7, 1–16. doi: 10.1186/s13068-014-0144-4

Detman, A., Mielecki, D., Chojnacka, A., Salamon, A., Błaszczyk, M. K., and Sikora, A. (2019). Cell factories converting lactate and acetate to butyrate: *Clostridium butyricum* and microbial communities from dark fermentation bioreactors. *Microb. Cell Factories* 18, 1–12. doi: 10.1186/s12934-019-1085-1

Diallo, M., Kengen, S. W., and López-Contreras, A. M. (2021). Sporulation in solventogenic and acetogenic Clostridia. *Appl. Microbiol. Biotechnol.* 105, 3533–3557. doi: 10.1007/s00253-021-11289-9

Diallo, M., Kint, N., Monot, M., Collas, F., Martin-Verstraete, I., Oost, J. V. D., et al. (2020). Transcriptomic and phenotypic analysis of a spoiie mutant in *Clostridium beijerinckii*. *Front. Microbiol.* 11:556064. doi: 10.3389/fmicb.2020.556064

Diender, M., Olm, I. P., Gelderloos, M., Koehorst, J. J., Schaap, P. J., Stams, A. J., et al. (2019). Metabolic shift induced by synthetic co-cultivation promotes high yield of chain elongated acids from syngas. *Sci. Rep.* 9, 1–11. doi: 10.1038/s41598-019-54445-y

Diender, M., Stams, A. J., and Sousa, D. Z. (2016). Production of medium-chain fatty acids and higher alcohols by a synthetic co-culture grown on carbon monoxide or syngas. *Biotechnol. Biofuels* 9, 1–11. doi: 10.1186/s13068-016-0495-0

Diez-Gonzalez, F., Russell, J. B., and Hunter, J. B. (1995). The role of an NAD-independent lactate dehydrogenase and acetate in the utilization of lactate by *Clostridium acetobutylicum* strain P262. *Arch. Microbiol.* 164, 36–42. doi: 10.1007/BF02568732

Drake, H. L., and Daniel, S. L. (2004). Physiology of the thermophilic acetogen *Moorella thermoacetica*. *Res. Microbiol.* 155, 422–36. doi: 10.1016/j.resmic.2004.03.003

Du, Y., Zou, W., Zhang, K., Ye, G., and Yang, J. (2020). Advances and applications of *Clostridium* co-culture systems in biotechnology. *Front. Microbiol.* 11:2842. doi: 10.3389/fmicb.2020.560223

Dwidar, M., Park, J. Y., Mitchell, R. J., and Sang, B. I. (2012). The future of butyric acid in industry. *Sci. World J.* 2012:471417. doi: 10.1100/2012/471417

Ebrahim, A., Lerman, J. A., Palsson, B. O., and Hyduke, D. R. (2013). COBRApy: constraints-based reconstruction and analysis for python. *BMC Syst. Biol.* 7:74. doi: 10.1186/1752-0509-7-74

Foster, C., Charubin, K., Papoutsakis, E. T., and Maranas, C. D. (2021). Modeling growth kinetics, interspecies cell fusion, and metabolism of a *Clostridium acetobutylicum/Clostridium ljungdahlii* syntrophic coculture. *mSystems* 6:e01325-20. doi: 10.1128/mSystems.01325-20

Freier, D., and Gottschalk, G. (1987). L(+)-lactate dehydrogenase of *Clostridium acetobutylicum* is activated by fructose-1,6-bisphosphate. *FEMS Microbiol. Lett.* 43, 229–233. doi: 10.1111/j.1574-6968.1987.tb02128.x

García-Jiménez, B., Torres-Bacete, J., and Nogales, J. (2021). Metabolic modelling approaches for describing and engineering microbial communities. *Comput. Struct. Biotechnol. J.* 19:226. doi: 10.1016/j.csbj.2020.12.003

Gottinger, A., Ladu, L., and Quitzow, R. (2020). Studying the transition towards a circular bioeconomy-a systematic literature review on transition studies and existing barriers. *Sustainability* 12:8990. doi: 10.3390/su12218990

Gu, C., Kim, G. B., Kim, W. J., Kim, H. U., and Lee, S. Y. (2019). Current status and applications of genome-scale metabolic models. *Genome Biol.* 20, 1–18. doi: 10.1186/s13059-019-1730-3

Hwang, H. W., Yoon, J., Min, K., Kim, M. S., Kim, S. J., Cho, D. H., et al. (2020). Two-stage bioconversion of carbon monoxide to biopolymers *via* formate as an intermediate. *Chem. Eng. J.* 389:124394. doi: 10.1016/j.cej.2020.124394

Ibarbalz, F. M., Pérez, M. V., Figuerola, E. L. M., and Erijman, L. (2014). The bias associated with amplicon sequencing does not affect the quantitative assessment of bacterial community dynamics. *PLoS ONE* 9:e99722. doi: 10.1371/journal.pone.0099722

Im, C., Valgepea, K., Modin, O., and Nygård, Y. (2022). *Clostridium ljungdahlii* as a biocatalyst in microbial electrosynthesis-Effect of culture conditions on product formation. *Bioresour. Technol. Rep.* 19:101156. doi: 10.1016/j.biteb.2022.101156

Keis, S., Sullivan, J. T., and Jones, D. T. (2001). Physical and genetic map of the *Clostridium saccharobutylicum* (formerly *Clostridium acetobutylicum*) NCP 262 chromosome. *Microbiology* 147, 1909–1922. doi: 10.1099/00221287-147-7-1909

Khandelwal, R. A., Olivier, B. G., Röling, W. F. M., Teusink, B., and Bruggeman, F. J. (2013). Community flux balance analysis for microbial consortia at balanced growth. *PLoS ONE* 8:e64567. doi: 10.1371/journal.pone.0064567

Kim, M., Park, B. G., Kim, E. J., Kim, J., and Kim, B. G. (2019). *In silico* identification of metabolic engineering strategies for improved lipid production in *Yarrowia lipolytica* by genome-scale metabolic modeling. *Biotechnol. Biofuels* 12, 1–14. doi: 10.1186/s13068-019-1518-4

Köpke, M., Gerth, M. L., Maddock, D. J., Mueller, A. P., Liew, F. M., Simpson, S. D., et al. (2014). Reconstruction of an acetogenic 2,3-butanediol pathway involving a novel NADPH-dependent primary-secondary alcohol dehydrogenase. *Appl. Environ. Microbiol.* 80:3394. doi: 10.1128/AEM.00301-14

Kremp, F., Roth, J., and Müller, V. (2020). The sporomusa type Nfn is a novel type of electron-bifurcating transhydrogenase that links the redox pools in acetogenic bacteria. *Sci. Rep.* 10, 1–14. doi: 10.1038/s41598-020-71038-2

Kuit, W., Minton, N. P., López-Contreras, A. M., and Eggink, G. (2012). Disruption of the acetate kinase (ACK) gene of *Clostridium acetobutylicum* results in delayed acetate production. *Appl. Microbiol. Biotechnol.* 94:729. doi: 10.1007/s00253-011-3848-4

Kumar, E., Gangwar, S., Ujor, B., Glycerol, V. C., Agyeman-Duah, E., Kumar, S., et al. (2022). Glycerol utilization as a sole carbon source disrupts the membrane architecture and solventogenesis in *Clostridium beijerinckii* NCIMB 8052. *Fermentation* 8:339. doi: 10.3390/fermentation8070339

Lee, H., Bae, J., Jin, S., Kang, S., and Cho, B.-K. (2022). Engineering acetogenic bacteria for efficient one-carbon utilization. *Front. Microbiol.* 13:865168. doi: 10.3389/fmicb.2022.865168

Liao, C., Seo, S. O., Celik, V., Liu, H., Kong, W., Wang, Y., et al. (2015). Integrated, systems metabolic picture of acetone-butanol-ethanol fermentation by *Clostridium acetobutylicum*. *Proc. Natl. Acad. Sci. U.S.A.* 112, 8505–8510. doi: 10.1073/pnas.1423143112

Loow, Y. L., Wu, T. Y., Jahim, J. M., Mohammad, A. W., and Teoh, W. H. (2016). Typical conversion of lignocellulosic biomass into reducing sugars using dilute acid hydrolysis and alkaline pretreatment. *Cellulose* 23, 1491–1520. doi: 10.1007/s10570-016-0936-8

Marcellin, E., Behrendorff, J. B., Nagaraju, S., Detissera, S., Segovia, S., Palfreyman, R. W., et al. (2016). Low carbon fuels and commodity chemicals from waste gases-systematic approach to understand energy metabolism in a model acetogen. *Green Chem.* 18, 3020–3028. doi: 10.1039/C5GC02708J

Milne, C. B., Eddy, J. A., Raju, R., Ardekani, S., Kim, P. J., Senger, R. S., et al. (2011). Metabolic network reconstruction and genome-scale model of butanol-producing strain *Clostridium beijerinckii* NCIMB 8052. *BMC Syst. Biol.* 5:130. doi: 10.1186/1752-0509-5-130

Monot, F., Martin, J. R., Petitdemange, H., and Gay, R. (1982). Acetone and butanol production by *Clostridium acetobutylicum* in a synthetic medium. *Appl. Environ. Microbiol.* 44, 1318–1324. doi: 10.1128/aem.44.6.1318-1324.1982

Mook, A., Beck, M. H., Baker, J. P., Minton, N. P., Dürre, P., and Bengelsdorf, F. R. (2022). Autotrophic lactate production from H_2 + CO_2 using recombinant and fluorescent FAST-tagged *Acetobacterium woodii* strains. *Appl. Microbiol. Biotechnol.* doi: 10.1007/s00253-022-11770-z

Moreira, J. P., Diender, M., Arantes, A. L., Boeren, S., Stams, A. J., Alves, M. M., et al. (2021). Propionate production from carbon monoxide by synthetic cocultures of *Acetobacterium wieringae* and propionigenic bacteria. *Appl. Environ. Microbiol.* 87:e0283920. doi: 10.1128/AEM.02839-20

Patakova, P., Branska, B., Sedlar, K., Vasylkivska, M., Jureckova, K., Kolek, J., et al. (2019). Acidogenesis, solventogenesis, metabolic stress response and life cycle changes in *Clostridium beijerinckii* NRRL B-598 at the transcriptomic level. *Sci. Rep.* 9, 1–21. doi: 10.1038/s41598-018-37679-0

Ragsdale, S. W., and Pierce, E. (2008). Acetogenesis and the wood-jungdahl pathway of co2 fixation. *Biochim. Biophys. Acta* 1784, 1873–1898. doi: 10.1016/j.bbapap.2008.08.012

Richardson, Y., Drobek, M., Julbe, A., Blin, J., and Pinta, F. (2015). "Chapter 8: Biomass gasification to produce Syngas," in *Recent Advances in Thermo-Chemical Conversion of Biomass*, eds A. Pandey, T. Bhaskar, M. Stäcker, and R. K. Sukumaran (Boston, MA: Elsevier), 213–250. doi: 10.1016/B978-0-444-63289-0.00008-9

Sakarika, M., Delmoitié, B., Ntagia, E., Chatzigiannidou, I., Gabet, X., Ganigué, R., et al. (2022). Production of microbial protein from fermented grass. *Chem. Eng. J.* 433:133631. doi: 10.1016/j.cej.2021.133631

Sar, T., Harirchi, S., Ramezani, M., Bulkan, G., Akbas, M. Y., Pandey, A., et al. (2022). Potential utilization of dairy industries by-products and wastes through microbial processes: a critical review. *Sci. Total Environ.* 810:152253. doi: 10.1016/j.scitotenv.2021.152253

Schwalm, N. D., Mojadedi, W., Gerlach, E. S., Benyamin, M., Perisin, M. A., and Akingbade, K. L. (2019). Developing a microbial consortium for enhanced metabolite production from simulated food waste. *Fermentation* 5:98. doi: 10.3390/fermentation5040098

Show, K. Y., Lee, D. J., Tay, J. H., Lin, C. Y., and Chang, J. S. (2012). Biohydrogen production: current perspectives and the way forward. *Int. J. Hydrog. Energy* 37, 15616–15631. doi: 10.1016/j.ijhydene.2012.04.109

Siemerink, M. A., Schwarz, K., Grimmler, C., Kuit, W., Ehrenreich, A., and Kengen, S. W. (2014). "Chapter 8: Comparative genomic analysis of the central metabolism of the solventogenic species *Clostridium acetobutylicum* ATCC 824 and *Clostridium beijerinckii* NCIMB 8052," in *Systems Biology of Clostridium*, 193–219. doi: 10.1142/9781783264414_0008

Sreekumar, S., Baer, Z. C., Pazhamalai, A., Gunbas, G., Grippo, A., Blanch, H. W., et al. (2015). Production of an acetone-butanol-ethanol mixture from *Clostridium acetobutylicum* and its conversion to high-value biofuels. *Nat. Protoc.* 10, 528–537. doi: 10.1038/nprot.2015.029

Tracy, B. P., Jones, S. W., Fast, A. G., Indurthi, D. C., and Papoutsakis, E. T. (2012). Clostridia: the importance of their exceptional substrate and metabolite diversity for biofuel and biorefinery applications. *Curr. Opin. Biotechnol.* 23, 364–381. doi: 10.1016/j.copbio.2011.10.008

Valgepea, K., Lemgruber, R. D. S. P., Abdalla, T., Binos, S., Takemori, N., Takemori, A., et al. (2018). H2 drives metabolic rearrangements in gas-fermenting *Clostridium autoethanogenum*. *Biotechnol. Biofuels* 11:55. doi: 10.1186/s13068-018-1052-9

Valgepea, K., Loi, K. Q., Behrendorff, J. B., Lemgruber, R. d. S., Plan, M., Hodson, M. P., et al. (2017). Arginine deiminase pathway provides ATP and boosts growth of the gas-fermenting acetogen *Clostridium autoethanogenum*. *Metab. Eng.* 41, 202–211. doi: 10.1016/j.ymben.2017.04.007

Xu, Z., Luo, Y., Mao, Y., Peng, R., Chen, J., Soteyome, T., et al. (2020). Spoilage lactic acid bacteria in the brewing industry. *J. Microbiol. Biotechnol.* 30, 955–961. doi: 10.4014/jmb.1908.08069

Yang, Y., Hoogewind, A., Moon, Y. H., and Day, D. (2016). Production of butanol and isopropanol with an immobilized *Clostridium*. *Bioprocess Biosyst. Eng.* 39, 421–428. doi: 10.1007/s00449-015-1525-1

frontiers | Frontiers in Microbiology

TYPE Original Research
PUBLISHED 24 January 2023
DOI 10.3389/fmicb.2022.1046661

Check for updates

OPEN ACCESS

EDITED BY
Durgesh K. Jaiswal,
Savitribai Phule Pune University, India

REVIEWED BY
Lucia Zifcakova,
Independent Researcher,
Okinawa, Japan
Xiaobo Liu,
Nanjing University of Science and Technology, China

*CORRESPONDENCE
Kirsten S. Hofmockel
✉ kirsten.hofmockel@pnnl.gov

SPECIALTY SECTION
This article was submitted to Microbiotechnology, a section of the journal Frontiers in Microbiology

RECEIVED 16 September 2022
ACCEPTED 21 December 2022
PUBLISHED 24 January 2023

CITATION
McClure R, Garcia M, Couvillion S, Farris Y and Hofmockel KS (2023) Removal of primary nutrient degraders reduces growth of soil microbial communities with genomic redundancy.
Front. Microbiol. 13:1046661.
doi: 10.3389/fmicb.2022.1046661

COPYRIGHT
© 2023 McClure, Garcia, Couvillion, Farris and Hofmockel. This is an open-access article distributed under the terms of the Creative Commons Attribution License (CC BY). The use, distribution or reproduction in other forums is permitted, provided the original author(s) and the copyright owner(s) are credited and that the original publication in this journal is cited, in accordance with accepted academic practice. No use, distribution or reproduction is permitted which does not comply with these terms.

Removal of primary nutrient degraders reduces growth of soil microbial communities with genomic redundancy

Ryan McClure[1], Marci Garcia[1], Sneha Couvillion[1], Yuliya Farris[1] and Kirsten S. Hofmockel[1,2]*

[1]Biological Sciences Division, Pacific Northwest National Laboratory, Richland, WA, United States, [2]Department of Agronomy, Iowa State University, Ames, IA, United States

Introduction: Understanding how microorganisms within a soil community interact to support collective respiration and growth remains challenging. Here, we used a model substrate, chitin, and a synthetic Model Soil Consortium (MSC-2) to investigate how individual members of a microbial community contribute to decomposition and community growth. While MSC-2 can grow using chitin as the sole carbon source, we do not yet know how the growth kinetics or final biomass yields of MSC-2 vary when certain chitin degraders, or other important members, are absent.

Methods: To characterize specific roles within this synthetic community, we carried out experiments leaving out members of MSC-2 and measuring biomass yields and CO_2 production. We chose two members to iteratively leave out (referred to by genus name): *Streptomyces,* as it is predicted *via* gene expression analysis to be a major chitin degrader in the community, and *Rhodococcus* as it is predicted *via* species co-abundance analysis to interact with several other members.

Results: Our results showed that when MSC-2 lacked Streptomyces, growth and respiration of the community was severely reduced. Removal of either *Streptomyces* or Rhodococcus led to major changes in abundance for several other species, pointing to a comprehensive shifting of the microbial community when important members are removed, as well as alterations in the metabolic profile, especially when Streptomyces was lacking. These results show that when keystone, chitin degrading members are removed, other members, even those with the potential to degrade chitin, do not fill the same metabolic niche to promote community growth. In addition, highly connected members may be removed with similar or even increased levels of growth and respiration.

Discussion: Our findings are critical to a better understanding of soil microbiology, specifically in how communities maintain activity when biotic or abiotic factors lead to changes in biodiversity in soil systems.

KEYWORDS

soil microbiome, primary degrader, chitin degradation, functional redundancy, synthetic community

Introduction

Microbial metabolism in soil is critical to a number of functions related to promotion of plant growth in the face of environmental or pathogen stress (Hannula et al., 2020; Tian et al., 2020) and to the cycling of carbon and other nutrients (Gougoulias et al., 2014; Scarlett et al., 2021). As carbon (C) enters the soil (either through plant exudates, plant litter or other means) there are multiple microbial metabolic pathways that support anabolic (cell growth and replication, increases in biomass) or catabolic (CO_2 respiration) activity. How microbial species or communities partition incoming carbon into either biomass or respiration pathways defines their carbon use efficiency (CUE; Li et al., 2014; Saifuddin et al., 2019). CUE can be examined in several ways, including at the ecological and population scale. When examining CUE with respect to communities it is defined as the gross biomass production per unit substrate taken up over short time scales. This definition only considers the uptake, not the subsequent loss of C as a function of microbial necromass and exudates (Geyer et al., 2016) but does factor in C lost through respiration as CO_2.

When quantifying the functions carried out by the soil microbiome, or when analyzing values such as CUE, viewing communities as the sum of individual members can lead to unidentified sources of variation. This is due to the fact that it is interactions between microbial species that define their metabolism and CUE values (Pan et al., 2021) not merely the sum of the individual community members in isolation (Saleem et al., 2019). The interaction network that emerges as these species exchange nutrients, compete for resources, or shift their phenotypes leads to certain species emerging as keystone members of the community. Microbial keystone species are defined as taxa with a large number of interactions with other members of the community and/or those that exert a large effect on the community structure or functioning (Banerjee et al., 2018). Keystone taxa may be those that carry out critical ecological functions in the community and, as a result, when they are lost, the community may show much less stability and activity (Xun et al., 2021).

Keystone species may be especially likely to emerge in small communities, with less opportunity for redundancy, when they are provided with complex carbon or nitrogen sources that not all community members can metabolize equally (Liu et al., 2021). The reduced size of these communities, both in terms of number of species and number of available metabolic processes, means that only a few members can play a role as keystone members or primary degraders in the community, and if these members are lost the community suffers. Keystone members are also defined by the environment. Under conditions with varied nutrient sources that many members can metabolize keystone members may be few. However, under conditions with a small number of nutrient sources, especially those that may be energetically expensive to metabolize, keystone members may be more important (Duan et al., 2022). Chitin is one such nutrient source that often promotes interspecies interactions when degraded. Previous work has shown that in a monoculture of a chitin degrading species only a small subset of cells actually produce chitinase and chitin breakdown products (chiefly N-acetyl-glucosamine, NAG) with the remaining cells subsisting off these breakdown products (Baty III et al., 2000a,b; Zhou et al., 2020). In addition, chitinase enzymes are often not cell associated (Itoh et al., 2013; Lobo et al., 2013; Johnson-Rollings et al., 2014) meaning the breakdown products can be more easily shared. In accordance with this, species have been found that contain NAG importers with no corresponding chitinase gene, suggesting they obtain NAG through the breakdown of chitin carried out by other species (Keyhani and Roseman, 1997). As chitin is an abundant C and nitrogen source in soil, keystone species in these communities may center around chitin breakdown with the primary chitin degraders in a community occupying the keystone positions. Even in communities that may have functional redundancy at the genomic level, the possibility for keystone species still exists. This is because genomic potential is not a direct predictor of phenotypic expression (Li et al., 2019). Environmental factors, including interspecies interactions, can alter the expression of a gene or enzyme, especially if this enzyme may be energetically unfavorable to synthesize (McClure et al., 2022).

Primary degraders and keystone species play important roles in soil microbiomes but the inherent complexity of this site, with thousands of species and metabolites and potentially millions of interactions, means that evaluating keystone species and how they may drive CUE can be difficult in the native soil. Recently, we sought to reduce this complexity through the generation of a model soil consortium (MSC). Previous work has developed MSC-1, a naturally evolved community of ~25 species (McClure et al., 2020) and MSC-2, a synthetic community of eight species isolated from MSC-1 (McClure et al., 2022). Within MSC-2 we identified two potential keystone species: a *Rhodococcus* species was found to be highly connected to other species in a co-abundance network of MSC-1 (McClure et al., 2020) while a *Streptomyces* species was found to be the primary, and perhaps only, chitin degrading species within the community (McClure et al., 2022). Here, we cultured MSC-2 lacking each of these species in turn and compared it to the complete MSC-2 community with reference to biomass accumulation, respiration, and ultimately CUE. We also collected and analyzed data showing the resulting community make up (amplicon analysis) and metabolite environment. Our results show how synthetic, representative microbial communities respond to the absence of different varieties of potential keystone species. These conclusions in turn can reveal how natural soil communities, and their C and nutrient cycling properties, may respond when primary degraders increase or decrease their abundance in response to changing environments.

Materials and methods

Growth of MSC-2 and MSC-2 subsets with chitin

A detailed description of MSC-2 is in our previous publication (McClure et al., 2022) but briefly this community is comprised of eight strains of common soil bacteria: a *Streptomyces* sp., *Neorhizobium tomejilense*, *Dyadobacter fermentans*, *Sphingopyxis fribergensis*, *Ensifer adhaerens*, *Variovorax beijingensis*, *Sinorhizobium meliloti* and a *Rhodococcus* sp. For simplicity each member is referred to by its genus name. To set up cultures of the complete MSC-2 community or of subcommunities lacking certain members, each MSC-2 strain was plated on an R2A agar plate and incubated at 20°C for 3 days. Following incubation, growth was collected from each plate and used to set up a 5 mL liquid culture, one for each of the eight members of MSC-2. These cultures were shaken at 150 rpm at 20°C overnight in 50 mL breathable falcon tubes containing R2A medium with 100 ppm chitin. Cells were then spun down for 5 minutes at 5,000 g, washed in R2A and spun down again before being resuspended in 5 mL of fresh R2A. Resuspended cultures were added to 95 mL of R2A with 100 ppm chitin in a 500 mL flask and shaken at 150 rpm at 20°C overnight. After overnight growth, cultures were spun down as above, washed with M9, spun down again, and resuspended in 10 mL of M9. M9 consisted of 12.8 g/L Na_2HPO_4-$7H_2O$, 3 g/L KH_2PO_4, 0.5 g/L NaCl, 1 g/L NH_4Cl, 4 mM $MgSO_4$, 100 uM $CaCl_2$, 1 mg/L biotin, 1 mg/L thymine, 1 mL/L of 1,000x wolfs trace minerals (comprised of the following per 1 l: HCl 1 mL, Na_4EDTA (tetrasodium) 0.5 g, $FeCl_3$ 2 g, H_3BO_3 0.05 g, $ZnCl_2$ 0.05 g, $CuCl_2$ 0.03 g, $MnCl_2$ 0.05 g $(NH_4)_2MoO_4$ 0.05 g, AlK (SO_4) 0.05 g, $CoCl_2$ 0.05 g, $NiCl_2$ 0.05 g) and 5 mL/L of vitamin solution (comprised of the following per 1 l: 10 mg each of Niacin, Pantothenate, Lipoic Acid, *p*-Aminobenzoic Acid, Thiamine B_1, Riboflavin B_2, Pyridoxine B_6 and Cobalamin B_{12} and 4 mg each of Biotin and Folic Acid). Additional biotin and thymine were added as that was found to lead to better growth of species.

Specific volumes of each strain were then collected and combined in a 50 mL falcon tube aiming for a final volume of 10 mL. Volumes were chosen so that cell numbers would be equal between all eight members using previously collected O.D. and colony forming unit (C.F.U.) data. Three different communities were made through combinations of MSC-2 members. One community consisted of all eight members of MSC-2 (MSC-2 Complete), one community consisted of all members except *Rhodococcus* (MSC-2-R), and one community consisted of all members except *Streptomyces* (MSC-2-S). The $O.D._{600}$ of each of the three communities was then adjusted by dilution to between 0.08–0.12 and chitin was added to a final concentration of 500 ppm. From these communities 9 mL was pulled and used to set up replicate tubes of each community (5 replicates of MSC-2 Complete, 5 replicates of MSC-2-R and 5 replicates of MSC-2-S, each containing 9 mL). Cultures were grown in 40 mL amber borosilicate tubes with snap top septa cap with shaking (150 rpm) at 20°C. Cell counts were collected every 24 h using an 11th edition Agilent Novocyte flow cytometer. For all samples chitin was allowed to settle for 5 min before cells were counted. CO_2 measurements were taken every day starting after the first 24 h using an EGM-4 environmental gas monitor. After 7 days of growth cell pellets were collected for 16S amplicon analysis and supernatants were collected for metabolomics analysis.

16S amplicon analysis

DNA was extracted from bacterial cell pellets using the ZymoBIOMICS DNA Miniprep Kit. 16S sequencing was carried out by GENEWIZ (South Plainfield, NJ). The proprietary workflow at GENEWIZ effectively amplifies the three variable regions of the16S rRNA (V3, V4, and V5) using paired end read Illumina technology. Following sequencing, the two sequences of each read pair were merged according to overlapping sequences. The read merge is deemed to be successful only if the overlapping sequence is least 20 bp long. After merging, undetermined bases (N) were removed from the resulting sequence and primer and adapter sequences were removed. The 5′ and 3′ bases with Q score lower than 20 were also removed. The sequences obtained were then aligned to UCHIME 'Gold' database to identify and remove chimera sequence. Sequences passing this filtering step are deemed as clean data ready for analysis. Clustering of OTUs and taxonomic identification was carried out *via* QIIME2 (Bolyen et al., 2019).

Metabolomics analysis

Metabolomic analysis of MSC-2 and MSC-2 subsets was carried out by gas chromatography mass spectrometry (GC–MS) as previously described (Cao et al., 2021). Samples were grouped into blocks and randomized for each experiment. GC–MS raw data processing was done with the Metabolite Detector software and metabolites were identified by matching experimental spectra and retention indices to an augmented version of FiehnLib (Kind et al., 2009). In addition, the NIST 14 GC–MS library was used to cross-validate spectral matching scores obtained by using the Agilent library and to provide identifications of unmatched metabolites. After removing outlier samples, four biological replicates were analyzed for MSC-2 and MSC-2-R and five biological replicates for MSC-2-S. Metabolomics data was processed using MetaboAnalyst 5.0 (Pang et al., 2022). The data was normalized by sample median and log transformed. Significant features were identified by a one-way ANOVA (value of p threshold >0.05) followed by the Tukey's HSD post-hoc analyses. The autoscaled metabolite abundances for significant and annotated metabolites was visualized as a heatmap and hierarchical clustering of the metabolites was done using Euclidean distance measure and Ward clustering algorithm. Metabolites in the MSC-2-S or MSC-2-R communities were then

compared to the complete MSC-2 and metabolites that shifted their abundance between communities with an adjusted *p*-value (by Benjamini-Hochberg) of less than 0.05 were the focus of our analysis.

Results

Respiration of MSC-2 and MSC-2 subsets

The complete MSC-2 community consists of eight members (referred to by their genus name for simplicity): *Streptomyces*, *Neorhizobium*, *Dyadobacter*, *Sphingopyxis*, *Ensifer*, *Variovorax*, *Sinorhizobium* and *Rhodococcus*. Previous work by our group has found that *Rhodococcus* occupies a central and important position in this community (McClure et al., 2020). This suggests that *Rhodococcus* may interact with many other species and its removal may disrupt key interaction networks. Additional work by our group has also found that *Streptomyces* is the primary degrader of chitin in this community (McClure et al., 2022). However, other species can grow using chitin as the sole C source and thus may act as chitin degraders when the primary degrader is removed. To explore the role of each different type of potential keystone species in the context of community growth and CUE (biomass accumulation vs. CO_2 production) we examined respiration rates and cell counts of three different communities: the complete 8-member MSC-2 community, MSC-2 lacking *Rhodococcus* (MSC-2-R) and MSC-2 lacking *Streptomyces* (MSC-2-S) under conditions where each of these communities was grown using chitin as the sole C source.

Approximately 24 h after the start of growth MSC-2-S and MSC-2-R have significantly lower CO_2 production compared to MSC-2 (Figure 1). By 53 h after the start of growth, the difference in CO_2 production between MSC-2-S and MSC-2 becomes more pronounced and the difference between MSC-2 and MSC-2-R becomes less as the MSC-2-R community begins to increase respiration. This trend continues to a timepoint collected 76 h after the start of growth; by this point MSC-2-R is producing more CO_2 compared to MSC-2 and this difference is statistically significant. Respiration levels of the three communities continue in this way until 173 h after the start of growth when CO_2 production by MSC-2-R is beginning to drop (continuing a decline started at 122 h) while the respiration rates of the complete MSC-2 community have continued to rise and are just beginning to peak. At the final timepoint of 173 h MSC-2-R has again fallen below MSC-2 in CO_2 production with this difference reaching statistical significance. Through this entire respiration assay the MSC-2-S communities show a very slight early increase in CO_2 production, but consistently remain far below both MSC-2 and MSC-2-R communities, in some cases showing CO_2 levels that are barely above background (collected from non-inoculated control tubes containing chitin only). Compared to MSC-2 communities, MSC-2-R communities show a faster rise in CO_2 production followed by a similarly early fall while MSC-2-S communities show consistently far less respiration.

Biomass of MSC-2 and MSC-2 subsets

Production of CO_2 represents one possible fate for C obtained through degradation of chitin. An alternative path for C is to be incorporated as biomass of microbial cells. To explore this, we also used cell counting to determine the number of bacterial cells at timepoints similar to the CO_2 assays shown above (Figure 2). The overall trend of these biomass assays mirrored the CO_2 assays. Cell counts in MSC-2-S communities were consistently lower than MSC-2, in most cases significantly so, this is despite cell counts at the start of the experiment showing the same amount for each community, indicating that they all begin at the same "starting line." Cell counts for all communities showed a drop at 53 h but began to generally show increases after that. By 102 h after the start of the growth assay the MSC-2-R community showed higher cell numbers compared to MSC-2. However, by the end of the assay, similar to the respiration levels, the cell counts in the MSC-2-R community had dropped below those of MSC-2 (though not significantly so). One major difference between the cell count assay and the CO_2 assay was at the end point of the experiment. Cell counts continued to increase for both MSC-2 and MSC-2-R even at 173 h. For respiration, in both communities, CO_2 production peaked at 148–173 h for MSC-2 and for MSC-2-R actually began to fall at 173 h (Figure 1). The collection of both respiration and biomass assays allow us to characterize CUE patterns for the communities across time. Early in the growth experiment CUE rates are low, respiration is dominant, and cell counts levels drop slightly. By 102 h after the start CUE rates begin to rise as biomass levels increase. By the end of the experiment at 173 h, CUE levels have maximized with biomass very high and respiration beginning to fall (MSC-2-R) or stabilizing (MSC-2). However, when viewing both respiration or biomass accumulation communities lacking *Streptomyces* (MSC-2-S) show far lower values across almost all timepoints when compared to either MSC-2 or MSC-2-R communities.

Amplicon analysis of MSC-2 and MSC-2 subsets

16S amplicon analysis was used to query the relative abundance of each species at the conclusion of the 7-day growth assay (Figure 3). In the MSC-2 community *Ensifer* was the dominant community member, comprising approximately 80% of the community with *Rhodococcus*, *Sphingopyxis*, *Sinorhizobium* and *Streptomyces* comprising most of the remaining 20%. When *Rhodococcus* was removed from the community, in MSC-2-R samples, *Ensifer* dropped in abundance from ~80% to ~60%. Table 1 shows the fold changes of other members of MSC-2 and how their abundances shift as a function of loss of *Rhodococcus*.

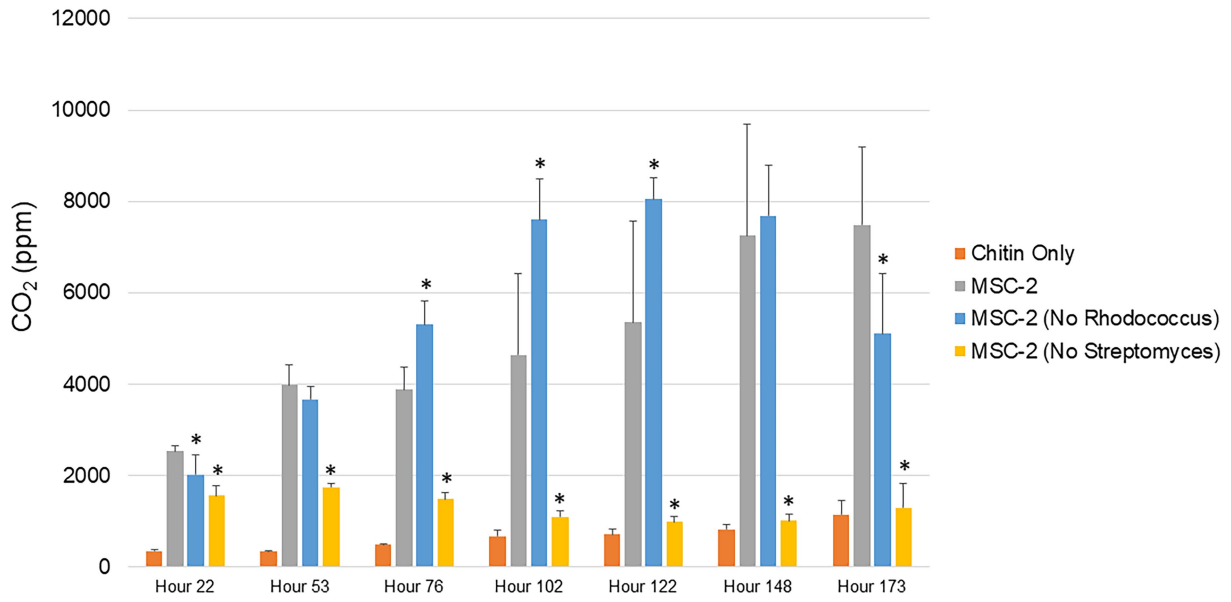

FIGURE 1
Respiration of MSC-2 and MSC-2 subset communities during chitin growth. CO_2 levels in parts per million are shown on the y-axis and timepoints ranging from 22 to 173h are shown on the x-axis. Orange bars are uninoculated samples containing only chitin, grey bars are complete MSC-2 communities, blue bars are MSC-2-R communities (lacking *Rhodococcus*), and yellow bars are MSC-2-S communities (lacing *Streptomyces*). Error bars indicate standard deviation and asterisks indicate that the community is statistically different from the MSC-2 community at that timepoint with a *p*-value of less than 0.05 using a Students *t*-test.

Aside from *Ensifer, Sinorhizobium* also showed a drop in abundance of nearly 2-fold. This drop in abundance for *Ensifer* and *Sinorhizobium* was concurrent with a relative increase in abundance for the other five members of this community. Of this *Dyadobacter* showed the greatest improvement with an approximately 10-fold increase in relative abundance. However, even with this increase *Dyadobacter* remained a low abundant member similar to what we have seen before (McClure et al., 2022) *Streptomyces* was more abundant and showed an increase of approximately 4-fold increase, going from ~3% to 10% in the absence of *Rhodococcus*. *Variovorax* also showed an increase in abundance as well.

We next compared the complete MSC-2 community to the community lacking *Streptomyces* (MSC-2-S). Without *Streptomyces* the community was much more even compared to the complete MSC-2 community and there was an even greater drop in *Ensifer*, the highly abundant member of MSC-2 (when compared to MSC-2-R). In MSC-2-S communities *Ensifer* dropped to ~36% with all other species increasing their relative abundance. Of these *Neorhizobium* had the biggest gain, going from 0.9% to more than 4%, a 15-fold increase. Interestingly, *Neorhizobium* did not show this magnitude increase in MSC-2-R samples even though *Ensifer* dropped there as well suggesting that the increase in *Neorhizobium* in MSC-2-S samples is due to lack of *Streptomyces*, not loss of *Ensifer*. *Rhodococcus* was the species that showed the next largest increase compared to MSC-2. *Rhodococcus* increased by more than 9-fold, going from ~4% to ~33% of the total community. *Sinorhizobium* also showed a ~3.7-fold increase in abundance. Like *Neorhizobium* this increase for *Sinorhizobium* was a very different response compared to that seen in the MSC-2-R community suggesting that it was lack of *Streptomyces*, not just a drop in *Ensifer* that led to this increase for *Sinorhizobium*. Other species also showed increases in abundance but their response in MSC-2-R and this community, MSC-2-S, were similar. All changes in abundance described in this section are statistically significant with a *p*-value of less than 0.05. It should be noted here that due to the nature of 16S sequencing the drop in *Ensifer* may open up more room on the sequencing flow cell allowing other species to show relative increases even if they are the same abundance. Species that show different responses in MSC-2-R and MSC-2-S communities, both of which lack *Ensifer*, are of interest as their response is likely not due to *Ensifer* abundance shifts but to true responses to the changing community. A PCA plot of all samples also showed clear delineation of the communities and that the variation between replicates was much smaller in the MSC-2-S community compared to the MSC-2 or MSC-2-R community (Supplementary Figure S1).

Metabolomic analysis of MSC-2 and MSC-2 subsets

We next examined the metabolic profile of MSC-2 and each of the subsets. Here, results were somewhat different from amplicon analysis. While MSC-2-R and MSC-2-S were both

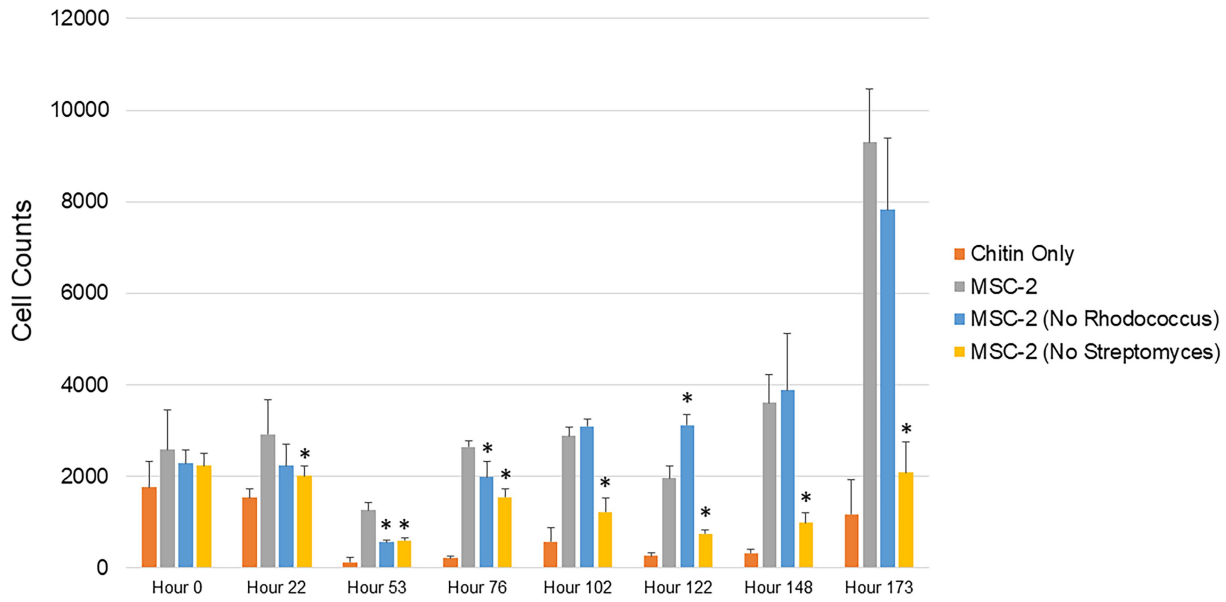

FIGURE 2
Cell counts of MSC-2 and MSC-2 subset communities during chitin growth. Cell counts are shown on the y-axis and timepoints ranging from 0 to 173h are shown on the x-axis. Orange bars are uninoculated samples containing only chitin, grey bars are complete MSC-2 communities, blue bars are MSC-2-R communities (lacking *Rhodococcus*), and yellow bars are MSC-2-S communities (lacing *Streptomyces*). Error bars indicate standard deviation and asterisks indicate that the community is statistically different from the MSC-2 community at that timepoint with a *p*-value of less than 0.05 using a Student's *t*-test.

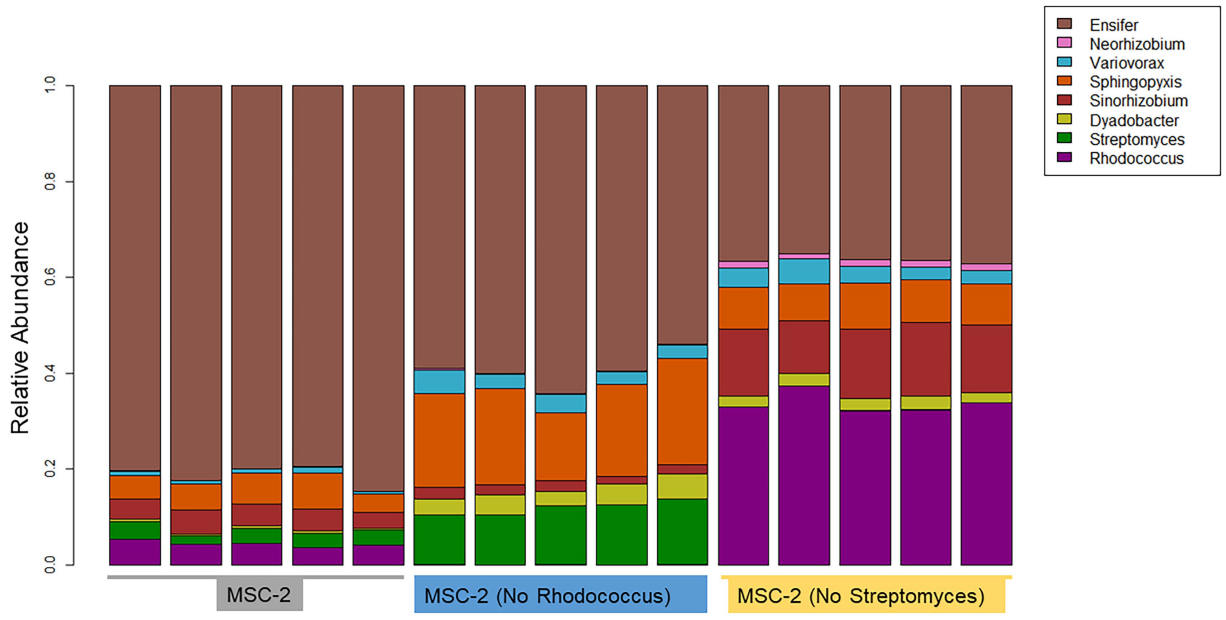

FIGURE 3
Taxonomic bar charts of MSC-2 members after chitin growth in MSC-2, MSC-2-R and MSC-2-S. Relative abundance is shown on the y-axis. MSC-2, MSC-2-R and MSC-2-S communities are grouped together on the *x*-axis. Color scheme assigned to each species is shown on the upper right.

distinct from MSC-2 (Supplementary Figure S2) a closer look at how metabolites differed shows that MSC-2-R was much more similar to MSC-2 compared to MSC-2-S. In fact, the MSC-2-S community was more similar to media blanks than either MSC-2 or MSC-2-R suggesting that without *Streptomyces* the metabolite profile of the environment shows the least change from starting

TABLE 1 Fold changes and *p*-values of member relative abundances in MSC-2-R and MSC-2-S communities.

MSC-2 member	Fold change		*p*-value	
	MSC-2-R/ MSC-2	MSC-2-S/ MSC-2	MSC-2-R vs. MSC-2	MSC-2-S vs. MSC-2
Rhodococcus	NA	9.07	NA	3.01E-09
Streptomyces	4.56	NA	8.91E-06	NA
Dyadobacter	10.71	6.81	2.04E-04	5.07E-07
Sinorhizobium	0.52	3.78	5.58E-04	9.86E-07
Sphingopyxis	3.84	1.84	1.10E-04	3.52E-04
Variovorax	4.49	5.18	6.80E-05	6.77E-04
Neorhizobium	2.18	15.84	5.22E-04	1.50E-07
Ensifer	0.82	0.53	4.70E-04	2.82E-08

conditions. Changes that did occur in the MSC-2-S community were, in many cases, the exact opposite for statistically significant metabolites compared to either MSC-2-R or the complete MSC-2 (Figure 4). We also looked in more detail at which specific metabolites were of higher or lower abundance in the MSC-2-R and MSC-2-S communities compared to the complete MSC-2. When comparing MSC-2-R to the complete MSC-2, 42 metabolites were differentially abundant. When comparing MSC-2-S to the complete MCS-2, 107 metabolites were differentially abundant. Table 2 shows some of the identified metabolites that were differentially abundant between the complete MSC-2 and the subcommunities. Focusing on metabolites that showed different fold changes in the MSC-2-R and MSC-2-S communities identified trehalose, adenine, succinic acid, N-carbamyl-L-glutamic acid, caffeic acid and mannobiose. Trehalose and succinic acid showed a decrease in communities lacking *Rhodococcus* and an increase in communities lacking *Streptomyces*. Adenine, N-carbamyl-L-glutamic acid, caffeic acid and mannobiose showed an increase in communities lacking *Rhodococcus* and a decrease in communities lacking *Streptomyces*.

Discussion

Within microbial communities, certain species often occupy important positions as primary degraders or keystone members. Here we explored how a defined community may respond when different kinds of keystone members (those highly connected to other members or those acting as primary degraders of nutrients) are removed. We found that when a keystone member defined by connectedness (*Rhodococcus*) was removed there was no negative effect on community growth or respiration, in fact the community did somewhat better. In contrast, when a keystone member defined by a chitin degradation phenotype (*Streptomyces*) was removed there was a severe loss of growth and respiration in the resulting community. Previous work (McClure et al., 2022) has strongly suggested that *Streptomyces* is the primary chitin degrader in the MSC-2 community. However, this same earlier study also showed that additional species are able to grow on chitin (as measured by increases in O.D.) even in monoculture. Despite redundancy in genomic potential and functional assays carried out in monoculture, functional redundancy (as measured by growth and respiration) was not expressed in the community context when the primary chitin degrader was removed. Why do these other species not emerge as alternative primary degraders and keystone members in the absence of *Streptomyces* to drive community growth to levels seen in the complete MSC-2 community? It may be that a without *Streptomyces* no species is able to act as a chitin degrader and that the minimal growth of the MSC-2-S community reflects necromass metabolism. While we do see that many of the MSC-2 species are able to grow on chitin in monoculture, phenotypes expressed in a community often do match those seen in monoculture (Heyse et al., 2019; Zuñiga et al., 2019), something we have also seen in our previous publications examining MSC-2 (McClure et al., 2022). Inhibitions between species may prevent one of the remaining chitin degrading members from expressing this phenotype and the community as a whole is stuck in its initial state (Geesink et al., 2018). This possibility is supported by the fact that the MSC-2-S community is still relatively even after 8 days, suggesting minimal growth and cell turnover and the fact that the metabolic profile is very similar to the initial growth media. Alternatively, some species may act as chitin degraders but they are simply not as efficient as *Streptomyces* so the community takes longer to reach high biomass levels. This is supported by our cell count measurements (Figure 2) showing that between hours 122 and 173 the CUE of the MSC-2-S community is high, biomass levels are increasing, and respiration is low, and that if the experiment had continued the MSC-2-S community may reach levels seen with the complete MSC-2. Our previous work (McClure et al., 2022) and others have shown variation among bacteria that can degrade chitin with regard to the rate that this takes place and how this drives subsequent growth (Brankatschk et al., 2011; Köllner et al., 2012).

However, we propose here that the lack of growth we see in the MSC-2-S community is related to the identity of the emerging chitin degrader in a community without *Streptomyces*. Our hypothesis is that without *Streptomyces*, *Rhodococcus* acts as the primary chitin degrader. However, the interactions that *Rhodococcus* has with other MSC-2 species means that chitin breakdown products generated by *Rhodococcus* are not shared efficiently with other MSC-2 members, or at least not as efficiently as when *Streptomyces* is the primary chitin degrader. This leads to slower overall growth of the MSC-2-S community. Multiple lines of evidence support this conclusion. First, in a version of MSC-2 lacking *Rhodococcus* the community actually grows better, as measured by biomass accumulation and respiration, compared to the complete MSC-2 community that contains *Rhodococcus*. This suggests possible antagonistic interactions that *Rhodococcus* may have with other species, possibly related to sharing of chitin breakdown products. The idea that *Rhodococcus* may be in

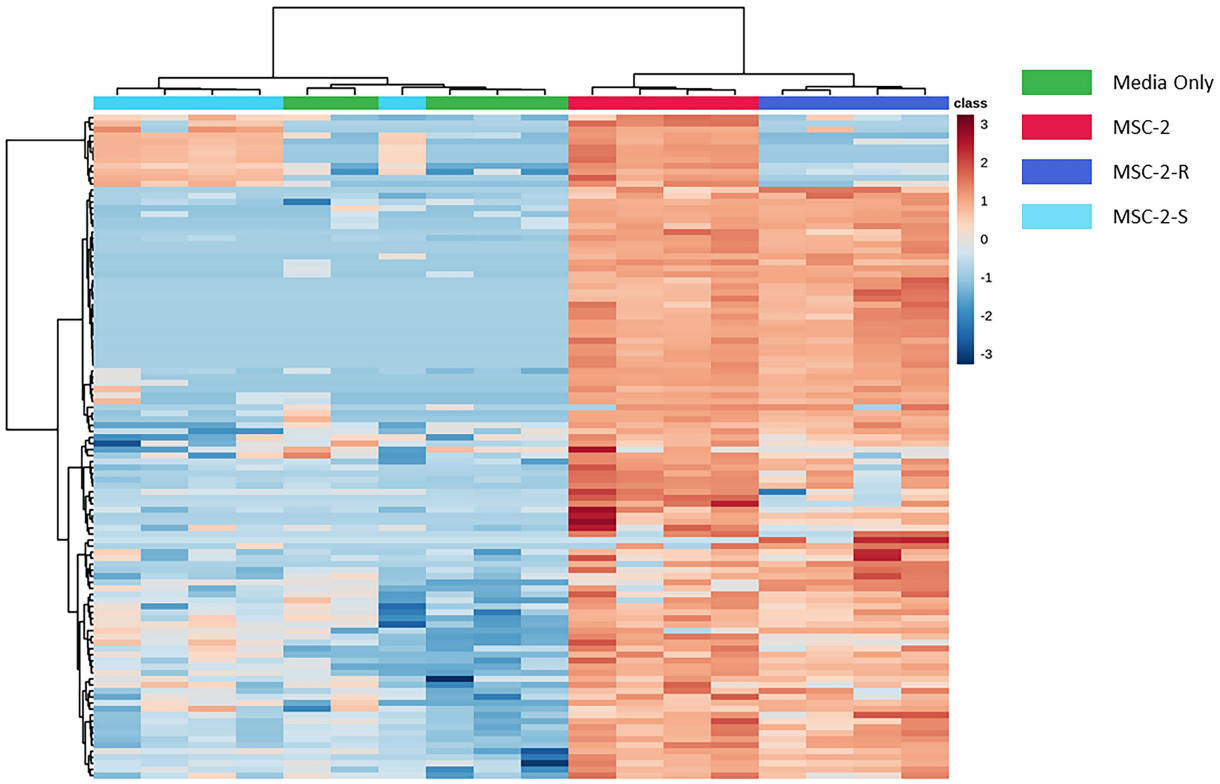

FIGURE 4
Heatmap of differentially abundant metabolites in MSC-2 communities, subsets and media controls. Both rows and columns are hierarchically clustered based on similarities in samples or metabolites, respectively, and color schemes indicate the sample type. Blue indicates that the metabolite is less abundant compared to all samples and red indicates that it is more abundant compared to all other samples. All metabolites included in the heatmap are statistically significant when comparing MSC-2-R to MSC-2 or when comparing MSC-2-S to MSC-2.

competitive rather that cooperative relationships is also supported by our previous network analysis showing negative co-abundances between *Rhodococcus* and other MSC-2 members including *Streptomyces* and *Variovorax* (McClure et al., 2020). Our observation here that *Streptomyces* and *Variovorax* actually increase their abundance when *Rhodococcus* is removed (Figure 3) supports these previous observations and our hypothesis here. A second line of evidence is related to the fact that *Rhodococcus* grows extremely well on chitin in monoculture (McClure et al., 2022), better than any other member of MSC-2, showing that it is able to make the most efficient use of chitin as a C source. Third, *Rhodococcus*' relative abundance is much higher in a community lacking *Streptomyces* (MSC-2-S) than in the complete MSC-2 community. In the complete MSC-2 community *Ensifer* is the dominant member, likely due to its large fundamental niche as we describe in a previous publication (McClure et al., 2022), but in the MSC-2-S community *Ensifer* is still abundant (~36% of the community), but it is virtually tied in abundance with *Rhodococcus* (~33% of the community). Without *Streptomyces* in the community to degrade chitin, *Rhodococcus* steps in as a chitin degrader. It's efficient use of chitin as a C source (seen in our previous publication (McClure et al., 2022)) means that the abundance of *Rhodococcus* increases. However, competitive interactions with other species (seen in our previous species co-abundance networks (McClure et al., 2020)) means that *Rhodococcus*-derived chitin breakdown products are not shared as efficiently and the community as a whole exhibits slow growth. This may take place even though chitin breakdown happens extracellularly, and breakdown products are at least in theory available to the whole community. *Rhodococcus* may possess cell associated chitinase enzymes that are not free floating, as has been seen with bacteria (Itoh et al., 2013). If this is the case, then NAG and other chitin breakdown products would be more available to *Rhodococcus* cells (since breakdown happens just adjacent to the cell) compared to other MSC-2 members. All of this means that even though *Rhodococcus* does well, its success does not translate to high biomass accumulation or respiration of the whole community.

The identity of some bacterial species as 'selfish', meaning they do not share breakdown products with other members, has been found in other systems (Reintjes et al., 2019, 2020; Manna et al., 2022). Many of these previous studies have found that a "selfish" phenotype is related to the expression of excreted extracellular enzymes that process C sources. Chitinase is known to be an extracellular enzyme; but while its excretion has been demonstrated in multiple studies for *Streptomyces* (which likely shares chitin breakdown products in MSC-2) (Joo, 2005; Narayana and Vijayalakshmi, 2009; Ray et al., 2019) it is less well known if

10.3389/fmicb.2022.1046661

TABLE 2 Fold changes of metabolites in MSC-2-R and MSC-2-S communities.

Metabolite	Fold change MSC-2-R/ MSC-2	Fold ChangeMSC-2-S/ MSC-2
Citramalic acid	0.491	0.035
Palmitic acid	1.254	2.155
Trehalose	0.922	3.176
Stearic acid	1.350	2.027
4-methyl-5-thiazoleethanol	1.607	2.902
3,4-dihydroxybenzoic acid (protocatechuic acid)	1.538	2.827
Adenine	1.527	0.024
Lactic acid	1.235	2.401
L-pyroglutamic acid	0.588	0.871
Succinic acid	0.920	1.491
2-isopropylmalic acid	0.073	0.002
N-carbamyl-L-glutamic acid	2.199	0.513
Caffeic acid	1.539	0.038
Porphine	1.224	2.512
5-hydroxymethyl-2-furoic acid	1.284	2.192
Mannobiose	2.454	0.455

this is the case for *Rhodococcus*. If *Rhodococcus* chitinase enzymes are extracellular but remain cell associated (and are not fully excreted) this may mean that *Rhodococcus* would not share chitin breakdown products as efficiently as *Streptomyces*. Supporting *Streptomyces* as a sharing species our analysis identified mannobiose as a metabolite that was much more abundant when *Streptomyces* was present vs. in a community lacking *Streptomyces*. This C source has been shown to be produced by *Streptomyces* and consumed by *Rhodococcus* (Ohashi et al., 2021).

Our identification here of a potential keystone species whose removal leads to better community growth and may be acting as a selfish member emphasizes that highly connected members are not necessarily those that promote community growth but only those that have an effect on community structure and functioning. In some cases, removing a highly connected member may be good for a community if that member has negative interactions with other community members, especially other keystone members. These conclusions will be of value when evaluating the application of certain species to native systems (Lopes et al., 2021) or predicting the response of communities when certain species are lost. If the definition of a keystone species includes those that are highly connected then keystone species may not always be those that are positive contributing members.

Previous work has shown in soil systems that diverse communities with redundancy are better able to respond to changes in the environment that may affect certain keystone members (Wagg et al., 2021). However, the results shown here suggest that even if diversity and redundancy for a particular pathway are present (i.e., chitin breakdown) communities may still not be able to survive the loss of a primary degrader keystone member if the new member filling this metabolic niche does not participate in the same sharing interactions. Our MSC-2 community had a great deal of redundancy related to chitin breakdown (5/8 species are able to metabolize chitin in monoculture (McClure et al., 2022)). Despite this, the communities' response to keystone species loss (*Streptomyces*) was driven not by the fact that there was redundancy in the system but primarily by the nature of next emerging primary degrading species (*Rhodococcus*) and the fact that it may limit the exchange of resources with other community members.

Aside from interaction networks and the identity of primary chitin degraders, these results also show how CUE shifts in a set of communities across time as they cycle a complex C source such as chitin. Species lacking *Rhodococcus* show more rapid increases and decreases in respiration compared to the complete MSC-2 community. As described above this may be due to *Rhodococcus* not facilitating growth of MSC-2 as well as *Streptomyces* but it also allows us to see how CUE shifts as communities are cultured. At 178 h CUE levels suddenly increase in MSC-2-R communities with a drop in respiration and a large increase in biomass. The complete MSC-2 community also shows a large increase in biomass at this timepoint and its respiration levels appear to be peaking suggesting that, if the experiment has been continued, it would have matched MSC-2-R's response with a drop in respiration. One possibility for this increase in CUE for both communities may be that the overall C pool is shifting as chitin is metabolized. In early timepoints much of the community may have been in a C starved and stressed state showing lower CUE (higher respiration and lower biomass accumulation; Schimel et al., 2007), since it appears that only a few species act as chitin degraders in MSC-2. However, as chitin is degraded (by *Streptomyces*, a sharing species) in the MSC-2 and MSC-2-R communities the C pool changes, and a number of new nutrients become available (N-acetyl-glucosamine and other chitin breakdown products). This removes the stress conditions for species and the CUE of the community as a whole increases as C is moved into a biomass accumulation pathway rather than a respiration/catabolic pathway. A more available C pool is supported by our previous work (McClure et al., 2022). These results suggest that changes in CUE can happen as a function of available carbon sources becoming more diversified and easier to metabolize by a greater number of community members. Shifts in C pools however, are a function of the species that are present. Metabolite profiles show that MSC-2-S communities show the least shift in their C pools compared to media only controls (Figure 4; equivalent to the carbon pools at the start of the experiment). This lack of shifting of C pools without *Streptomyces* is likely one reason why this community shows slower growth.

Conclusion

We show here how a chitin degrading synthetic community of soil microbes, MSC-2, responds to loss of certain keystone members. Lack of a primary degrader (*Streptomyces*) causes a collapse in community growth and respiration even when other members have the genomic potential to fill the same metabolic niche. Even if diversity and redundancy are in place, if subsequent chitin degraders that step up in the absence of a primary degrader do not share metabolites, then the community cannot thrive. As soil microbiomes continue to shift in response to changing environments keystone species may bloom or die off and other species will likely emerge to replace them. The accepted paradigm is that diversity will allow for greater resilience due to the larger number of species available to fill required metabolic niches. While this is still true the results presented here show that simple redundancy of pathways is not enough. If the emerging species filling the metabolic niche does not possess the same sharing phenotype and interaction network, then the community will not grow as well. These results also show how synthetic communities can be used to better understand processes in native systems and will be of value when considering genomic redundancy in soil communities' and how this gives the soil microbiome the ability to respond to changes that may take place over the next decades due to a changing climate.

Data availability statement

All 16s data has been deposited to the PNNL DataHub, a public facing repository here: https://data.pnnl.gov/group/nodes/dataset/33294. Users must be login with an ORCID. All metabolomics data has been deposited in MASSIVE here https://massive.ucsd.edu/ProteoSAFe/dataset.jsp?accession=MSV000090720.

Author contributions

RM, KH, and MG designed the experiments. MG and YF carried out the experiments and analyzed growth and respiration data. RM analyzed amplicon data. SC analyzed and interpreted metabolomics data. RM wrote the manuscript and KH led the overall project. All authors contributed to the article and approved the submitted version.

Funding

This program is supported by the U. S. Department of Energy, Office of Science, through the Genomic Science Program, Office of Biological and Environmental Research, under FWP 70880. PNNL is a multi-program national laboratory operated by Battelle for the DOE under Contract DE-AC05-76RLO 1830. A portion of this work was performed in the William R. Wiley Environmental Molecular Sciences Laboratory (EMSL), a national scientific user facility sponsored by Office of Biological and Environmental Research and located at PNNL.

Conflict of interest

The authors declare that the research was conducted in the absence of any commercial or financial relationships that could be construed as a potential conflict of interest.

Publisher's note

All claims expressed in this article are solely those of the authors and do not necessarily represent those of their affiliated organizations, or those of the publisher, the editors and the reviewers. Any product that may be evaluated in this article, or claim that may be made by its manufacturer, is not guaranteed or endorsed by the publisher.

Supplementary material

The Supplementary material for this article can be found online at: https://www.frontiersin.org/articles/10.3389/fmicb.2022.1046661/full#supplementary-material

SUPPLEMENTARY FIGURE S1
PCA of amplicon data from MSC-2 communities and subsets. Colors of samples are shown in the upper right. To remove differentially effects of the leave out aspect of the experiment this PCA includes amplicon data from all members of MSC-2 except for *Rhodococcus* and *Streptomyces*.

SUPPLEMENTARY FIGURE S2
PCA of metabolic from MSC-2 communities, subsets and media controls. Colors of samples are shown in the upper right.

References

Banerjee, S., Schlaeppi, K., and Van Der Heijden, M. G. (2018). Keystone taxa as drivers of microbiome structure and functioning. *Nat. Rev. Microbiol.* 16, 567–576. doi: 10.1038/s41579-018-0024-1

Baty III, A. M., Eastburn, C. C., Diwu, Z., Techkarnjanaruk, S., Goodman, A. E., and Geesey, G. G. (2000a). Differentiation of chitinase-active and non-chitinase-active subpopulations of a marine bacterium during chitin degradation. *Appl. Environ. Microbiol.* 66, 3566–3573. doi: 10.1128/AEM.66.8.3566-3573.2000

Baty III, A. M., Eastburn, C. C., Techkarnjanaruk, S., Goodman, A. E., and Geesey, G. G. (2000b). Spatial and temporal variations in chitinolytic gene expression and bacterial biomass production during chitin degradation. *Appl. Environ. Microbiol.* 66, 3574–3585. doi: 10.1128/AEM.66.8.3574-3585.2000

Bolyen, E., Rideout, J. R., Dillon, M. R., Bokulich, N. A., Abnet, C. C., Al-Ghalith, G. A., et al. (2019). Reproducible, interactive, scalable and extensible microbiome data science using QIIME 2. *Nat. Biotechnol.* 37, 852–857. doi: 10.1038/s41587-019-0209-9

Brankatschk, R., Töwe, S., Kleineidam, K., Schloter, M., and Zeyer, J. (2011). Abundances and potential activities of nitrogen cycling microbial communities along a chronosequence of a glacier forefield. *ISME J.* 5, 1025–1037. doi: 10.1038/ismej.2010.184

Cao, X., Pan, X., Couvillion, S. P., Zhang, T., Tamez, C., Bramer, L. M., et al. (2021). Fate, cytotoxicity and cellular metabolomic impact of ingested nanoscale carbon dots using simulated digestion and a triculture small intestinal epithelial model. *NanoImpact* 23:100349. doi: 10.1016/j.impact.2021.100349

Duan, L., Li, J.-L., Yin, L.-Z., Luo, X.-Q., Ahmad, M., Fang, B.-Z., et al. (2022). Habitat-dependent prokaryotic microbial community, potential keystone species, and network complexity in a subtropical estuary. *Environ. Res.* 212:113376. doi: 10.1016/j.envres.2022.113376

Geesink, P., Tyc, O., Küsel, K., Taubert, M., Van De Velde, C., Kumar, S., et al. (2018). Growth promotion and inhibition induced by interactions of groundwater bacteria. *FEMS Microbiol. Ecol.* 94:fiy164. doi: 10.1093/femsec/fiy164

Geyer, K. M., Kyker-Snowman, E., Grandy, A. S., and Frey, S. D. (2016). Microbial carbon use efficiency: accounting for population, community, and ecosystem-scale controls over the fate of metabolized organic matter. *Biogeochemistry* 127, 173–188. doi: 10.1007/s10533-016-0191-y

Gougoulias, C., Clark, J. M., and Shaw, L. J. (2014). The role of soil microbes in the global carbon cycle: tracking the below-ground microbial processing of plant-derived carbon for manipulating carbon dynamics in agricultural systems. *J. Sci. Food Agric.* 94, 2362–2371. doi: 10.1002/jsfa.6577

Hannula, S. E., Ma, H. K., Perez-Jaramillo, J. E., Pineda, A., and Bezemer, T. M. (2020). Structure and ecological function of the soil microbiome affecting plant-soil feedbacks in the presence of a soil-borne pathogen. *Environ. Microbiol.* 22, 660–676. doi: 10.1111/1462-2920.14882

Heyse, J., Buysschaert, B., Props, R., Rubbens, P., Skirtach, A. G., Waegeman, W., et al. (2019). Coculturing bacteria leads to reduced phenotypic heterogeneities. *Appl. Environ. Microbiol.* 85, e02814–e02818. doi: 10.1128/AEM.02814-18

Itoh, T., Hibi, T., Fujii, Y., Sugimoto, I., Fujiwara, A., Suzuki, F., et al. (2013). Cooperative degradation of chitin by extracellular and cell surface-expressed chitinases from *Paenibacillus* sp. strain FPU-7. *Appl. Environ. Microbiol.* 79, 7482–7490. doi: 10.1128/AEM.02483-13

Johnson-Rollings, A. S., Wright, H., Masciandaro, G., Macci, C., Doni, S., Calvo-Bado, L. A., et al. (2014). Exploring the functional soil-microbe interface and exoenzymes through soil metaexoproteomics. *ISME J.* 8, 2148–2150. doi: 10.1038/ismej.2014.130

Joo, G.-J. (2005). Purification and characterization of an extracellular chitinase from the antifungal biocontrol agent *Streptomyces halstedii*. *Biotechnol. Lett.* 27, 1483–1486. doi: 10.1007/s10529-005-1315-y

Keyhani, N. O., and Roseman, S. (1997). Wild-type *Escherichia coli* grows on the chitin disaccharide, N, N'-diacetylchitobiose, by expressing the cel operon. *Proc. Natl. Acad. Sci. U. S. A.* 94, 14367–14371. doi: 10.1073/pnas.94.26.14367

Kind, T., Wohlgemuth, G., Lee, D. Y., Lu, Y., Palazoglu, M., Shahbaz, S., et al. (2009). FiehnLib: mass spectral and retention index libraries for metabolomics based on quadrupole and time-of-flight gas chromatography/mass spectrometry. *Anal. Chem.* 81, 10038–10048. doi: 10.1021/ac9019522

Köllner, K. E., Carstens, D., Keller, E., Vazquez, F., Schubert, C. J., Zeyer, J., et al. (2012). Bacterial chitin hydrolysis in two lakes with contrasting trophic statuses. *Appl. Environ. Microbiol.* 78, 695–704. doi: 10.1128/AEM.06330-11

Li, J., Mau, R. L., Dijkstra, P., Koch, B. J., Schwartz, E., Liu, X.-J. A., et al. (2019). Predictive genomic traits for bacterial growth in culture versus actual growth in soil. *ISME J.* 13, 2162–2172. doi: 10.1038/s41396-019-0422-z

Li, J., Wang, G., Allison, S. D., Mayes, M. A., and Luo, Y. (2014). Soil carbon sensitivity to temperature and carbon use efficiency compared across microbial-ecosystem models of varying complexity. *Biogeochemistry* 119, 67–84. doi: 10.1007/s10533-013-9948-8

Liu, X., Wang, Y., and Gu, J.-D. (2021). Ecological distribution and potential roles of Woesearchaeota in anaerobic biogeochemical cycling unveiled by genomic analysis. *Comput. Struct. Biotechnol. J.* 19, 794–800. doi: 10.1016/j.csbj.2021.01.013

Lobo, M. D. P., Silva, F. D. A., Landim, P. G. D. C., Da Cruz, P. R., De Brito, T. L., De Medeiros, S. C., et al. (2013). Expression and efficient secretion of a functional chitinase from *Chromobacterium violaceum* in *Escherichia coli*. *BMC Biotechnol.* 13, 1–15. doi: 10.1186/1472-6750-13-46

Lopes, M. J. D. S., Dias-Filho, M. B., and Gurgel, E. S. C. (2021). Successful plant growth-promoting microbes: inoculation methods and abiotic factors. *Front. Sustain. Food Syst.* 5:606454. doi: 10.3389/fsufs.2021.606454

Manna, V., Zoccarato, L., Banchi, E., Arnosti, C., Grossart, H. P., and Celussi, M. (2022). Linking lifestyle and foraging strategies of marine bacteria: Selfish behaviour of particle-attached bacteria in the northern Adriatic Sea. *Environ. Microbiol. Rep.* 14, 549–558. doi: 10.1111/1758-2229.13059

Mcclure, R., Farris, Y., Danczak, R., Nelson, W., Song, H.-S., Kessell, A., et al. (2022). Interaction networks are driven by community-responsive phenotypes in a chitin-degrading consortium of soil microbes. *Msystems* 7:e0037222. doi: 10.1128/msystems.00372-22

Mcclure, R., Naylor, D., Farris, Y., Davison, M., Fansler, S. J., Hofmockel, K. S., et al. (2020). Development and analysis of a stable, reduced complexity model soil microbiome. *Front. Microbiol.* 11:1987. doi: 10.3389/fmicb.2020.01987

Narayana, K. J., and Vijayalakshmi, M. (2009). Chitinase production by Streptomyces sp. ANU 6277. *Braz. J. Microbiol.* 40, 725–733. doi: 10.1590/S1517-83822009000400002

Ohashi, K., Hataya, S., Nakata, A., Matsumoto, K., Kato, N., Sato, W., et al. (2021). Mannose-and Mannobiose-specific responses of the insect-associated cellulolytic bacterium *Streptomyces* sp. Strain SirexAA-E. *Appl. Environ. Microbiol.* 87, e02719–e02720. doi: 10.1128/AEM.02719-20

Pan, Z., Chen, Y., Zhou, M., and Mcallister, T. A. (2021). Microbial interaction-driven community differences as revealed by network analysis. *Comput. Struct. Biotechnol. J.* 19, 6000–6008. doi: 10.1016/j.csbj.2021.10.035

Pang, Z., Zhou, G., Ewald, J., Chang, L., Hacariz, O., Basu, N., et al. (2022). Using MetaboAnalyst 5.0 for LC–HRMS spectra processing, multi-omics integration and covariate adjustment of global metabolomics data. *Nat. Protoc.* 17, 1735–1761. doi: 10.1038/s41596-022-00710-w

Ray, L., Panda, A. N., Mishra, S. R., Pattanaik, A. K., Adhya, T. K., Suar, M., et al. (2019). Purification and characterization of an extracellular thermo-alkali stable, metal tolerant chitinase from *Streptomyces chilikensis* RC1830 isolated from a brackish water lake sediment. *Biotechnol. Rep.* 21:e00311. doi: 10.1016/j.btre.2019.e00311

Reintjes, G., Arnosti, C., Fuchs, B., and Amann, R. (2019). Selfish, sharing and scavenging bacteria in the Atlantic Ocean: a biogeographical study of bacterial substrate utilisation. *ISME J.* 13, 1119–1132. doi: 10.1038/s41396-018-0326-3

Reintjes, G., Fuchs, B. M., Amann, R., and Arnosti, C. (2020). Extensive microbial processing of polysaccharides in the south pacific gyre via selfish uptake and extracellular hydrolysis. *Front. Microbiol.* 11:583158. doi: 10.3389/fmicb.2020.583158

Saifuddin, M., Bhatnagar, J. M., Segrè, D., and Finzi, A. C. (2019). Microbial carbon use efficiency predicted from genome-scale metabolic models. *Nat. Commun.* 10, 1–10. doi: 10.1038/s41467-019-11488-z

Saleem, M., Hu, J., and Jousset, A. (2019). More than the sum of its parts: microbiome biodiversity as a driver of plant growth and soil health. *Annu. Rev. Ecol. Evol. Syst.* 50, 145–168. doi: 10.1146/annurev-ecolsys-110617-062605

Scarlett, K., Denman, S., Clark, D. R., Forster, J., Vanguelova, E., Brown, N., et al. (2021). Relationships between nitrogen cycling microbial community abundance and composition reveal the indirect effect of soil pH on oak decline. *ISME J.* 15, 623–635. doi: 10.1038/s41396-020-00801-0

Schimel, J., Balser, T. C., and Wallenstein, M. (2007). Microbial stress-response physiology and its implications for ecosystem function. *Ecology* 88, 1386–1394. doi: 10.1890/06-0219

Tian, L., Lin, X., Tian, J., Ji, L., Chen, Y., Tran, L. P., et al. (2020). Research advances of beneficial microbiota associated with crop plants. *Int. J. Mol. Sci.* 21:1792. doi: 10.3390/ijms21051792

Wagg, C., Hautier, Y., Pellkofer, S., Banerjee, S., Schmid, B., and Van Der Heijden, M. G. (2021). Diversity and asynchrony in soil microbial communities stabilizes ecosystem functioning. *elife* 10:e62813. doi: 10.7554/eLife.62813

Xun, W., Liu, Y., Li, W., Ren, Y., Xiong, W., Xu, Z., et al. (2021). Specialized metabolic functions of keystone taxa sustain soil microbiome stability. *Microbiome* 9, 1–15. doi: 10.1186/s40168-020-00985-9

Zhou, J., Liu, X., Yuan, F., Deng, B., and Yu, X. (2020). Biocatalysis of heterogenously-expressed chitosanase for the preparation of desirable chitosan oligosaccharides applied against phytopathogenic fungi. *ACS Sustain. Chem. Eng.* 8, 4781–4791. doi: 10.1021/acssuschemeng.9b07288

Zuñiga, C., Li, C.-T., Yu, G., Al-Bassam, M. M., Li, T., Jiang, L., et al. (2019). Environmental stimuli drive a transition from cooperation to competition in synthetic phototrophic communities. *Nat. Microbiol.* 4, 2184–2191. doi: 10.1038/s41564-019-0567-6

frontiers | Frontiers in Microbiology

TYPE Original Research
PUBLISHED 08 February 2023
DOI 10.3389/fmicb.2023.1017167

Check for updates

OPEN ACCESS

EDITED BY
Durgesh K. Jaiswal,
Savitribai Phule Pune University, India

REVIEWED BY
Ram Krishna,
Directorate of Onion and Garlic Research (ICAR), India
Anca Macovei,
The University of Pavia, Italy

*CORRESPONDENCE
Vishal Prasad
✉ vp.iesd@bhu.ac.in

SPECIALTY SECTION
This article was submitted to Microbiotechnology, a section of the journal Frontiers in Microbiology

RECEIVED 11 August 2022
ACCEPTED 16 January 2023
PUBLISHED 08 February 2023

CITATION
Shankar A and Prasad V (2023) Potential of desiccation-tolerant plant growth-promoting rhizobacteria in growth augmentation of wheat (*Triticum aestivum* L.) under drought stress.
Front. Microbiol. 14:1017167.
doi: 10.3389/fmicb.2023.1017167

COPYRIGHT
© 2023 Shankar and Prasad. This is an open-access article distributed under the terms of the Creative Commons Attribution License (CC BY). The use, distribution or reproduction in other forums is permitted, provided the original author(s) and the copyright owner(s) are credited and that the original publication in this journal is cited, in accordance with accepted academic practice. No use, distribution or reproduction is permitted which does not comply with these terms.

Potential of desiccation-tolerant plant growth-promoting rhizobacteria in growth augmentation of wheat (*Triticum aestivum* L.) under drought stress

Ajay Shankar and Vishal Prasad*

Institute of Environment and Sustainable Development, Banaras Hindu University, Varanasi, India

Wheat (*Triticum aestivum* L.) yield and physiology are adversely affected due to limited water availability. However, desiccation-tolerant plant growth-promoting rhizobacteria (DT-PGPR) are potential candidates that can overcome the negative impacts of water stress. In the present study, a total of 164 rhizobacterial isolates were screened for desiccation tolerance up to −0.73 MPa osmotic pressure, of which five isolates exhibited growth and expression of plant growth properties under the influence of desiccation stress of −0.73 MPa. These five isolates were identified as *Enterobacter cloacae* BHUAS1, *Bacillus cereus* BHUAS2, *Bacillus megaterium* BHUIESDAS3, *Bacillus megaterium* BHUIESDAS4, and *Bacillus megaterium* BHUIESDAS5. All five isolates exhibited plant growth-promoting properties and production of exopolysaccharide (EPS) under the impact of desiccation stress. Furthermore, a pot experiment on wheat (variety HUW-234) inoculated with the isolates *Enterobacter cloacae* BHUAS1, *Bacillus cereus* BHUAS2, and *Bacillus megaterium* BHUIESDAS3 exhibited a positive influence on the growth of wheat under the condition of water stress. A significant improvement in plant height, root length, biomass, chlorophyll and carotenoid content, membrane stability index (MSI), leaf relative water content (RWC), total soluble sugar, total phenol, proline, and total soluble protein, were recorded under limited water-induced drought stress in treated plants as compared with non-treated plants. Moreover, plants treated with *Enterobacter cloacae* BHUAS1, *Bacillus cereus* BHUAS2, and *Bacillus megaterium* BHUIESDAS3 depicted improvement in enzymatic activities of several antioxidant enzymes such as guaiacol peroxidase (POD), catalase (CAT), and ascorbate peroxidase (APX). Beside this significant decrease in electrolyte leakage, H_2O_2 and malondialdehyde (MDA) contents were also recorded in treated plants. From the results obtained, it is evident that *E. cloacae* BHUAS1, *B. megaterium* BHUIESDAS3, and *B. cereus* BHUAS2 are the potential DT-PGPR having the capability to sustain growth and yield, alleviating the deleterious effect of water stress in wheat.

KEYWORDS

antioxidant, wheat, PGPR, drought, osmotic potential, antioxidative enzymes

1. Introduction

Wheat is the second most important food grain after rice and provides 20% of the calories consumed by the world's population, with a total annual production of ~700 million tons worldwide (Qaseem et al., 2019). In rainfed areas, wheat cultivation faces heavy yield loss because of the irregular supply of water during the grain filling stage (Qaseem et al., 2019). Drought stress typically results in osmotic and oxidative stresses, which alter the physiological, biochemical, and molecular characteristics of plants and ultimately reduce crop yield. The decrease in plant growth and yield because of low water availability is essentially caused by altered plant water relations, reduced photosynthesis, oxidative stress at the cellular level, membrane degradation, and inhibited enzymatic activities. Any fluctuations in optimal values of physiological functions indicate the abnormality in plant health and their surrounding environmental conditions (Gangadhar et al., 2016; Batool et al., 2020). It is a serious challenge for breeders and practitioners to develop such a variety having genetic structure for high yield and resistance to abiotic stress for ensuring a sustainable agroecosystem under ever increasing environmental stresses (Lulsdorf et al., 2013; Batool et al., 2020). Genetic modification and transgenic methods have also been used for tolerance against drought in the case of many crops but their acceptance is under question due to social, ethical, and political issues (Jaiswal et al., 2022). Because of limited genetic diversity and ecological restrictions, further expansion in this way may be restricted for crop improvement (Xu and Zhou, 2006; Batool et al., 2020). On the other hand, crop management strategies to increase tolerance against adverse conditions can be a good option to overcome the impact and improve the yield under abiotic environmental stresses (Batool et al., 2020). In the past few years, plant-associated microorganisms such as plant growth-promoting rhizobacteria (PGPR) have gained attention for increasing crop productivity as well as their abiotic stress tolerance capabilities. The favorable impact in form of plant growth promotion has been reported in several crops (Saharan and Nehra, 2011; Adesemoye and Egamberdieva, 2013; Batool et al., 2020). The PGPR have been testified in improving seed germination, development of root and shoot, increasing biomass and chlorophyll content, soluble sugars and phenols, antioxidants, and water movement activity to maintain relative water content and uptake of nutrients in several studies (Meng et al., 2016; Sprenger et al., 2018; Batool et al., 2020). The PGPR represent a variety of root-colonizing bacterial species, which possess the ability to provide resistance to plants against several of the abiotic and biotic stressors owing to their root-colonizing capability (Mayak et al., 2004; Glick et al., 2007; Ngumbi and Kloepper, 2016). The mechanism behind the PGPR-mediated drought tolerance includes modification of root architecture, osmotic tolerance, managing oxidative stresses through biosynthesis of phytohormones and ACC-deaminase, reactive oxygen species (ROS) scavenging antioxidants, and production of exopolysaccharides (EPS), which help in biofilm formation for maintaining moisture availability in the root zone (Ngumbi and Kloepper, 2016; Vurukonda et al., 2016; Jochum et al., 2019). The soil having low water availability imposes desiccation stress on the resident microorganism. Bacteria that tolerate low water availability could be more viable and beneficial in such types of stressful soils; hence, the bacterial strains with higher tolerance toward desiccation stress perform better for plant growth promotion in such soils (Vilchez and Manzanera, 2011; Molina-Romero et al., 2017). Several bacteria such as *Rhizobium leguminosarum* (Casteriano et al., 2013), *Pseudomonas putida* mt-2 (Chang et al., 2007), *Bradyrhizobium japonicum* (Streeter, 2003), *Pseudomonas putida* KT2440 (van de Mortel et al., 2004), *Azospirillum brasilense* Sp7 (Molina-Romero et al., 2017), and *Pseudomonas putida* GAP-P45 (Sandhya et al., 2009) have been reported for their capabilities to tolerate desiccation stress as well as provide plant beneficial activities under drought stress in plants (Muñoz-Rojas, 2018). With this knowledge and background studies, the present study was carried out to isolate and characterize desiccation-tolerant plant growth-promoting bacteria and evaluate their efficacy in overcoming the negative impacts of low water-induced drought stress in wheat plants.

2. Materials and methods

2.1. Sampling site and physicochemical analysis of soil

A total of 24 rhizospheric soil samples were collected from roots of different crops grown in agricultural soils of the Hamirpur district of Uttar Pradesh, located between 25°27′00″ to 25°57′00″ N latitude and 79°11′00″ to 80°19′00″ E longitude with an area of 4139.09 km^2 in the Bundelkhand plateau of the Ganga River Basin India, having various crops grown such as wheat, linseed, pigeon pea, mustard, pea, and gram. The soil physicochemical properties including soil moisture (SM), temperature (T), pH, water holding capacity (WHC), and soil texture along with soil nutrients such as organic carbon (OC), nitrogen (N), potassium (K), and phosphorus (P) were measured and analyzed using standard methodologies (Pawar and Shah, 2009).

2.2. Isolation and characterization of rhizobacteria

The isolation of rhizobacteria was performed by serial dilution using a plating technique on nutrient agar (NA) medium (Gouzou et al., 1993; Sandhya et al., 2009). The various bacterial isolates obtained were screened for desiccation tolerance in tryptone soya broth (TSB) medium having different water potentials (−0.05, −0.15, −0.30, −0.45, and −0.73 MPa) prepared using PEG-6,000 in an appropriate amount (Michel and Kaufmann, 1973; Sandhya et al., 2009). The desiccation-tolerant isolates obtained were further characterized based on their morphological characters such as shape, size, colony structure, gram staining, and biochemical properties (amylase, catalase, cellulase, citrate utilization, protease, and urease test) (Cappuccino and Sherman, 1992; Kammoun et al., 2008; Pereira and Castro, 2014). For molecular identification, bacterial genomic DNA of selected bacterial isolates was extracted using the method described by Sambrooke et al. (1989). The amplification of 16S rDNA genes was performed by polymerase chain reaction using universal primers 27F (5′-AGAGTTTGATCCTGGCTCAG-3′) and 1492R (5′-GTTACCTTGTTACGACTT-3′). The evolutionary genetics were studied using comparative molecular analysis, and the phylogenetic tree was constructed using MEGA-X (Kumar et al., 2004; Jaiswal et al., 2019).

2.3. Evaluation of plant growth-promoting (PGP) attributes and exopolysaccharide production of selected bacterial isolates

The PGP attributes of selected desiccation-tolerant bacterial isolates were carried out using established methods. Indole acetic acid (IAA) production was analyzed using the method of Bric et al. (1991), solubilization of insoluble phosphorus (P) was done by the method of Mehta and Nautiyal (2001), production of siderophore was analyzed using the method given by Schwyn and Neilands (1987), and production of ACC deaminase enzyme was estimated by calculating the quantity of α-ketobutyrate liberated along with ammonia after deamination of ACC was done by the method of Honma and Shimomura (1978) and Penrose and Glick (2003). All analyses were carried out in non-stress as well as desiccation stress (−0.73 MPa) under *in vitro* conditions. The estimation of protein content was done by the Bradford (1976) method. The exopolysaccharide (EPS) was estimated using a modification of the methods described by Bramhachari and Dubey (2006) and Kumar et al. (2011) under non-stress as well as under the condition of desiccation stress.

2.4. Application of selected bacterial isolates BHUAS1, BHUAS2, and BHUIESDAS3 on wheat

2.4.1. Inoculum preparation and growing conditions

On the basis of the expression of PGP traits under the impacts of desiccation stress (−0.73 MPa), three bacterial isolates *Enterobacter cloacae* BHUAS1, *Bacillus megaterium* BHUIESDAS3, and *Bacillus cereus* BHUAS2 were selected for the evaluation of their growth-promoting effects on wheat plants grown under limited water condition. For the treatment of wheat seeds, the selected bacterial strains were grown in a 250 ml conical flask at 30 ± 2°C at 120 rpm for 24 h in a TSB medium. The bacterial cell density was maintained at 1×10^7 cells/ml. For experiment work, wheat (*Triticum aestivum* L. var. HUW-234) seeds were procured from the seed bank of the Institute of Agricultural Sciences, Banaras Hindu University, Varanasi. Seeds were sterilized with 70% ethanol for 2 min followed by 0.1% $HgCl_2$ for 3 min. In the next step, seeds were washed five times with sterile distilled water. After soaking in 1% CMC (adherent) for at least 10 h at room temperature, seeds were used for bacterial coating. Seeds were coated enough with bacterial cell suspension in double volume (1×10^7 cells/ml) for 24 h. Three different treatments along with untreated control seeds were used — (1) **C:** Control (untreated) seeds, (2) **T1:** *Enterobacter cloacae* BHUAS1 coated seeds, (3) **T2:** *Bacillus megaterium* BHUIESDAS3 coated seeds, and (4) **T3:** *Bacillus cereus* BHUAS2 coated seeds.

The pot experiment was carried out at the Institute of Environment and Sustainable Development, Banaras Hindu University (25°15′44.17″ N latitude and 82°59′41.59″), Varanasi. The potting mixture used for the experiment contained 10 kg soil (9 kg of garden soil and 1 kg of farm yard manure) filled in a plastic pot of dimension 30cm × 20cm (height × width). The soil used in the experiment was from the garden of the Institute of Environment and Sustainable Development, Banaras Hindu University, Varanasi, India, mixed with farm yard manure and moistened before use. The final soil mix was found to have 12.9% sand, 36.9% clay, and 50.1% silt with water holding capacity of 41.2%. The pH and electrical conductivity (EC) of the soil were 6.94 μS/cm and 45.2 μS/cm, respectively. The organic carbon (OC), nitrogen (N), and available *P* in the soil were 0.6%, 52.71 kg/ha, and 49.5 kg/ha, respectively. The untreated and treated seeds were sown in plastic pots containing potting mixture. The pots were arranged in two sets: (1) Set I — non-stress (2) Set II — water stress on the basis of watering conditions. Each set has 12 pots with four types of treatment in triplicates, which have three bacterial treatments (T1: BHUAS1, T2: BHUIESDAS3, and T3: BHUAS2) and one control/untreated (C) pot. The seeds were allowed to germinate under environmental conditions and after germination thinning was performed by removing 50% of the seedling. At 10 DAS, 500 ml of sterilized tap water was added to each pot in both sets. At 20 DAS, watering was done again by adding 500 ml of sterilized tap water only in Set I (non-stress), while water limiting condition was induced by escaping watering in Set II (water stress). The total number of seeds germinated on each day was recorded. The percentage of seed germination was calculated on the basis of data recorded after 7 days. After 35 days, wheat plants were harvested, and different plant indices such as fresh weight, dry weight, root length, and shoot length were recorded using a standard protocol.

2.4.2. Physiological analysis

2.4.2.1. Electrolyte leakage

The electrolyte leakage (EL) was measured using the method described by Gonzalez and Gonzalez-Vilar (2003). Ten discs of wheat leaves were cut and placed in a test tube containing 10 ml of distilled water to estimate EL. The preliminary electrical conductivity (EC1) was measured. The tubes were kept at 10°C for 24 h before being placed in a 95°C water bath for 20 min. The samples were cooled, and the final electrical conductivity (EC2) was measured. The following formula was used to calculate the EL:

$$\text{EL}\,(\%) = \frac{\text{EC1}}{\text{EC2}} \text{ x } 100$$

where EL represents electrolyte leakage and EC represents electrical conductivity.

2.4.2.2. Membrane stability index

The membrane stability index (MSI) was calculated using a conductivity probe by following the modified method of Khanna-Chopra and Selote (2007). For this, a 1 cm piece of leaf was cut and washed with distilled water before being placed in test tubes with 10 ml of distilled water. The tubes were kept in a water bath at 40°C for 30 min. After that, tubes were taken out of the water bath and cooled down. A conductivity probe was used to measure the initial electrical conductivity (EC1). The samples were placed in a 100°C water bath for another 10 min. After cooling the samples, the final electrical conductivity (EC2) was measured again. The MSI was calculated using the formula as follows:

$$\text{MSI} = \left[1 - \left(\frac{\text{EC1}}{\text{EC2}}\right)\right] \text{ x } 100$$

where MSI is Membrane Stability Index and EC represents electrical conductivity.

2.4.2.3. Relative water content

The relative water content (RWC) of leaves was determined using the standard method described by Teulat et al. (2003). For this, 1 g of

fresh leaves were kept in 50 ml of distilled water in a 100 ml flask for 5 h at room temperature. The turgid weight was recorded, and the samples were oven dried for 2 h at 70°C to calculate the dry weight. The RWC was determined as follows:

$$\text{RWC}\,(\%) = \frac{\text{FW} - \text{DW}}{\text{TW} - \text{DW}} \text{ x } 100$$

2.4.3. Measurement of chlorophyll and carotenoid contents

Precisely weighed 0.5 g of the fresh leaf of wheat plant was placed in a test tube containing 10 ml of 80% acetone covered with a cap to stop evaporation of acetone and kept in dark overnight in a refrigerator at 4°C. The leaf sample along with acetone was then transferred to a mortar and pestle and homogenized. Furthermore, the homogenized sample was centrifuged at 10,000 rpm for 15 min at 4°C. The supernatant was transferred to a different tube, and then 0.5 ml of it was mixed with 4.5 ml of 80% acetone. This mixture was then analyzed for chlorophyll-a, chlorophyll-b, total chlorophyll, and carotenoids. The absorbance of the extracted sample was recorded by spectrophotometer (Thermo-Scientific, Evolution-201) at 645 and 663 nm for chlorophyll estimation and at 480 and 510 nm for carotenoids (Arnon, 1949; Sumanta et al., 2014). The calculation was done by using the following formula:

$$\text{Chlorophyll a}\,(\text{mg/g}) = \frac{12.3 \times \text{OD}\,(663\text{nm}) - 0.85 \times \text{OD}\,(645\text{nm})}{\text{d} \times 1000 \times \text{weight}\,(\text{g})} \text{ x V}$$

$$\text{Chlorophyll b}\,(\text{mg/g}) = \frac{19.3 \times \text{OD}\,(645\text{nm}) - 3.6 \times \text{OD}\,(663\text{nm})}{\text{d} \times 1000 \times \text{weight}\,(\text{g})} \text{ x V}$$

$$\text{Total chlorophyll}\,(\text{mg/g}) = \frac{20.2 \times \text{OD}\,(645\text{nm}) - 8.02 \times \text{OD}\,(663\text{nm})}{\text{d} \times 1000 \times \text{weight}\,(\text{g})} \text{ x V}$$

$$\text{Carotenoids}\,(\text{mg/g}) = \frac{7.6 \times \text{OD}\,(480\text{nm}) - 1.49 \times \text{OD}\,(510\text{nm})}{\text{d} \times 1000 \times \text{weight}\,(\text{g})} \text{ x V}$$

where

d = length of cuvette (1 cm), V = volume of extract (ml)

2.4.4. Biochemical analysis

2.4.4.1. Total soluble sugar

The method given by Dubois et al. (1956) was used to estimate the plant's total soluble sugar using phenol sulphuric acid (PSA). For the total sugar analysis in the wheat plant, 0.1 g of fresh leaves were placed in 5 ml of 80% methanol and heated in a water bath for 1 h at 70°C. A 0.5 ml aliquot of this solution was taken and mixed with 0.5 ml of phenol (5%) and 1.5 ml of H_2SO_4 (96%). The solutions were thoroughly mixed and incubated in dark for 1 h at room temperature. After 1 h, the reaction mixture was thoroughly mixed by gentle shaking, and the absorbance at 490 nm was measured using a spectrophotometer (Thermo-Scientific, Evolution-201). The total sugar content was expressed as mg/g fresh tissue weight and calculated using the following formula:

$$\text{Soluble sugar}\,(\text{mg/g}) = \frac{\text{OD of sample x K value (20)}}{\text{weight of fresh tissue (0.5g)}} \text{ x Dilution factor}$$

2.4.4.2. Total phenol

A total of 0.1 g of fresh leaf sample was homogenized in 2 ml of 80% methanol and heated for 15 min at 70°C to estimate total phenol (Zieslin and Ben-Zaken, 1993). After this, 1 ml of methanolic extract was mixed with 5 ml of distilled water and 250 µl of Folin–Ciocalteau reagent (1N). Following that, 1 ml of saturated sodium carbonate (20%) was added, and the mixture was incubated at 25°C for 30 min. A spectrophotometer was used to measure the absorbance at 725 nm (Thermo-Scientific, Evolution-201). The phenolic content was calculated using a Gallic acid standard curve and expressed as g GAE g^{-1} fresh weight.

2.4.4.3. Proline and total soluble protein

Free proline in wheat plants was determined by the colorimetric method described by Bates et al. (1973). For this, 0.5 g of fresh leaf samples were homogenized with 10 ml of 3% aqueous sulfosalicylic acid, and the residue was removed by centrifugation at 12,000 rpm for 10 min at 4°C. From this, 1 ml of supernatant was taken and mixed with an equal volume of acid–ninhydrin and glacial acetic acid (1:1, v/v) in a test tube. The mixture was boiled for 1 h at 100°C. The reaction was terminated immediately by placing in ice water for 5 min and subsequently, 2 ml of toluene was added and vortexed for 2 min for the extraction of proline present in the mixture. The upper aqueous phase (wine red color) in toluene containing chromophores warmed at room temperature was collected, and its absorbance was recorded in a spectrophotometer (Thermo-Scientific, Evolution-201) at 520 nm. The proline concentration was calculated by using the L-proline standard curve and reported as µmol g^{-1} FW. The estimation of total protein concentration in wheat plants was determined according to the Bradford (1976) method.

2.4.4.4. Reactive oxygen species, lipid peroxidation, and antioxidant enzymatic activities

Reactive oxygen species (ROS), lipid peroxidation (assessed by estimating malondialdehyde: MDA content), and antioxidant enzymatic activities were estimated in the leaf using the following methods. For the assay, 0.5 g of fresh leaves were cut and homogenized in a pre-chilled mortar and pestle with ice cold potassium phosphate (50 mM) extraction buffer (pH 7.0) and 0.4% (w/v) polyvinyl pyrrolidone (PVP). Furthermore, this homogenous mixture was centrifuged at 12,000 rpm for 30 min at 4°C. Then the supernatant was collected and used as a crude extract for the aforementioned assays using a UV-VIS spectrophotometer (Thermo-Scientific, Evolution-201).

The amount of H_2O_2 was measured using the method described by Alexieva et al. (2001). For this, the reaction mixture containing 0.5 ml of crude extract, 0.5 ml of 0.1 M potassium phosphate buffer, and 2 ml of KI (1 M) solution was incubated at room temperature in dark. The absorbance was recorded at 390 nm and 0.1% TCA was used as blank. The amount of H_2O_2 was calculated using a standard curve prepared using dilutions of a working standard of 100 µM of H_2O_2.

The MDA content was determined by a slight modification of the method described by Heath and Packer (1968) using thiobarbituric acid (TBA). For this, crude extract (0.3 ml) was mixed with 1.2 ml of 2-thiobarbituric acid (0.5% w/v) prepared in 20% trichloroacetic acid (TCA). The mixture was incubated at 95°C for 30 min. After that, the reaction was stopped by immediately immersing the tubes in an ice bath, and the mixture was centrifuged at 12,000 rpm for 10 min. The absorbance of the supernatant was measured using a UV-VIS

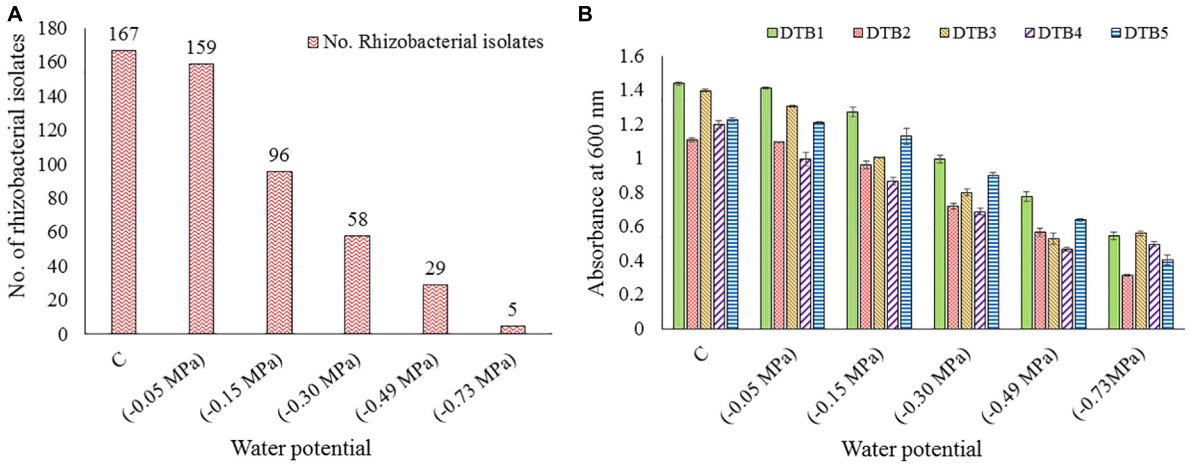

FIGURE 1
(A) Total number of different bacterial isolates obtained from various soil samples and further surviving isolate count at various levels of desiccation stress imposed by PEG-6000, **(B)** growth performance of five selected desiccation-tolerant bacterial isolates at various levels of desiccation stress imposed by PEG-6000.

spectrophotometer at 532 and 600 nm (Thermo-Scientific, Evolution-201). For non-specific absorbance, the absorbance at 600 nm was subtracted from the absorbance at 532 nm. The MDA concentration was determined using an extinction coefficient of 155 $mM^{-1}cm^{-1}$.

$$\text{MDA content} = \frac{\text{OD (532nm)} - \text{OD (600nm)}}{155} \text{x1000}$$

Peroxidase (POD) activity was determined by adding 100 μL of enzyme extract in a reaction mixture (3.0 ml) containing 1.0 ml of 100 mM phosphate buffer (pH 7.0), 0.3 ml of 0.1 mM EDTA, 0.6 ml of 5.0 mM guaiacol, and 1.0 ml of 15 mM H_2O_2 described by Urbanek et al. (1991). The reaction started after the enzyme was added. In a UV-VIS spectrophotometer, the absorbance increased for 90 s at 470 nm (Thermo-Scientific, Evolution-201). The amount of tetraguaiacol formed was quantified using its molar extinction coefficient (26.6 $mM^{-1}cm^{-1}$), and enzyme activity was expressed as mol min^{-1} mg^{-1} protein.

For CAT activity, 200 μl of enzyme extract was added to the reaction mixture (3.0 ml) containing 1.5 ml of 50 mM phosphate buffer (pH 7.0), 300 μl of 0.1 M H_2O_2, and 1.0 ml of distilled water. The CAT activity was assayed using a spectrophotometer by monitoring the decrease in the absorbance of H_2O_2 at 240 nm (Bin et al., 2010; Batool et al., 2020). The reaction was started by adding an aliquot of the enzyme to the reaction mixture. The absorbance change was monitored 90 s after the reaction began. The absorbance difference (A240) was divided by the H_2O_2 molar extinction coefficient (39.4 $M^{-1}cm^{-1}$). The enzyme activity was expressed in mol min^{-1} mg^{-1} protein.

The activity of APX was measured using a slightly modified method developed by Nakano and Asada (1981). 200 μl of enzyme extract was added to the reaction mixture of 50 mM sodium phosphate buffer (pH 7.0), 0.2 mM EDTA, and 0.5 mM ascorbic acid. H_2O_2 was added to a final concentration of 0.1 mM to start the reaction. The oxidation of ascorbic acid was detected as a decrease in the absorbance at 290 nm using a UV-VIS spectrophotometer (Thermo-Scientific, Evolution-201) 90 s after the reaction began. The difference in absorbance was divided by the ascorbate molar extinction coefficient (2.8 $mM^{-1}cm^{-1}$). The enzyme activity was expressed as nmol of H_2O_2 $min^{-1}mg^{-1}$ protein taking into consideration that 1.0 mol of ascorbate is required for the reduction of 1.0 mol of H_2O_2.

2.5. Statistical analysis

All the data obtained were considered for correlation analysis (5% significance levels) and illustrated as a graph. The results were expressed as mean ± SD of three independent replicates. Analysis of variance (ANOVA) was done followed by Duncan's multiple range test (DMRT) to compare the means and determine the significant differences between each treatment. The level of statistical significance was set to $P < 0.05$.

3. Results

3.1. Soil characteristics, isolation, and screening of desiccation-tolerant rhizobacteria

The pH of the soil samples varied from slightly acidic (6.35) to alkaline (9.13). On average, soil comprised 41.38% clay, 36.86% silt, and 21.76% sand content. The average SM was observed to be 21.5%. The average value for temperature, EC, and WHC was 17.9°C, 68.8 μs/cm, and 45.4%, respectively. The nutrients N, P, and K were estimated to be 30.32, 133.04, and 284.01 kg/ha, respectively, whereas the OC content was 1.36%. A total of 167 rhizobacteria were isolated, which were further screened for desiccation tolerance. Only five isolates were observed to survive and grow at maximum desiccation stress of 0.73 MPa (**Figure 1A**). They were named as DTB1, DTB2, DTB3, DTB4, and DTB5. Among them, isolate DTB3 showed maximum growth at −0.73 MPa water potential. The overall growth behavior of all five isolates was observed to be in the following order DTB3 > DTB1 > DTB4 > DTB5 > DTB2 (**Figure 1B**) at −0.73 MPa.

3.2. Morphological, biochemical, and molecular characterization of bacterial isolates

All the isolates were rod shaped among which four were Gram positive, whereas one isolate was Gram negative (Table 1). Isolate DTB1 exhibited positive activity for catalase, citrate, and urease. Isolate DTB2 was positive for catalase, cellulase, and urease. Isolate DTB3 was positive for catalase, cellulase, urease, and protease. Isolate DTB4 showed positive activity for amylase, catalase, cellulase, citrate, urease, and protease, while isolate DTB5 was positive for amylase, catalase, cellulase, urease, and protease (Table 1).

Blast similarity analysis revealed that bacterial isolate DTB1 exhibited 92% similarity with *Enterobacter cloacae* strain PANS11, DTB2 showed 96% similarity with *Bacillus megaterium* strain IPNR61, DTB3 had 99% similarity with *B. megaterium strain 02-A7*, DTB4 showed 100% similarity with *B. megaterium* strain CEBZ144, and DTB5 showed 99.71% similarity with *B. cereus* strain SRE1. The sequences were deposited in the NCBI Gene-Bank database and assigned accession numbers MN173899, MN402912, MN402759, MN403305, and MN165497 were obtained. The phylogenetic analysis revealed three different clusters (Figure 2) of which cluster III had a majority of assemblage (14) consisting of three isolates of *B. megaterium* BHUIESDAS3 (DTB2), *B. megaterium* BHUIESDAS4 (DTB3), and *B. megaterium* BHUIESDAS5 (DTB4). *B. cereus* BHUAS2 (DTB5) was clustered with five other bacterial species in cluster I. Cluster II had *E. cloacae* BHUAS1 (DTB1) with five reference bacterial species.

3.3. Estimation of IAA, P-solubilisation, siderophore, ACCD, and EPS

The strains *Enterobacter cloacae* BHUAS1, *Bacillus megaterium* BHUIESDAS3, *Bacillus megaterium* BHUIESDAS4, *Bacillus megaterium* BHUIESDAS5, and *Bacillus cereus* BHUAS2 exhibited production of IAA, solubilization of insoluble phosphate, production of siderophore, and ACC deaminase activity under desiccation stress (−0.73 MPa water potential) (Figure 3). Expression of all PGP properties was observed under the impacts of desiccant by all the strains with a significant increase in EPS production under desiccation stress. *Enterobacter cloacae* BHUAS1 was observed to produce the highest amount of IAA under desiccation stress followed by *Bacillus cereus* BHUAS2, *Bacillus megaterium* BHUIESDAS3, *Bacillus megaterium* BHUIESDAS4, and *Bacillus megaterium* BHUIESDAS5 (Figure 3A). The amount of soluble phosphate was found significantly high in *Enterobacter cloacae* BHUAS1 under stress as well as desiccation challenge in comparison to others (Figure 3B). Furthermore, the production of siderophore was observed to be significantly high again in the case of *Enterobacter cloacae* BHUAS1 under no stress as well as desiccation stress in comparison to others (Figure 3C). *Enterobacter cloacae* BHUAS1 was also observed to produce the highest amount of ACC deaminase both under control as well as desiccation stress (Figure 3D). The EPS production was highest in *Bacillus cereus* BHUAS2 (6.31 g L^{-1}), followed by *Enterobacter cloacae* BHUAS1 (5.95 g L^{-1}), *Bacillus megaterium* BHUIESDAS4 (4.93 g L^{-1}), *Bacillus megaterium* BHUIESDAS3 (4.55 g L^{-1}), and *Bacillus megaterium* BHUIESDAS5 (3.66 g L^{-1}) (Figure 3E).

3.4. Growth improvement in wheat under limited water-induced drought stress

Bacterial treatment was observed to have a substantial effect on seed germination as compared with non-treated seeds. Highest seed germination was observed with *Enterobacter cloacae* BHUAS1 (T1) (88.89%) followed by *Bacillus cereus* BHUAS2 (T3) (88.78%) and *Bacillus megaterium* BHUIESDAS3 (T2) (85.56%), while control showed 77.78% germination of total seed sown after 7 days. The stress imposed by limited water availability led to a significant reduction in the growth dynamics of the plant (Figure 4). Plants with bacterial treatment showed better performance under drought than plants without bacterial treatment. It was observed that during the condition of water stress, plant height was increased by 32, 29, and 30% in T1, T2, and T3 inoculated plants, respectively, in comparison to un-inoculated control plants (Figure 4A). Root length was increased by 49, 45, and 47% in T1, T2, and T3 inoculated plants, respectively, than plants without inoculation (control) under water stress (Figure 4B). Similarly, under water stress, fresh weight of plant was enhanced by 23, 16, and 14% in case of T1, T2, and T3 treated plants, respectively, than in untreated control plants (Figure 4C), while dry weight was improved by 29, 24, and 26% in plants treated with T1, T2, and T3, respectively, as compared with un-inoculated control plant (Figure 4D).

3.5. Changes in leaf chlorophyll and carotenoid content

The plant pigments such as total chlorophyll and carotenoid of wheat plants were increased in bacterial treated plants under the influence of water stress (Figure 5). During water stress, total chlorophyll was enhanced by 10, 13, and 11% in plants with T1, T2, and T3 treatment, respectively, as compared to plants without bacterial inoculation. The T1 treated plants showed maximum chlorophyll content (Figure 5A). Similarly, under water stress, carotenoid content was also improved in wheat plants with bacterial treatment over the untreated control plants. During water stress conditions, carotenoid content increased by 13, 19, and 12% in T1, T2, and T3 treated plants, respectively, than plants without bacterial treatment (Figure 5B).

3.6. Changes in plant physiological parameters

Changes in physiological traits such as EL, RWC, and MSI are calculated under water stress in wheat plants as shown in Figure 6.

The water stress resulted in an increased level of electrolyte leakage (EL) in wheat plants (Figure 6A). However, under water stress, plants having bacterial inoculation showed a decrease in EL than in plants without bacterial treatment. During water stress, EL decreased by 18, 22, and 21% in T1, T2, and T3 treated wheat plants, respectively, as compared with un-inoculated plants.

The water stress was also observed to decrease the relative water content (RWC) and membrane stability index (MSI). However, under water stress, wheat plants with bacterial treatments exhibited an increment in RWC than plants without bacterial treatment (Figure 6B). Under stress conditions, RWC was enhanced by 44, 31,

TABLE 1 Morphological and biochemical characteristics of five selected desiccation-tolerant rhizobacterial isolates.

Characteristics		Desiccation-tolerant rhizobacterial isolates				
		DTB1	DTB2	DTB3	DTB4	DTB5
Morphological						
Colony morphology-	Form	Circular	Circular	Circular	Circular	Irregular
	Elevation	Convex	Crateriform	Crateriform	Raised	Flat
	Margin	Entire	Entire	Entire	Undulate	Undulate
	Color	Off white	Cream Yellow	Cream Yellow	Cream Yellow	White
	Appearance	Slimy	Slimy	Slimy	Slimy	Slightly Slimy
Cell morphology-	Gram's test	Negative	Positive	Positive	Positive	Positive
	Shape	Rod	Rod	Rod	Rod	Rod
Biochemical						
Amylase		–	–	–	+	+
Catalase		+	+	+	+	+
Cellulase		–	+	+	+	+
Citrate		+	–	–	+	–
Protease		–	–	+	+	+
Urease		+	+	+	+	+

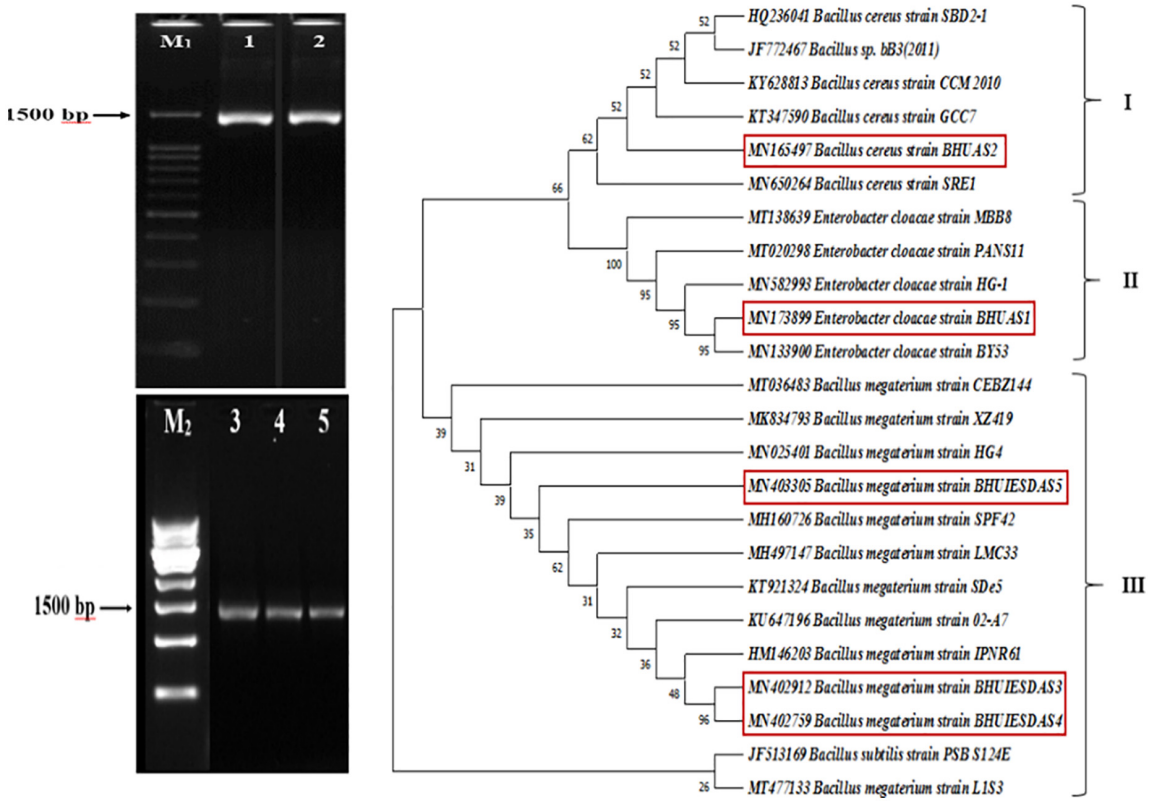

FIGURE 2
Gel-electrophoresis image showing the 1,500 bp amplified product of 16S rDNA gene from the five selected desiccation-tolerant rhizobacterial isolates 1-DTB1, 2-DTB5, 3-DTB2, 4-DTB3, and 5-DTB4. M1 is a 100 bp ladder and M2 is a 500 bp ladder. Phylogenetic tree obtained by the UPGMA method and bootstrap clustering showing the similarity relatedness of the selected rhizobacterial isolates and their relative position in respective clusters.

and 38% in plants inoculated with T1, T2, and T3, respectively, in comparison to plants without treatment.

The membrane stability decreased under water stress in wheat plants. However, under water stress, the plants with bacterial treatments showed an increase in MSI than plants without bacterial inoculation (Figure 6C). During water stress, MSI was improved by 44, 43, and 33% in plants with T1, T2, and T3 bacterial treatments, respectively, than in plants without bacterial treatment.

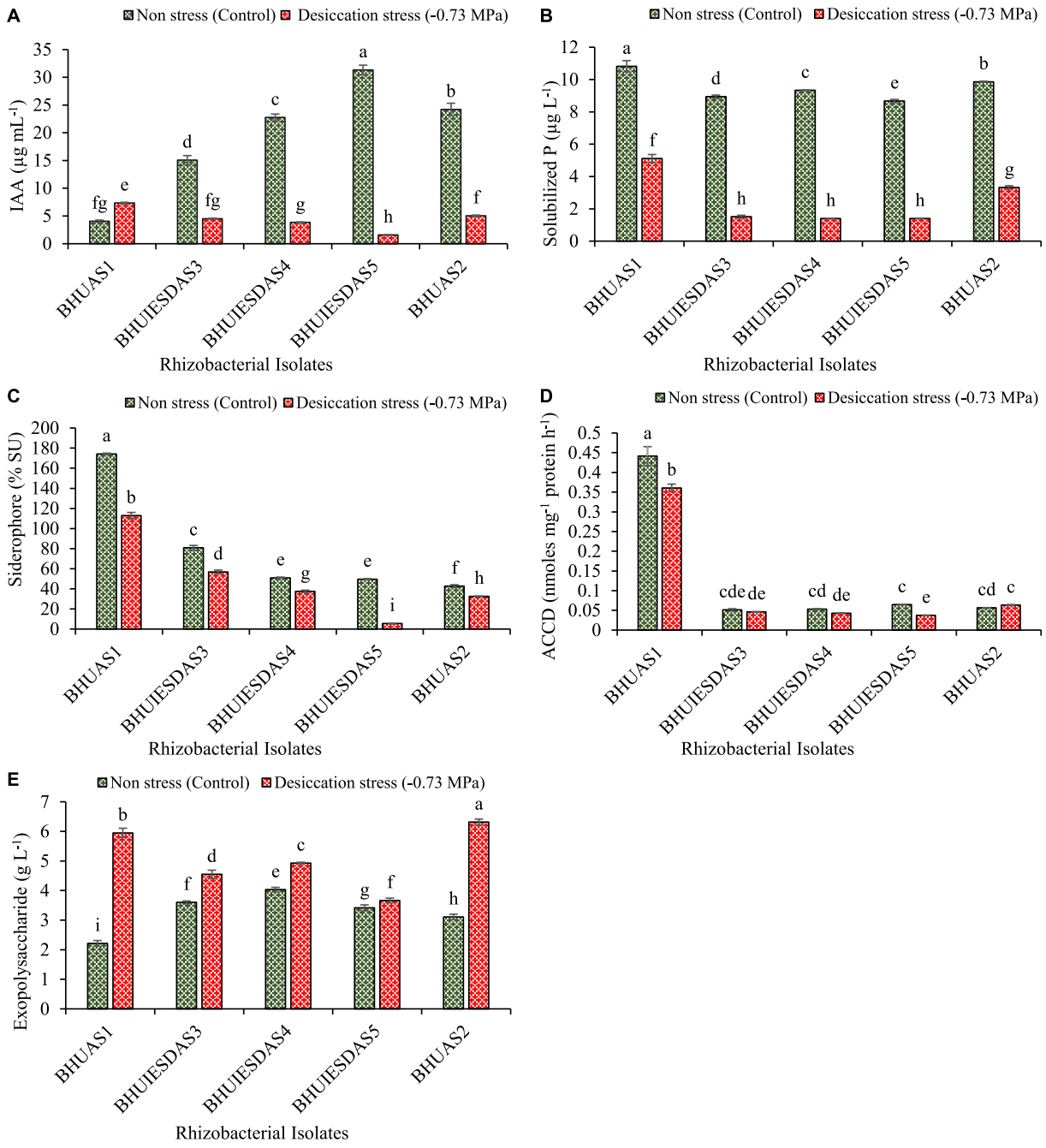

FIGURE 3
Expression of plant growth-promoting features of five selected desiccation-tolerant bacterial strains under non-stress and impacts of desiccation stress **(A)** amount of IAA produced, **(B)** amount of solubilized phosphate liberated, **(C)** amount of Fe chelating siderophore produced, **(D)** amount of ACC deaminase expressed, and **(E)** amount of exopolysaccharide produced. The different alphabets indicate statistically significant differences between each treatment (DMRT $p < 0.05$).

3.7. Changes in lipid peroxidation and reactive oxygen species

Changes in malondialdehyde (MDA) and reactive oxygen species (ROS) such as hydrogen peroxide (H_2O_2) under water stress are calculated in wheat plants as shown in Figure 7.

The water stress led to an increase in lipid peroxidation quantitated by the synthesis of MDA (Figure 7A). However, bacterial treated plants depicted a lower production of MDA in comparison to plants without bacterial inoculation under both no stress as well as water stress. The MDA content was decreased by 28, 22, and 31% in the case of plants treated with T1, T2, and T3, respectively, as compared to plants without any treatment under water stress.

Due to water stress, H_2O_2 production was increased in wheat plants (Figure 7B). However, plants having bacterial treatments showed a lower amount of H_2O_2 produced under water stress than plants without bacterial treatments. In wheat plants under water stress, H_2O_2 production decreased by 49%, 42%, and 51% in bacterial treatments T1, T2, and T3, respectively, in comparison to plants without treatments.

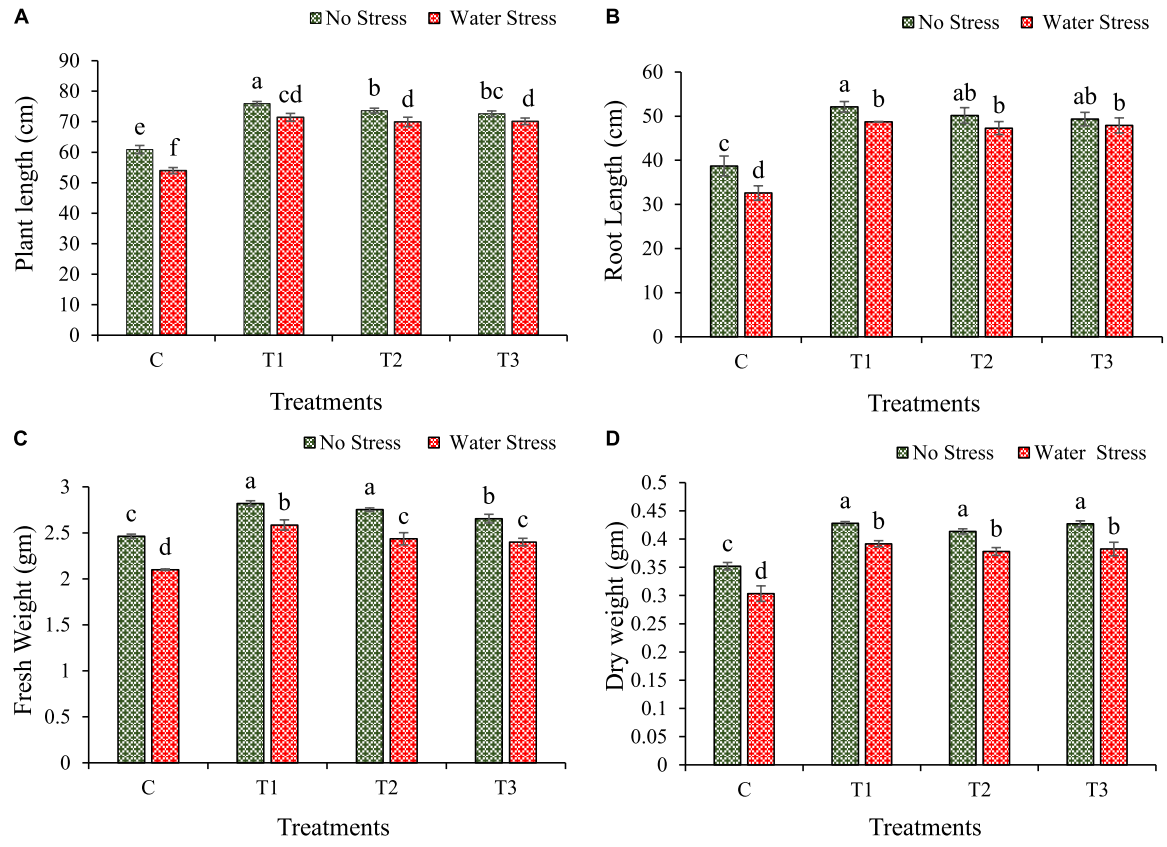

FIGURE 4
Impacts of bacterial treatments (T1 — *Enterobacter cloacae* BHUAS1, T2–*Bacillus megaterium* BHUIESDAS3, and T3 — *Bacillus cereus* BHUAS2) on various morpho-physiological features of wheat plants under the influence of water-induced drought stress **(A)** plant height, **(B)** root length, **(C)** fresh weight, and **(D)** dry weight. Data are presented as means ± SD of three replicates. The different alphabets indicate statistically significant differences between each treatment (DMRT $p < 0.05$).

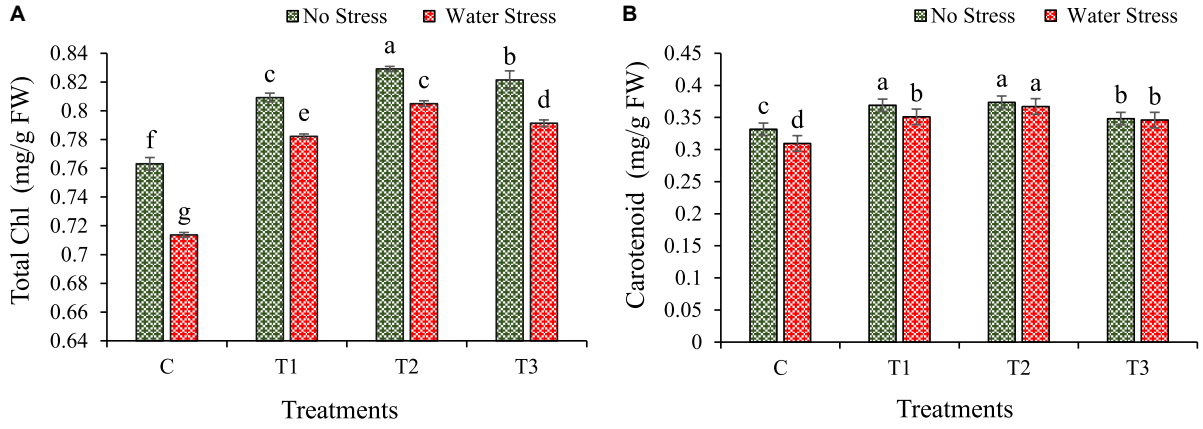

FIGURE 5
Impacts of bacterial treatments (T1 — *Enterobacter cloacae* BHUAS1, T2 — *Bacillus megaterium* BHUIESDAS3, and T3 — *Bacillus cereus* BHUAS2) on various biochemical contents of wheat plants under the influence of water-induced drought stress **(A)** total chlorophyll and **(B)** carotenoid. The different alphabets indicate statistically significant differences between each treatment (DMRT $p < 0.05$).

3.8. Changes in antioxidant enzyme activities

Water stress mostly activates the production of antioxidant enzymes and modulates plant physiology. It was found that during water stress, the production of ascorbate peroxidase (APX), catalase (CAT), and peroxidase (POD) increased in inoculated plants more than in un-inoculated plants (Figure 8).

The activity of APX was increased under water stress in wheat plants and was found higher than in no stress conditions (Figure 8A). However, plants with bacterial treatments T1, T2, and T3 showed an increase in APX activity by 70, 50, and 87%, respectively, in

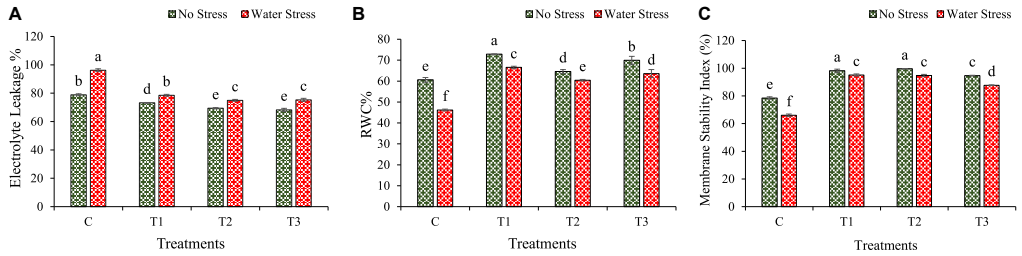

FIGURE 6
Impacts of bacterial treatments (T1 — *Enterobacter cloacae* BHUAS1, T2 — *Bacillus megaterium* BHUIESDAS3, and T3 — *Bacillus cereus* BHUAS2) on various features of wheat plants under the influence of water-induced drought stress **(A)** electrolyte leakage (EL), **(B)** relative water content (RWC), and **(C)** membrane stability index (MSI). The different alphabets indicate statistically significant differences between each treatment (DMRT $p < 0.05$).

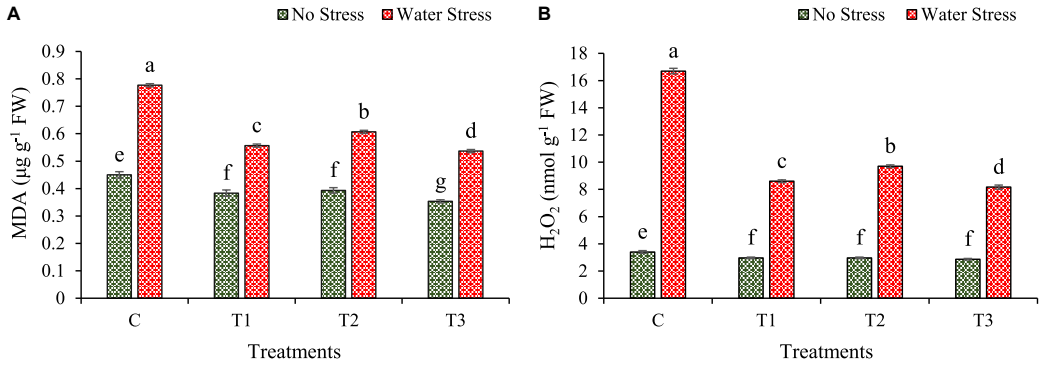

FIGURE 7
Impacts of bacterial treatments (T1 — *Enterobacter cloacae* BHUAS1, T2 — *Bacillus megaterium* BHUIESDAS3, and T3 — *Bacillus cereus* BHUAS2) on various features of wheat plants under the influence of water-induced drought stress **(A)** malondialdehyde (MDA) and **(B)** hydrogen peroxide (H_2O_2). The different alphabets indicate statistically significant differences between each treatment (DMRT $p < 0.05$).

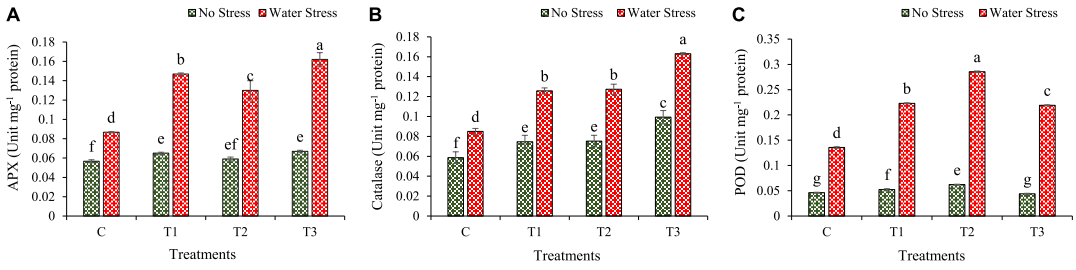

FIGURE 8
Impacts of bacterial treatments (T1 — *Enterobacter cloacae* BHUAS1, T2 — *Bacillus megaterium* BHUIESDAS3, and T3 — *Bacillus cereus* BHUAS2) on activities of various antioxidant enzymes of wheat plants under the influence of water-induced drought stress **(A)** ascorbate peroxidase (APX), **(B)** catalase (CAT), and **(C)** peroxidase (POD). The different alphabets indicate statistically significant differences between each treatment (DMRT $p < 0.05$).

comparison to plants without bacterial treatment under water stress conditions.

Under water stress, the CAT activity increased. It was found higher under water stress as compared with no stress. During water stress condition, the plants having bacterial treatments depicted higher CAT activity as compared with un-inoculated plants (Figure 8B). The CAT activity was increased by 48, 50, and 92%, respectively in plants treated with T1, T2, and T3 over control plants under water stress.

Similarly, the POD activity also increased significantly under water stress. The plants with bacterial treatments showed higher POD activity as compared to plants without bacterial treatments under water stress condition (Figure 8C). The POD activity increased by 64, 111, and 62%, respectively, in plants inoculated with T1, T2, and T3 as compared to plants without bacterial treatment under water stress.

3.9. Changes in the production of biochemicals

The production of soluble sugar was increased under the impact of water stress than no stress in wheat plants (Figure 9A). During water stress, the plants inoculated with bacterial isolates showed higher production than plants without inoculation. The production of total soluble sugar was increased by 99, 95, and 82% in plants

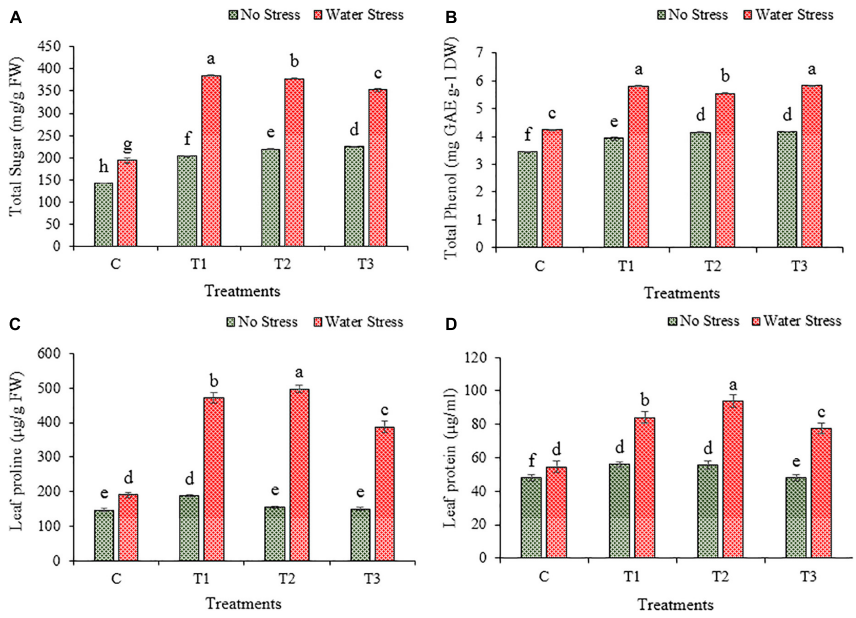

FIGURE 9
Impacts of bacterial treatments (T1- *Enterobacter cloacae* BHUAS1) (T2- *Bacillus megaterium* BHUIESDAS3) (*Bacillus cereus* BHUAS2) on various features of wheat plants under the influence of water induced drought stress **(A)** total sugar, **(B)** total phenol, **(C)** proline content, and **(D)** protein content. The different alphabets indicate statistically significant differences between each treatment (DMRT $p < 0.05$).

treated with bacteria T1, T2, and T3, respectively, than in un-inoculated plants under water stress.

The content of phenol increased due to water stress in wheat plants (**Figure 9B**). Under water stress conditions, the plants with bacterial treatments showed higher phenol content as compared to plants without bacterial inoculation. The phenol content was increased by 37, 31, and 38% in wheat plants with inoculation of T1, T2, and T3, respectively, in comparison to plants without any treatment under water stress.

Due to water stress, the proline content was increased significantly in wheat plants (**Figure 9C**). More production of proline was observed in plants having inoculation with bacterial isolates than in un-inoculated plants. The proline content was increased by 148, 161, and 104% in T1, T2, and T3 treated plants, respectively, than plants without bacterial treatment under water stress.

Similarly, water stress resulted in an increased production of total soluble protein in wheat plants (**Figure 9D**). Under water stress, the plants inoculated with bacterial isolates depicted higher production of soluble protein than plants without bacterial treatment. The production of total soluble protein increased by 54, 72, and 42% in plants with the application of T1, T2, and T3, respectively, than in plants without bacterial application under water stress.

4. Discussion

Drought is one of the most disastrous abiotic stressors in agriculture, with particular importance in wheat cultivars because of their vulnerability to low water which results in a significantly decreased physiological growth and yield under the impact of drought (Gaju et al., 2009; Qaseem et al., 2019). The history of the use of plant beneficial microorganisms such as PGPR in agriculture is too old, and it has been increasing day by day in enhancing plant's tolerance to different adverse environmental stresses including drought (Lizana et al., 2006; Batool et al., 2020). The establishment of the association of soil with plant roots created a rhizosphere system in which plants secreted exudates for inhabiting microflora so that they could flourish with the food and other nutrients such as C, N, and *P* (Jaiswal et al., 2022). The bacteria-associated roots of the plant play a crucial role in plant growth and development through different mechanisms (Chouhan et al., 2021; Jaiswal et al., 2022). Most often bacteria present in soil face the condition of desiccation due to water deficit, which leads to the development of a natural tolerance in them for growth and survival under water deficit conditions (Potts, 1994; Alpert, 2005). In the present study, the count of bacterial isolates obtained differently from soil samples was 167, which displayed a significant variation in their physicochemical properties. The variations in parameters such as WHC, SOC, *P*, and K are known to have a major impact on soil fertility including the growth behavior of bacteria (Kumar et al., 2013; Laldinthar and Dkhar, 2015; Wiesmeier et al., 2019; Garnaik et al., 2020). Bacterial isolates obtained were screened under different water potentials and also their plant growth-promoting traits were evaluated *in vitro*. Out of 167 rhizobacterial isolates, only five isolates survived at −0.73 MPa and were considered desiccation-tolerant. These bacterial strains were further characterized molecularly as *Enterobacter cloacae* BHUAS1, *Bacillus megaterium* BHUIESDAS3, *Bacillus megaterium* BHUIESDAS4, *Bacillus megaterium* BHUIESDAS5, and *Bacillus cereus* BHUAS2. These bacterial strains produced several enzymes such as amylase, catalase, cellulase, citrate, protease, and urease, which have been reported to have soil and plant beneficial effects (Bennett and Wallsgrove, 1994; Jaiswal et al., 2019).

The bacterial isolates selected also produced IAA, siderophore, and ACC deaminase enzyme, and they also solubilized insoluble phosphate under the impacts of desiccation stress. Studies reported that such beneficial PGP traits of bacteria positively influence plant growth and development during stressed conditions by increasing

nutrient accessibility and protection against oxidative damage (Glick et al., 2007; Saikia et al., 2018). Studies have shown a positive impact of bacteria synthesized IAA on the morphology of plant roots as well as seed germination and growth of seedlings under the condition of osmotic stress, and they also help in the bio-fortification of micronutrients such as Zn, Se, Fe, and others (Ngumbi and Kloepper, 2016; Saikia et al., 2018; Khanna et al., 2022). Furthermore, phosphate solubilizing rhizobacteria isolated from drought-impacted agroecosystems was observed to be more beneficial for the improvement of plant health under the availability of limited water conditions (Sarma and Saikia, 2014). All five isolates tested here were efficient phosphate solubilizers both in control as well as under water stress. The isolates were also an efficient producer of siderophore under desiccation stress. Siderophore plays an essential role in maintaining the bioavailability of iron near the root zone (Sorty et al., 2016). Such siderophore producing bacteria have also been reported as a defensive agent for plants against heavy metal injury (Burd et al., 2000). The enzyme ACC deaminase producing rhizobacteria helps plants to tolerate stress by decreasing ethylene production through its deamination activity, which dissociates ACC into α-ketobutyrate and ammonia, thus inhibiting the production of stress-induced ethylene and thereby another downstream signaling (Glick, 2014; Gupta and Pandey, 2019). All five desiccation-tolerant rhizobacterial isolates tested here exhibited excellent ACC deaminase activity. The desiccation-tolerant rhizobacteria having ACC deaminase activity have been observed to trigger plant growth by increasing seed germination and pigment content under no stress (control) and desiccation stress by decreasing the level of ethylene along with increased production of ROS scavenging enzymes (Barnawal et al., 2012; Egamberdieva et al., 2019; Mukhtar et al., 2020). All five desiccation-tolerant bacterial strains exhibited significant activity of various antioxidant enzymes under no stress (control) and desiccation stress condition (**Figure 3D**). Thus, ACC deaminase activity along with other PGP properties has been observed to put an additive impact on plant growth and development under limited water condition (Saikia et al., 2018).

The desiccation-tolerant bacterial isolates secreted high amounts of EPS at −0.73 MPa water potential showing that limited availability of water induced the EPS production in them. The EPS produced by root adhered bacteria enhances the permeability of roots in soil by making soil aggregates and also maintains a positive water potential around the root zone, which results in improved water uptake and growth of the plant (Roberson and Firestone, 1992; Ali et al., 2014). These EPS produced by bacteria also protect seedling growth during water stress (Miller and Wood, 1996; Alami et al., 2000; Sandhya et al., 2009).

The present study also showed a protective role of desiccation-tolerant bacterial isolates in coping with the negative effects of water stress. Plant growth parameters got reduced under low water availability in non-treated plants. However, a significant increment in plant growth features was observed (**Figure 4**) in bacterial inoculated plants. In a study using pepper and tomato plants, inoculating the roots with PGPR was found to have improved biomass in comparison to un-inoculated plants under water stress conditions (Mayak et al., 2004; Kalozoumis et al., 2021). The isolate *E. cloacae* BHUAS1 was one of the most effective strains with higher EPS production showing significant improvement in fresh and dry weight of wheat seedlings under water limiting conditions in comparison to untreated control plants. Similar results have been reported where EPS producing bacteria was significantly effective in reducing the negative effect of water stress on fresh weight, dry weight, and root and shoot length of the maize plant (Naseem and Bano, 2014; Vurukonda et al., 2016).

A major consequence of water stress was observed as a reduction in the chlorophyll content of wheat plants (**Figure 5**). During water stress, chloroplast gets damaged, which results in photoinhibition that reduces the ATP intake in the C_3 cycle due to the low rate of electron transportation (Izanloo et al., 2008; Batool et al., 2020). The chlorophyll content should be enough to improve photosynthesis or stomatal conductance under water limiting conditions since two-thirds of the crop's green part is actively involved in accumulating the light to drive photosynthesis (Ji et al., 2010; Batool et al., 2020). Therefore, the rate of photosynthesis is directly proportional to the amount of photosynthetic pigment (chlorophyll) per unit leaf area. Furthermore, the plant's water status in form of leaf RWC and MSI treated with plant beneficial rhizobacteria are considered essential to keep up the stomatal conductance for CO_2 exchange and execution of photosynthesis as well as proper operation of the electron transport system (Batool et al., 2020).

The amount of ROS and MDA accumulated in wheat plants under water stress conditions and in treatments with desiccation-tolerant bacterial strains showed a significant ameliorating impact on bacterial isolates (**Figure 7**). The amount of oxidative stress determines the intercellular concentration of MDA (Lulsdorf et al., 2013). The accumulation of MDA activates the cascade of signals characterized by various physiological aberrations in a cell such as a cell membrane becoming more permeable, decreased chlorophyll content, breakdown of macromolecules such as nucleic acids and proteins causing nutrients to remobilize extensively and premature senescence, and finally decreased crop growth and development. The MDA and ROS contents were observed to increase in un-inoculated plants during water stress (**Figure 7**), which is implicated in the reduced amount and capacity of antioxidants in wheat plants. It is well-reported that photosynthetic inhibition leads to the accumulation of ROS in cells and its organelles (Lulsdorf et al., 2013). Hence, it becomes mandatory to control the synthesis and accumulation of ROS within plant cells in order to check the damage caused by them in plants (Saneoka et al., 2004; Mahajan and Tuteja, 2005). Wheat plants having bacterial treatments showed lower MDA and ROS contents as compared to plants without bacteria showing an increased ROS scavenging ability under water stress.

The bacterial treated plants also exhibited higher activities of enzymes APX, CAT, and POD, and lower MDA and ROS contents (**Figure 8**). The results depicted that the synthesis of a suitable ROS scavenging antioxidant system in water-stressed plants under bacterial treatments might have boosted photosynthesis in treated plants. Similar results had been reported by Banik et al. (2016) in which it was concluded that bacterial treatment in *Agrostis palustris* showed drought tolerance by means of inhibiting cell membrane damage, decreased MDA production, and increased osmotic regulation.

Plants are reported to have the capability to regulate water relations in order to maintain cellular integrity during water stress conditions through osmotic adjustment by producing compatible solutes such as various soluble sugars, phenol, proline, and soluble proteins (Saharan and Nehra, 2011; Banik et al., 2016). These compatible solutes help plants to maintain cell turgidity and volume of the cell when water potential crucial for maintaining cell metabolism declines (Saneoka et al., 2004; Fischer, 2008; Batool et al., 2020). In addition, the osmolytes also assist in the repossession of metabolic activities of cells after overcoming stress (Abid et al., 2016).

Overall water unavailability was observed to impose a serious influence on wheat stress plant growth, yield, and physiological as well as biochemical functions. However, bacterial treatments helped the wheat plant to sustain its development and other functions proficiently, under the impacts of low water-induced drought stress. Wheat plants having bacterial treatments maintained higher biomass and root and shoot length. The plants with bacterial inoculation showed better MSI, RWC, chlorophyll, and carotenoid. These plants further displayed lower MDA and ROS and higher enzymatic activity of APX, CAT, and POD along with elevated production of soluble sugars, phenol, proline, and soluble protein. These isolates characterized may be used as potential candidates for the improvement in growth and yield of wheat under conditions of low water availability or any other similar stress.

Data availability statement

The original contributions presented in this study are included in this article/supplementary material, further inquiries can be directed to the corresponding author.

Author contributions

AS collected the samples, executed the experiments and data analysis, comprehended the study, arranged the figures, and wrote the first draft. VP edited the manuscript. Both authors conceived the study and approved the final manuscript.

Acknowledgments

The authors are thankful to SERB (ECR/2018/000941) for providing financial support. AS is also thankful to the University Grant Commission, New Delhi, India, for providing fellowship during the study period.

Conflict of interest

The authors declare that the research was conducted in the absence of any commercial or financial relationships that could be construed as a potential conflict of interest.

Publisher's note

All claims expressed in this article are solely those of the authors and do not necessarily represent those of their affiliated organizations, or those of the publisher, the editors and the reviewers. Any product that may be evaluated in this article, or claim that may be made by its manufacturer, is not guaranteed or endorsed by the publisher.

References

Abid, M., Tian, Z., Ata-Ul-Karim, S. T., Liu, Y., Cui, Y., Zahoor, R., et al. (2016). Improved tolerance to post-anthesis drought stress by pre-drought priming at vegetative stages in drought-tolerant and-sensitive wheat cultivars. *Plant Physiol. Biochem.* 106, 218–227. doi: 10.1016/j.plaphy.2016.05.003

Adesemoye, A. O., and Egamberdieva, D. (2013). "Beneficial effects of plant growth-promoting rhizobacteria on improved crop production: Prospects for developing economies," in *Bacteria in agrobiology: Crop productivity*, eds D. K. Maheshwari, M. Saraf, and A. Aeron (Berlin: Springer), 45–63. doi: 10.1007/978-3-642-37241-4_2

Alami, Y., Achouak, W., Marol, C., and Heulin, T. (2000). Rhizosphere soil aggregation and plant growth promotion of sunflowers by an exopolysaccharide-producing *Rhizobium* sp. strain isolated from sunflower roots. *Appl. Environ. Microbiol.* 66, 3393–3398. doi: 10.1128/AEM.66.8.3393-3398.2000

Alexieva, V., Sergiev, I., Mapelli, S., and Karanov, E. (2001). The effect of drought and ultraviolet radiation on growth and stress markers in pea and wheat. *Plant Cell Environ.* 24, 1337–1344. doi: 10.1046/j.1365-3040.2001.00778.x

Ali, S. Z., Sandhya, V., and Venkateswar Rao, L. (2014). Isolation and characterization of drought-tolerant ACC deaminase and exopolysaccharide-producing fluorescent *Pseudomonas* sp. *Ann. Microbiol.* 64, 493–502. doi: 10.1007/s13213-013-0680-3

Alpert, P. (2005). The limits and frontiers of desiccation-tolerant life. *Integr. Comp. Biol.* 45, 685–695. doi: 10.1093/icb/45.5.685

Arnon, D. I. (1949). Copper enzymes in isolated chloroplasts. Polyphenoloxidase in *Beta vulgaris*. *Plant Physiol.* 24:1. doi: 10.1104/pp.24.1.1

Banik, P., Zeng, W., Tai, H., Bizimungu, B., and Tanino, K. (2016). Effects of drought acclimation on drought stress resistance in potato (*Solanum tuberosum* L.) genotypes. *Environ. Exp. Bot.* 126, 76–89. doi: 10.1016/j.envexpbot.2016.01.008

Barnawal, D., Bharti, N., Maji, D., Chanotiya, C. S., and Kalra, A. (2012). 1-Aminocyclopropane-1-carboxylic acid (ACC) deaminase-containing rhizobacteria protect *Ocimum sanctum* plants during waterlogging stress via reduced ethylene generation. *Plant Physiol. Biochem.* 58, 227–235. doi: 10.1016/j.plaphy.2012.07.008

Bates, L. S., Waldern, R. O., and Teare, I. D. (1973). Rapid determination of free proline for water-stress studies. *Plant Soil* 39, 205–207. doi: 10.1007/BF00018060

Batool, T., Ali, S., Seleiman, M. F., Naveed, N. H., Ali, A., Ahmed, K., et al. (2020). Plant growth promoting rhizobacteria alleviates drought stress in potato in response to suppressive oxidative stress and antioxidant enzymes activities. *Sci. Rep.* 10, 1–9. doi: 10.1038/s41598-020-73489-z

Bennett, R. N., and Wallsgrove, R. M. (1994). Secondary metabolites in plant defence mechanisms. *New Phytol.* 127, 617–633. doi: 10.1111/j.1469-8137.1994.tb02968.x

Bin, T., Xu, S. Z., Zou, X. L., Zheng, Y. L., and Qiu, F. Z. (2010). Changes of antioxidative enzymes and lipid peroxidation in leaves and roots of waterlogging-tolerant and waterlogging-sensitive maize genotypes at seedling stage. *Agric. Sci. China* 9, 651–661. doi: 10.1016/S1671-2927(09)60140-1

Bradford, M. M. (1976). A rapid and sensitive method for the quantitation of microgram quantities of protein utilizing the principle of protein-dye binding. *Anal. Biochem.* 72, 248–254. doi: 10.1016/0003-2697(76)90527-3

Bramhachari, P. V., and Dubey, S. (2006). Isolation and characterization of exopolysaccharide produced by *Vibrio harveyi* strain VB23. *Lett. Appl. Microbiol.* 43, 571–577. doi: 10.1111/j.1472-765X.2006.01967.x

Bric, J. M., Bostock, R. M., and Silverstone, S. E. (1991). Rapid in situ assay for indoleacetic acid production by bacteria immobilized on a nitrocellulose membrane. *Appl. Environ. Microbiol.* 57, 535–538. doi: 10.1128/aem.57.2.535-538.1991

Burd, G. I., Dixon, D. G., and Glick, B. R. (2000). Plant growth-promoting bacteria that decrease heavy metal toxicity in plants. *Can. J. Microbiol.* 46, 237–245. doi: 10.1139/w99-143

Cappuccino, J., and Sherman, N. (1992). *Biochemical activities of microorganisms. Microbiology, a laboratory manual*. San Francisco, CA: The Benjamin/Cummings Publishing Co, 188–247.

Casteriano, A., Wilkes, M. A., and Deaker, R. (2013). Physiological changes in rhizobia after growth in peat extract may be related to improved desiccation tolerance. *Appl. Environ. Microbiol.* 79, 3998–4007. doi: 10.1128/AEM.00082-13

Chang, W.-S., Van De Mortel, M., Nielsen, L., Nino De Guzman, G., Li, X., and Halverson, L. J. (2007). Alginate production by *Pseudomonas putida* creates a hydrated microenvironment and contributes to biofilm architecture and stress tolerance under water-limiting conditions. *Am. Soc. Microbiol.* 189, 8290–8299. doi: 10.1128/JB.00727-07

Chouhan, G. K., Verma, J. P., Jaiswal, D. K., Mukherjee, A., Singh, S., de Araujo Pereira, A. P., et al. (2021). Phytomicrobiome for promoting sustainable agriculture and food security: Opportunities, challenges and solutions. *Microbiol. Res.* 248:126763. doi: 10.1016/j.micres.2021.126763

Dubois, M., Gilles, K. A., Hamilton, J. K., and Rebers, P. T. (1956). Colorimetric method for determination of sugars and related substances. *Anal. Chem.* 28, 350–356. doi: 10.1021/ac60111a017

Egamberdieva, D., Wirth, S., Bellingrath-Kimura, S. D., Mishra, J., and Arora, N. K. (2019). Salt-tolerant plant growth promoting rhizobacteria for enhancing crop productivity of saline soils. *Front. Microbiol.* 10:2791. doi: 10.3389/fmicb.2019.02791

Fischer, R. A. (2008). The importance of grain or kernel number in wheat: A reply to Sinclair and Jamieson. *Field Crops Res.* 105, 15–21. doi: 10.1016/j.fcr.2007.04.002

Gaju, O., Reynolds, M. P., Sparkes, D. L., and Foulkes, M. J. (2009). Relationships between large-spike phenotype, grain number, and yield potential in spring wheat. *Crop Sci.* 49, 961–973. doi: 10.2135/cropsci2008.05.0285

Gangadhar, B. H., Sajeesh, K., Venkatesh, J., Baskar, V., Abhinandan, K., Yu, J. W., et al. (2016). Enhanced tolerance of transgenic potato plants over-expressing non-specific lipid transfer protein-1 (StnsLTP1) against multiple abiotic stresses. *Front. Plant Sci.* 7:1228. doi: 10.3389/fpls.2016.01228

Garnaik, S., Sekhon, B. S., Sahoo, S., and Dhaliwal, S. S. (2020). Comparative assessment of soil fertility status of various agroecological regions under intensive cultivation in Northwest India. *Environ. Monit. Assess.* 192, 1–18. doi: 10.1007/s10661-020-08290-6

Glick, B. R. (2014). Bacteria with ACC deaminase can promote plant growth and help to feed the world. *Microbiol. Res.* 69, 30–39. doi: 10.1016/j.micres.2013.09.009

Glick, B. R., Cheng, Z., Czarny, J., and Duan, J. (2007). "Promotion of plant growth by ACC deaminase-producing soil bacteria," in *New perspectives and approaches in plant growth-promoting rhizobacteria research*, eds P. A. H. M. Bakker, J. M. Raaijmakers, G. Bloemberg, M. Höfte, P. Lemanceau, and B. M. Cooke (Dordrecht: Springer), 329–339. doi: 10.1007/978-1-4020-6776-1_8

Gonzalez, L., and Gonzalez-Vilar, M. (2003). "Determination of relative water content," in *Handbook of plant ecophysiology techniques*, ed. M. J. Reigosu (Dordrecht: Kluwer Academic), 207–212. doi: 10.1007/0-306-48057-3_14

Gouzou, L., Burtin, G., Philippy, R., Bartoli, F., and Heulin, T. (1993). Effect of inoculation with *Bacillus polymyxa* on soil aggregation in the wheat rhizosphere: Preliminary examination. *Geoderma* 56, 479–491. doi: 10.1016/0016-7061(93)90128-8

Gupta, S., and Pandey, S. (2019). ACC deaminase producing bacteria with multifarious plant growth promoting traits alleviates salinity stress in French bean (*Phaseolus vulgaris*) plants. *Front. Microbiol.* 10:1506. doi: 10.3389/fmicb.2019.01506

Heath, R. L., and Packer, L. (1968). Photoperoxidation in isolated chloroplast I. Kinetics and stoichiometry of fatty acid peroxidation. *Arch. Biochem. Biophys.* 125, 189–198. doi: 10.1016/0003-9861(68)90654-1

Honma, M., and Shimomura, T. (1978). Metabolism of 1-aminocyclopropane-1-carboxylic acid. *Agric. Biol. Chem.* 42, 1825–1831. doi: 10.1080/00021369.1978.10863261

Izanloo, A., Condon, A. G., Langridge, P., Tester, M., and Schnurbusch, T. (2008). Different mechanisms of adaptation to cyclic water stress in two South Australian bread wheat cultivars. *J. Exp. Bot.* 59, 3327–3346. doi: 10.1093/jxb/ern199

Jaiswal, D. K., Krishna, R., Chouhan, G. K., de Araujo Pereira, A. P., Ade, A. B., Prakash, S., et al. (2022). Bio-fortification of minerals in crops: Current scenario and future prospects for sustainable agriculture and human health. *Plant Growth Regul.* 28, 1–8. doi: 10.1007/s10725-022-00847-4

Jaiswal, D. K., Verma, J. P., Krishna, R., Gaurav, A. K., and Yadav, J. (2019). Molecular characterization of monocrotophos and chlorpyrifos tolerant bacterial strain for enhancing seed germination of vegetable crops. *Chemosphere* 223, 636–650. doi: 10.1016/j.chemosphere.2019.02.053

Ji, X., Shiran, B., Wan, J., Lewis, D. C., Jenkins, C. L., Condon, A. G., et al. (2010). Importance of pre-anthesis anther sink strength for maintenance of grain number during reproductive stage water stress in wheat. *Plant Cell Environ.* 33, 926–942. doi: 10.1111/j.1365-3040.2010.02130.x

Jochum, M. D., Mcwilliams, K. L., Borrego, E. J., Kolomiets, M. V., Niu, G., Pierson, E. A., et al. (2019). Bioprospecting plant growth-promoting rhizobacteria that mitigate drought stress in grasses. *Front. Microbiol.* 10:2106. doi: 10.3389/fmicb.2019.02106

Kalozoumis, P., Savvas, D., Aliferis, K., Ntatsi, G., Marakis, G., Simou, E., et al. (2021). Impact of plant growth-promoting rhizobacteria inoculation and grafting on tolerance of tomato to combined water and nutrient stress assessed via metabolomics analysis. *Front. Plant Sci.* 12:670236. doi: 10.3389/fpls.2021.670236

Kammoun, R., Naili, B., and Bejar, S. (2008). Application of a statistical design to the optimization of parameters and culture medium for α-amylase production by *Aspergillus oryzae* CBS 819.72 grown on gruel (wheat grinding by-product). *Bioresour. Technol.* 99, 5602–5609. doi: 10.1016/j.biortech.2007.10.045

Khanna, K., Kumar, P., Ohri, P., and Bhardwaj, R. (2022). Harnessing the role of selenium in soil–plant-microbe ecosystem: Ecophysiological mechanisms and future prospects. *Plant Growth Regul.* 14, 1–21. doi: 10.1007/s10725-022-00830-z

Khanna-Chopra, R., and Selote, D. S. (2007). Acclimation to drought stress generates oxidative stress tolerance in drought-resistant than-susceptible wheat cultivar under field conditions. *Environ. Exp. Bot.* 60, 276–283. doi: 10.1016/j.envexpbot.2006.11.004

Kumar, M. A., Anandapandian, K. T. K., and Parthiban, K. (2011). Production and characterization of exopolysaccharides (EPS) from biofilm forming marine bacterium. *Brazil. Arch. Biol. Technol.* 54, 259–265. doi: 10.1590/S1516-89132011000200006

Kumar, M. V., Lakshmi, G., and Madhuvani, P. (2013). Appraisal of soil fertility status in salt-affected soils of Ongole division, Prakasam district, Andhra Pradesh. *J. Indian Soc. Soil Sci.* 61, 333–340.

Kumar, S., Tamura, K., and Nei, M. (2004). MEGA3: Integrated software for molecular evolutionary genetics analysis and sequence alignment. *Brief. Bioinf.* 5, 150–163. doi: 10.1093/bib/5.2.150

Laldinthar, R., and Dkhar, M. (2015). Relationship between soil bacterial population and various physico-chemical properties at two broadleaved forest stands of Meghalaya differing in altitudes. *Transcriptomics* 3, 1–7.

Lizana, C., Wentworth, M., Martinez, J. P., Villegas, D., Meneses, R., Murchie, E. H., et al. (2006). Differential adaptation of two varieties of common bean to abiotic stress: I. Effects of drought on yield and photosynthesis. *J. Exp. Bot.* 57, 685–697. doi: 10.1093/jxb/erj062

Lulsdorf, M. M., Yuan, H. Y., Slater, S. M., Vandenberg, A., Han, X., Zaharia, L. I., et al. (2013). Endogenous hormone profiles during early seed development of *C. arietinum* and *C. anatolicum*. *Plant growth Regul.* 71, 191–198. doi: 10.1007/s10725-013-9819-2

Mahajan, S., and Tuteja, N. (2005). Cold, salinity and drought stresses: An overview. *Arch. Biochem. Biophys.* 444, 139–158. doi: 10.1016/j.abb.2005.10.018

Mayak, S., Tirosh, T., and Glick, B. R. (2004). Plant growth-promoting bacteria that confer resistance to water stress in tomatoes and peppers. *Plant Sci.* 166, 525–530. doi: 10.1016/j.plantsci.2003.10.025

Mehta, S., and Nautiyal, C. S. (2001). An efficient method for qualitative screening of phosphate-solubilizing bacteria. *Curr. Microbiol.* 43, 51–56. doi: 10.1007/s002840010259

Meng, S., Zhang, C., Su, L., Lim, Y., and Zhao, Z. (2016). Nitrogen uptake and metabolism of *Populus simonii* in response to PEG-induced drought stress. *Environ. Exp. Bot.* 123, 78–87. doi: 10.1016/j.envexpbot.2015.11.005

Michel, B. E., and Kaufmann, M. R. (1973). The osmotic potential of polyethylene glycol 6000. *Plant Physiol.* 51, 914–916. doi: 10.1104/pp.51.5.914

Miller, K. J., and Wood, J. M. (1996). Osmoadaptation by rhizosphere bacteria. *Ann. Rev. Microbiol.* 50, 101–137. doi: 10.1146/annurev.micro.50.1.101

Molina-Romero, D., Baez, A., Quintero-Hernández, V., Castañeda-Lucio, M., Fuentes-Ramírez, L. E., Bustillos-Cristales, M. D. R., et al. (2017). Compatible bacterial mixture, tolerant to desiccation, improves maize plant growth. *PLoS One* 12:e0187913. doi: 10.1371/journal.pone.0187913

Mukhtar, T., Rehman, S. U., Smith, D., Sultan, T., Seleiman, M. F., Alsadon, A. A., et al. (2020). Mitigation of heat stress in *Solanum lycopersicum* L. by ACC-deaminase and exopolysaccharide producing Bacillus cereus: Effects on biochemical profiling. *Sustainability* 12:2159. doi: 10.3390/su12062159

Muñoz-Rojas, J. (2018). Desiccation-tolerant rhizobacteria maintain their plant growth-promoting capability after experiencing extreme water stress. *Scifed J. Appl. Microbiol.* 1, 15–17.

Nakano, Y., and Asada, K. (1981). Hydrogen peroxide is scavenged by ascorbate specific peroxidase in spinach chloroplasts. *Plant Cell Physiol.* 22, 867–880.

Naseem, H., and Bano, A. (2014). Role of plant growth-promoting rhizobacteria and their exopolysaccharide in drought tolerance of maize. *J. Plant Interact.* 9, 689–701. doi: 10.1080/17429145.2014.902125

Ngumbi, E., and Kloepper, J. (2016). Bacterial-mediated drought tolerance: Current and future prospects. *Appl. Soil Ecol.* 105, 109–125. doi: 10.1016/j.apsoil.2016.04.009

Pawar, D. R., and Shah, K. M. (2009). *Laboratory testing procedure for soil and water sample analysis*. Pune: Government of Maharashtra Water Resources Department, Directorate of Irrigation Research and Development Pune.

Penrose, D. M., and Glick, B. R. (2003). Methods for isolating and characterizing ACC deaminase-containing plant growth-promoting rhizobacteria. *Physiol. Plant.* 118, 10–15. doi: 10.1034/j.1399-3054.2003.00086.x

Pereira, S. I., and Castro, P. M. (2014). Phosphate-solubilizing rhizobacteria enhance *Zea mays* growth in agricultural P-deficient soils. *Ecol. Eng.* 73, 526–535. doi: 10.1016/j.ecoleng.2014.09.060

Potts, M. (1994). Desiccation tolerance of prokaryotes. *Microbiol. Rev.* 58, 755–805. doi: 10.1128/mr.58.4.755-805.1994

Qaseem, M. F., Qureshi, R., and Shaheen, H. (2019). Effects of pre-anthesis drought, heat and their combination on the growth, yield and physiology of diverse wheat (*Triticum aestivum* L.) genotypes varying in sensitivity to heat and drought stress. *Sci. Rep.* 9:6955. doi: 10.1038/s41598-019-43477-z

Roberson, E. B., and Firestone, M. K. (1992). Relationship between desiccation and exopolysaccharide production in a soil *Pseudomonas* sp. *Appl. Environ. Microbiol.* 58, 1284–1291. doi: 10.1128/aem.58.4.1284-1291.1992

Saharan, B. S., and Nehra, V. (2011). Plant growth promoting rhizobacteria: A critical review. *Life Sci. Med. Res.* 21:30.

Saikia, J., Sarma, R. K., Dhandia, R., Yadav, A., Bharali, R., Gupta, V. K., et al. (2018). Alleviation of drought stress in pulse crops with ACC deaminase producing rhizobacteria isolated from acidic soil of Northeast India. *Sci. Rep.* 8, 1–16. doi: 10.1038/s41598-018-21921-w

Sambrooke, J., Fritsch, E., and Maniatis, T. (1989). *Molecular cloning: A laboratory manual*, 2nd Edn. New York, NY: Cold Spring Harbor Press.

Sandhya, V., Sk, Z. A., Grover, M., Reddy, G., and Venkateswarlu, B. (2009). Alleviation of drought stress effects in sunflower seedlings by the exopolysaccharides producing *Pseudomonas putida* strain GAP-P45. *Biol. Fertil. Soils* 46, 17–26. doi: 10.1007/s00374-009-0401-z

Saneoka, H., Moghaieb, R. E., Premachandra, G. S., and Fujita, K. (2004). Nitrogen nutrition and water stress effects on cell membrane stability and leaf water relations in *Agrostis palustris* Huds. *Environ. Exp. Bot.* 52, 131–138. doi: 10.1016/j.envexpbot.2004.01.011

Sarma, R. K., and Saikia, R. (2014). Alleviation of drought stress in mung bean by strain *Pseudomonas aeruginosa* GGRJ21. *Plant Soil* 377, 111–126. doi: 10.1007/s11104-013-1981-9

Schwyn, B., and Neilands, J. (1987). Universal chemical assay for the detection and determination of siderophores. *Anal. Biochem.* 160, 47–56. doi: 10.1016/0003-2697(87)90612-9

Sorty, A. M., Meena, K. K., Choudhary, K., Bitla, U. M., Minhas, P., and Krishnani, K. (2016). Effect of plant growth promoting bacteria associated with halophytic weed (*Psoralea corylifolia* L) on germination and seedling growth of wheat under saline conditions. *Appl. Biochem. Biotechnol.* 180, 872–882. doi: 10.1007/s12010-016-2139-z

Sprenger, H., Erban, A., Seddig, S., Rudack, K., Thalhammer, A., Le, M. Q., et al. (2018). Metabolite and transcript markers for the prediction of potato drought tolerance. *Plant Biotechnol. J.* 6, 939–950. doi: 10.1111/pbi.12840

Streeter, J. (2003). Effect of trehalose on survival of *Bradyrhizobium japonicum* during desiccation. *J. Appl. Microbiol.* 95, 484–491. doi: 10.1046/j.1365-2672.2003.02017.x

Sumanta, N., Haque, C. I., Nishika, J., and Suprakash, R. (2014). Spectrophotometric analysis of chlorophylls and carotenoids from commonly grown fern species by using various extracting solvents. *Res. J. Chem. Sci.* 9, 63–69.

Teulat, B., Zoumarou-Wallis, N., Rotter, B., Ben Salem, M., Bahri, H., and This, D. (2003). QTL for relative water content in field grown barley and their stability across Mediterranean environments. *Theor. Appl. Genet.* 108, 181–188. doi: 10.1007/s00122-003-1417-7

Urbanek, H., Kuzniak-Gebarowska, E., and Herka, K. (1991). Elicitation of defence responses in bean leaves by *Botrytis cinerea* polygalacturonase. *Acta Physiol. Plant.* 13, 43–50.

van de Mortel, M., Chang, W.-S., and Halverson, L. (2004). Differential tolerance of *Pseudomonas putida* biofilm and planktonic cells to desiccation. *Biofilms* 1, 361–368. doi: 10.1017/S1479050504001528

Vilchez, S., and Manzanera, M. (2011). Biotechnological uses of desiccation-tolerant microorganisms for the rhizoremediation of soils subjected to seasonal drought. *Appl. Microbiol. Biotechnol.* 91, 1297–1304. doi: 10.1007/s00253-011-3461-6

Vurukonda, S., Vardharajula, S., Shrivastava, M., and Skz, A. (2016). Multifunctional *Pseudomonas putida* strain FBKV2 from arid rhizosphere soil and its growth promotional effects on maize under drought stress. *Rhizosphere* 1, 4–13. doi: 10.1016/j.rhisph.2016.07.005

Wiesmeier, M., Urbanski, L., Hobley, E., Lang, B., Von Lützow, M., Marin-Spiotta, E., et al. (2019). Soil organic carbon storage as a key function of soils-A review of drivers and indicators at various scales. *Geoderma* 333, 149–162. doi: 10.1016/j.geoderma.2018.07.026

Xu, Z. Z., and Zhou, G. S. (2006). Combined effects of water stress and high temperature on photosynthesis, nitrogen metabolism and lipid peroxidation of a perennial grass *Leymus chinensis*. *Planta* 224, 1080–1090. doi: 10.1007/s00425-006-0281-5

Zieslin, N., and Ben-Zaken, R. (1993). Peroxidase activity and presence of phenolic substances in peduncle of rose flower. *Plant Physiol. Biochem.* 31, 333–339.

frontiers | Frontiers in Microbiology

TYPE Original Research
PUBLISHED 16 February 2023
DOI 10.3389/fmicb.2022.1024005

Check for updates

OPEN ACCESS

EDITED BY
Durgesh K. Jaiswal,
Savitribai Phule Pune University,
India

REVIEWED BY
Lei Wang,
University of Nebraska-Lincoln,
United States
Zhengliang Qi,
Qilu University of Technology, China

*CORRESPONDENCE
Juan Zhang
✉ zhangj@jiangnan.edu.cn
Guocheng Du
✉ gcdu@jiangnan.edu.cn

SPECIALTY SECTION
This article was submitted to Microbiotechnology, a section of the journal Frontiers in Microbiology

RECEIVED 20 August 2022
ACCEPTED 16 December 2022
PUBLISHED 16 February 2023

CITATION
Wu X, Cai W, Zhu P, Peng Z, Zheng T, Li D, Li J, Zhou G, Zhang J and Du G (2023) Function-driven design of *Bacillus kochii* and *Filobasidium magnum* co-culture to improve quality of flue-cured tobacco. *Front. Microbiol.* 13:1024005. doi: 10.3389/fmicb.2022.1024005

COPYRIGHT
© 2023 Wu, Cai, Zhu, Peng, Zheng, Li, Li, Zhou, Zhang and Du. This is an open-access article distributed under the terms of the Creative Commons Attribution License (CC BY). The use, distribution or reproduction in other forums is permitted, provided the original author(s) and the copyright owner(s) are credited and that the original publication in this journal is cited, in accordance with accepted academic practice. No use, distribution or reproduction is permitted which does not comply with these terms.

Function-driven design of *Bacillus kochii* and *Filobasidium magnum* co-culture to improve quality of flue-cured tobacco

Xinying Wu[1,2,3], Wen Cai[4], Pengcheng Zhu[1,4], Zheng Peng[1,2], Tianfei Zheng[1,2], Dongliang Li[4], Jianghua Li[1,2], Guanyu Zhou[1,2], Juan Zhang[1,2]* and Guocheng Du[1,5]*

[1]School of Biotechnology, Jiangnan University, Wuxi, China, [2]Science Center for Future Foods, Jiangnan University, Wuxi, China, [3]School of Liquor and Food Engineering, Guizhou University, Guiyang, China, [4]Technical Research Center, China Tobacco Sichuan Industrial Co., Ltd., Chengdu, China, [5]The Key Laboratory of Carbohydrate Chemistry and Biotechnology, Ministry of Education, Jiangnan University, Wuxi, China

Flue-cured tobacco (FCT) is an economical raw material whose quality affects the quality and cost of the derived product. However, the time-consuming and inefficient spontaneous aging is the primary process for improving the FCT quality in the industry. In this study, a function-driven co-culture with functional microorganisms was built in response to the quality-driven need for less irritation and more aroma in FCT. The previous study has found that *Bacillus kochii* SC could degrade starch and protein to reduce tobacco irritation and off-flavors. The *Filobasidium magnum* F7 with high lipoxygenase activity was screened out for degrading higher fatty acid esters and terpenoids to promote the aroma and flavor of FCT. Co-cultivation with strain SC and F7 obtained better quality improvement than mono-culture at an initial inoculation ratio of 1:3 for 2 days, representing a significant breakthrough in efficiency and a reduction in production costs compared to the more than 2 years required for the spontaneous aging process. Through the analysis of microbial diversity, predicted flora functions, enzyme activities and volatile compositions within the mono- and co-cultivation, our study showed the formation of a function-driven co-culture between two strains through functional division of labor and nutritional feeding. Herein, the function-driven co-culture via bioaugmentation will become an increasingly implemented approach for the tobacco industry.

KEYWORDS

co-culture, bioaugmentation, *Bacillus kochii*, *Filobasidium magnum*, function-driven design, flue-cured tobacco

Introduction

Microbial groups have diverse metabolic capabilities and play an active role in various natural processes. Various functional strains have been screened for application in different industries *via* mono-culture (De Melo Pereira et al., 2020). Recently, co-cultivation has attracted attention because it has the potential to achieve higher biomass, create higher-quality products (Charubin and Papoutsakis, 2019; Shahab et al., 2020), and aid in the biotransformation of harmful substances (Hernández-Adame et al., 2021; Ke et al., 2021), even for multiple demands (Canon et al., 2020). However, the stability of co-cultivation remains the biggest challenge of this methodology. Therefore,

developing the appropriate strategies to enhance collaborative relationships between strains is necessary.

Tobacco (*Nicotiana tabacum L.*) is a global economic crop usually made into flue-cured tobacco (FCT). Due to the differences in climate and plant-related soil and agronomic practices in different regions and environments, not all tobacco can be made into high-quality raw materials. Hence, FCT must be stored in an aging warehouse for spontaneous aging under natural conditions. The aging process is essential for improving the quality of FCT in tobacco industry production. During the two-year aging process, the macromolecular components of FCT are degraded or converted into aroma-causing compounds through the synergistic action of microorganisms, enzymes, and chemical oxidation. Nevertheless, some FCT does not still meet product demands after this process due to the low efficiency of spontaneous aging, which becomes the FCT with quality defects to reduce the utilization and increase the cost of raw materials in the enterprise. Consequently, finding an effective method to improve the quality of defective FCT is necessary. Artificial aging using functional strains has recently received increasing attention (Su et al., 2011). In industrial production, the noted quality deficiencies of FCT are primarily irritation, off-flavor, and lack of aroma. Excessive starch in FCT can cause irritation (Han et al., 2010; Wang et al., 2021). The high protein and total nitrogen content are negatively correlated with the off-flavor and irritation of FCT (Cao et al., 2020; Shen et al., 2022). So, the degradation of starch and protein in FCT helps to improve the quality of the final product, in which the formed reducing sugars and amino acids contribute to the aftertaste and sweetness of the product (Feizi et al., 2020). The high fatty acid (HFA) esters (such as linolenic acid, linoleic acid, and palmitic acid esters) could lead to irritation and astringency, and the modest degradation of HFA esters increases the concentration and softness of the smoking gas (Swain and Stedman, 1962; Yang et al., 2018). Terpenoids are important aroma precursors in FCT, as in many plants. Specifically, carotenoids are major terpenoids in FCT that are degraded into various flavors and aromas, such as safranal, beta-damascone, beta-cyclocitral, and megastigmatrienones so on (Leffingwell, 1999).

However, it is usually difficult for a single strain to meet the multiple requirements for quality improvement in FCT simultaneously. Therefore, we established a co-culture to enhance fragrance while reducing irritation using complementary functional strategies. We obtained *Bacillus kochii* strain SC from the tobacco microflora (accession number MZ198211) derived from previous studies (Wu et al., 2021). Strain SC has an excellent ability to secrete neutral protease and alpha-amylase. Although the *B. kochii* SC bioaugmentation enhanced the softness and decreased the irritation of FCT, the aroma still needed to be improved based on the evaluation panel feedback (Wu et al., 2021). Therefore, screening for strains enabling excellent aroma production capacity to compensate for the lack of aroma in FCT is of substantial importance. It has been confirmed that the oxidative degradation of carotenoids in plants involves dioxygenases and that lipoxygenase (LOX, EC 1.13.11.12) plays a significant role in this process (Lyu et al., 2021). LOX is also regarded as a critical enzyme in fatty acid metabolism, one of the main pathways for synthesizing aromas or flavors in fruits (Li et al., 2021). Therefore, it is expected that the screened strains with high LOX incorporated with *B. kochii* SC to produce good quality-enhancing effects.

Because FCT cannot be sterilized with conventional sterilization methods and processed in an open environment, the pure cultivation of functional strains is impossible. So bioaugmentation makes much practical sense in tobacco fermentation. Bioaugmentation aims to inoculate functional microorganisms into the natural biological system in order to enhance the effects of the mixed microbial system (Atasoy and Cetecioglu, 2020). Bioaugmentation has also been applied to improve the quality and yield of traditional foods (Chai et al., 2020; Viesser Jéssica et al., 2020). Herein, we demonstrated a method for the quality improvement of raw materials using bioaugmentation with co-culture.

In the present study, strain F7 with high production of LOX was screened from the tobacco microflora and identified as *Filobasidium magnum*. *F. magnum* is commonly found in the natural environment (Ken et al., 2013; Zhu et al., 2021) and is closely related to fruit flavor formation as the dominant endophyte of fruits (Sayed et al., 2021). *F. magnum* F7 were co-cultured with *B. kochii* SC with the functionally complementary and evaluated with their impact on FCT quality under an optimized mix rate and fermenting time. The potential motivation for improving quality by co-culture was presented by profiling the microbial diversity, functional enzyme activities, and volatile components.

Materials and methods

Screening and identification of functional strains

Screening

The screening protocol for the evaluated functional strains is visualized in Figure 1, including the collection of tobacco microbe mixture, the initial screening of strains, and the re-screening of LOX-secreting strains.

Collection of tobacco microbe mixture: the mixture of tobacco microbes was collected following the previous method (Wu et al., 2021). In brief, a 10 ± 0.1 g of FCT sample was transferred into 200 ml sterilized PBS (phosphate buffer solution; 0.1 mol/l, pH 7.2) and then shocked, sonicated and filtered. The filtrate was centrifuged at 7,000 × g for 10 min. The resulting deposit was resuspended with sterile PBS and then stained with 7-AAD (BD Pharmingen, New Jersey, United States) for 20 min. The multi-strain suspension was filtered through a 40 μm filter and diluted to biomass at an absorbance of 0.3 (optical density: OD600). According to the method described in the previous study (Wu et al., 2021), 1 ml of suspension was transferred into the sample tank of the flow cytometer (FACSARia III cell sorter of BD Biosciences, United States), and single cells were sorted into 96-well plate for culture.

Initial screening of strains: after cultivation, strains formed [colonies in Luria-Bertani (LB) Agar or Bengal Red (BR) Agar]. The strains were then enriched into 96 deep well plates filled with LB broth at 37°C, 400 rpm for 24–72 h, or BR broth at 30°C, 400 rpm for 72–120 h. The addition of FCT extract to the LB and BR media resulted in a yellow–brown color and a strong absorbance of 460 nm measured by spectrophotometry. FCT extract was prepared by reference to Zorn's method (Zorn et al., 2003). In brief, 20 g of tobacco powder was extracted with a co-solvent of Tween 80 and dichloromethane, and then the solvent was filtered and evaporated off at 40°C and 25 kPa. The residue was re-dissolved in 10 ml of water and sterile-filtered (0.45 μm, Millipore). At last, FCT extract was uniformly dispersed into a sterile medium. After proliferation, the strains with lighter colored medium

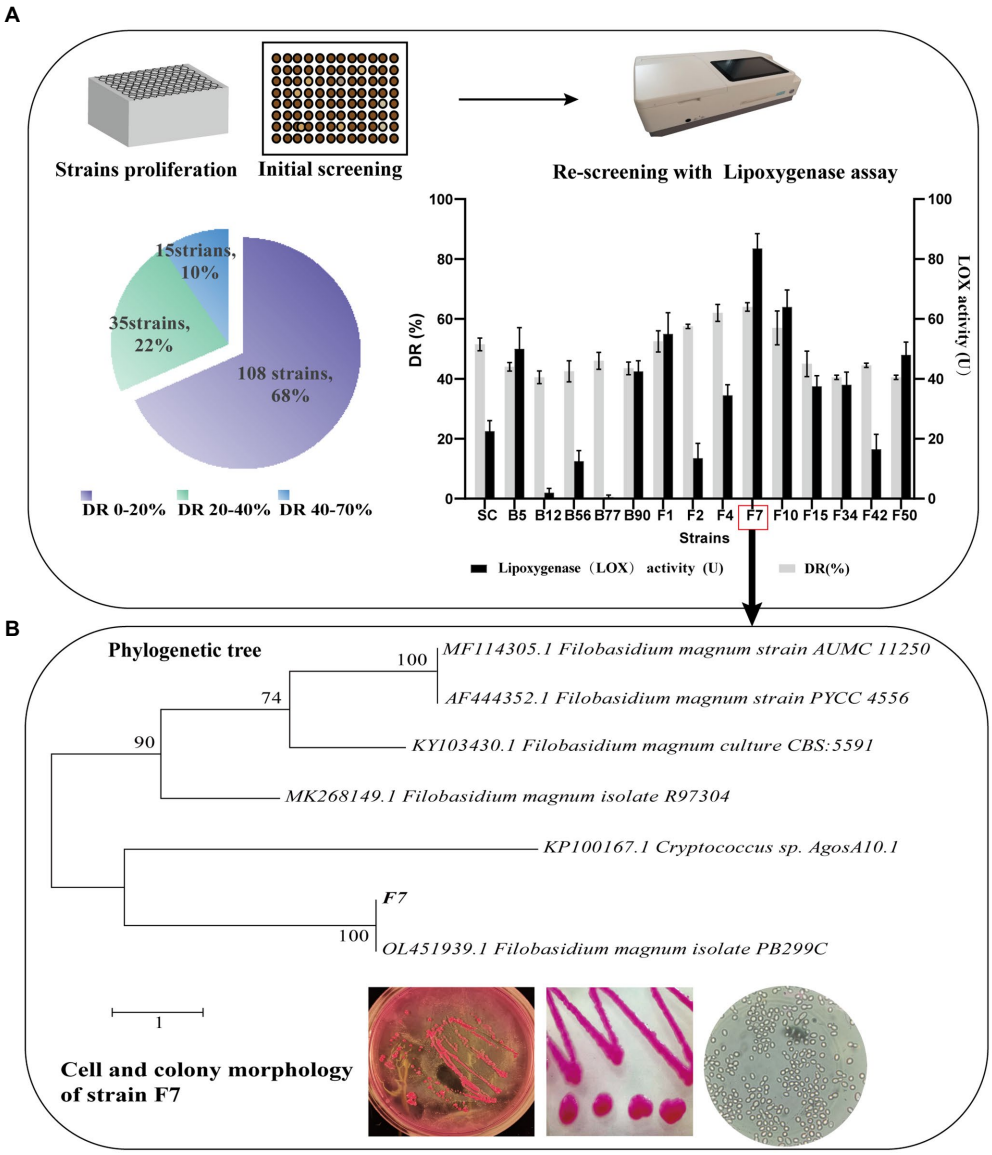

FIGURE 1
Screening **(A)** and identification **(B)** of functional microorganisms.

would be initially screened into a new deep well plate for re-culture regarding their potential to enhance FCT aroma.

Re-screening of LOX-secreting strains: the functional strains were re-screened using a LOX activity assay. LOX activity assay method referred to Lyu's method (2021). Eighty microliter of crude enzyme supernatant reacted with 920 µl substrate, which was mixed with 10 µl linoleic acid, 5 µl Tween 20, 1 ml NaOH (sodium hydroxide, 0.10 mol/l) and 4 ml PBS (0.20 mol/l, pH 6.5), diluted to 29 ml. The absorbance was kinetically determined at 234 nm. One unit of LOX activity (U) was defined as a change in absorbance of 0.1 per mL of suspension per min. The strain with the highest LOX activity was isolated from the pure culture.

Functional strain identification

After morphological and colony identification of the strain with the highest LOX activity, taxonomic identification was carried out. Fungi colony identification was performed using the internal transcribed spacer region (ITS) sequencing. Genomic DNA was extracted with a Fungi Genomic DNA Extraction Kit (Solarbio Science & Technology Co. Ltd. Beijing, China). The following primers were used for ITS1-5.8S rRNA-ITS2 region amplification: ITS1 (5′-TCCGTAGGTGAACC TGCGG-3′) and ITS4 (5′-TCCTCCGCTTATTGATATGC-3′). PCR was performed following Ni's method (2021) (Rocío et al., 2020), and PCR products were sequenced by Sangon Biotech Co., Ltd. (Shanghai, China). The sequencing data were blasted against NCBI (U.S. National Center for Biotechnology Information) database. The phylogenetic tree of the evaluated strain was mapped in MEGA software (molecular evolutionary genetics analysis, version 7.0.26[1]) using maximum parsimony analysis. The identified functional strain was named strain F7.

1 https://www.megasoftware.net

Bioaugmentation of functional strains

In the present study, the FCT with quality defects was used as an object of bioaugmentation and collected from China Tobacco Si Chuan Industrial Co Ltd. (Chengdu County, Sichuan Province, China). This FCT underwent spontaneous aging for 2 years in a factory setting. However, the quality of the FCT still failed to meet production requirements due to high irritation, heavy impurities, and a lack of aroma. The defective FCT evaluated herein was Yunyan 87, among the main varieties of light-flavor FCT widely planted in China. Before bioaugmentation with functional strains, FCT was pre-treated by slicing them into picadura. The bioaugmentation with functional strains was prepared as follows. Single colonies of strain SC or F7 grown on LB/BR agar plates were inoculated into 5 ml broth for further growth. When the growth reached 7–8 log CFU (colony forming units)/mL, the colony's suspension was mixed thoroughly with FCT at 20% inoculum. Under 85% relative humidity, mono-culture with strain SC and F7 were incubated at 37°C and 30°C, respectively, and co-culture was incubated at 30°C. The culture is stirred once every 4 h. After bioaugmentation, FCT samples were ground into powder in liquid nitrogen and were stored at -80°C for further analysis. Meanwhile, the control group was treated with equal amounts of sterile water. The culture time and proportions of two strains in co-culture were optimized according to the quality evaluation of FCT.

FCT quality evaluation

We strictly followed the FCT quality evaluation standards delineated within China's tobacco industry (YC/T138-1998, YC/T496-2014) and national standards (GB/T102212012, GB/T12310-2012). The different tests and descriptive tests are the standards' primary sensory evaluation methods. Panelists with excellent individual qualifications included two females and five males. The quality evaluations were conducted on a nine-point quality scale. Quality scores lower than four points are considered unacceptable quality, and a score of five to seven is acceptable; when the score is seven or higher, the sample quality matches the superior quality. There were eight evaluation indicators: aromatic intensity, aromatic quantity, pleasant odor, smoke intensity, smoke quantity, softness, sweetness, and aftertaste. The total score of quality evaluation was the sum of all indicators.

Profiling of microbial diversity

DNA extraction and PCR amplification

Referring to Su's study (2011) with some modifications, 10 ± 0.1 g of sample was added into 200 ml sterilized PBS (0.1 mol/l, pH 7.2) and shaken at 220 r/min, 30°C for 2 h, then sonicated for 5 min and filtered by the sterile absorbent gauze. The filtrate was first centrifuged at 500 × g for 10 min to remove FCT fragments, then repeated the above experimental steps two to three times. The microbial sediment was collected by centrifugation at 10,000 × *g* for 10 min. Then the sediment was resuspended by sterile deionized water. One milliliter of suspension was used to extract the metagenomic DNA from the FCT microflora using the DNeasy PowerSoil Kit.

The metagenomic DNA was used as the template for gene amplification. The V4-V5 region of the bacteria 16S rRNA gene was amplified with barcoded universal primers (515F: 5′-GTGCCAGCMGCCGCGGTAA-3′; 907R: 5′-CCGTCAATTCMTTTRAG TTT-3′). ITS sequencing of the fungal rRNA gene was amplified with the primer (ITS1F: 5′-CTTGGTCATTTAGAGGAAGTAA-3′; ITS2: 5′-GCTGCGTTCTTCATCGATGC-3′). PCR program was set to 98°C for 2 min, 30 cycles of 98°C for 15 s, 55°C for 30 s, 72°C for 30 s, and finally, an extension at 72°C for 5 min. After purification and recovery using magnetic beads, the amplicons were subjected to biological analysis.

Bacterial and fungal diversity analysis

Equal amounts of the amplicons were measured with paired-end 2 × 250 bp (base pair) sequencing on the Illlumina MiSeq platform (Illumina, San Diego, CA, United States). Bioinformatic analysis was performed on the raw sequence data2 using QIIME2 software (2019.4[2]; Bokulich et al., 2018). The non-singleton amplicon sequence variant (ASV) taxonomy of the 16S rRNA genes was blasted against the Silva database,[3] and the ASVs of ITS genes were blasted against the UNITE database.[4] The sequencing data have been submitted to NCBI (accession numbers: PRJNA762207 for bacterial sequences and PRJNA764574 for fungal sequences). The data randomly extracted from sequences in each sample were flattened to reach a uniform depth for analyzing the relative abundances of ASVs.

Microflora function prediction

The PICRUSt2 (Phylogenetic Investigation of Communities by Reconstruction of Unobserved States) software package was used to predict the potential genetic functions based on the 16S rRNA or ITS sequence. The MetaCyc database[5] was used to predict the primary and secondary metabolic pathways (Dayalan et al., 2019).

Analysis of starch content

The sample powder was prepared with a grinder (TL-48R, Jingxin, Shanghai, China) at 60 Hz for 90 s. Starch contents in samples were determined using a continuous flow analyzer (Wang et al., 2021). Briefly, 0.2 ± 0.01 g of FCT powder was added to 25 ml of 80% ethanol-sodium chloride saturated solution (at a volume ratio of 3:1) and was ultrasonically treated for 25 min and then centrifuged at 8,000 × *g* for 10 min to remove the pigment. Starch was extracted by adding 15 ml of 40% perchloric acid to the sediment and sonicating it for 15 min. The filtrate was collected after adding another 15 ml of deionized water. The starch in the filtrate was analyzed colorimetrically at 570 nm by reaction with iodine using a Bruker FT-NIR spectrometer (Flyer MATRIX-F, Bruker, Germany) under acidic conditions based on the industry standard (YC/T 216–2013).

Analysis of enzymatic activity

2.5 ± 0.1 g of sample powder was added into 30 ml sterilized PBS (0.2 mol/l, pH 6.5) and was shocked at 220 r/min, 30°C for 1 h. The supernatant was collected by centrifuging (10,000 × *g*) at 4°C for

2 https://qiime2.org
3 https://www.arb-silva.de/
4 https://unite.ut.ee/
5 https://metacyc.org/

10 min. The LOX activity was assayed according to the above method. Neutral protease activity was determined by the Folin color method (Li et al., 2017). One unit of neutral protease activity was defined as 1 μg tyrosine produced from casein per hour at 40°C, pH 7.0. The alpha-amylase activity was determined by DNS (Suraiya et al., 2018). One unit of alpha-amylase activity was defined as 1 mg of reducing sugar produced from soluble starch per minute at 60°C and pH 6.0. Enzyme activity is expressed as activity units per gram of dried sample powder (DW).

Profiling of volatile compositions

FCT volatiles was profiled using untargeted metabolomics based on HP-SPME-GC-TOF-MS (gas chromatography time-of-flight mass spectrometry with headspace solid-phase micro-extraction). A 2.00 ± 0.01 g FCT powder was placed in the 20 ml headspace bottle with 1 μl internal standard (1 μg/ml tritiated naphthalene dissolved in dichloromethane, Supelco, Aladdin). Volatiles were extracted by SPME fiber assembled with DVB/CAR/PDC (divinylbenzene/carboxyl/polydimethylsiloxane, 50/30 μm) at 60°C for 30 min.

The volatile components of samples were detected with a GC-TOP-MS system (Pegasus BT; LECO, St. Joseph, Michigan, United States) coupled with Agilent 7890A GC and Agilent DB-5MS column (30 m × 250 μm × 0.25 μm, J&W Scientific, Folsom, CA, United States). The chromatographic conditions c the column flow was 1 ml/min; the inlet temperature was 250°C; the heating temperature was maintained at 40°C for 2 min and then increased to 250°C at a rate of 10°C/min for 6 min; the ion source adopted the electron bombardment model, the electron energy was 70 eV; the transmission line and ion source temperature were 280°C and 210°C, respectively; the mass spectrometry data were retrieved in full-scan mode (range, 33–400 atomic mass units at a rate of 3 specs/s), and the data acquisition rate was 10 specs/s.

The raw peaks extraction, data baseline filtering, and calibration, alignment, deconvolution analysis, peak identification, and integration were executed with the support of Chroma TOF 4.3X software (LECO Corp., St. Joseph, MI, United States) and the LECO-Fiehn Rtx5 database (Li et al., 2020). The compositions matched NIST (U.S. National Institute of Standards and Technology) and Wiley library[6]) databases regarding retention indices and mass spectra. Identified compounds with matching scores of over 700 were further analyzed. Peaks detected in <50.0% of samples or RSDs (relative standard deviations) of peak areas >30.0% were removed. Using MetaboAnalyst5.0 software,[7] a PLS-DA (partial least squares-discriminant analysis) model of samples was constructed to identify differential compounds according to VIP (Variable importance of projection) values of >1 and *p*-values of <0.05.

Statistical analysis

Data were displayed as mean ± standard deviation. The volatile components were analyzed using six replicate samples, and other results were performed at three parallels. Bar charts and sample variances were depicted using GraphPad Prism 6 software (GraphPad, San Diego, CA, United States).

Results

Construction of co-cultivation

With the goal of co-cultivation with *B. kochii* SC to comprehensively improve the quality of FCT, we screened functional microorganisms with high LOX activity from the FCT microflora. Following the screening protocol (Figure 1), 158 well-grown strains were obtained from colonies grown in 96 shallow-well plates. In the initial screening, the decolorization of the medium by the strains was compared with uninoculated samples. The percentage of color reduction was defined as the decolorization rate (DR). Fifteen strains achieved a high DR of 40–70%. Strain F7 had the highest DR and LOX activities of 64 ± 5.6% and 83.5 ± 2.2 U/ml, respectively. As a result, strain F7 was selected as a study subject.

The phylogenetic tree of strain F7 and microscopic imaging under the magnification of 100 × 1.25 are shown in Figure 1. The cells of strain F7 were spherical or ovoid, and some cells showed asexual reproduction with monopolar budding, which was the distinctive feature judged as yeast. The colonies of strain F7 were characterized by smooth, convex, rounded edges, moist, sticky, and easy to pick up. Strain F7 colonies were milky white when grown on malt extract agar. When strain F7 was cultured in RB, the colonies appeared purplish red, due to the entry of medium pigments into the cells. The phylogenetic tree was constructed by the neighbor-joining method with the bootstrap values at the edge of each node. The blast analysis of ITS1 gene domain sequences of strain F7 reveals a closer related *F. magnum*. Therefore, strain F7 is identified as a strain of *F. magnum*, and the sequence has been submitted to the GenBank database (NCBI; accession number, MZ351194).

Effects of bioaugmentation on quality attributes

We dynamically studied the changes in quality attributes of mono and co-cultivation with different fermentation times. Following the quality evaluation criteria of FCT, difference and descriptive tests with negative controls were performed in our study to highlight the quality-enhancing effect of bioaugmentation with functional strains on FCT with quality defects. Mono-culture SC and F7 fermentation for 2.5 days and 2 days, respectively, obtained the highest quality evaluation scores, as shown in Figures 2A,B, with statistically significant differences between the bioaugmentation and control samples ($p < 0.001$, two-tailed). The quality evaluation score was the highest when SC and F7 were co-cultivated for 2 days at the initial inoculation ratio of 1:3 (Figure 2C). There was also a statistically significant quality enhancement in co-culture compared to the control and mono-culture samples ($p < 0.001$, two-tailed). According to Figure 2D, bioaugmentation with SC favored softness and pleasant odor, while mono-culture of F7 contributed to aroma intensity and aroma quality. Based on functional complementarity, co-cultivation obtained comprehensive quality improvements, obviously enhancing aroma-related attributes, softness and pleasant odor, simultaneously increasing the sweetness and aftertaste of the FCT. The control group had a score of <5 for each evaluation attribute, while the test group using co-culture scored over 5.

6 https://onlinelibrary.wiley.com
7 https://metaboanalyst.ca

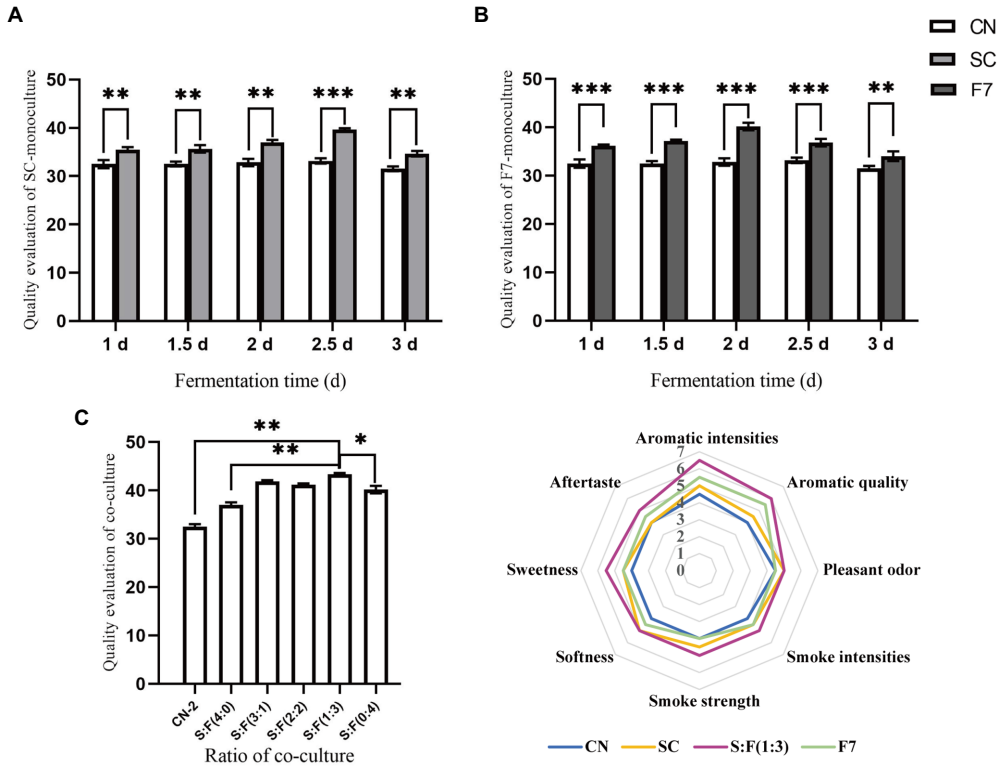

FIGURE 2
Dynamic analysis of FCT quality response to *Bacillus kochii* SC mono-culture **(A)**, *Filobasidium magnum* F7 mono-culture **(B)**, co-cultivation at different mixing ratios **(C)**, and sub-quality indicators evaluation of co-cultivation **(D)**. CN represents the control group. SC represents *B. kochii* SC mono-culture samples. F7 represents *F. magnum* F7 mono-culture samples. S:F represents the sample of *B. kochii* SC-*F. magnum* F7 co-culture. Error bars represent the standard deviation of the samples (triplicate). *p* value represents by an asterisk "*" (*: $0.01<p\leq0.05$; **: $0.001<p\leq0.01$, ***: $p\leq0.001$; ns: no significant difference).

The aroma intensity and aroma quality increased significantly, reaching over 6 points.

Motivation related to quality improvement

The intervention of functional strains altered the diversity of natural consortia on tobacco and the activity of secreted enzymes and additionally affected the chemical composition of FCT through metabolism and/or catalysis.

Changes in microbial diversity

This study applied microbial assembly from different phylogenetic groups to bioaugmentation. A total of 413,098 16S rRNA and 384,294 ITS1-5.8S rRNA-ITS2 high-quality sequences were obtained individually from 12 samples. Each deduplicated sequence was defined as ASVs. After data was flattened using a rarefaction method, the relative abundance of ASVs was observed at the same sequencing depth (18,232 bacterial and 5,443 fungal ASVs per sample) (Supplementary Tables 1, 2). The microbial diversity of the controls differed statistically significantly from that observed within bio-inoculation samples (Figures 3A,B). Based on the alpha-diversity analysis of bacterial and fungal communities (Supplementary Tables 3, 4), Goods-coverage indices are higher than 99%, which suggests the sequencing results with high coverage in a gene library of samples. Observed species and Chao1 indices can characterize data richness, whereas Shannon and Simpson indices indicate the diversity and evenness of a sample (Su et al., 2020). Consequently, the bio-inoculation samples had less complex diversity and lower richness than the control group ($p<0.05$) due to the intervention of functional microorganisms.

Regarding the relative abundance of functional strains, there was no statistically significant difference in bacterial flora between the bio-inoculated samples. In contrast, there was a significant difference in fungal flora between mono-culture with strain F7 and co-culture with strain F7 and SC, which should be due to the intervention of strain SC in the co-culture. According to the findings presented in Figures 3A,B, 18 bacterial genera and 14 fungal genera had a relative abundance greater than 1% in the control group spontaneously fermented at 85% relative humidity and 30°C for 2 days. However, there was less complex diversity in bio-inoculation samples. The relative abundance of *B. kochii* SC was close to 100% because of its outstanding growth properties. The relative abundance of strain F7 was elevated from 2% (control group) to 90.73% (co-cultivation). Strain F7 developed more readily in co-culture (90.73%) than in monoculture (64.68%), suggesting that strain SC was a good promoter of strain F7. Consequently, additional research is needed to verify how strain SC promoted the growth of strain F7. In bioaugmentation, functional strains dominate, contributing to serving the purpose of bioaugmentation (Viesser Jéssica et al., 2020).

PICRUSt2 software was used to predict the functional abundance of consortia according to the marker gene sequences. According to

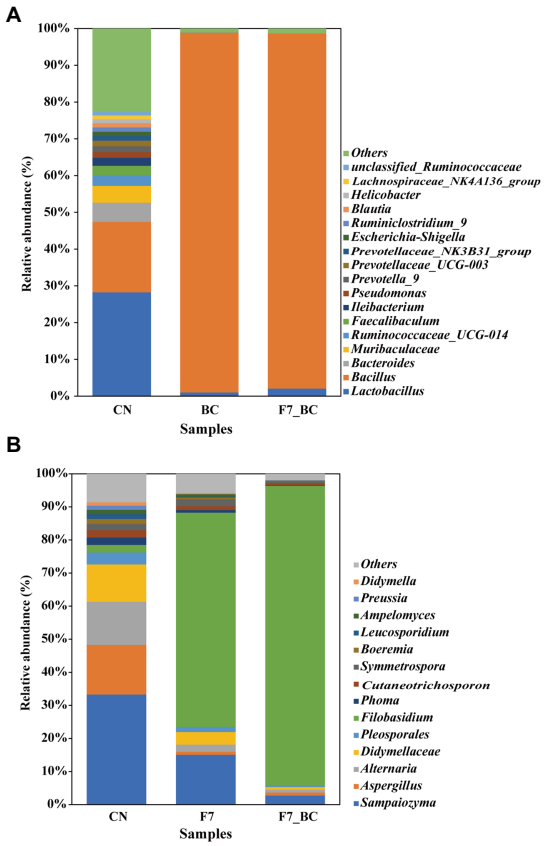

FIGURE 3
Analysis of bacterial **(A)** and fungal **(B)** diversity.

Caspi R's study (2008), the prediction of MetaCyc metabolic pathways approached the reliability of macroeconomic analysis (Caspi et al., 2008). Biosynthesis and degradation/ utilization/ assimilation metabolism pathways had a higher relative abundance than the others as shown in Supplementary Figure 1. Pathways associated with microbial growth, including carbohydrate degradation, glycolysis, and amino acid synthesis, have a fairly high relative abundance in bacterial communities. The pathways associated with flavor formation, including secondary metabolite degradation in bacterial flora and fatty acid/lipid degradation in fungal flora, showed a higher abundance. Analyzing important differential metabolic pathways with genera composition in Figures 4A,B, *Bacillus* showed a high abundance of amino acid synthesis pathways, consistent with its high protease activity phenotype, and *Filobasidium* could promote the oxidative pathway by secreting a highly active LOX. Unsaturated, saturated C6 and C9 volatile aldehydes/alcohols are generated through the LOX pathway, essential flavor contributors to fruits, vegetables, and herbs (Wilfried et al., 2008).

Dynamic changes in functional enzyme activity

As shown in Figure 5, the enzymatic activity of neutral protease, alpha-amylase, LOX behaved differently in mono-culture and co-cultivation. All samples showed the highest activities of enzymes when fermented for 2 days, with low enzyme activities found in the control group. Our study found high neutral protease and alpha-amylase activity in strain SC mono-culture and co-culture. However, there was no statistical difference between the control and the mono-culture with strain F7 (Figures 5A,B). It could be assumed that strain F7 did not secrete neutral protease and α-amylase. Collaboration of microbial communities may lead to higher α-amylase activity in co-culture than in mono-culture, but additional research is needed. LOX activity could be detected in all samples, but the activity in the mono-, co-culture with strain F7 was higher than in other samples (Figure 5C). Strain F7 was able to secrete LOX, consistent with the predicted results of colony function (Figure 4B). In Figure 5D, starch degradation was higher in the mono-, co-culture with strain SC, while there was no statistically significant change in the mono-culture with strain F7. The overall high enzyme activity in co-cultivation should result from the mutual promotion between the two strains, which may be why co-cultivation can result in substantial quality improvement.

Changes in flavor-associated volatile composition

The flavor-associated volatile compositions have an essential impact on the quality of FCT (Yin et al., 2016). As the main conclusion of our manuscript titled "Profiling the role of microorganisms in quality improvement of the aged flue-cured tobacco" (Submitted for publication), HFA/lipid metabolism, terpenoid degradation, and the formation of Maillard reaction products are the key metabolic pathways involved in the quality improvement of FCT during spontaneous aging. 191 volatiles volatiles were detected using the untargeted metabolomes based on HP-SPME-GC/MS. There were 54 carbonyl compounds, 37 alkanes and alkenes, 35 heterocyclic compounds, 28 esters, 15 aromatic hydrocarbons, 15 alcohols and phenols and 10 acids (Supplementary Table 5). Samples can be distinguished within 95% confidence intervals using unsupervised PCA (principal components analysis) (Figure 6A). In the present evaluation, two principal components contribute 50.9% of the total variance. There is an excellent distinction between the control and bioaugmented groups. In addition, we constructed supervised PLS-DA models. Cross-validation showed that these models had good predictive without over-fitting (R2Y and Q2 were close to 1, as shown in Figure 6B). Given the criteria of VIP values of >1.0 and p-values of <0.05, 64 differential metabolites were identified, including 17 compounds related to terpene metabolism, 13 compounds related to fatty acid and lipid metabolism and 13 compounds related to Maillard reaction (Supplementary Table 6).

The heat maps of some differential metabolites are shown in Figure 7. In fatty acid and lipid metabolism, *Filobasidium* showed a high capacity for fatty acid oxidation that promoted the degradation of HFA esters. HFA esters include pentadecanoic acid methyl ester, hexadecanoic acid methyl ester and 9,12,15-octadecatrienoic acid methyl ester and so on. Meanwhile, simple esters have the highest content in the bioaugmentation with strain F7_SC and F7, in which 2-phenylethyl acetate had the highest content in co-culture; Most products related to Maillard reaction were at their highest level in bioaugmentation with SC. Terpenoid metabolism products are essential flavors in tobacco, especially the degradation products of carotenoids and cembrene (Ni et al., 2021). However, strain SC and strain F7 both showed the capacity to promote the degradation of aromatic precursors and the accumulation of aromas in terpenoid metabolism. While F7 demonstrated a better capacity than SC in the present study.

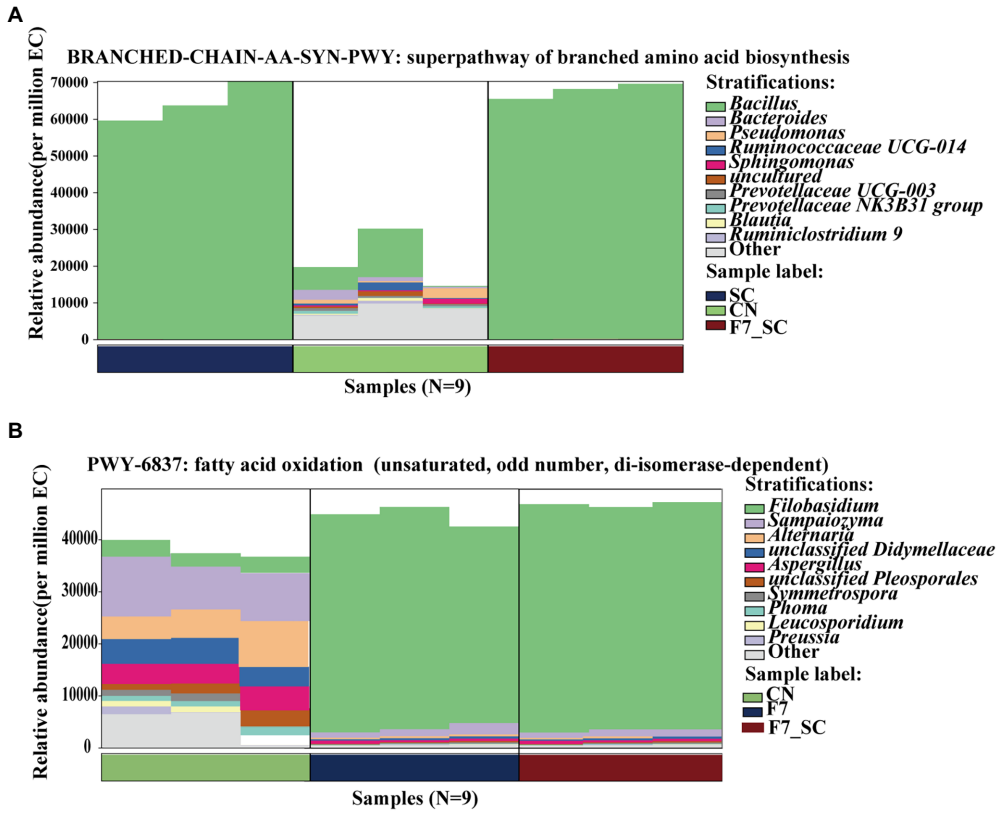

FIGURE 4
Maps of the genera composition in the differential MetaCyc metabolic pathway of bacterial **(A)** and fungal **(B)** consortia. CN represents the control group. SC represents *B. kochii* SC mono-culture. F7 represents *F. magnum* F7 mono-culture. F7-SC represents *F. magnum* F7-*B. kochii* SC co-culture.

Discussions

In our study, flow cytometry is a powerful method for screening and isolating single cells through high-throughput equipment compared to traditional plate isolation methods (Vitelli et al., 2021). *Via* flow cytometry, the obtained library of tobacco microbes can provide a screening source for functional microbial. The purpose of the initial screening was to obtain microorganisms that could lighten the color of the medium added FCT extract. Pigment in the FCT extract consists of polyphenols, carotenoids, and rutinosides. These compounds are essential precursors of flavor and aroma (Maldonado-Robledo et al., 2003) and transformed or degraded by the action of enzymes or microorganisms. Which leads to a color change in the medium. Thus, the initially screened strains were considered to have the potential to enhance FCT aroma. Based on the ability of the strain to secrete LOX and the effect on FCT flavor, *F. magnum* strain F7 was re-screened. *F. magnum* is one of the dominant genera of fungi in microbial communities of FCT through diversity analysis described in our previous study (Wu et al., 2021). *F. magnum* was also found in the Lhalu Wetland and the rhizosphere soil of the Hami melon orchards in Xinjiang, China (Guo et al., 2018; Zhu et al., 2021). *F. magnum* has also been isolated from the larval midgut of stag beetle, which could degrade biodegradable plastic films (Ken et al., 2013). It was likewise found as an endophytic fungus in the vineyard environment and was closely associated with the formation of grape flavor (Sayed et al., 2021). Unfortunately, we could not conclude whether strain F7 was a tobacco endophyte. With our limited knowledge, a lipoxygenase-producing *Filobasidium* was first screened from FCT *in situ* to promote aroma.

The evaluated test object was FCT with quality defects that had not yet met quality demands. The highest quality score was obtained in bioaugmentation with strain SC and F7 co-cultured for 2 days at the initial inoculation ratio of 1:3. Consequently, the FCT with quality defects (control group) was upgraded from unacceptable quality to acceptable quality to become the qualified raw materials (test group). It was a noticeable and significant improvement in quality for the evaluated FCT. The apparent effect of co-culture on FCT quality implied a synergistic relationship between the two strains and the native consortia. Similarly, Chai et al. (2020) enhanced acetoin accumulation in vinegar fermentation through bioaugmentation of *Lactobacillus casei* and *Acetobacter pasteurianus*, with an initial ratio of 1:1. Canon et al. (2020) developed co-cultures of functionally complementary lactic acid bacteria to ferment a new food with target flavor attributes. It shows that assembling different functional strains through co-culture can achieve better results than those obtained through mono-culture. Good quality improvement was achieved in only 2 days with the co-culture bioaugmentation method. This represents a significant breakthrough in efficiency and a reduction in production costs compared to the more than 2 years required for the spontaneous aging process.

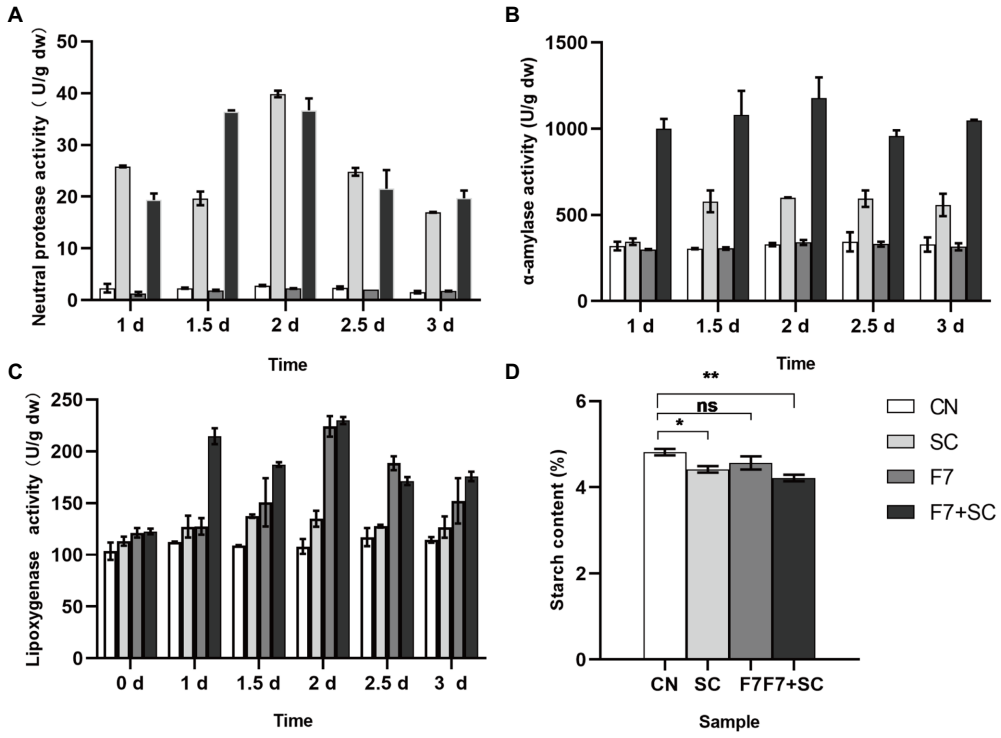

FIGURE 5
Dynamic analysis of neutral protease activities **(A)**, alpha-amylase activities **(B)**, lipoxygenase (LOX) activities **(C)**, and starch content **(D)** response to bio-inoculation. CN represents the control group. SC represents *B. kochii* SC mono-culture. F7 represents *F. magnum* F7 mono-culture. F7-SC represents *F. magnum* F7-*B. kochii* SC co-culture. Error bars represent the standard deviation of the samples (triplicate). *p* value represents by an asterisk "*" (*: $0.01<p\leq0.05$; **: $0.001<p\leq0.01$, paired, *t*-test; ns: no significant difference).

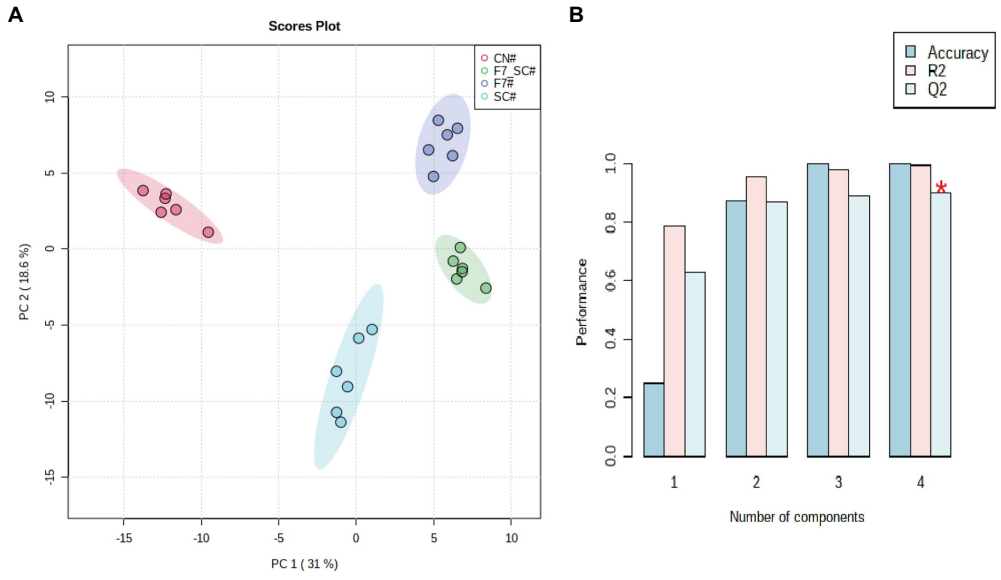

FIGURE 6
Profiling the volatile compositions in FCT with bio-cultivation. Principal component analysis **(A)** and cross-validation of PLS-DA (R2:0.9945; Q2:0.9355) of the volatile compositions in FCT with bio-cultivation **(B)**.

To understand the motivation of co-culture in promoting quality, we compared the differences between the control and bioaugmentation group (mono- and co-cultivation) from different dimensions. Microbial diversity analysis indicated that the intervention of functional strains decreased the diversity and richness of microbial community. Strains F7 and SC dominate overwhelmingly in the flora. Meanwhile, the relative abundance of strain F7 in the co-culture was higher than in the mono-culture. *Bacillus* is ubiquitous and can produce diverse enzymes to degrade different organisms, such as alpha-protease (Yogesh and Halami, 2015), amylase (Ullah et al., 2021)

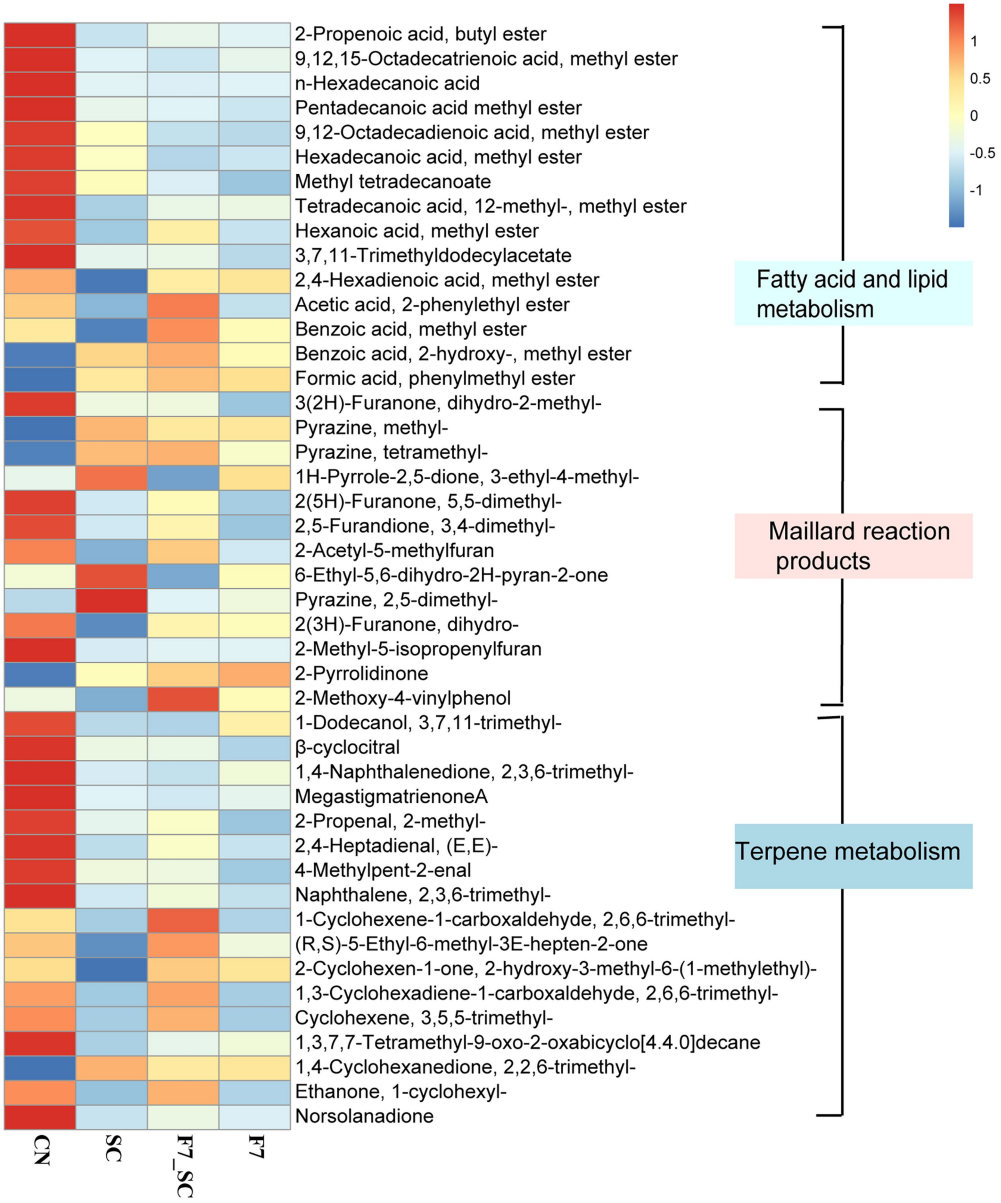

FIGURE 7
Heat map of key differential metabolites between control and bio-cultivation groups. CN represents the control group. SC represents *B. kochii* SC mono-culture. F7 represents *F. magnum* F7 mono-culture. F7-SC represents *F. magnum* F7-*B. kochii* SC co-culture.

and lipase (Adetunji and Olaniran, 2021). *F. magnum* could secrete lipase and pectinase (Li et al., 2017). In the present study, the high activities of neutral protease and α-amylase in strain SC promoted the degradation of protein and starch into small molecular carbohydrates and amino acids, which provided more nutrients for the growth and metabolism of F7 in the co-culture.

Meanwhile, the analysis of flora genes functions, enzyme activities, and various components in the mono- and co-culture modes suggested the excellent performance of the co-culture based on function-driven design. Changes in the composition resulted from microbial metabolism and created a change in quality characteristics. As shown in Figure 2, the bioaugmentation with SC enhanced the attributes of softness and pleasant odor, while F7 mono-culture contributed to the intensities and quality of aroma. Co-cultivation with two functional strains obtained comprehensive quality improvements. *F. magnum* F7 with high LOX might affect fatty acid, lipid metabolism and terpene metabolism. *B. kochii* SC with high proteases and amylases mainly promoted the accumulation of Maillard reaction products by accelerating the formation of amino acids and reducing sugars. The co-cultivation with two strains achieved a higher accumulation of flavor-related substances by complementary functions.

In Figure 7, HFA esters can degrade into volatile carbonyl compounds (Han et al., 2010) to alleviate irritation and off-flavor, and promotes the accumulation of flavor-related degradation products. 2-phenylethyl acetate is a very valuable flavor compound that provides a stronger fruity character in wine (Viana et al., 2009). Benzoic acid methyl ester is a food-grade oral favor additive (Zheng et al., 2021). Most Maillard reaction products can offer a sweet, nutty, or popcorn-like flavor (Hinneh et al., 2018), in which 1H-Pyrrole-2,5-dione, 3-ethyl-4-methyl- has been reported as a flavor marker in dark tea (strongly associated with an aged fragrance) and 2,5-dimethylpyrazine

offers a cocoa flavor (Zhang et al., 2021). As well, the degradation of terpenoids contributes to the lessening of irritation and the formation of flavors. Cembrene could be degraded into solanone with a peculiar flavor and mellowed aroma (Zorn et al. 2003; Popova et al., 2020). 2,6,6-trimethyl-1,3-cyclohexadiene-1-carboxaldehyde (also known as safranal) increases the sweetness and has been identified as an aroma-active compound in dark tea (Zhang et al., 2021). 2,6,6-trimethyl-1-cyclohexene-1-carboxaldehyde and beta-damascone are important degradation products of carotenoids and have floral and fruity scents (Popova et al., 2020).

Through the analysis of microbial diversity, gene function, enzyme activity and volatile compositions within the mono- and co-cultivation, our study showed the formation of a good co-culture between two strains through functional division of labor and nutritional feeding. It took only 2 days of bioaugmentation with co-cultivation to obtain comprehensive quality improvements in the study subject, clearly enhancing aroma-related attributes, softness and pleasant odor, simultaneously increasing the sweetness and aftertaste of FCT. However, functional strains were overwhelmingly dominant in the flora through the bioaugmentation technique. The impact of other microorganisms on the composition of FCT needs to be studied more. We demonstrated that a co-culture method could more effectively meet target needs than previous approaches using a function-driven design. Bioaugmentation with co-cultivation will become a promising approach to the economically targeted promotion of the quality of raw materials suitable for industrialized production with rough handling.

Data availability statement

The datasets presented in this study can be found in online repositories. The names of the repository/repositories and accession number(s) can be found in the article/Supplementary material.

Author contributions

XW: data curation, methodology, formal analysis, and writing — original draft. WC: methodology and data curation. PZ: methodology and investigation. ZP: writing-editing and data visualization. TZ: data visualization. DL: resources and funding acquisition. JL: writing — conceptualization and reviewing. GZ: data visualization. JZ: writing — editing and supervision. GD: funding acquisition and writing — reviewing. All authors contributed to the article and approved the submitted version.

Funding

Our work was funded by the 2020 Major Science and Technology Special Project of China Tobacco Corporation (110,202,001,040 XJ-02) and the Major Science and Technology Special Project of China Tobacco Sichuan Industrial Co., Ltd. (KJSB201808020001).

Conflict of interest

WC, PZ, and DL were employed by China Tobacco Sichuan Industrial Co., Ltd.

The remaining authors declare that the research was conducted in the absence of any commercial or financial relationships that could be construed as a potential conflict of interest.

Publisher's note

All claims expressed in this article are solely those of the authors and do not necessarily represent those of their affiliated organizations, or those of the publisher, the editors and the reviewers. Any product that may be evaluated in this article, or claim that may be made by its manufacturer, is not guaranteed or endorsed by the publisher.

Supplementary material

The Supplementary material for this article can be found online at: https://www.frontiersin.org/articles/10.3389/fmicb.2022.1024005/full#supplementary-material

References

Adetunji, A. I., and Olaniran, A. O. (2021). Production strategies and biotechnological relevance of microbial lipases: a review. *Braz. J. Microbiol.* 52, 1257–1269. doi: 10.1007/s42770-021-00503-5

Atasoy, M., and Cetecioglu, Z. (2020). Butyric acid dominant volatile fatty acids production: bio-augmentation of mixed culture fermentation by clostridium butyricum. *J. Environ. Chem. Eng.* 8:104496. doi: 10.1016/j.jece.2020.104496

Bokulich, N. A., Kaehler, B. D., Rideout, J. R., Dillon, M., Bolyen, E., Knight, R., et al. (2018). Optimizing taxonomic classification of marker-gene amplicon sequences with QIIME 2's q2-feature-classifier plugin. *Microbiome* 6:90. doi: 10.1186/s40168-018-0470-z

Canon, F., Mariadassou, M., Maillard, M. B., Falentin, H., Parayre, S., Madec, M. N., et al. (2020). Function-driven Design of Lactic Acid Bacteria co-cultures to produce new fermented food associating Milk and Lupin. *Front. Microbiol.* 11:584163. doi: 10.3389/fmicb.2020.584163

Cao, J. L., Cheng, J. Q., Li, Y. P., Wu, C. L., and Zhang, J. L. (2020). Research progress on the relationship between routine chemical composition and smoking quality of flue-cured tobacco. *Hubei Agric. Sci.* 59, 253–262. doi: 10.14088/j.cnki.issn0439-8114

Caspi, R., Altman, T., Billington, R., Dreher, K., Foerster, H., Fulcher, C. A., et al. (2008). The metacyc database of metabolic pathways and enzymes and the biocyc collection of pathway/genome databases. *Nucl. Acids Res.* 36, D623–D631. doi: 10.1093/nar/gkm900

Chai, L. J., Qiu, T., Lu, Z. M., Deng, Y. J., Zhang, X. J., Shi, J. S., et al. (2020). Modulating microbiota metabolism via bioaugmentation with lactobacillus casei and Acetobacter pasteurianus to enhance acetoin accumulation during cereal vinegar fermentation. *Food Rev. Int. Ont.* 138:109737. doi: 10.1016/j.foodres.2020.109737

Charubin, K., and Papoutsakis, E. T. (2019). Direct cell-to-cell exchange of matter in a synthetic clostridium syntrophy enables CO2 fixation, superior metabolite yields, and an expanded metabolic space. *Metab. Eng.* 52, 9–19. doi: 10.1016/j.ymben.2018.10.006

Dayalan, S., Xia, J., Spicer, R. A., Salek, R., Roessner, U. (2019). Metabolome Analysis. In encyclopedia of Bioinformatics and Computational Biology. eds. *Ranganathan S., Gribskov M., Nakai K., Schönbach C. (Cambridge, MA, USA: Academic Press)* 396–409.

De Melo Pereira, V. G. D., Neto, D. P. D., Junqueira, A. C. D., Karp, S. G., Letti, L. A. J., and Magalhães Júnior, A. I. (2020). A review of selection criteria for starter culture development in the food fermentation industry. *Food Rev. Int.* 36, 135–167. doi: 10.1080/87559129.2019.1630636

Feizi, R., Jorfi, S., and Takdastan, A. (2020). Bioremediation of phenanthrene-polluted soil using *Bacillus kochii* AHV-KH14 as a halo-tolerant strain isolated from compost. *Environ. Health Eng. Manag.* 7, 23–30. doi: 10.34172/EHEM.2020.04

Guo, X. F., Ji, D., Long, Q. W., Bai, B. J., Wang, H. J., and Cao, Y. P. (2018). Spatial dynamics of yeast community and its relationship with environmental factors in Lhalu wetland, Tibet. *Acta Microbiol Sin.* 58, 1167–1181. doi: 10.13343/j.cnki.wsxb.20170311

Han, G. H., Yan, K. Y., Zhao, M. Q, and Yin, Q. Y. (2010). *Tobacco Chemistry*. Beijing: China Agriculture Press.

Hernández-Adame, N. M., López-Miranda, J., Martínez-Prado, M. A., La Cisneros-de Cueva, S., Rojas-Contreras, J. A., and Medrano-Roldán, H. (2021). Increase in Total petroleum hydrocarbons removal rate in contaminated mining soil through bioaugmentation with autochthonous fungi during the slow bioremediation stage. *Water Air Soil Pollut.* 232, 221–232. doi: 10.1007/s11270-021-05051-0

Hinneh, M., Semanhyia, E., Van de Walle, D., Ade, W., Tzompa-Sosa, D. A., Scalone, G. L. L., et al. (2018). Assessing the influence of pod storage on sugar and free amino acid profiles and the implications on some Maillard reaction related flavor volatiles in Forastero cocoa beans. *Food Rev. Int.* 111:607. doi: 10.1016/j.foodres.2018.05.064

Ke, T., Zhang, J., Tao, Y., Zhang, C., Zhang, Y., Xu, Y. H., et al. (2021). Individual and combined application of cu-tolerant bacillus spp. enhance the cu phytoextraction efficiency of perennial ryegrass. *Chemosphere* 263:127952. doi: 10.1016/j.chemosphere.2020.127952

Ken, S., Hironori, S., and Yukiko, S. (2013). Affinity purification and characterization of a biodegradable plastic-degrading enzyme from a yeast isolated from the larval midgut of a stag beetle *Aegus laevicollis*. *Appl. Microbiol. Biotechnol.* 97, 7679–7688. doi: 10.1007/s00253-012-4595-x

Leffingwell, J. C. (1999). *Basic Chemical Constituents of Tobacco Leaf and Differences among Tobacco Types*, New Jersey: Blackwell Science Ltd, 265–284.

Li, J. F., Lin, T., Ren, D. D., Wang, T., Tang, Y., Wang, Y. W., et al. (2021). Transcriptomic and Metabolomic studies reveal mechanisms of effects of CPPU-mediated fruit-setting on attenuating volatile attributes of melon fruit. *Agronomy* 11:1007. doi: 10.3390/agronomy11051007

Li, M. M., Song, J. L., Ma, Q. Y., Kong, D. L., Zhou, Y. Q., Jiang, X., et al. (2020). Insight into the characteristics and new mechanism of Nicosulfuron biodegradation by a pseudomonas sp LAM1902. *J. Agric. Food Chem.* 68:826. doi: 10.1021/acs.jafc.9b06897

Li, Z. Y., Zhou, X. L., Zhou, B., Dong, M. H., Wang, Y. X., Yang, L. Y., et al. (2017). Diversity and extracellular enzymes of yeasts from Chenghai Lake in winter. *Mycosystema* 36, 177–185.

Lyu, Y., Bi, J. F., Chen, Q. Q., Li, X., Wu, X. Y., Hou, H. N., et al. (2021). Discoloration investigations of freeze-dried carrot cylinders from physical structure and color-related chemical compositions. *J. Sci. Food Agric.* 101, 5172–5181. doi: 10.1002/jsfa.11163

Maldonado-Robledo, G., Rodriguez-Bustamante, E., Sanchez-Contreras, A., Rodriguez-Sanoja, R., and Sanchez, S. (2003). Production of tobacco aroma from lutein. Specific role of the microorganisms involved in the process. *Appl. Microbiol. Biotechnol.* 62, 484–488. doi: 10.1007/s00253-003-1315-6

Ni, H., Jiang, Q. X., Lin, Q., Ma, Q. Q., Wang, L., Weng, S. Y., et al. (2021). Enzymatic hydrolysis and auto-isomerization during β-glucosidase treatment improve the aroma of instant white tea infusion. *Food Chem.* 342:128565. doi: 10.1016/j.foodchem.128565

Popova, V. T., Ivanova, T. A., Stoyanova, A. S., Nikolova, V. V., Docheva, M. H., Hristeva, T. H., et al. (2020). Chemical constituents in leaves and aroma products of Nicotiana rustica L. tobacco. Int. J. *Food Stud.* 9, 146–159. doi: 10.7455/ijfs/9.1.2020.2

Rocío, U. M., Percy, O. G., Alberto, C. B., Gretty, K. V., and Carmen, T. A. (2020). Diversity of endophytic plant-growth microorganisms from Gentianella weberbaueri and Valeriana pycnantha, highland Peruvian medicinal plants. *Microbiol. Res.* 233:126413. doi: 10.1016/j.micres.2020.126413

Sayed, S. M., El-Shehawi, A. M., Elarnaouty, S. A., Al-Otaibi, S. A., El-Shazly, S. S., Alotaibi, R., et al. (2021). Molecular characterization of endophytic fungal communities associated with Vitis vinifera L. at Taif region of Saudi Arabia. *J. Environ. Biol.* 42, 177–185. doi: 10.22438/jeb/42/2/MRN-1577

Shahab, R. L., Brethauer, S., Davey, M. P., Smith, A. G., Vignolini, S., Luterbacher, J. S., et al. (2020). A heterogeneous microbial consortium producing short-chain fatty acids from lignocellulose. *Science* 369:1214. doi: 10.1126/science.Abb1214

Shen, H., Ge, J., Wang, Y. F., Shang, G. M. Z., Fang, C. N., Gou, X. Q., et al. (2022). Correlation analysis of free amino acid and other major nitrogen compounds and sensory quality of flue-cured tobacco in FuJian. *Acta Tabacaria Sinica* 28, 18–26. doi: 10.16472/j.chinatobacco.2021.206

Su, C., Gu, W., Zhe, W., Zhang, K. Q., Duan, Y. Q., and Yang, J. K. (2011). Diversity and phylogeny of bacteria on Zimbabwe tobacco leaves estimated by 16S rRNA sequence analysis. *Appl. Microbiol. Biotechnol.* 92, 1033–1044. doi: 10.1007/s00253-011-3367-3

Su, C., Zhang, K. Z., and Cao, X. Z. (2020). Effects of Saccharomycopsis fibuligera and Saccharomyces cerevisiae inoculation on small fermentation starters in Sichuan-style Xiaoqu liquor. *Food Rev. Int. Ottawa* 137:109425. doi: 10.1016/j.foodres.2020.109425

Suraiya, S., Lee, J. M., Cho, H. J., Jang, W. J., Kim, D. G., Kim, Y. O., et al. (2018). Monascus spp. fermented brown seaweeds extracts enhance bio-functional activities. *Food Biosci.* 21, 90–99. doi: 10.1016/j.fbio.2017.12.005

Swain, A. P., and Stedman, R. L. (1962). Analytical study on the higher fatty acids of tobacco. *J. Assoc. Off. Agr. Chem.* 45, 536–540. doi: 10.1093/jaoac/45.3.536

Ullah, I., Khan, M. S., Khan, S. S., Ahmad, W., Zheng, L. J., Shah, S. U., et al. (2021). Identification and characterization of thermophilic amylase producing bacterial isolates from the brick kiln soil. *Saudi J. Biol. Sci.* 28, 970–979. doi: 10.1016/j.sjbs.2020.11.017

Viana, F., Gil, J. V., Vallés, S., and Manzanares, P. (2009). Increasing the levels of 2-phenylethyl acetate in wine through the use of a mixed culture of Hanseniaspora osmophila and Saccharomyces cerevisiae. *Int. J. Food Microbiol.* 135, 68–74. doi: 10.1016/j.ijfoodmicro.2009.07.025

Viesser Jéssica, A., Melo, P., De Gilberto, V., Carvalho, N., Pedro, D., De Rogez, H., et al. (2020). Co-culturing fructophilic lactic acid bacteria and yeast enhanced sugar metabolism and aroma formation during cocoa beans fermentation. *Int. J. Food Microbiol.* 339:109015. doi: 10.1016/j.ijfoodmicro.109015

Vitelli, M., Budman, H., Pritzker, M., and Tamer, M. (2021). Applications of flow cytometry sorting in the pharmaceutical industry: a review. *Biotechnol. Prog.* 37:e3146. doi: 10.1002/btpr.3146

Wang, H. G., Dong, W. J., Dou, Y. Q., Mao, X. X., Zhang, J. X., Yang, K., et al. (2021). Research of correlationship between starch content and sensory quality of flue-cured tobacco. *Southwest China J. Agric. Sci.* 30, 1533–1537. doi: 10.16213/j.cnki.scjas.2017.7.012

Wilfried, S., Rachel, D. R., and Efraim, L. (2008). Biosynthesis of plant-derived flavor compounds. *Plant J.* 54, 712–732. doi: 10.1111/j.1365-313X.2008.03446.x

Wu, X. Y., Cai, W., Zhu, P. C., Peng, Z., Zheng, T. F., Li, D. L., et al. (2022). (2022) profiling the role of microorganisms in quality improvement of the aged flue-cured tobacco. *BMC Microbiol.* 22:197. doi: 10.1186/s12866-022-02597-9

Wu, X. Y., Zhu, P. C., Li, D. L., Zheng, T. F., Cai, W., Li, J. H., et al. (2021). Bioaugmentation of bacillus amyloliquefaciens–*Bacillus kochii* co-cultivation to improve sensory quality of flue-cured tobacco. *Arch. Microbiol.* 203, 5723–5733. doi: 10.1007/s00203-021-02556-4

Yang, L. Y., Yang, S. L., Li, J. Y., Pang, T., He, B., and Gong, M. (2018). Research advances on metabolism of higher fatty acids in Nicotiana tabacum and its affecting factors. *Biotechnol. Bull.* 33, 51–60. doi: 10.13560/j.cnki.biotech.bull.1985.2017-0391

Yin, F., Zhang, X. M., Song, S. Q., Han, T., and Karangwa, E. (2016). Identification of aroma types and their characteristic volatile compounds of Chinese faint-scent cigarettes based on descriptive sensory analysis and GC–MS and partial least squares regression. *Eur. Food Res. Technol.* 242, 869–880. doi: 10.1007/s00217-015-2593-9

Yogesh, D., and Halami, P. M. (2015). A fibrin degrading serine metallo protease of Bacillus circulans with α-chain specificity. *Food Biosci.* 11, 72–78. doi: 10.1016/j.fbio.2015.04.007

Zhang, H., Wang, J. J., Zhang, D. D., Zeng, L., Liu, Y. A., Zhu, W., et al. (2021). Aged fragrance formed during the post-fermentation process of dark tea at an industrial scale. *Food Chem.* 342:128175. doi: 10.1016/j.foodchem.2020.128175

Zheng, T. Z., Sai, H., Leng, X. P., Sadeghnezhad, E., Li, T., Pervaiz, T., et al. (2021). Profiling analysis of volatile and non-volatile compounds in *Vitis Vinifera* berries (cv. Chardonnay) and spontaneous bud mutation. *Front. Nutr.* 8:715528. doi: 10.3389/fnut.2021.715528

Zhu, S. S., Lei, Y. H., Wang, C. W., Yu, M., Wang, C. C., and Sun, Y. F. (2021). Patterns of yeast diversity distribution and its drivers in rhizosphere soil of Hami melon orchards in different regions of Xinjiang. *BMC Microbiol.* 21:170. doi: 10.1186/s12866-021-02222-1

Zorn, H., Breithaupt, D. E., Takenberg, M., Schwack, W., and Berger, R. G. (2003). Enzymatic hydrolysis of carotenoid esters of marigold flowers (*Tagetes erecta* L.) and red paprika (*Capsicum annuum* L.) by commercial lipases and Pleurotus sapidus extracellular lipase. *Enzym. Microb. Technol.* 32, 623–628. doi: 10.1016/S0141-0229(03)00020-6

frontiers | Frontiers in Microbiology

TYPE Review
PUBLISHED 30 March 2023
DOI 10.3389/fmicb.2023.1138401

Check for updates

OPEN ACCESS

EDITED BY
Tarun Belwal,
Zhejiang University,
China

REVIEWED BY
Debdulal Banerjee,
Vidyasagar University,
India
Sunil Kumar Deshmukh,
The Energy and Resources Institute (TERI),
India
Benevides Costa Pessela,
Spanish National Research Council (CSIC),
Spain

*CORRESPONDENCE
Sanjay Kumar Singh
✉ sksingh@aripune.org
Paras Nath Singh
✉ pnsingh@aripune.org

SPECIALTY SECTION
This article was submitted to Microbiotechnology, a section of the journal Frontiers in Microbiology

RECEIVED 05 January 2023
ACCEPTED 09 March 2023
PUBLISHED 30 March 2023

CITATION
Pawar KS, Singh PN and Singh SK (2023) Fungal alkaline proteases and their potential applications in different industries. *Front. Microbiol.* 14:1138401. doi: 10.3389/fmicb.2023.1138401

COPYRIGHT
© 2023 Pawar, Singh and Singh. This is an open-access article distributed under the terms of the Creative Commons Attribution License (CC BY). The use, distribution or reproduction in other forums is permitted, provided the original author(s) and the copyright owner(s) are credited and that the original publication in this journal is cited, in accordance with accepted academic practice. No use, distribution or reproduction is permitted which does not comply with these terms.

Fungal alkaline proteases and their potential applications in different industries

Kadambari Subhash Pawar[1,2], Paras Nath Singh[1,2]* and Sanjay Kumar Singh[1,2]*

[1]National Fungal Culture Collection of India (NFCCI), Biodiversity and Palaeobiology Group (Fungi), MACS' Agharkar Research Institute, Pune, Maharashtra, India, [2]Savitribai Phule Pune University, Pune, India

The consumption of various enzymes in industrial applications around the world has increased immensely. Nowadays, industries are more focused on incorporating microbial enzymes in multiple processes to avoid the hazardous effects of chemicals. Among these commercially exploited enzymes, proteases are the most abundantly used enzymes in different industries. Numerous bacterial alkaline proteases have been studied widely and are commercially available; however, fungi exhibit a broader variety of proteases than bacteria. Additionally, since fungi are often recognized as generally regarded as safe (GRAS), using them as enzyme producers is safer than using bacteria. Fungal alkaline proteases are appealing models for industrial use because of their distinct spectrum of action and enormous diversity in terms of being active under alkaline range of pH. Unlike bacteria, fungi are less studied for alkaline protease production. Moreover, group of fungi growing at alkaline pH has remained unexplored for their capability for the production of commercially valuable products that are stable at alkaline pH. The current review focuses on the detailed classification of proteases, the production of alkaline proteases from different fungi by fermentation (submerged and solid–state), and their potential applications in detergent, leather, food, pharmaceutical industries along with their important role in silk degumming, waste management and silver recovery processes. Furthermore, the promising role of alkali–tolerant and alkaliphilic fungi in enzyme production has been discussed briefly. This will highlight the need for more research on fungi growing at alkaline pH and their biotechnological potential.

KEYWORDS

alkaline proteases, classification, fermentation, alkaliphilic fungi, pH

1. Introduction

Enzymes are biocatalysts and are involved in nearly all biological reaction. Enzymes have been used in beer, wine, vinegar production, and cheese making since prehistoric time. The enzymes used in these processes were not pure and well–characterized. They were generally produced by micro–organisms that were spontaneously growing. Later, selected strains of micro–organisms were being used to produce enzymes on a large scale, followed by their purification. This development has made a remarkable contribution to the rectification of industrial processes. Further development of industrial enzymes has been revolutionized through directed mutation, protein engineering, and genetic engineering (Sharma, 2019). Currently, various enzymes are used in industries like lipases, proteases, amylases, cellulases,

xylanases, etc. However, proteases remain the dominant type of enzyme as they are extensively valuable for multiple processes in detergents, dairy, food, paper, and pulp industries. Proteases hold about 60% shares of total enzymes sold commercially every year (Rao et al., 1998; Savitha et al., 2011; Figure 1). In 2019, the worldwide protease market was 2.76 billion USD, and expected to increase over the period of 2019–2024 with the annual growth rate of 6.1% (Choudhary et al., 2022). Among various proteases, alkaline proteases contribute the largest sector of the enzyme market, especially in the detergent industry (Abidi et al., 2011). Alkaline proteases are active at neutral to alkaline pH range and require either Asp-His-Ser triad (serine protease) or metal ions (metalloprotease) to act on the substrate (Choudhary et al., 2022). Alkaline proteases are preferred over the other types of proteases because of their ability to sustain under the alkaline pH without losing the action specificity. Owing to this fact, they have long been used in various industries, exclusively in the detergent industry. As an excellent and diverse enzyme reservoir, micro–organisms are extensively used for enzyme production to meet the current demand for proteases in various industries. Consequently, researchers keep searching for novel micro-organisms secreting alkaline proteases with desirable properties (Matkawala et al., 2021). In 1971, the first report was published regarding the production of alkaline protease by bacterium (*Bacillus* sp. strain 221) (Horikoshi, 1999). Since then, several bacterial and fungal genera have been studied for alkaline protease activity and exploited for their commercial production. In industrial processes, fungal proteases are the choice of enzymes over bacterial enzymes as they can be produced using low–cost substrate coupled with high and rapid productivity (Naeem et al., 2022). One more advantage of fungi over bacteria is biomass separation from production media; the mycelia can be easily removed from the broth, simplifying downstream processes (Souza et al., 2015; Arya et al., 2021). Therefore, the demand for fungal proteases for their extensive applications in various industries is increasing worldwide. The present review article deals with fungal alkaline proteases, their production, characterization, and applications in different fields.

2. Classification of proteases

In accordance with the Nomenclature Committee of the International Union of Biochemistry and Molecular Biology (IUBMB), proteases belong to subgroup 4 of hydrolases (group 3) (Barrett, 1997). The proteases have been primarily categorized based on three essential criteria: (1) site of action; (2) chemical nature of the active site; (3) evolutionary relationship with respect to their structure. On the basis of site of action, proteases are classified as exo–peptidases and endo–peptidases. Proteases acting near the termini of the polypeptide chain are placed under the group of exo–peptidases. In contrast, endo–peptidases act on the peptide bond in the internal region of the polypeptide chain, as free amino acid or carboxyl group negatively affects the enzyme activity. Exo–peptidases are further clustered into carboxypeptidases (acting near C terminus) and aminopeptidases (acting near N terminus). Based on the chemical nature of the active site, proteases were previously grouped into four major groups: serine proteases, cysteine proteases, aspartic proteases and, metalloproteases (Rawlings and Barrett, 1993). After discovering three more types of proteolytic enzymes, (1) threonine protease, (2) glutamic protease and, (3) asparagine peptide lyase, the hierarchy of proteolytic enzyme was made in 1993 was redefined. As per the online database for peptidases and their inhibitors (MEROPS), seven types of proteolytic enzymes have been described (Rawlings et al., 2018). Serine proteases contain serine residue at their catalytic site used for their catalytic activity (Polgár, 2005). They show their activity at both neutral and alkaline pH with an optimum range of 7.0 to 11.0. Serine proteases that are effective at highly alkaline pH are clustered as serine alkaline proteases, which is a major subclass of serine proteases with optimum pH around 10. Subtilisin of bacterial origin is the second–largest subclass of serine proteases effective at alkaline pH (Rao et al., 1998; Ekici et al., 2008). Second group, Cysteine proteases, also known as thiol proteases contain catalytic triad of amino acids, Cys-His-Asn (Verma et al., 2016). They are optimally active at neutral pH (Barrett and Rawlings, 2001). The third group, Aspartic proteases, has a dyad of two highly conserved aspartic acid residues (Friedman and Caflisch, 2010). Being maximally active at low pH (3.0–4.0), they are usually known as acidic proteases. Fourth group, Metallo–proteases are known for a characteristic of their obligation for divalent metal ion (zinc, cobalt, copper, nickel, manganese, and iron) to activate water which acts as a nucleophile to catalyze the reaction (Rawlings and Barrett, 1995). In 1995, threonine protease was discovered as the fifth catalytic type of protease while resolving the proteasome structure from *Thermoplasma acidophilum*. Out of fourteen, three subunits of peptidase of proteasome had N–terminal threonine that

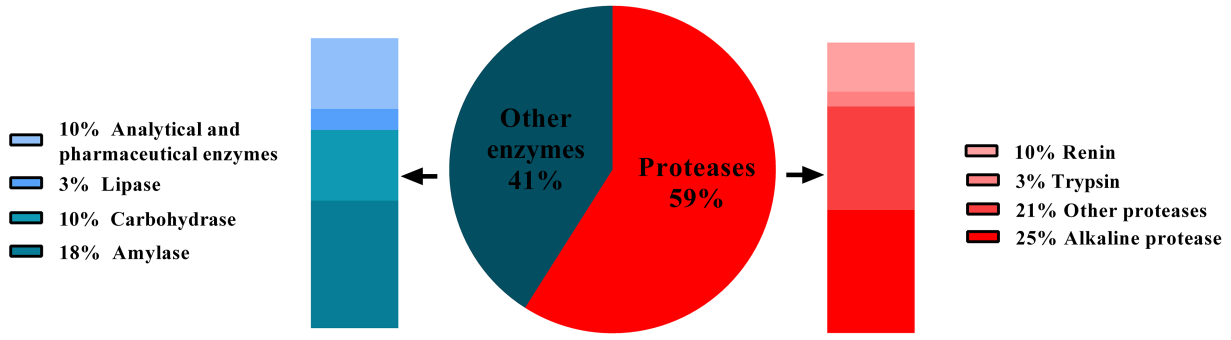

FIGURE 1
Contribution of types of proteases (red portion) in annual sales of the total enzyme. Source: adapted and modified from reference (Rao et al., 1998).

TABLE 1 Classification of proteolytic enzymes.

Type of proteolytic enzymes	Amino acids involved in active site	Mode of action*	Examples
(A) Exopeptidase			
(1) Aminopeptidase	–		–
Dipeptidyl peptidase (3.4.14)	–		–
Tripeptidyl peptidase (3.4.16–3.4.18)			
(2) Carboxypeptidase			–
Dipeptidase (3.4.19)	–		–
Peptidyl dipeptidase	–		–
Serine type carboxypeptidase	Ser-Asp-His		–
Metallocarboxypeptidase	–		–
Cysteine type carboxypeptidase (3.4.15)	–		–
(B) Endopeptidase			
Serine endopeptidase (3.4.21)	Asp-His-Ser		Chymotrypsin, trypsin, subtilisin
Cysteine endopeptidase (3.4.22)	Cys-His-Asn		Papain
Aspartic endopeptidase (3.4.23)	Asp-Asp		Pepsin, chymosin
Metalloendopeptidase (3.4.24)	His-His-Glu		Gelatinase, collagenase
Threonine endopeptidase (3.4.25)	N–terminal Thr		Proteasome endopeptidase complex
Endopeptidases of unknown catalytic mechanism (3.4.99)	–		–

The meaning of symbol * is as follows : Blue balls represent terminal amino acids; Brown balls represent amino acid residues from the internal polypeptide region. Slanting Red line indicated the site of cleavage.

participated in catalysis by acting as a nucleophile (Brannigan et al., 1995; Seemüller et al., 1995). The sixth type of protease was identified in 2004 as glutamic peptidases. The catalytic site of glutamic protease has a catalytic dyad of glutamic acid and glutamine (Fujinaga et al., 2004). In 2011, a new type of proteolytic enzyme termed asparagine peptide lyase was discovered, which uses asparagine residue of their active site for peptide bond cleavage. The active site of this enzyme contains Asp-Asn amino acids. Unlike all other proteolytic enzymes, this type of enzyme does not require hydrolysis (use of water molecule for lysis) to catalyze the reaction. Hence, they are not peptidase but peptide lyase (Rawlings et al., 2011). Detailed classification of these proteolytic enzymes according to the MEROPS database has been summarized in Table 1 (Fernandes et al., 2023).

Based on the evolutionary relationship, proteases are divided into different clans (also known as super families) that represent various protease families sharing a common ancestor in the evolution process (Argos, 1987). As per the recent data available on MEROPS database (Rawlings et al., 2018), proteolytic enzymes have been divided into 271 families, which are assembled into 56 clans. As of now, 53 families of serine peptidases, 96 families of cysteine peptidases, 16 families of aspartic peptidases, 76 families of metallopeptidases, 6 families of threonine peptidases, 2 families of glutamic peptidases, 10 families of asparagine lyases, 2 families of mixed catalytic type and 10 of unknown catalytic type have been identified (Rawlings and Bateman, 2019).

3. Production of fungal alkaline proteases

Alkaline proteases can be synthesized on a bulk scale using fungal isolates by submerged (Smf) and solid–state fermentation (SSF). Different fungi have been reported showing alkaline protease production potential (Table 2). Various cost–effective substrates like wheat bran, oil seed cakes, soybean bran, rice bran have been reported to give a considerable yield of the enzyme under SSF (Germano et al., 2003; Agrawal et al., 2004; Xiao et al., 2015; Novelli et al., 2016; Ram and Yepuru, 2018; Rukmi and Purwantisari, 2020). Although SSF offers volumetric productivity using cheaper substrates, superior monitoring and process control are still associated with Smf. Among fungi, *Aspergillus* sp. was found to be more prominent in the production of alkaline proteases. In a study, the regulation of alkaline protease production has been analyzed using both wild–type and mutant *Aspergillus nidulans*. This study describes an experiment to show the effect of carbon, nitrogen, and sulfur compounds on enzyme production regulation; when any of these compounds in the medium is withheld (Cohen, 1973). In another report, alkaline protease obtained from the cultures of *Aspergillus niger* strain Z1 in Czapek dox medium containing 1% casein can withstand the temperature up to 90°C and retained 48.4% of its original activity for 15 min. This alkaline protease has been reported to have its optimum activity at temperature 40°C and pH 9.0 (Coral et al., 2003). *Aspergillus tamarii* was tested for alkaline protease production, and its growth conditions

TABLE 2 List of fungi producing alkaline proteases and characteristics of proteases.

Genus	Fungal isolate	Fermentation type	Optimum pH	Optimum temperature	Substrate	Purification step	Type of protease	References
Aspergillus	*Aspergillus niger* Z1	Smf	9.0	40°C	Czapek Dox medium	Ethanol precipitation	Serine protease	Coral et al. (2003)
	Aspergillus clavatus ES1	Smf	8.5	50°C	$CaCl_2.7H_2O$, KH_2PO_4, Na_2HPO_4, $MgSO_4.7H_2O$, $ZnCl_2$, NaCl, whole *Sardinella* (*Sardinella aurita*) fish flour, wheat bran	Acetone treatment, Sephadex G-100 gel filtration, CM-Sepharose separation	Serine protease	Hajji et al. (2007)
	Aspergillus tamarii NRRL 20818	SSF	9.0	30°C	Wheat bran	Ammonium sulphate precipitation, DEAE-cellulose, DEAE-cellulose	Serine protease	Anandan et al. (2007)
		Smf	7.0–10.0	30°C	Glucose, peptone, skimmed milk, yeast extract, Na_2HPO_4, $NaNO_3$			
	Aspergillus parasiticus	SSF	8.0	40°C	Wheat bran	Acetone precipitation, DEAE-Sephadex A-50 Flow through, Gel filtration (FPLC)	Serine protease	Tunga et al. (2003)
	Aspergillus terreus (IJIRA 6.2)	SSF	8.5	37°C	Wheat bran	DEAE-Sephadex A25, phosphocellulose column, hydroxyapatite column, casein-Sepharose column, Sephacryl-S-300 column	Serine protease	Chakrabarti et al. (2000)
	Aspergillus ochraceus BT21	Smf	9.0	50°C	Dextrin, peptone, K_2HPO_4, $MgSO_4$, KCl, $FeSO_4$	Sephacryl S-200 gel filtration chromatography, Ion-exchange chromatography	Serine protease	El-Khonezy et al. (2021)
Trametes	*Trametes cingulata* CTM10101	Smf	9.0	60°C	Potato dextrose broth	Ammonium sulphate precipitation, Fast protein liquid chromatography	Serine protease	Omrane Benmrad et al. (2016)
Trichoderma	*Trichoderma atroviride F6*	Smf	8.0–9.0	50°C	whole-feather medium	Ammonium sulphate precipitation, DEAE–cellulose column	Serine protease	Cao et al. (2008)
	Trichoderma longibrachiatum	Smf	9.0	40°C	KH_2PO_4, Na_2HPO_4, $CaCl_2.7H_2O$, $MgSO_4.7H_2O$, NaCl, $ZnCl_2$, different agro-industrial products	Ammonium sulphate precipitation	Unidentified	Chandra Behera et al. (2021)
Penicillium	*Penicillium* sp.	SSF	9.0	45°C	Wheat bran	–	Unidentified	Agrawal et al. (2004)
	Penicillium chrysogenum X5	Smf	10.0	80°C	Yellow lentil flour, tryptone, glucose, $CaCl_2$, KH_2PO_4, K_2HPO_4, trace elements	Ammonium sulphate precipitation, UNO Q-12 FPLC	Serine protease	Benmrad et al. (2018)
	Penicillium rubidurum	Smf	8.0	40°C	KH_2PO_4, Na_2HPO_4, $CaCl_2.7H_2O$, $MgSO_4.7H_2O$, NaCl, $ZnCl_2$, different agro-industrial products	Ammonium sulphate precipitation	Unidentified	Chandra Behera et al. (2021)
Fusarium	*Fusarium* sp. BLB	Smf	9.5	50°C	soybean powder, glucose, polypepton, yeast extract, KH_2PO_4, $MgSO_4$	Ammonium sulphate precipitation, CM-Toyopearl 650 M column elution, Superdex 75 HR 10/30 column	Serine protease	Ueda et al. (2007)

(Continued)

10.3389/fmicb.2023.1138401

TABLE 2 (Continued)

Genus	Fungal isolate	Fermentation type	Optimum pH	Optimum temperature	Substrate	Purification step	Type of protease	References
Ophiostoma	*Ophiostoma piceae* 387 N	Smf	7.0–9.0	40°C	$CaCl_2.2H_2O$, KH_2PO_4, Na_2HPO_4, $MgSO_4.7H_2O$, potassium hydrogen phthalate	hydrophobic interaction chromatography, Ammonium sulphate precipitation	Unidentified	Abraham and Breuil (1996)
Myceliophthora	*Myceliophthora* sp.	SSF	9.0	50°C	Wheat bran	–	Unidentified	Zanphorlin et al. (2010)
		Smf	7.0	50°C	Casein, $(NH_4)_2SO_4$, $MgSO_4.7H_2O$, NH_4NO_3			
Engyodontium	*Engyodontium album* BTMFS10	SSF	11.0	60°C	Wheat bran	Ammonium sulphate precipitation, Ion-exchange chromatography (DEAE)	Unidentified	Chellappan et al. (2006)
Clonostachys	*Clonostachys rosea*	Smf	9.0–10.0	60°C	Glucose, gelatin, peptone, yeast extract	Ammonium sulphate precipitation, HiPrep Phenyl FF column, SOURCE 15Q	Serine protease	Li et al. (2006)
Botrytis	*Botrytis cinerea*	Smf	8.0	50°C	Yeast extract, glucose, gelatin/soy protein	Ammonium sulphate precipitation, Superdex G-75 gel filtration, Anion-exchange chromatography with SP-Sepharose	Unidentified	Abidi et al. (2011)
Beauveria	*Beauveria* sp. MTCC 5184	Smf	9.0	50°C	Glucose, yeast extract, mustard seed cake	Ammonium sulphate precipitation, DEAE-cellulose column	Serine protease	Shankar et al. (2011)
Conidiobolus	*Conidiobolus coronatus* ATCC PTA–4132	Smf	9.0	28°C	MGYP broth	–	Unidentified	Laxman et al. (2005)
Microsporum	*Microsporum canis* strain IHEM 10157	Smf	9.0	55°C	Cat keratine, Glucose, inositol, pyridoxine, thiamine	Affinity based chromatography using bacitracin agarose	Subtilisin-like serine protease	Mignon et al. (1998)
Chrysosporium	*Chrysosporium keratinophilum*	Smf	9.0	90°C	keratin suspension, lactose, $MgSO_4.7H_20$, $FeSO_4.7H_20$, $ZnSO_4.7H_20$, peptone	cold-acetone precipitation, gel-filtration on Sephadex G-75	Unidentified	Dozie et al. (1994)

10.3389/fmicb.2023.1138401

were optimized in solid–state fermentation using wheat bran and submerged fermentation to maximize yield. The isolate was found to produce maximum enzyme at pH 9.0 and temperature 30°C in both fermentation types and required 65% moisture content in wheat bran (Anandan et al., 2007). Moreover, in the first report aimed to optimize production of alkaline protease by *Aspergillus clavatus*, it has been reported that the enzyme was highly active at pH 9.5 and 40°C temperature. The isolate showed the highest proteolytic activity (38 U/mL), when the medium was supplemented with 1% glucose and casein. Among tested nitrogen sources, NH_4NO_3 (0.2% w/v) was reported as the best nitrogen source and showed 27 U/mL enzyme activity (Tremacoldi and Carmona, 2005).

Further a report is available based on activity of bleach stable alkaline protease by the newly isolated *Aspergillus clavatus* ES1 (Hajji et al., 2007). The enzyme showed a 7.5–fold rise in specific activity when purified by acetone precipitation, gel filtration (Sephadex G–100), and ion–exchange chromatography (CM–Sepharose), with 29% recovery having optimum activity at 50°C and pH 8.5. In another study, alkaline protease obtained from *Aspergillus terreus* was studied for its use in detergent formulation. This monomeric enzyme with molecular weight 16 ± 1 kDa showed 148.9 U/mg enzyme activity. Casein was the best substrate over gelatin with 12.8 U/mL Vmax and 5.4 mg/mL Km. The enzyme was active from pH 8.0–12.0, showing optimum activity at pH 11.0 (Niyonzima and More, 2015). Additionally a literature is available (Ke et al., 2018) in which the successful expression of truncated alkaline protease in Pichia pastoris KM71 from *Aspergillus sojae* GIM3.33 using the RT–PCR technique has been described. This recombinant alkaline protease had 400.4 ± 40.5 U/mL enzyme activity up to three days after induction using methanol and was optimally active at pH 10.0 and temperature 45°C. A recent study was focused on the production of alkaline protease using *Aspergillus* sp. isolated from an Ethiopian food, Injera, and the use of response surface methodology (RSM) for process optimization. RSM optimization found that pH 8.24, 30.5°C, and 0.316% sucrose concentration gave the maximum enzyme activity (166.4221 U/mL) (Mustefa Beyan et al., 2021).

Besides *Aspergillus*, very few other fungal genera have been reported for alkaline protease production. In a study, assessment of the protease production by *Fusarium oxysporum* f. sp. *dianthi* race 2 (Fod) using cell wall extracts of susceptible and resistant cultivars of carnation (*Dianthus caryophyllus* L.) has been described (Rodríguez et al., 2017). This study was aimed to reveal the protease–assisted pathogenicity in Fod–carnation interaction. In the presence of cell wall extract of susceptible carnation, Fod produced maximum protease enzymes. Serine protease (trypsin), one of the three isoenzymes secreted by the fungus, was further studied for its identification and biochemical characterization. The enzyme was highly active at pH 8.0 and 50°C temperature, which was then purified using gel filtration (Sephadex G–75), DEAE–cellulose ion exchange, and affinity chromatography (Benzamidine Sepharose 6B). The molecular weight of this protease was 54 kDa, showing Km of 0.31 mg/mL and Vmax of 24.7 µmol/min. Further an interesting study is available on alkaline protease produced by *Clonostachys rosea* (syn. *Gliocladium roseum*) in which the enzyme was studied for its role in infecting nematodes. Its biochemical characterization has been performed upon purification of enzyme using ammonium sulfate precipitation, HiLoad 16/10 Phenyl Sepharose FF column, and anion exchange column (SOURCE 15Q 4.6/100 PE column). The enzyme exhibited highest activity at 60°C temperature and pH 9.0–10.0. Nematicidal studies revealed that the crude enzyme was superior in nematode immobilization than the purified enzyme with 80 ± 5% nematicidal activity (Li et al., 2006). Further the fibrinolytic alkaline protease (M.W. 27 kD) produced from *Fusarium* sp. BLB isolated from plant leaf (*Hibiscus*) has been characterized (Ueda et al., 2007). Purification of the enzyme was carried out by $(NH_4)_2SO_4$ precipitation and column chromatography (CM–Toyopearl 650 M and Superdex 75). The enzyme had its maximum fibrinolytic activity at pH 9.5 and temperature 50°C. In another study, from the culture of *Penicillium chrysogenum* X5 the thermostable serine alkaline protease was purified, and its biochemical characterization was done. The results revealed that the enzyme was active at 10.0 pH and 80°C temperature. Enzyme purification was done by following three steps which include heat treatment at 80°C/10 min, $(NH_4)_2SO_4$ precipitation (30–50%) and dialysis, and anion exchange chromatography (UNO Q–12) using the FPLC system. To evaluate its compatibility with laundry detergents, the enzyme was tested for its wash performance by using it as an additive with detergents. Results revealed that, the enzyme improved the performance of laundry detergent to clean the egg and blood stains on the fabric (Benmrad et al., 2018). A new alkaline protease obtained from *Penicillium nalgiovense* showed its optimum activity at pH 8.0, 35°C temperature, and 0.25 M NaCl concentration. $(NH_4)_2SO_4$ precipitation, dialysis, and ultrafiltration increased the enzyme activity by 12–fold. The molecular mass (45.2 kDa) was confirmed by ESI–MS analysis (Papagianni and Sergelidis, 2014). One more species of *Penicillium* has been studied for the production of alkaline protease using SSF (Xiao et al., 2015). From fermented fish sauce, 30 fungi were isolated based on morphology, among which only *P. citrinum* YL–1 showed enzyme activity. Under Plackett–Burman design, three significant variables like peptone concentration, initial pH, and moisture content were chosen for increasing enzyme yield. The influence of these variables on production of alkaline protease was studied using Box–Behnken design. Another study, focused on fungal isolate *Conidiobolus coronatus* from *Entomophthorales* order, showed the usage of alkaline protease for gelatin degradation and silver recovery from x–ray film. The obtained enzyme was active at 40°C and pH 9.0 with 1.35 U/mL specific activity (Shankar et al., 2010). *Scopulariopsis* spp. was used to produce alkaline protease with a molecular mass of 15 ± 1 kD showing 138.1 U/mg specific activity. The optimum pH of this enzyme was 9.0, while the enzyme was active and stable between the pH 8.0 to 12.0. The enzyme was optimally active at temperature 50°C. The enzyme had 4.3 mg/mL Km and 15.9 U/mL Vmax, using casein as a substrate. As the enzyme was found to be stable in the presence of surfactants, oxidizing and bleaching agents, active at high temperatures and alkaline pH, exhibiting wide range of substrate specificity and compatibility with detergents, its consumption in the detergent formulation has been highly recommended (Niyonzima and More, 2014).

4. Applications of alkaline proteases

Fungal alkaline proteases have a several applications, predominantly in the detergent and food industries. Fungal alkaline proteases are envisioned to have wide–ranging uses in other fields like bioremediation and leather treatment, etc. (Kumar and Takagi, 1999). Table 3 highlights some of the crucial uses of fungal alkaline proteases.

4.1. Detergent industry

Proteases are essential and standard additives in detergents, as they can remove all kinds of proteinaceous materials (Nehra et al., 2002). The first enzymatic formulation named "Brunus" was prepared in 1913, containing crude pancreatic extract and sodium carbonate (Razzaq et al., 2019). A detergent containing a bacterial enzyme with the trade name "BIO–40" was marketed for the first time in 1956 (Kumar et al., 2008). Proteases act against a wide range of substrates, making it worthwhile to remove stains of foodstuff, blood, and body secretions. Characteristics such as stability at alkaline pH and high temperature, ability to withstand with surfactants, oxidizing and chelating agents will make alkaline proteases an indispensable candidate for their application in the detergent industry (Sharma, 2019).

Many researchers studied the compatibility of alkaline protease with detergents to make it sound as a detergent additive. In a report it is presented that the alkaline protease produced by *Conidiobolus coronatus* (NCL 86.8.20) retained its 90% of activity at a lower concentration (0.05 mg/mL–1) in commercial detergent solution after 1 h of incubation at 40°C; suggesting its possible use in detergents (Phadatare et al., 1993). Alkaline serine–protease of *Aspergillus clavatus* ES1 showed extreme stability (100%) in non–ionic surfactant [5% (v/v) tween 80 and triton X–100]; however, enzyme retained its 90% of activity when tested with 0.1% SDS (strong anionic surfactant). Also, the enzyme showed moderate stability towards 1% (w/v) and 2% (w/v) sodium perborate, retaining 71 and 53% activity, respectively (Hajji et al., 2007). In another study, similar results were obtained for the protease produced by *Scopulariopsis* spp., where an increase in protease activity with Tween–80, SDS, and Triton X–100 with retention of 50% enzyme activity in the commercial detergents (enzymatic and nonenzymatic) was obtained (Niyonzima and More, 2014). Another alkaline protease of *Aspergillus* species (*A. niger* and *A. terreus*) retained 50–80% of its initial activity in the presence of various commercially available detergents such as Tide, Hattic, Savo, Surf, Henko, Persil, Wheel, and Aerial (Ali, 2008; Devi et al., 2008). Further a team of researchers studied the compatibility of enzymes produced by two fungal isolates, *Graphium putredinis, Trichoderma harzianum*, and an intergenetically developed fusant. All three enzymes were stable towards SDS and sodium perborate with retention of 58.25–73.82% and 61.58–70.24% of residual activity, respectively, while enzyme from fusant was highly stable than parents with 76.74% of activity when tested for its compatibility with commercial detergent Rin Advanced (Savitha et al., 2011). Similar studies were focused on the compatibility and incorporation of alkaline protease produced by *Aspergillus niger* and *Aspergillus* sp. DHE7 as an additive in detergent formulation (Pundir et al., 2012; El-Ghonemy and Ali, 2021). Recent literature highlighted the introduction of third-generation cold-adapted alkaline proteases to the detergent industry which were found to have excellent activity and stability in surfactants and bleaches (Suresh and Dass, 2022).

4.2. Leather industry

In leather–processing industries, alkaline proteases have extensive applications in various processes like soaking, debating, and depilating of skin and hides. This enzymatic treatment removes unwanted pigments, increases the skin area, and produces a clean hide (Arora, 2003). Alkaline proteases accelerate the dehairing process, as the attack of protease on the hair follicle at higher pH makes the hair removal process easy. Conventionally, this has been carried out using chemicals like a saturated solution of lime and sodium sulfide to treat an animal hide; but this is a very expensive and produces intensely polluting effluent (Anwar and Saleemuddin, 1998). A very few studies have been reporting the application of fungal alkaline protease in the leather industry. A study was aimed on the potential use of alkaline protease produced by *Aspergillus flavus* in the tannery as a depilation agent (Malathi and Chakraborty, 1991). Also, from experimental data, it was confirmed that enzymatic treatment increased the tensile strength, stitch tear strength, bursting strength of leather as compared to control. A similar study has reported using alkaline protease as a dehairing agent in tannery (Pal et al., 1996). Further, the potential use of protease obtained from *Conidiobolus coronatus* has been studied in soaking, dehairing, and bating animal skin/ hide (Khandelwal, 2013).

4.3. Food industry

The production of cheese is the primary application of proteases in the dairy industry. For good flavor and texture development, proteolysis plays a vital role (Fox, 1982). Protease hydrolyses kappa casein and stabilizes micelle formation, which prevents coagulation. Proteases obtained from fungi such as *A. oryzae, Rhizomucor miechie, R. pusillus* are extensively used as coagulants for cheese production in the dairy industry (Neelakantan et al., 1999). Besides the dairy industry, alkaline protease was used in meat tenderization because of its potential to hydrolyze connective tissue and muscle fiber (Ellaiah et al., 2002).

4.4. Pharmaceutical industry

The vast diversity and specificity of fungal proteases are significant advantages in developing effective therapeutic agents. Protease obtained from *Aspergillus oryzae* has been applied to cure the digestive disorders like lytic enzyme deficiency syndromes by its oral administration (Rani et al., 2012). Alkaline protease produced by *Aspergillus niger* LCF 9 is used for therapeutic application because of its collagenolytic activity (Barthomeuf et al., 1992). Fibrinogen, fibrin, and blood clot were hydrolyzed efficiently by proteases obtained from *Aspergillus* strains (El-Shora and Metwally, 2008). Treatments for illnesses including Dupuytren's disease, Peyronie's disease, wound healing, burns, glaucoma, intervertebral disc herniation, debridement, keloid, vitrectomy, and cellulite involve alkaline protease with collagenase activity (Gurumallesh et al., 2019). In burns and wound treatment, immobilized subtilisins have been formulated as soft gel-based formulae, ointments, and bandage materials (Matkawala et al., 2021).

4.5. Waste management

Keratin is the primary protein found in waste from the poultry and leather industry. Because of its compactly packed polypeptide, which is stabilized by strong disulfide bonds and some weak

TABLE 3 Application of fungal alkaline proteases in different industries.

Fungal isolates	Application	References
Conidiobolus brefeldianus	Dehairing of skins/hides	Khandelwal et al. (2015)
Conidiobolus coronatus ATCC PTA–4132	Silver recovery from photographic film	Shankar et al. (2010)
Penicillium sp.	Soy protein hydrolysis	Agrawal et al. (2004)
Aspergillus niger LCF 9	Collagenolytic activity	Barthomeuf et al. (1992)
Fusarium sp. BLB	Fibrinolytic activity	Ueda et al. (2007)
Aspergillus niger DEF 1	Fibrinolytic activity	Lanka et al. (2017)
Aspergillus strain KH 17	Fibrinolytic activity	Palanivel et al. (2013)
Scopulariopsis spp.	Detergent formulation	Niyonzima and More (2014)
Penicillium godlewskii SBSS 25	Detergent formulation	Sindhu et al. (2009)
Trametes cingulata CTM10101	Detergent formulation	Omrane Benmrad et al. (2016)
Graphium putredinis, Trichoderma harzianum	Detergent formulation	Savitha et al. (2011)
Aspergillus sp. DHE7	Detergent formulation	Suresh and Dass (2022)
Penicillium chrysogenum X5	bio–additive for textile processing	Benmrad et al. (2018)
Trichoderma longibrachiatum, Aspergillus niger	Blood stain removal	Suryawanshi and Pandya (2017)
Aspergillus oryzae NRRL–447	Keratinolytic activity	Ali et al. (2011)
Aspergillus spp.	Keratinolytic activity	Kim (2003)
Cunninghamella echinulata	Keratinolytic activity	More et al. (2013)
Fusarium oxysporum	Keratinolytic activity	Prolo et al. (2020)
Chrysosporium tropicum	Keratinolytic activity	Koutb et al. (2022)
Conidiobolus coronatus (NCIM 1238)	to resolve the racemic mixtures of DL–phenylalanine and DL–phenylglycine	Sutar et al. (1992)

interaction, makes it difficult to degrade. Fungal alkaline proteases have been accessed by many researchers for the degradation of keratin. A study has been done on the degradation of keratin using proteases from five species of *Aspergillus* (*A. flavus, A. niger, A. fumigatus, A. terreus*, and *A. nidulans*). Among them, protease from *A. niger* degraded maximum keratin of chicken feathers with 28 μg/mL of cysteine release followed by *A. flavus, A. fumigatus, A. nidulans,* and *A. terreus* (Kim, 2003). Protease from *A. oryzae* has also been reported to degrade feather keratin with the release of various essential (threonine, isoleucine, methionine, leucine, tyrosine, valine, histidine, and lysine) and non–essential (glycine, serine, alanine, phenylalanine, glutamic acid, aspartic acid, and arginine) amino acids and ammonia. Released amino acids and ammonia from the waste can be further used as fertilizer or additives in feed (Ali et al., 2011). In another study, ten dermatophytes from the soil was isolated and studied to biodegrade human and animal hair. Among ten dermatophytes, *Chrysosporium indicum* degraded human hair with maximum weight loss (56.66%); whereas, *Microsporum gypseum* and *Trichophyton verrucosum* degraded animal hair with 49.34% weight loss (Sharma et al., 2011).

4.6. Silk degumming

The proteases are significant candidates in the silk industry for silk degumming or sericin removal from silk. Rough texture of the raw silk fiber is due to the presence of sericin in the peripheral region of fiber. Degumming of silk before dyeing, helps to improve the sheen, texture, and color of cloth. Various fungal proteases have been used for silk degumming. The literature is available on the comparative study of silk degumming using Marseille's soap and enzyme from *Conidiobolus* species (Gulrajani et al., 2000). Fungal protease showed 19.8% weight loss after incubation of 3 h at 37°C, while degumming with Marseille's soap gave 20.5% weight loss on the incubation of 1.5 h at boiling temperature. Successful degumming at a lower temperature will make enzymatic degumming a cost–effective process compared to chemical degumming. One more study based on a similar approach reported comparing degumming by six microbial proteases (4 fungal and 2 actinomycetes) and conventional method using alkali and soap. Among tested proteases of microbial origin, *Conidiobolus brefeldianus* MTCC 5185 and *Actinomycete*–2 (BOA–3) showed best results with 21.10 ± 0.67 and 21.78 ± 0.99% weight loss, respectively, in a short time which is similar to the weight loss (21.40 ± 0.75%) by conventional method (More et al., 2013).

4.7. Silver recovery

The photography industry uses a large quantity of silver in the preparation of light–sensitive emulsion. Used X–ray film has been found to contain around 1.5 to 2.0% silver in the gelatin layers. Silver recovery from X–ray films by conventional methods, mainly by combustion of X–ray films, causes pollution in environment. Hence, the hydrolysis of the gelatin present on the X–ray films using fungal alkaline proteases can be used as an alternative option for silver recovery (Sharma et al., 2019). In one of the studies, protease obtained

from *Conidiobolus coronatus* showed 5% weight loss in x–ray film with the silver recovery of 3.87% (w/w) of sludge weight and 0.2% (w/w) of x–ray film weight, respectively (Shankar et al., 2010). Similarly from one more study, the recovery of 0.135 gm of silver from 40 gm of x–ray film has been reported with 0.335% yield using protease produced by *Aspergillus versicolor* PF/F/107, suggesting an eco–friendly way to the silver from used x–ray films (Choudhary, 2013).

5. Alkaliphilic/alkali-tolerant fungi as a potential source of alkaline enzymes

Primarily most of the fungal species are known to grow at weakly acidic to neutral pH and only handful of researchers has reported on the fungi which can grow at alkaline pH as well. Consequently, these groups of alkaliphilic and alkali–tolerant fungi have remained unexplored for their capability for production of commercially valuable products that are stable at alkaline pH.

A research done in Japan on the distribution of alkalophilic and alkali–tolerant fungi from the limestone caves soil in Japan revealed that approximately one–third (30.8%) of the isolates had the optimum pH in the alkaline range. Fungal species belonging to genera *Acremonium* and *Chrysosporium* were found to be predominant at alkaline pH. (Nagai et al., 1998). A recent study for understanding the evolution alkaliphily in fungi has described the diversity of weak alkali–tolerant to alkaliphilic fungi from soils around the basin of soda lakes in Asia and Africa. It shows the wide of alkaliphilic trait throughout ascomycota division of fungi. Fungi belonging to *Emericellopsis* lineage (*Emericellopsis alkalina*) of order *Hypocreales*, along with fungi from *Plectosphaerellaceae* (*Sodiomyces species, Acrostalagmus luteoalbus*), *Pleosporaceae* (*Alternaria* sect. *Soda*), *Chaetomiaceae* (*Thielavia* sp.) families, were found to be strong alkalitolerants and effective alkaliphiles. Moderate alkali–tolerant fungi included members of genus *Scopulariopsis*, *Fusarium*, *Cladosporium* and Acremonium–like species. While, *Penicillium* sp., *Purpureocillium lilacinum*, and *Alternaria alternata* species showed weak alkali tolerance (Grum Grzhimaylo et al., 2016). In another such study from Thailand, 490 fungi were isolated from various mycological samples, including tree–holes, roots, leaf litter, wood, and soil at pH 11. A total of 324 (66%) isolates were screened for alkaline enzymes like Arabinanase, amylase, potato–galactanase, and protease. This screening revealed that most of these alkali–tolerant fungal isolates were able to produce at least one of the listed enzymes, and a few strains were positive for the activity of all four enzymes (Kladwang et al., 2003).

This dig at the literature highlights the gap in research to produce alkaline enzymes, especially industrially important alkaline proteases from alkaliphilic and alkali–tolerant fungi. This will lead to the production of more promising alkaline enzymes and can ease the wide range of industrially important reactions that are done at alkaline conditions.

6. Conclusion

Global consumption of various enzymes, especially microbial proteases, in industrial applications is increasing because of their wide range of applications in different industries. To meet the existing demand and rapid and easy production, the exploitation of other alternative microbial sources like fungi becomes essential. Fungal proteases are emerging as the best alternative and possess numerous commercial applications. The present comprehensive review describes the alkaline proteases obtained from fungi of different genera and their potential applications in various industries. Meager studies of fungal alkaline proteases leave the scope for research in alkaline proteases from fungi for their industrial applications, which will be helpful for future research worldwide. This review also highlights the need to study the alkaliphily trait spread among fungi, the diversity of alkali-tolerant and alkaliphilic fungi, and their use for the production of various alkaline enzymes. Moreover, due to their intrinsic adaptation to withstand the alkalinity, these enzymes can be used as a promising alternative for current alkaline enzymes produced by fungi growing at acidic to neutral pH.

Author contributions

All authors listed have made a substantial, direct, and intellectual contribution to the work and approved it for publication.

Acknowledgments

Authors thank Director, MACS' Agharkar Research Institute, Pune for providing the necessary facilities to carry out the research work. KP also acknowledges the S. P. Pune University for providing the admission to Ph.D. degree and University Grant Commission (UGC), New Delhi for granting Senior Research Fellowship (SRF).

Conflict of interest

The authors declare that the research was conducted in the absence of any commercial or financial relationships that could be construed as a potential conflict of interest.

Publisher's note

All claims expressed in this article are solely those of the authors and do not necessarily represent those of their affiliated organizations, or those of the publisher, the editors and the reviewers. Any product that may be evaluated in this article, or claim that may be made by its manufacturer, is not guaranteed or endorsed by the publisher.

References

Abidi, F., Chobert, J. M., Haertlé, T., and Marzouki, M. N. (2011). Purification and biochemical characterization of stable alkaline protease Prot–2 from *Botrytis cinerea*. *Process Biochem.* 46, 2301–2310. doi: 10.1016/j.procbio.2011.09.010

Abraham, L. D., and Breuil, C. (1996). Isolation and characterization of a subtilisin–like serine proteinase secreted by the sap–staining fungus *Ophiostoma piceae*. *Enzym. Microb. Technol.* 18, 133–140. doi: 10.1016/0141-0229(95)00098-4

Agrawal, D., Patidar, P., Banerjee, T., and Patil, S. (2004). Production of alkaline protease by *Pddenicillium* sp. under SSF conditions and its application to soy protein hydrolysis. *Process Biochem.* 39, 977–981. doi: 10.1016/S0032-9592(03)00212-7

Ali, U. F. (2008). Utilization of whey amended with some agro–industrial by–products for the improvement of protease production by *aspergillus terreus* and its compatibility with commercial detergents. *Res. J. Agric. Biol. Sci.* 4, 886–891.

Ali, T. H., Ali, N., and Mohamed, L. A. (2011). Production, purification and some properties of extracellular keratinase from feathers–degradation by *aspergillus oryzae* NRRL–447. *J. Appl. Sci. Environ. Sanit.* 6, 123–136.

Anandan, D., Marmer, W. N., and Dudley, R. L. (2007). Isolation, characterization and optimization of culture parameters for production of an alkaline protease isolated from *aspergillus tamarii*. *J. Ind. Microbiol. Biotechnol.* 34, 339–347. doi: 10.1007/s10295-006-0201-5

Anwar, A., and Saleemuddin, M. (1998). Alkaline proteases: a review. *Bioresour. Technol.* 64, 175–183. doi: 10.1016/S0960-8524(97)00182-X

Argos, P. (1987). A sensitive procedure to compare amino acid sequences. *J. Mol. Biol.* 193, 385–396. doi: 10.1016/0022-2836(87)90226-9

Arora, D. K.. *Handbook of Fungal Biotechnology*. Boca Raton: CRC press. (2003). 287–297.

Arya, P. S., Yagnik, S. M., Rajput, K. N., Panchal, R. R., and Raval, V. H. (2021). Understanding the basis of occurrence, biosynthesis, and implications of thermostable alkaline proteases. *Appl. Biochem. Biotechnol.* 193, 4113–4150. doi: 10.1007/s12010-021-03701-x

Barrett, A. J. (1997). Nomenclature Committee of the International Union of biochemistry and molecular biology (NC-IUBMB). Enzyme nomenclature. Recommendations 1992. Supplement 4: corrections and additions. *Eur. J. Biochem.* 250, 1–6. doi: 10.1111/j.1432-1033.1997.001_1.x

Barrett, A. J., and Rawlings, N. D. (2001). Evolutionary lines of cysteine peptidases. *Biol. Chem.* 382, 727–734. doi: 10.1515/bchm.2001.382.5.727

Barthomeuf, C., Pourrat, H., and Pourrat, A. (1992). Collagenolytic activity of a new semi–alkaline protease from *aspergillus Niger*. *J. Ferment. Bioeng.* 73, 233–236. doi: 10.1016/0922-338X(92)90168-T

Benmrad, M. O., Moujehed, E., Elhoul, M. B., Mechri, S., Bejar, S., Zouari, R., et al. (2018). Production, purification, and biochemical characterization of serine alkaline protease from *Penicillium chrysogenum* strain X5 used as excellent bio–additive for textile processing. *Int. J. Biol. Macromol.* 119, 1002–1016. doi: 10.1016/j.ijbiomac.2018.07.194

Brannigan, J. A., Dodson, G., Duggleby, H. J., Moody, P. C., Smith, J. L., Tomchick, D. R., et al. (1995). A protein catalytic framework with an N-terminal nucleophile is capable of self-activation. *Nature* 378, 416–419. doi: 10.1038/378416a0

Cao, L., Tan, H., Liu, Y., Xue, X., and Zhou, S. (2008). Characterization of a new keratinolytic *Trichoderma atroviride* strain F6 that completely degrades native chicken feather. *Lett. Appl. Microbiol.* 46, 389–394. doi: 10.1111/j.1472-765X.2008.02327.x

Chakrabarti, S. K., Matsumura, N., and Ranu, R. S. (2000). Purification and characterization of an extracellular alkaline serine protease from *aspergillus terreus* (IJIRA 6.2). *Curr. Microbiol.* 40, 239–244. doi: 10.1007/s002849910048

Chandra Behera, B., Kumar Sethi, B., Mohapatra, S., Thatoi, H., and Ranjan, M. R. (2021). Bio-production of alkaline protease by *Trichoderma longibrachiatum* and *Penicillium rubidurum* using different agro-industrial products. *Nov. Res. Microbiol. J.* 5, 1241–1255. doi: 10.21608/nrmj.2021.178300

Chellappan, S., Jasmin, C., Basheer, S. M., Elyas, K. K., Bhat, S. G., and Chandrasekaran, M. (2006). Production, purification and partial characterization of a novel protease from marine *Engyodontium album* BTMFS10 under solid state fermentation. *Process Biochem.* 41, 956–961. doi: 10.1016/j.procbio.2005.10.017

Choudhary, V. (2013). Recovery of silver from used X–ray films by *aspergillus versicolor* protease. *J. Acad. Ind. Res.* 2, 39–41.

Choudhary, K., Mankar, M. K., and Sahay, S. (2022). "Extremophilic enzymes: catalytic features and industrial applications" in *Extremophilic fungi: Ecology, Physiology and Applications* (Singapore: Springer Nature Singapore), 273–314.

Cohen, B. L. (1973). Regulation of intracellular and extracellular neutral and alkaline proteases in *aspergillus nidulans*. *Microbiology* 79, 311–320. doi: 10.1099/00221287-79-2-311

Coral, G., Arikan, B. U., Unaldi, M. N., and Guvenmez, H. A. (2003). Thermostable alkaline protease produced by an *aspergillus Niger* strain. *Ann. Microbiol.* 53, 491–498.

Devi, M. K., Banu, A. R., Gnanaprabhal, G. R., Pradeep, B. V., and Palaniswamy, M. (2008). Purification, characterization of alkaline protease enzyme from native isolate *aspergillus Niger* and its compatibility with commercial detergents. *Indian J. Sci. Technol.* 1, 1–6. doi: 10.17485/ijst/2008/v1i7.8

Dozie, I. N., Okeke, C. N., and Unaeze, N. C. (1994). A thermostable, alkaline-active, keratinolytic proteinase from *Chrysosporium keratinophilum*. *World J. Microbiol. Biotechnol.* 10, 563–567. doi: 10.1007/BF00367668

Ekici, Ö. D., Paetzel, M., and Dalbey, R. E. (2008). Unconventional serine proteases: variations on the catalytic Ser/his/asp triad configuration. *Protein Sci.* 17, 2023–2037. doi: 10.1110/ps.035436.108

El-Ghonemy, D. H., and Ali, T. H. (2021). Effective bioconversion of feather–waste keratin by Thermo–surfactant stable alkaline keratinase produced from *aspergillus* sp. DHE7 with promising biotechnological application in detergent formulations. *Biocatal. Agric. Biotechnol.* 35:102052. doi: 10.1016/j.bcab.2021.102052

El-Khonezy, M. I., Elgammal, E. W., Ahmed, E. F., and Abd-Elaziz, A. M. (2021). Detergent stable thiol-dependant alkaline protease produced from the endophytic fungus *aspergillus ochraceus* BT21: purification and kinetics. *Biocatal. Agric. Biotechnol.* 35:102046. doi: 10.1016/j.bcab.2021.102046

Ellaiah, P., Srinivasulu, B., and Adinarayana, K. (2002). A review on microbial alkaline proteases. *J. Sci. Ind. Res.* 61, 690–704.

El-Shora, H. M., and Metwally, M. A. (2008). Production, purification and characterization of proteases from whey by some fungi. *Ann. Microbiol.* 58, 495–502. doi: 10.1007/BF03175548

Fernandes, V. D., Deepika, M., Ajith, S., and Pramod, T. (2023). "Versatile action, properties, application and mechanism of eco-friendly microbial enzyme-proteases" in *Enzymes-Mechanisms and Action* (Delhi India: Jaya Publishing House), 155.

Fox, P. F. (1982). Proteolysis in milk and dairy products. *Biochem. Soc. Trans.* 10, 282–284. doi: 10.1042/bst0100282

Friedman, R., and Caflisch, A. (2010). On the orientation of the catalytic dyad in aspartic proteases. *Proteins* 78, NA–1582. doi: 10.1002/prot.22674

Fujinaga, M., Cherney, M. M., Oyama, H., Oda, K., and James, M. N. (2004). The molecular structure and catalytic mechanism of a novel carboxyl peptidase from *Scytalidium lignicolum*. *Proc. Natl. Acad. Sci. U. S. A.* 101, 3364–3369. doi: 10.1073/pnas.0400246101

Germano, S., Pandey, A., Osaku, C. A., Rocha, S. N., and Soccol, C. R. (2003). Characterization and stability of proteases from *Penicillium* sp. produced by solid–state fermentation. *Enzym. Microb. Technol.* 32, 246–251. doi: 10.1016/S0141-0229(02)00283-1

Grum Grzhimaylo, A. A., Georgieva, M. L., Bondarenko, S. A., Debets, A. J., and Bilanenko, E. N. (2016). On the diversity of fungi from soda soils. *Fungal Divers.* 76, 27–74. doi: 10.1007/s13225-015-0320-2

Gulrajani, M. L., Agarwal, R., and Chand, S. (2000). Degumming of silk with a fungal protease. *Indian J. Fibre Text Res.* 25, 138–142.

Gurumallesh, P., Alagu, K., Ramakrishnan, B., and Muthusamy, S. (2019). A systematic reconsideration on proteases. *Int. J. Biol. Macromol.* 128, 254–267. doi: 10.1016/j.ijbiomac.2019.01.081

Hajji, M., Kanoun, S., Nasri, M., and Gharsallah, N. (2007). Purification and characterization of an alkaline serine–protease produced by a new isolated *aspergillus clavatus* ES1. *Process Biochem.* 42, 791–797. doi: 10.1016/j.procbio.2007.01.011

Horikoshi, K. (1999). Alkaliphiles: some applications of their products for biotechnology. *Microbiol. Mol. Biol. Rev.* 63, 735–750. doi: 10.1128/MMBR.63.4.735-750.1999

Ke, Y., Yuan, X., Li, J., Zhou, W., Huang, X., and Wang, T. (2018). High–level expression, purification, and enzymatic characterization of a recombinant *aspergillus sojae* alkaline protease in *Pichia pastoris*. *Protein Expr. Purif.* 148, 24–29. doi: 10.1016/j.pep.2018.03.009

Khandelwal, H. B.. (2013) Production, purification and characterization of fungal alkaline protease and its applications. Ph.D. Thesis. Pune: University of Pune.

Khandelwal, H. B., More, S. V., Kalal, K. M., and Laxman, R. S. (2015). Eco–friendly enzymatic dehairing of skins and hides by *C. brefeldianus* protease. *Clean Technol. Environ. Policy* 17, 393–405. doi: 10.1007/s10098-014-0791-y

Kim, J. D. (2003). Keratinolytic activity of five *aspergillus* species isolated from poultry farming soil in Korea. *Mycobiology* 31, 157–161. doi: 10.4489/MYCO.2003.31.3.157

Kladwang, W., Bhumirattana, A., and Hywel Jones, N. (2003). Alkaline–tolerant fungi from Thailand. *Fungal Divers.* 13, 69–83.

Koutb, M. M., Hassan, E. A., Morsy, F. M., and Bagy, M. M. (2022). Optimization of keratinase production by keratinolytic fungus *Chrysosporium tropicum* and its potentiality in bidegradation of chicken feathers. *J. Umm Al-Qura Univ. Appl. Sci.* 20, 1–7. doi: 10.1007/s43994-022-00020-7

Kumar, D., Savitri, T. N., Verma, R., and Bhalla, T. C. (2008). Microbial proteases and application as laundry detergent additive. *Res. J. Microbiol.* 3, 661–672. doi: 10.3923/jm.2008.661.672

Kumar, C. G., and Takagi, H. (1999). Microbial alkaline proteases: from a bioindustrial viewpoint. *Biotechnol. Adv.* 17, 561–594. doi: 10.1016/S0734-9750(99)00027-0

Lanka, S., Anjali, C. H., and Pydipalli, M. (2017). Enhanced production of alkaline protease by *Aspergillus niger* DEF 1 isolated from dairy form effluent and determination of its fibrinolytic ability. *Afr. J. Microbiol. Res.* 11, 440–449. doi: 10.5897/AJMR2016-8379

Laxman, R. S., Sonawane, A. P., More, S. V., Rao, B. S., Rele, M. V., Jogdand, V. V., et al. (2005). Optimization and scale up of production of alkaline protease from *Conidiobolus coronatus*. *Process Biochem.* 40, 3152–3158. doi: 10.1016/j.procbio.2005.04.005

Li, J., Yang, J., Huang, X., and Zhang, K. Q. (2006). Purification and characterization of an extracellular serine protease from *Clonostachys rosea* and its potential as a pathogenic factor. *Process Biochem.* 41, 925–929. doi: 10.1016/j.procbio.2005.10.006

Malathi, S., and Chakraborty, R. (1991). Production of alkaline protease by a new *aspergillus flavus* isolate under solid–substrate fermentation conditions for use as a depilation agent. *Appl. Environ. Microbiol.* 57, 712–716. doi: 10.1128/aem.57.3.712-716.1991

Matkawala, F., Nighojkar, S., Kumar, A., and Nighojkar, A. (2021). Microbial alkaline serine proteases: production, properties and applications. *World J. Microbiol. Biotechnol.* 37, 63–62. doi: 10.1007/s11274-021-03036-z

Mignon, B., Swinnen, M., Bouchara, J. P., Hofinger, M., Nikkels, A., Pierard, G., et al. (1998). Purification and characterization of a 315 kDa keratinolytic subtilisin-like serine protease from *Microsporum canis* and evidence of its secretion in naturally infected cats. *Med. Mycol.* 36, 395–404. doi: 10.1080/02681219880000631

More, S. V., Khandelwal, H. B., Joseph, M. A., and Laxman, R. S. (2013). Enzymatic degumming of silk with microbial proteases. *J. Nat. Fibers* 10, 98–111. doi: 10.1080/15440478.2012.761114

More, S. S., Lakshmi Sridhar, D., Prakash, S. N., Vishwakarma, J., and Umashankar, S. (2013). Purification and properties of a novel fungal alkaline keratinase from *Cunninghamella echinulata*. *Turk J. Biochem.* 38, 68–74. doi: 10.5505/tjb.2013.37928

Mustefa Beyan, S., Venkatesa Prabhu, S., Mumecha, T. K., and Gemeda, M. T. (2021). Production of alkaline proteases using *aspergillus* sp. isolated from *Injera*: RSM–GA based process optimization and enzyme kinetics aspect. *Curr. Microbiol.* 78, 1823–1834. doi: 10.1007/s00284-021-02446-4

Naeem, M., Manzoor, S., Abid, M. U. H., Tareen, M. B. K., Asad, M., Mushtaq, S., et al. (2022). Fungal proteases as emerging biocatalysts to meet the current challenges and recent developments in biomedical therapies: an updated review. *J. Fungi* 8:109. doi: 10.3390/jof8020109

Nagai, K., Suzuki, K., and Okada, G. (1998). Studies on the distribution of alkalophilic and alkali–tolerant soil fungi II: fungal flora in two limestone caves in Japan. *Mycoscience* 39, 293–298. doi: 10.1007/BF02464011

Neelakantan, S., Mohanty, A. K., and Kaushik, J. K. (1999). Production and use of microbial enzymes for dairy processing. *Curr. Sci.* 77, 143–148.

Nehra, K. S., Dhillon, S., Chaudhary, K., and Singh, R. (2002). Production of alkaline protease by *aspergillus* sp. under submerged and solid substrate fermentation. *Indian J. Microbiol.* 42, 43–47.

Niyonzima, F. N., and More, S. (2014). Purification and properties of detergent–compatible extracellular alkaline protease from *Scopulariopsis* spp. *Prep. Biochem. Biotechnol.* 44, 738–759. doi: 10.1080/10826068.2013.854254

Niyonzima, F. N., and More, S. S. (2015). Purification and characterization of detergent–compatible protease from *aspergillus terreus* gr. 3. *Biotech* 5, 61–70. doi: 10.1007/s13205-014-0200-6

Novelli, P. K., Barros, M. M., and Fleuri, L. F. (2016). Novel inexpensive fungi proteases: production by solid state fermentation and characterization. *Food Chem.* 198, 119–124. doi: 10.1016/j.foodchem.2015.11.089

Omrane Benmrad, M., Moujehed, E., Ben Elhoul, M., Zaraî Jaouadi, N., Mechri, S., Rekik, H., et al. (2016). A novel organic solvent–and detergent–stable serine alkaline protease from *Trametes cingulata* strain CTM10101. *Int. J. Biol. Macromol.* 91, 961–972. doi: 10.1016/j.ijbiomac.2016.06.025

Pal, S., Banerjee, R., Bhattacharyya, B. C., and Chakraborty, R. (1996). Application of a proteolytic enzyme in tanneries as a depilating agent. *J. Am. Leather Chem. Assoc.* 91, 59–63.

Palanivel, P., Ashokkumar, L., and Balagurunathan, R. (2013). Production, purification and fibrinolytic characterization of alkaline protease from extremophilic soil fungi. *Int J Pharm. Bio. Sci* 4, 101–110.

Papagianni, M., and Sergelidis, D. (2014). Purification and biochemical characterization of a novel alkaline protease produced by *Penicillium nalgiovense*. *Appl. Biochem. Biotechnol.* 172, 3926–3938. doi: 10.1007/s12010-014-0824-3

Phadatare, S. U., Deshpande, V. V., and Srinivasan, M. C. (1993). High activity alkaline protease from *Conidiobolus coronatus* (NCL 86.8.20): enzyme production and compatibility with commercial detergents. *Enzym. Microb. Technol.* 15, 72–76. doi: 10.1016/0141-0229(93)90119-M

Polgár, L. (2005). The catalytic triad of serine peptidases. *Cell. Mol. Life Sci.* 62, 2161–2172. doi: 10.1007/s00018-005-5160-x

Prolo, T., Izidoro, S. C., de Lima, V. A., Maia, G. A., and Knob, A. (2020). Adding value to a recalcitrant and problematic waste: the use of dog hair for fungal keratinolytic protease production. *Biocatal. Biotransformation* 38, 343–356. doi: 10.1080/10242422.2020.1746770

Pundir, R. K., Rana, S., and Tyagi, H. (2012). Studies on compatibility of fungal alkaline protease with commercially available detergents. *Int. J. Modern Biochem.* 1, 41–56.

Ram, R. M., and Yepuru, S. K. (2018). Production of alkaline pro tease from *aspergillus oryzae* isolated from seashore of bay of Bengal. *J. Appl. Nat. Sci.* 10, 1210–1215. doi: 10.31018/jans.v10i4.1905

Rani, M. R., Prasad, N. N., and Sambasivarao, K. R. (2012). Optimization of cultural conditions for the production of alkaline protease from a mutant *aspergillus Flavus* AS2. *Asian J. Exp. Biol. Sci.* 3, 565–576.

Rao, M. B., Tanksale, A. M., Ghatge, M. S., and Deshpande, V. V. (1998). Molecular and biotechnological aspects of microbial proteases. *Microbiol. Mol. Biol. Rev.* 62, 597–635. doi: 10.1128/MMBR.62.3.597-635.1998

Rawlings, N. D., and Barrett, A. J. (1993). Evolutionary families of peptidases. *Biochem. J.* 290, 205–218. doi: 10.1042/bj2900205

Rawlings, N. D., and Barrett, A. J. (1995). Evolutionary families of metallopeptidases. *Methods Enzymol.* 248, 183–228. doi: 10.1016/0076-6879(95)48015-3

Rawlings, N. D., Barrett, A. J., and Bateman, A. (2011). Asparagine peptide Lyases: a seventh catalytic type of proteolytic enzymes. *J. Biol. Chem.* 286, 38321–38328. doi: 10.1074/jbc.M111.260026

Rawlings, N. D., Barrett, A. J., Thomas, P. D., Huang, X., Bateman, A., and Finn, R. D. (2018). The MEROPS database of proteolytic enzymes, their substrates and inhibitors in 2017 and a comparison with peptidases in the PANTHER database. *Nucleic Acids Res.* 46, D624–D632. doi: 10.1093/nar/gkx1134

Rawlings, N. D., and Bateman, A. (2019). Origins of peptidases. *Biochimie* 166, 4–18. doi: 10.1016/j.biochi.2019.07.026

Razzaq, A., Shamsi, S., Ali, A., Ali, Q., Sajjad, M., Malik, A., et al. (2019). Microbial proteases applications. *Front. Bioeng. Biotechnol.* 7, 1–20. doi: 10.3389/fbioe.2019.00110

Rodríguez, K. L., Higuera, B. L., and Martínez, S. T. (2017). Induction of proteases secreted by *fusarium oxysporum* f. sp. *Dianthi* in the presence of carnation root cell walls. Biochemical characterization of a serine protease. *J. Plant Pathol.* 99, 609–617.

Rukmi, I., and Purwantisari, S. (2020). The production of alkaline protease from *aspergillus flavus* DUCC K225 on rice bran containing medium. *J. Phys. Conf. Ser.* 1524:012058. doi: 10.1088/1742-6596/1524/1/012058

Savitha, S., Sadhasivam, S., Swaminathan, K., and Lin, F. H. (2011). Fungal protease: production, purification and compatibility with laundry detergents and their wash performance. *J. Taiwan Inst. Chem. Eng.* 42, 298–304. doi: 10.1016/j.jtice.2010.05.012

Seemüller, E., Lupas, A., Stock, D., Löwe, J., Huber, R., and Baumeister, W. (1995). Proteasome from *Thermoplasma acidophilum*: a threonine protease. *Science* 268, 579–582. doi: 10.1126/science.7725107

Shankar, S., More, S. V., and Laxman, R. S. (2010). Recovery of silver from waste X–ray film by alkaline protease from *Conidiobolus coronatus*. *J. Sci. Eng. Technol.* 6, 60–69. doi: 10.3126/kuset.v6i1.3311

Shankar, S., Rao, M., and Laxman, R. S. (2011). Purification and characterization of an alkaline protease by a new strain of *Beauveria* sp. *Process Biochem.* 46, 579–585. doi: 10.1016/j.procbio.2010.10.013

Sharma, N. (2019). A review on fungal alkaline protease. *J. Emerg. Technol. Innov. Res.* 6, 261–273. doi: 10.1729/Journal.22354

Sharma, M., Gat, Y., Arya, S., Kumar, V., Panghal, A., and Kumar, A. (2019). A review on microbial alkaline protease: an essential tool for various industrial approaches. *Ind. Biotechnol.* 15, 69–78. doi: 10.1089/ind.2018.0032

Sharma, M., Sharma, M., and Rao, V. M. (2011). In vitro biodegradation of keratin by dermatophytes and some soil keratinophiles. *Afr. J. Biochem. Res.* 5, 1–6.

Sindhu, R., Suprabha, G. N., and Shashidhar, S. (2009). Optimization of process parameters for the production of alkaline protease from *Penicillium godlewskii* SBSS 25 and its application in detergent industry. *Afr. J. Microbiol. Res.* 3, 515–522.

Souza, P. M., Bittencourt, M. L., Caprara, C. C., Freitas, M. D., Almeida, R. P., Silveira, D., et al. (2015). A biotechnology perspective of fungal proteases. *Braz. J. Microbiol.* 46, 337–346. doi: 10.1590/S1517-838246220140359

Suresh, A. J., and Dass, R. S. (2022). "Cold-adapted fungi: evaluation and comparison of their habitats, molecular adaptations and industrial applications" in *Survival Strategies in Cold-Adapted Microorganisms* (Singapore: Springer), 31–61.

Suryawanshi, H. K., and Pandya, N. D. (2017). Screening, identification of alkaline proteases producing fungi from soil of different habitats of Amalner Tahsil [Maharashtra] and their applications. *Int. J. Appl. Sci. Biotechnol.* 5, 397–402. doi: 10.3126/ijasbt.v5i3.18304

Sutar, I. I., Srinivasan, M. C., and Vartak, H. G. (1992). Production of an alkaline proteinase from *Conidiobolus coronatus* and its use to resolve DL–phenylalanine and DL–phenylglycine. *World J. Microbiol. Biotechnol.* 8, 254–258. doi: 10.1007/BF01201873

Tremacoldi, C. R., and Carmona, E. C. (2005). Production of extracellular alkaline proteases by *aspergillus clavatus*. *World J. Microbiol. Biotechnol.* 21, 169–172. doi: 10.1007/s11274-004-2724-0

Tunga, R., Shrivastava, B., and Banerjee, R. (2003). Purification and characterization of a protease from solid state cultures of *Aspergillus parasiticus*. *Process Biochem.* 38, 1553–1558. doi: 10.1016/S0032-9592(03)00048-7

Ueda, M., Kubo, T., Miyatake, K., and Nakamura, T. (2007). Purification and characterization of fibrinolytic alkaline protease from *fusarium* sp BLB. *Appl. Microbiol. Biotechnol.* 74, 331–338. doi: 10.1007/s00253-006-0621-1

Verma, S., Dixit, R., and Pandey, K. C. (2016). Cysteine proteases: modes of activation and future prospects as pharmacological targets. *Front. Pharmacol.* 7, 1–12. doi: 10.3389/fphar.2016.00107

Xiao, Y. Z., Wu, D. K., Zhao, S. Y., Lin, W. M., and Gao, X. Y. (2015). Statistical optimization of alkaline protease production from *Penicillium citrinum* YL–1 under solid–state fermentation. *Prep. Biochem. Biotechnol.* 45, 447–462. doi: 10.1080/10826068.2014.923450

Zanphorlin, L. M., Facchini, F. D., Vasconcelos, F., Bonugli-Santos, R. C., Rodrigues, A., and Sette, L. D. (2010). Production, partial characterization, and immobilization in alginate beads of an alkaline protease from a new thermophilic fungus *Myceliophthora* sp. *J. Microbiol.* 48, 331–336. doi: 10.1007/s12275-010-9269-8

frontiers | Frontiers in Microbiology

TYPE Review
PUBLISHED 27 April 2023
DOI 10.3389/fmicb.2023.1132770

Check for updates

OPEN ACCESS

EDITED BY
Durgesh K. Jaiswal,
Savitribai Phule Pune University,
India

REVIEWED BY
Parvaze Wani,
Crescent University, Abeokuta,
Nigeria
Ravindra Kumar,
Indian Council of Agricultural Research (ICAR),
India
Manish Kumar,
Amity University, Gwalior,
India

*CORRESPONDENCE
Mohammad Shahid
✉ shahidfaiz5@gmail.com
Udai B. Singh
✉ udaiars.nbaim@gmail.com
Prakash Singh
✉ prakash201288@gmail.com

†These authors have contributed equally to this work and share first authorship

SPECIALTY SECTION
This article was submitted to Microbiotechnology, a section of the journal Frontiers in Microbiology

RECEIVED 27 December 2022
ACCEPTED 20 March 2023
PUBLISHED 27 April 2023

CITATION
Shahid M, Singh UB, Khan MS, Singh P, Kumar R, Singh RN, Kumar A and Singh HV (2023) Bacterial ACC deaminase: Insights into enzymology, biochemistry, genetics, and potential role in amelioration of environmental stress in crop plants. *Front. Microbiol.* 14:1132770. doi: 10.3389/fmicb.2023.1132770

COPYRIGHT
© 2023 Shahid, Singh, Khan, Singh, Kumar, Singh, Kumar and Singh. This is an open-access article distributed under the terms of the Creative Commons Attribution License (CC BY). The use, distribution or reproduction in other forums is permitted, provided the original author(s) and the copyright owner(s) are credited and that the original publication in this journal is cited, in accordance with accepted academic practice. No use, distribution or reproduction is permitted which does not comply with these terms.

Bacterial ACC deaminase: Insights into enzymology, biochemistry, genetics, and potential role in amelioration of environmental stress in crop plants

Mohammad Shahid[1*†], Udai B. Singh[1*†], Mohammad Saghir Khan[2], Prakash Singh[3*], Ratan Kumar[4], Raj Narian Singh[5], Arun Kumar[6] and Harsh V. Singh[1]

[1]Plant-Microbe Interaction and Rhizosphere Biology Lab, ICAR-National Bureau of Agriculturally Important Microorganisms (NBAIM), Mau, Uttar Pradesh, India, [2]Department of Agricultural Microbiology, Faculty of Agricultural Sciences, Aligarh Muslim University, Aligarh, Uttar Pradesh, India, [3]Department of Plant Breeding and Genetics, Veer Kunwar Singh College of Agriculture, Bihar Agricultural University, Dumraon, India, [4]Krishi Vigyan Kendra, Rohtas, Bihar Agricultural University, Bikramganj, Bihar, India, [5]Directorate of Extension Education, Bihar Agricultural University, Bhagalpur, Bihar, India, [6]Swamy Keshwanand Rajasthan Agriculture University, Bikaner, Rajasthan, India

Growth and productivity of crop plants worldwide are often adversely affected by anthropogenic and natural stresses. Both biotic and abiotic stresses may impact future food security and sustainability; global climate change will only exacerbate the threat. Nearly all stresses induce ethylene production in plants, which is detrimental to their growth and survival when present at higher concentrations. Consequently, management of ethylene production in plants is becoming an attractive option for countering the stress hormone and its effect on crop yield and productivity. In plants, ACC (1-aminocyclopropane-1-carboxylate) serves as a precursor for ethylene production. Soil microorganisms and root-associated plant growth promoting rhizobacteria (PGPR) that possess ACC deaminase activity regulate growth and development of plants under harsh environmental conditions by limiting ethylene levels in plants; this enzyme is, therefore, often designated as a "stress modulator." TheACC deaminase enzyme, encoded by the *AcdS* gene, is tightly controlled and regulated depending upon environmental conditions. Gene regulatory components of *AcdS* are made up of the LRP protein-coding regulatory gene and other regulatory components that are activated *via* distinct mechanisms under aerobic and anaerobic conditions. ACC deaminase-positive PGPR strains can intensively promote growth and development of crops being cultivated under abiotic stresses including salt stress, water deficit, waterlogging, temperature extremes, and presence of heavy metals, pesticides and other organic contaminants. Strategies for combating environmental stresses in plants, and improving growth by introducing the *acdS* gene into crop plants *via* bacteria, have been investigated. In the recent past, some rapid methods and cutting-edge technologies based on molecular biotechnology and omics approaches involving proteomics, transcriptomics, metagenomics, and next generation sequencing (NGS) have been proposed to reveal the variety and potential of ACC deaminase-producing PGPR that thrive under external stresses. Multiple stress-tolerant ACC deaminase-producing PGPR strains have demonstrated great promise in providing plant resistance/tolerance to various stressors and, therefore, it could be advantageous over other soil/plant microbiome that can flourish under stressed environments.

KEYWORDS
environnemental stress, ethylene, plants, PGPR, ACC deaminase, mode of action

Introduction

Plant growth and productivity are affected by myriad complex factors, both physiological and environmental, including plant genotype, soil physical and chemical characteristics, availability of nutrients, and other variables (Schwachtje et al., 2019). In addition, crop growth and yield may be stressed by several biotic and abiotic factors, i.e., salinity, drought, temperature, mechanical wounding, waterlogging, organic contaminants, heavy metals and other xenobiotics (Gupta et al., 2013; Gull et al., 2019). As a consequence of these factors, ~35–50% yield loss has beed reported so far in major crops globally (Stallworth et al., 2020). Abiotic stresses are therefore considered as a primary influence affecting agricultural production worldwide.

Global food supplies must be increased to fulfil the increasing demands of rapidly-growing populations (Place et al., 2017). Response to several biotic and nutritional challenges in plant husbandry can be resolved using chemical pesticides, fertilizers, and other agrochemicals. However, using non-biological methods to address problems posed by abiotic stressershas its share of difficulties. Plants respond to external challenges by altering production of certain hormones, which promotes the synthesis of stress-related proteins that afford protection against the negative effects of stressors (Gupta et al., 2020). In this regard, ethylene is considered as the most common phytohormone mediating stress response in many crop plants (Tiwari et al., 2020). In contrast, when ethylene production exceeds a certain threshold, it becomes "stress ethylene." Excessive levels of ethylene adversely affect proliferation of roots, shoots, and other yield parameters and, thus, hamper overall plant performance (Klay et al., 2018; Mog et al., 2018). The detrimental impacts of the high ethylene levels can be reduced by various soil/plant-colonizing microbiomes that contain the essential enzyme ACC deaminase (Glick, 2014; Saikia et al., 2018). ACC deaminase (ACCD) converts the harmful form of ethylene to a non-toxic state (Das and Osborne, 2018). The ACCD decreases ethylene levels in plants by breaking down ACC into α-ketobutyrate ($C_4H_6O_3$) and ammonia (Bharti and Barnawal, 2019) which in turn allow roots/shoots or entire plants to grow normally (Glick, 2014). Thus, ACCD permits plants to thrive in challenging environments by reducing harmful concentrations of ethylene (Han et al., 2015; Ravanbakhsh et al., 2017; Sarkar et al., 2018a,b). ACC serves as the originator of ethylene in plants (Ouaked et al., 2003). "Induced systemic tolerance" refers to the inherent characteristics of assigning tolerance to abiotic stressors through ACCD activity and some redundant PGPR processes to alleviate stresses in host plants (Arya et al., 2018; Carlson et al., 2020). Therefore, PGPR equipped with ACCD activity are essential organisms that play a major role in the reduction/mitigation of the toxic effects of several environmental stressors such as salinity, drought, heavy metals, and organic pollutants (Table 1). The production of the stress hormone, ethylene, and its impact on plants while growing under stress has previously been explained. Taking relevant papers into account, the present review describes the importance of ethylene in plant physiology and the function of bacterial ACC deaminase in reducing stress-induced ethylene levels in plants, thereby circumventing the negative effects of environmental stressors.

Ethylene: Biosynthesis, physiology, regulation, and stress response in plants

Ethylene, the smallest and simplest gaseous phytohormone produced by plants, regulates a suite of biological and functional processes in plants (Light et al., 2016; Fernandez-Moreno and Stepanova, 2019). Processes regulated by ethylene include seedling germination, ripening/maturation of fruit, senescence, development of root hairs and nodules, elongation of roots, and epinasty (Zhang et al., 2016; Zhu et al., 2016; Sun et al., 2019; Figure 1).

Ethylene production in plants is primarily influenced by environmental factors and depends on the degree and intensity of environmental variables. The identification of ethylene as a plant growth regulator was revealed by early leaf shedding, geotropism of etiolated pea seedlings when exposed to lighting gas, and the ripening/maturation of plant organs when exposed to kerosene combustion gas (Pierik et al., 2006; Glick et al., 2007a).

A wide array of biotic and abiotic factors (e.g., salinity, drought, waterlogging, flooding, agrochemicals, pesticides, heavy metals, organic and inorganic pollutants, phytopathogens) inducesethyleneproduction in plants (Gontia-Mishra et al., 2014). Henceforth, the ethylene produced under such environmental stresses is regarded as "stress ethylene" (Glick, 2014). The stress ethylene triggers genes to be transcribed and further expressed, resulting in plant senescence. Ethylene biosynthesis in plants follows a relatively straightforward system where methionine is converted to S-adenosyl methionine (SAM) by the enzyme SAM synthetase that is subsequently used as a substrate by ACC synthase to generate 1-aminocyclopropane-1-carboxylic acid (ACC). The ACC generated in this process acts as precursor for ethylene production by the action of enzyme ACC oxidase.

ACCD: Biochemical properties and mode of action

When ACC deaminase was identified in soil microorganisms for the first time, it was demonstrated to transform ACC to ammonia (NH_3) and α-ketobutyrate, which were subsequently metabolized by microbes (Honma and Shimomura, 1978). ACCD is a pyridoxal PO_4^{3-}-dependent enzyme. In order to activate the enzyme, about 3.0 mol of pyridoxal PO_4^{3-} (enzyme bound) mol^{-1} of enzyme or 1.0 mol $trimeric^{-1}$subunitis required (Honma, 1985; Karthikeyan et al., 2004). This enzyme was first purified from *Pseudomonas* sp. strain ACP; however, strains of *P. chloroaphis* 6G5 (Klee et al., 1991) and *P. putida* GR12-2 (Jacobson et al., 1994) have also been utilized for partial purification of ACCD. The molecular mass and shape of

TABLE 1 Examples of ACC deaminase producing PGPR.

PGPR strains	Source	ACC deaminase activity (nmol α-ketobutyrate mg protein^{-1} h^{-1})	Reference
Achromobacter xylosooxidans A551	*Pisum sativum* rhizosphere	400 ± 4.0	Belimov et al. (2009)
Burkholderia cepacia PSBB1	*Vicia faba* rhizosphere	–	Shahid and Khan (2018)
Pseudomonas putida UW4	–	3,030 ± 60	Hontzeas et al. (2006)
Rhizobium leguminosarum 128C53K	*Pisum sativum* rhizosphere	5.0 ± 1.0	Belimov et al. (2005)
Serratia proteamaculans	Rhizosphere region of salt-affected *T. aestivum* (L.)	276 ± 00	Zahir et al. (2009)
Serratia marcescens BC-3	Rhizosphere soils of salt and petroleum amended *E. crusgali* plants	38,520 ± 00	Liu et al. (2015)
Bacillus pumilus SB1-ACC3	*Oryza sativa* (L.) rhizosphere	1,460 ± 00	Bal et al. (2013)
Bacillus licheniformis B2r	Salinity-stressed rhizosphere soils	860 ± 00	Chookietwattana and Maneewan (2012)
Bacillus sp. MR4	Rhizosphere soils of *Arabidopsis thaliana* (L.) and *Festuca rubra* (L.)	15,920 ± 00	Grobelak et al. (2018)
Bacillus cereus LB1	Tissue of *Carthamus tinctorius* (L.)	2,400 ± 00	Hemida and Reyad (2018)
Bacillus aerius SB1	Tissue of *Carthamus tinctorius* (L.)	1,800 ± 00	Hemida and Reyad (2018)
Pseudomonas sp. R3	Rhizosphere soil of *Arabidopsis thaliana* (L.) and *Festuca rubra* (L.)	23,490 ± 00	Grobelak et al. (2018)
Mesorhizobium ciceri strain LMS-1 (pRKACC)	–	2,305 ± 00	Nascimento et al. (2012)
Sinorhizobium meliloti KYA71 and KYA40	Soil and Water Research Institute (Iran)	326,136 ± 00	Khosravi et al. (2014)
Serratia ficaria	Salinity-stressed rhizosphere soils	326 ± 00	Nadeem et al. (2010)
Pseudomonas sp. ST3	Rhizosphere soil of *Ipomoea aquatica* (L.)	900 ± 00	Trung et al. (2016)
Enterobacter aerogenes	Rhizosphere soil of salt-treated *Zea mays* (L.)	341 ± 00	Nadeem et al. (2007)
Enterobacter sp. CS1	-	170 ± 00	Huang et al. (2013)
Enterobacter cloacae ZNP-4	*Ziziphus nullifera* (L.) rhizosphere soil	188.90 ± 9.3	Singh et al. (2022)
Pseudomonas sp. TR15a	Contaminated rhizosphere of *Trifoliumrepens* (L.)	53.74 ± 00	Kumar et al. (2021)
Bacillus amyloliquefaciens	Pearl millet rhizosphere	2196.23 ± 00	Murali et al. (2021)
Ensifer adhaerens KS23	Rhizosphere soil of leguminous crop	174.2 ± 00	Katiyar et al. (2021)
Achromobacter sp.	Rhizosphere soil	4.90 ± 00	Sun et al. (2022)
Streptomyces hydrogenans DH16		363 ± 00	Kaur and Manhas (2022)

enzyme isolated from all three sources appear to be identical. *Pseudomonas* sp. strain ACP was found to have a native size of 110–112 KDa, while *P. putida* GR12-2 had a native size of 105 KDa. In nature, this enzyme is found in the trimeric form with ~36,500 Da mass subunit.

At pH 6.0 and pH 9.0, the absorption maxima of pure ACC deaminase from *Pseudomonas* sp. were 416 and 326 nm, respectively (Honma, 1985). The 326 nm band observed at pH 9.0 could represent the activation form of ACCD to which inhibitors and substrates strongly bind (Jacobson et al., 1994). The published range of K_m values for enzyme extracts from various bacteria at pH 8.5 is 1.5–17.4 mM, indicating that the enzyme has a low affinity for ACC. Following second-order kinetics, the total efficiency ($k_{cat}/_{km}$) of ACC deaminase is around 690 $M^{-1}S^{-1}$. The ACC deaminase K_m value for 1-amino cyclopropane 1-carboxylate has been established using enzyme extracts from microorganisms at pH 8.5 (Klee et al., 1991). Several bacterial species produced ACCD enzyme and their activity was evaluated over a broad pH range and at pH 8.0 to 8.5 showing highest activity. The optimal temperature for ACC deaminase activity is 30°C (Glick et al., 1998).

Because ACC deaminase is an inducible enzyme, its production is triggered when its substrate, ACC, is present. In *P. putida* strain GR12-2 and *Pseudomonas* sp. strain ACP GR12-2, the lowest level of substrate for induction was determined to be 100 nM. ACCD induction is a lengthy and complex procedure. Within a few hours of incubation with the substrate, the enzyme expresses its activity which, steadily declines thereafter (Jha et al., 2012). In a minimal medium supplied with $(NH_4)_2SO_4$ (ammonium sulfate) as Nsource, the basal level of enzyme activity was observed. It was further demonstrated that growing bacteria in a minimal medium that contained ACC as

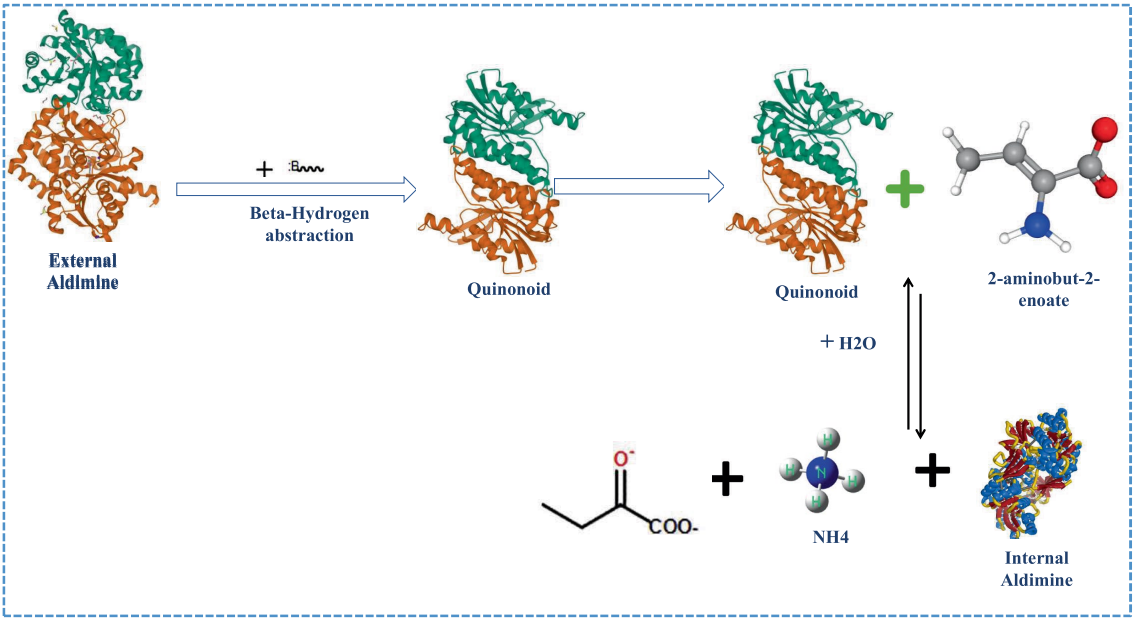

FIGURE 1
Elucidation of route1 (Direct β-hydrogen extraction) for ACC metabolism by ACC deaminase.

the only N source led to increased enzyme activity, suggesting that the substrate ACC had a direct relationship with induction of enzyme activity (Honma, 1983). Expression of ACCD and the activation of other amino acids such as *L*-alanine, *DL*-alanine, and *D*-serine, increase to a lesser degree than in the case of ACC. Furthermore, both ACC and amino-isobutyric acid ($C_4H_9NO_2$) produced a similar degree of enzyme activity in *Pseudomonas* sp. strain ACP (Honma, 1983). According to Glick et al. (1998), ACC is released from plant roots or seeds, ingested by soil microbiota, and hydrolysed to ammonia and α-ketobutyrate. The quantum of ACC outside the plant root, however, decreases due to ACC absorption and hydrolysis. The equilibrium between levels of internal and external ACC is also maintained by the exudation of excess ACC into the rhizosphere. As a result, a reduction in ACC levels reduces the production of stress hormone ethylene in host plants and stimulating growth of the plant (Glick et al., 1998).

L-isomers of amino acids such as *L*-alanine, *L*-serine, *L*-homoserine, and *L*-aminobutyric acid inhibit ACC deaminase competitively, with *L*-alanine and *L*-serine exhibiting greatest inhibition. ACC deaminase isolated from *Pseudomonas* sp. can also use ACC-related compounds like 2-alkyl-ACC and vinyl-ACC as substrates. Strain ACP, although the enzyme has a peculiar preference for *D*-amino acids, being inactive with any *L*-amino acids or derivatives. According to NMR research, a proton is removed from the β-carbon of *D*-alanine but not from the *L*-isomer. These findings support the stero-specific breakage of the cyclopropane ring during ACC deamination, which explains the deamination of *D*-amino acids and many substituted *D*-alanines. The iodoacetamide derivative 1,5 N-iodoacetamidoethyl-1-aminonapthalene-5-sulfonic acid (1,5-I-AEDANS) inactivates ACC deaminase more effectively in the presence of *D*-alanine than iodoacetamide. During inactivation, a thiol group in cysteine residue 162 is altered, as it is the aldimine connection between pyridoxal phosphate and lysine residue 51 (Honma et al., 1993). The primary feature of the ACC deaminase-catalyzed process is the opening of the ACC cyclopropane ring. The most likely method for cleaving the cyclopropane bond appear to be nucleophilic addition and elimination, although the full reaction mechanism is unknown (Thibodeaux and Liu, 2011).

Enzymology of ACC deaminase

The deamination of ACC, the precursor of the gaseous phytohormone ethylene, is carried out by the tryptophan synthase beta (β) superfamily enzyme ACC deaminase (EC 3.5.99.7), which is dependent on the pyridoxal 5′-phosphate (PLP) molecule. To initiate the ACC deaminase enzyme activity, 1 mol pyridoxal phosphate (vitamin B6) works as a firmly bound cofactor (Singh et al., 2015). It is found in the cytoplasm of bacterial cells and has a molecular mass of 35–42 kDa (Gamalero and Glick, 2015). PLP is thought to be an inducible enzyme that requires a substrate, ACC, at a concentration of <100 nM to activate the process. By switching ACC deaminase-producing bacterial strains from nutrient-rich growth media to minimal media containing ACC as its sole N source, the induction of enzymatic activity by substrate, ACC, is proven. Other amino acids such as *D*-alanine, *L*-alanine, *D*-valine, 2-alkyl-ACC, vinyl-ACC, and 2-aminoisobutyric acid, all of which are similar to ACC in structure and behavior, can also activate ACC deaminase. Furthermore, 2-aminoisobutyric acid has the same ability to stimulate activity as ACC (Malerba et al., 1996).

Activation of ACCD has been observed at various pH levels. The pH range 8.5–9.0 has, however, been found to impart the highest efficiency for the substrate and competing inhibitors. The *L*-amino acids or their derivatives decrease the activation of ACC deaminase. At pH 9.0, the ACC deaminase absorption spectra showed the strongest band at 326 nm. The activity of *Pseudomonas putida* strain GR12-2 ACC deaminase was reported to be highest at 30°C (Jacobson

et al., 1994). At pH 8.5, enzyme K_m value ranged from 1.5 to ~17.4 mM, indicating that it does not have a strong affinity for ACC (Hontzeas et al., 2004). The enzyme has a catalytic efficiency of roughly 690 M^{-1} S^{-1} ($k_{cat/km}$) (Klee et al., 1994). Because ACC oxidase has a stronger affinity for ACC than ACC deaminase, the lower $K_m$values indicate that ACC deaminase should be present in higher concentrations (100–1,000 fold) in order to utilize the ACC substrate before ACC oxidase and hence reduce ethylene levels (Glick et al., 1998).

Mechanism of ACC deaminase enzymatic reaction

Stressed plants generate ACC, which is hydrolyzed by the microbial enzyme ACC deaminase to α-ketobutyrateand ammonia, thus reducing stress-induced ethylene and related growth inhibition. The elimination reaction and addition of nucleophiles that breaks the cyclopropane ring is the fundamental feature of the ACC deaminase-catalyzed second-order process (Glick et al., 2007a,b). Two possible mechanisms by which ACC deaminase carried out the deamination of its substrate ACC (Walsh et al., 1981; Zhao et al., 2003) include: (i) Direct β-hydrogen extraction in whichLys-mediated hydrolytic reactions break the cyclopropane ring when a hydrogen atom is extracted from the ACC substrate (Figure 1); and (ii) Nucleophilic addition followed by β-hydrogen extraction where ACCcarbon is attacked nucleophilically, and the cyclopropane ring is opened *via* *Lys*51-mediated hydrogen abstraction. The internal aldimine (imine analogue of aldehyde group) is located between the ACC deaminase lysine residue and pyridoxal phosphate cofactor. The trans-aldimination process occurs when the ACC amino group displaces the *L*-lysine residue from the enzyme active site, leading to the production of external aldimine *via* an aminyl intermediate that is present in both proposed pathways (Hontzeas et al., 2006). In route 1, a Lys basic residue on an external aldimine removes the methylene proton directly, forming quinonoid, which results in the formation of a new quinonoid molecule by protonation and electronic configuration (Joshi et al., 2012). The process continues with quinonoid nucleophilic attack by basic lysine amino residues, yielding another quinonoid and 2-aminobut-2-enoate, which is then reversibly hydrolyzed to provide 2-oxobutanoate and an ammonium ion, restoring the internal aldimine (Ose et al., 2003). Following the formation of external aldimine, route 2 departs from route 1 by performing a nucleophilic attack on the proton of the β-carbon of ACC (pro-S), resulting in the synthesis of quinonoid, followed by hydrogen removal from the carbon of ACC (pro-R). Following quinonoid production, the steps are identical to route 1 (Ose et al., 2003).

The ACC deaminase gene and its expression

ACC deaminase gene

As previously mentioned, the *AcdS* gene encoding ACC deaminase has been identified in various bacterial and fungal species. ACC deaminase has recently been discovered in a variety of Gram-negative bacteria (Gontia-Mishra et al., 2017), fungi (Rauf et al., 2021), endophytes (Sofy et al., 2021) and rhizobia (Saghafi et al., 2019). An ACC deaminase gene has been identified in several species, notably *R. leguminosarum* bv. *Trifoli* and *Mesorhizobium loti* MAFF303099. The degree of ACC deaminase expression, however, differs from one organism to another. A portion of the *AcdS* gene was amplified and examined in a variety of environmental isolates using a universal pair of primers. Various workers have developed several pairs of primers to identify the presence of the bacterial *AcdS* gene. Only a few bacterial species have had the entire genetic makeup and function of the ACCD gene described (Duan et al., 2013). It has also been discovered that the nucleotide sequences of the *AcdS* gene are very similar to those of two other genes, i.e., *dcyD* and *yedO*, which encode for another PLP-dependent enzyme, D-cysteine sulfhydralase. Earlier studies have shown that certain genes previously thought to code for ACC deaminase activity also code for D-cysteine desulfhydrase (Riemenschneider et al., 2005). Nascimento et al. (2014) used *Pseudomonas* sp. strain UW-4 as a reference to evaluate the key protein residues recognized to be crucial for ACC deaminase function, including *Leu*322, *Glu*296, *Ser78*, *Tyr*295 and *Lys*51. Any alteration in residues at certain sites was considered to indicate D-cysteine desulfhydrase.

With few exceptions, the *AcdS* gene in the majority of bacterial species is chromosomal DNA-borne. In symbiotic bacteria *M. loti* (symbiont of *lotus* spp.), the ACC deaminase gene is associated with nitrogen fixation genes and might be regulated by *NifA*, which is known to activate *nif* gene expression in association with the product of *rpoN* gene (Ma et al., 2003a). Only a small fraction of the putative *AcdS* gene has been shown to encode active enzyme (Glick et al., 2013).

Regulation of ACC deaminase

AcdS is highly controlled, whose expression varies with O_2level, quantity of substrate, and product accumulation. With few exceptions, regulation of the *AcdS*gene in various bacterial taxa is poorly understood. Li et al. (2000) presented the model for regulating ACC deaminase genes in *P. putida* strain UW-4. Regulatory elements for the expression of ACC deaminase gene consist of regulatory gene *AcdR* located 5′ upstream of ACC deaminase structural gene (*AcdS*), promoter regions for binding of regulatory proteins like Lrp box for binding of Lrp protein, *AcdB* box for binding regulatory protein *AcdB*, FNR box for binding of fumarate and nitrate reductase protein, and CRP box for binding of cAMP receptor protein (Figure 2). The LRP creates an active octamer in the presence of ACC, which binds to an ACC-*AcdB*complex (Gupta and Pandey, 2019). Glycerophosphoryl diester phosphodiesterase is encoded by the gene dB, which forms a complex with ACC. By attaching to the promoter region of *AcdS*, this triparental complex promotes its transcription. In other bacteria studied for *AcdS* gene expression, *AcdB*has not been demonstrated to play a function. Leucine, which is generated from α-ketobutyrate, a breakdown product of the ACCD-catalyzed process, inhibits expression of the ACC deaminase gene. As the quantity of leucine rises, it favors creation of inactive LRP dimers, which prevents the *AcdS* gene from being transcribed (Figure 2).

The regulatory mechanism that controls *AcdS* expression differs from bacterial species to species. The majority of bacteria have *AcdR* encoding LRP or related sequences, according to results of the IMG database analysis. LRP-like protein and the 70 promoters are also implicated in the regulation of the *AcdS* gene in *Bradyrhizobium japonicum* USDA 110 and *Rhizobium*

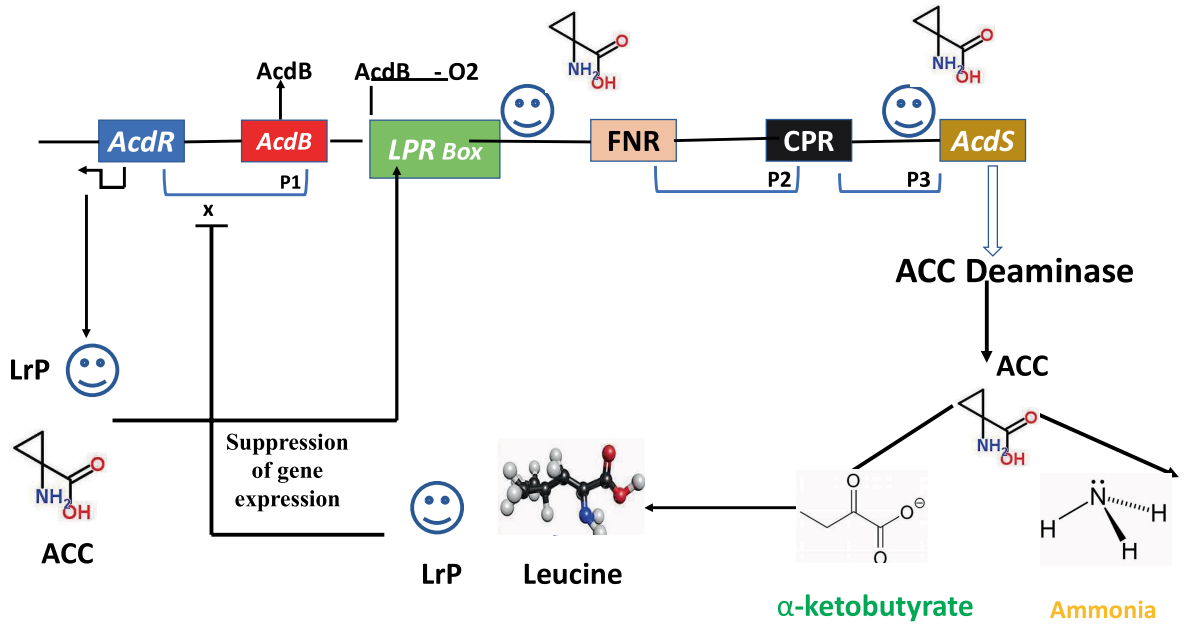

FIGURE 2
Regulatory circuits of *AcdS* gene expression in *Pseudomonas putida* UW4 and related bacteria. *AcdR*, regulatory gene for ACC deaminase; *AcdB*, encoding for glycerophosphoryl diester phosphodiester; LRP, leucine responsive protein; FNR, fumarate nitrate reductase protein; CRP, c-AMP receptor protein; *AcdS*, gene for encoding ACC deaminase.

leguminosarum bv. *Viciae* 128 C53K (Kaneko et al., 2002; Ma et al., 2003a). According to the evolutionary analysis of the *AcdS* and *AcdR*gene evolved in a similar fashion. Instead of the *AcdR* gene, *Burkholderia* sp. CCGE 1002 and *B. phymatum* STM 815 have two copies (megaplasmid and the other on the second chromosome) of the *AcdS* gene. In smaller replicons, these shards of evidence point to chromosomal rearrangement or gene insertion events. Some bacteria, such as *Achromobacterxylosooxidans* A-551 and *Variovoraxparrdoxus* 5C2, lack all the regulatory components as observed in the model bacterium *P. putida* UW4.In *M. loti*, the upstream elements of *AcdS* and *nifH* contain *nifA1* and *nifA2* (regulatory N_2 fixing unit) and σ^{54} RNA polymerase sigma recognition site. It was hypothesized that expression of ACC deaminase in *M. loti* required the symbiotic nitrogen fixing regulatory gene *nifA*2 (Nukui et al., 2006).

The *nifA2* encoded protein *NifA2* interacts with σ^{54} RNA polymerase, favoring *AcdS* transcription. The *nifA1* also affects transcription of the *AcdS* gene to some extent; however, its role in expression of *AcdS* is not fully understood (Nukui et al., 2006; Figure 3). The *AcdS* gene is expressed in root nodules, which minimizes the negative effects of ethylene-induced senescence and increases the concentration of fixed nitrogen in nodules. The activity of ACC deaminase is commonly measured in free-living organisms; however, in *M. loti*, it was only found in symbiotic nodules (Uchiumi et al., 2004).

It must be emphasized that, unlike free-living bacteria, ACC deaminase among nodule-forming rhizobia does not reduce ethylene levels throughout the plant and, hence, cannot be employed to protect plants from various stresses (Ferguson and Mathesius, 2014; Vargas et al., 2017). Furthermore, the amount of ACCD produced in the nodule is only 2–10% of the amount produced by free-living bacteria.

The *GntR* protein coding gene is presentadjacent to the*AcdS* gene in various *Meiothermus* and *Actinobacteria*. This suggests that some downstream components may be involved in ACC deaminase expression control as well. The lack of a promoter region in some members of these genera clearly suggests that control of *AcdS* gene transcription is mediated by the interaction of the *AcdS*gene with a downstream element close to thatgene. *Brenneria* sp. EniD312, *Burkholderiaxenovorans* LB4000, and *Pantoea* sp. are examples of *Actinobacteria* and *Proteobacteria*. At-9B, a transcription regulatory element belonging to the *LysR* family was identified near the *AcdS* gene. However, it is still not clear howACC deaminase specifically functions in such organisms. Therefore, to fully comprehend the mechanism of ACC deaminase regulation and function in various bacterial genera, additional genetic and biochemical research is required.

When triggered by ACC, the putative ACC deaminase gene in *M. loti* MAFF303099 contains no regulatory elements and shows no enzyme activity (Ma et al., 2003b). ACC concentrations as low as 1 M promote ACC deaminase expression in *R. leguminosarum* bv. *Viciae* 128C53K. The introduction of the ACC deaminase and its regulatory gene from *R. leguminosarum* bv. *Viciae* 128C53K to a *S. meliloti* strain resulted in an increase in *Medicago sativa* nodulation efficiency (Ma et al., 2004). Furthermore, in terms of nodulation, the latter strain outperformed the wild type (Ma et al., 2004).

ACC deaminase producing PGPR: Ecological significance

The relevance of PGPR having ACCD activity in reducing the effects of stress ethylene has been extensively studied. When ACCD-producing bacteria are present on the root surface of a stressed plant, they function as ACC reservoirs, reducing ethylene levels in the plant

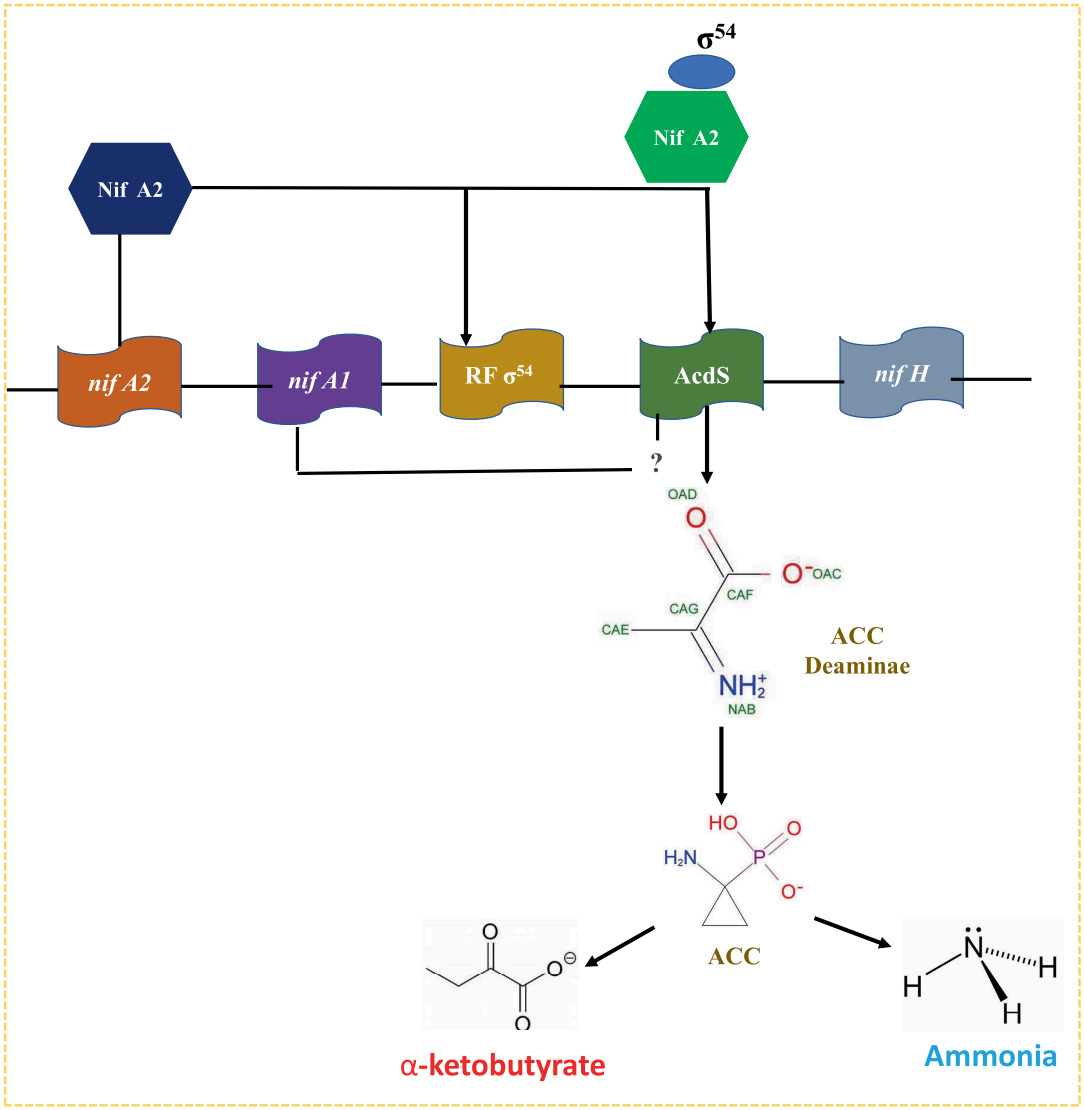

FIGURE 3
A model for *acds* gene regulation in nitrogen fixing *Mesorhizobium* sp. Expression of *acds* is positively regulated by $NIFA_2$ protein which binds to σ^{54} and switch on transcription of *AcdS* gene. $Nifa_1$ is also required in regulation of *AcdS* but its role is not well-understood.

and promoting root development. Because of their extensive root growth, plants inoculated with ACCD harboring PGPR may have better tolerance to a variety of environmental challenges. Several environmental stresses (salinity, flooding, extreme temperatures, heavy metal toxicity, water deficit, nutrient deficiency, and pathogenicity) are the key limiting factors for agricultural production and productivity across the globe. It is presumed that global climate change might augment the occurrence and magnitude of environmental stresses, i.e., abiotic and biotic in the near future (Saleem et al., 2007; Timmusk et al., 2011). These stresses cause significant reduction in the crop growth and yield of stressed plants. It is well established that ethylene production increased significantly under environmental stressed condition especially in stress-sensitive crop varieties. This is commonly known as "stress ethylene" produced as a consequence of abiotic and biotic stresses. On the other hand it is well known that the ACC deaminase-producing organisms were much abundant in the rhizosphere of wild barley (*Hordeum spontaneum*) growing in a stressed environment than they were in a similar (nearby) less stressed environment (Timmusk et al., 2011). Under stresses conditions, rhizospheric and endophytic bacterial/microorganisms produces ACC deaminase which break the ACC (prerequisite of ethylene production) to α-ketobutyrate and ammonia and thereby diminishes level of "stresses ethylene" in the stressed host plants. Few reports indicated that *Methylobacterium* spp. (phytopathogenic in nature) modulate plant growth and development by decreasing environmental stress, immobilizing heavy metals, degrading toxic organic compounds and even inhibiting plant pathogens (Reinhold-Hurek and Hurek, 2011; Brader et al., 2014; Santoyo et al., 2016; Shahzad et al., 2017; Ek-Ramos et al., 2019). A number of bacteria have been discovered in soil/rhizosphere that can utilize ACC as a sole source of nitrogen, are capable of alleviating different environmental stresses, and can support improved growth and overall performance of agricultural crops (Chauhan et al., 2017; Figure 4). Plant synthesis of ethylene is also regarded as a stress response, and is closely linked

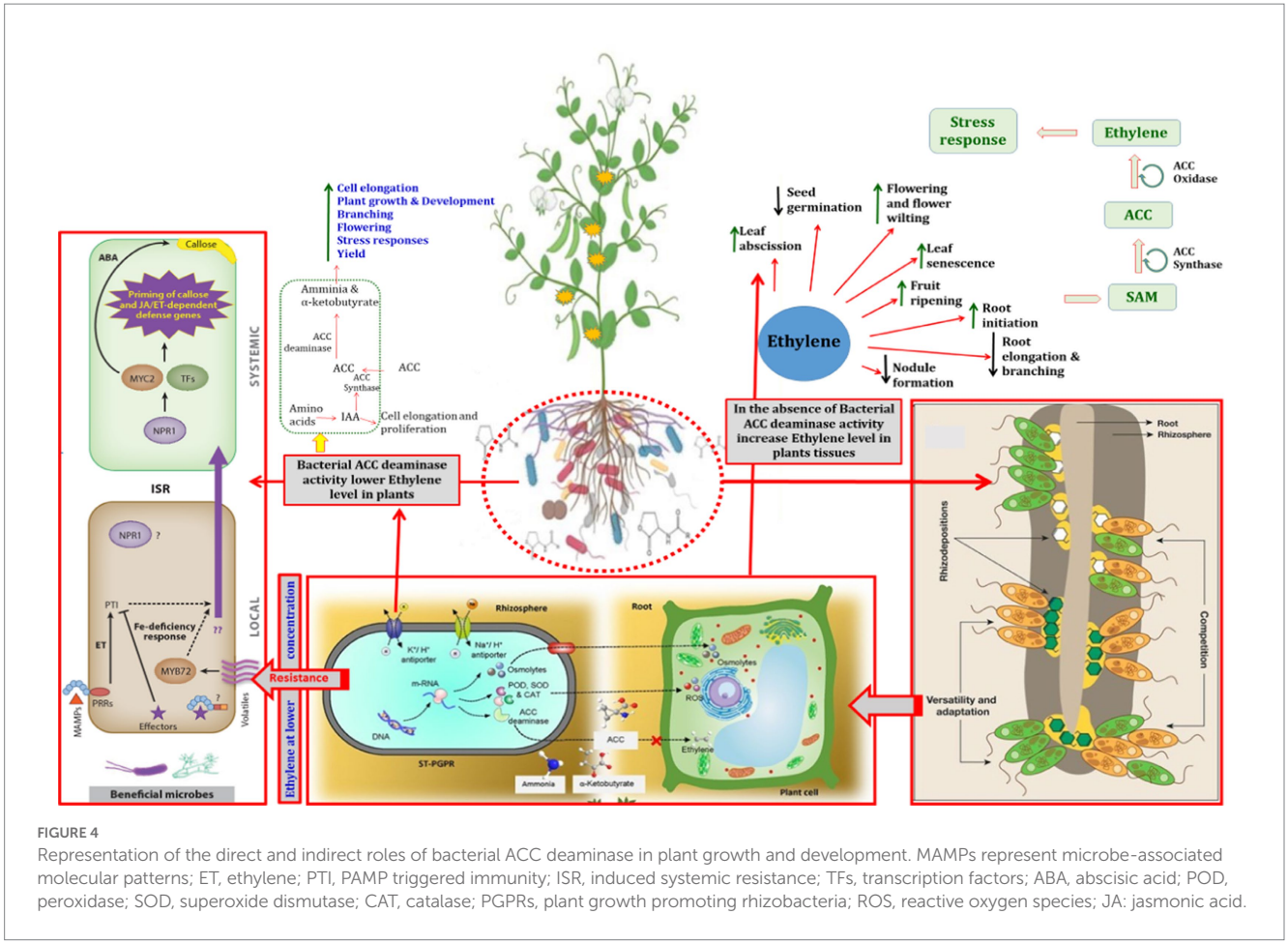

FIGURE 4
Representation of the direct and indirect roles of bacterial ACC deaminase in plant growth and development. MAMPs represent microbe-associated molecular patterns; ET, ethylene; PTI, PAMP triggered immunity; ISR, induced systemic resistance; TFs, transcription factors; ABA, abscisic acid; POD, peroxidase; SOD, superoxide dismutase; CAT, catalase; PGPRs, plant growth promoting rhizobacteria; ROS, reactive oxygen species; JA: jasmonic acid.

to a variety of stress factors including as waterlogging, salinity, presence of heavy metals, and nutrient deficiencies (Dimkpa et al., 2009). It may be possible to apply phytoremediation at contaminated sites by taking advantage of the variation in ACC deaminase activity among microbial species under extreme environmental conditions (Glick, 2005). By biotransforming toxic substances, rhizodegradation mediated by root exudates, and/or detoxification of heavy metals, ACC deaminase-producing bacteria support plants in phytoremediation and enable host plants to thrive under challenging conditions (Qin et al., 2014). By expanding the plant root system and improving root access to soil, ACC deaminase rhizospheric bacterial populations can accelerate rhizo-remediation (Kalsoom et al., 2022). With modified root structure and architecture, inorganic pollutants are more effectively absorbed by the plant. According to Belimov et al. (2005), increased root growth was positively correlated with increased bacterial ACC deaminase activity when cadmium accumulated in plant tissue. Synthesis of minimal quantities of ethylene in leguminous plants has been shown to disrupt the *Nod* factor involved in the signal transduction pathway, which was prevented by rhizobial inoculation (Guinel, 2015). As a result, PGPR-produced ACC deaminase shields plants from the detrimental effects of ethylene when exposed to abiotic stress (Sapre et al., 2018a,b). Some widely acclaimed bacterial genera synthesizing ACC deaminase include *Achromobacter* (Sun et al., 2022), *Brevibacterium linens* (Choi et al., 2022), *Bacillus amyloliquefaciens* (Murali et al., 2021), *Ensiferadhaerens* (Katiyar et al., 2021), *Variovorax* sp. (Bessadok et al., 2020), *Enterobacter* sp. (Sagar et al., 2020), *Rhizobium* (Saghafi et al., 2019), *Bradyrhizobium* (Greetatorn et al., 2019), *Pseudomonas* (Nascimento et al., 2019), *Bacillus* (Din et al., 2019), *Burkholderia*, *Enterobacter*, *Serratia* (Zafar-ul-Hye et al., 2019), *Azotobacter* (Rizvi and Khan, 2018), *Achromobacter* (Shahid et al., 2019a,b), and *Acinetobacter*, *Alcaligenes* (Gontia-Mishra et al., 2017). Table 1 lists certain PGPR-containing ACC deaminase activity (ACCD) positive bacteria.

Biochemistry of ACC deaminase

ACC deaminase is a multimeric enzyme in the tryptophan synthase β-superfamily of pyridoxal phosphate-binding proteins (Glick et al., 2007a,b; Gamalero and Glick, 2015) and is cytoplasmically localized. It has a subunit of mass of ~35–42kD, whereas its natural size is between 100 and 112 kD (Raghuwanshi and Prasad, 2018). This enzyme does not have high affinity for the substrate (1.5–6.0 mM). As a co-factor, pyridoxal phosphate is required for ACC deaminase activity (Glick et al., 2007a,b), and is required for activity of ACC synthase, which catalyzes the synthesis of ACC. Enzyme ACCD exists in the microbial community in very low quantities, and in comparison, to ACC deaminase, ACC oxidase has a substantially higher affinity for ACC (Singh et al., 2015). The level of ethylene in bacterial species depends primarily on activities of ACC oxidase and ACC deaminase (Glick, 2014). Amino acids such as *L*-alanine, *DL*-alanine, and *DL*-valine also stimulate enzyme activity to a modest degree, whereas 4-aminobutanoic acid can stimulate enzyme activity to about the same degree as ACC (Honma, 1983; Raghuwanshi and Prasad, 2018). At pH

8.5, the substrate ACC, as well as the competing inhibitors *L*-alanine and *L*-serine has maximum affinity (Hontzeas et al., 2006; Stress, 2018). The *acdS* genes present in certain bacteria and numerous fungi belonging to different genera are thought to have originated from a collective progenitor (Nascimento et al., 2014). Vertical gene transfer is widespread in many bacteria, while horizontal gene transfer, such as inter-kingdom transfer, also occurs occasionally. The structural genes (*acdS*) and regulatory genes (*acdR*) of ACC deaminase genes have been reported in numerous rhizobacterial groups including endophytic, rhizospheric and root nodulating rhizobia such as *Rhizobium* spp. (Kumar et al., 2016), *Bradyrhizobium* spp. (Greetatorn et al., 2019), *Mesorhizobium* spp. (Senthilkumar et al., 2016) and non-rhizobial groups such as *Burkholderia* spp. (Sarkar et al., 2018a,b), *Pseudomonas* spp. (Azadikhah et al., 2019), *Achromobacter* spp. (Chandra et al., 2020), *Enterobacter* spp. (Kruasuwan and Thamchaipenet, 2018), *Azotobacter* spp. (Viscardi et al., 2016), *Bacillus* spp. (Din et al., 2019), and *Leclercia* spp. (Kang et al., 2019). Regardless, however, even if certain strains of a genus and species possess an *acdS* gene, not all strains of that genus and species have ACCD.

Bioinoculation impact of ACC deaminase-producing PGPR: Management of biotic and abiotic stresses

Plants may be exposed to a wide range of environmental stresses, both biotic and biotic. ACCD-containing bacterial species safeguards plants from the deleterious impacts of environmental stresses including drought, salinity, high temperature, waterlogging, excess pesticides, heavy metals, and other xenobiotic contaminants by decreasing the activity of stressor-induced ethylene (Figure 4; Ali and Kim, 2018; Danish et al., 2020; Misra and Chauhan, 2020). The utilization of ACCD-positive PGPR for mitigating multiple abiotic stresses and their positive response on plants appears in Table 2.

In general, every plant has innate ability to withstand the adverse effects of the environment. However, under such stressed conditions, a number of physio-biochemical cascades activated and deactivated upon sensing the type of stresses. Among them, certain phytohormones play important role in stresses plants (Babalola et al., 2003; Glick et al., 2012). However, a number of microorganisms present either in rhizosphere, phyllosphere or endosphere of the plants play crucial role in the sensing and transducing signal to the plants under stressed conditions in coordinated manner. It is well established that ethylene at lower concentration worked as signaling molecules and regulate several gene expression, transcription and translation lead to overall plant development (Shaharoona et al., 2006; Yim et al., 2012; Bal et al., 2013; Ek-Ramos et al., 2019). In contrast, ethylene at higher concentration causes programme cell death, accelerating abscission, aging, inhibiting root elongation, senescence, leaf and fruit drop, etc. Under such circumstances, ACC deaninase either produced by plant or microorganisms cleave the ACC and lowering down the production of excess amount of ethylene even under stressed condition (Glick et al., 1998). Further, microorganisms synthesizing IAA along with endogenous plant IAA could accelerate the amalgamation of the enzyme ACC synthase translating the compound S-adenosyl methionine to ACC being the immediate precursor of ethylene in higher plants (Glick, 2012). It was revealed that phyllosphere methylobacteria distributed in the rice leaves produce the enzyme ACC deaminase, which control the ethylene concentrations level in the rice plant (Chinnadurai et al., 2009). The beneficial impact of ACCD-positive PGPR in the alleviation of various stresses is briefly discussed in the following sections.

Salinity stress

Salinity is a critical environmental stress that strongly influences plant productivity worldwide (Pirasteh-Anosheh et al., 2016; Hussain et al., 2019; Singh S. et al., 2021; Singh U. B. et al., 2021). Among the total global cultivable area, ~20% of area suffer from salinity stress; as a direct result of irrigation, this situation is becoming more serious (Kataria and Verma, 2018; Singh U. B. et al., 2021). Globally, the land area affectted by salinity/sodicity is estimated to be over 800 million hectares (MH) (FAO, 2008; Rengasamy, 2010; Dixit et al., 2015). Salinity affects plant physiology *via* differing mechanisms including disruption of chlorophyll synthesis, increased levels of photorespiration and transpiration, and fluctuation in homeostasis in plant cells (Miller et al., 2010; Sahu et al., 2021). Nutrient imbalance due to salinity stress is another variable that adversely affects plant growth and yield (Singh U. B. et al., 2021). This imbalance interrupts proper uptake and transport of nutrients to growing shoots and that ultimately causes mineral deficiencies in the plant (Panda et al., 2017; Singh U. B. et al., 2021). High levels of salt result in oxidative burst of cellular organelles. Increased production of ROS follows, which damages the plasma membrane and adversely affectscellular metabolism and homeostasis. Salinity causes overproduction of ethylene which increases abscission of leaves and petals, and accelerates organ senescence that ultimately leads to premature death of the plant (Zahir et al., 2009; Singh S. et al., 2021). ACCD-containing PGPR have been used to resolve salinity stress in several crops including vegetables and legumes (Shahid et al., 2021a, 2022a,b,c). These PGPR transform ACC to NH_3 and α-ketobutyrate, which the plant uses as a source of nitrogen, while also mitigating the deleterious effects of salt stress (Siddikee et al., 2012; Barnawal et al., 2014). Even in rather saline environment, salt-tolerant and ACCD-producing bacteria can thrive, and their beneficial characteristics assist plants in overcoming the impacts of stress (Thijs et al., 2014; Han et al., 2021; Sagar et al., 2022).

Microorganisms that survive and flourish in media containing sodium chloride (NaCl) up to 1–33% are known as halotolerant bacteria (Arora et al., 2017; Kumar M. et al., 2019; Singh et al., 2020b). Substantial literature is available on salt-tolerant ACCD-producing PGPR strains that can safeguard plants against the harmful effects of salt. Wang C. et al. (2016), Wang P. et al. (2016), and Wang Q. et al. (2016) found that the ACCD-synthesizing *V. paradoxus* 5C-2 reduced the negative effects of NaCl in pea by enhancing water relations and ion homeostasis, as well as increasing plant growth, dry biomass, chlorophyll synthesis, and yield when pea was grown in a saline environment. Halotolerant strains of *Enterobacter*, *Bacillus* and *Acinetobacter* containing ACCD genes increased plant height, biomass, leaf-to-stem ratio, leaf relative water content (LRWC), production of leaf chlorophyll and nutrient status of *Medicago sativa* (L.) plants cultivated in salinity-stressed agricultural soil (Daur et al., 2018). The early nodulation process and growth of common beans cultivated under high levels of salt stress have been shown to be stimulated by the endophytic bacterium *Serratia grimesii* BXF-1 (Tavares et al., 2018). In a similar study, Ji et al. (2020) reported that *Glutamicibacter* sp. strain YD-01 tolerated exceedingly high salt levels.

TABLE 2 Selected examples of ACCD synthesizing PGPR strains in alleviation of abiotic and biotic stress.

S. No.	ACC deaminase producing PGPR	Source	Used against/ host plant	Stress	Application response	References
Salinity stress						
1	*Bacillus mycoides* PM-35	Rhizosphere soil	*Zea mays* (L.)	–	Enhanced chlorophyll, soluble sugar and protein content and capacity to scavenge radical ions	Ali et al. (2022a)
2	*Enterobacter cloacae* ZNP-4	*Ziziphus nummularia*	*T. aestivum* (L.)	–	Increased growth parameters like shoot (41%) and root length (31%), fresh plant weight (28%), dry biomass (29%) and leaf chlorophyll	Singh et al. (2022)
3	*Enterobacter cloacae* PM23	Rhizosphere soil	*Zea mays* (L.)	–	Enhanced the power of radical scavenging, relative water content (RWC), soluble sugars, proteins, phenolic content, total flavonoid content in salt-treated *Z. mays* plants	Ali et al. (2022b)
4	*Bacillus marisflavi* CHR JH 203 and *Bacillus cereus* (BST YS1-42)	Leguminous crop	*Pisum sativum* (L.)	–	Increased dry biomass, biochemical constituents (carbohydrates, protein, reducing soluble sugars, leaf chlorophyll, phenolics and flavonoids)	Gupta et al. (2021)
5	*Glutamicibacter* sp. YD01	Rhizosphere of *Oryza sativa*	*Oryza sativa* (L.)	–	Decreased levels of Na^+ ion buildup and, electrolyte leakage; improved plant development	Ji et al. (2020)
6	*Bacillus aryabhattai* EWR29	Wheat rhizosphere soil	*T. aestivum* (L.)	–	Mitigated the negative impact of NaCl, significantly enhanced growth, and reduced proline content	Farahat et al. (2020)
7	*Paenibacillus* sp. ACC-06 and *Aneurinibacillusaneurinilyticus* ACC-02	*Allium sativum* (L.) rhizosphere soil	*Phaseolus vulgaris* (L.)	–	Negatively affected NaCl-induced pressure and enhanced biological properties (length, fresh weight, biomass) and photosynthetic capability of plant	Gupta and Pandey (2019)
8	*Serratia grimesii* BXF1	Rhizosphere soil	*Phaseolus vulgaris* (L.)	–	Promoted formation of early root nodules and growth; improved the symbiotic attributes of plants	Tavares et al. (2018)
9	*Bacillus, Acinetobacter* and *Enterobacter*	Soil	*Medicago sativa* (L.)	–	Height, leaf-to-stem ratio, fresh weight, dry biomass, pigments used for photosynthetic energy, nitrogen, phosphorus and potassium content all increased in the plants.	Daur et al. (2018)
10	*Enterobacter* sp.	Soil	*Oryza sativa* (L.)	–	Lowered antioxidative enzymatic responses and NaCl-induced ethylene in bacteria-treated plants; improved plant yield and productivity	Sarkar et al. (2018a,b)
11	*Klebsiella* sp.	Rhizosphere of *T. aestivum*	*Avena sativa* (L.)	–	Reduced salt stress and boosted plant development in salt-stressed soil. Expression profiles of the *rbcL* and *WRKY*1 genes were positively regulated	Sapre et al. (2018a,b)
12	*Pseudomonas* sp., *Bacillus cereus* and *Bacillus* sp.	*Brassica napus* rhizosphere	*Festuca rubra and Brassica napus* (L.)	–	Potentially ameliorated the salinity and enhanced the physiological and biochemical traits of plants	Grobelak et al. (2018)
13	*Bacillus cereus* LB1 and *Bacillus aerius* SB1	Rhizosphere soil	*Carthamus tinctorus*	–	Mitigated toxicity of NaCl and promoted vegetative growth of plant	Hemida and Reyad (2018)
14	*Pseudomonas frederiksbergensis*	Soil	*Capsicum annum* (L.)	–	Increased resistance of plants to NaCl stress observed in bacterial treated plants, as evidenced by increased antioxidant enzymatic activity responsiveness in leaf tissue and lowered hydrogen ion concentrations	Chatterjee et al. (2017)

(Continued)

10.3389/fmicb.2023.1132770

TABLE 2 (Continued)

S. No.	ACC deaminase producing PGPR	Source	Used against/ host plant	Stress	Application response	References
15	*Bacillus licheniformis* HSW-16	Rhizosphere of *T. aestivum*	*Triticum aestivum* (L.)	–	ACCD-positive PGPR strain positively influenced plant growth by relieving toxic effect of salts	Singh and Jha (2016)
16	*Paenibacilluslentimorbus* B-30488	Rhizosphere soil	*Lycopersicon esculentum*	–	Suppressed growth of phytopathogens and inhibited southern blight disease in tomato; improved overall plant growth	Dixit et al. (2016)
17	*Dietzianatronolimnaea*	Rhizosphere soil	*Triticum aestivum* (L.)	–	Halotolerant PGPR strain increased different antioxidant defensive enzymes and stressor metabolites thus improving salt tolerance ability of plant	Bharti et al. (2016)
18	*Pseudomonas putida*	Desert regions of Rajasthan	*C. arietinum* (L.)	–	Relieved salt-induced toxicity and modulated the growth, physiology, biochemical properties and expression of various stress-related genes	Tiwari et al. (2016)
19	*Variovorax paradoxus* 5C-2	Soil	*Pisum sativum* (L.)	–	Loweredthe proline and MDA content and antioxidant enzymes and enhanced the plant growth	Wang C. et al. (2016), Wang P. et al. (2016), and Wang Q. et al. (2016)
20	*Pseudomonas* sp. ST3	Root nodule of *Vigna unguiculata*	*Vigna unguiculata* (L.)	–	Improved the plant water-relation status, ionic balance, biological attributes, and photosynthetic machinery of peas by relieving the NaCl-induced toxic effect	Trung et al. (2016)
21	*Bacillus* sp., *Zhihengliuellahalotolerans* and *Staphylococcus succinus*	Root nodule of *T. aestivum*	*Triticum estivum* (L.)	–	Improved ion balance, nutritional content and homeostasis	Orhan (2016)
22	*Variovorax paradoxus* 5C-2	Root nodule of *P. sativum*	*P. sativum* (L.)	–	Water uptake, ionic homeostasis, overall growth, dry phyto-mass accumulation, leaf chlorophyll and grain yield of pea plants significantly improved	Wang C. et al. (2016), Wang P. et al. (2016), and Wang Q. et al. (2016)
23	*Pseudomonas stutzeri* A1501	Rhizosphere of *O. sativa*	*Oryza sativa* (L.)	–	Restricted level of salts and improved the development and yield features of plant	Han et al. (2015)
24	*Pseudomonas fluorescens* YsS6	Soil	*Lycopersicum esculentum* (L.)	–	Augmented seedling germination, vigor index (SVI), plant length (root and shoot) and plant dry biomass	Ali et al. (2014)
25	*Bacillus flexus, Isoptericola dokdonensis* and *Arthrobacter soli*	Inner tissues of *Limonium sinense*	*L. sinense* (L.)	–	Protected against salinity effects; increased the flavenoid accumulation	Qin et al. (2014)
26	*Rhizobium leguminosarum*	Pea root nodule	*P. sativum* (L.)	–	Augmented lengths of shoots and roots, dry biomass, chlorophyll synthesis, LHb content and nutrient uptake of plants	Ahmad et al. (2013)
27	*Pseudomonas putida* UW4	Soil	*Lycopersicum esculentum* (L.)	–	Increased expression of mRNA in different ROS-scavenging enzymes and stressor metabolites, i.e., proline	Yan et al. (2013)
Drought stress						
28	*Bacillus megaterium* (MU2)	Maize rhizosphere soil	*T. aestivum* (L.)	–	Potentially increased germination indices, vigor indices (SVI), plant fresh weight and dry biomass	Rashid et al. (2022)
29	*Pseudomonas* sp.	Rhizosphere soil of cereal crop	*Arabidopsis thaliana* (L.)	–	Increased plant survival, LRWC, chlorophyll, glycine betaine, stressor proline, and malondialdehyde content in drought-induced *A. thaliana* plants by 95, 59, 30, 38, 23, and 43%, respectively	Yasmin et al. (2022)

(Continued)

10.3389/fmicb.2023.1132770

TABLE 2 (Continued)

S. No.	ACC deaminase producing PGPR	Source	Used against/ host plant	Stress	Application response	References
30	*Serratia marcescens* and *Pseudomonas* sp.	Rhizosphere of cereal crops	*T. aestivum* (L.)	–	Both strains potentially improved ROS, water status, osmolyte accumulation, chlorophyll and carotenoids content in plant leaves	Khan and Singh (2021)
31	*Enterobacter cloacae* 2WC2	*Withaniacoagulans* plant	*Zea mays* (L.)	–	Morpho-biological parameters, RWC and antioxidant defence enzymes of PEG-treated plants increased following application of *E. cloacae* strain 2WC2	Maqbool et al. (2021)
32	*Bacillus velezensis* strain D_3	Rhizosphere soil of rain-fed area		–	Photosynthetic capacity, stomatal conductance, vapor pressure, water-use efficiency, and transpiration rate all improved	Nadeem et al. (2021)
33	*Enterobacter* HS9 and *Bacillus* G9	Soil	*Mucuna pruriens* (L.)	–	Improved water uptake, rate of respiration and synthesis of chlorophyll	Saleem et al. (2018)
34	*Ochrobactrumpseudogrignonense* RJ12, *Pseudomonas* sp. RJ-15 and *Bacillus subtilis* RJ-46	Drought-affected rhizosphere soils	*Vigna mungo* and *P. sativum* (L.)	–	Germination attributes, plant length (root and shoot) and dry biomass enhanced	Saikia et al. (2018)
35	*Mitsuaria* sp. and *Burkholderia*	*Arabidopsis thaliana*	*A. thaliana* and *Zea mays* (L.)	–	Lowered evapotranspiration; altered proline, MDA, and levels of plant hormones.	Huang et al. (2017)
36	*Bacillus pumilus* and *Bacillus firmus*	Rhizosphere of *Solanum tuberosum*	*S. tuberosum* (L.)	–	Enhanced proline content in tubers; greater mRNA expression levels of several ROS scavenging enzymes responsible for increased plant tolerance to salt and drought stress.	Gururani et al. (2013)
37	*Bacillus cereus* AR156, *Bacillus subtilis* SM21 and *Serratia* sp. XY21	Soil	*Cucumis sativus* (L.)	–	Root:shoot ratio and vegetative growth increased	Wang et al. (2012)
38	*Pseudomonas fluorescens* ACC-5	Nodule	*Pisum sativum* (L.)	–	Increased water uptake by plants	Zahir et al. (2008)
39	*Pseudomonas* sp.	Drought-stressed soil	*Pisum sativum* (L.)	–	Increased plant height, leaf-to-stem ratio, fresh plant weight, dry biomass, chlorophyll a, b, and total chlorophyll; increased N, P, and K contents.	Arshad et al. (2008)
Heavy metal stress						
40	*Bacillus gibsonii* (PM11) and *Bacillus xiamenensis* (PM14)	Industrially polluted rhizosphere	*Linumusitatissimum* (L.)	–	Incresed fresh and dry biomass, chlorophyll content, proline concentration, and antioxidant enzymatic activity of plants	Zainab et al. (2020)
41	*Agrobacterium fabrum* and *Leclercia adecarboxylata*	Metal-contaminated rhizosphere	*Zea mays* (L.)	–	Potentially alleviated Cr toxicity and improved the overall growth of plants by reducing metal uptake	Danish et al. (2019)
42	*Rhizobium leguminosarum bv. viciae* 1066S	Metal-contaminated rhizosphere	*Pisum sativum* (L.)	–	Increased shoot biomass, nodulation, nitrogen fixation, water usage efficiency (WUE), and nutritional mineral uptake	Belimov et al. (2019)
43	*Agrobacterium fabrum* (CdtS5) and *Stenotrophomonas maltophilia* (CdtS7)	Cd-contaminated wheat rhizophere	*Tritium estivum* (L.)	Cd	Alleviated Cd toxicity and lowered uptake of Cd; improved growth, chlorophyll content and yield attributes of wheat	Zafar-Ul-Hye et al. (2018)
44	Combination of *Pseudomonas* sp., *Bacillus cereus* and *Bacillus* sp.	Rhizosphere soil	*Festuca rubra* and *Brassica napus* (L.)	Heavy metals	Sequestered the metal, reduced proline, MDA and antioxidant enzymes, reduced metal levels within the plant	Grobelak et al. (2018)
45	*Azotobacter chroococcum*	Metal-contaminated rhizosphere	*Zea mays* (L.)	Heavy metals	Detoxified the metals and increased biological and physiological parameters of the plant	Rizvi and Khan (2018)

(Continued)

10.3389/fmicb.2023.1132770

TABLE 2 (Continued)

S. No.	ACC deaminase producing PGPR	Source	Used against/ host plant	Stress	Application response	References
46	*Pseudomonas aeruginosa*	Metal-polluted soil	*C. arietinum* (L.)	Heavy metals	Enhanced root length, shoot length, biomass, chlorophyll formation, nodulation, symbiotic attributes and seed yield of plant	Saif and Khan (2018)
47	*Enterobacter aerogenes* MCC 3092	Rhizosphere of *Oryza sativa*	*Oryza sativa* (L.)	Cd	Alleviated phytotoxicity of Cd, reduced level of ethylene, antioxidant enzymes (CAT, SOD, POD), increased growth and chlorophyll content of plants	Pramanik et al. (2018)
48	*Enterobacter ludwigii* (HG 2) and *Klebsiella pneumonia*	*Alternanthera sessilis* and *Cyperus esculentus* rhizosphere	*T. aestivum* (L.)	Cr	Much improved growth promotion of wheat seedlings.	Gontia-Mishra et al. (2016)
49	*Enterobacter* sp., *Serratia* sp. and *Klebsiella* sp.	Rhizospheres of plants growing in mining waste	*Helianthus annuus* (L.)	Pb	Lowered toxicity of Cd, promoted growth features of plants	Carlos et al. (2016)
50	*Pseudomonas fluorescens* and *Bacillus thuringiensis*	Rhizosphere of *Zea mays*	*T. aestivum* (L.)	Cr	Improved plant growth and decreased Cr accumulation in roots and shoots	Shahzadi et al. (2013)
51	*Pseudomonas stutzeri* A1501	–	*Oryza sativa* (L.)	Ni	increased metal tolerance of plants	Han et al. (2015)
52	*Azotobacter* sp.	Metal-contaminated rhizosphere	*Zea mays* (L.)	Pb	Lowered Pb toxicity and enhanced plant biometric parameters, biomass production, chlorophyll *a* and *b* and carotenoids, protein, proline, glutathione *S*-transferase and enzymes of POD and CAT	Hassan et al. (2014)
53	*Ochrobactrum* sp. and *Bacillus* spp.	Slag disposal site	*Oryza sativa* (L.)	Heavy metals	Mitigated toxicity of heavy metals, reduced ethylene level and enhanced overall growth of plants	Pandey et al. (2013)
Organic pollutant stress						
54	*Burkholderia* sp.	Soil	Assorted vegetables	Organic pollutant	Lowered phenol toxicity, thus increasing overall functioning of plants	Chen et al. (2017)
55	*Enterobacter intermedius*, *Bacillus circulans* and *Serratia carnosus*	*Z. mays* and *per nigrum* Rhizosphere soil	*Z. mays* (L.)	Organic pollutant	Improvement in vegetative development of plant was quite noticeable	Ajuzieogu et al. (2015)
56	*Pseudomonas aeruginosa* SLC-2and *Serratia marcescens* BC-3	Contaminated soil	*Avena sativa* (L.)	Organic pollutant	Degraded/detoxified the pollutant and improved biological properties and yield of plants even in petroleum-contaminated soil	Liu et al. (2015)
57	*Acinetobacter* sp.	Ploysycyclic aromatic hydrocarbon (PAHs)-contaminated soil	*A. sativa* (L.)	Organic pollutant	DegradedPAHs and hydrocarbons; decreased level of MDA, free proline content and ROS-scavenging enzymes; increased overall performance of plants	Xun et al. (2015)
58	*Pseudomonas aeruginosa* and *Serratia marcescens*	Rhizosphere of Echinochloa	*A. Sativa* (L.)	Organic pollutant	A pronounced increase in *A. sativa* plants	Liu et al. (2015)
Agrochemicals stress						
59	*Burkholderiacepacia*	Cabbage rhizosphere	*C. arietinum* (L.)	Pesticide	Alleviated toxicity of glyphosate; enhanced overall plant growth and performance	Shahid and Khan (2018)
60	*Rhizobium leguminosarum*	Root nodules of pea	*P. sativum* (L.)	Pesticide	Improved length, biomass, symbiotic features, nutrient uptake and seed attributes of plants under kitazin stress	Shahid et al. (2019a,b)

(Continued)

10.3389/fmicb.2023.1132770

TABLE 2 (Continued)

S. No.	ACC deaminase producing PGPR	Source	Used against/ host plant	Stress	Application response	References
Biotic stress						
61	*Pseudomonas putida*	*Withaniasomnifera* rhizosphere soil	*Papaver somniferum* (L.)	*Peronospora* sp. causing downy mildew disease	Biochemical and physiological (stomatal behavior and rate of transpiration) parameters significantly increased	Barnawal et al. (2017)
62	*Bacillus xiamenensis* PM14	Sugarcane rhizosphere	*Saccharum officinarum* L.	*Colletotrichum falcatum* causing red rot disease	Potentially suppressed symptoms of disease, enhanced plant growth, enhanced production of defensive enzymes and content of proline	Xia et al. (2020)
63	*Pseudomonas* sp. strain S3	rhizospheric soil of turmeric (*Curcuma longa*)	*Solanum lycopersicum* (L.)	*Rhizoctonia solani*	Improved morphological features, photosynthetic attributes and osmolytes in plants	Pandey and Gupta (2020)
64	*Paenibacilluslentimorbus* B-30488	rhizospheric soil of tomato	*Solanum lycopersicum* (L.)	*Sclerotiumrolfsii* causing southern blight diseases	Controlled the disease, increased defense enzymes and improved plant growth attributes	Dixit et al. (2016)
65	*Delftiatsuruhatensis* WGR-UOM-BT1	*Rauwolfia serpentina* Rhizosphere	*Solanum lycopersicum* (L.)	*Fusarium oxysporum*	Protected plant from fungal disease; significantly improved characteristic growth features of tomato	Prasannakumar et al. (2015)

When treated as a biological inoculant to *Oryza sativa* (L.), this strain exhibited low levels of Na^+ buildup and decreased electrolyte leakage (EL) during salt treatment, as well as increased plant productivity. In a similar study, two NaCl-tolerant and ACCD-positive PGPR, *Aneurinibacillusaneurinilyticus* ACC-02 and *Paenibacillus* sp. ACC-06, imparted a positive response to morphological attributes (length and biomass), biochemical features, and yield of salt-treated *Phaseolus vulgaris* (L.) by limiting the negative effects of NaCl (Gupta and Pandey, 2019). Wheat (*Triticum aestivum* L.) plants cultivated in saline-sodic soil treated with fertilizer and ACCD positive strains of *S. succinus*, *Zhihengliuella halotolerans* and *Bacillus* sp., either alone or in combination, grew and yielded better than those cultivated in soil treated solely with NaCl (Orhan, 2016; Singh U. B. et al., 2021).

Sapre et al. (2018a,b) reported that a salt-tolerant and ACCD-producing PGPR strain of *Klebsiella* sp. was inoculated to *Avena sativa* plants treated with varying levels of NaCl. The PGPR strain improved plant development under salt stress and progressively regulated the *rbcL* and *WRKY*1 gene expression profiles.

Drought stress

Insufficient availability of water, referred to as drought, unfavorably affects crop productivity. Under drought stress many plants physiological and biochemical effects including reduction in water potential, turgor loss, wilting, stomatal closure, and alteration in structures of membranes and proteins are reported (Kaushal and Wani, 2016). Drought stress is documented to slow plant growth, resulting in lower yields, necessitating the use of drought-resistant plant growth techniques. Several researchers have utilized ACCD-producing and drought-tolerant PGPR strains for ameliorating water stress. ACCD-positive PGPR strains *Ochrobactrumpseudogrignonense* RJ-12, *Pseudomonas* sp. RJ-15 and *B. subtilis* RJ-46 were isolated from drought-stressed rhizosphere soil and utilized as bioinoculants to *Vigna mungo* and *Pisum sativum* cultivated under drought stress. ThePGPR strains increased the germination attributes, morphological features and dry weight accumulation in plants (Saikia et al., 2018). Saleem et al. (2018) reported that two ACCD-containing drought-resistant *Enterobacter* HS-9 and *Bacillus* G-9 strains improved overall growth of *Mucuna pruriens* cultivated in drought-stressed conditions. In another crop-based study, two strains of *Bacillus* (*B. pumilus* and *B. firmus*) were reported to enhance the expression levels of mRNA of several ROS scavenging enzymes, and decreased proline concentration in drought-stressed tubers (Gururani et al., 2013). Additionally, the inoculation of ACCD-producing drought-tolerant PGPR strains of *Burkholderia*and *Mitsuaria* sp. recovered from the rhizosphere of *Arabidopsis thaliana* were reported to lower evapotranspiration rate as well as levels of proline and malondialdehyde. Levels of phytohormones were also altered (Huang et al., 2017).

Waterlogging stress

Flooding is a common abiotic stress that impacts a wide range of plants. During flooding, plant roots experience anoxia (lack of oxygen), prompting production of ACC that oxidizes ethylene as it moves within the plant. The secreted ethylene has negative consequences on leaves, such as epinasty (rapid nastic motions), chlorosis, necrosis, and lower fruit output (Paul et al., 2016). To eliminate the epinasty response in plants, ethylene production inhibitors likeCO_2, cobalt chloride, 7-chloro-4-ethoxycarbonylmethoxy-5-methyl-2,1,3-benzothiadiazole,

L-α-(2-aminoethoxyvinyl)-glycine (AVG), silver nitrate, and 1-methylcyclopropene (1-MCP) have been used (Jackson, 2008). In addition to these, ACCD-synthesizing PGPR operate as an ACC sink, and their application reduces ethylene levels significantly, protecting plants from flooding stress (Ali and Kim, 2018). Tolerance against waterlogging stress in rice seedlings was enhanced by ACC deaminase-synthesizing *Streptomyces* sp. GMKU 336. The bacteria reduced levels of ethylene and improved root elongation, biomass production, leaf area and chlorophyll content (Jaemsaeng et al., 2018). Etesami et al. (2014) reported that ACC deaminase-positive endophytic *P. fluorescens* strain REN_1 significantly elongated rice roots, endophytically colonized plants and promoted development of seedlings under waterlogged conditions. Barnawal et al. (2012) observed that ACC deaminase PGPR strains protected *Ocimum sanctum* (L.) plants against waterlogging. Compared to waterlogged plants without bacterial inoculation, the selected bacteria modulated the negative alterations in stress-induced ethylene production, decreased the lipid peroxidation and proline content, and substantially increased the chlorophyll concentration and foliar nutrient uptake in *O. sanctum* plant. Furthermore, ACCD-containing PGPR strains (*P. putida* ATCC17399/pRK415, *Enterobacter cloacae* UW4 and *E. cloacae* CAL2) enhanced various physiological reactions of *S. lycopersicum* (L.) under flooding stress (Grichko and Glick, 2001).

Agrochemical stress

Agrochemicals including pesticides, herbicides and fungicides are among the most significant anthropogeniccompounds that adversely affect microbial physiology (Shahid et al., 2019a,b, 2020), composition and functions (Ataikiru et al., 2019; Shahid et al., 2021b; Shahid and Khan, 2022a,b), soil fertility (Sanchez-Hernandez, 2019) and crop productivity (Shahid et al., 2018a,b; Khan et al., 2020). Stress ethylene production causes the agrochemical to obstruct plant development viaunknown mechanisms. Several beneficial pesticide-tolerant soil microbes (PGPR) are reported which can degrade pesticides (Shahid et al., 2019a,b, 2021c; Shahid and Khan, 2019). In addition, a plentiful ACC deaminase-positive and pesticide-tolerant PGPR has been shown to support legumes grown in degraded or stressed soils (Zaidi et al., 2016; Ahmed et al., 2017; Rizvi et al., 2017; Zaidi et al., 2017). Shahid and Khan (2018) reported that glyphosate-tolerant PGPR strain *Burkholderiacepacia* PSBB1 isolated from the contaminated rhizosphere of *Vicia faba* produced considerable ACC deaminase and alleviated the toxicity of the herbicide, and enhanced overall growth and performance of chickpea plants raised in herbicide-amended soil.

Heavy metal stress

Soil pollution by heavy metals has become one of the greatest environmental and agronomic challenges worldwide (Ashraf et al., 2019). Certain heavy metals including Zn, Cu, and Co are used by plants in trace quantities; however, they become toxic at higher concentrations and cause deleterious effects to plant growth and development (Dixit et al., 2015). Roots are primarily responsible for nutritient (including metal) uptake by plants. Stress ethylene is produced in soils having high concentrations of heavy metals, which limits root morphogenesis (Saif et al., 2017). Numerous reports existin the literature regarding utilization of metal-tolerant and ACCD-generating PGPR strains capable of optimizing plant growth under heavy metal-stressed conditions (Płociniczak et al., 2014; Pramanik et al., 2018; Manoj et al., 2020). ACCD-positive PGPR support phytoremediation by increasing the uptake of harmful metals by enlarging/improving root growth under metal stress (Santos et al., 2019). In this regard, several agronomists and microbiologists have isolated metal-tolerant and ACCD-producing PGPR strains from different contaminated sites for use as potent bioinoculants for various crops grown in soils contaminated with heavy metals. For instance, single or co-inoculation of metal-tolerating ACCD-producing PGPR strains such as *Bacillus* sp., *B. cereus* and *Pseudomonas* sp. to *Festuca rubra* and *Brassica napus* plants resulted in substantial increases in plant growth and yield (Grobelak et al., 2018). Pandey et al. (2013) reported that metal-tolerant ACCD-positive PGPR strains of *Ochrobactrum* sp. and *Bacillus* spp., when used with rice plantsgrown in heavy metal-contaminated soils, mitigate the toxic effect of metals, reduced ethylene levels and enhanced overall growth of plants. Similarly, two Cr-tolerant PGPR strains, *Enterobacter ludwigii* and *Klebsiella pneumonia*, significantly reduced the toxicity of Cr and promoted seedling germination, and increased protein and carbohydrate content of wheat plants even in the presence of high concentrations of Cr (Gontia-Mishra et al., 2016). Other PGPR strains like *Pseudomonas fluorescens* and *Bacillus thuringiensis* (Shahzadi et al., 2013), *Achromobacter xylosoxidans* and *Bacillus pumilus* (Chandra et al., 2019), *Enterobacter* sp., *Serratia* sp. and *Klebsiella* sp. (Carlos et al., 2016), and *Enterobacter aerogenes* MCC 3092 (Pramanik et al., 2018) are also reported to alleviate toxic ethylene levels vis-à-vis enhanced growth of crops.

Temperature (chilling and heat) stress

Extreme (low or high) temperatures cause substantial losses in yield and productivity of crops (Lesk et al., 2016; Wang C. et al., 2016; Wang P. et al., 2016; Wang Q. et al., 2016). Temperature extremes cause plants to modify many metabolic processes (Yadav, 2010). Temperature changes cause drastic alteration in membrane shape, catalytic characteristics, enzyme performance, and nutrient transport (Subramanian et al., 2016). Low temperatures (between 0 and 15°C) cause yield losses in a variety of tropical and subtropical crops. Cold stress generally slows rate of germination, reduces growth, causes yellowing (chlorosis) of leaves, and reduces tiller formation (Yadav, 2010). Chilling causes lesions on leaf surfaces, discoloration, and rapid senescence in horticultural crops due to reduced chlorophyll production. Chilling, like other environmental stresses, results in production of ethylene which inhibits overall plant development. The use of ACCD-synthesizing bacterial strains in *Vitis vinifera* (L.) and *Solanum lycopersicum* (L.) was reported to alleviate chilling stress (Theocharis et al., 2012; Subramanian et al., 2016). Some cold-tolerant and ACCD-negative PGPR strains, *viz.*, *P. frederiksbergensis*, *Sphingomonasfaeni* and *Flavobacterium* sp. were transformed with a plasmid pRKACCharboring the *acdS* gene from *Pseudomonas putida* UW4. The role of these altered PGPRs that overexpressed the *acdS* gene in alleviating chilling stress in *S. lycopersicum* (L.), *Setariaitalica* (L.) and *Eleusine coracana*was investigated (Subramanian et al., 2015; Srinivasan et al., 2017).

Air pollution stress

Sulfur dioxide (SO_2), ozone (O_3), nitrogen oxides (NOx), and volatile organic compounds (VOCs) are anthropogenicand naturally-occurring pollutants that impart negative impacts to human health and ecosystems (Sharma et al., 2013). Atmospheric pollutants deleteriously affect plants by inhibiting enzyme systems and metabolic

activities (Saxena and Kulshrestha, 2016). The increased synthesis of ethylene in plants in response to air pollutants is well documented, and is thought to be one of the key regulators in plant tolerance to air pollution stress, particularly O_3 exposure (Rao and Davis, 2001). According to one study, inhibition of the ethylene expressing gene resulted in considerable reduction of O_3-induced leaf damage in tomato plants (Moeder et al., 2002). As a result, bacteria that produce ACC deaminase have received greater attention as a stress management tool for plants suffering from air pollution.

Nutrient deficiency

Excessive application of chemical fertilizers in agriculture is costly, andosols considered a potential source of soil and water pollution (Kumar R. et al., 2019). A variety of beneficial ACC deaminase-synthesizing bacteria are known to boost productivity and efficiency of fertilized crops, either directly or indirectly. At low fertilizer application rates, PGPR ACC deaminase activity may reduce ethylene concentrations in wheat plants exposed to nutritional stress by hydrolyzing ACC to α-ketobutyrate and NH_3 (Hemissi et al., 2019). The authorsfurther claim that PGPR, which comprise ACCD-generating bacteria, might be used in concert with fertilizers to boost nutrient intake and plant development. Multiple studies have demonstrated the critical role of microbially-synthesized ACC deaminase in promoting plant growth, which allows them to withstand abiotic stress and ultimately create a symbiotic interaction between plants and the native rhizosphere (Tahir et al., 2006).

Stress from other organic contaminants

Rapid worldwide industrial development and modernization has resulted in the manufacture and release of significant volumes of hazardous organic pollutants into natural habitats. Polycyclic aromatic hydrocarbons (PAHs), petroleum, and other xenobiotics based on hydrocarbons are known to limit crop productivity (Jajoo, 2017; Li et al., 2019). Most plants are stressed by the presence of organic pollutants in soil, which causes them to produce more ethylene. However, the exact mechanisms of excessive ethylene production remain unknown. Organic contaminants such as refrigerants and organic solvents are reported to be degraded by several bacterial species belonging to different genera. In the presence of organic pollutants, ACCD-producing PGPRs have consistently improved plant development (Xun et al., 2015). PGPR can also aid in plant-mediated remediation (phytoremediation) by bio-transforming harmful substances to innocuous forms. ACCD-producing PGPR is known to play a significant role in elongation of roots and overall plant growth, which explains why host plants are superior at phytoremediating organic chemicals. Phenol-degrading PGPR strain *Burkholderia* sp. isolated from phenol-contaminated soil was reported to reduce the phytotoxicity of phenol and improve growth and biochemical activities in plants (Chen et al., 2017). Similarly, ACCD-producing and petroleum-degrading PGPR strains *S. marcescens* BC-3 and *P. aeruginosa* SLC-2 augmented the growth and physiological properties of *Avena sativa* grown in petroleum-contaminated soil (Liu et al., 2015). An ACCD-producing and PAHs-tolerant soil bacterium *Acinetobacter* sp., when applied to *A. sativa* plants cultivated in hydrocarbon-contaminated soil, decreased the MDA, antioxidant enzymes, and free proline contents of shoot tissues and increased yield, photosynthetic pigments, and protein content of plants (Xun et al., 2015). In, another study, two PGPR-degrading *P. aeruginosa* and *S. marcescens* strains isolated from the rhizosphere of *Echinochloa* promoted the growth of *Ascophyllum sativum* (Liu et al., 2015). Application to polluted soil of *Microbacterium* sp. strain F10a-R containing ACC deaminase enzymes and other multifarious PGP features resulted in elimination of pyrene and phenanthrene, both hazardous PAHs, and boosted wheat growth (Sheng et al., 2009).

Biotic stress

Pathogen attack

Plants often respond to attack/infection of bacterial pathogens, fungal pathogens, viruses, and nematodes by increasing ethylene levels in their tissue (Van Loon et al., 2006). Soil application of potent ACCD-producing PGPR strains may reduce injuries from induced ethylene triggered by numerous pathogenic bacteria such as *Agrobacterium tumefaciens* (Toklikishvili et al., 2010), *Pseudomonas syringae* pv. tomato (Indiragandhi et al., 2008), and *Erwinia* spp. (Wang et al., 2000), and those caused by phytopathogenic fungi such as *Pythium aphanidermatum* (El-Tarabily, 2013), *P. ultimum* (Wang et al., 2000), and *Pyriculariaoryzae* (Amutharaj et al., 2012). The PGPR either directly or indirectly inhibit pathogen development by synthesizing a variety of antimicrobial metabolites (Singh et al., 2016a, 2020a). The efficiency and efficacy of varying species and genera of ACC deaminase-producing PGPR strains have demonstrated a positive effect in the suppression of different diseases caused by phytopathogens (Singh et al., 2016b; Shahid et al., 2017). *Bursaphelenchusxylophilus* is a pathogenic nematode commonly known as pine/wood nematode and is associated with by pine wilt disease. This nematode was suppressed by ACC deaminase-containing *B. subtilis* (Nascimento et al., 2013). In an *in-vitro* study, Al-Shwaiman et al. (2022) reported that multi-stress tolerant and biocontrol agent *Beijerinckiafluminensis* supressed the growth of major fungal phytopathogens (*Aletrnariaalternata*, *Rhizoctonia solani*, *Fusariumoxysporum*, *Ustilaginoidea virens*) by producing defensive extracellular enzymes. Dixit et al. (2016) assessed the plant growth-regulating and biocontrol efficiency of ACC deaminase-producing strain *Paenibacilluslentimorbus* B-30488, which suppresses the growth of fungal pathogens and inhibits southern blight disease in tomatoes. Additionally, ACCD containing *Pseudomonas putida* recovered from *Withaniasomnifera* (L.) rhizosphere soil and applied to*Peronospora* sp. causing downy mildew disease infected *Papaver somniferum* (L.) plants. It was observed that the potential ACCD candidate significantly modulated the biochemical and physiological (stomatal behavior and rate of transpiration) parameters by reducing the incidence of disease in plant (Barnawal et al., 2017; Malviya et al., 2020). Based on these data, inoculation of ACC deaminase-containing bacteria to crops suffering from pathogenic stress can protect the plants effectively. In addition, ACCD-synthesizing PGPR strains lower the quantity of ethylene generated in plants infected with soil-borne and foliar disease (Glick, 2014).

Certain plant growth-promoting microorganisms produce the enzyme ACC deaminase, which indirectly promote plant growth by lowering down the ethylene level in plants (Glick, 1995). Under biotic stressed condition, ACC deaminase transcriptionally regulated differently by several biotic factors (Gontia-Mishra et al., 2014). Few reports indicated that *Methylobacterium* spp. (phytopathogenic in nature) modulate plant growth by inhibiting plant pathogens indirectly. ACCD producting *Methylobacterium* spp. synthesized certain polymer degrading

pectinase and cellulase, suggesting that they can indirectly induce systemic resistance during pathogen attack (Chinnadurai et al., 2009; Tsolakidou et al., 2019). Under biotic stressed condition, PGPMs produce ACC deaminase which modulates the level of ethylene by hydrolyzing ACC, a precursor of ethylene, in ammonia and a-ketobutyrate (Babalola et al., 2003; Nascimento et al., 2014). The lower concentration of ethylene induced jasmonate dependent pathways in plants which further modulate synthesis of antioxidative biomolecules which in turn reduce the synthesis of reactive oxygen species and superoxide radicals and protect plants from programme cell death against invasion caused by hemi-biotroph and necrotroph. In contrast, ET dependent pathways lead to PCD in the plants attacked by obligate and biotrophs which restrict colonization and invasion of the pathogen. Some time, elevated ET cause premature leaf and fruit drop in the plants attacked by biotrophs (Etesami et al., 2020).

Concluding remarks and future prospects

In agricultural systems worldwide, environmentally-benign management approaches are necessary to improve food security in the face of constantly changing agro-climatic conditions. The current review focuses on the interaction and mechanistic action of ACCD-synthesizing rhizobacteria on abiotic and biotic stress tolerance induction. It is well recognized that multiple stress-tolerant ACC deaminase-synthesizing bacterial strains are advantageous over other conventional bacterial strains, and can thrive in sufficient numbers in new and stressful environments to impart favorable impacts to crop plants. Under abiotic- and biotic-stressed situations, powerful PGPR strains enhance crop growth and production. Keeping in mind the many significant environmental hazards encountered in agronomic practices from anthropogenic and natural factors, there is an urgent need for a major paradigm shift in agricultural practices. The costs associated with generating and modifying transgenic plants capable of tolerating biotic and abiotic stresses are substantial. To overcome this problem, focus has shifted to the identification and development of ACCD-containing PGPR formulations that support plants in combatting stressed environmental conditions. The survival of such beneficial PGPR strains under harsh circumstances poses a challenge for their large-scale production, yet the exploitation of a powerful PGPR strain is likely to provide wide-ranging solutions to problems in modern agriculture. Research has demonstrated that ethylene balance is crucial for plant growth and development under abiotic stress conditions, and application of PGPR bacteria may be useful in protecting plants from such stresses. Therefore, rhizobacteria should be screened for ACC deaminase production. Utilizing ACC deaminase-synthesizing bacterial strains as biological inoculants for abiotic stress management could be critical for long-term sustainability of agriculture. Furthermore, uncovering the essential mechanistic action of these PGPR strains will help to expand the applicability of this technology.

Author contributions

MS and MK conceived and designed the study. MS, MK, US, PS, and HS performed the literature search. MS wrote the first draft of the manuscript. MS and US prepared the figures and artwork. MS, MK, US, RK, RS, and AK edited the manuscript. MS, PS, and AM formatted the reference as per Journal's style. All authors contributed to the article and approved the submitted version.

Funding

This work is funded by Network Project on Application of Microorganisms in Agriculture and Allied Sectors (AMAAS), Indian Council of Agricultural Research, New Delhi.

Acknowledgments

MS is thankful to DST-SERB for the National Post-Doctoral Fellowship (PDF/2022/000970). The authors MS and US would like to thank the ICAR-NBAIM for providing research facilities. Thanks to John Pichtel, Ball State University (United States) for assistance with the manuscript. Authors have picked-up some of the figures/artwork to prove their concept and acknowledged the Social cites for valuable help. We would like to extend their sincere thanks to the Network Project on Application of Microorganisms in Agriculture and Allied Sectors (AMAAS), Indian Council of Agricultural Research, New Delhi, for providing financial support to carry out the research.

Conflict of interest

The authors declare that the research was conducted in the absence of any commercial or financial relationships that could be construed as a potential conflict of interest.

The reviewer RK declared a shared affiliation with the authors MS, US, and HS to the handling editor at the time of review.

Publisher's note

All claims expressed in this article are solely those of the authors and do not necessarily represent those of their affiliated organizations, or those of the publisher, the editors and the reviewers. Any product that may be evaluated in this article, or claim that may be made by its manufacturer, is not guaranteed or endorsed by the publisher.

References

Ahmad, E., Khan, M. S., and Zaidi, A. (2013). ACC deaminase producing *pseudomonas putida* strain PSE3 and *rhizobium leguminosarum* strain RP2 in synergism improves growth, nodulation and yield of pea grown in alluvial soils. *Symbiosis (Philadelphia, PA)* 61, 93–104. doi: 10.1007/s13199-013-0259-6

Ahmed, B., Zaidi, A., Khan, M. S., Rizvi, A., Saif, S., and Shahid, M. (2017). "Perspectives of plant growth promoting rhizobacteria in growth enhancement and sustainable production of tomato" in *Microbial strategies for vegetable production*, eds. Zaidi, A., Khan, M. (Cham: Springer), 125–149.

Ajuzieogu, C. A., Ibiene, A. A., and Stanley, H. O. (2015). Laboratory study on influence of plant growth promoting rhizobacteria (PGPR) on growth response and tolerance of *Zea mays* to petroleum hydrocarbon. *Afr. J. Biotechnol.* 14, 2949–2956. doi: 10.5897/AJB2015.14549

Ali, S., Charles, T. C., and Glick, B. R. (2014). Amelioration of high salinity stress damage by plant growth-promoting bacterial endophytes that contain ACC deaminase. *Plant Physiol. Biochem.* 80, 160–167. doi: 10.1016/j.plaphy.2014.04.003

Ali, S., and Kim, W. C. (2018). Plant growth promotion under water: decrease of waterlogging-induced ACC and ethylene levels by ACC deaminase-producing bacteria. *Front. Microbiol.* 9:1096. doi: 10.3389/fmicb.2018.01096

Ali, B., Wang, X., Saleem, M. H., Azeem, M. A., Afridi, M. S., Nadeem, M., et al. (2022a). *Bacillus mycoides* PM35 reinforces photosynthetic efficiency, antioxidant defense, expression of stress-responsive genes, and ameliorates the effects of salinity stress in maize. *Life* 12:219. doi: 10.3390/life12020219

Ali, B., Wang, X., Saleem, M. H., Sumaira, , Hafeez, A., Afridi, M. S., et al. (2022b). PGPR-mediated salt tolerance in maize by modulating plant physiology, antioxidant defense, compatible solutes accumulation and bio-surfactant producing genes. *Plan. Theory* 11:345. doi: 10.3390/plants11030345

Al-Shwaiman, H. A., Shahid, M., Elgorban, A. M., Siddique, K. H., and Syed, A. (2022). *Beijerinckiafluminensis* BFC-33, a novel multi-stress-tolerant soil bacterium: deciphering the stress amelioration, phytopathogenic inhibition and growth promotion in *Triticum aestivum* (L.). *Chem* 295:133843. doi: 10.1016/j.chemosphere.2022.133843Get

Amutharaj, P., Sekar, C., and Natheer, S. E. (2012). Intergeneric microbial co aggregates: bio inoculation effect of ACC deaminase positive wild type strains of *pseudomonas* and *Paenibacillus*, as co aggregates, on the maximization of ISR against *Pyriculariaoryzae* in upland rice cv. ASD-19. CIB Tech. *J. Microbiol.* 1, 57–66.

Arora, S., Singh, A. K., and Sahni, D. (2017). "Bioremediation of salt-affected soils: challenges and opportunities" in *Bioremediation of salt affected soils: an Indian perspective*, eds. Arora, S., Singh, A., Singh, Y. (Cham: Springer), 275–301.

Arshad, M., Shaharoona, B., and Mahmood, T. (2008). Inoculation with *pseudomonas* spp. containing ACC deaminase partially eliminates the effects of drought stress on growth, yield, and ripening of pea (*Pisum sativum* L.). *Pedosphere* 18, 611–620. doi: 10.1016/S1002-0160(08)60055-7

Arya, B., Komala, B. R., Sumalatha, N. T., Surendra, G. M., and Gurumurthy, P. R. (2018). PGPR induced systemic tolerance in plant. *Int. J.Curr. Microbiol. Appl. Sci.* 7, 453–462.

Ashraf, S., Ali, Q., Zahir, Z. A., Ashraf, S., and Asghar, H. N. (2019). Phytoremediation: environmentally sustainable way for reclamation of heavy metal polluted soils. *Ecotoxicol. Environ. Safe* 174, 714–727. doi: 10.1016/j.ecoenv.2019.02.068

Ataikiru, T. L., Okpokwasili, G. S. C., and Okerentugba, P. O. (2019). Impact of pesticides on microbial diversity and enzymes in soil. *Public Administration Series--Bibliography*, 4, 1–16. doi: 10.9734/sajrm/2019/v4i230104

Azadikhah, M., Jamali, F., Nooryazdan, H. R., and Bayat, F. (2019). Growth promotion and yield enhancement of barley cultivars using ACC deaminase producing *Pseudomonas fluorescens* strains under salt stress. *Spanish J. Agric. Res.* 17:16. doi: 10.5424/sjar/2019171-13828

Babalola, O. O., Osir, E. O., Sanni, A. I., Odhiambo, G. D., and Bulimo, W. D. (2003). Amplification of 1-amino-cyclopropane-1-carboxylic (ACC) deaminase from plant growth promoting rhizobacteria in Striga-infested soil. *African J. Biotechnol.* 2, 157–160. doi: 10.5897/AJB2003.000-1032

Bal, H. B., Nayak, L., Das, S., and Adhya, T. K. (2013). Isolation of ACC deaminase PGPR from rice rhizo-sphere and evaluating their plant growth promoting activity under salt stress. *Plant Soil* 366, 93–105. doi: 10.1007/s11104-012-1402-5

Barnawal, D., Bharti, N., Maji, D., Chanotiya, C. S., and Kalra, A. (2012). 1-Aminocyclopropane-1-carboxylic acid (ACC) deaminase-containing rhizobacteria protect *Ocimum sanctum* plants during waterlogging stress via reduced ethylene generation. *Plant Physiol. Biochem.* 58, 227–235. doi: 10.1016/j.plaphy.2012.07.008

Barnawal, D., Bharti, N., Maji, D., Chanotiya, C. S., and Kalra, A. (2014). ACC deaminase-containing *Arthrobacter protophormiae* induces NaCl stress tolerance through reduced ACC oxidase activity and ethylene production resulting in improved nodulation and mycorrhization in *Pisum sativum*. *J. Plant Physiol.* 171, 884–894. doi: 10.1016/j.jplph.2014.03.007

Barnawal, D., Pandey, S. S., Bharti, N., Pandey, A., Ray, T., Singh, S., et al. (2017). ACC deaminase-containing plant growth-promoting rhizobacteria protect *Papaversomniferum* from downy mildew. *J. Appl. Microbiol.* 122, 1286–1298. doi: 10.1111/jam.13417

Belimov, A. A., Dodd, I. C., Hontzeas, N., Theobald, J. C., Safronova, V. I., and Davies, W. J. (2009). Rhizosphere bacteria containing 1-aminocyclopropane1-carboxylate deaminase increase yield of plants grown in drying soil via both local and systemic hormone signalling. *New Phytol.* 181, 413–423. doi: 10.1111/j.1469-8137.2008.02657.x

Belimov, A. A., Hontzeas, N., Safronova, V. I., Demchinskaya, S. V., Piluzza, G., Bullitta, S., et al. (2005). Cadmium-tolerant plant growth-promoting bacteria associated with the roots of Indian mustard (*Brassica juncea* L. Czern.). *Soil Biol. Biochem.* 37, 241–250. doi: 10.1016/j.soilbio.2004.07.033

Belimov, A. A., Zinovkina, N. Y., Safronova, V. I., Litvinsky, V. A., Nosikov, V. V., Zavalin, A. A., et al. (2019). Rhizobial ACC deaminase contributes to efficient symbiosis with pea (*Pisum sativum* L.) under single and combined cadmium and water deficit stress. *Environ. Exp. Bot.* 167:103859. doi: 10.1016/j.envexpbot.2019.103859

Bessadok, K., Navarro-Torre, S., Pajuelo, E., Mateos-Naranjo, E., Redondo-Gómez, S., Caviedes, M. Á., et al. (2020). The ACC-deaminase producing bacterium *Variovorax* sp. CT7. 15 as a tool for improving *Calicotomevillosa* nodulation and growth in arid regions of Tunisia. *Microorganisms* 8:541. doi: 10.3390/microorganisms8040541

Bharti, N., and Barnawal, D. (2019). "Amelioration of salinity stress by PGPR: ACC deaminase and ROS scavenging enzymes activity" in *PGPR amelioration in sustainable agriculture 85–10*, eds. Amit Kishore Singh, Ajay Kumar and Pawan Kumar Singh (Woodhead Publishing. Elsevier).

Bharti, N., Pandey, S. S., and Barnawal, D. (2016). Plant growth promoting rhizobacterial *Dietzianatronolimnaea* modulates the expression of stress responsive genes providing protection of wheat from salinity stress. *Sci. Rep.* 6:34768. doi: 10.1038/srep34768

Brader, G., Compant, S., Mitter, B., Trognitz, F., and Sessitsch, A. (2014). Metabolic potential of endophytic bacteria. *Curr. Opin. Biotechnol.* 27, 30–37. doi: 10.1016/j.copbio.2013.09.012

Carlos, M. H. J., Stefani, P. V. Y., and Janette, A. M. (2016). Assessing the effects of heavy metals in ACC deaminase and IAA production on plant growth-promoting bacteria. *Microbiol. Res.* 188-189, 53–61. doi: 10.1016/j.micres.2016.05.001

Carlson, R., Tugizimana, F., Steenkamp, P. A., Dubery, I. A., Hassen, A. I., and Labuschagne, N. (2020). Rhizobacteria-induced systemic tolerance against drought stress in *Sorghum bicolor* (L.) Moench. *Microbiol. Res.* 232:126388. doi: 10.1016/j.micres.2019.126388

Chandra, D., Srivastava, R., Glick, B. R., and Sharma, A. K. (2020). Rhizobacteria producing ACC deaminase mitigate water-stress response in finger millet (*Eleusine coracana* (L.) Gaertn.). *3 Biotech* 10:65. doi: 10.1007/s13205-019-2046-4

Chandra, D., Srivastava, R., Gupta, V. V., Franco, C. M., and Sharma, A. K. (2019). Evaluation of ACC-deaminase-producing rhizobacteria to alleviate water-stress impacts in wheat (*Triticumaestivum* L.) plants. *Canadian J. Microbiol.* 65, 387–403. doi: 10.1139/cjm-2018-0636

Chatterjee, P., Samaddar, S., Anandham, R., Kang, Y., Kim, K., Selvakumar, G., et al. (2017). Beneficial soil bacterium *pseudomonas frederiksbergensis* OS261 augments salt tolerance and promotes red pepper plant growth. *Front. Plant Sci.* 8:705. doi: 10.3389/fpls.2017.00705

Chauhan, P. S., Anandham, R., Han, G. H., and Sa, T. (2017). Erratum to: isolation, characterization, and use for plant growth promotion under salt stress, of ACC deaminase-producing halotolerant bacteria derived from coastal soil. *J. Microbiol. Biotechnol.* 20, 1577–1584. doi: 10.4014/jmb.1007.07011

Chen, J., Li, S., and Xu, B. (2017). Characterization of *Burkholderia* sp. XTB-5 for phenol degradation and plant growth promotion and its application in bioremediation of contaminated soil. *Land Degrad. Dev.* 28, 1091–1099. doi: 10.1002/ldr.2646

Chinnadurai, C., Balachandar, D., and Sundaram, S. P. (2009). Characterization of 1-aminocyclopropane-1-carboxylate deaminase producing methylobacteria from phyllosphere of rice and their role in ethylene regulation. *World J. Microbiol. Biotechnol.* 25, 1403–1411. doi: 10.1007/s11274-009-0027-1

Choi, J., Roy Choudhury, A., Walitang, D. I., Lee, Y., and Sa, T. (2022). ACC deaminase-producing *Brevibacterium linens* RS16 enhances heat-stress tolerance of rice (*Oryza sativa* L.). *Physiol. Planta.* 174:e13584. doi: 10.1111/ppl.13584

Chookietwattana, K., and Maneewan, K. (2012). Selection of efficient salt-tolerant bacteria containing ACC deaminase for promotion of tomato growth under salinity stress. *Soil Environ.* 31, 30–36.

Danish, S., Kiran, S., Fahad, S., Ahmad, N., Ali, M. A., Tahir, F. A., et al. (2019). Alleviation of chromium toxicity in maize by Fe fortification and chromium tolerant ACC deaminase producing plant growth promoting rhizobacteria. *Ecotoxicol. Environ. Saf* 185:109706. doi: 10.1016/j.ecoenv.2019.109706

Danish, S., Zafar-ul-Hye, M., Mohsin, F., and Hussain, M. (2020). ACC-deaminase producing plant growth promoting rhizobacteria and biochar mitigate adverse effects of drought stress on maize growth. *PLos One* 15:e0230615. doi: 10.1371/journal.pone.0230615

Das, A., and Osborne, J. W. (2018). "Bioremediation of heavy metals" in *Nanotechnology, food security and water treatment*, eds. Gothandam, K., Ranjan, S., Dasgupta, N., Ramalingam, C., Lichtfouse, E. (Cham: Springer), 277–311.

Daur, I., Saad, M. M., Eida, A. A., Ahmad, S., Shah, Z. H., Ihsan, M. Z., et al. (2018). Boosting alfalfa (*Medicago sativa* L.) production with rhizobacteria from various plants in Saudi Arabia. *Front. Microbiol.* 9:477. doi: 10.3389/fmicb.2018.0047

Dimkpa, C., Weinand, T., and Asch, F. (2009). Plant–rhizobacteria interactions alleviate abiotic stress conditions. *Plant Cell Environ.* 32, 1682–1694. doi: 10.1111/j.1365-3040.2009.02028.x

Din, B. U., Sarfraz, S., Xia, Y., Kamran, M. A., Javed, M. T., Sultan, T., et al. (2019). Mechanistic elucidation of germination potential and growth of wheat inoculated with exopolysaccharide and ACC-deaminase producing *bacillus* strains under induced salinity stress. *Ecotoxicol. Environ. Saf.* 183:109466. doi: 10.1016/j.ecoenv.2019.109466

Dixit, R., Agrawal, L., Gupta, S., Kumar, M., Yadav, S., Chauhan, P. S., et al. (2016). Southern blight disease of tomato control by 1-aminocyclopropane-1-carboxylate (ACC) deaminase producing *Paenibacilluslentimorbus* B-30488. *Plant Sign. Behav.* 11, 1–36. doi: 10.1080/15592324.2015.1113363

Dixit, R., Malaviya, D., Pandiyan, K., Singh, U. B., Sahu, A., Shukla, R., et al. (2015). Bioremediation of heavy metals from soil and aquatic environment: an overview of principles and criteria of fundamental processes. *Sustain.* 7, 2189–2212. doi: 10.3390/su7022189

Duan, J., Jiang, W., Cheng, Z., Heikkila, J. J., and Glick, B. R. (2013). The complete genome sequence of the plant growth-promoting bacterium *pseudomonas* sp. UW4. *PLoS One* 8:e58640. doi: 10.1371/journal.pone.0058640

Ek-Ramos, M. J., Gomez-Flores, R., Orozco-Flores, A. A., Rodríguez-Padilla, C., González-Ochoa, G., and Tamez-Guerra, P. (2019). Bioactive products from plant-endophytic gram-positive bacteria. *Front. Microbiol.* 10:463. doi: 10.3389/fmicb.2019.00463

El-Tarabily, K. A. (2013). Biocontrol of damping-off and root and crown rots of cucumber caused by *Pythium aphanidermatum* by ACC deaminase producing endophytic actinomycetes. *Phytopathology* 103:40.

Etesami, H., Mirseyed Hosseini, H., and Alikhani, H. A. (2014). Bacterial biosynthesis of 1-aminocyclopropane-1-caboxylate (ACC) deaminase, a useful trait to elongation and endophytic colonization of the roots of rice under constant flooded conditions. *Physiol. Mol. Biol. Plants* 20, 425–434. doi: 10.1007/s12298-014-0251-5

Etesami, H., Noori, F., Ebadi, A., and Reiahi Samani, N. (2020). "Alleviation of stress-induced ethylene-mediated negative impact on crop plants by bacterial ACC deaminase: perspectives and applications in stressed agriculture management" in *Plant microbiomes for sustainable agriculture by A*. eds. R. Meena, et al. (Springer, Singapore: Springer Nature Switzerland AG), 287–315.

FAO (2008). FAO land and plant nutrition management service. Available at: http://www.fao.org/ag/agl/agll/spush

Farahat, M. G., Mahmoud, M. K., Youseif, S. H., Saleh, S. A., and Kamel, Z. (2020). Alleviation of salinity stress in wheat by ACC deaminase-producing *bacillus aryabhattai* EWR29 with multifarious plant growth-promoting attributes. *Plant Arch.* 20, 417–429.

Ferguson, B. J., and Mathesius, U. (2014). Phytohormone regulation of legume-rhizobia interactions. *J. Chemical Ecol.* 40, 770–790. doi: 10.1007/s10886-014-0472-7

Fernandez-Moreno, J. P., and Stepanova, A. N. (2019). Monitoring ethylene in plants: genetically encoded reporters and biosensors. *Small Methods* 4:1900260. doi: 10.1002/smtd.201900260

Gamalero, E., and Glick, B. R. (2015). Bacterial modulation of plant ethylene levels. *PlantPhysiol.* 169, 13–22. doi: 10.1104/pp.15.00284

Glick, B. R. (1995). The enhancement of plant growth by free-living bacteria. *Can. J. Microbiol.* 41, 109–117. doi: 10.1139/m95-015

Glick, B. R. (2005). Modulation of plant ethylene levels by the bacterial enzyme ACC deaminase. *FEMS Microbiol. Lett.* 251, 1–7. doi: 10.1016/j.femsle.2005.07.030

Glick, B. R. (2012). Plant growth-promoting bacteria: mechanisms and applications. *Scientifica* 2012:963401, 1–15. doi: 10.6064/2012/963401

Glick, B. R. (2014). Bacteria with ACC deaminase can promote plant growth and help to feed the world. *Microbiol. Res.* 169, 30–39. doi: 10.1016/j.micres.2013.09.009

Glick, B. R., Cheng, Z., Czarny, J., and Duan, J. (2007a). "Promotion of plant growth by ACC deaminase-producing soil bacteria" in *New perspectives and approaches in plant growth-promoting Rhizobacteria research*, eds. Bakker, P. A. H. M., Raaijmakers, J. M., Bloemberg, G., Höfte, M., Lemanceau, P., Cooke, B. M. (Dordrecht: Springer), 329–339.

Glick, B. R., Penrose, D. M., and Li, J. (1998). A model for the lowering of plant ethylene concentrations by plant growth-promoting bacteria. *J. Theoretical Biol.* 190, 63–68. doi: 10.1006/jtbi.1997.0532

Glick, B. R., Todorovic, B., Czarny, J., Cheng, Z., Duan, J., and McConkey, B. (2007b). Promotion of plant growth by bacterial ACC deaminase. *Critical Review Plant Sci.* 26, 227–242. doi: 10.1080/07352680701572966

Glick, B. R., Nascimento, F. X., Vicente, C. S. L., Barbosa, P., Espada, M., Mota, M., et al (2013). Evidence for the involvement of ACC deaminase from Pseudomonas putida UW4 in the biocontrol of pine wilt disease. *caused by Bursaphelenchus xylophilus. Biocontrol* 58, 427–433. doi: 10.1007/s10526-012-9500-0

Gontia-Mishra, I., Sapre, S., Kachare, S., and Tiwari, S. (2017). Molecular diversity of 1-aminocyclopropane-1-carboxylate (ACC) deaminase producing PGPR from wheat (*Triticum aestivum* L.) rhizosphere. *Plant Soil* 414, 213–227. doi: 10.1007/s11104-016-3119-3

Gontia-Mishra, I., Sapre, S., and Sharma, A. (2016). Alleviation of mercury toxicity in wheat by the interaction of mercury-tolerant plant growth-promoting rhizobacteria. *J. Plant Growth Reg.* 35, 1000–1012. doi: 10.1007/s00344-016-9598-x

Gontia-Mishra, I., Sasidharan, S., and Tiwari, S. (2014). Recent developments in use of 1-aminocyclopropane-1-carboxylate (ACC) deaminase for conferring tolerance to biotic and abiotic stress. *Biotechnol. Lett.* 36, 889–898. doi: 10.1007/s10529-014-1458-9

Greetatorn, T., Hashimoto, S., Sarapat, S., Tittabutr, P., Boonkerd, N., Uchiumi, T., et al. (2019). Empowering rice seedling growth by endophytic *Bradyrhizobium* sp. SUTN 9-2. *Lett. Appl. Microbiol.* 68, 258–266. doi: 10.1111/lam.13114

Grichko, V. P., and Glick, B. R. (2001). Amelioration of flooding stress by ACC deaminase-containing plant growth-promoting bacteria. *Plant Physiol. Biochem.* 39, 11–17. doi: 10.1016/S0981-9428(00)01212-2

Grobelak, A., Kokot, P., Świątek, J., Jaskulak, M., and Rorat, A. (2018). Bacterial ACC deaminase activity in promoting plant growth on areas contaminated with heavy metals. *J. Ecol. Eng.* 19, 150–157. doi: 10.12911/22998993/89818

Guinel, F. C. (2015). Ethylene, a hormone at the center-stage of nodulation. *Front. Plant Sci.* 6, 1–21. doi: 10.3389/fpls.2015.01121

Gull, A., Lone, A. A., and Wani, N. U. I. (2019). "Biotic and abiotic stresses in plants" in *Abiotic and Biotic Stress in Plants* (London, United Kingdom: Intech Open).

Gupta, A., Bano, A., Rai, S., Kumar, M., Ali, J., Sharma, S., et al. (2021). ACC deaminase producing plant growth promoting rhizobacteria enhance salinity stress tolerance in *Pisumsativum*. *3 Biotech* 11, 514–517. doi: 10.1007/s13205-021-03047-5

Gupta, K., Dey, A., and Gupta, B. (2013). Plant polyamines in abiotic stress responses. *Acta Physiol.Plant.* 35, 2015–2036. doi: 10.1007/s11738-013-1239-4

Gupta, S., and Pandey, S. (2019). Unravelling the biochemistry and genetics of ACC deaminase-an enzyme alleviating the biotic and abiotic stress in plants. *Plant Gene.* 18:100175. doi: 10.1016/j.plgene.2019.100175

Gupta, A., Sinha, R., Fernandes, J. L., Abdelrahman, M., Burritt, D. J., and Tran, L. S. P. (2020). Phytohormones regulate convergent and divergent responses between individual and combined drought and pathogen infection. *Critical Reviews Biotech.* 40, 320–340. doi: 10.1080/07388551.2019.1710459

Gururani, M. A., Upadhyaya, C. P., Baskar, V., Venkatesh, J., Nookaraju, A., and Park, S. W. (2013). Plant growth-promoting rhizobacteria enhance abiotic stress tolerance in *Solanum tuberosum* through inducing changes in the expression of ROS-scavenging enzymes and improved photosynthetic performance. *J. Plant Growth Regul.* 32, 245–258. doi: 10.1007/s00344-012-9292-6

Han, Y., Wang, R., Yang, Z., Zhan, Y., Ma, Y., Ping, S., et al. (2015). 1-aminocyclopropane-1-carboxylate deaminase from *pseudomonas stutzeri* A1501 facilitates the growth of rice in the presence of salt or heavy metals. *J. Microbiol. Biotechnol.* 25, 1119–1128. doi: 10.4014/jmb.1412.12053

Han, L., Zhang, H., Xu, Y., Li, Y., and Zhou, J. (2021). Biological characteristics and salt-tolerant plant growth-promoting effects of an ACC deaminase-producing Burkholderiapyrrocinia strain isolated from the tea rhizosphere. *Arch. Microbiol.* 203, 2279–2290. doi: 10.1007/s00203-021-02204-x

Hassan, W., Bano, R., Bashir, F., and David, J. (2014). Comparative effectiveness of ACC-deaminase and/or nitrogen-fixing rhizobacteria in promotion of maize (*Zea mays* L.) growth under lead pollution. *Environ. Sci. Pollut. Res.* 21, 10983–10996. doi: 10.1007/s11356-014-3083-5

Hemida, K. A., and Reyad, A. M. M. (2018). Improvement salt tolerance of safflower plants by endophytic bacteria. *J. Hort. Plant Res.* 5, 38–56. doi: 10.18052/www.scipress.com/JHPR.5.38

Hemissi, I., Hammami, R., Hachana, A., Arfaoui, H., and Sifi, B. (2019). Fertilizer-dependent efficiency of *Mesorhizobium* strain for improving growth, nutrient uptake and grain yield of durum wheat (*Triticum turgidium* L.) variety. *J. New Sci.* 61, 3885–3891.

Honma, M. (1983). Enzymatic determination of 1-aminocyclopropane-1-carboxylic acid. *Agric. Biol. Chem.* 47, 617–618.

Honma, M. (1985). Chemically reactive sulfhydryl groups of 1-aminocyclopropane-1-carboxylate deaminase. *Agric. Biol. Chem.* 49, 567–571. doi: 10.1080/00021369.1985.10866774

Honma, M. (1993). "Stereospecific reaction of 1-aminocyclopropane-1-carboxylate deaminase" in *Cellular and molecular aspects of the plant hormone ethylene* (Dordrecht: Springer), 111–116.

Honma, M., Kawai, J., and Yamada, M. (1993). Identification of the reactive sulfhydryl group of 1-aminocyclopropane-1-carboxylate deaminase. *Biosci. Biotechnol. Biochem.* 57, 2090–2093. doi: 10.1271/bbb.57.2090

Honma, M., and Shimomura, T. (1978). Metabolism of 1-aminocyclopropane-1-carboxylic acid. *Agric. Biol. Chem.* 42, 1825–1831. doi: 10.1080/00021369.1978.10863261

Hontzeas, N., Hontzeas, C. E., and Glick, B. R. (2006). Reaction mechanisms of the bacterial enzyme 1-aminocyclopropane-1-carboxylate deaminase. *Biotechnol. Adv.* 24, 420–426. doi: 10.1016/j.biotechadv.2006.01.006

Hontzeas, N., Zoidakis, J., Glick, B. R., and Abu-Omar, M. M. (2004). Expression and characterization of 1-aminocyclopropane-1-carboxylate deaminase from the rhizobacterium *pseudomonas putida* UW4: a key enzyme in bacterial plant growth promotion. *Biochim. Biophysica Acta-Proteins Proteom.* 1703, 11–19. doi: 10.1016/j.bbapap.2004.09.015

Huang, C. H., Hsiang, T., and Trevors, J. T. (2013). Comparative bacterial genomics: defining the minimal core genome. *Anton. Leeuw.* 103, 385–398. doi: 10.1007/s10482-012-9819-7

Huang, X. F., Zhou, D., Lapsansky, E. R., Reardon, K. F., Guo, J., Andales, M. J., et al. (2017). *Mitsuaria* sp. and *Burkholderia* sp. from *Arabidopsis* rhizosphere enhance drought tolerance in *Arabidopsis thaliana* and maize (*Zea mays* L.). *Plant Soil* 419, 523–539. doi: 10.1007/s11104-017-3360-4

Hussain, S., Shaukat, M., Ashraf, M., Zhu, C., Jin, Q., and Zhang, J. (2019). *Salinity stress in arid and semi-arid climates: effects and management in field crops*. Climate change and agriculture. Intech Open.

Indiragandhi, P., Anandham, R., Kim, K., Yim, W. J., Madhaiyan, M., and Sa, T. M. (2008). Induction of defense responses in tomato against *pseudomonas syringae*pv. Tomato by regulating the stress ethylene level with *Methylobacteriumoryzae* CBMB20 containing 1-aminocyclopropane-1carboxylate deaminase. *World J. Microbiol. Biotechnol.* 24, 1037–1045. doi: 10.1007/s11274-007-9572-7

Jackson, M. B. (2008). Ethylene-promoted elongation: an adaptation to submergence stress. *Ann. Bot.* 101, 229–248. doi: 10.1093/aob/mcm237

Jacobson, C. B., Pasternak, J. J., and Glick, B. R. (1994). Partial purification and characterization of 1-aminocyclopropane-1-carboxylate deaminase from the plant growth promoting rhizobacterium *pseudomonas putida* GR12-2. *Canadian J. Microbiol.* 40, 1019–1025. doi: 10.1139/m94-16

Jaemsaeng, R., Jantasuriyarat, C., and Thamchaipenet, A. (2018). Positive role of 1-aminocyclopropane-1-carboxylate deaminase-producing endophytic *Streptomyces* sp. GMKU 336 on flooding resistance of mung bean. *Agric. Natural Res.* 52, 330–334. doi: 10.1016/j.anres.2018.09.008

Jajoo, A. (2017). "Effects of environmental pollutants polycyclic aromatic hydrocarbons (PAH) on photosynthetic processes" in *Photosynthesis: structures, mechanisms, and applications* (Cham, eds. Hou, H., Najafpour, M., Moore, G., Allakhverdiev, S. Springer), 249–259.

Jha, C. K., Annapurna, K., and Saraf, M. (2012). Isolation of Rhizobacteria from *Jatrophacurcas* and characterization of produced ACC deaminase. *J. Basic Microbiol.* 52, 285–295. doi: 10.1002/jobm.201100113

Ji, J., Yuan, D., Jin, C., Wang, G., Li, X., and Guan, C. (2020). Enhancement of growth and salt tolerance of rice seedlings (*Oryza sativa* L.) by regulating ethylene production with a novel halotolerant PGPR strain *Glutamicibacter* sp. YD01 containing ACC deaminase activity. *Acta Physiol. Plant.* 42:42. doi: 10.1007/s11738-020-3034-3

Joshi, M., Srivastava, R., Sharma, A. K., and Prakash, A. (2012). Screening of resistant varieties and antagonistic *fusarium oxysporum* for biocontrol of *fusarium* wilt of chilli. *J. Plant Pathol. Microbiol.* 03, 1–6. doi: 10.4172/2157-7471.1000134

Kalsoom, A., Batool, R., and Jamil, N. (2022). Beneficial rhizospheric associated traits of chromate resistant bacteria for remediation of Cr (VI) contaminated soil. *Biorem. J.*, 16, 1–19. doi: 10.1080/10889868.2022.2054930

Kaneko, T., Nakamura, Y., Sato, S., Minamisawa, K., Uchiumi, T., Sasamoto, S., et al. (2002). Complete genomic sequence of nitrogen-fixing symbiotic bacterium *Bradyrhizobium japonicum* USDA110. *DNA Res.* 9, 189–197. doi: 10.1093/dnares/9.6.189

Kang, S. M., Shahzad, R., Bilal, S., Khan, A. L., Park, Y. G., Lee, K. E., et al. (2019). Indole-3-acetic-acid and ACC deaminase producing *Leclerciaadecarboxylata* MO1 improves *Solanum lycopersicum* L. growth and salinity stress tolerance by endogenous secondary metabolites regulation. *BMC Microbiol.* 19:80. doi: 10.1186/s12866-019-1450-6

Karthikeyan, S., Zhou, Q., Zhao, Z., Kao, C. L., Tao, Z., Robinson, H., et al. (2004). Structural analysis of *pseudomonas* 1-aminocyclopropane-1-carboxylate deaminase complexes: insight into the mechanism of a unique pyridoxal-5′-phosphate dependent cyclopropane ring-opening reaction. *Biochemist* 43, 13328–13339. doi: 10.1021/bi048878g

Kataria, S., and Verma, S. K. (2018). "Salinity stress responses and adaptive mechanisms in major glycophytic crops: the story so far" in *Salinity responses and tolerance in plants*, eds. Kumar, V., Wani, S., Suprasanna, P., Tran, LS. (Cham: Springer), 1, 1–39.

Katiyar, P., Dubey, R. C., and Maheshwari, D. K. (2021). ACC deaminase-producing *Ensiferadhaerens* KS23 enhances proximate nutrient of *Pisum sativum* L. cultivated in high altitude. *Arch. Microbiol.* 203, 2689–2698. doi: 10.1007/s00203-021-02250-5

Kaur, T., and Manhas, R. K. (2022). Evaluation of ACC deaminase and indole acetic acid production by *Streptomyces hydrogenans* DH16 and its effect on plant growth promotion. *Biocat. Agric. Biotech.* 42:102321. doi: 10.1016/j.bcab.2022.102321

Kaushal, M., and Wani, S. P. (2016). Plant growth-promoting rhizobacteria: drought stress alleviators to ameliorate crop production in drylands. *Ann. Microbiol.* 66, 35–42. doi: 10.1007/s13213-015-1112-3

Khan, S., Shahid, M., Khan, M. S., Syed, A., Bahkali, A. H., Elgorban, A. M., et al. (2020). Fungicide-tolerant plant growth-promoting rhizobacteria mitigate physiological disruption of white radish caused by fungicides used in the field cultivation. *Int. J. Environ. Res. Public Health* 17:7251. doi: 10.3390/ijerph17197251

Khan, A., and Singh, A. V. (2021). Multifarious effect of ACC deaminase and EPS producing *pseudomonas* sp. and *Serratia marcescens* to augment drought stress tolerance and nutrient status of wheat. *World J.Microbiol. Biotech.* 37, 198–117. doi: 10.1007/s11274-021-03166-4

Khosravi, H., Alikhani, H. A., Yakhchali, B., and Kharkhane, A. A. (2014). Isolation, cloning and sequence analysis of 1-aminocyclopropane-1-carboxylate deaminase gene from native *Sinorhizobiummeliloti*. *Iran. J. Biotech.* 12, 50–56. doi: 10.15171/ijb.1000

Klay, I., Gouia, S., Liu, M., Mila, I., Khoudi, H., Bernadac, A., et al. (2018). Ethylene response factors (ERF) are differentially regulated by different abiotic stress types in tomato plants. *Plant Sci.* 274, 137–145. doi: 10.1016/j.plantsci.2018.05.023

Klee, H. J., Hayford, M. B., Kretzmer, K. A., Barry, G. F., and Kishore, G. M. (1991). Control of ethylene synthesis by expression of a bacterial enzyme in transgenic tomato plants. *Plant Cell* 3, 1187–1193. doi: 10.1105/tpc.3.11.1187

Klee, H. J., Romano, C. P., and Binns, A. (1994). The roles of phytohormones in development as studied in transgenic plants. *Critic. Review Plant Sci.* 13, 311–324. doi: 10.1080/07352689409701918

Kruasuwan, W., and Thamchaipenet, A. (2018). 1-aminocyclopropane-1-carboxylate (ACC) deaminase-producing endophytic diazotrophic *Enterobacter* sp. EN-21 modulates salt–stress response in sugarcane. *J. Plant Growth Regul.* 37, 849–858. doi: 10.1007/s00344-018-9780-4

Kumar, P., Dubey, R. C., Maheshwari, D. K., and Bajpai, V. (2016). ACC deaminase producing *rhizobium leguminosarum* rpn5 isolated from root nodules of *Phaseolus vulgaris* L. *Bangladesh J. Bot.* 45, 477–484.

Kumar, M., Etesami, H., and Kumar, V. (2019). *Saline soil-based agriculture by halotolerant microorganisms* Springer.

Kumar, R., Kumar, R., and Prakash, O. (2019). Chapter-5 the impact of chemical fertilizers on our. *Environ. Ecosyst.* 35:69.

Kumar, A., Maleva, M., Bruno, L. B., and Rajkumar, M. (2021). Synergistic effect of ACC deaminase producing pseudomonas sp. TR15a and siderophore producing *Bacillus aerophilus* TR15c for enhanced growth and copper accumulation in *Helianthus annuus* L. *Chemosphere* 276:130038. doi: 10.1016/j.chemosphere.2021.130038

Lesk, C., Rowhani, P., and Ramankutty, N. (2016). Influence of extreme weather disasters on global crop production. *Nature* 529, 84–87. doi: 10.1038/nature16467

Li, J., Ovakim, D. H., Charles, T. C., and Glick, B. R. (2000). An ACC deaminase minus mutant of *Enterobactercloacae* UW4No longer promotes root elongation. *Cur. Microbiol.* 41, 101–105. doi: 10.1007/s002840010101

Li, Z., Wang, W., and Zhu, L. (2019). Effects of mixed surfactants on the bioaccumulation of polycyclic aromatic hydrocarbons (PAHs) in crops and the bioremediation of contaminated farmlands. *Sci. Total Environ* 646, 1211–1218. doi: 10.1016/j.scitotenv.2018.07.349

Light, K. M., Wisniewski, J. A., Vinyard, W. A., and Kieber-Emmons, M. T. (2016). Perception of the plant hormone ethylene: known-knowns and known-unknowns. *J. Biol. Inorganic Chem.* 21, 715–728. doi: 10.1007/s00775-016-1378-3

Liu, J. L., Xie, B. M., Shi, X. H., Ma, J. M., and Guo, C. H. (2015). Effects of two plant growth-promoting rhizobacteria containing 1-aminocyclopropane-1carboxylate deaminase on oat growth in petroleum-contaminated soil. *Int. J. Environ. Sci. Technol.* 12, 3887–3894. doi: 10.1007/s13762-015-0798-x

Ma, W., Charles, T. C., and Glick, B. R. (2004). Expression of an exogenous 1-aminocyclopropane-1-carboxylate deaminase gene in *Sinorhizobiummeliloti* increases its ability to nodulate alfalfa. *Appl. Environ. Microbiol.* 70, 5891–5897. doi: 10.1128/AEM.70.10.5891-5897.2004

Ma, W., Guinel, F. C., and Glick, B. R. (2003a). *Rhizobium leguminosarum* biovar viciae 1-aminocyclopropane-1-carboxylate deaminase promotes nodulation of pea plants. *Appl. Environ. Microbiol.* 69, 4396–4402. doi: 10.1128/AEM.69.8.4396-4402.2003

Ma, W., Sebestianova, S. B., Sebestian, J., Burd, G. I., Guinel, F. C., and Glick, B. R. (2003b). Prevalence of 1-aminocyclopropane-1-carboxylate deaminase in *rhizobium* spp. *Antonie Van Leeuwenhoek* 83, 285–291. doi: 10.1023/A:1023360919140

Malerba, M., Crosti, P., and Bianchetti, R. (1996). 2-Aminoisobutyric acid prevents the substrate-induced inactivation of ACC-synthase without inhibiting the enzyme. *Plant Sci.* 113, 131–138. doi: 10.1016/0168-9452(95)04294-6

Malviya, D., Singh, U. B., Singh, S., Sahu, P. K., Pandiyan, K., Kashyap, A. S., et al. (2020). "Microbial interactions in the rhizosphere contributing crop resilience to biotic and abiotic stresses" in *Rhizosphere microbes*. eds. Sharmaet al. (Singapore: Springer), 1–33.

Manoj, S. R., Karthik, C., Kadirvelu, K., Arulselvi, P. I., Shanmugasundaram, T., Bruno, B., et al. (2020). Understanding the molecular mechanisms for the enhanced phytoremediation of heavy metals through plant growth promoting rhizobacteria: a review. *J. Environ.Manag.* 254:109779. doi: 10.1016/j.jenvman.2019.109779

Maqbool, S., Amna, A., Mehmood, S., Suhaib, M., Sultan, T., and Munis, M. (2021). Interaction of acc deaminase and antioxidant enzymes to induce drought tolerance in *Enterobacter cloacae* 2wc2 inoculated maize genotypes. *Pak. J. Bot.* 53. doi: 10.30848/PJB2021-3(28)

Miller, G., Susuki, N., and Ciftci-Yilmaz, S. (2010). Reactive oxygen species homeostasis and signalling during drought and salinity stresses. *Plant Cell Environ.* 33, 453–467. doi: 10.1111/j.1365-3040.2009. 02041.x

Misra, S., and Chauhan, P. S. (2020). ACC deaminase-producing rhizosphere competent *bacillus* spp. mitigate salt stress and promote *Zea mays* growth by modulating ethylene metabolism. *3 Biotech* 10, 119–114. doi: 10.1007/s13205-020-2104-y

Moeder, W., Barry, C. S., Tauriainen, A. A., Betz, C., Tuomainen, J., Utriainen, M., et al. (2002). Ethylene synthesis regulated by biphasic induction of 1-aminocyclopropane-1-carboxylic acid synthase and 1-aminocyclopropane-1-carboxylic acid oxidase genes is required for hydrogen peroxide accumulation and cell death in ozone-exposed tomato. *Plant Physiol.* 130, 1918–1926. doi: 10.1104/pp.009712

Mog, B., Adiga, D., and Nayak, M. G. (2018). Role of plant growth hormones in cashew: key strategy for modifying crop performance. *Int. J. Curr. Microbiol. App. Sci.* 7, 1470–1484. doi: 10.20546/ijcmas.2018.707.174

Murali, M., Singh, S. B., Gowtham, H. G., Shilpa, N., Prasad, M., Aiyaz, M., et al. (2021). Induction of drought tolerance in *Pennisetum glaucum* by ACC deaminase producing PGPR-*bacillus amyloliquefaciens* through antioxidant defense system. *Microbiol. Res.* 253:126891. doi: 10.1016/j.micres.2021.126891

Nadeem, S. M., Ahmad, M., Tufail, M. A., Asghar, H. N., Nazli, F., and Zahir, Z. A. (2021). Appraising the potential of EPS-producing rhizobacteria with ACC-deaminase activity to improve growth and physiology of maize under drought stress. *Physiol. Plant.* 172, 463–476. doi: 10.1111/ppl.13212

Nadeem, S. M., Zahair, Z. A., Naveed, M., and Arshad, M. (2007). Preliminary investigations on inducing salt tolerance in maize through inoculation with rhizobacteria containing ACC deaminase activity. *Can. J. Microbiol.* 53, 1141–1149. doi: 10.1139/W07-081

Nadeem, S. M., Zahir, Z. A., Naveed, M., Asghar, H. N., and Arshad, M. (2010). Rhizobacteria capable of producing ACC deaminase may mitigate salt stress in wheat. *Soil Sci. Soc. Am. J.* 74, 533–542. doi: 10.2136/sssaj2008.0240

Nascimento, F., Brígido, C., Alho, L., Glick, B. R., and Oliveira, S. (2012). Enhanced chickpea growth-promotion ability of a *Mesorhizobium* strain expressing an exogenous ACC deaminase gene. *Plant Soil* 353, 221–230. doi: 10.1007/s11104-011-1025-2

Nascimento, F. X., Rossi, M. J., Soares, C. R., McConkey, B. J., and Glick, B. R. (2014). New insights into 1-aminocyclopropane-1-carboxylate (ACC) deaminase phylogeny, evolution and ecological significance. *PLoS One* 9:e99168. doi: 10.1371/journal.pone.0099168

Nascimento, F. X., Tavares, M. J., Franck, J., Ali, S., Glick, B. R., and Rossi, M. J. (2019). ACC deaminase plays a major role in *Pseudomonas fluorescens* YsS6 ability to promote the nodulation of alpha-and beta proteobacteria rhizobial strains. *Arch.Microbiol.* 201, 817–822. doi: 10.1007/s00203-019-01649-5

Nascimento, F. X., Vicente, C. S., Barbosa, P., Espada, M., Glick, B. R., Mota, M., et al. (2013). Evidence for the involvement of ACC deaminase from *pseudomonas putida* UW4 in the biocontrol of pine wilt disease caused by *Bursaphelenchusxylophilus*. *Biol. Control* 58, 427–433. doi: 10.1007/s10526-012-9500-0

Nukui, N., Minamisawa, K., Ayabe, S. I., and Aoki, T. (2006). Expression of the 1-aminocyclopropane-1-carboxylic acid deaminase gene requires symbiotic nitrogen-fixing regulator gene nifA2 in Mesorhizobium loti MAFF303099. *Appl. Environ. Microbiol.* 72, 4964–4969. doi: 10.1128/AEM.02745-05

Orhan, F. (2016). Alleviation of salt stress by halotolerant and halophilic plant growth-promoting bacteria in wheat (*Triticum aestivum*). *Brazilian J. Microbiol.* 47, 621–627. doi: 10.1016/j.bjm.2016.04.001

Ose, T., Fujino, A., Yao, M., Watanabe, N., Honma, M., and Tanaka, I. (2003). Reaction intermediate structures of 1-aminocyclopropane-1-carboxylate deaminase: insight into PLP-dependent cyclopropane ring-opening reaction. *J. Biol. Chem.* 278, 41069–41076. doi: 10.1074/jbc.M305865200

Ouaked, F., Rozhon, W., Lecourieux, D., and Hirt, H. (2003). A MAPK pathway mediates ethylene signaling in plants. *EMBO J.* 22, 1282–1288. doi: 10.1093/emboj/cdg131

Panda, A., Rangani, J., Kumari, A., and Parida, A. K. (2017). Efficient regulation of arsenic translocation to shoot tissue and modulation of phytochelatin levels and antioxidative defense system confers salinity and arsenic tolerance in the halophyte *Suaeda maritima*. *Environ. Exp. Bot.* 143, 149–171. doi: 10.1016/j.envexpbot.2017.09.007

Pandey, S., Ghosh, P. K., Ghosh, S., De, T. K., and Maiti, T. K. (2013). Role of heavy metal resistant *Ochrobactrum* sp. and *bacillus* spp. strains in bioremediation of a rice cultivar and their PGPR like activities. *J. Microbiol.* 51, 11–17. doi: 10.1007/s12275-013-2330-7

Pandey, S., and Gupta, S. (2020). Evaluation of *pseudomonas* sp. for its multifarious plant growth promoting potential and its ability to alleviate biotic and abiotic stress in tomato (*Solanumlycopersicum*) plants. *Sci. Rep.* 10, 1–15. doi: 10.1038/s41598-020-77850-0

Paul, M. V., Iyer, S., Amerhauser, C., Lehmann, M., van Dongen, J. T., and Geigenberger, P. (2016). Oxygen sensing via the ethylene response transcription factor RAP2. 12 affects plant metabolism and performance under both normoxia and hypoxia. *Plant Physiol.* 172, 141–153. doi: 10.1104/pp.16.00460

Pierik, R., Tholen, D., Poorter, H., Visser, E. J., and Voesenek, L. A. (2006). The Janus face of ethylene: growth inhibition and stimulation. *Trends Plant Sci.* 11, 176–183. doi: 10.1016/j.tplants.2006.02.006

Pirasteh-Anosheh, H., Ranjbar, G., Pakniyat, H., and Emam, Y. (2016). Physiological mechanisms of salt stress tolerance in plants: an overview. *Plant-Environ. Interact. Responses Approaches Mitigate Stress*, 141–160. doi: 10.1002/9781119081005.ch8

Place, F., Meybeck, A., Colette, L., de Young, C., Gitz, V., Dulloo, E., et al (2017). Food security and sustainable resource use? What are the resource challenges to food security.

Płociniczak, T., Sinkkonen, A., and Romantschuk, M. (2014). Characterization of *Enterobacterintermedius* MH8b and its use for the enhancement of heavy metals uptake by *Sinapis alba* L. *Appl. Soil Ecol.* 63, 1–7. doi: 10.1016/j.apsoil.2012.09.009

Pramanik, K., Mitra, S., Sarkar, A., and Maiti, T. K. (2018). Alleviation of phytotoxic effects of cadmium on rice seedlings by cadmium resistant PGPR strain *Enterobacter aerogenes* MCC 3092. *J. Hazard. Mater.* 351, 317–329. doi: 10.1016/j.jhazmat.2018.03.009

Prasannakumar, S. P., Gowtham, H. G., Hariprasad, P., Shivaprasad, K., and Niranjana, S. R. (2015). *Delftiatsuruhatensis* WGR–UOM–BT1, a novel rhizobacterium with PGPR properties from *Rauwolfia serpentina* (L.) Benth. Ex Kurz also suppresses fungal phytopathogens by producing a new antibiotic—AMTM. *Lettt. Appl. Microbiol.* 61, 460–468. doi: 10.1111/lam.12479

Qin, S., Zhang, Y. J., Yuan, B., Xu, P. Y., Xing, K., Wang, J., et al. (2014). Isolation of ACC deaminase-producing habitat-adapted symbiotic bacteria associated with halophyte *Limonium sinense* (Girard) Kuntze and evaluating their plant growth-promoting activity under salt stress. *Plant Soil* 374, 753–766. doi: 10.1007/s11104-013-1918-3

Raghuwanshi, R., and Prasad, J. K. (2018). "Perspectives of rhizobacteria with ACC deaminase activity in plant growth under abiotic stress" in *Root biology*, eds. Giri, B., Prasad, R., Varma, A. (Cham: Springer), 303–321.

Rao, M. V., and Davis, K. R. (2001). The physiology of ozone induced cell death. *Planta* 213, 682–690. doi: 10.1007/s004250100618

Rashid, U., Yasmin, H., Hassan, M. N., Naz, R., Nosheen, A., Sajjad, M., et al. (2022). Drought-tolerant *bacillus megaterium* isolated from semi-arid conditions induces systemic tolerance of wheat under drought conditions. *Plant Cell Rep.* 41, 549–569. doi: 10.1007/s00299-020-02640-x

Rauf, M., Awais, M., Ud-Din, A., Ali, K., Gul, H., Rahman, M. M., et al. (2021). Molecular mechanisms of the 1-aminocyclopropane-1-carboxylic acid (ACC) deaminase producing *Trichoderma asperellum* MAP1 in enhancing wheat tolerance to waterlogging stress. *Front. Plant Sci.* 11:2213. doi: 10.3389/fpls.2020.614971

Ravanbakhsh, M., Sasidharan, R., Voesenek, L. A., Kowalchuk, G. A., and Jousset, A. (2017). ACC deaminase-producing rhizosphere bacteria modulate plant responses to flooding. *J. Ecol.* 105, 979–986. doi: 10.1111/1365-2745.12721

Reinhold-Hurek, B., and Hurek, T. (2011). Living inside plants: bacterial endophytes. *Curr. Opin. Plant Biol.* 14, 435–443. doi: 10.1016/j.pbi.2011.04.004

Rengasamy, P. (2010). Soil processes affecting crop production in salt-affected soils. *FunctionalPlant Biol.* 37, 613–620. doi: 10.1071/FP09249

Riemenschneider, A., Wegele, R., Schmidt, A., and Papenbrock, J. (2005). Isolation and characterization of ad-cysteine desulfhydrase protein from Arabidopsis thaliana. *FEBS J.* 272, 1291–1304. doi: 10.1111/j.1742-4658.2005. 04567.x

Rizvi, A., and Khan, M. S. (2018). Heavy metal induced oxidative damage and root morphology alterations of maize (*Zea mays* L.) plants and stress mitigation by metal tolerant nitrogen fixing *Azotobacter chroococcum*. *Ecotoxicol. Environ. Safe.* 157, 9–20. doi: 10.1016/j.ecoenv.2018.03.063

Rizvi, A., Zaidi, A., Khan, M. S., Saif, S., Ahmed, B., and Shahid, M. (2017). Growth improvement and management of vegetable diseases by plant growth-promoting rhizobacteria. *In Microbial Strategies for Vegetable Production. eds. Zaidi, A., Khan, M. Springer, Cham.*. doi: 10.1007/978-3-319-54401-4_5

Sagar, A., Rai, S., Ilyas, N., Sayyed, R. Z., Al-Turki, A. I., El Enshasy, H. A., et al. (2022). Halotolerant rhizobacteria for salinity-stress mitigation: diversity, mechanisms and molecular approaches. *Sustainability* 14:490. doi: 10.3390/su14010490

Sagar, A., Sayyed, R. Z., Ramteke, P. W., Sharma, S., Marraiki, N., Elgorban, A. M., et al. (2020). ACC deaminase and antioxidant enzymes producing halophilic *Enterobacter* sp. PR14 promotes the growth of rice and millets under salinity stress. *Physiol. Molecular Biol. Plants* 26, 1847–1854. doi: 10.1007/s12298-020-00852-9

Saghafi, D., Ghorbanpour, M., Ajirloo, H. S., and Lajayer, B. A. (2019). Enhancement of growth and salt tolerance in *Brassica napus* L. seedlings by halotolerant *rhizobium* strains containing ACC-deaminase activity. *Plant Physiol. Rep.* 24, 225–235. doi: 10.1007/s40502-019-00444-0

Sahu, P. K., Singh, S., Singh, U. B., Chakdar, H., Sharma, P. K., Sarma, B. K., et al. (2021). Inter-genera colonization of *Ocimumtenuiflorum* endophytes in tomato and their complementary effects on Na^+/K^+ balance, oxidative Stress regulation, and root architecture under elevated soil salinity. *Front. Microbiol.* 12:744733. doi: 10.3389/fmicb.2021.744733

Saif, S., and Khan, M. S. (2018). Assessment of toxic impact of metals on proline, antioxidant enzymes, and biological characteristics of *Pseudomonas aeruginosa* inoculated *Cicer arietinum* grown in chromium and nickel-stressed sandy clay loam soils. *Environ.Monit. Assess.* 190, 290–218. doi: 10.1007/s10661-018-6652-0

Saif, S., Khan, M. S., Zaidi, A., Rizvi, A., and Shahid, M. (2017). Metal toxicity to certain vegetables and bioremediation of metal-polluted soils. *In Microbial Strategies for Vegetable Production. eds. Zaidi, A., Khan, M. Springer, Cham*. doi: 10.1007/978-3-319-54401-4_8

Saikia, J., Sarma, R. K., Dhandia, R., Yadav, A., Bharali, R., Gupta, V. K., et al. (2018). Alleviation of drought stress in pulse crops with ACC deaminase producing rhizobacteria isolated from acidic soil of Northeast India. *Sci. Rep.* 8:3560. doi: 10.1038/s41598-018-21921-w

Saleem, M., Arshad, M., Hussain, S., and Bhatti, A. S. (2007). Perspective of plant growth promoting rhizobacteria (PGPR) containing ACC deaminase in stress agriculture. *J. Ind. Microbiol. Biotechnol.* 34, 635–648. doi: 10.1007/s10295-007-0240-6

Saleem, A. R., Brunetti, C., Khalid, A., Della Rocca, G., Raio, A., and Emiliani, G. (2018). Drought response of *Mucuna pruriens* (L.) inoculated with ACC deaminase and IAA producing rhizobacteria. *PLoS One* 13, 1–18. doi: 10.1371/journal.pone.0191218

Sanchez-Hernandez, J. C. (2019). Biochar mitigates the impact of pesticides on soil enzyme activities. *Biorem. Agric. Soils*, 193–216. doi: 10.1201/9781315205137-10

Santos, E., Pires, F. R., Ferreira, A. D., Egreja Filho, F. B., Madalão, J. C., Bonomo, R., et al. (2019). Phytoremediation and natural attenuation of sulfentrazone: mineralogy influence of three highly weathered soils. *Int. J. Phytoremediation* 21, 652–662. doi: 10.1080/15226514.2018.1556583

Santoyo, G., Moreno-Hagelsieb, G., del Carmen Orozco-Mosqueda, M., and Glick, B. R. (2016). Plant growth-promoting bacterial endophytes. *Microbiol. Res.* 183, 92–99. doi: 10.1016/j.micres.2015.11.008

Sapre, S., Gontia-Mishra, I., and Tiwari, S. (2018a). Klebsiella sp. confers enhanced tolerance to salinity and plant growth promotion in oat seedlings (*Avena sativa*). *Microbiol. Res.* 206, 25–32. doi: 10.1016/j.micres.2017.09.009

Sapre, S., Gontia-Mishra, I., and Tiwari, S. (2018b). "ACC deaminase-producing bacteria: a key player in alleviating abiotic stresses in plants" in *Plant growth promoting Rhizobacteria for agricultural sustainability* (Singapore: Springer), 267–291.

Sarkar, A., Ghosh, P. K., Pramanik, K., Mitra, S., Soren, T., Pandey, S., et al. (2018a). A halotolerant *Enterobacter* sp. displaying ACC deaminase activity promotes rice seedling growth under salt stress. *Res.Microbiol.* 169, 20–32. doi: 10.1016/j.resmic.2017.08.005

Sarkar, A., Pramanik, K., Mitra, S., Soren, T., and Maiti, T. K. (2018b). Enhancement of growth and salt tolerance of rice seedlings by ACC deaminase-producing *Burkholderia* sp. MTCC 12259. *J. Plant Physiol.* 231, 434–442. doi: 10.1016/j.resmic.2017.08.005

Saxena, P., and Kulshrestha, U. (2016). "Biochemical effects of air pollutants on plants" in *Plant responses to air pollution*, Kulshrestha, U., Saxena, P. (eds) (Singapore: Springer), 59–70.

Schwachtje, J., Whitcomb, S. J., Firmino, A. A., Zuther, E., Hincha, D. K., and Kopka, J. (2019). Induced, imprinted and primed metabolic responses of plants to changing environments: do plants store and process information by metabolic imprinting and metabolic priming? *Front. Plant Sci.* 10:106. doi: 10.3389/fpls.2019.00106

Senthilkumar, M., Paulraj, S., Alagupalamuthirsolai, M., Singh, M., and Singh, J. (2016). Synergistic effect of *Mesorhizobiumciceri* and 1-amino cyclopropane 1-carboxylate (ACC) deaminase producing rhizobacteria on chickpea growth and yield. *J. Food Legumes* 29, 37–42.

Shaharoona, B., Arshad, M., and Zahir, Z. A. (2006). Effect of plant growth promoting rhizobacteria containing ACC-deaminase on maize (*Zea mays* L.) growth under axenic conditions and on nodulation in mung bean (*Vigna radiata* L.). *Lett. Appl. Microbiol.* 42, 155–159. doi: 10.1111/j.1472-765X.2005.01827.x

Shaharoona, B., Jamro, G. M., Zahir, Z. A., Arshad, M., and Memon, K. S. (2007). Effectiveness of various *pseudomonas* spp. and *Burkholderiacaryophylli* containing ACC-deaminase for improving growth and yield of wheat (*Triticum aestivum* L.). *J. Microbiol. Biotechnol.* 17, 1300–1307. doi: 10.1016/j.soilbio.2006.03.024

Shahid, M., Ahmed, B., and Khan, M. S. (2018a). Evaluation of microbiological management strategy of herbicide toxicity to greengram plants. *Biocat. Agric. Biotech.* 14, 96–108. doi: 10.1016/j.bcab.2018.02.009

Shahid, M., Ahmed, B., Zaidi, A., and Khan, M. S. (2018b). Toxicity of fungicides to *Pisum sativum*: a study of oxidative damage, growth suppression, cellular death and morpho-anatomical changes. *RSC Adv.* 8, 38483–38498. doi: 10.1039/C8RA03923B

Shahid, M., Al-Khattaf, F. S., Danish, M., Atef Hatamleh, A., Mohamed, A., and Ali, S. (2022a). PGPR *Kosakoniaradicincitans* KR-17 increases the salt tolerance of radish by regulating ion-homeostasis, photosynthetic molecules, redox potential, and stressor metabolites. *Front. Plant Sci.* 13:2270. doi: 10.3389/fpls.2022.919696

Shahid, M., Ameen, F., Maheshwari, H. S., Ahmed, B., AlNadhari, S., and Khan, M. S. (2021a). Colonization of *Vigna radiata* by a halotolerant bacterium *Kosakoniasacchari* improves the ionic balance, stressor metabolites, antioxidant status and yield under NaCl stress. *Appl. Soil Ecol.* 158:103809. doi: 10.1016/j.apsoil.2020.103809

Shahid, M., and Khan, M. S. (2018). Glyphosate induced toxicity to chickpea plants and stress alleviation by herbicide tolerant phosphate solubilizing *Burkholderiacepacia* PSBB1 carrying multifarious plant growth promoting activities. *3 Biotech* 8, 131–117. doi: 10.1007/s13205-018-1145-y

Shahid, M., and Khan, M. S. (2019). Fungicide tolerant *Bradyrhizobium japonicum* mitigate toxicity and enhance greengram production under hexaconazole stress. *J. Environ. Sci.* 78, 92–108. doi: 10.1016/j.jes.2018.07.007

Shahid, M., and Khan, M. S. (2022a). Tolerance of pesticides and antibiotics among beneficial soil microbes recovered from contaminated rhizosphere of edible crops. *Cur. Res. Microbial Sci.* 3:100091. doi: 10.1016/j.crmicr.2021.100091

Shahid, M., and Khan, M. S. (2022b). Ecotoxicological implications of residual pesticides to beneficial soil bacteria: a review. *Pesticide Biochem. Physiol* 188:105272. doi: 10.1016/j.pestbp.2022.105272

Shahid, M., Khan, M. S., Syed, A., Marraiki, N., and Elgorban, A. M. (2021b). *Mesorhizobiumciceri* as biological tool for improving physiological, biochemical and antioxidant state of *Cicer aritienum* (L.) under fungicide stress. *Sci. Rep.* 11, 1–18. doi: 10.1038/s41598-021-89103-9

Shahid, M., Khan, M. S., and Zaidi, A. (2020). Fungicide toxicity to legumes and its microbial remediation: a current perspective. *Pestic. Crop Prod. Physiol. Biochem. Action*, 15–33. doi: 10.1002/9781119432241.ch2

Shahid, M., Manoharadas, S., Altaf, M., and Alrefaei, A. F. (2021c). Organochlorine pesticides negatively influenced the cellular growth, morphostructure, cell viability, and biofilm-formation and phosphate-solubilization activities of *Enterobacter cloacae* strain EAM 35. *ACS Omega.* 6, 5548–5559. doi: 10.1021/acsomega.0c05931

Shahid, M., Shah, A. A., Basit, F., Noman, M., Zubair, M., Ahmed, T., et al. (2019a). *Achromobacter* sp. FB-14 harboring ACC deaminase activity augmented rice growth by upregulating the expression of stress-responsive CIPK genes under salinity stress. *Brazilian J. Microbiol.* 51, 719–728. doi: 10.1007/s42770-019-00199-8

Shahid, M., Singh, U. B., Ilyas, T., Malviya, D., Vishwakarma, S. K., Shafi, Z., et al. (2022c). Bacterial inoculants for control of fungal diseases in *Solanum lycopersicum L.* (tomatoes): a comprehensive overview. *In Rhizosphere Microbes. Microorganisms for Sustainability, eds. Singh, U.B., Sahu, P.K., Singh, H.V., Sharma, P.K., Sharma, S. K. vol 40. Springer, Singapore.*, 311–339. doi: 10.1007/978-981-19-5872-4_1

Shahid, M., Zaidi, A., Ehtram, A., and Khan, M. S. (2019b). *In vitro* investigation to explore the toxicity of different groups of pesticides for an agronomically important rhizosphere isolate *Azotobacter vinelandii*. *Pesticide Biochem. Physiol* 157, 33–44. doi: 10.1016/j.pestbp.2019.03.006

Shahid, M., Zaidi, A., Khan, M., Rizvi, A., Saif, S., and Ahmed, B. (2017). Recent advances in management strategies of vegetable diseases. *In Microbial Strategies for Vegetable Production. eds. Zaidi, A., Khan, M. Springer, Cham.* doi: 10.1007/978-3-319-54401-4_9

Shahid, M., Zeyad, M. T., Syed, A., Singh, U. B., Mohamed, A., Bahkali, A. H., et al. (2022b). Stress-tolerant endophytic isolate *Priestiaaryabhattai* BPR-9 modulates physio-biochemical mechanisms in wheat (*Triticum aestivum* L.) for enhanced salt tolerance. *Int. J. Environ. Res. Public Health* 19:10883. doi: 10.3390/ijerph191710883

Shahzad, R., Khan, A. L., Bilal, S., Asaf, S., and Lee, I. J. (2017). Plant growth-promoting endophytic bacteria versus pathogenic infections: an example of *bacillus amyloliquefaciens* RWL-1 and *fusarium oxysporum* f. sp. *lycopersici* in tomato. *Peer J.* 5:e3107. doi: 10.7717/peerj.3107

Shahzadi, I., Khalid, A., Mahmood, S., Arshad, M., Mahmood, T., and Aziz, I. (2013). Effect of bacteria containing ACC deaminase on growth of wheat seedlings grown with chromium contaminated water. *Pak. J. Bot.* 45, 487–494.

Sharma, S. B., Jain, S., Khirwadkar, P., and Kulkarni, S. (2013). The effects of air pollution on the environment and human health. *Indian J. Res. Pharmacy Biotech.* 1, 391–396.

Sheng, X. F., He, L. Y., Zhou, L., and Shen, Y. Y. (2009). Characterization of *microbacterium* sp. F10a and its role in polycyclic aromatic hydrocarbon removal in low-temperature soil. *Can. J. Microbiol.* 55, 529–535. doi: 10.1139/W09-005

Siddikee, M. A., Chauhan, P. S., and Sa, T. (2012). Regulation of ethylene biosynthesis under salt stress in red pepper (*Capsicum annuum* L.) by 1-aminocyclopropane-1-carboxylic acid (ACC) deaminase-producing halotolerant bacteria. *J. Plant Growth Regul.* 31, 265–272. doi: 10.1007/s00344-011-9236-6

Singh, R. P., and Jha, P. N. (2016). A halotolerant bacterium *bacillus licheniformis* HSW-16 augments induced systemic tolerance to salt stress in wheat plant (*Triticum aestivum*). *Front. Plant Sci.* 7:1890. doi: 10.3389/fpls.2016.01890

Singh, U. B., Malviya, D., Singh, S., Imran, M., Pathak, N., Alam, M., et al. (2016a). Compatible salt-tolerant rhizosphere microbe-mediated induction of phenylpropanoid cascade and induced systemic responses against *Bipolarissorokiniana* (Sacc.) shoemaker causing spot blotch disease in wheat (*Triticum aestivum* L.). *Appl. Soil Ecol.* 108, 300–306. doi: 10.1016/j.apsoil.2016.09.014

Singh, U. B., Malviya, D., Singh, S., Pradhan, J. K., Singh, B. P., Roy, M., et al. (2016b). Bio-protective microbial agents from rhizosphere eco-systems trigger plant defense responses provide protection against sheath blight disease in rice (*Oryza sativa* L.). *Microbiol. Res.* 192, 300–312. doi: 10.1016/j.micres.2016.08.007

Singh, U. B., Malviya, D., Singh, S., Singh, P., Ghatak, A., Imran, M., et al. (2021). Salt-tolerant compatible microbial inoculants modulate physio-biochemical responses enhance plant growth, Zn biofortification and yield of wheat grown in saline-sodic soil. *Int. J. Environ. Res. Public Health* 18:9936. doi: 10.3390/ijerph18189936

Singh, R. P., Pandey, D. M., Jha, P. N., and Ma, Y. (2022). ACC deaminase producing rhizobacterium *Enterobactercloacae* ZNP-4 enhance abiotic stress tolerance in wheat plant. *PLoS One* 17:e0267127. doi: 10.1371/journal.pone.0267127

Singh, R. P., Shelke, G. M., Kumar, A., and Jha, P. N. (2015). Biochemistry and genetics of ACC deaminase: a weapon to "stress ethylene" produced in plants. *Front. Microbiol.* 6:937. doi: 10.3389/fmicb.2015.00937

Singh, S., Singh, U. B., Malviya, D., Paul, S., Sahu, P. K., Trivedi, M., et al. (2020a). Seed biopriming with microbial inoculant triggers local and systemic defense responses against *Rhizoctonia solani* causing banded leaf and sheath blight in maize (*Zea mays* L.). *Int. J. Environ. Res. Public Health* 17:1396. doi: 10.3390/ijerph17041396

Singh, S., Singh, U. B., Trivdi, M., Malviya, D., Sahu, P. K., Roy, M., et al. (2021). Restructuring the cellular responses: connecting microbial intervention with ecological fitness and adaptiveness to the maize (*Zea mays* L.) grown in saline–sodic soil. *Front. Microbiol.* 11:568325. doi: 10.3389/fmicb.2020.568325

Singh, S., Singh, U. B., Trivedi, M., Sahu, P. K., Paul, S., Paul, D., et al. (2020b). Seed biopriming with salt-tolerant endophytic *Pseudomonas geniculata*-modulated biochemical responses provide ecological fitness in maize (*Zea mays* L.) grown in saline sodic soil. *Int. J. Environ. Res. Public Health* 17:253. doi: 10.3390/ijerph17010253

Sofy, M. R., Aboseidah, A. A., Heneidak, S. A., and Ahmed, H. R. (2021). ACC deaminase containing endophytic bacteria ameliorate salt stress in *Pisum sativum* through reduced oxidative damage and induction of antioxidative defense systems. *Environ. Sci. Pollut. Res.* 28, 40971–40991. doi: 10.1007/s11356-021-13585-3

Srinivasan, R., Mageswari, A., and Subramanian, P. (2017). Exogenous expression of ACC deaminase gene in psychrotolerant bacteria alleviates chilling stress and promotes plant growth in millets under chilling conditions. *Indian J. Exp. Biol.* 55, 463–468.

Stallworth, S., Schumaker, B., Fuller, M. G., and Tseng, T. M. (2020). "Consequences and mitigation strategies of biotic and abiotic Stress in Rice (*Oryza sativa* L.)" in *Plant Stress physiology* (eds. Akbar Hossain Intech Open)

Stress, A. (2018). Perspectives of Rhizobacteria with ACC deaminase activity in plant growth under. *Root Biology* 52:303. doi: 10.1007/978-3-319-75910-4_12

Subramanian, P., Kim, K., and Krishnamoorthy, R. (2016). Cold stress tolerance in psychrotolerant soil bacteria and their conferred chilling resistance in tomato (*Solanum lycopersicum* mill.) under low temperatures. *PLoS One* 11:e0161592. doi: 10.1371/journal.pone.0161592

Subramanian, P., Krishnamoorthy, R., and Chanratana, M. (2015). Expression of an exogenous 1-aminocyclopropane-1-carboxylatedeaminase gene in psychrotolerant bacteria modulates ethylene metabolism and cold induced genes in tomato under chilling stress. *Plant Physiol. Biochem.* 89, 18–23. doi: 10.1016/j.plaphy.2015.02.003

Sun, L., Zhang, X., Ouyang, W., Yang, E., Cao, Y., and Sun, R. (2022). Lowered cd toxicity, uptake and expression of metal transporter genes in maize plant by ACC deaminase-producing bacteria *Achromobacter* sp. *J. Hazard. Mater.* 423:127036. doi: 10.1016/j.jhazmat.2021.127036

Sun, L. R., Zhao, Z. J., and Hao, F. S. (2019). NADPH oxidases, essential players of hormone signalings in plant development and response to stresses. *Plant Signal. Behav.* 14:1657343. doi: 10.1080/15592324.2019.1657343

Tahir, M., Arshad, M., Naveed, M., Zahir, Z. A., Shaharoona, B., and Ahmad, R. (2006). Enrichment of recycled organic waste with N fertilizer and PGPR containing ACC-deaminase for improving growth and yield of tomato. *Soil Environ.* 31, 23–15.

Tavares, M. J., Nascimento, F. X., Glick, B. R., and Rossi, M. J. (2018). The expression of an exogenous ACC deaminase by the endophyte *Serratia grimesii* BXF 1 promotes the early nodulation and growth of common bean. *Letter Appl. Microbiol.* 66, 252–259. doi: 10.1111/lam.12847

Theocharis, A., Bordiec, S., Fernandez, O., Paquis, S., Dhondt-Cordelier, S., Baillieul, F., et al. (2012). *Burkholderiaphytofirmans*PsJN primes *Vitis vinifera* L. and confers a better tolerance to low non-freezing temperatures. *Mol. Plant-Microbe Interact.* 25, 241–249. doi: 10.1094/MPMI-05-11-0124

Thibodeaux, C. J., and Liu, H. W. (2011). Mechanistic studies of 1-aminocyclopropane-1-carboxylate deaminase: characterization of an unusual pyridoxal 5′-phosphate-dependent reaction. *Biochemist* 50, 1950–1962. doi: 10.1021/bi101927s

Thijs, S., Weyens, N., Sillen, W., Gkorezis, P., Carleer, R., and Vangronsveld, J. (2014). Potential for plant growth promotion by a consortium of stress-tolerant 2, 4-dinitrotoluene-degrading bacteria: isolation and characterization of a military soil. *Microbial Biotech.* 7, 294–306. doi: 10.1111/1751-7915.12111

Timmusk, S., Paalme, V., Pavlicek, T., Bergquist, J., Vangala, A., Danilas, T., et al. (2011). Bacterial distribution in the rhizosphere of wild barley under contrasting microclimates. *PLoS One* 6:e17968. doi: 10.1371/journal.pone.0017968

Tiwari, S., Gupta, D., Fatima, A., Singh, S., and Prasad, S. M. (2020). "Phytohormonal metabolic engineering for abiotic stress in plants: new avenues and future prospects" in *Plant life under changing environment*, eds. Durgesh Kumar Tripathi, Vijay Pratap Singh, Naleeni Ramawat (Academic Press), 543–576.

Tiwari, S., Lata, C., Chauhan, P. S., and Nautiyal, C. S. (2016). *Pseudomonas putida* attunes morphophysiological, biochemical and molecular responses in *Cicer arietinum* L. during drought stress and recovery. *Plant Physiol. Biochem.* 99, 108–117. doi: 10.1016/j.plaphy.2015.11.001

Toklikishvili, N., Dandurishvili, N., Vainstein, A., Tediashvili, M., Giorgobiani, N., and Lurie, S. (2010). Inhibitory effect of ACC deaminase producing bacteria on crown gall formation in tomato plants infected by *agrobacterium tumefaciens* or *A. vitis*. *Plant Pathol.* 59, 1023–1030. doi: 10.1111/j.1365-3059.2010. 02326.x

Trung, N. T., Hieu, H. V., and Thuan, N. H. (2016). Screening of strong 1-aminocyclopropane-1-carboxylate deaminase producing bacteria for improving the salinity tolerance of cowpea. *Appl. Micro Open Access* 2:1000111. doi: 10.4172/amoa.1000111

Tsolakidou, M. D., Pantelides, L. S., Tzima, A. K., Kang, S., Paplomatas, E. J., and Tsaltas, D. (2019). Disruption and overexpression of the gene encoding ACC (1-aminocyclopropane-1-carboxylic acid) deaminase in soil-borne fungal pathogen *Verticillium dahliae* revealed the role of ACC as a potential regulator of virulence and plant defense. *Mol. Plant-Microbe Interact.* 32, 639–653. doi: 10.1094/MPMI-07-18-0203-R

Uchiumi, T., Ohwada, T., Itakura, M., Mitsui, H., Nukui, N., Dawadi, P., et al. (2004). Expression islands clustered on the symbiosis island of the Mesorhizobium loti genome. *J. Bacteriol.* 186, 2439–2448. doi: 10.1128/JB.186.8.2439-2448.2004

Van Loon, L. C., Geraats, B. P. J., and Linthorst, H. J. M. (2006). Ethylene as a modulator of disease resistance in plants. *Trends Plant Sci.* 11, 184–191. doi: 10.1016/j.tplants.2006.02.005

Vargas, L. K., Volpiano, C. G., Lisboa, B. B., Giongo, A., Beneduzi, A., and Passaglia, L. M. P. (2017). *Potential of rhizobia as plant growth-promoting rhizobacteria* Springer International Publishing, 153–174.

Viscardi, S., Ventorino, V., Duran, P., Maggio, A., De Pascale, S., Mora, M. L., et al. (2016). Assessment of plant growth promoting activities and abiotic stress tolerance of *Azotobacter chroococcum* strains for a potential use in sustainable agriculture. *J. Soil Sci. Plant Nut.* 16, 848–863. doi: 10.4067/S0718-95162016005000060

Walsh, C., Pascal, R. A. Jr., Johnston, M., Raines, R., Dikshit, D., Krantz, A., et al. (1981). Mechanistic studies on the pyridoxal phosphate enzyme 1-aminocyclopropane-1-carboxylate deaminase from *pseudomonas* sp. *Biochemist* 20, 7509–7519. doi: 10.1021/bi00529a028

Wang, Q., Dodd, I. C., Belimov, A. A., and Jiang, F. (2016). Rhizosphere bacteria containing 1-aminocyclopropane-1-carboxylate deaminase increase growth and photosynthesis of pea plants under salt stress by limiting Na1 accumulation. *Funct. Plant Biol.* 43, 161–172. doi: 10.1071/FP15200

Wang, C., Knill, E., Glick, B. R., and Défago, G. (2000). Effect of transferring 1-aminocyclopropane-1-carboxylic acid (ACC) deaminase genes into *Pseudomonas fluorescens* strain CHA0 and its gacA derivative CHA96 on their growth-promoting and disease-suppressive capacities. *Can. J. Microbiol.* 46, 898–907. doi: 10.1139/w00-07

Wang, C., Wang, F., Zhang, Q., and Liang, W. (2016). Individual and combined effects of tebuconazole and carbendazim on soil microbial activity. *Eur. J. Soil Bio. J.* 72, 6–13. doi: 10.1016/j.ejsobi.2015.12.005

Wang, C. J., Yang, W., Wang, C., Gu, C., Niu, D. D., Liu, H. X., et al. (2012). Induction of drought tolerance in cucumber plants by a consortium of three plant growth-promoting rhizobacterium strains. *PLoS One* 7:e52565. doi: 10.1371/journal.pone.0052565

Wang, P., Zhang, Z., Chen, Y., Wei, X., Feng, B., and Tao, F. (2016). How much yield loss has been caused by extreme temperature stress to the irrigated rice production in China? *Clim. Chang.* 134, 635–650. doi: 10.1007/s10584-015-1545-5

Xia, Y., Farooq, M. A., Javed, M. T., Kamran, M. A., Mukhtar, T., Ali, J., et al. (2020). Multi-stress tolerant PGPR *Bacillusxiamenensis* PM14 activating sugarcane (*Saccharum officinarum* L.) red rot disease resistance. *Plant Physiol. Biochem.* 151, 640–649. doi: 10.1016/j.plaphy.2020.04.016

Xun, F., Xie, B., and Liu, S. (2015). Effect of plant growth-promoting bacteria (PGPR) and arbuscular mycorrhizal fungi (AMF) inoculation on oats in saline-alkali soil contaminated by petroleum to enhance phytoremediation. *Environ. Sci. Pollut. Res.* 22, 598–608. doi: 10.1007/s11356-014-3396-4

Yadav, S. K. (2010). Cold stress tolerance mechanisms in plants: a review. *Agron. Sustain. Dev.* 30, 515–527. doi: 10.1051/agro/2009050

Yan, K., Shao, H., Shao, C., Chen, P., Zhao, S., and Brestic, M. (2013). Physiological adaptive mechanisms of plants grown in saline soil and implications for sustainable saline agriculture in coastal zone. *Acta Physiol. Plant.* 35, 2867–2878. doi: 10.1007/s11738-013-1325-7

Yasmin, H., Bano, A., Wilson, N. L., Nosheen, A., Naz, R., Hassan, M. N., et al. (2022). Drought-tolerant *pseudomonas* sp. showed differential expression of stress-responsive genes and induced drought tolerance in *Arabidopsis thaliana*. *Physiol. Planta.* 174:e13497. doi: 10.1111/ppl.13497

Yim, W. J., Woo, S. M., Kim, K. Y., and Sa, T. M. (2012). Regulation of ethylene emission in tomato (*Lycopersicon esculentum* mill.) and red pepper (*Capsicum annuum* L.) inoculated with ACC deaminase producing *Methylobacterium* spp. *Korean J. Soil Sci. Fertilizer* 45, 37–42.

Zafar-ul-Hye, M., Danish, S., Abbas, M., Ahmad, M., and Munir, T. M. (2019). ACC deaminase producing PGPR *bacillus amyloliquefaciens* and *agrobacterium fabrum* along with biochar improve wheat productivity under drought stress. *Agronomy* 9:343. doi: 10.3390/agronomy9070343

Zafar-Ul-Hye, M. U., Shahjahan, A., Danish, S. U., Abid, M. U., and Qayyum, M. F. (2018). Mitigation of cadmium toxicity induced stress in wheat by acc-deaminase containing PGPR isolated from cadmium polluted wheat rhizosphere. *Pak. J. Bot.* 50, 1727–1734.

Zahir, Z. A., Ghani, U., Naveed, M., Nadeem, S. M., and Asghar, H. N. (2009). Comparative effectiveness of *pseudomonas* and *Serratia* sp. containing ACC deaminase for improving growth and yield of wheat (*Triticum aestivum* L.) under salt-stressed conditions. *Arch. Microbiol.* 191, 415–424. doi: 10.1007/s00203-009-0466-Y

Zahir, Z. A., Munir, A., Asghar, H. N., Shaharoona, B., and Arshad, M. (2008). Effectiveness of rhizobacteria containing ACC deaminase for growth promotion of peas (*Pisum sativum*) under drought conditions. *J. Microbiol. Biotechnol.* 18, 958–963.

Zaidi, A., Khan, M. S., Ahmad, E., Saif, S., Rizvi, A., and Shahid, M. (2016). Growth stimulation and management of diseases of ornamental plants using phosphate solubilizing microorganisms: current perspective. *Acta Physiol. Planta.* 38, 1–21. doi: 10.1007/s11738-016-2133-7

Zaidi, A., Khan, M. S., Saif, S., Rizvi, A., Ahmed, B., and Shahid, M. (2017). "Role of nitrogen-fixing plant growth-promoting rhizobacteria in sustainable production of vegetables: current perspective" in *Microbial strategies for vegetable production*, Zaidi, A., Khan, M. (eds) (Cham: Springer), 49–79.

Zainab, N., Din, B. U., Javed, M. T., Afridi, M. S., Mukhtar, T., Kamran, M. A., et al. (2020). Deciphering metal toxicity responses of flax (*Linumusitatissimum* L.) with exopolysaccharide and ACC-deaminase producing bacteria in industrially contaminated soils. *Plant Physiol. Biochem.* 152, 90–99. doi: 10.1016/j.plaphy.2020.04.039

Zhang, H., Li, A., Zhang, Z., Huang, Z., Lu, P., Zhang, D., et al. (2016). Ethylene response factor TERF1, regulated by ethylene-INSENSITIVE3-like factors, functions in reactive oxygen species (ROS) scavenging in tobacco (*Nicotiana tabacum* L.). *Sci. Rep.* 6:29948. doi: 10.1038/srep29948

Zhao, Z., Chen, H., Li, K., Du, W., He, S., and Liu, H. W. (2003). Reaction of 1-amino-2-methylenecyclopropane-1-carboxylate with 1-aminocyclopropane-1-carboxylate deaminase: analysis and mechanistic implications. *Biochemist* 42, 2089–2103. doi: 10.1021/bi020567n

Zhu, T., Deng, X., Zhou, X., Zhu, L., Zou, L., Li, P., et al. (2016). Ethylene and hydrogen peroxide are involved in brassinosteroid-induced salt tolerance in tomato. *Sci. Rep.* 6:35392. doi: 10.1038/srep35392

Frontiers in Microbiology

Explores the habitable world and the potential of microbial life

The largest and most cited microbiology journal which advances our understanding of the role microbes play in addressing global challenges such as healthcare, food security, and climate change.

Discover the latest Research Topics

See more →

Frontiers

Avenue du Tribunal-Fédéral 34
1005 Lausanne, Switzerland
frontiersin.org

Contact us

+41 (0)21 510 17 00
frontiersin.org/about/contact